ROCK DRILLING WITH IMPREGNATED DIAMOND MICROBITS

DUNCAN EDMUND MILLER

A THESIS PRESENTED TO FULFIL THE
REQUIREMENTS FOR THE DEGREE OF
DOCTOR OF PHILOSOPHY
OF THE
UNIVERSITY OF CAPE TOWN

1986

ABSTRACT

A fully instrumented laboratory drilling rig was designed and used to drill a variety of rock types with impregnated diamond microbits. The rocks, selected to represent a wide range of properties, were characterised by optical petrography and by the measurement of uniaxial compressive strength and relative abrasion resistance. A computer controlled electronic data logging system was used to record the power consumption, the rotational velocity, the bit thrust, the torque and the penetration rate. Tests were conducted under set thrust and under set rate of advance conditions to determine the effect of varying the bit pressure, rotational velocity, diamond mesh size and concentration, and rock type on the dependent drilling variables of diamond wear, bit wear, rock fracture, torque, power consumption, penetration rate and reactive load. The drilling efficiency was monitored by calculating the specific energy of drilling from the power consumption corrected for the power losses in the machine and from the generated torque, the latter being more sensitive. The diamond wear on a used bit was evaluated under the optical microscope by classifying each exposed stone into one of ten wear categories. The rock fracture was evaluated by scanning electron microscopy of the drilled surfaces, and by particle size distribution analysis of the drilling detritus. On the basis of the results a performance model for impregnated diamond bit drilling was formulated in which a critical stress threshold per actively drilling diamond must be exceeded for steady drilling to take place with any specific combination of bit and rock type. The optimum drilling thrust at which the specific energy is at a minimum and the penetration rate at a maximum for a given rock and bit configuration, occurs marginally above the thrust required for all the exposed diamonds to be in contact with the rock. The effective bit pressure and the rock type characteristics are crucial determinants for diamond wear type development and hence for the drilling performance within the operating range. The transition from suboptimal to optimal drilling conditions has been described in terms of the characteristic diamond wear, the specific energy, and the coefficient of friction between the bit and the rock. The mechanism of diamond wear and rock fracture are discussed with reference to the results of the optical and

scanning electron microscopy of worn diamonds and the rock detritus. It is concluded that a variety of rock properties affects the drilling performance, sometimes unpredictably and that the realistic drilling of any specific rock is necessary to determine its resistance to drilling. The necessary approach is demonstrated in detail for a single rock type, norite, for which it is shown the transition takes place at a pressure of approximately 400 MPa per actively drilling stone irrespective of the diamond size or concentration. A discussion of rock drillability testing demonstrates that experimental drilling with microbits has a valid role in the realistic evaluation of drillability and in the study of the complex fracture and wear mechanisms that must be understood for the application and rational design of appropriate bits.

ACKNOWLEDGEMENTS

My thanks are due to my supervisor, Professor Anthony Ball, to the staff and students of the Materials Engineering Department of the University of Cape Town, and to my friends for their assistance. Specific contributions of individuals will be noted in the appropriate places in the text. Financial support from Boart Research Centre in Krugersdorp and the CSIR is gratefully acknowledged as is the practical assistance of members of the Boart Research Centre staff in discussing the course of the research and for manufacturing the bits.

CONTENTS

PAGE

PAGE

PAGE

LIST OF FIGURES

PAGE

PAGE

PAGE

PAGE

PAGE

PAGE

PAGE

PAGE

PAGE

PAGE

PAGE

PAGE

PAGE

LIST OF TABLES

PAGE

PAGE

CHAPTER 1

INTRODUCTION

1.1 A SHORT HISTORY OF ROCK DRILLING AND INDUSTRIAL DIAMOND USE

Rock drilling has a long history with a very sparse record. Tubular drills rotating under pressure with quartz grit as an abrasive are thought to have been used by the ancient Egyptians for obtaining cores in hard rock, and a thousand years ago the Chinese were using percussion drilling to extract water and salt from wells up to 1,2 km deep (Norling undated).

The earliest known written account of the use of diamond is a description of a diamond engraving tool written about 300 BC by Brahman Kautilya (Hughes 1980). The first mention of the use of diamond grit as an abrasive was by Pliny in AD 77 but it was only in AD 1757 that the first known description of a hand operated diamond tipped rock drill appeared. During the nineteenth and early twentieth century the use of natural whole stones in tooling applications expanded with innovations in rock drilling, stone cutting, lathe tools, wire-drawing dies and grinding wheels.

In the 1920's industrial boart or natural industrial diamond was introduced in the USA and found a growing market in industry (Bullen & Bailey 1979). The introduction and initial development of impregnated diamond bits using boart or reject grade industrial diamond took place before 1940 (Wilson 1941). It was only in 1951 that the first experiments were done on the controlled crushing of natural boart to provide material for the expanded demand in industry for diamond abrasive (Rainer 1980) and in 1953 the first synthetic diamond was produced in Sweden by ASEA (Liander 1980). Since 1970, synthetic diamond grit has been used increasingly extensively as an abrasive with a wide range of crystal shapes, strengths and size distributions available (Bullen 1983).

1.2 DIAMOND DRILLING BITS

There are three main types of diamond drilling bits currently available. Surface set crowns consist of a hard metal matrix set with regular arrays of natural whole stones, often on geometrically complicated surfaces specifically designed for different applications. Impregnated diamond bits are made by mixing a suitable powdered metal with the appropriate diamond grit, natural or synthetic, and sintering at high temperature to produce impregnated drilling pads mounted on a threaded shank. In the last decade polycrystalline diamond compacts have been developed that are analogous to sintered tungsten carbide-cobalt. The compacts are available in a variety of shapes; either with hard metal supports or free, for different applications including setting as cutting elements in rotary drills. Polycrystalline diamond components are being used increasingly where formerly surface set or impregnated drills were used. However, as the creation of the compact involves a further production step it is still economical to use the more conventional tools except for specialised applications. The attributes and behaviour of these new diamond materials are being explored currently (Brookes & Hooper 1982, Brookes & Lambert 1982, Atkins 1985). A comparison of the performance of drills set with polycrystalline inserts with surface set or impregnated bits is not yet possible.

Surface set diamond crowns are designed so that the placement and degree of protrusion of the relatively large diamonds protects the matrix from wear. As drilling proceeds the diamonds themselves develop wear flats which eventually impede the operation of the bit and necessitate the application of a greater thrust force to maintain penetration. Eventually the bit has to be reset, to replace broken, lost or excessively worn stones with new ones. Salvage credit is available on the useful stones left in worn out bits. Surface set bits are used extensively in oil prospecting and the drilling of softer formations, as well as in hard rock drilling to a more limited extent.

Impregnated diamond bits are more appropriate to hard rock drilling and civil engineering applications (Busch 1979) where the "polishing" of the diamonds of a surface set bit would be severe. The impregnated bit is designed so that under correct operating conditions, fresh diamonds are

exposed continually by a process of balanced matrix wear in order to maintain the appropriate number of cutting points for a sustained penetration rate. An appropriately selected bit operated at the correct rate of advance should drill steadily for its lifetime which is determined by the wear rate of the matrix (Paone & Madson 1966).

It is important that the differences in the modes of operation of surface set and impregnated diamond bits be understood for their efficient use. If correctly used impregnated diamond bits operate at lower thrusts albeit with lower penetration rates than surface set bits. They are consumed totally and can be operated without resetting thus allowing for a longer down-hole life. The advantages of hard rock drilling with impregnated bits have been summarised by Hammerback (1969). The bits are robust and not easily damaged by drilling through broken or hard rock or in use by inexperienced drillers working under minimal supervision. Because of the lower thrusts required, the tendency for the hole to deflect is reduced and a straighter hole and smoother core are produced. There is correspondingly less friction between the drill string and the side walls. Since the bit is consumed to expose all the diamonds no resetting, or administrative record of diamond salvage is required. The cost of drilling hard rock can be lowered as the bit costs drop and a longer active operational life may be possible under suitable conditions. Impregnated diamond bits are not advantageous in drilling soft or very abrasive rocks as it is difficult to maintain close control of the clearance between the rock and the bit matrix and hence to control the flushing and removal of cuttings (Adamson 1946).

The performance of surface set bits has been enhanced in some cases by crystallographic orientation of the diamonds to present the hardest vector to the surface being cut. This is an expensive and uneconomical procedure in the production of an impregnated bit (Rowlands 1971). Hence exact placement of the diamonds is not achieved in the production of impregnated diamond bits and the distribution of stones is assumed to be random.

1.3 THE NEED FOR FUNDAMENTAL INFORMATION

It is widely agreed upon that there is a crucial lack of fundamental information on the operation of impregnated diamond bits despite their

use for over forty years. In 1966 Paone and Madson observed that very little was known about the performance of impregnated diamond bits. The basic mechanism of drilling is still obscure (Maurer 1967, Graham 1972) and what information there is tends to be largely subjective (Rowlands 1971). Bailey & Dean (1967) described the motivations of fundamental research into rock drilling. These included the need for a description of the fracture process in rocks and the enhancement of performance prediction models. These goals are still valid and unfulfilled. More specifically, research into the performance of impregnated bits has generally failed to distinguish between suboptimal performance (with insufficient bit matrix wear to achieve steady drilling) and stable performance (eg. Paone & Madson 1966, Spink 1972). There is a lack of knowledge about some of the fundamental variables in the drilling system. For instance, almost nothing is known about the effect of changing diamond size; the nature of detritus produced by drilling has not been studied in detail; and the wear of the diamonds and the matrix in impregnated bit drilling is largely unresearched.

1.4 THE MERITS OF LABORATORY TESTING

The major advantage of laboratory testing of impregnated diamond bit drilling is the ease with which the drilling parameters - eg. thrust, rotational speed, flushing rate and pressure - can be controlled and monitored. Field drilling rigs have rudimentary instrumentation generally unsuitable for taking useful measurements. Large blocks of rock are unwieldy but laboratory testing obviates the problem of transporting the drilling rig to investigate different rock types. In the case of scaled microbit drilling the reduced cost of the smaller bits is an added advantage, making it possible to run numerous tests at limited expense. Bullen (1984) has listed the main disadvantages of laboratory drilling. The drill string dynamics and the problem of deflection cannot be investigated as the holes drilled are necessarily short; and the rock material drilled in the laboratory is usually relatively free from fractures and realistic discontinuities. These limitations are not significant in research aimed at describing the basic mechanisms of impregnated diamond bit drilling but must be taken into consideration when laboratory results are projected into field performance.

1.5 THE AIMS OF THE PRESENT RESEARCH

The primary aim of the research presented in this thesis was to study the interaction between the rock and the impregnated diamond drill bit with the intention of describing the processes occurring at the rock bit interface. This required the establishment and the evaluation of the performance of a fully instrumented laboratory drilling rig for testing the behaviour of impregnated diamond microbits under realistic drilling conditions of thrust and rotational speed and at realistic penetration rates. The drilling performance was investigated both under set rate of advance and set thrust conditions in a variety of rock types. As the events at the drill tip could not be observed directly they were studied indirectly by monitoring drilling performance, diamond wear and the damage to the rock. The effects of changing operating parameters and diamond size have also been studied intensively in a single rock type to provide basic information necessary for an evaluation of drilling mechanisms in general.

1.6 THE STRUCTURE OF THIS THESIS

The literature survey in Chapter 2 summarises the published information on impregnated diamond bit drilling. After a brief historical introduction the summary takes the form of a presentation of the results of experimental drilling with impregnated diamond bits, followed by a discussion of some aspects common to the different investigations. Reviews of the pertinent literature on the strength and wear of diamonds and on rock fracture conclude the chapter. Chapter 3 consists of a detailed description of the design and operation of the instrumented laboratory drilling machine constructed for testing impregnated diamond microbits. The drilling test procedure as well as the main ancillary testing methods are described in Chapter 4. The presentation of results in Chapter 5 is restricted to an exposition of the results with minimum comment. The discussion is reserved for Chapter 6 where inferences drawn from the results are combined with information from the literature in an assessment of the research. The conclusions in Chapter 7 are a summary of the research presented in this thesis and directions for further work are suggested.

CHAPTER 2

LITERATURE SURVEY

2.1 EXPERIMENTAL DRILLING WITH IMPREGNATED DIAMOND BITS

The relatively few papers which deal explicitly with experimental impregnated diamond bit drilling will be summarised chronologically with emphasis on results significant to this work. A review of specific topics pertinent to experimental rock drilling will follow the summaries. More detailed discussion will be found in Chapter 6.

One of the first reports on impregnated diamond drill bits was written by Wilson in 1941. It briefly described sintering methods, different matrix compositions, the process of bit face reconditioning by sandblasting, and the need for high speed drilling machines. In 1957 two papers on the subject appeared in the Proceedings of the Seventh Annual Drilling Symposium at the University of Minnesota. The first, by Reid (1957) described the advantages of using impregnated diamond bits for drilling a hard haematite ore. Their performance was better than that of surface set bits only in the harder areas of the iron formation but the impregnated bits had the advantage of being less vulnerable to damage and malfunction when used by inexperienced drillers with less supervision. In the second paper, McWilliams (1957) claimed that more extensive use of impregnated bits would be possible if there were proper instruction in their use, taking into account the differences in operating techniques between the impregnated and familiar surface set bits. It was found that impregnated bits needed to operate at an appropriate feed rate and required at least slightly abrasive rock for maintenance of balanced bit wear and stable operation.

The first major comparative study of drilling with impregnated diamond bits was reported by Paone & Madson (1966). Drillability tests were done in the laboratory and in the field on a wide variety of well characterised rock types. Full-scale bits were used to test the effects

of rotational speed and thrust on penetration rate and drilling performance. The highest penetration rates were obtained with the combination of the highest thrust and rotational speed. But bit wear, assessed by visual inspection, was greater at high speeds. At constant thrust, the increase of the penetration rate with increasing rotational speed was found to be linear.

With increasing thrust at a nominally constant rotational speed, the increase in penetration rate was not linear but increased at a diminishing rate until stalling occurred. The rate of increase was greatest for softer rocks at low rotary speeds and for harder rocks at higher speeds. Harder rocks were drilled more effectively at higher speeds. Below a threshold value of torque, penetration did not take place which indicated that a critical input of energy was required before rock failure could occur. With increasing torque the increase in penetration rate was linear up to a critical value of torque above which the penetration rate increased more slowly. This was considered to be due to an unspecified inherent rock property. In rocks with a uniaxial compressive strength over about 175 MPa the penetration rates of impregnated bits did not vary significantly with increasing compressive or tensile rock strength (see Fig. 2:1). Relative abrasiveness was found to influence penetration rate, while the estimated percentage of "free quartz" determined the life of the bit. For low values of strength, abrasiveness and quartz content, small changes in a property resulted in a large change in penetration rate or bit life. But for high values of rock strength the drilling performance was less affected by fairly substantial changes in the rock properties.

Paone, Bruce & Virciglio (1966) showed by statistical regression analysis of the data of Paone & Madson (1966) that no single rock physical property was a reliable predictor of drilling performance and that all the rock properties were strongly correlated with each other. Equations for the prediction of penetration rate based on laboratory and field tests had only Young's modulus, shear modulus and thrust in common although abrasiveness percentage quartz and compressive strength were also sighificant.

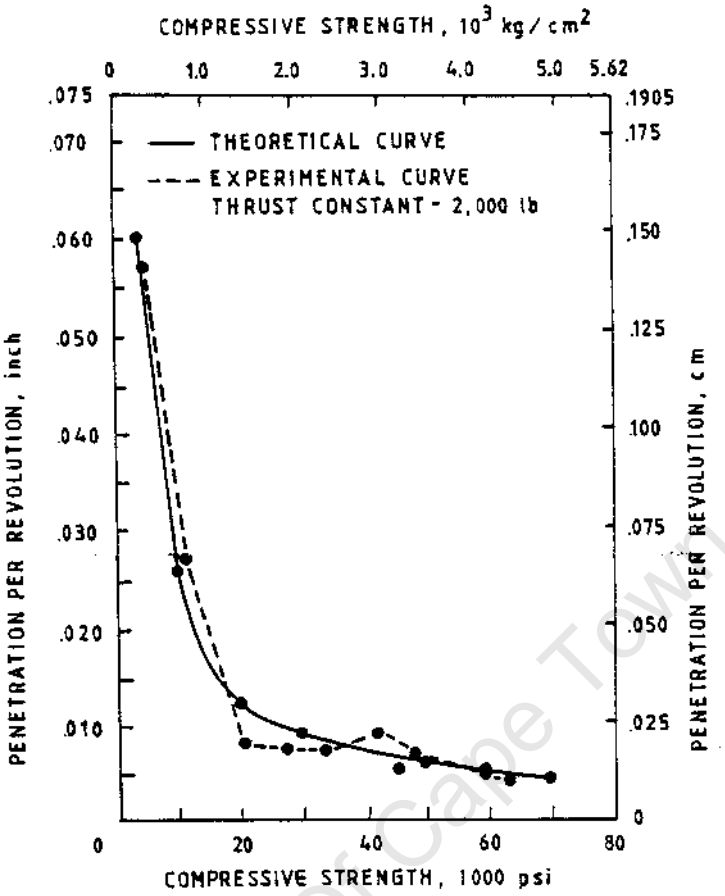

FIGURE 2.1 : Relationship of theoretical and experimental curves for drillability based on compressive strength (after Paone & Madson 1966)

The effect of additives in the drill flushing medium was investigated by Selim, Schultz & Strebig (1969) and further reported on by Strebig, Schultz & Selim (1969) and Strebig, Selim and Schulz (1971). Quartzite was drilled with a range of thrusts and rotational speeds in laboratory tests using standard small narrow-kerf bits. A wear coefficient for the bit was calculated from the drilling performance and not by direct measurement. All the additives used - glycerine, ethylene glycol and anionic detergent - increased the penetration rate (see Fig. 2.2) with a maximum at the highest rotational speed for all concentrations. A torque threshold for penetration was found to exist and was ascribed to the sliding friction between the bit and the rock, assuming that no plastic ploughing took place. The energy per unit volume drilled was constant over a range in which the relationship between torque and penetration rate at a given thrust was linear. The energy per unit volume drilled

was higher with the use of additives than with plain water because of the increased torque transmitted to the rock. No evidence was found that the strength of the rock had been reduced by the additives. All the additives reduced the wear coefficient relative to water and decreased the need to resharpen the bit. This is consistent with the results of similar research using surface set bits (Westwood & Mills 1977, Cooper 1979). Fracture of the diamonds was not recorded. It was suggested that the additives in moderate concentration acted as wetting agents, increased the heat transfer from the diamonds to the coolant and thus inhibited their wear by oxidation and/or graphitisation.

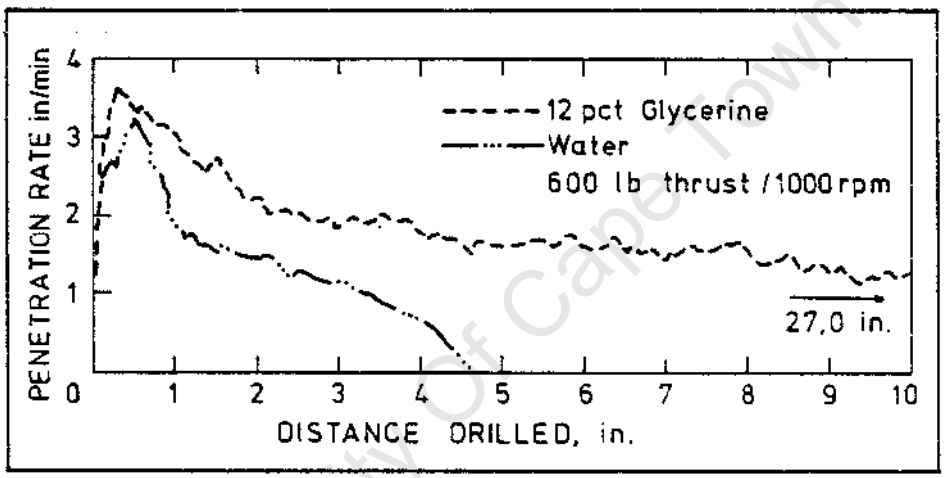

FIGURE 2.2 : Comparison of penetration rates with glycerine and with water (after Selim et al 1969)

The first laboratory tests using impregnated diamond microbits appear to have been those of Spink (1972). Short holes were drilled in a variety of rock types to determine the degree of plastic response of rock, the feasibility of reducing it, and the effect of drilling at low bit pressures. As the gross specific energy values obscured the variation in net specific energy the specific energy was calculated from the gross power consumption after calibration for power losses in the drilling machine at all the operational speeds (Fig. 2.3). The method is described in Moller & Spink (1973). The bits used consisted of a bronze matrix with 100/120 US mesh diamonds in unspecified concentration drilled at a range of rotational speeds and at relatively low bit pressures under set thrust conditions. There was no account of bit or diamond wear.

High bit speeds and pressures were needed to produce penetration in the stronger rocks. In terms of specific energy the optimum bit pressures were much lower than those used conventionally. It was suggested that at low bit pressures most of the work was converted to frictional heat and at high pressures it contributed to enhanced plasticity. Suppression of plastic deformation seemed to be possible by increasing the rotational speed at bit pressures near the optimum. Paradoxically, in some rock types the rate of penetration was reduced at intermediate bit pressures.

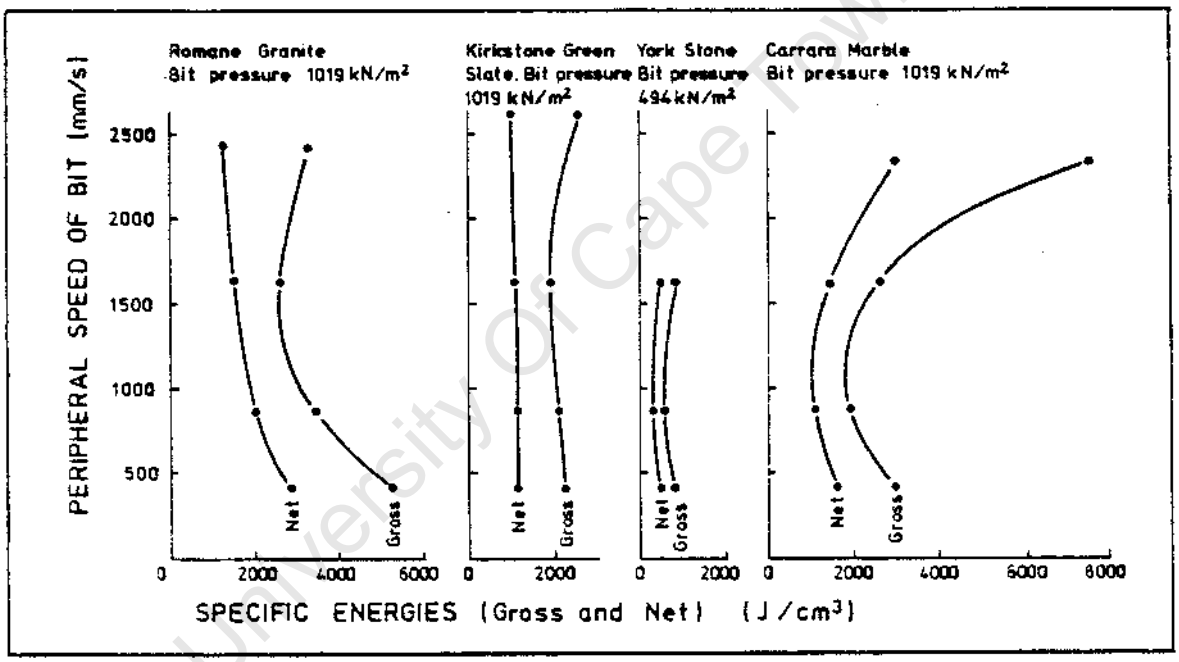

FIGURE 2.3 : Corresponding gross and net specific energies for a series of drilling experiments in various rocks (after Moller & Spink 1973)

Busch & Hill (1975) studied the effect of bit pressure and rotational speed on penetration rate and performance for thin walled bits with two different matrices and a natural processed diamond type of 30/40 US mesh at 75 concentration. (A concentration of 100 is conventionally defined as having 0,88 grams of diamond per cubic centimetre of impregnation, or approximately 25% by volume). As dulling behaviour was being studied resharpening was not carried out. Bit wear was estimated qualitatively.

Plain and reinforced concretes were drilled with a laboratory rig at a realistic range of rotational speeds and bit pressures. Increased bit pressure influenced penetration rate more strongly than increased rotational speed and the softer matrix produced higher penetration rates for each combination (Fig. 2.4). Dulling of the bits at low pressures was indicated by a drop in penetration rate and the smooth appearance of the bit face after drilling. High pressures were required to maintain self sharpening of the bit but this increased the bit wear. Plasticity of the reinforcing bars produced a sharp drop in penetration rate and resulted in a smooth appearance to the face of the bit after drilling through the steel. Economic optimisation of the drilling process was discussed in terms of balancing the tool cost represented by bit wear rate, and the time cost determined by penetration rate.

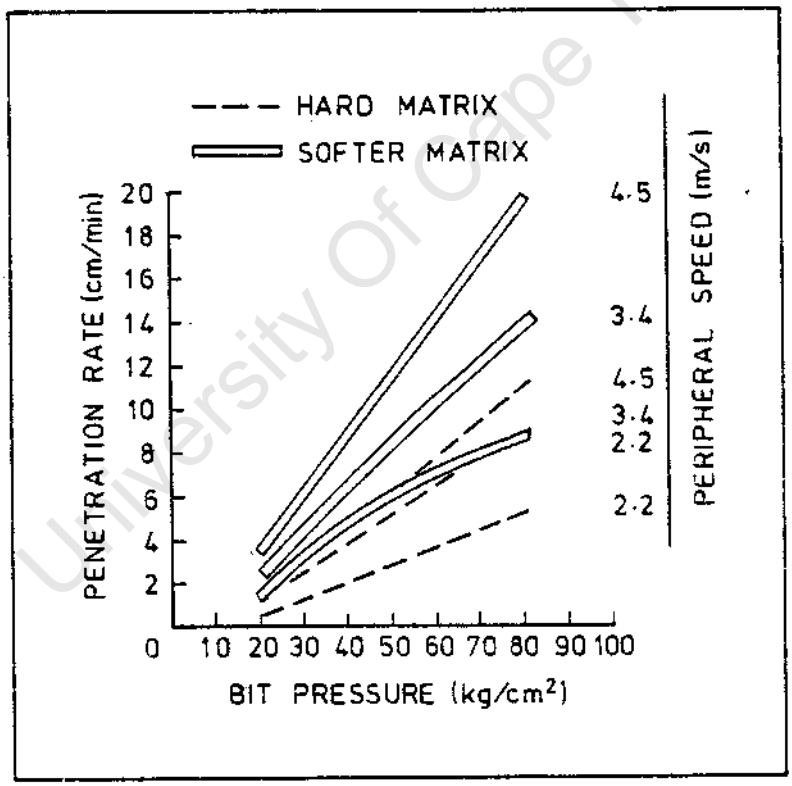

FIGURE 2.4 : Penetration rate against bit pressure in plain cured concrete (after Busch & Hill 1975)

Sullen & Bailey (1979) tested full-scale impregnated diamond bits with a laboratory rig and drilled granite at a variety of set rates of penetration instead of set bit pressure. The bits contained three types of diamonds of different strengths - SDA 100S, SDA 100 and SDA - with a size of 25/35 mesh and at 50 concentration in a hard matrix. Axial bit

wear was measured at regular intervals in a special jig. The tests were conducted to evaluate the performance of synthetic diamond grit in hard rock drilling. At low penetration rates the stronger diamonds polished more rapidly and impeded the progress of the drill. As the penetration rate was increased stronger diamonds were needed to penetrate the rock effectively (Fig. 2.5). Stronger diamonds used at high penetration rates reduced the drilling time but the bit wear increased. For a given type of diamond the bit wear was reduced by a drop in penetration rate with a corresponding increase in drilling time. It was stated that using stronger diamonds at higher penetration rates did not necessarily require increased loads as the stones may maintain their protrusion and ability to drill effectively. The diamonds polished below a threshold thrust force. For stable operation an important relationship existed between diamond grit type and set penetration rate.

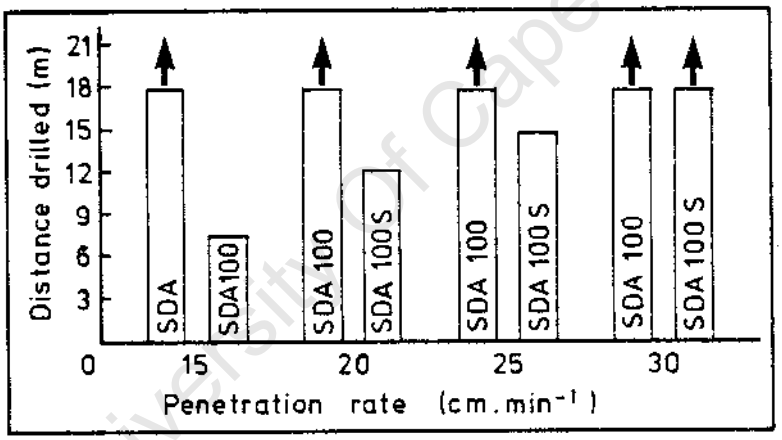

FIGURE 2.5 : Distance drilled as a function of penetration rate in granite (after Bullen & Bailey 1979)

Bamford, Brown & Siribumrungsukha (1979) briefly summarised tests in three rock types at various set thrusts with microbits ranging from 10 to 70 concentration. Strong rocks required a high thrust to maintain steady drilling. Similar trends in results were obtained for microbit and full-scale bit drilling tests. A concentration of 30 produced the highest penetration rate in sandstone but bit wear was lower using a 40 concentration bit, although it drilled slightly less effectively (Fig. 2.6). A bit reconditioning procedure was established by drilling a set distance into abrasive sandstone at moderate bit pressure. Three other tests with full-scale bits were described, two drilled in the field and one in the laboratory on an artificial rock. These tests indicated that

quantification of rock properties might be possible from the complete drilling records kept in cases where rock core recovery was not complete.

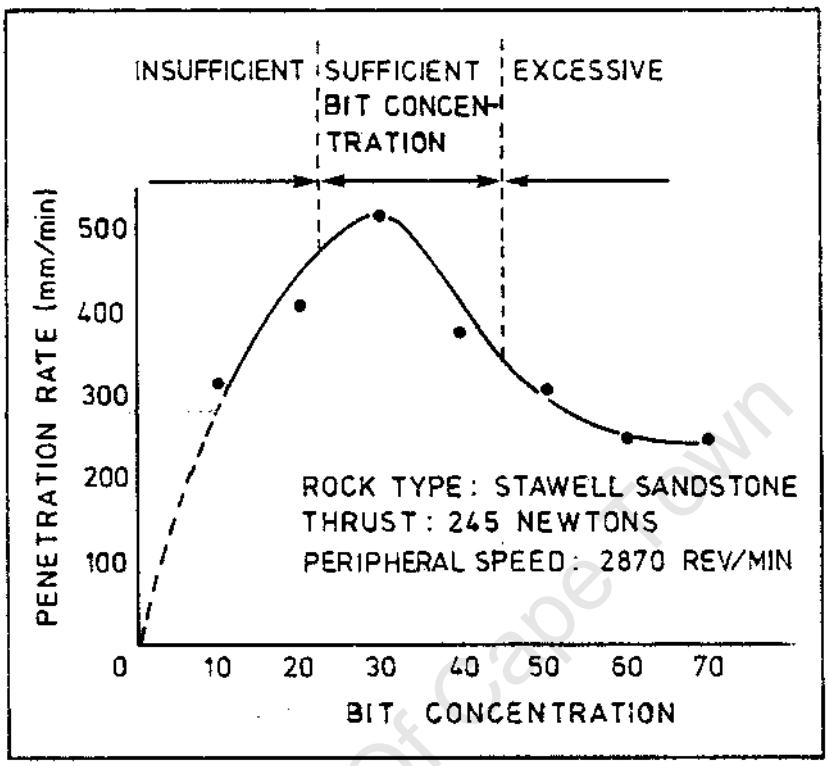

FIGURE 2.6 : Penetration rate against bit concentration in drilling sandstone (after Bamford et al 1979)

A comparative study of full-scale and microbits was carried out by Siribumrunsukha (1980). The stated aims of the research were to investigate the effects of bit wear on penetration rate; to determine the possibility of bit reconditioning after dulling; the standardisation of drilling data; the effects of diamond concentration, thrust and rotational speed on penetration rate; and the relationship between drillability and mechanical rock properties. Seven rock types with a wide variety of measured physical properties were drilled with a range of rotational speeds and thrusts. The impregnated microbits had fairly wide kerfs and contained stones of about 40 US mesh in concentrations from 10 to 70 in steps of 10. Resharpening was achieved by drilling a set distance in sandstone as described in the paper by Bamford et al (1979) which contained a summary of these tests. The full-scale bits were thin walled bits with 40 US mesh diamonds in 40 concentration. The laboratory drilling rig for use with the microbits was similar in concept to the one described by Spink (1972). As it was used as an initial guide for the

design of the machine used for the research reported on in this thesis its operation will be described in some detail. A 0,37 kW bench drill was modified by the addition of a wheel to the load arm. Thrusts provided by variable weights were calibrated with a proving ring in static loading under the bit. Drilling time was measured with a stopwatch, and the power consumption monitored by a graduated wattmeter read at no load and at the midpoint of each drilling increment. Torque was determined from the deflection of a calibrated strain-gauged beam attached to a turntable holding the specimen. Difficulty was experienced in measuring some of the very low torques generated in the tests. The drilling variables were read at least once during each drilling increment of between 70 and 90 mm. Axial bit wear was measured in a specially designed rig with a vernier micrometer reading to 0,002 mm.

The full-scale bits were drilled using a 0,75 kW radial arm drill operating at a rather low rotational velocity and intermediate thrusts. Power consumption was read from a wattmeter, penetration from a scaled dial on the machine, and time recorded by a stopwatch. The flushing rates were kept constant for each of the two machine configurations. An abrasive index was calculated from the recorded drilling variables using a formula based on an analysis of surface set bit performance and valid only if progressive dulling of the bit occurred with a resulting decrease in penetration rate. This was indeed the case for most the tests reported on by Siribumrungsukha (1980).

It was found that for a given diamond concentration and combination of rock type and rotational speed there was an optimum load that gave a maximum penetration rate. In strong rocks, at all rotational speeds, the initial penetration rate was linear with respect to thrust below a level causing damage to the diamonds or the matrix (Fig. 2.7). Bit clogging and matrix contact with the rock occurred at high thrusts in softer rocks. Penetration rate and torque depended linearly on drilling distance while specific energy varied exponentially. The computed abrasive ihdex was reduced as thrust increased but the 'abrasive index increased with an increase in rotational speed. The initial penetration per revolution decreased with rotational speed but the net initial penetration rate increased linearly with rotational speed for low speeds and deviated from this at high speeds. Increasing thrust caused a decrease in specific ehergy for the stronger rocks while for lower

strength rocks an optimum thrust existed within the available thrust range. Increasing the thrust was found to be preferable to increasing the rotational speed in order to increase the penetration rate in strong rocks. Diamond wear was not evaluated but was assumed to be due to abrasion and graphitisation and/or oxidation. Matrix wear by abrasion was thought to predominate over wear by erosion. Reconditioning of the bit was carried out by drilling in abrasive sandstone to remove 0,5 mm of matrix to expose fresh stones. Adequate diamond exposure or protrusion was important when drilling soft rocks to prevent bit matrix contact with the rock. By comparison of results for drilling with full-scale and microbits it was found that rock drillability and drilling behaviour could be predicted from the performance of the microbits if similar bit pressures, linear velocities and concentrations were used for both sizes of bit. For the harder rocks drillability showed some dependance on uniaxial compressive strength, tensile strength, and Sklerograph rebound hardness (Siribumrungsukha 1980: 45). It was maintained that the best method of determining rock drillability was by experimental drilling because petrographic characteristics crucially affected drillability.

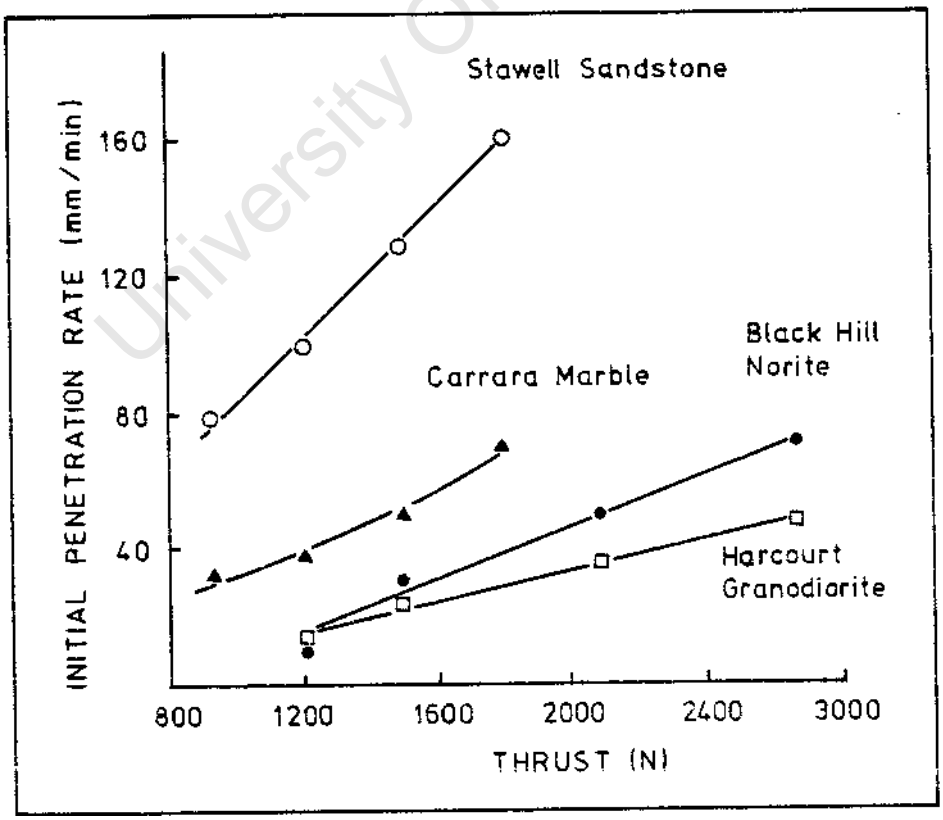

FIGURE 2.7 : Initial penetration rate against thrust; full-scale impregnated bits at 385 rpm rotational speed (from Siribumrungsukha 1980)

Bullen (1983, 1984) described tests drilled in granite with full-scale diamond bits to compare the performance of synthetic and natural diamond and to evaluate drilling under set thrust or set penetration rate conditions with bits of different kerf width.

For tests comparing synthetic SDA 100 and natural EMBS the bits contained 30/40 US mesh grit at 75 concentration in an unspecified matrix. These tests were drilled at set rotational speeds and at set rate of advance. The monitored variables were thrust, torque, penetration rate and drilling distance. Axial bit wear was measured accurately in a special jig that took into account differential_ wear across the wide kerf profile. It was found that at the given rate of advance and rotational speed the synthetic grit was advantageous and displayed controlled fracture. The natural grit was too friable and could not maintain sufficient protrusion thereby reducing the specific bit life, presumably through excessive bit wear.

The bits with two different kerf widths used in the comparison of drilling performance under set thrust and set penetration rate contained SDA 100 30/40 US mesh at 60 concentration. Bit wear and drilling parameters were measured in the same way as in the previous tests. Two rotational speeds, and a realistic range of bit pressures or alternatively a set penetration rate of 100 mm/min were used. The narrower kerf width bits were more efficient than the wide kerf width bits in terms of bit wear and penetration rate while the axial wear rates of the two types of bits were not significantly affected by a change in rotational speed. It was found that under constant thrust conditions the penetration rate decreased progressively due to polishing of the diamonds (Fig. 2.8). Increased speed of rotation, breaking the stones physically, or redressing the bit were required to make the bit operate efficiently again. The torque measurement was useful in monitoring the bit performance. Efficient drilling required the correct selection of penetration rate which depended on the bit design, diamond type and rock type. Bit pressure fluctuations were considered a necessary and natural consequence of a proposed three stage mechanism of cyclical bit wear required to keep the bit open and operating successfully.

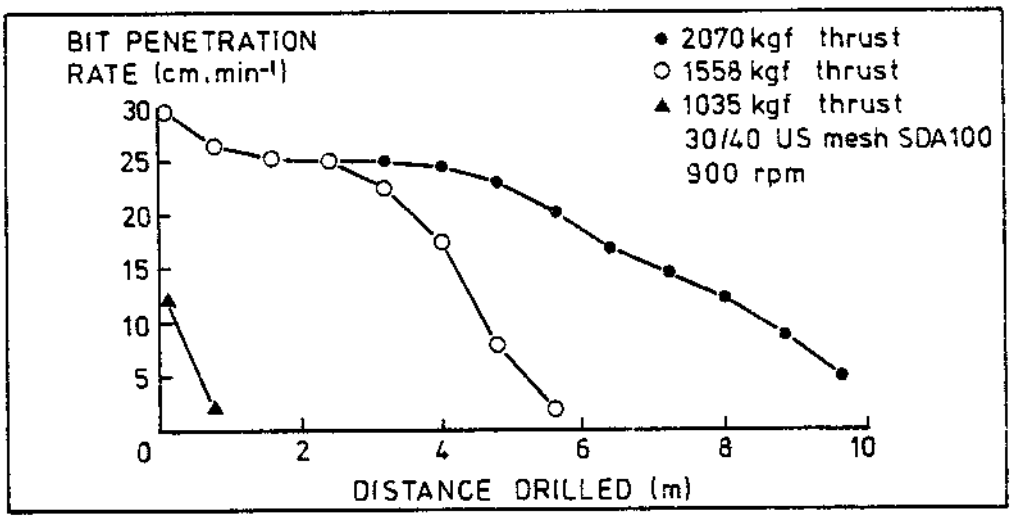

FIGURE 2.8 : Penetration rate against distance drilled at constant thrust (after Bullen 1984)

2.2 STEADY STATE DRILLING WITH IMPREGNATED DIAMOND BITS

The primary objective in drilling with an impregnated diamond bit is to achieve a constant penetration rate throughout the life of the bit. This depends on the bit geometry and formulation as well as the drilling parameters (Busch & Hill 1975). Efficient drilling in terms of the above criterion is not easily achieved when drilling under set thrust conditions. However, at appropriate set rates of advance the bit load is free to respond to changes in the condition of the bit face and in theory a steady penetration rate can be maintained for the life of the bit (Bullen 1983). In a number of the reported studies the tests conducted at set thrusts have failed to meet this criterion and have suffered progressive decrease in penetration rate with drilling distance (See Fig. 2.8). Paone & Madson (1966) did not distinguish between tests in which drilling progressed steadily and those in which the bit needed to be reconditioned by increasing the thrust temporarily or by sandblasting the bit when the penetration rate became unacceptably low. The tests done by Spink (1972) were too short for any systematic drop in penetration rate to be noticed except in the most resistant rocks. Busch & Hill (1975) recognised that relatively high bit pressures were necessary to maintain constant penetration rates in medium to hard rocks. Most of the tests reported by Bamford et al (1979) and Siribumrungsukha (1980) showed a decrease in penetration rate with drilling distance at set thrust, indicating suboptimal behaviour.

2.3 PREDICTIVE EQUATIONS FOR THE PENETRATION RATE OF IMPREGNATED DIAMOND BITS

Several attempts have been made to establish predictive equations for drilling with impregnated diamond bits. These equations are intended to predict the penetration rate of the drill, often in the undesirable situation of drilling with a diminishing penetration rate under set thrust force. The equations are quoted here to illustrate their diversity of form. For more detailed description of their variables the reader is referred to the original papers.

Paone et al (1966) performed statistical regression analysis on the results of drilling tests in a wide variety of rock types with a diversity of measured physical properties. Two different predictive equations for laboratory and field drilling with full-scale bits were obtained. The most successful empirical predictor equation for laboratory diamond drilling with impregnated bits was as follows:

$$Y = 0{,}0001997+0{,}0006714X1-0{,}04279X3-0{,}0001273X5-0{,}03448X7+0{,}1135X8$$

where Y = penetration per revolution
X1 = coded thrust
X3 = coded reciprocal of compressive strength
X5 = reciprocal of relative abrasiveness
X7 = coded reciprocal of shear modulus
X8 = coded reciprocal of static Young's modulus.

The empirically determined predicator equation for field diamond drilling with impregnated bits was as follows:

$$Y = -0{,}0004340+0{,}0003407X1+0{,}006761X7+0{,}001079X8+0{,}0007856X9$$

where Y = penetration per revolution
X1 = coded thrust
X7 = coded reciprocal of shear modulus
X8 = coded reciprocal of static Young's modulus
X9 = reciprocal of quartz content.

Both equations include thrust, rock strength terms and terms related to petrographic factors such as quartz content and relative abrasiveness. Although it was claimed that these equations could predict drilling

performance all the standard rock properties were found to be highly intercorrelated (Clarke 1982) and the usefulness of these equations is questionable even under the suboptimal drilling conditions from which they have been derived.

Selim et al (1969) and Strebig et al (1971) described the decreasing penetration rate of impregnated bits in tests conducted with flushing fluid additives using an equation derived from reliability theory to predict the diminishing penetration rate in terms of decreasing reliability due to wear of the bit. The penetration rate was expressed as a percentage of the initial penetration rate.

$$dx/dt = P_o e^{-\lambda(x-y)^{\beta}}$$

where dx/dt = penetration rate

P_o = constant

λ = failure rate (or wear coefficient)

y = location parameter

β = Weibull shape parameter

Determination of the Weibull shape parameter (by a method in William 1964 cited by Selim et al 1969) allowed A to be calculated and used as an evaluation of bit reliability or as a wear coefficient to express the drilling efficiency. This method allowed the relative performance of the drill in suboptimal conditions to be tested using different additives without direct measurement of wear.

Siribumrungsukha (1980) adopted an equation established by Tsoutrelis (1969a) to describe the progressive decrease in penetration rate due to diamond wear by the production of wear flats on surface set bits. Provided that progressive blunting occurred during the drilling the only variables required to determine the initial penetration rate and the abrasive index were drilling distance and time.

$$x = Vo/b\ (1\text{-}e\text{-}bt)$$

where x = distance drilled

V_o = initial penetration rate

b = abrasive index

t = drilling time.

As noted by Siribumrungsukha (1980) none of the above methods required direct measurement of diamond wear; but all of them assumed a non-uniform penetration rate. A number of other attempts have been made to predict drilling performance with surface set bits. These include a proportional relationship between penetration rate and thrust and rotational speed (Sasaki, Yamakado, Shiohara & Tobe 1962); a work equilibrium equation balancing the sum of work done by thrust and torque with the energy required to penetrate the rock (Paone & Bruce 1963); a model of ploughing a rigid-plastic Coulomb material (Rowley & Appl 1969); and a model considering equivalent blades (Peterson 1976). These are not very relevant to impregnated bit drilling because none of them account for diamond fracture or bit matrix wear. No published mathematical model of operation of impregnated diamond bits operating in the desirable stable mode of constant penetration rate and load has been found.

A conceptual model of impregnated diamond bit drilling has been formulated at Boart Research Centre (Cooper & Adams 1983). The model focuses on the gap between the bit matrix and the rock being drilled. There must be clearance or a minimum gap at the bit face for drilling to occur. This gap is thought to be maintained by the erosive action of the slurry on the bit matrix. If the slurry is not erosive enough then fresh diamonds are not exposed and excessive wear flats develop which hinder the drilling. If the slurry is too erosive then rapid matrix wear and diamond loss result, reducing the bit life. According to this model if all the pertinent variables are controlled correctly then the optimal gap could be achieved and maintained. The consequence would be steady drilling at a constant penetration rate.

Cooper & Adams (1983) considered four types of diamond behaviour viz. the generation of wear flats, fracture by micro- and macrochipping, premature loss by pull-out, and "shear" of the diamonds near the matrix surface. The advance per revolution was assumed to be the fundamental operating parameter which had to be set correctly for the maintenance of an optimal operating gap with a given bit formulation and rock type (Fig. 2.9). The "operating box" was defined as the region in which stable drilling occurred or in which drilling could be maintaihed by altering the drilling parameters appropriately.

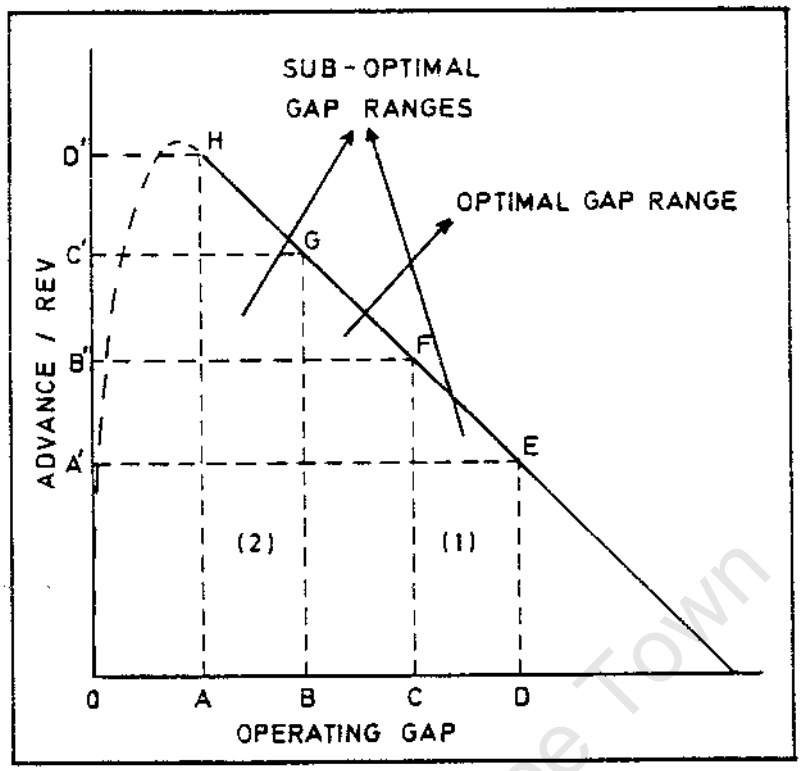

FIGURE 2.9 : Theoretical relationship between rate of advance and operating gap (after Cooper & Adams 1983)

Aspects of this model have been tested on the full size laboratory drilling machine installed at Boart Research Centre (Boswell 1983) and on the laboratory drill at the University of Cape Town.

2.4 THE DETERMINATION OF ROCK DRILLABILITY WITH IMPREGNATED DIAMOND BITS

Drillability is a loosely defined term used to denote the ease of drilling a particular rock with a particular drilling system. It depends on the drilling tools, operating conditions, and on the properties of the rock. For a detailed review of rock drillability see Singh (1973).

It is important to be able to predict the resistance of the rock to being drilled by a particular type of bit in order to calculate the cost of commercial drilling operations (Clarke 1982). Drillability studies have usually been conducted using surface set bits (eg. Paone & Bruce 1963) or specially shaped drill bits (Tsoutrelis 1969a) with some consideration made for bit wear (Singh 1973). Drillability values determined for surface set bits are not considered valid for impregnated bits due to

differences in the coefficient of friction and the drilling mechanisms of the two types of diamond bits (ibid). Paone et al (1966) found that bit thrust and Young's modulus, shear modulus, compressive strength, abrasiveness and quartz content of the rock were important in determining the drillability with impregnated diamond bits and that no single rock property could be used as a reliable indicator of drillability. Bailey & Dean (1967) considered the unconfined rock compressive strength and shear strength important but warned that all results could not be correlated satisfactorily using these two values alone. Spink (1972) and Siribumrungsukha (1980) found that petrographic factors such as free quartz content, grain size and mineralogy had significant and sometimes crucial influence on the rock drillability. Nevertheless Clarke (1982) observed that if the forces between the bit and the rock are related to the strength characteristics of a rock the compressive or tensile shear strengths should form a simple index of drillability. The computed "drilling strength" of many rocks appears to approximate the compressive strength which is a direct function of tensile and shear strength in most rocks (ibid).

This relationship is the basis of a method for determining the compressive strengths of rocks in situ or in the laboratory from drilling data. Tsoutrelis (1969b) devised a method based on an empirically determined relationship between uniaxial compressive strength and the initial penetration rate at a given thrust. At the end of a detailed review of rock drillability studies Singh (1973) concluded that the best way to determine drillability is by drilling the rock in question with a full-scale bit or a suitably scaled microbit with due care taken in reproducing the realistic drilling parameters. This indicates the need for standardised laboratory testing to formulate guidelines for drilling any particular rock.

2.5 THE DRILLING MECHANISM WITH IMPREGNATED DIAMOND BITS

The motivations for modelling rock failure mechanisms in the drilling process were discussed by Bailey and Dean (1967). Attempts at improving predictions of drilling performance have had only limited success when approached from a consideration of fundamental mechanisms. The objective of increasing the understanding of the attrition process itself has been

even less successful. More needs to be be known about the stress conditions in the rock beneath the bit. Current knowledge of fracture processes cannot be applied without a detailed knowledge of the loading geometry. Information is lacking on the propagation of microfractures and the effect of multiple passes of a diamond over the same track. A review of the literature on the drilling mechanisms with impregnated diamond bits shows that these deficiencies in knowledge still exist.

Single diamond scratching tests on glass, quartz and silica glass by Graham (1972) using diamonds of different radius produced cracks that were very complicated. Material removal was due to the interaction of a variety of crack types including Hertzian and longitudinal cracks. The formation of characteristic "chatter cracks" was a statistical process, with the least cracking taking place on a dry surface. The pattern appeared to be affected by diamond size. Small radius stones left a roughened abrasion track on glass with a fine powdered debris. Large radius stones produced chipping and Hertzian cracks in silica glass and quartz, with larger chips formed by a deep cracking system at higher loads (Fig. 2.10).

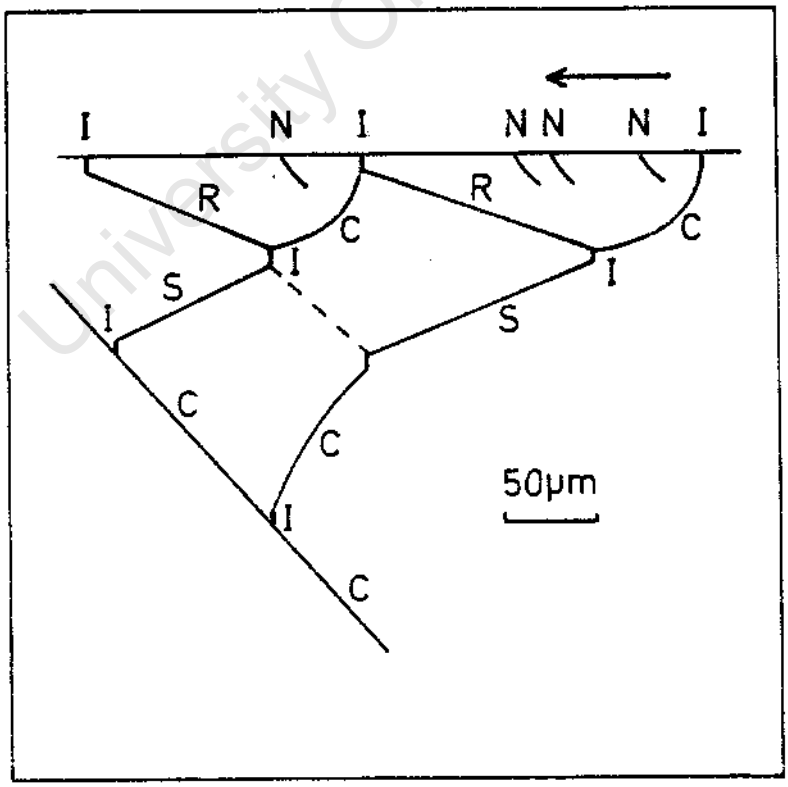

FIGURE 2.10 : Network of deep cracking in glass showing the complexity of damage induced by a sliding indentor: I - reverse crack, N - normal Hertzian crack, R - radial crack, C - circumferential crack, S - smooth crack (after Graham 1972)

Glover (1980) tested the effect of multiple passes over the same track in quartz and found that a diamond point at low loads and low rates of traverse could fail to produce a visible track until after a number of passes. Hertzian cracking was predominant, with subsurface shear cracking and failure by delamination if the coefficient of friction was sufficiently low.

Single diamond scoring of microsyenite (a crystalline igneous rock) by Rowlands (1972) indicated that a threshold thrust was required to remove material. A second pass removed less material than the inital cut particularly for tests above the experimentally determined optimum load of 6 kgf. Much of this material was excavated from the bottom of the furrow rather than from the sides. The displacement between successive parallel cuts had a strong influence on the volume of material broken out from the ridge between adjacent furrows.

Rock drilling has been seen as a grinding 'or comminution process (Adamson 1946, Spink 1972). Failure of the rock, and the necessary wear of the matrix of an impregnated diamond bit, can only take place if the forces applied to the rock through the combination of rotational speed, thrust and applied torque are high enough to create sufficient stress to induce fracture (Paone & Madson 1966). Penetration takes place if the thrust force and tangential force on each operating diamond point exceed the failure strength of the rock and the friction between the bit and rock (Clarke 1982). Optimum bit pressures exist (Rowlands 1972) below which no penetration can take place and above which energy is lost to increased friction, heat and fusion of the bit to the rock (Spink 1972).

The surface failure of the rock in drilling has been described in terms of three major components (Pfleider & Blake 1953, Paone & Madson 1966, Rowlands 1971, Clarke 1982). (i) The normal thrust force causes axial penetration, plastic deformation of the contact zone, crushing beneath the indenter and consequent tension cracks and lateral shear cracks. (ii) Rotation causes impact and compression ahead of the indentor, tensional failure of the rock behind it, the creation of additional lateral shear planes, and a ploughing action that excavates precracked material. (iii) Further fracture by shear to the free surfaces on ridges between the tracks of individual diamonds is important.

The shape of the indenting diamond point has an effect on the fracture mechanism and the detritus produced (Maurer 1967). Lundberg (1974) confirmed that the use of indenters with small internal apical angles caused a preponderance of chipping to take place in granite while crushing was predominant beneath indenters with greater apex angles (see Fig. 2.11). Rounder points are thought to cause crushing and sharper points produce more chipping (Norling undated). Paone & Tandanand (1966) described crushing as the consequence of high local compressive stress and chipping as the result of subsurface fractures extending to a free surface. Cleavage of individual mineral grains and shearing along planes inclined to the principal stresses were thought to be the predominant failure mechanisms in rock drilling (ibid). Spink (1972) advocated the use of low loads to maximise fracture by Hertzian cracking and to minimise the effects of inefficient ploughing. A more detailed description of these mechanisms can be found in Appendix 1.

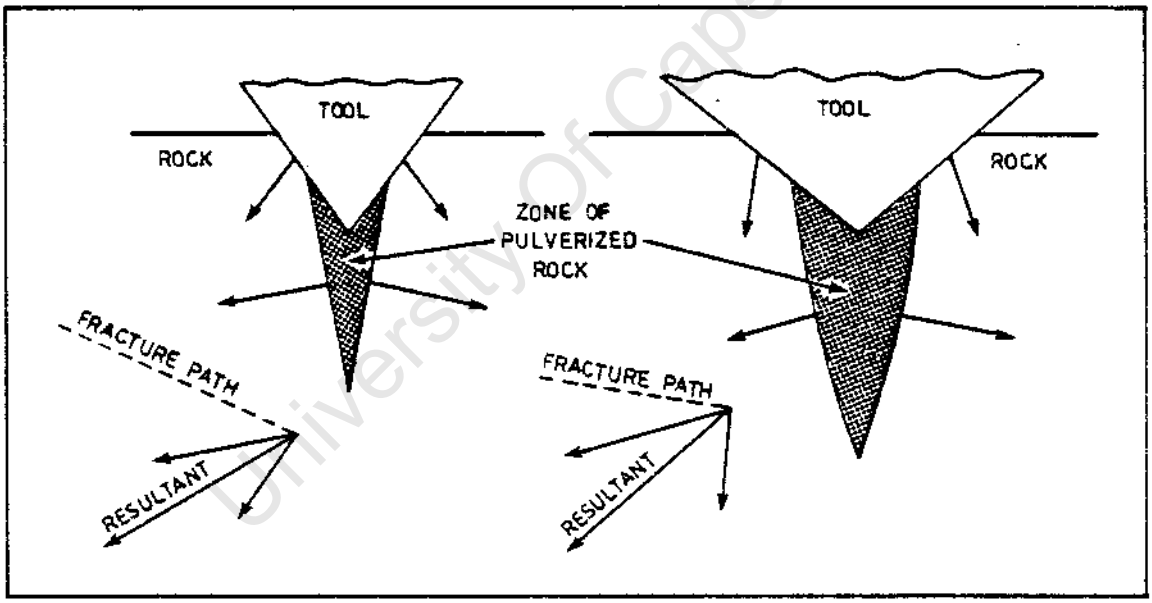

FIGURE 2.11 : Influence of wedge angle on size of crushed zone beneath an indenter (after Maurer 1967)

The rock resistance comprises a bearing resistance to the vertical load force and a frictional resistance to the applied torque (Paone & Madson 1966). The abrasive mechanism of drilling is thought to generate variable resistance because of the intermittent shearing of asperities and the variable properties of the rock due to its granular texture (Clarke 1982). This could be the cause of the vibration associated with many drilling enterprises (Rowlands 1971).

The actual rock deformation can involve both plastic and brittle behaviour depending on the drilling circumstances. Plastic effects are particularly important when drilling at depth under high confining pressures (Cheatham & Gnirk 1967). This applies particularly to drilling using a drilling mud and surface set bits. The high environmental pressure changes the mode of failure from predominantly brittle fracture to plastic ploughing (Garner 1967). Deformation at these high pressures and at high temperatures is thought to be due to intergranular fracture, intergranular gliding and recrystallistion (Paone & Tandanand 1966). Plastic processes in drilling with impregnated diamond bits have been discussed by Spink (1972). Plastic deformation could be due to crystallographic twinning, dislocation movement and mineralogical phase changes, as well as softening and melting. Spink suggested that the use of high rotational speeds could suppress plastic work by increasing the strain rate despite unavoidable plastic deformation in rock drilling.

No reported studies of the appearance and nature of the damaged zone at the bottom of a hole drilled with an impregnated diamond bit or of the characteristics of the drilling detritus are known. Some general observations exist however. If the rock matrix is easily sheared so that individual grains can be released, as in a soft sandstone or weakly cemented quartzite, then the physical properties of individual mineral grains do not affect the drilling process substantially (Rowlands 1971). Harder rocks, such as a well cemented quartzite, can be expected to undergo both intergranular and transgranular fracture (Ball 1972, 1974).

The size and shape of drilling detritus and the appearance of the bottom of the hole after laboratory drilling in a variety of rocks with a surface set bit have been described by Pfleider & Blake (1953). The tests were drilled at low rotational speeds so that the bit could be lifted off the bottom of the hole rapidly to minimise the distance over which the thrust decreased. Different minerals had very diverse responses. Drilled quartz particles were angular with conchoidal fractures and only rarely were they internally shattered. Felspar formed irreaular or flat cleaved fragments and were often smeared out into "mashed flakes" of rock flour compacted into curled chips. Biotite formed sheets or "books" plucked from the rock by the relatively large diamonds. Marble (composed of calcite) formed a fine rock flour, mashed flakes and lumps of caked material compacted under the force transmitted

by the diamonds. These "cakes" were characteristic of the detritus of finer grained, softer rocks. Limestone produced fine particles of rock flour and some caked lumps. Sandstone detritus consisted entirely of fractured quartz particles and excavated grains. Detritus from taconite (a hard, dense jaspilite rock containing iron ore) consisted of chips of quartz and magnetite as well as mashed flakes. In trap rock (a volcanic rock) the softer minerals were crushed and mashed and the harder silicates fractured. A high rate of advance produced slightly coarser particles especially in the sandstone and finer particles were produced by higher rotational speeds, perhaps by increased comminution of reground particles. The "cakes" tended to plug the bit by compacting between and on the diamonds. This inhibited penetration. The drilled granite looked "shattered" at the bottom of the hole with a frosted appearance due to refraction and reflection of light from cracked silicate mineral grains. Although quartz had developed deep fractures not much material had been released as secondary chips. The felspar had broken along cleavage planes, as had the biotite unless it was cut perpendicular to its basal plane. The marble and limestone had material caked on the bottom of the hole. The poorly cemented sandstone revealed plucking of the grains. It was concluded that each mineral constituent had behaved in a highly individual manner (Pfleider & Blake 1953).

One study has included a size distribution analysis of particles derived from impregnated diamond bit drilling. Paone & Madson (1966) found size analysis unhelpful in trying to explain higher penetration rates in quartzite over taconite because all the particles had been reground. This obscured any meaningful distinction in primary particle size.

2.6 ENERGY IN ROCK DRILLING

Since the penetration rate in drilling is proportional to the power transmitted to the rock (Hammerback 1969) it is important to understand the process of energy transfer to the rock. Such an understanding will allow an evaluation of the resistive forces impeding the drilling process and assist in minimising their effect (Clarke 1982). The partitioning of the energy imput is difficult to determine and varies with rock type as well as bit configuration and mode of operation. It has been estimated

that approximately half the work required to fracture rock is expenaed on loading the bulk of the rock. The other half is used in actually crushing material beneath the diamonds (Simon 1963). The energy used in cracking and releasing rock chips is considered to be negligible by comparison. The various types of energy expenditure in drilling have been listed by Spink (1972). Useful energy creates new surfaces. Some elastic strain energy is used in creating cracks but most is dissipated as heat and some in elastic hysteresis. Plastic work at crack tips consumes an irreducible amount of energy as stress is removed and cracks cease to propagate. Other plastic work involves strain hardening and ploughing of material, which can absorb considerable energy under certain conditions. Regrinding of detritus beneath the bit wastes further energy. Friction between the diamonds and the rock, and between the bit matrix, rock, and slurry are unavoidable but should be minimised. Energy wastage is thought to be highest when drilling in an abrasive mode. This is at least in part due to friction being higher in an abrasive rather than Hertzian fracture mode (Spink 1972).

The friction between the bit and the rock is in itself complex and depends on the thrust, the rock strength, the rotational speed, the diamond exposure and matrix contact. When there is little protrusion of the diamonds and contact between the rock and the bit matrix occurs then most of the energy is dissipated as friction (Paone & Madson 1966). An average value for the coefficient of friction of 0,4 for rock drilling has been estimated from experimental penetration rates obtained under controlled conditions (Clarke 1982).

The friction between the bit and the rock in turn significantly affects the torque transmitted to the rock. There is a threshold torque required for drilling which is determined by the friction between the bit and the rock (Paone & Madson 1966). The torque is a function both of friction between the rock and the bit, and the fracture process. As such, it is a measure of the resistive forces in the rock opposing rotation of the bit (Clarke 1979).

The resistance of the rock to being drilled determines the energy required to drill a unit volume of rock. The gross specific energy is strictly speaking specific to the particular drilling configuration

(Moller & Spink 1973) but has been used to compare the efficiency of different drilling bits and techniques. It has been found empirically that most rock drilling operations approach an optimal specific energy with a minimum value of the order of the compressive strength of the material being drilled (Bailey & Dean 1967). Above a power threshold the specific energy is generally found to be nearly constant within the effective operating range in which torque and penetration rate are linearly related (Teale 1965, Simon 1963, Maurer 1967, Bailey & Dean 1967). Fracture due to the thrust component has been estimated to be 0.2 percent of the fracture caused by the rotary component; thus the specific energy can be defined essentially in terms of the rotary component (Teale 1965):

$$e_r = (2\,rr\,/A)\,(TO)$$

where e_r = specific energy
A = area of hole
T = torque
P = penetration per revolution

Teale (ibid) observed that for a given drill configuration the minimum specific energy often involves relatively low thrust forces, and penetration rates below the maximum rates available if higher thrusts were used. It is therefore unrealistic to compare the operating efficiency of different drilling systems on the basis of specific energy alone (Maurer 1967). Since the power supply costs in drilling are usually insignificant in comparison with the time costs, consideration of methods of transmitting greater power to the rock has been advised. On the other hand it has been shown that it is possible in some situations to make significant reductions in the specific energy of the process. Research with this aim in view has been advocated (Bailey & Dean 1967).

2.7 SELF SHARPENING BEHAVIOUR AND THE ROLE OF THE MATRIX IN IMPREGNATED DIAMOND BIT DRILLING

Impregnated diamond bits were originally produced with the aim of their being self-sharpening, like a grinding wheel. It was found that soft

matrices led to rapid loss of diamond grit and that hard matrices required sandblasting to combat the effect of polishing of the retained diamonds (Wilson 1941, Paone & Madson 1966). It is still the aim of manufacturers and users of impregnated diamond bits to maintain steady penetration with a balanced matrix wear rate (Clarke 1979, Bullen 1984). Attempts have been made to control matrix wear behaviour by adding abrasives or introducing controlled porosity (Cooper & Adams 1983). With the modern development of wireline drilling with the core retracted up the barrel (Savage 1985) and the planning of very deep holes with wireline drilling extending 15 km into the crust (Barber 1985, Svendsen 1985) it is even more imperative to drill effectively for the full life of the bit.. Self-sharpening is crucial to achieving this goal.

The bit matrix wear and the diamond wear are intimately related. The wear of diamond saw blades has been described in terms of the diamond wear by Ertingshausen (1985). Under some conditions wear was apparently steady while under others it was cyclical. A segment which had just passed through a maximum wear phase had a relatively large proportion of freshly exposed stones. These progressed through a phase characterised by a high incidence of broken diamonds and wear flats to a minimum wear phase with large wear flats and a large proportion of pull-out holes. It was suggested that two mechanisms operated simultaneously. (i) Freshly exposed diamonds developed wear flats. The forces on the diamonds increased and they started to break down. Splinters were dislodged and lost. (ii) The points of freshly exposed diamonds broke off and the diamonds developed wear flats. They were subsequently pulled out of the matrix by cutting forces exceeding the strength of the bond. The matrix wear itself was not discussed.

Bamford et al (1979) described the matrix wear in drilling by two mechanisms. (i) Erosion by fine particles in the flushing medium. (ii) Abrasion by direct contact between the matrix and the rock (possibly with fragments trapped between them). Abrasion was thought to account for high rates of matrix wear in bits with low concentration of diamonds. Matrix wear was found to be very low with diamond concentrations of 50 to 70 and this hindered the exposure of fresh stones.

Bullen & Bailey (1979) found that diamond strength affected the process of stable operation. Strong diamonds drilling under low loads polished rapidly in hard rocks and required an increase in load to a point where penetration could not be maintained due to lack of power. However, if sufficiently high loads were used initially then penetration could be maintained with the stronger diamonds. The load was observed to fluctuate in a "saw tooth" manner as the bit surface regenerated itself intermittently. This load fluctuation at set rate of advance was also reported by Selim et al (1969).

Little experimental work has been published about the role of the bit matrix itself in impregnated diamond bit drilling. Wilson (1941) listed the metals used as cobalt, cobalt and tungsten carbide, steel, and brass. Modern practice (anon 1985) tends to favour tungsten or a mixture of tungsten and tungsten carbide with a cobalt binder to hold the diamond both mechanically and chemically (Fig. 2.12). The matrix metal is mixed in powdered form with the diamond grit and sintered at temperatures ranging from about 700 °C to well over 1000 °C depending on the metal involved. It is generally recognised that a combination of suitable operating parameters and the correct matrix material for a given rock type are required to keep a bit "open" so that it can drill of (Paone & Madson 1966, Spink 1972). Ideally the matrix must be abraded at the correct rate to complement wear of the exposed diamonds so that fresh points are continually available (Clarke 1979).

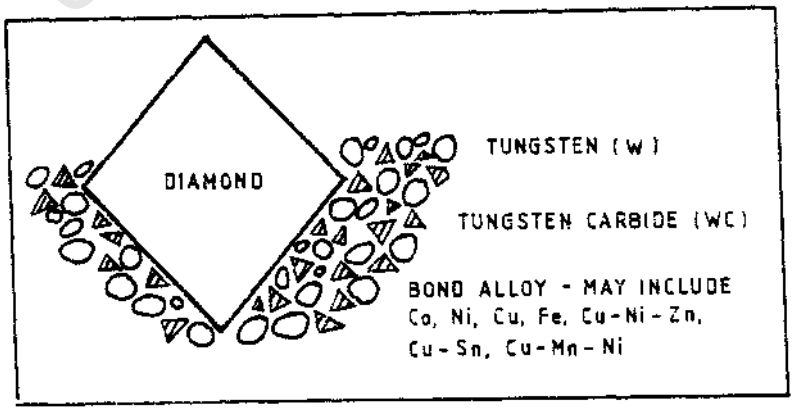

FIGURE 2.12 : The functions of the W and WC in the bit matrix are achieved only if they are effectively bonded together with the appropriate auxillary metals (after anon 1985)

A cyclical process involving the wear of diamonds and consequent load increase, followed by rapid stripping of the matrix to expose fresh stones has been proposed by Bullen (1984). In practice this can be difficult to achieve and fairly high thrust and slightly abrasive rock are required to maintain the controlled breakdown of the grit/matrix system (Paone & Madson 1966, Busch & Hill 1975). The mechanism of matrix wear in stable drilling conditions has not been studied in detail, but the bit can "close" due to insufficient matrix wear or the generation of excessive wear flats on the diamonds. The matrix can be stripped off by a temporary increase in thrust or removed by sandblasting to expose fresh stones (Wilson 1941, Paone & Madson 1966).

2.8 THE PROPERTIES OF DIAMOND RELEVANT TO DIAMOND DRILLING

The superlative hardness of diamond is the most important property determining its original choice as the abrasive material in hard rock drilling. The related properties of abrasion resistance and toughness as well as thermal conductivity are considered crucial in modern applications (Atkins 1983).

The indentation hardness of diamond is extreme when measured by any method but appears to be load dependent with higher measured hardness values resulting from the use of lower indenting loads (Brookes 1979). The mechanism governing this phenomenon is not clear but may involve the homogeneity of slip beneath the indenter. The anisotropy of the hardness follows predictions based on a 11111 <110> slip system (see Fig. 2.13) suggesting an important if small degree of plastic flow at room temperatures. However, diamond is essentially brittle below 1600 °C at atmospheric pressure (Evans 1976). Dislocation movement has not been observed in diamonds at room temperature (Hanninck & Gane 1974). The strong convalent C-C bonds produce a high Peierls force (Brookes 1979) while the dissolved nitrogen in the synthetic type lb diamonds also inhibits dislocation movement (Welch 1982). At high temperature dislocations are mobile and plastic deformation is possible (Evans 1976, Tabor 1979).

Diamond graphitises in air at about 700 °C with the formation of a carbonaceous film on the surface. Above 1000 °C in air it transforms rapidly to amorphous carbon (Bowden & Tabor 1965). However, the very high thermal conductivity allows diamond tools to be used at relatively high temperatures because the heat is conducted away from the working surface efficiently (Field & Freeman 1981).

The abrasion resistance of diamond has been studied extensively by Wilks and Wilks (1965, 1979, 1982, 1984). It is anisotropic with the degree of anisotropy apparently affected by the method of abrasion. Good quality synthetic stones have been found to be as abrasion resistant as good quality natural stones. The mechanism of abrasion has not been established but seems to be a mechanical process, as opposed to a chemical or thermal one. The particles produced are estimated to be about 5 nm in size (ibid).

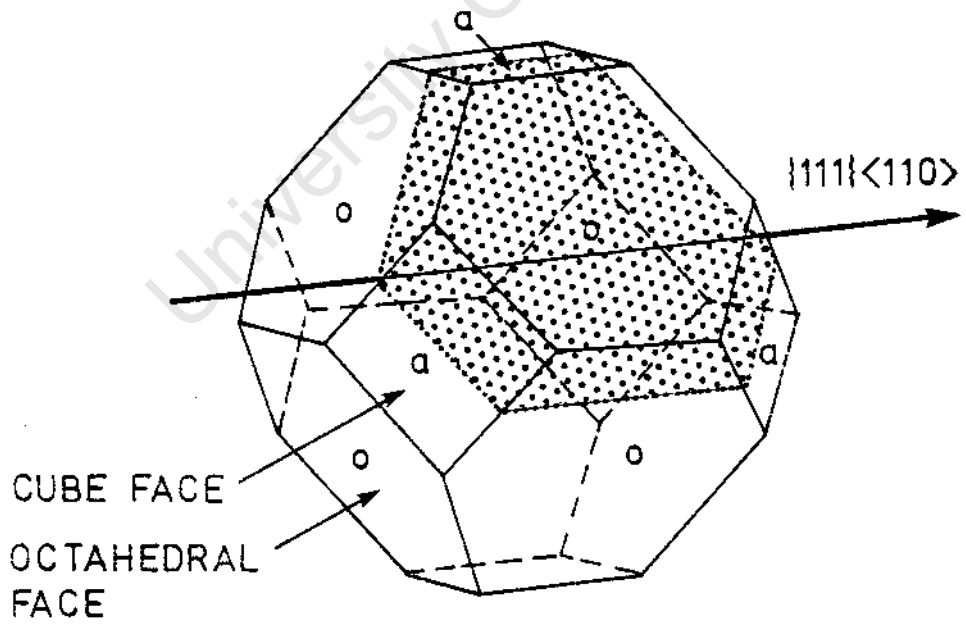

FIGURE 2.13 : Idealised form of a cubo-octahedral diamond showing a {111} plane and <110> direction

The gradual reduction in the resistance to abrasion of a diamond surface has been reported and ascribed to a fatigue mechanism (Crompton, Hirst & Howse 1973). If a diamond surface is subjected to cyclic stressing breakdown of the surface occurs after a finite incubation period (Tabor 1979). The length of the incubation depends on the hardness of the material rubbing against the diamond. Hence it is concluded that some precise and uniform fatigue mechanism occurs in the diamond (Wilks & Wilks 1979) whereby "under the conditions of repeated sliding the cumulative effect of micro-deformation may result in the mechanical breakdown of a hard crystal by another which is much softer" (Brookes 1979). It has been suggested that the fatigue damage consists in the progressive opening up of extremely small microcracks until they reach observable dimensions. These have not been seen however (Wilks & Wilks 1979). Bowden & Tabor (1965) have observed that in a diamond under repeated impact the development of surface cracks is sudden. These cracks may be the result of cumulative growth of subcritical microcracks initiated at surface defects.

The coincidence of the slip systems and the cleavage planes in diamond makes it difficult to distinguish between cracks and slip lines (Brookes & Lambert 1982). Steps between 20 nm and 2000 nm high on 11111 planes have been observed on stressed diamond surfaces, especially those subjected to elevated temperatures (Seal 1981). A small indentor can produce plastic deformation at room temperature without forming cracks at the edge of the circle of contact (Bowden & Tabor 1965). Slip is presumably involved despite the lack of evidence of dislocation movement at room temperature. The close correspondence of measured fracture surface energy and the theoretical value for surface energy for 11111 cleavage implies that there is little or no dislocation movement in the stress field at the tip of a propagating crack in a diamond at room temperature (Field & Freeman 1981). The fracture mechanism of diamond has been observed to be strain rate dependent. At very low strain rates crystallographic fracture is preceded by the formation of ring and cone cracks which do not have time to develop under higher strain rates (Levitt & Nabarro 1966).

The wear of diamond in a general machining application has been described by Brookes (1979) in terms of four mechanisms. (i) Diffusion of carbon into steel workpiece materials is due to the ease with which carbon dissolves in iron and other carbide forming metals. (ii) Thermal shock is usually insignificant because of the high thermal conductivity of diamond. (iii) Plastic deformation is important only at high temperatures. (iv) Mechanical abrasion and thermally enhanced attrition account for most of the wear. To these must be added failure by fracture and cleavage. Tool stones are particularly susceptible to fracture on impact with hard inclusions in softer material (Wong 1981).

The wear of diamonds specifically in rock drilling was described by Perrott (1979) as (i) attrition by mechanical action to produce wear flats, (ii) brittle fracture by direct impact on exposed stones and (iii) thermal fatigue producing cracking that propagates into the bulk of the stone. A classification by Bailey & Bullen (1979) of diamond wear in rock sawing listed the wear as (i) "good" with no wear, (ii) "wear flat" probably due to abrasion, (iii) "wear flat and rough" in which the wear flats were broken by impact, (iv) "rough" with no smooth areas, and (v) holes produced by pull-out due to mechanical loading or loss of the stone by disintegration. Ertingshausen (1985) used a simpler classification for diamond wear in sawing. Rounding was thought to be due to "thermal stresses" and microfracture due to mechanical stress. Unworn stones, striated wear flats, stones broken by microfracture, and pull-outs were described. The wear of diamonds used as cutting tools in precision machining of aluminium was described by Wong (1981) as consisting of (i) "normal" wear to produce a smooth rounded edge, (ii) chipping, (iii) line effects, visible on the workpiece, attributed to slip steps on the diamonds and (iv) catastrophic failure by impact with a hard inclusion.

Brookes & Hooper (1982) described the wear of a diamond aggregate tool tip. Wear flats developed initially with "smooth grooving" and some fracture. This was followed by a more extensive breakdown of the surface to form a network of blocks about ten microns in size. It was suggested that a fatigue type mechanism operated whereby repeated impacts initiated cracks at flaws in the material or extended microcracks produced by the smooth grooving. Twinning (Woods 1971) may have given rise to the blocky structure. The wear of diamond and cubic boron nitride grits in

machining steel and alumina with electroplated nibs was studied by Hitchiner & Wilks (1983). The diamond performed better than the softer CBN on alumina and less well on steel because of the chemical affinity of carbon for steel. Both abrasives wore primarily by the development of wear flats which determined the life of the nib, although fractured grits were also observed. Further work on the wear of ABN abrasive in grinding steel was reported by Stokes and Valentine (1984). The wear of the grit was described as (i) attritious wear, (ii) essential grit fracture with regenerative cutting edges, designated as "microfracture" as opposed to undesirable "macrofracture" caused by cleavage, (iii) wheel loading apparent as metal smeared over the grit and bond surfaces, (iv) pull outs due to mechanical stress.

The description of wear flats produced either by mechanical abrasion or by a thermally activated process; and fracture of some sort, either microfracture or more extensive cleavage fracture, are common to all the classifications. Diamonds do not outperform CBN in machining ferrous metals because of the chemical enhancement of diamond wear by diffusion of the carbon into the workpiece. However, it is interesting that both diamond and the boron nitride display regenerative microfracture.

The abrasion mechanisms are not well understood but may involve a fatigue mechanism operating with an incubation period (Crompton et al 1973) followed by the removal of small fragments and subsequent mechanical abrasion (Wilks & Wilks 1979). At high temperatures graphitisation contributes to the degradation. Cleavage processes play an important role even on a microscale (Field and Freeman 1981). Observable wear damage consists of fractured stones and relatively smooth wear flats. The development of wear flats is strongly dependent on the nature of the material being abraded by the diamond (Hitchener & Wilks 1983). Polycrystalline diamond appears to wear by similar mechanisms as do single crystals; with the fragmentation of individual grains into blocks about 10 microns in size after an initial incubation period. Diamond fatigue is thought to be induced by repeated impact and the opening of microcracks, or the activation of intrinsic faults (Dunn & Lee 1979, Brookes & Hooper 1982). Microfracture is important in maintaining a desirable degree of sharpness in some polycrystalline diamond compacts used in rock drilling (Atkins 1983).

The strength of individual diamonds, either grains in a compact or as single crystals is obviously important in controlling the process of microfracture. Smaller diamond particles may have greater strength due to fewer intrinsic defects. Hence larger stones fracture at lower stresses although they are capable of carrying higher net loads (Field & Freeman 1981). The fracture strength of synthetic stones decreases with increasing metal inclusion and nitrogen content (Field 1979).

The friction properties of diamond have been ascribed to the surface roughness but are poorly understood (Tabor 1979). The high elastic modulus prevents small surface asperities from deforming readily. As a result adhesion between a diamond surface and a moving diamond indenter is negligible. The friction is anisotropic which may be explained by the microtopography of crystallographically orientated asperities. The friction rarely exceeds 0,2 and is hardly changed by lubrication. It may be load dependent (ibid). The friction of a given diamond surface appears to rise after multiple passes (Wilks & Wilks 1979) which may be due to damage produced by the sliding process itself (Enamoto & Tabor 1980). The friction between diamond and other hard materials is due not to plastic deformation but to the interaction of the surface asperities (Seal 1981) involved at the sliding surface interface in a process as yet not understood (Tabor 1979).

CHAPTER 3

LABORATORY DRILLING MACHINE

3.1 THE REQUIREMENTS

A laboratory drilling rig based on a commercially available machine and capable of simulating realistic drilling conditions using 20 mm diameter microbits was sought. The work of Spink (1972) and Siribumrungsukha (1980) using laboratory drilling machines had shown that experiments with small-scale rigs were promising. Tests conducted by the staff of Boart Research Centre using a full-scale laboratory rig provided some indications of the required operating capabilities.

i) The machine had to be capable of operating in two different modes; viz. set advance per revolution to simulate the behaviour of screw feed machines, and set thrust to simulate machines operating under constant thrust.

ii) Using 20 mm diameter microbits a rotational velocity of at least 3000 rpm was required to achieve a realistic linear speed in excess of 2 ms^{-1} (see footnote) for individual diamonds.

iii) The power available from the motor had to be as high as possible at the required high rotational speeds to enable a wide range of bit thrusts and rates of advance to be investigated without stalling the motor.

iv) The power feed facility essential for set rate of advance tests had to be capable of being modified easily to operate at rates between 0,01 mm/rev and 0,1 mm/rev - an order of magnitude less than the rates available on most industrial drilling machines.

v) The geometry of the machine had to be appropriate. To conserve space it had to operate vertically, needed a vertical travel which would allow 100 mm deep holes to be drilled on each test-run, and have sufficient distance between the spindle nose and table to accommodate the specimen clamp, turntable, splash guard and rock specimen, and leave working space.

NOTE: Throughout this thesis the abbreviation ms^{-1} has been used to denote metres per second

3.2 DESCRIPTION OF THE DRILLING MACHINE

The drilling machine used was based on a power-fed Arboga 2512GM pillar mounted machine (see Fig. 3.1) with specifications as listed in Table 3.1. It was levelled and securely mounted with bolts to the concrete floor of the laboratory.

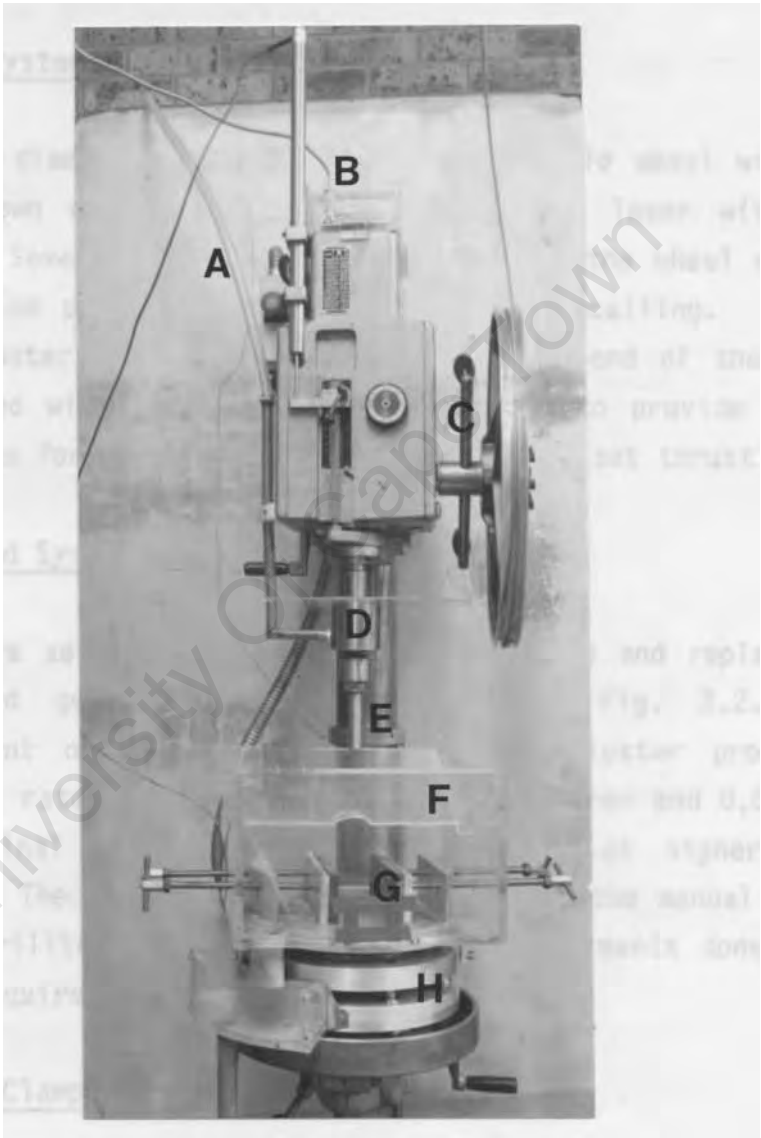

FIGURE 3.1 : The modified Arboga drilling machine (photographed by Mr B. Greeves)

A : Water Feed hose
B : Rotation meter
C : Manual feed lever
D : Water swivel
E : Drill bit
F : Splash box
G : Specimen clamp
H : Turntable discs

TABLE 3.1 : Drilling machine specifications

Maximum spindle speed	: 3500 rpm
Motor size	: 1 kW
Spindle internal taper	: Morse no. 3
Maximum quill movement	: 110 mm
Maximum distance from spindle nose to table	: 900 mm

3.2.1 Loading System

A 460 mm diameter cast light alloy motorcycle wheel with the rim turned down was fitted to the manual feed lever with a steel sleeve. Several turns of wire rope around the wheel were passed to a teflon pulley mounted in the concrete ceiling. A 10 litre plastic water container suspended from the end of the wire rope was filled with variable amounts of water to provide a constant load force for those tests carried out under set thrust.

3.2.2 Power Feed System

The entire set feed rate gearbox was removed and replaced with a redesigned gear cluster, illustrated in Fig. 3.2. Simple replacement of gears 11 and 12 in the cluster provided four different rates of advance between 0,011 mm/rev and 0,044 mm/rev. The original gearbox was used for tests at higher rates of advance. The gears were engaged by twisting the manual feed lever of the drilling machine through 90% Experiments done under set thrust required the gears to be disengaged.

3.2.3 Specimen Clamp and Turntable

The rock specimens to be drilled were held in a clamp on a three tier turntable and surrounded by a perspex splash guard (see Fig. 3.3 & 3.4). The clamp and guard box could accommodate specimens with maximum dimensions of 150 x 100 x 100 mm, with cylindrical or cuboid specimens held firmly by mahogany faced clamps. The splash box, with inclined covers, had a central hole to accommodate the drill string. Water emptied from a corner drain into a gutter attached to the bottom disc of the turntable to allow for the

relative movement of the upper disc. From the gutter it drained through a flexible pipe to a floor drain, or to a collecting bucket if required. The three aluminium discs were assembled with a large thrust bearing between the upper two to allow for free rotation of the upper disc. The upper pair in turn could move vertically in response to the load, by means of vertical linear bearings in the bottom disc which was bolted with T-bolts to the table of the drilling machine.

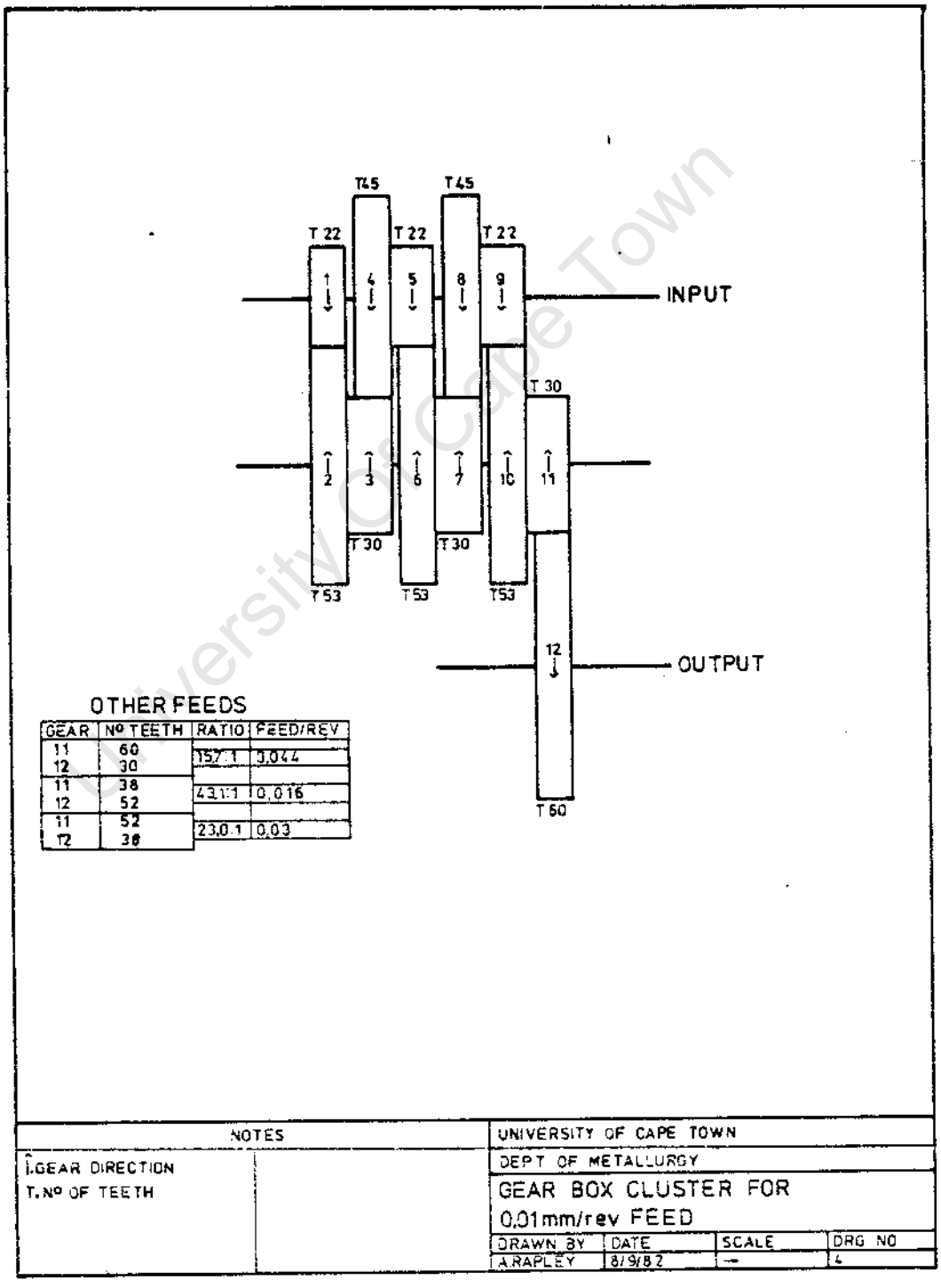

FIGURE 3.2 : Diagram of the redesigned gear cluster assembly

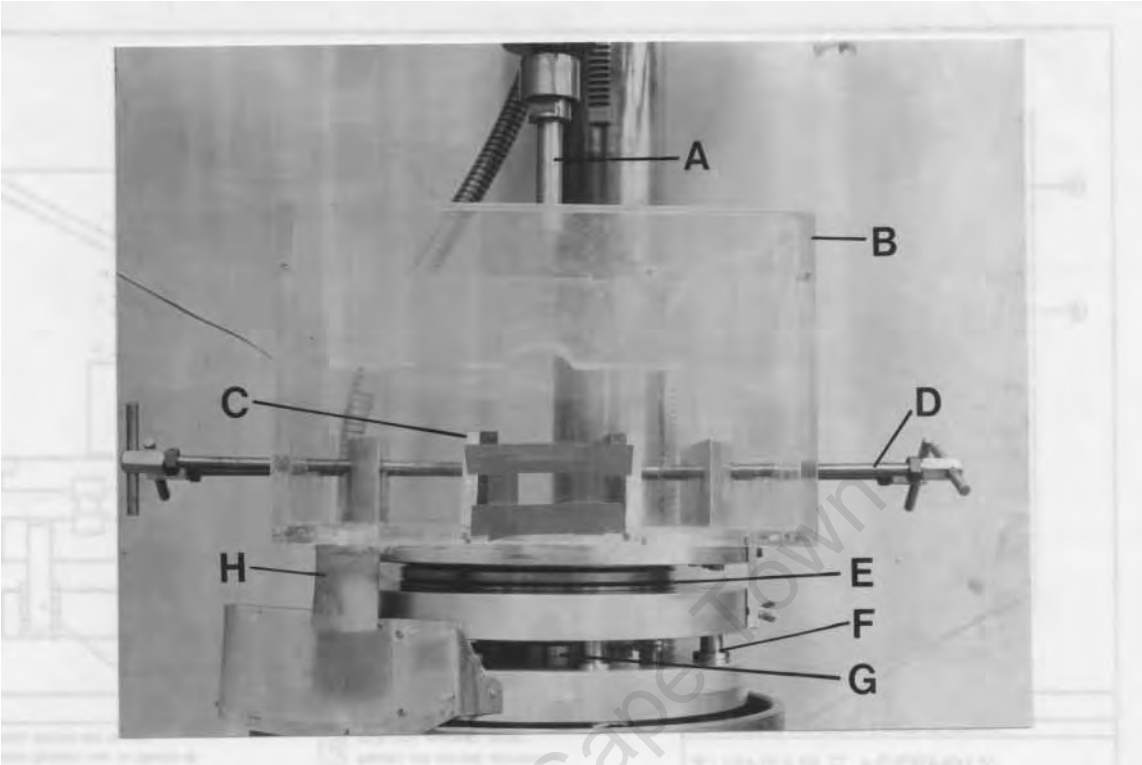

FIGURE 3.3 : The Arboga machine showing detail of the turntable, specimen holder and bit assembly (photographed by Mr B. Greeves)

A : Drill bit shaft
B : Splash guard
C : Specimen clamps
D : Clamping screws
E : Thrust and bearing
F : Linear bearing
G : Load cell
H : Drain

The table was clamped centrally so that the drill bit was on axis with respect to the turntable. The entire splash box assembly with the two upper aluminium discs could be lifted off the load cell mounted in the bottom disc by withdrawing the six steel dowels from the linear bearings. All the bearings were lubricated frequently with WD-40 water repellant aerosol lubricant.

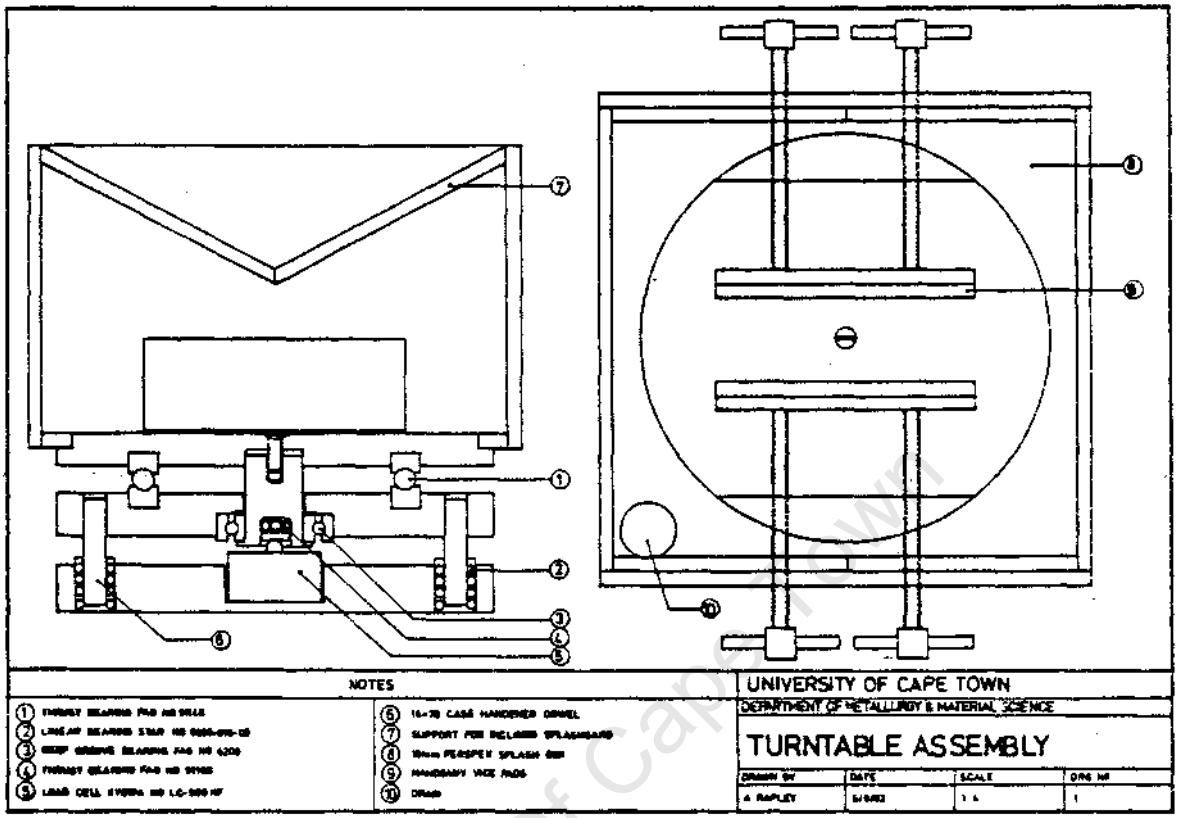

FIGURE 3.4 : Diagram of the turntable assembly

3.2.4 Water Flushing System

Water from the mains supply was fed through a NIXON cylindrical perspex flowmeter with a rider indicating the flow in litres per hour and then through a FERRIS pressure guage reading in kPa. Flow rate was controlled by adjusting a tap. An alternative flow route selected by another tap allowed a flexible hose to be used for flushing out the splash box and as a drain for the entire water feed system. The flow of flushing and cooling water at a pressure of about 200 kPa was maintained between 300 litres per hour and 400 litres per hour. Water entered the drill string through a waterswivel designed to be used at high spindle speeds and at high pressures with water as the cooling medium. The seals (GACO MIM 2547) were easily replaced. The upper end of the waterswivel fitted the Morse taper of the drill spindle and the lower end accepted the bit shaft (see Fig. 3.5).

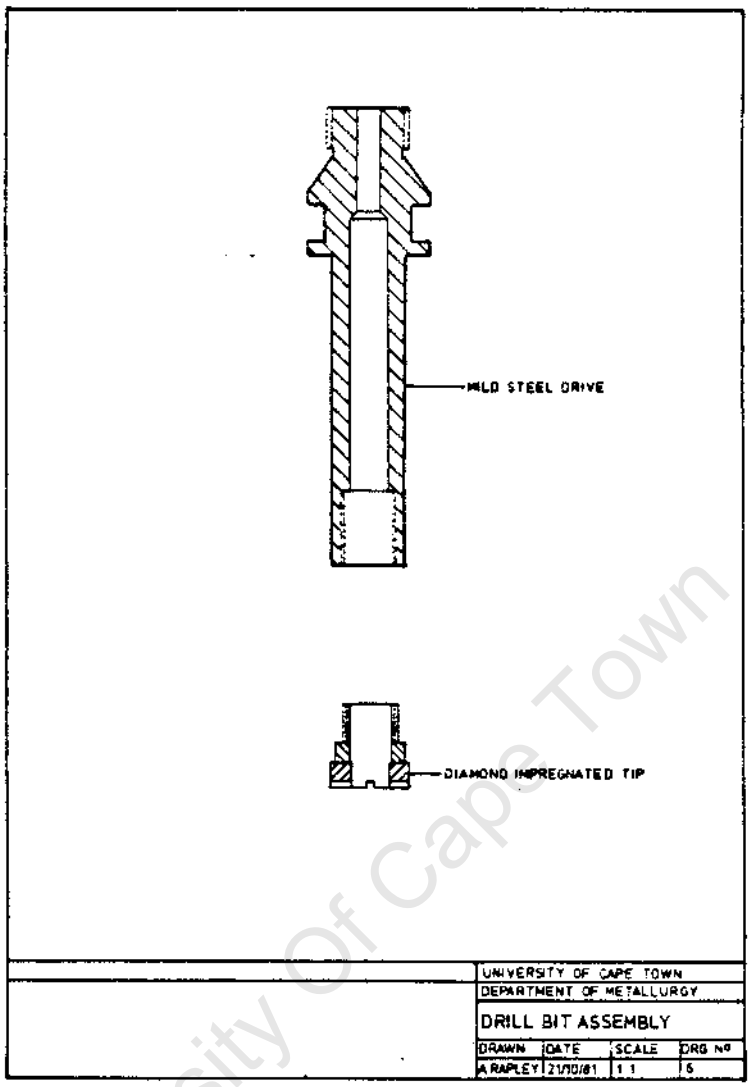

FIGURE 3.5 : Diagram of the drill bit assembly

3.3 ELECTRONIC INSTRUMENTATION

Five variables were measured continuously and recorded electronically to provide a detailed record of each drilling test and the data from which to calculate the results.

3.3.1 Power Consumption Measurement

The gross power consumed by the drilling machine and the drilling process was measured with a three phase wattmeter in the main power line. The wattmeter - a SINEAX model 56-1P1-052 - had an output of 10 mA DC current proportional to power consumption.

The wattmeter was calibrated according to the method described by Moller & Spink (1973) to allow the measurement of gross power consumption to be corrected for load dependent power losses in the drilling machine. The resulting net power consumption (representing the useful output) was used for calculating the specific energy of drilling for comparison with the specific energy calculated from the measurement of torque.

3.3.2 Rotational Speed Measurement

The rotational frequency of the drilling machine spindle was measured at the top of the machine where the spindle projected to accept a lift-off drive gear. A hollow cylindrical brass crown with two vertical blades was mounted on top of the spindle so that rotation caused the blades to obstruct the optical path of a MONSANTO MCA 8 opto-isolator. The output passed through a converter to produce an output voltage proportional to the rotational frequency. The opto-isolator was mounted above the crown on the inside of a perspex cover made to fit snugly over the top of the motor housing.

3.3.3 Load Measurement

The vertical load force exerted on the rock by the drill bit was measured with a load cell set into the base disc of the specimen turntable. The load cell was a KYOWA LC-500 KF waterproof model with a 500 kgf capacity, allowing bit pressures of up to 30 MPa to be used.

3.3.4 Torque Measurement

The upper disc of the turntable, capable of rotating on the large thrust bearing, was restrained by a rigid steel beam clamped to the bottom of this disc and impinging on a minature load cell attached to a steel upright on the drill table mount. The load cell - a KYOWA LM-5KA model with a 5 kgf capacity - produced an output voltage proportional to the torque force experienced by the rock. The load cell was preferable to a strain-gauged beam for

measuring low torques because of difficulties experienced in calibrating a robust beam at the very low torques generated by using high rotational speeds.

3.3.5 Penetration Measurement

The position of the drill bit was measured by a DC LVDT - a model D2/3000A supplied by RDP Electronics - with a 150 mm linear range covering the full travel of the quill. The transducer was mounted on the front of the motor housing and the spring loaded probe impinged on a projecting bar attached to the quill. The position of the drill bit could be monitored reliably to within 5 microns.

3.3.6 Interface Board

An excitation and interface board (see Fig. 3.6) designed by Dr P.A. Fox provided the required, excitation voltages for the two load cells, the LVDT and the opto-isolator. It also incorporated the power source for the wattmeter and a frequency to voltage converter for the output of the rotation monitor. Instrument amplifiers with switch selectable gains boosted the output signal of the transducers. This power supply and interface board was mounted on the drilling machine to reduce the length of cables between the transducers and the instrument amplifiers. A multicore cable connected the instrument amplifiers to a data-logger.

3.3.7 Data-logger and Controlling Computer

The data-logger used was a Hewlett-Packard 3497A Data Acquisition and Control Unit with a number of optional plug-in assemblies. Its central facility is a fully programmable 51/2 digit voltmeter with 1 microvolt sensitivity, capable of up to 300 readings per second in 31/2 digit mode.

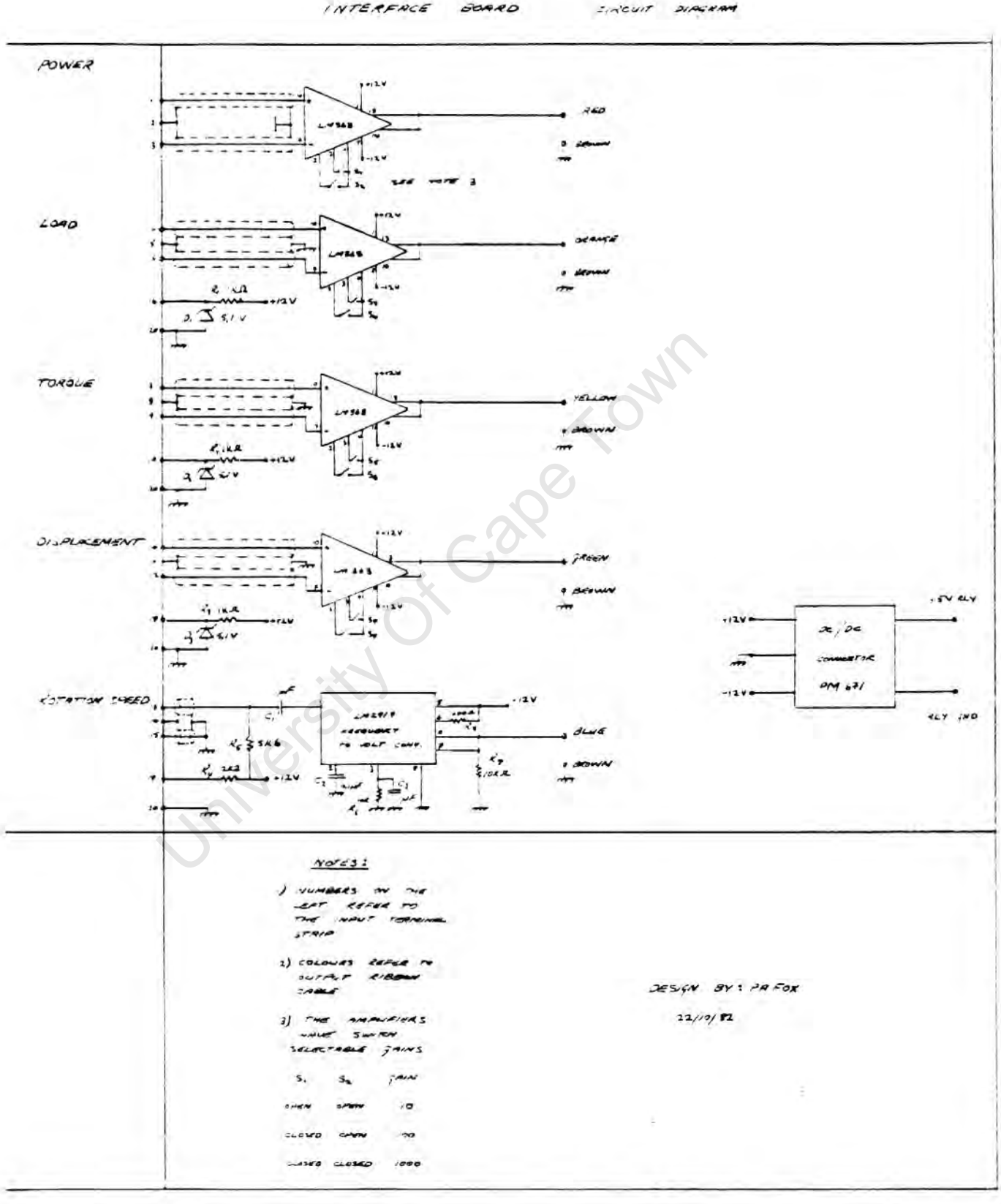

FIGURE 3.6 : Circuit diagram of the current source and interface board

In conjunction with a 19 channel relay multiplexer assembly and internal memory buffer this allowed rapid monitoring of the outputs of the five measuring instruments on the drilling machine to provide a detailed record otherwise unobtainable. Programming and control of the data-logger were achieved with an HP 85 micro-computer which was also used for subsequent storage of data and computation of results.

3.4 CALIBRATION OF THE MEASURING INSTRUMENTS

3.4.1 Penetration LVDT

The LVDT activation voltage produced by the current source was measured with a digital millivolt meter as 2,497 V DC. Linearity of the LVDT response and the calibration equation given by the manufacturers were checked by recording the instrument output for twelve positions of the transducer and fitting a straight line by least squares regression. The regression coefficient for this line was 1,0 and the manufacturer's calibration equation was confirmed.

POSITION (mm) OUTPUT VOLTAGE x 29.3

3.4.2 Thrust Load Cell

The load cell activation voltage was measured as 8,762 V DC. The formula for calibrating load force given by the manufacturer was checked by using it to calculate the weight of the specimen turntable assembly from the output it produced from the load cell. The addition of a 10 kg weight and recalculation of the results confirmed the manufacturer's calibration equation.

LOAD (kgf) OUTPUT VOLTAGE x 1000 x 0,3332/ACTIVATION VOLTAGE

where 0,3332 is a calibration constant characteristic of the class of load cell and was supplied by the manufacturer.

To allow for comparison of thrust values for tests using bits of different face areas the load force values were converted into bit pressure values. In order to do this the average bit face area of the microbits to be used had to be determined. Sixteen new bits were photographed and the images measured with a digital analyser. The total area of 96 drill face pads was measured. The average area was calculated as 24,37 mm^2 with a standard deviation of 1,77 mm^2. The mean value was used in computing the toal bit face pad area of each bit at 146 x 10^{-6} m^2. Using this value of bit face area and the calibration equation given for the load cell the bit pressure was calculated using the following formula.

$$\text{PRESSURE } (MNm^{-2}) = \text{OUTPUT VOLTAGE} \times \frac{1000 \times 0,3332}{8,762} \times \frac{9,8 \times 10^{-6}}{146 \times 10^{-6}}$$

3.4.3 Torque Load Cell

The activation voltage of the torque load cell was measured as 4,817 V DC. The manufacturer's calibration formula was given as:

LOAD (kfg) = (OUTPUT VOLTAGE/ACTIVATION VOLTAGE)/0,1856

where 0,1856 is a factory measured calibration constant.

The distance from the centre of the turntable to the nub of the torque load cell was 260 mm so the torque could be calculated from the load cell output with the followihg formula.

$$\text{TORQUE (Nm)} = \text{OUTPUT VOLTAGE} \times \frac{0,260 \times 9,8}{4,817 \times 0,1856}$$

This formula was checked by clamping a substantial rod centrally in the specimen vice, fitting a torque wrench to the top of the rod and loading this column by lowering the quill of the drill under an applied load of 1 kN onto the back of the torque wrench. Eight voltage output readings were taken for manually applied torques in the range 2,5 Nm to 6 Nm. The regression coefficient

for the best least squares linear fit to these points was 0,992. The formula for the best fit line confirmed the given calibration formula.

3.4.4 Rotation Meter

The rotation meter mounted on the top of the spindle of the drill was calibrated using a xenon strobe. Eight readings were taken of the output voltage at speeds in the range 780 rpm to 3720 rpm determined by freezing the first order image of the brass turret with adjustment of the xenon strobe frequency. The best fit regression line had a coefficient of 1,0 and the following formula was adopted.

ROTATIONAL FREQUENCY (rpm) = OUTPUT VOLTAGE x 907,7

Using a bit diameter of 20 mm the maximum surface linear speed (or peripheral speed) of the bit was given by the following formula.

$$\text{LINEAR SPEED } (ms^{-1}) = \text{OUTPUT VOLTAGE} \times \frac{\pi \times 20}{1000} \times \frac{907,7}{60}$$

3.4.5 Wattmeter

A standard calibrated wattmeter was used to calibrate the recording wattmeter. Ten readings were taken of the voltage output of the recording wattmeter at different power outputs up to 1 kW. The regression coefficient for the best fit straight line was 1,0 and the following formula determined.

POWER CONSUMPTION (W) = OUTPUT VOLTAGE x 199,8 - 0,423

3.4.6 Machine Losses

Power losses in the drilling machine accounted for much of the energy consumed. Moller & Spink (1973) described a procedure for reliable calibration of these losses so that the power consumption of the drilling machine could be used in calculations of specific energy of drilling. Three tests had to be done.

i) Locked rotor test

A clamp was attached to the top of the drill spindle to prevent rotation. Power was applied to the stator windings from a variac at proportions of the rated full-load current of 2,5 A. Readings of voltage, current, and power consumption were taken at 5% to 120% (in 5% steps) of the rated full-load current. There is a linear relationship between these losses (so-called "copper losses") and the gross power consumption.

ii) Fixed losses test

The drive gears were disengaged and the power consumption of the motor measured at 380 V. This recorded power consumption constituted a fixed loss (so-called "iron losses").

iii) Drill string loss test

The drilling machine was run at 380 V with no applied load, the water circulating in the swivel and with the full drill string in place at 3500 rpm (the rotational speed used for most of the subsequent tests) with the feed gears both engaged and disengaged. The power consumption for each configuration was measured. The loss of power in the feed gears was negligible.

The three sets of tests described above were were collated into a table listing the percentage efficiency of the drilling machine at various levels of power consumption (see Table 3.2). The relationship was linear over the tested range (Fig. 3.7) with the least squares best fit line having a regression coefficient of 0,999. At higher values of power consumption than those measured in these tests the relationship was not strictly linear as can be seen from the trend of the highest values plotted. Higher values could not be tested due to thermal overloading of the motor during the locked rotor tests when the cooling fan could not operate.

The effective power output of the entire machine at a nominal speed of 3500 rpm was determined by the following formula.

POWER OUTPUT (W) = (POWER INPUT x 0,718) - 405,0

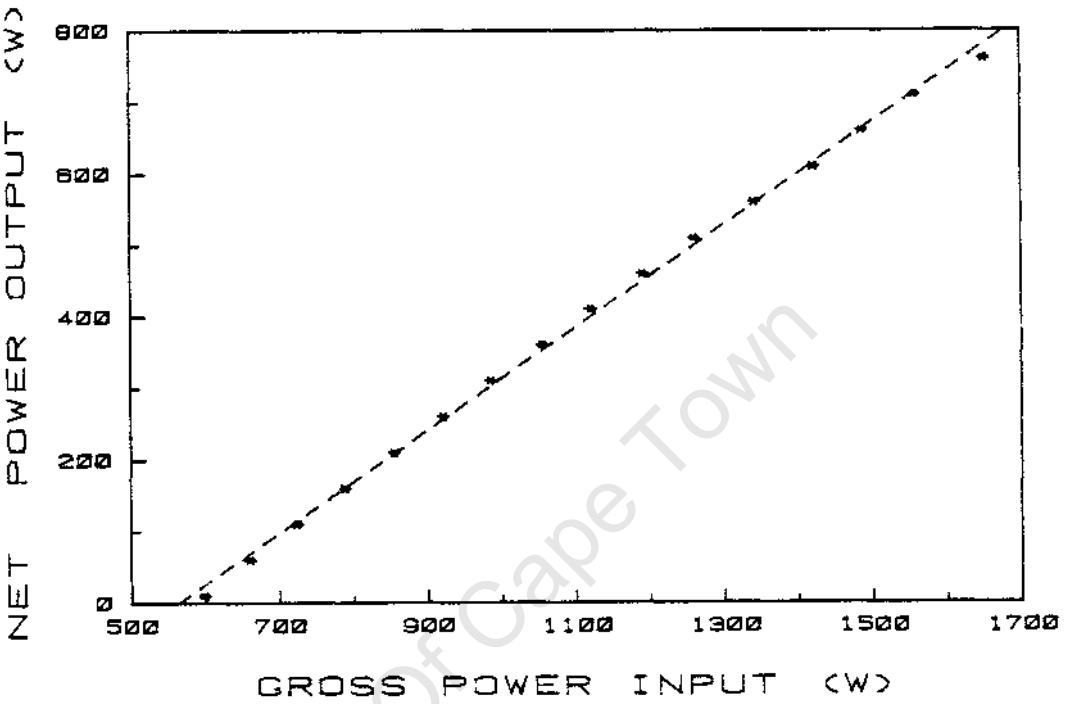

FIGURE 3.7 : Calibration plot of net power output against gross power consumption at 3500 rpm

TABLE 3.2 : Abbreviated table illustrating the calculation of percentage efficiency of the drilling machine under various loads at 3500 rpm

1	2	3	4	5=3+4	6	7=2-6	8=5+6+7	9
Rated Motor Output		Motor Losses			Drill	Overall Efficiency		
		Copper	Iron	Total	Losses	Net Output	Gross Input	Effic.
%	W	W	W	W	W	W	W	%
120	1200	350	100	450	440	760	1650	46,0
115	1150	306	100	406	440	710	1556	45,6
110	1100	286	100	386	440	660	1486	44,4
105	1050	270	100	370	440	610	1420	43,0
100	1000	240	100	340	440	560	1340	41,8
95	950	210	100	310	440	510	1260	40,5
90	900	190	100	290	440	460	1190	38,7
85	850	170	100	270	440	410	1120	36,6
80	800	155	100	255	440	360	1055	34,1
75	750	135	100	235	440	310	985	31,5

3.5 COMPUTER PROGRAMMING

The computer available for programming and control of the data-logger was an HP85 micro-computer. The controlling program, written in HP BASIC, consists of three major sections and is listed in Appendix 2 along with a more detailed commentary.

i) The first section, preceded by a short initializing routine, recalibrates the power losses in the drilling machine before each test. The seals in the water swivel suffered significant degradation with operational life, resulting in a decreasing loss of energy to friction in the ageing seals. This necessitated the recalibration before each test to ensure that the net power output values calculated from the gross power consumption were valid.

ii) The section controlling the actual drilling test starts with a request for details of the test to be run. Test parameters recorded are rock type, a description of the bit, mode of operation (set thrust or set rate of advance) and sampling rate. This is dependent on the expected length of the test because the HP85 has limited memory capacity and only 600 sets of data can be retained during each test. All the channels with the exception of the output of the LVDT are sampled for zero reference readings. The wattmeter output is then monitored as rapidly as possible in order to sense the beginning of the test which is identified by the rapid rise in power consumption. The program then jumps to the test routine in which the data-logger samples each of the five instrument channels very rapidly at regular intervals and stores the values internally. These are then read by the HP85 during the interval before the next timer controlled sampling instruction. There is insufficient time to write this data directly to disc storage during the active testing so it is stored internally in the interim and transfered to disc at the end of the test.

iii) A concluding section calculates and prints summarised results that act as a temporary record of the test.

More detailed results and plots are produced by another program "B" which will not be described in detail. It is included in Appendix 2 with programs "C" and "D". The plots act as a visual record of each test (see Figs. 5.13 & 5.24). Program "C" computes summary tables and tables of standardised results (eg. Appendix 5). Program "D" compiles summary tables of all the results (see Appendix 4).

The plots of results in Chapter 5 were produced with the aid of a plotting program written for the HP85 computer by Mr K. Barker.

CHAPTER 4

TEST MATERIALS AND EXPERIMENTAL METHODS

In this chapter the design and formulation of the bits used are described as well as the composition and structure of the materials drilled. This is followed by a description of the experimental and analytical methods used in the research program. The drilling test procedure is described as well as the associated testing and measuring techniques used both before and after the test to obtain ancillary information.

4.1 BIT DESIGN

The geometry of the microbits was the same in all cases. The outer and inner diameters were 20 mm and 12 mm respectively with six 2 mm wide waterways symmetrically placed. With the available drill spindle speeds these dimensions allowed testing up to a bit peripheral speed of 3,5 ms^{-1}; this is comparable with field conditions. Given the diameter of the bit, the kerf was very wide so six waterways were chosen instead of the more conventional four. This produced a bit face area of 146 mm^2. A value in this region was convenient and made it easier to generate realistic operating bit pressures without using an unwieldy weight to create the load.

All the bits were made using a bronze matrix (80/20 Cu/Sn) on a threaded mild steel shank. They were manufactured by Boart Research Centre by pressing a mixture of bronze powder and the appropriate quantity of diamond grit into a Nimonic mould and sintering at 725 $^{\circ}C$ in an inverted position with the steel shank in place. This produced an impregnated diamond drill bit with a supposedly random distribution of diamonds in the matrix. The waterways were of a standard depth, extending almost to the base of the 5 mm deep impregnation. The excess bronze coating the shank adjacent to the waterways had to be removed from both the inside and the ouside of the bit with a hacksaw. The impregnation was 1 mm wider than the steel shank so the channels produced by this operation allowed water to reach the waterways.

The diamonds used in the bits were all De Beers SDA 100. This diamond saw abrasive was chosen because of its intermediate strength and previous use in other experimental drilling programs (Bullen & Bailey 1979, Bullen 1983). Its cubo-octahedral shape gives the individual stones a blocky form with truncated points and they more closely approach a spherical shape than other untreated synthetics. The sizes of the diamonds ranged from 20 US mesh to 80 US mesh, mostly graded in 10 mesh intervals. Diamond concentration was usually 30 except for one test series using 50 concentration bits. An intermediate bit formulation consisting of 40/50 mesh SDA 100 grit in 30 concentration was used as a standard bit in many of the tests. A concentration of 30 was chosen so that a reasonable number of individual diamonds would be exposed for the evaluation of diamond wear after a test.

Three so-called monolayer bits were designed by Mr C. Franks and produced at Boart Research Centre. These were of standard dimensions but had a single layer of exposed diamonds set in the matrix in a regular pattern like a surface set bit. Two incorporated 30/40 mesh diamonds, the other had 20/30 mesh stones.

4.2 THE MATERIALS DRILLED

In this section the rock types and other materials drilled will be described with emphasis on the characteristics particularly relevant to drilling. Petrographic descriptions of the rock types drilled are given in Appendix 3. The rock types were chosen with the intention of including a full range of properties important in drilling; from strong and non-abrasive, through strong and abrasive, soft and abrasive, to soft and non-abrasive. The single crystal materials were chosen because of the predominance or importance of these minerals in some of the rock types. All the rock specimens were delivered sawn by Boart Research Centre into approximately 100 x 100 x 100 mm cubes.

4.2.1 Rock Types

Eight different rock types were drilled. Photographs at a uniform magnification of thin sections of each rock type appear together for comparison in Fig. 4.1.

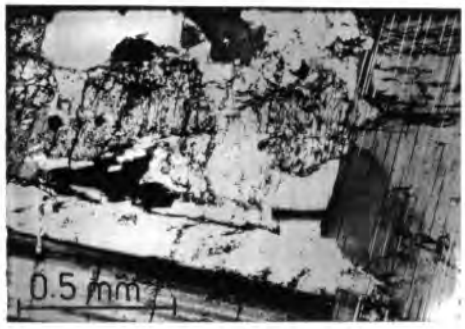

A: LIGHT NORITE

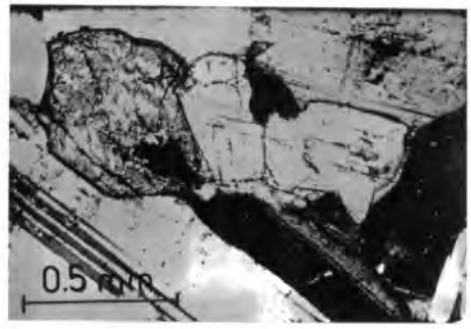

B: DARK NORITE

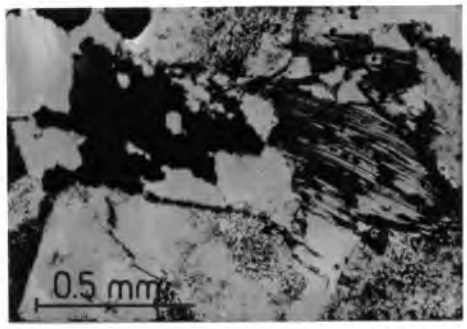

C: CAPE GRANITE

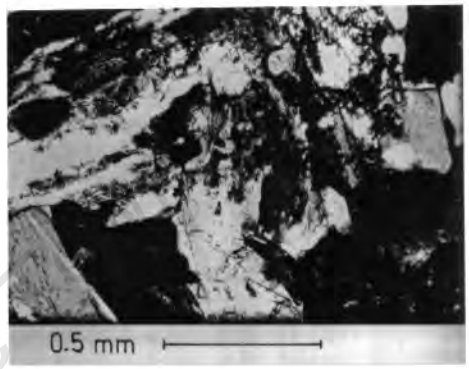

D: QUARTZ SYENITE

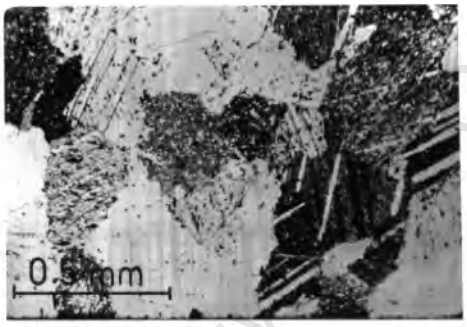

E: MARBLE

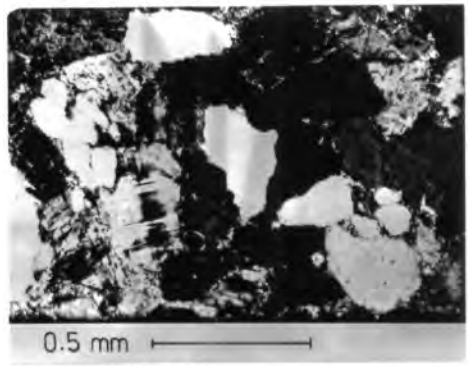

F: SANDSTONE

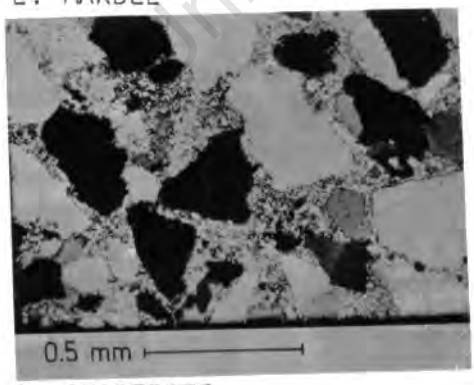

G: QUARTZITE

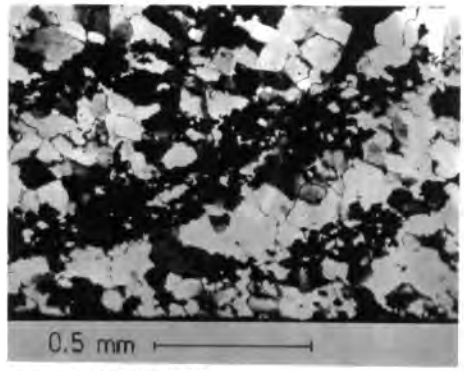

H: JASPILITE

FIGURE 4.1 : Photomicrographs of petrographic thin sections of the eight rock types drilled. Magnification 40X, under crossed polars to enhance contrast between minerals.

"Dark" Norite

A very fresh gabbro norite, this rock consists of about 60 percent plagioclase felspar and the balance of pyroxene. Both of these minerals have well developed cleavage. The rock is fairly coarse grained with an average grain size between 2 and 3 mm. Containing no quartz this rock was expected to be moderately strong and not very abrasive. It was the material selected for most of the tests into the drilling mechanism because of its intermediate properties in terms of drilling behaviour and its traditional role at Boart Research Centre as an experimental drilling material.

"Light" Norite

This gabbro norite is very similar in composition to the "dark" norite. These two norites were expected to behave very similarly.

"Cape" Granite

The predominant mineral in this rock, alkali felspar forms large crystals between 4 and 10 mm long, with interstitial and irregular grains of quartz and minor quantities of plagioclase felspar, biotite and opaque minerals. The felspars have well developed cleavage but the quartz, forming very angular grains was expected to be abrasive as well as contributing to the strength of the rock.

Quartz Syenite

This rock, known colloquially as "red granite", contains much less quartz then the Cape granite. It consists primarily of plagioclase felspar, hornblende (an amphibole), and a pyroxene all in large crystals averaging about 4 mm long. These minerals all have well developed cleavage. Thus the degree of fracturing and alteration lead to the expectation that this rock would have a moderate strength and not be particularly abrasive.

Marble

This recrystallised limestone consists almost entirely of intergrown grains of calcite with an average grain size of 0,5 mm. Calcite has a very easy cleavage and is soft with a Mohs hardness of 3. The rock was expected to be weak and unabrasive.

Sandstone

This sedimentary rock contains mostly moderately angular quartz grains about 0,5 mm in diameter, with a micaceous matrix and a minor quantity of felspar and fragments of cherty material. It was expected that the high percentage of weakly cemented quartz grains would make this rock particularly weak but highly abrasive.

Quartzite

The moderately angular grains making up this rock have been recrystallised to some extent and been cemented by a fine grained siliceous matrix. The rock was expected to be of moderate strength but the abrasiveness could not be predicted.

Jaspilite

The extremely fine grained nature of the microcrystalline quartz predominant in this rock was expected to make this material particularly difficult to drill due to its being both very strong and non-abrasive.

4.2.2 Minerals

The minerals drilled were all single crystal blocks, natural or synthetic and selected for freedom from gross inclusions but incorporating their natural or grown-in flaws. Making thin sections of these materials for illustration was pointless because under the petrographic microscope the field would be uniform except for cleavage traces and micro-inclusions.

Felspar

Large blocks of natural microcline felspar (Amazonite) were selected for apparent freedom from cracks and trimmed to shape by utilising the prominent cleavage and where necessary by diamond sawing of parallel faces for clamping. Because of this geometry drilling was perpendicular to a prominent cleavage plane. This material was chosen to correspond to the felspar in the norite, granite and syenite and to enable a comparison to be made of the mineralogy of the detrital grains produced by drilling these materials.

Calcite

Blocks of natural single crystal calcite (Iceland spar) were processed in the same way as the felspar. This material was used for comparison with the polycrystalline marble.

Quartz

Synthetic quartz bars produced for the electronics industry were obtained from STC, Boksburg in sufficient size to enable drilling parallel to the z or c axis (Z direction) for distances of about 60 mm. Unfortunately this necessitated drilling through the seed plate and the adjacent planes of grown-in flaws and bubbles. The quartz was drilled for comparison with the quartzite and sandstone.

4.3 BIT OPENING AND RECONDITIONING

The faces of new bits were flat with no stones exposed. The bits had been sintered in an inverted position so the stones immediately below the surface presented flat faces on initial exposure, presumably due to their having settled on the bottom of the mould during the pressing stage. This layer of orientated diamonds had to be stripped from the bit before testing to avoid spurious drilling behaviour due to the flats presented and to expose suitably sharp stones in nominally random crystallographic orientations and positions on the bit face.

Reconditioning of worn bits intended for re-use was necessary to remove a sufficient depth of impregnation to expose a new set of fresh stones. The procedure was intended to be equivalent to the initial bit opening process but as the stones to be removed were already exposed, only about half the previous depth of impregnation had to be removed to achieve the standardisation.

Initial experimentation with drilling new bits into abrasive sandstone established the bit opening procedure. Measurement of impregnation removed and visual inspection of the diamonds under 10 X magnification showed that with new 40/50 mesh standard bits drilling about 0,5 m (or 6 holes) into sandstone at 5 MPa bit pressure with the water flow rate at maximum (about 600 l/hr) had the required effect of removing the first layer of orientated stones (see Table 4.1). Reconditioning of the 40/50 mesh bits required drilling about 0,3 m (or 4 holes) into sandstone under the same conditions. Bits with coarser diamonds drilled the sandstone with much less matrix wear so they were first opened in a very abrasive and harder HIPPO 80 ceramic brick and then the bit face condition was standardised by drilling 0,5 m in sandstone under the conditions described above. Reconditioning was achieved by drilling 0,5 m in sandstone directly with the coarser bits. Bits with finer mesh diamonds needed proportionally shorter drilling in sandstone to remove the required depth of impregnation. The finest 60/80 mesh bits were adequately opened and reconditioned by drilling only one approximately 85 mm deep hole.

TABLE 4.1 : Results of bit conditioning tests to remove orientated stones

Bit pressure (MPa)	4	5	6
Bit mass loss (g)	1,28	1,32	1,49
Linear bit wear (mm)	0,59	0,55	1,08
Orientated stones	11	0	0

4.4 BIT WEAR MEASUREMENT

Bit wear was measured in two ways. Axial or linear bit wear represented the retreat of the bit face as the bronze impregnation wore away. Bit mass loss recorded the total bit wear including loss of material from the

sides of the bit and loss due to change in the bit profile through rounding of the face or coning towards the inner diameter.

4.4.1 Linear Bit Wear

This was measured in two ways. A rough estimate of axial bit wear was obtained from the change in height of the most protuberant point on the bit. This was measured by lowering the bit on the drilling machine under no applied load onto a steel reference cylinder and reading the output of the LVDT position transducer before and after each test. This method was replaced by the use of a micrometer jig for all but the earliest tests. The results of the initial method were not representative of the bit face as a whole.

The micrometer jig is a mild steel block with a V-groove terminated at one end by a 25 mm high hardened steel post with an inward facing vertical 60° edge and at the other end by a vernier micrometer reading to 0,001 mm. The bit to be measured was screwed firmly into a threaded hole at one end of a brass cylinder 25 mm in diameter, placed in the groove with a bit face pad up against the vertical edge of the post, and the screw of the micrometer tightened for the reading to be taken (see Fig. 4.2). The average of twelve readings taken at different positions of the bit face were used as the bit height value. The difference between this value before and after a• drilling test constituted the linear bit wear. This value was normalised to 1 m to take into account the effect of different test lengths.

4.4.2 Bit Mass Loss

This was taken as the difference between the bit mass recorded on a four place balance before and after each test with the bit cleaned ultrasonically to remove dust or drilling detritus before taking the reading. This value was also normalised to 1 metre.

4.5 DRILLING TEST PROCEDURE

After the opening of a newly numbered bit, or reconditioning of a used one, it was cleaned ultrasonically, dried and weighed to determine the initial bit mass. The initial bit height was measured with the micrometer jig and both these values noted with the test number, bit number, diamond mesh size, and desired set rate of advance or bit pressure (if operating under set thrust), and the material to be drilled.

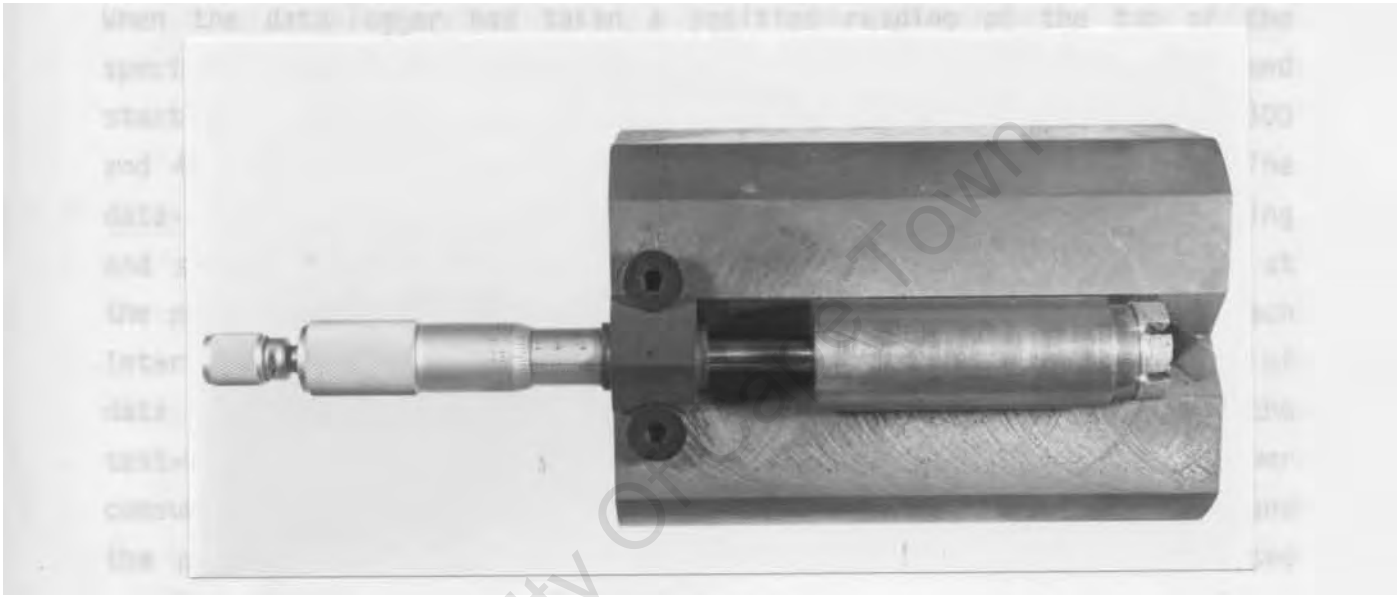

FIGURE 4.2 : Photograph of the micrometer jig with a bit in position to measure the extent of linear bit wear (photographed by Mr B. Greeves)

The computer program "A" controlling the data-logger was loaded from disc to the HP85 computer and the drilling machine was switched on and run for ten minutes to warm up with the water circulating in the swivel. Then the data-logger took the appropriate readings from the wattmeter to recalibrate the power losses in the drilling machine (described in detail in the previous chapter). The drill and water were then turned off. With the data and time set on the data-logger the program prompted the operator to enter further details of the test; viz. the operating conditions (set rate of advance or set thrust), and selection of a sampling rate. Zero readings were automatically taken on all instrument channels except the position transducer and then the operator was prompted to lower the bit - screwed firmly into the bit holder which in turn was screwed into the water swivel and tightened with a wrench - onto

the steel reference cylinder to record the initial bit height reading electronically. Replacement of the cylinder with the specimen to be drilled followed, the turntable was unclamped, the flexible detritus drain directed to a collecting bucket if necessary and the bit loaded onto the rock specimen. The required feed gears had been selected before the outset or at this stage the appropriate weight was applied to the loading wheel to generate the desired bit pressure which was checked electronically.

When the data-logger had taken a position reading of the top of the specimen the computer prompted the operator to switch on the water and start the drill. The water flow rate was rapidly adjusted to between 300 and 400 1/hr and maintained there by re-adjustment if necessary. The data-logger sensed the onset of drilling, took a reference time reading and started sampling the five instrument channels in rapid sequence at the preselected interval (every one, two or three seconds). During each interval the measurements were read by the computer and the number of data sets already read displayed on the data-logger. At the end of the test-run when stopping the drill was sensed through the drop in power consumption the data-logger ceased sampling and read both the time and the position of the bottom of the hole. Elapsed time and accumulated drilling distance were displayed by the computer and the test was either continued with the drilling of another hole and the results concatenated to produce one long test record, or terminated. If a disc of rock from the bottom of the hole was required then for one test-run the specimen was raised on two lateral 6 mm square steel bars. This enabled the drill to penetrate far enough for ring cracks to form in the test material at the bottom of the hole so that the water pressure could force a disc of rock out into the 6 mm gap.

Tests were ideally terminated after drilling 16 holes in one block of material or after 600 sets of data had accummulated. Non-ideal termination occurred when there was a deficiency of test material or stalling 'due to thermal overloading of the motor stopped the drill. Termination of the test involved switching off the water, clamping the turntable to avoid damage to the torquemeter load cell, removing the specimen, washing it and flushing the splash box with water from the flexible hose to drive all the detritus into the collecting buckets, and

lowering the unloaded drill string once again onto the steel reference cylinder for a terminal bit height reading. The raw data, corrected only for initial non-zero readings on the transducers, was stored in duplicate on the appropriate computer discs while the bit was being removed from the bit holder. After cleaning, drying and weighing to determine the final bit mass value, the final bit wear value was measured on the micrometer jig. A note was made in the test record book of normalised linear bit wear and mass loss, the total distance drilled, the bit profile, whether a punch-through disc had been made and detritus collected, and the nature of the termination. The computer then printed out preliminary results on its internal thermal printer to act as a temporary record of the test to accompany the bit.

4.6 RESULT CALCULATIONS AND RECORDS

Under control of program "B" the computer recomputed the test results and produced plots of selected variables (eg. Figs. 5.13 & 5.24). The formulae used in these calculations are included in Appendix 2. The first page of each record consisted of the details of the test as well as the computed variables; viz. the test number, the data and time of the test, the material drilled, the bit description, the set parameter (thrust or rate of advance), test duration, sampling interval, distance drilled, mean power output, mean bit pressure, mean linear bit speed, mean torque generated, mean advance per revolution, average specific energy of drilling calculated from the corrected wattmeter readings, average specific energy of drilling calculated from the torquemeter readings, and the specific linear bit wear measured by the data-logger. As they became available other data (such as the detritus size distribution) associated with the test were added to this record page.

The print-out for each test included six plots illustrating the progress of the test as recorded by the sequential sampling routine. These plots acted as a visual record of the entire test and allowed the drilling peformance to be evaluated conveniently at a glance. The following plots were produced:

i) Power consumed against drilling distance
ii) Generated torque against drilling distance

iii) Penetration against drilling time

iv) Bit pressure against drilling distance (for set rate of advance tests) or advance per revolution against drilling distance (for set thrust tests)

v) Specific energy of drilling calculated from the wattmeter readings against drilling distance

vi) Specific energy of drilling calculated from the torquemeter output against drilling distance.

Summary tables of results for the tests produced by Program "D" incorporated the normalised bit wear and bit mass loss data measured independently of the drilling machine as well as other data measured subsequent to the drilling test.

4.7 DIAMOND WEAR EVALUATION

The worn diamonds on a used bit have been observed to display certain characteristic features and it was proposed by Cooper & Adams (1983) that these features may be classifiable into three categories. These have been expanded into ten categories (Miller 1984) and an attempt has been made to associate the drilling performance of a bit with the predominance of a particular diamond wear type.

The classification of these features on a used bit was done under 40 X magnification using a Nikon optical stereo microscope. The 40/50 mesh bits typically had between 100 and 150 features to classify; finer mesh bits had significantly more and so with these bits the features on only three of the six pads were classified. The bits with stones coarser than 40 mesh had fewer features and were less taxing to evaluate.

The wear features included diamonds showing different types of wear and fracture as well as different degrees of exposure, and both shallow and deep holes left in the matrix by the loss of stones. The definition and designation of categories used in the classification are presented in Table 4.2 and typical examples are illustrated in Fig. 4.3,

TABLE 4.2 : Categories of diamond wear

TYPE	DEFINITION
0a	: Unworn stone only just protruding from the matrix
0b	: Unworn stone exposed for more than 4 of its diameter
la	: Worn stone displaying rounded corners or edges
lb	: Worn stone displaying well developed wear flats
2a	: Worn stone cracked or chipped but essentially integral
2b	: Worn stone fractured into multiple sharp points
3a	: Fresh hole in matrix associated with recent loss of stone
3b	: Shallow hole in matrix representing an earlier loss
4a	: Stone cleaved or broken off flush with the matrix
4b	: Stone worn down flush with or pressed into the matrix

Classification of a particular stone or feature was necessarily subjective using these criteria and occassionally it was difficult to assign a designation with confidence. The diamond wear types graded into each other and some distinctions were more difficult to make than others. Type 0 (a & b) stones were clearly distinct from the others. Type la grade into Type lb and the pitted and roughened surfaces of some Type lb stones could look similar to Type 2b wear. Type 3a grades into Type 3b, but since these were not strictly speaking diamond wear features they were readily distinct from other categories. Confusion between Type 4a and Type 2b wear was sometimes a problem. Despite these reservations this classification was useful and since it was done throughout by only one person it could be expected to be as consistent as possible. The location of each classified feature was recorded on a special diagram with the wear type designation. The incidence of particular types of wear was determined by counting and calculating the percentage frequencies for each type on a given bit.

4.8 DETRITUS PARTICLE SIZE DISTRIBUTION MEASUREMENT

The detritus collected in a series of 20 litre buckets during a drilling test was allowed to settle for about 15 minutes and then the excess water carefully decanted. All the sediment was transfered to a 1 litre beaker and oven dried at 50 $^{\circ}$C overnight. Then the beaker and sediment were

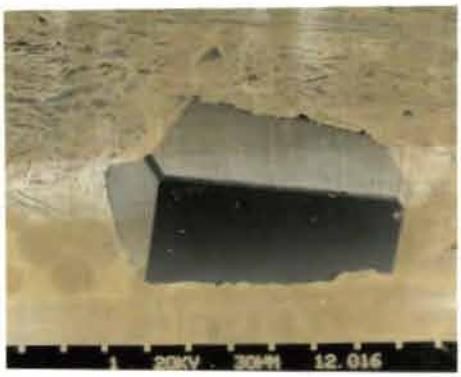

Type 0a

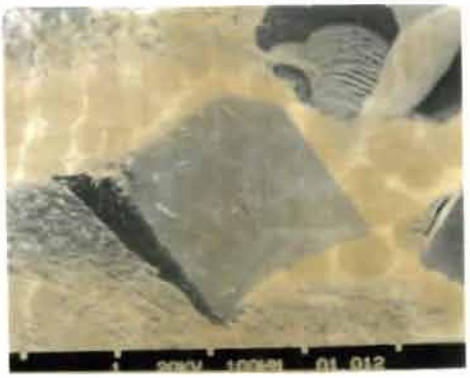

Type 0b

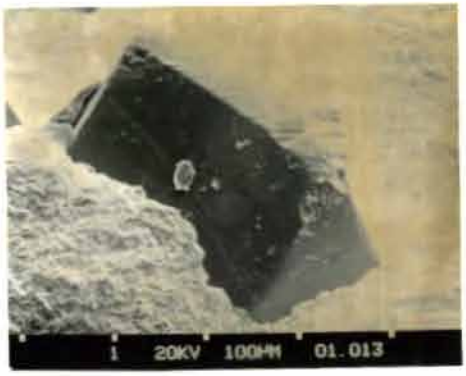

Type 1a

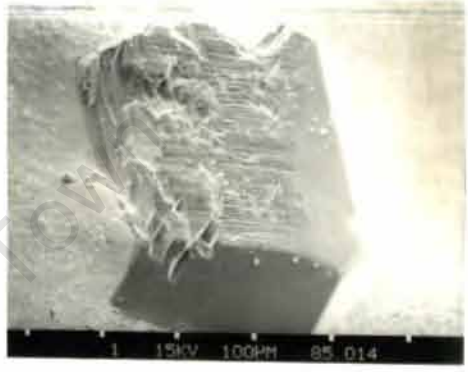

Type 1b

Type 2a

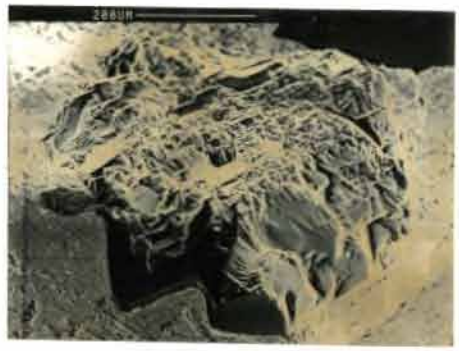

Type 2b

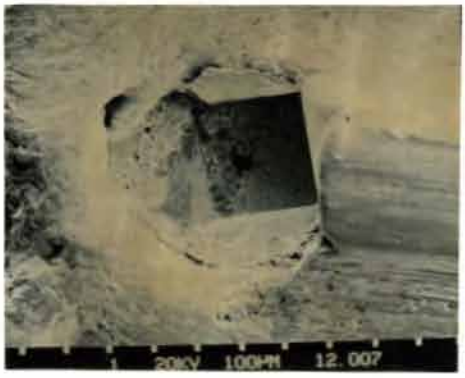

Type 3a

Type 4a

FIGURE 4.3 : Scanning electron micrographs of typical examples of common diamond wear types

weighed together, a detergent deflocculant added and all the detritus washed in a 63 micron sieve on an automatic shaker for about 20 minutes until all the fine material had been separated. The retained coarse fraction was replaced in the beaker, dried and weighed after which the beaker was weighed alone. Values for total detrital mass and mass of fine fraction were used to calculate the percentage fines (% MUD) under 63 microns in size. Occasionally these figures had to be adjusted to accommodate the subsequent removal of large spalls over 2 mm in size from the cleaned coarse fraction. The sand sized material (between 63 microns and 2 mm) was then split repetitively with a partitioned riffle splitter to produce two representative sub-samples, each with a mass of about 2,5 g. These were retained, one for particle size distribution analysis, the other as a reserve or for examination of the grains in the microscope.

The semi-automatic hydraulic settling tube housed in the Department of Marine Geosciences, University of Cape Town was used. It has been described in detail by Flemming (1977). The tube is a vertically mounted water filled transparent PVC pipe with an internal diameter of 140 mm and a fall height of about 2 m. The sample is introduced to the water surface mechanically and a chart recorder starts moving simultaneously. A scale pan suspended from a very sensitive electronic balance at the top of the tube by thin cords records the increase of mass as the particles settle, the larger particles arriving first. The amplified signal from the balance is plotted by the chart recorder as a sigmoidal graph of mass increase against time. For each sample this graph has to be digitised by hand; thirty measurement being taken at set intervals to transfer the data to computer cards.

Execution of the program ABS.SETTLEPROG/TEMP (described by Flemming 1977, p. 179) on the Sperry 1100 mainframe computer calculates statistics for the sample including deciles, median, mean, standard deviation, skewness, and kurtosis for the percentage frequency by mass of particle size plotted on a negative log-normal scale. A convenient summary plot was also available on request and this was added to the test record (see Fig. 4.4). The frequency percent scale of these plots refers to the peaked curve and the cumulative percent to the smooth curve. The

abscissa is in units of phi, a negative log scale conventionally used by sedimentologists to describe particle size distributions because these tend to be log-normal and dominated by fine particles. Phi is defined as the negative logarithm to the base two of the particle diameter "d" in mm divided by 1 mm to produce a dimensionless number (Blatt, Middleton & Murray 1972):

$$phi = -\log_2 d/1\ mm$$

The value for mean particle size and standard deviation were recorded from the computer print-outs for each sample and transferred with the value for the percentage finer than 63 microns (% MUD) to the summary tables of results (see Appendix 4).

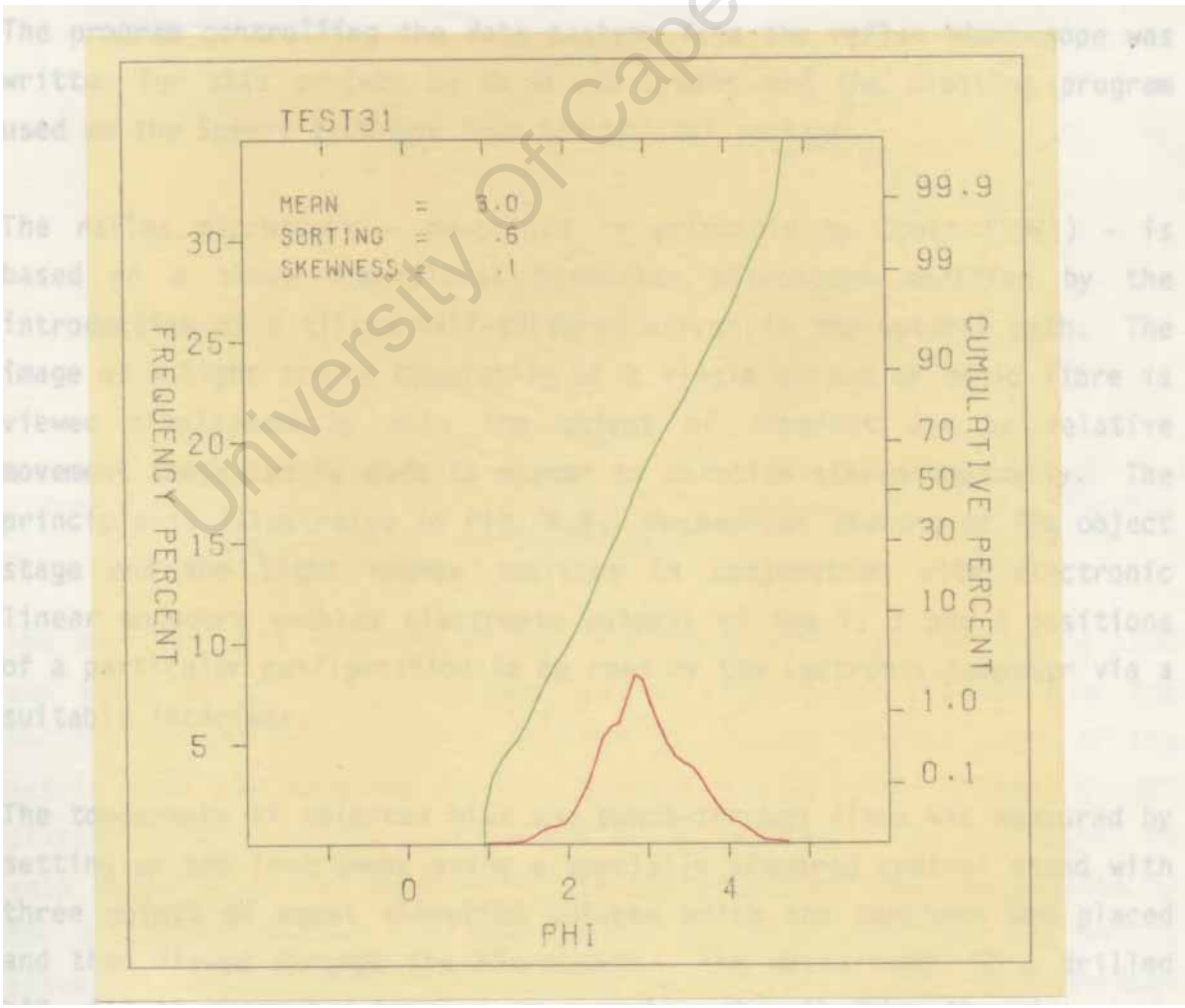

FIGURE 4.4 : A computer drawn plot of detrital particle size distribution determined by hydraulic settling

4.9 SCANNING ELECTRON MICROSCOPY (SEM)

All the punch-through rock discs, selected bits and detritus samples were glued onto numbered aluminium stubs and prepared for SEM by cleaning ultrasonically and washing in alcohol to remove all loose material and then sputter coated with gold. The specimens were viewed in the SEM at an accelerating voltage of 20 KeV with a specimen tilt of 15°.

4.10 MEASUREMENT OF BIT TOPOGRAPHY

The protrusion of the diamonds before and after drilling with bits of different diamond mesh size, as well as the topography of the matrix of these bits and the punch-through discs produced by them were measured using a reflex microscope and Tectronix display terminal. Contoured plots were produced by the Sperry 1100 computer and a Calcomp plotter. The program controlling the data capture from the reflex microscope was written for this project by Mr H van Gyssen and the plotting program used on the Sperry 1100 was from the SACLANT package.

The reflex microscope - described in principle by Scott (1981) - is based on a three dimensional binocular microscope modified by the introduction of a tilted half-silvered mirror in the optical path. The image of a light source consisting of a single strand of optic fibre is viewed simultaneously with the object of interest and by relative movement these can be made to appear to coincide stereoscopically. The principle is illustrated in Fig. 4.5. Mechanical gearing of the object stage and the light source position in conjunction with electronic linear encoders enables electronic outputs of the X, Y and Z positions of a particular configuration to be read by the Tectronix computer via a suitable interface.

The topography of selected bits and punch-through discs was measured by setting up the instrument using a specially prepared control stand with three mints of equal elevation between which the specimen was placed and then viewed through the microscope. The measurement of a drilled bit will be described here as an example. By adjusting the microscope focus and positioning the light spot coincident with the apex of the exposed diamonds the X, Y and Z co-ordinates of each of these points

were read by the computer and stored in a data file on tape. The bit matrix relief was measured by sighting 1000 points, more or less evenly spaced over the bit face. The elevation and lateral position of individual points could be determined to within 10 microns.

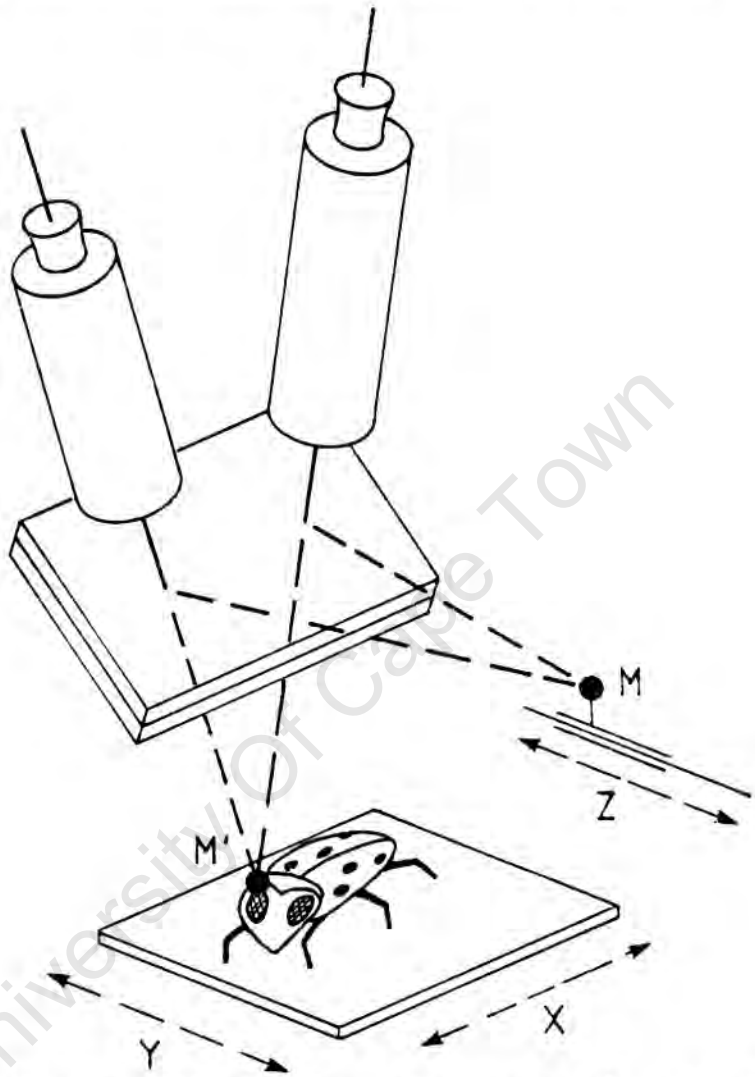

FIGURE 4.5 : A diagram illustrating the principle of the reflex microscope (after Scott 1981)

The position data recorded on tape was transferred to the Sperry 1100 and after being subject to some routine editing was processed by the SACLANT gridder and contourer programs to produce contour plots of the matrix with any required contour interval and with the diamond points plotted as spot heights. Fig. 4.6 is an example. The protrusion of each stone above the adjacent matrix was estimated from these plots by the difference between the spot height for that stone and the matrix elevation interpolated from neighbouring contours. The punch-through disc relief plots had of course no spot heights.

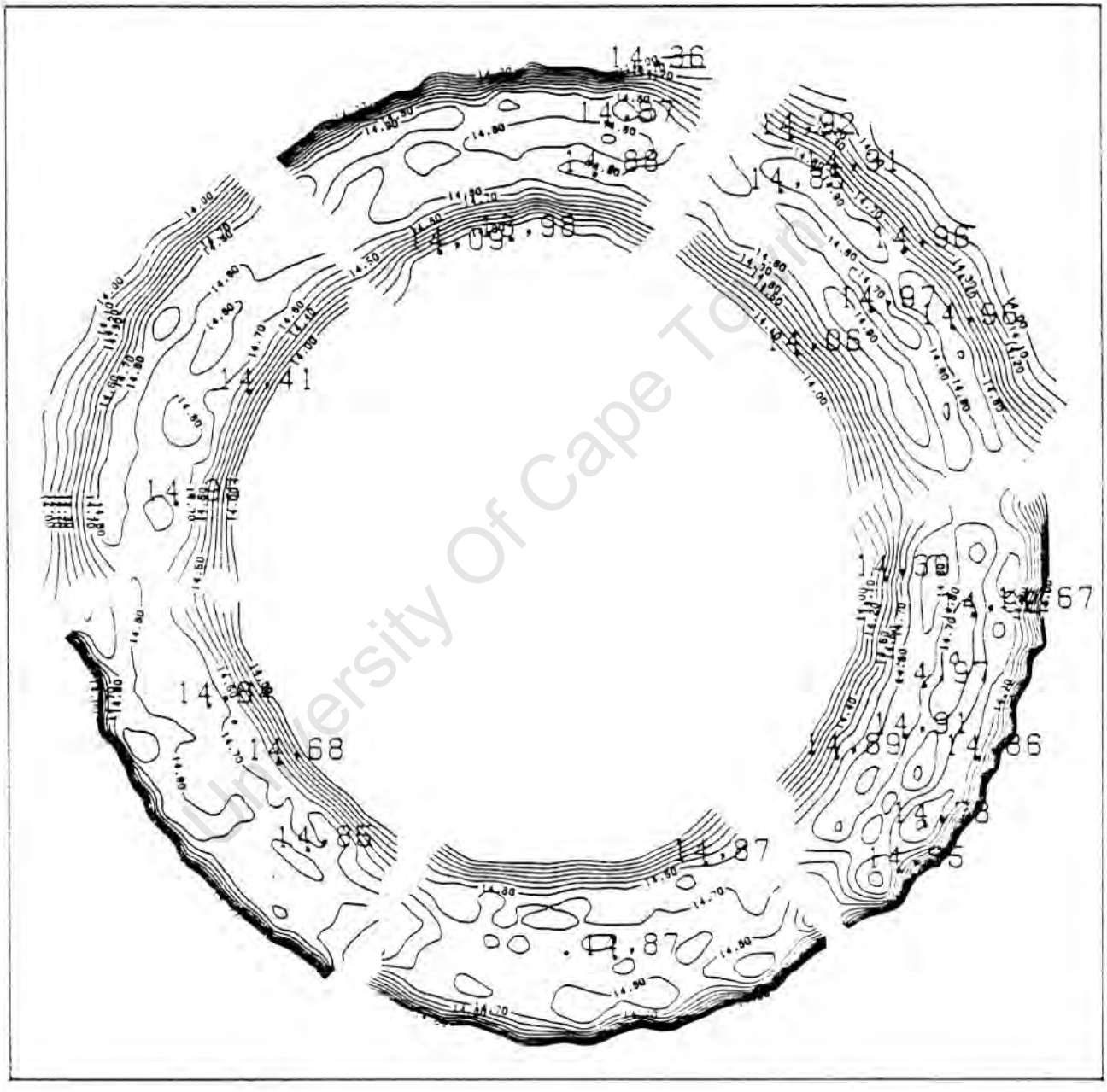

FIGURE 4.6 : Computer drawn contour diagram of the relief of a bit face measured with the reflex microscope showing the spot heights of the exposed stone above an arbitrary datum

4.11 DIGITAL IMAGE ANALYSIS

The measurement of the average bit face area to be used in the calculation of bit pressure from load data and the measurement of the diamond distribution within the bit matrix were both carried out using a digital analyser and a program written for its routine operation by Mrs V. Frith (1983). The equipment consists of a digitising tablet connected to a Tectronics computer with a disc drive and printer. The bit face area was measured by digitising the perimeters of photographic images of the pads of sixteen drill bits and calculating the average area using all 96 pads. The diamond distribution in the matrix was determined using the same program but measuring the lineal intercept length of the photographic images of the diamonds exposed in sections of impregnated pads prepared and polished at Boart Research Centre. The frequency percent distribution of distances between individual stones was used as a measurement of the distribution of the stones themselves.

4.12 COMPRESSIVE STRENGTH TESTS OF DIAMONDS AND TEST MATERIALS

Compressive strength tests were carried out on individual diamonds and on selected rocks and minerals. The diamonds, selected from 40/50 mesh grit, were well formed unworn stones with at least two well developed parallel faces. The relevant face areas of each stone were measured under the optical stereo microscope and then the diamond was carefully transferred to the compression testing machine. The two cylindrical anvils were of synthetic single crystal corundum, each ground with one flat end face polished using an Ultra-Tec precision lapidary machine. The diamond was compressed to failure between these polished faces. Fig. 4.7 illustrates the loading arrangement with the lower anvil mounted on a ball bearing free to rotate in a cup to accommodate any non-parallelism of the diamond faces.

FIGURE 4.7 : A photograph of the supports and corundum anvils used in the compressive strength tests of single diamond crystals (photographed by Mr B. Greeves)

The relative compressive strengths of selected rocks and minerals were measured by testing cores recovered from drilling tests. These were trimmed by diamond grinding to have two parallel flat end faces and were compressed to failure in uniaxial compression in an Instron machine.

4.13 RELATIVE ABRASION RESISTANCE TESTS

Selected rocks and minerals were subjected to abrasion tests on a pin and belt rig which has been described by Noel (1981). The test

consisted of loading a prepared core vertically with a 5 kgf weight so that the prepared specimen face rested on a supported commercial abrasive belt charged with 100 mesh silicon carbide grit. The belt was run at a speed of 0,03 ms^{-1} for three runs each of 1,22 m with the specimen moving across the belt on a screw feed so it continuously encountered fresh abrasive. The mass of the specimen was determined to five decimal places before and after each test-run and the loss due to abrasion calculated from the average mass loss for the three runs. Relative abrasion resistance was calculated by dividing the mass loss for each specimen by the value of mass lost for single crystal quartz which was the most resistant material tested.

4.14 REPRODUCIBILITY

The reproducibility of the drilling test results was determined with two independent series of tests. The first series consisted of twelve consecutive tests under nominally identical conditions drilled at set thrust, to test the accuracy of the measured drilling variables. The second series comprised the results of six tests drilled under nominally similar conditions at set rate of advance, and spaced over two months of testing, to determine the long term reproducibility.

4.14.1 Reproducibility Tests at Set Thrust

The following test conditions were used for the twelve reproducibility tests at set thrust:

Bit - Cu/Sn 80/20 matrix, 40/50 mesh diamond, concentration 30, SDA 100 grit
Rotational velocity - 3500 rpm (about 4 ms^{-1} peripheral bit speed)
Bit pressure - 6 MPa
Rock type - norite
Test length - 6 runs (0,5 to 0,6 m)

Four bits were used, with three tests drilled with each. The fresh bits were opened by drilling in sandstone to remove more than 0,5 mm of impregnation. They were standardised between tests by drilling 4 holes, sufficient to remove at least another

0,34 mm of matrix to expose fresh stones. These tests (TESTS 32 to 43 inclusive) were designed to fall in the zone of effective, quasi-stable drilling (Mode 2) in norite with the given bit formulation. One test (TEST 42) displayed dulling behaviour (Mode 1) with a steadily decreasing penetration rate and low bit torque values indicating a poor couple between the bit and the rock.

4.14.2 Reproducibility Tests at Set Rate of Advance

The six drilling tests (TESTS 78, 79, 86, 87, 94, 95) at a set rate of advance of 0,044 mm/rev were drilled in norite using the standard bit formulation. These tests varied in length but were all longer than 1 m. As they were drilled at a set rate of advance comparison between their results is valid.

4.14.3 Calculation of Percentage Error

The formula used for the calculation of percentage error was the conventional one for determining the error at the 90% confidence level associated with a single test.

$$\% \text{ ERROR } 90\% \text{ level} = 165s/VTI$$

where s = sample standard deviation
$N = 1$ in the case of a single test
$\bar{x}$ = sample mean

The percentage error calculated in this way applied strictly speaking only to a single test drilled under conditions identical to those used to obtain the reproducibility sample. Since these tests were designed to fall within the quasi-stable Mode 2 region of operation it was expected that single tests outside this region would have a greater associated error. However, since it was stable behaviour that was of greatest interest it was more desirable to determine the expected error in that region than to do the much larger number of tests necessary to establish the intrinsically larger error associated with less stable conditions.

were read by the computer and stored in a data file on tape. The bit matrix relief was measured by sighting 1000 points, more or less evenly spaced over the bit face. The elevation and lateral position of individual points could be determined to within 10 microns.

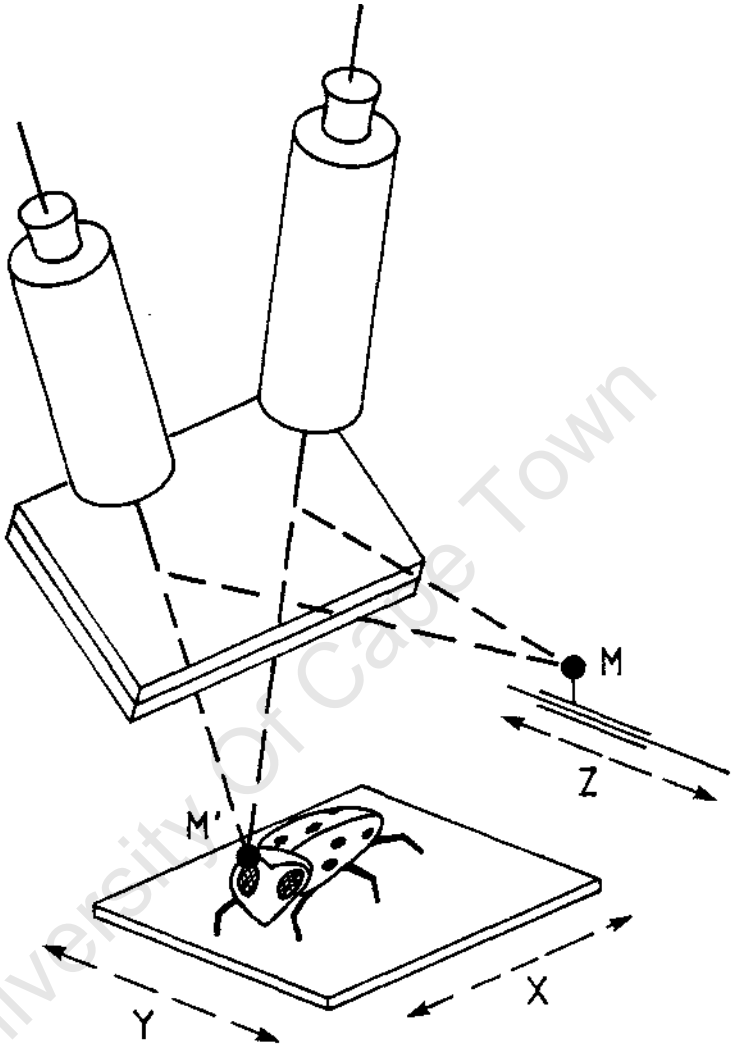

FIGURE 4.5 : A diagram illustrating the principle of the reflex microscope (after Scott 1981)

The position data recorded on tape was transferred to the Sperry 1100 and after being subject to some routine editing was processed by the SACLANT gridder and contourer programs to produce contour plots of the matrix with any required contour interval and with the diamond points plotted as spot heights. Fig. 4.6 is an example. The protrusion of each stone above the adjacent matrix was estimated from these plots by the difference between the spot height for that stone and the matrix elevation interpolated from neighbouring contours. The punch-through disc relief plots had of course no spot heights.

The results of the reproducibility tests are summarised in Table 4.3. The results for the set thrust test series are presented twice with the values from TEST 42 excluded from the calculations of the second set of results. The errors associated with the drilling variables and detritus size distribution analysis for this second set of calculations were not higher than 15%. The errors associated with the bit characteristics and wear behaviour were much higher. The third set of results, derived from the selected set rate of advance tests had greater associated errors for all the drilling variables except mean bit torque. However, these were still not higher than 25%.

TABLE 4.3 : Results of the reproducibility tests (see footnote)

	SET THRUST SERIES (n=12)		SET THRUST SERIES (n=11) EXCLUDING TEST 42		SET RATE OF ADVANCE SERIES (n=6)	
	$\bar{x}$ S	% ERROR	$\bar{x}$ S	% ERROR	$\bar{x}$ S	% ERROR
Mean Power Output (W)	816 ± 102	21	840 ± 62	12	445 ± 45	17
Mean Bit Pressure (MPa)	6,19 ± 0,09	2	6,20 ± 0,08	2	4,21 ± 0,42	16
Mean Bit Speed (ms^{-1})	3,87 ± 0,08	3	3,86 ± 0,09	4	3,84 ± 0,29	16
Mean Bit Torque (Nm)	2,13 ± 0,24	19	2,18 ± 0,17	13	1,20 ± 0,06	8
Average Advance Per Rev (mm/rev)	0,058 ± 0,08	23	0,060 ± 0,005	14	0,046 ± 0,006	22
Average Specific Energy [W] ($MJ \cdot m^{-3}$)	1145 ± 78	11	1135 ± 74	11	799 ± 107	22
Average Specific Energy [T] ($MJ \cdot m^{-3}$)	1156 ± 91	13	1138 ± 69	10	830 ± 124	25
Specific Bit Wear (mm/m)	0,738 ± 0,38	85	0,78 ± 0,37	78	0,21 ± 0,07	55
Net Bit Mass Loss (g)	0,373 ± 0,13	58	0,396 ± 0,110	46	0,16 ± 0,05	52
Diamond Wear Type % : 0	16 ± 5	52	16 ± 5	52	25 ± 5	33
1	10 ± 5	83	9 ± 3	62	22 ± 3	23
2	31 ± 3	43	32 ± 7	36	21 ± 4	31
3	40 ± 4	17	40 ± 4	17	32 ± 4	21
4	4 ± 2	83	3 ± 2	77	1 ± 1	165
Total Count	128 ± 12	15	127 ± 12	16	129 ± 10	13
Detritus: Mean	3,16 ± 0,11	6	3,14 ± 0,10	5	3,06 ± 0,04	2
S.D.	0,56 ± 0,05	15	0,56 ± 0,05	15	0,51 ± 0,05	16
% MUD	-	-	-	-	79 ± 2	4

NOTE: Throughout this thesis the quantities and errors have not been rounded to their appropriate accuracy

The errors associated with the detritus size distribution analyses were comparable with those of the set thrust tests. The bit wear and performance errors were high but mostly lower than those associated with the set thrust tests. The diamond wear figures indicated that the set thrust series of tests (excluding TEST 42) drilled with Mode 2 behaviour - with Type 2 diamond wear predominant over Type 1 - but that the set rate of advance tests were borderline between Mode 1 and Mode 2, with a balance between Type 1 and Type 2 diamond wear.

The high variability associated with the measurement of average advance per revolution in the set rate of advance tests series was due to the way in which this value was calculated. All of the relevant tests were in fact conducted at a set rate of advance of 0,044 mm/rev set by the gearing of the drilling machine. However, the calculated penetration rate value was obtained by dividing the net penetration recorded by the LVDT, associated with a small but significant error, by the total number of revolutions calculated from the rotation meter output which has a significantly larger error associated with it. The average advance per revolution and both the average specific energy values suffered from the combination of errors associated with the measurement of the individual drilling variables used in calculating these computed variables.

CHAPTER 5

RESULTS

The results are presented in three sections, viz. the results of tests on the materials used in the experimental drilling, the results from the drilling tests, and the results of the ancillary tests which were aimed at clarifying aspects of the drilling behaviour.

5.1 RELATIVE ABRASION RESISTANCE AND UNCONFINED COMPRESSIVE STRENGTH OF TEST ROCK AND MINERALS

Relative abrasion resistance and unconfined compressive strength were determined using 30 mm lengths of 10 mm diameter core of all the materials drilled except single crystal calcite. The easy cleavage of calcite made core recovery impossible. Relative abrasion resistance was measured by dry abrasion of preground specimens under a load of 5 kgf sliding over a 100 mesh SiC belt for 3,66 m at a speed of 0,03 ms^{-1}. R.A.R. is defined as follows:

$$R.A.R. = \frac{\text{MASS LOSS OF QUARTZ}}{\text{MASS LOSS OF MATERIAL}}$$

The relative compressive strengths were determined in an Instron machine operating at a cross-head speed of 0,254 mm/min. The results are tabulated in Table 5.1 and ranked from highest relative abrasion resistance to lowest. The latter have the greatest associated variability. The R.A.R. values are very reproducible for the more abrasion resistant materials. The variability associated with the compressive strength values does not exceed 35%.

There is no direct correlation between compressive strength and relative abrasion resistance for all the materials. However, for the purposes of this work, the drilled materials were classified as having low, moderate or high drilling resistance according to Table 5.2.

TABLE 5.1 : Results of relative abrasion resistance and compressive strength tests

MATERIAL	MASS LOSS (g) (n = 3)	R.A.R.	MEAN LOAD (kgf) (n = 4)	COMPRESSIVE STRENGTH (MPa) (n = 4)
Single Crystal Quartz	0,0321±0,0007	1±0,001	2880± 962	360±120
Jaspilite	0,0397±0,0017	0,809±0,002	3918±1060	489±132
Granite	0,0564±0,0034	0,569±0,003	1491± 381	186± 48
Dark Norite	0,0683±0,0019	0,470±0,002	2297± 280	287± 35
Light Norite	0,0729±0,0021	0,440±0,002	1676± 223	209± 28
Quartzite	0,0736±0,0035	0,436±0,004	1998± 699	250± 87
Syenite	0,0802±0,0061	0,400±0,006	1413± 214	176± 27
Single Crystal Felspar	0,0813±0,0029	0,395±0,003	1755± 823	219±103
Sandstone	0,8865±0,0685	0,036±0,069	332± 48	41± 6
Marble	1,1200±0,0387	0,029±0,039	1069± 433	138± 36

TABLE 5.2 : Classification of drilling resistance

R.A.R.	COMPRESSIVE STRENGTH	DRILLING RESISTANCE
<0,1	<150 MPa	Low
0,1 - 0,7	150 - 300 MPa	Moderate
>0,7	>300 MPa	High

5.2 COMPRESSIVE STRENGTH TESTS ON DIAMONDS

Diamonds released from worn bits by boiling in aqua regia were examihed under the optical stereo microscope. Well formed, unworn stones were selected for compression testing between polished single crystal corundum anvils. The crystals displayed the clear cubo-octahedral habit of SDA 100 synthetic diamonds with crystallographically orientated radial arms of inclusions (Fig. 5.1). Measurement of the cube face area of the crystals enabled the pressure at failure load to be calculated. Each

test damaged the laboriously cut and polished anvils and only three tests were possible. Two of these were successful. The third was rejected because the anvils were too badly damaged to support the diamond properly. The mean peak load of the two successful tests was 77 kg t 13%, representing a failure stress of 4,44 GPa.

FIGURE 5.1 : Photograph of typical SDA 100 crystals showing cubo-octahedral habit and crystallographically orientated radial arms of inclusions of metallic flux. The yellowish colour is due to the high dissolved nitrogen content in these synthetic diamonds.

5.3 DIAMOND DISTRIBUTION IN THE BIT MATRIX

Eighteen polished sections from six standard microbits were received, two of which consisted of badly broken segments and were discarded. The remaining sixteen consisted of four vertical radial sections, six vertical transverse sections, and six horizontal sections parallel to the bit face. These sections were photographed using a stereo optical microscope. The enlarged prints were analysed with a semi-automatic digitiser using a computer program which calculated the frequency in

predetermined intervals of inter-diamond matrix lengths measured along linear traverses (Frith 1983). The plot of the distribution of the distances between the stones for all the sections represents the distribution of diamonds three dimensionally in the bit matrix and is similar to the negative exponential distribution to be expected if the distribution of the diamonds is random (Fig. 5.2). The average inter-diamond spacing was 2,08 mm and should be a function of the diamond size and concentration, not of the distribution. A x^2 test indicated that there was no significant difference between the observed inter-diamond spacing and a calculated negative exponential distribution with a mean value of 2,08 mm. It is concluded that the diamonds in these six bits tested were essentially randomly distributed.

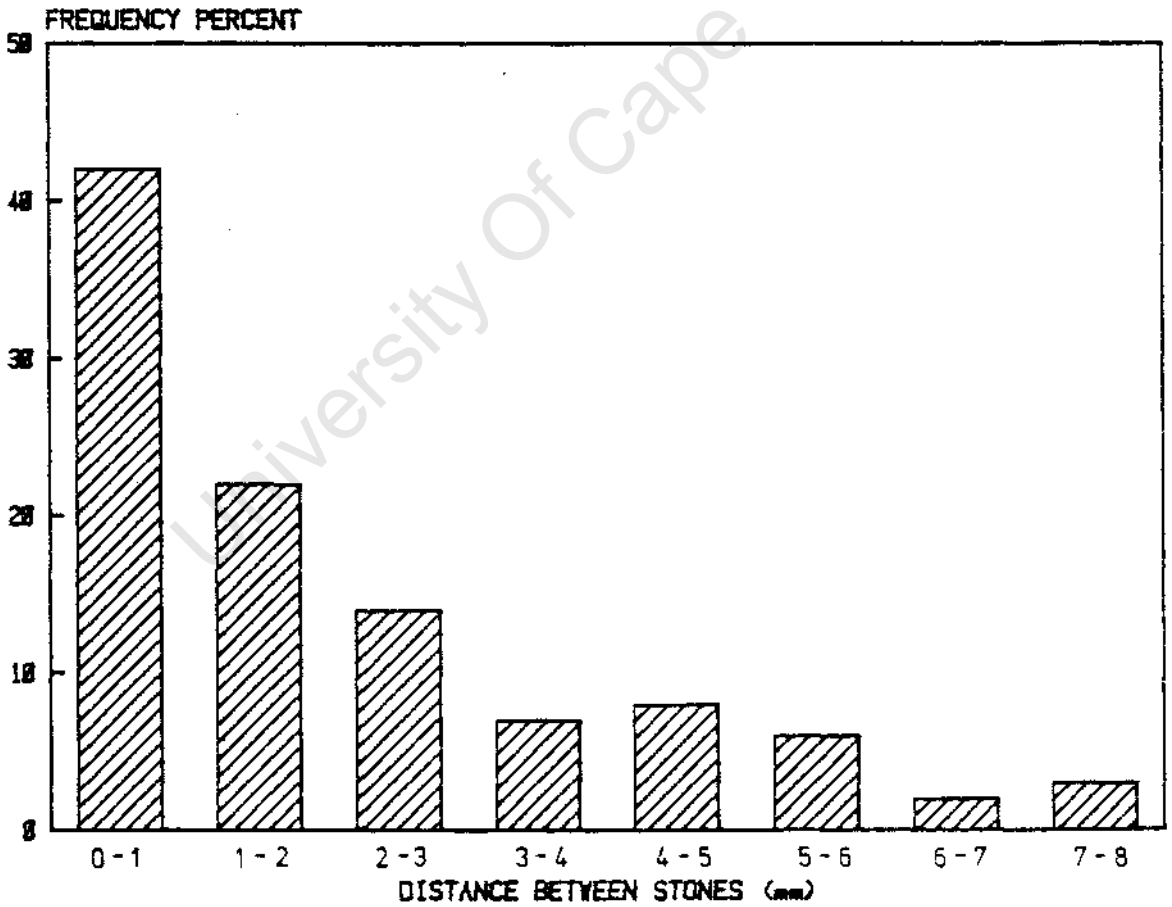

FIGURE 5.2 : Distribution of inter-diamond spacing in the bit matrix of six standard microbits

5.4 DRILLING TESTS

The actual drilling tests were carried out either at set rate advance or under set thrust. The test conditions are summarised in Table 5.3. Unless otherwise specified the rotational velocity was nominally 3500 rpm and the water flushing rate was between 300 1/hr and 400 1/hr at a pressure of about 200 kPa. Obviously in such a test series mishaps can occur. A few spurious results had to be eliminated from the result plots. However, apparently negative results were occasionally informative in unexpected ways. These are discussed when appropriate. The results of all the drilling tests are tabulated in Appendix 4.

TABLE 5.3 : Summary of drilling test conditions

DRILLING PARAMETER	MATERIAL	DIAMOND MESH
Set Thrust	Norite	40/50
Set Rate of Advance	Norite	40/50
Set Rotational Speed	Norite	40/50
Set Rate of Advance	Norite	Range
Set Thrust	Norite	Range
Set Rate of Advance	Quartzite	Range
Set Rate of Advance	Variety	40/50
Set Thrust	Variety	40/50

5.4.1 Tests in Norite at Set Thrust with Standard Bits

Twenty tests (TESTS 53-72) were drilled in norite with standard microbits (40/50 mesh, SDA 100, concentration 30 in a bronze matrix) at a nominal rotational velocity of 3500 rpm and at set thrusts producing bit pressures ranging from 2 MPa to 13 MPa. All the tests were either of 10 minutes duration or were stopped after drilling 16 holes (about 1,4 m) if this occurred in less than 10 minutes. Punch-through discs of rock for SEM were produced at four pressures ranging from 7 MPa to 13 MPa. After each test diamond wear type analysis of the worn bit and particle size distribution analysis of the drilling detritus were done. The tests were designed to evaluate the general performance of the drilling machine and to determine the response of norite to drilling under set thrust conditions. The upper load limit of the

drilling machine in this configuration was reached at about 13 MPa bit pressure when the machined stalled and the motor cut out due to overloading. Consequently the results of the test drilled at this pressure are less valid. The full set of results is presented in Figs. 5.3 to 5.17.

Relationships Between the Drilling Variables

There was a linear relationship between the required power output and the bit pressure from 2 MPa to 12 MPa (Fig. 5.3) with a least squares linear best fit of y = 184,58 x - 261,22 (r = 0,99). There was also a linear relationship between the bit pressure and the generated torque (Fig. 5.4) with a least squares best fit line of y = 0,47 x - 0,64 (r = 0,99) excluding the result for the test at 13 MPa.

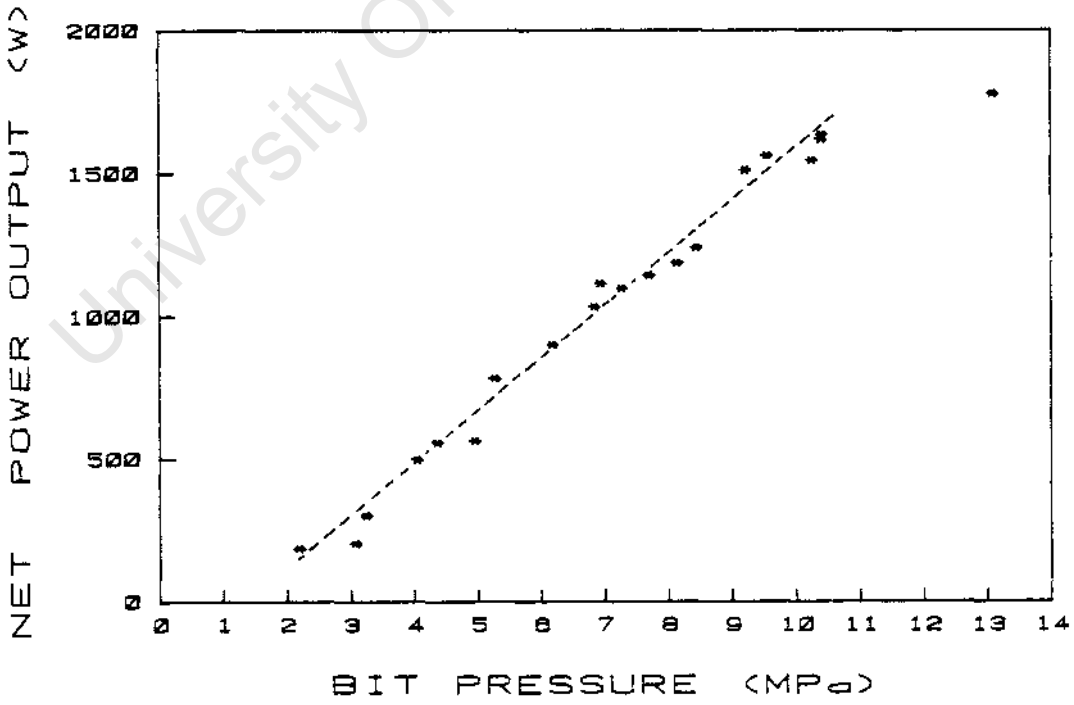

FIGURE 5.3 : Plot showing the linear relationship between net power consumption and bit pressure up to the stalling point for tests drilled in norite at set thrust

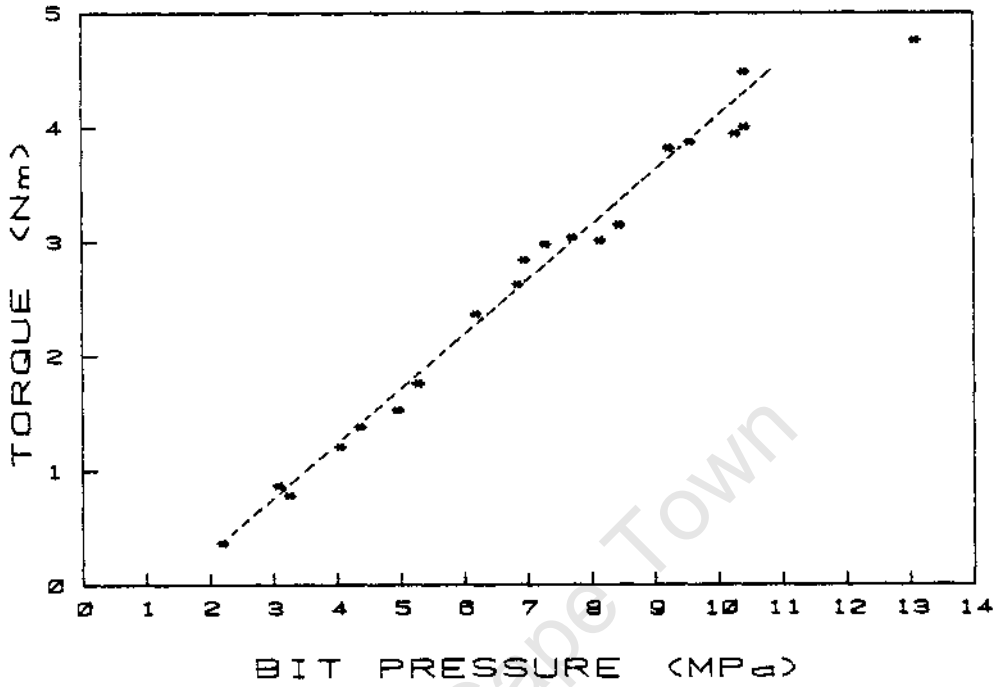

FIGURE 5.4 : Plot showing the linear relationship between torque and bit pressure up to the stalling point for tests drilled in norite at set thrust

The drilling machine was set at a nominal rotational speed of 3500 rpm for these tests but above 6 MPa bit pressure there was a trend of decreasing linear bit speed (or peripheral speed) with increasing bit pressure (Fig. 5.5). Owing to this tendency to stall the measured rotational velocities were used in calculating the subsequent results to avoid the distortion introduced by assuming a constant velocity. The advance per revolution increased steadily with increasing bit pressure between 2 MPa and 5 MPa. At higher bit pressure the penetration rate was constant because of the drop in speed and assumed an average value of 0,11 mm/rev ± 12,5% up to the load limit of the machine. A minimum bit pressure in the region of 2 MPa was required to produce any penetration at all (see Fig. 5.6).

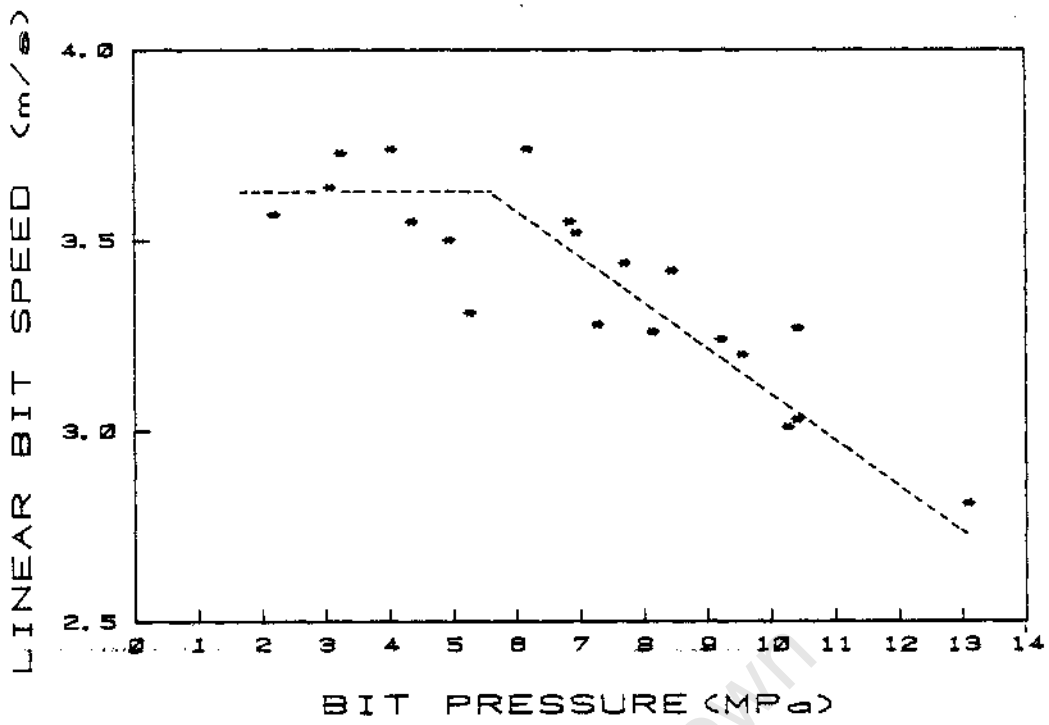

FIGURE 5.5 : Plot showing the linear decrease in rotational velocity with increasing bit pressure above 5 MPa for tests drilled in norite at set thrust

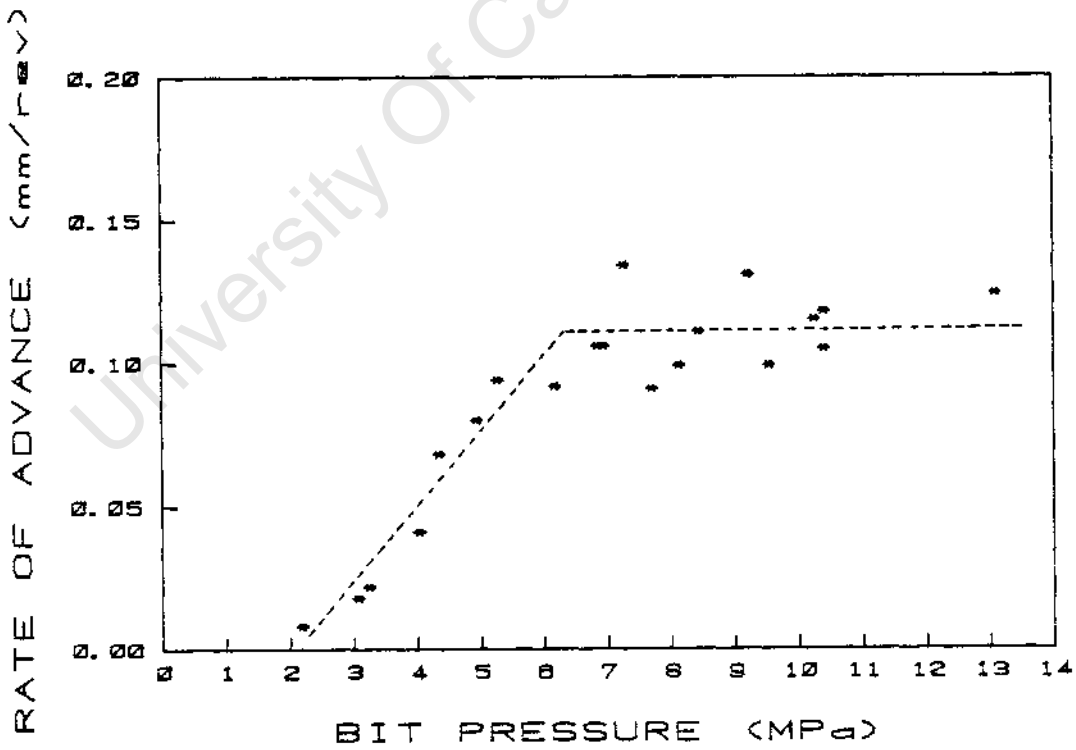

FIGURE 5.6 : Plot of results of tests drilled in norite at set thrust showing a linear increase in rate of advance with increasing bit pressure up to 5 MPa and a uniform rate of advance at higher bit pressure up to stalling point

The specific energy results calculated independently from the power consumption and the generated torque both had similar values and trends relative to the bit pressure (Figs. 5.7 & 5.8). Both sets of results had an optimal minimum of about 600 MJm^{-3} at 5 MPa and rose steeply at lower value of bit pressure to a theoretically infinite value below the threshold of penetration at 2 MPa. At the bit pressures above the optimum the specific energy rose more gently and steadily up to the load limit of the machine.

Bit Wear and Diamond Wear

Bit wear was recorded as linear bit wear and bit mass loss. The linear bit wear results were normalised to 10 minutes duration. Three tests drilled at steady penetration rates but stopped prematurely due to partial bit failure through excessive wear of the inner diameter. The normalised results fell into two groups (see Fig. 5.9). The tests drilled at lower bit pressures with decreasing penetration rates had low bit wear values. At higher bit pressures much higher linear bit wear values were associated with steady penetration rates but decreased rotational velocity. The, same two groups were evident in the bit mass loss data, normalised to 1 m drilling distance (see Fig. 5.10). The scatter was greater in the bit wear results of the group of tests drilled at higher bit pressures, indicating less direct dependency of bit wear on thrust in this region of stable drilling.

The results suggest a significant transition in the region of 5 MPa bit pressure. Inspection of the preliminary computer output for individual tests showed that the transition from diminishing penetration rate at constant thrust (Mode 1 behaviour) to stable drilling at constant penetration rate (Mode 2 behaviour) took place around 5 MPa. This was supported by the analysis of diamond wear counts. Above 5 MPa microfractured stones, Type 2 wear, predominated over stones exhibiting the wear flats and smooth rounding of Type 1 wear (Fig. 5.11). The loss of stones by pull-out (Type 3 wear), the exposure of fresh stones (Type 0 wear), and wear by macrofracture (Type 4 wear) were each nearly constant over all pressures with their values averaging 40%, 20% and 2% respectively (Fig. 5.12).

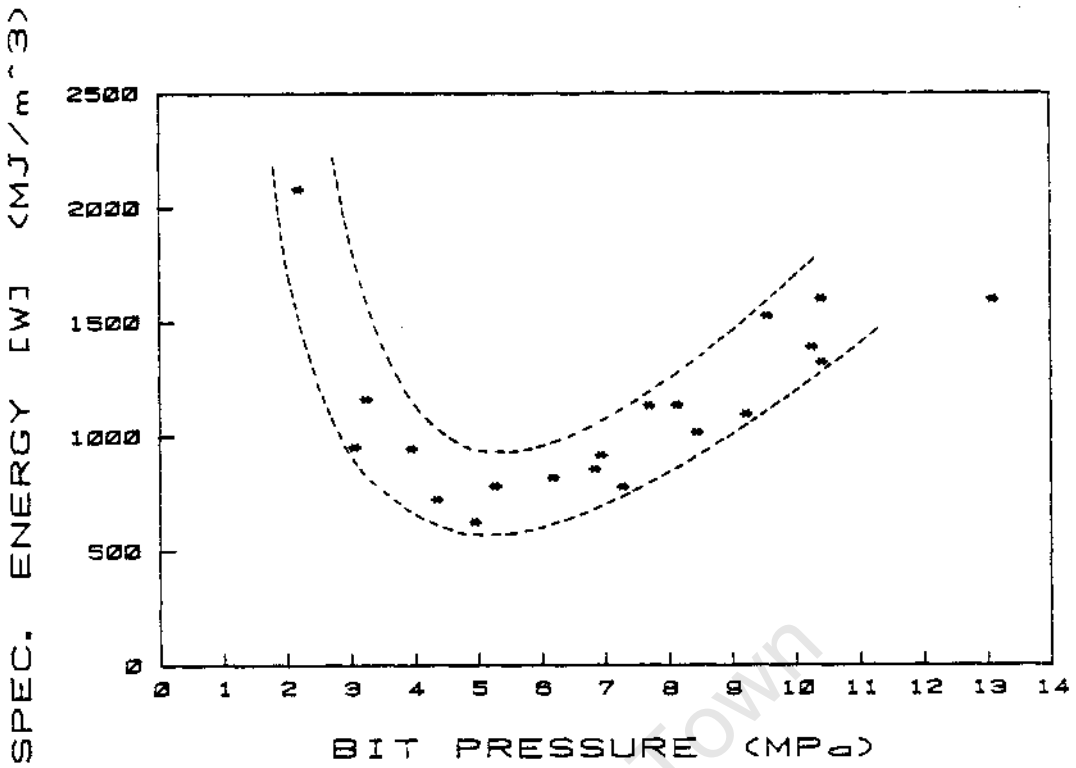

FIGURE 5.7 : Plot of specific energy calculated from the wattmeter output against bit pressure for tests in norite at set thrust, indicating a minimum value of specific energy at about 5 MPa bit pressure

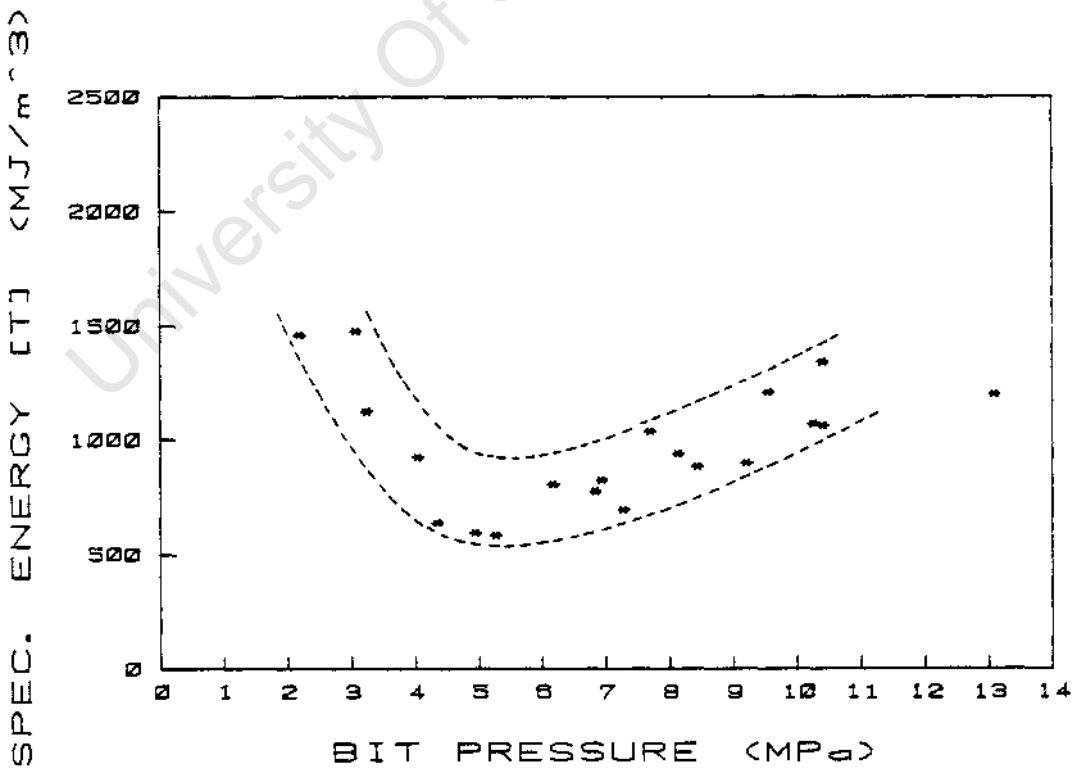

FIGURE 5.8 : Plot of specific energy calculated from the torquemeter output against bit pressure for tests in norite at set thrust indicating a minimum value of specific energy at about 5 MPa bit pressure

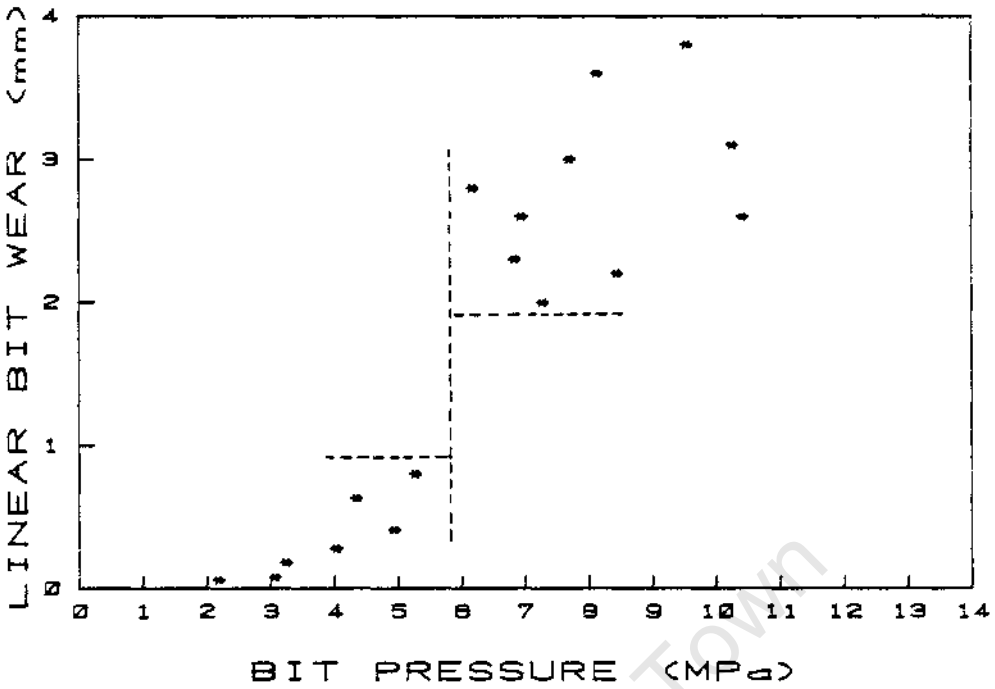

FIGURE 5.9 : Plot of linear bit wear against bit pressure for tests drilled in norite at set thrust, indicating two groups of results with a boundary between 5 MPa and 6 MPa bit pressure

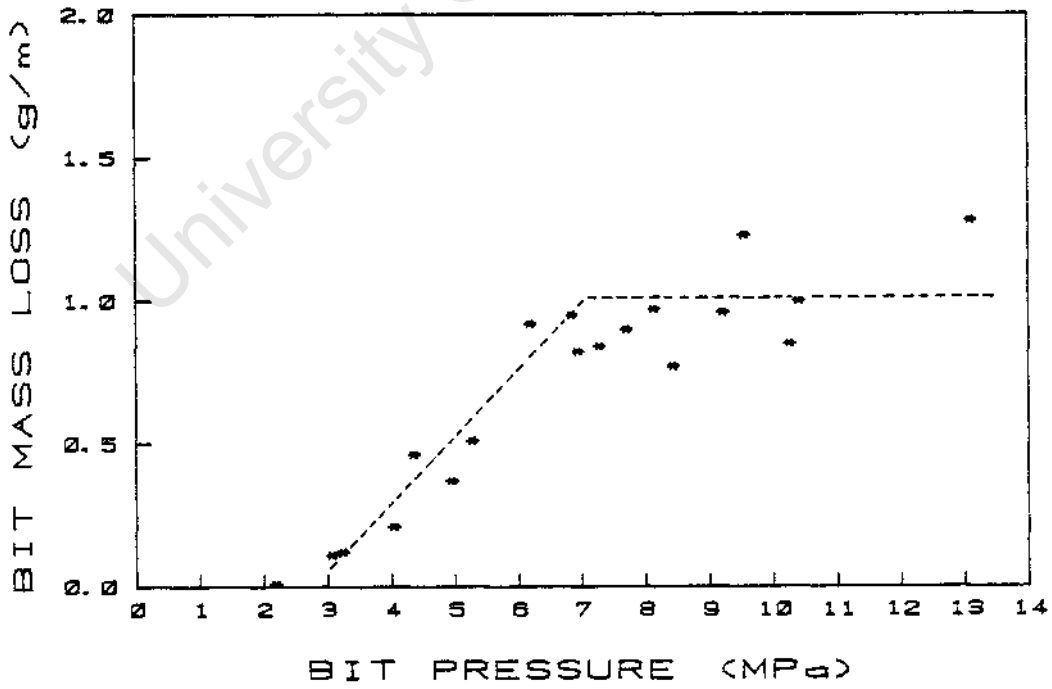

FIGURE 5.10 : Plot of results of tests drilled in norite at set thrust showing a linear increase in specific bit mass loss with increasing bit pressure up to between 5 MPa and 6 MPa and a more uniform but higher bit mass loss at higher bit pressures

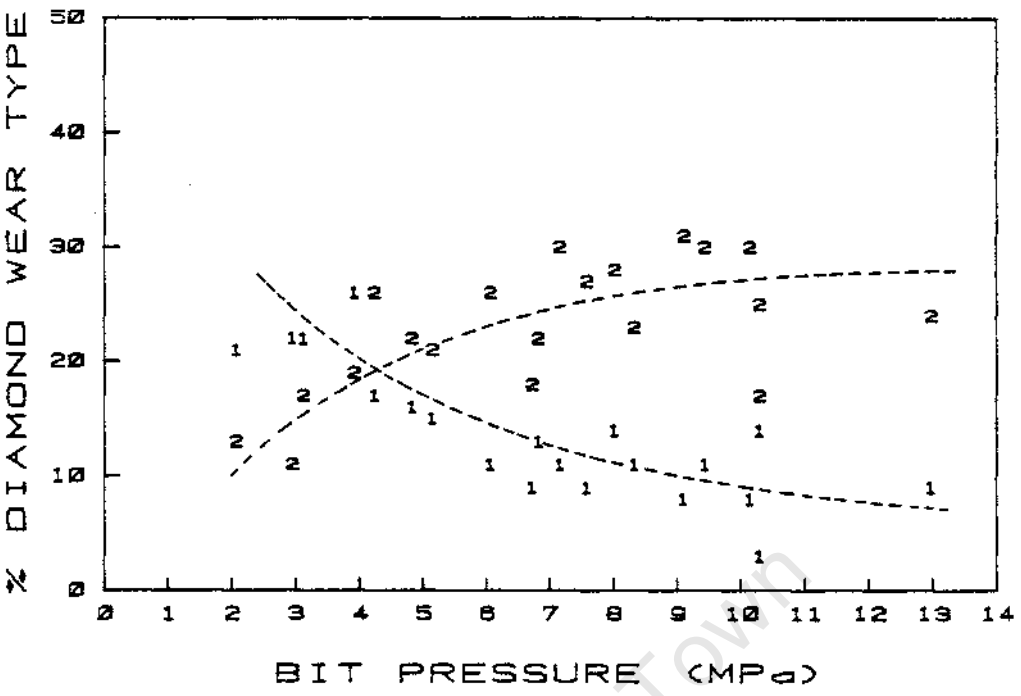

FIGURE 5.11 : Plot of diamond wear type percentage against bit pressure for tests drilled in norite at set thrust, showing the change in predominant wear type at about 5 MPa bit pressure

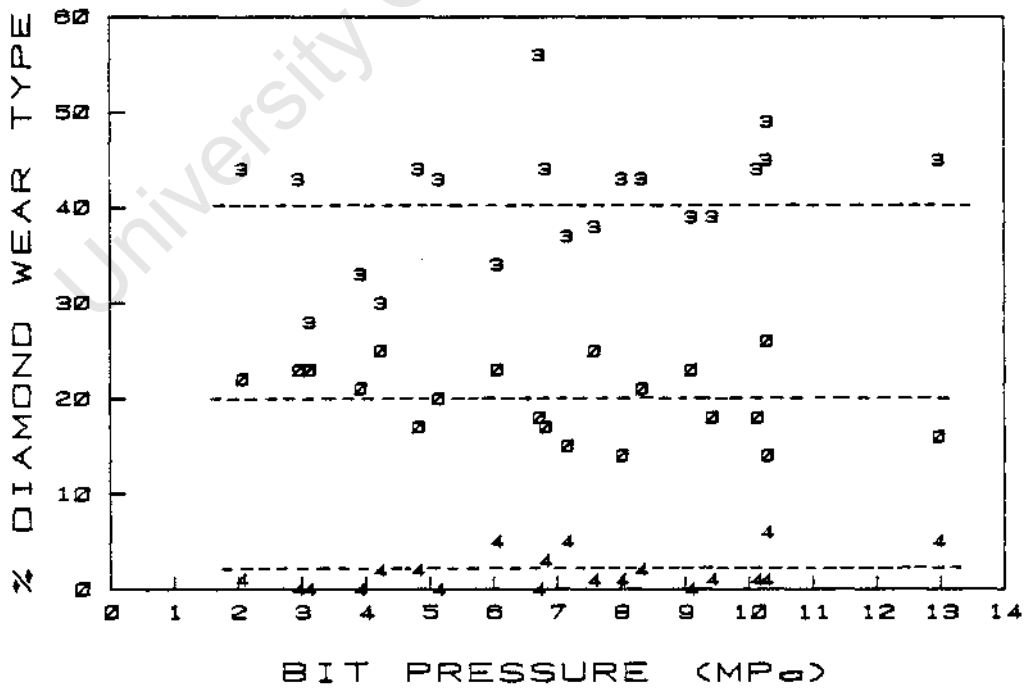

FIGURE 5.12 : Plot of diamond wear type percentages against bit pressure for tests drilled in norite at set thrust showing uniformity in percentages of Type 0, Type 3, and Type 4 wear at all bit pressures

TEST 67 was selected as an example of typical stable Mode 2 behaviour. The mean bit pressure of 5,26 MPa was optimal in terms of specific energy and was just above the threshold of Mode 2 behaviour. The preliminary plots of results and diamond wear counts reflected the stable drilling of the Mode 2 regime (see Fig. 5.13). The power required and the torque generated dropped slightly over the first 300 mm of drilling as the bit settled in and then they remained constant, as did the penetration rate. The advance per revolution fluctuated about an essentially constant average value of 0,1 mm/rev. Both the specific energy measurements remained stable and constant. The spikiness of some of the result plots was caused by stopping and restarting the machine between each test run. From the diamond wear record it can be seen that Type 2 wear predominated over Type 1 wear. In particular Type 2b wear - heavily microfractured stones - predominated over Type lb wear characterised by well developed wear flats.

The results of this test were typical of Mode 2 behaviour and will be contrasted with the results of typical Mode 1 behaviour presented in the next section. The bit used for TEST 67 was studied in the SEM and selected stones were photographed to illustrate the wear features (Fig. 5.14(a - e)).

The Type 0 wear example had slight rounding of the exposed edges but was otherwise unworn (Fig. 5.14(a)). Type 1 wear was characterised by the development of wear flats and the rounding of exposed points and edges. The example illustrated in Fig. 5.14(b) showed grooving parallel to the direction of rotation (horizontal) and crystallographically orientated incipient cleavage cracks across the exposed edge. Type 2 wear displayed by the example in Fig. 5.14(c) consisted of cleavage controlled microfracture which presented a multitude of small points to the rock surface. Type 3 wear consisted in the complete loss of a stone by pull-out (Fig. 5.14(d)). Type 4 wear was distinguished by conchoidal microfracture leading to the rapid breakdown of the stone until it was effectively flush with the matrix (Fig. 5.14(e)).

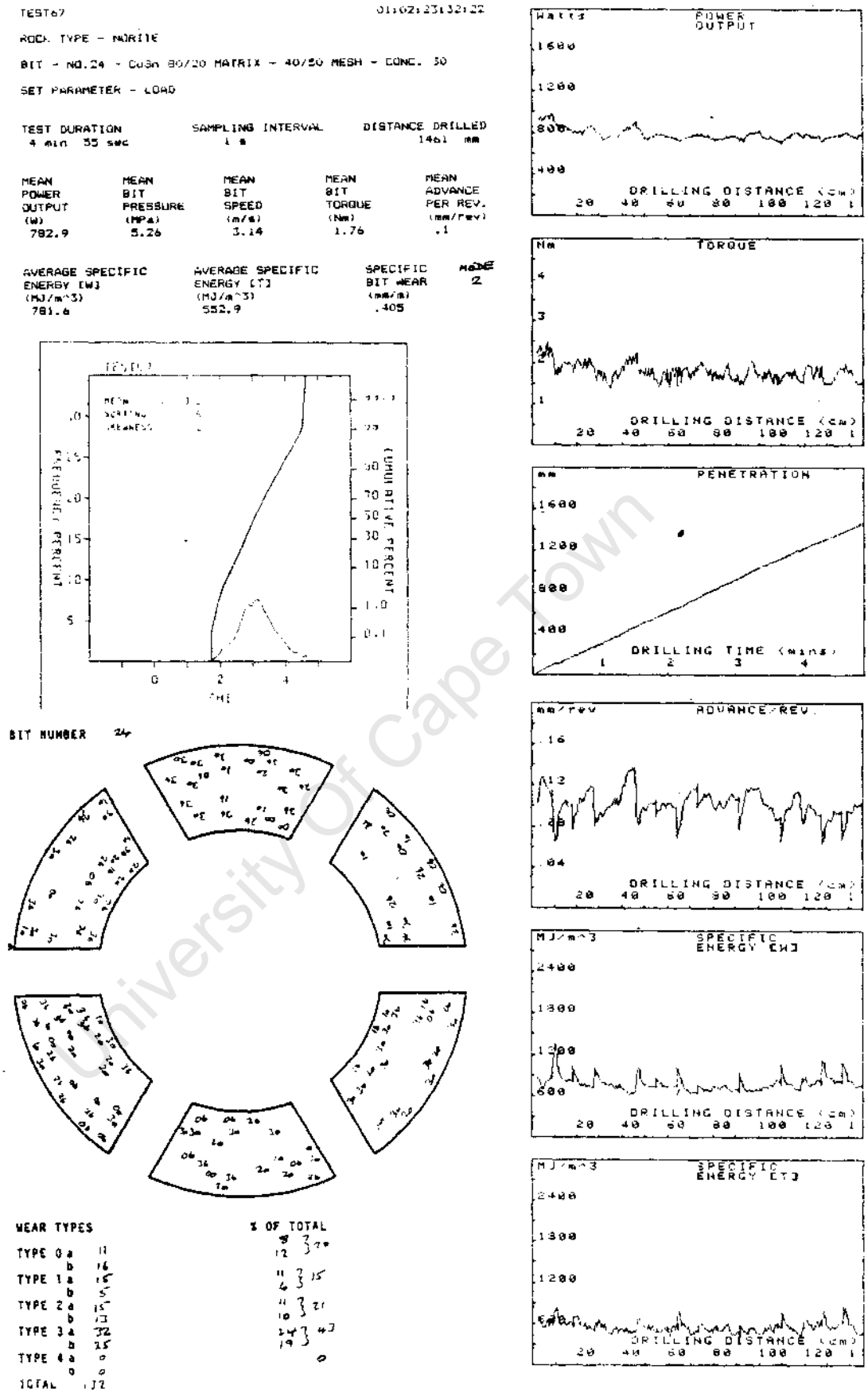

FIGURE 5.13 : Full graphical record of TEST 67, typical of mode 2 behaviour, with constant penetration rate and a predominance of Type 2 diamond wear over Type 1 wear

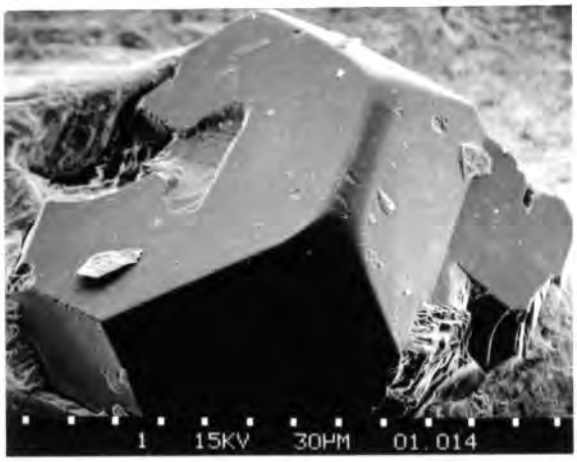

(a) : Type 0 wear - recently exposed stone showing minimal wear

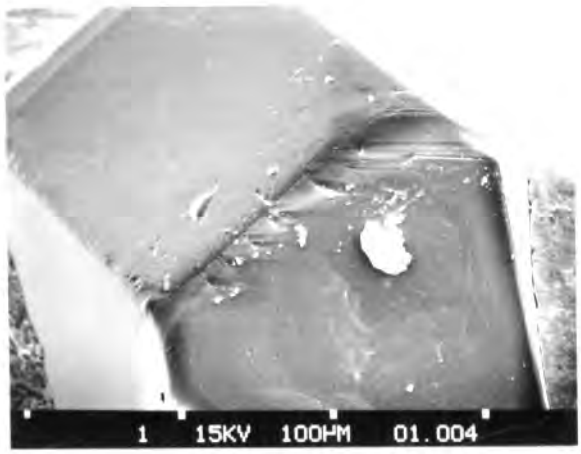

(b) : Type 1 wear - development of grooved wear flat and cleavage cracks on exposed diagonal edge

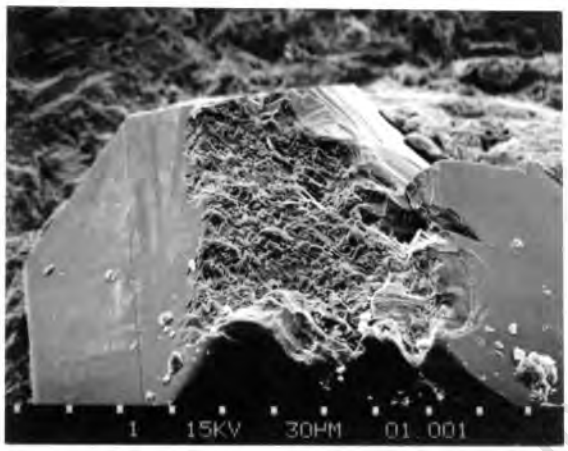

(c) : Type 2 wear - cleavage controlled microfracture

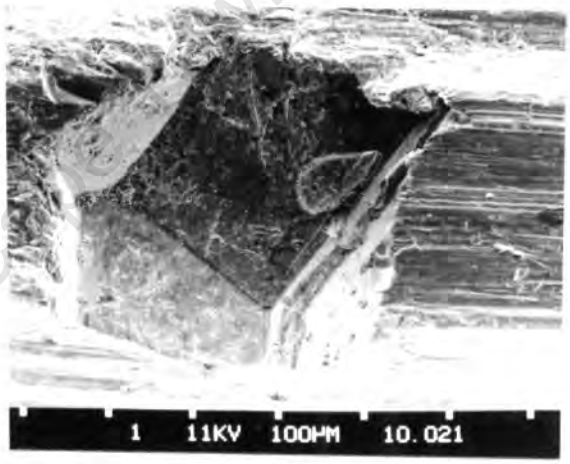

(d) : Type 3 wear - loss of stone by pull-out, leaving a hole

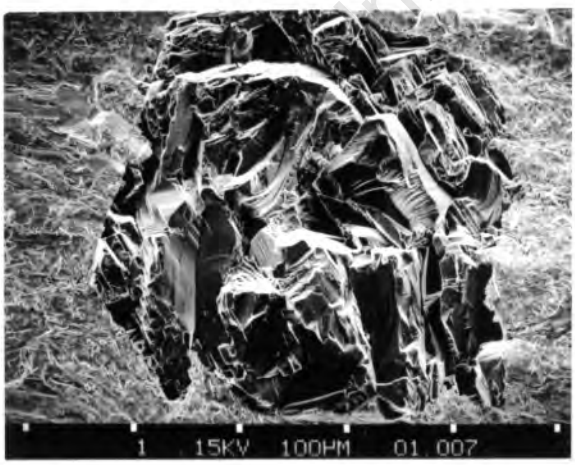

(e) : Type 4 wear - conchoidal macrofracture

FIGURE 5.14 : Selected examples of diamond wear from a bit drilled in norite at 5,26 MPa in Mode 2

Analysis of the Drilling Detritus and Drilling Tracks

The particle size distribution analysis of the drilling detritus showed no significant variation in mean particle size diameter, for the size fraction between 2 mm and 63 micron. The overall mean particle diameter in the 2 mm to 63 micron range was 3,123 ± 0,085 phi or about 0,115 mm ± 2,7% (Fig. 5.15). (The particle size distributions are plotted in units of phi to allow the standard deviations of the log-normal distributions to be plotted as symmetrical bars). There was a minimum in the percentage of particles finer than 63 micron at about 5,5 MPa (Fig. 5.16).

Discs of rock were punched through at the end of tests drilled at four bit pressures ranging from 7 MPa to 13 MPa and photographed in the SEM. The tracks left at the bottom of the holes looked similar for all the specimens. Norite is composed primarily of felspar and pyroxene both of which have well developed angular cleavage which dominated the appearance of the tracks (Fig. 5.17(a - d)). All of them showed the ubiquitous presence of what looked like plastic tracks in the norite. They were in fact mashed flakes composed of compacted (and in some instances sintered) rock flour smeared over a substrate of finely broken norite. These flakes tended to occupy the bottom of grooves caused by the passage of individual diamonds. Most of them were removed by the flushing during drilling or by the ultrasonic cleaning required to clear the fine particles that otherwise obscured the drilled rock surfaces. The angular felspar cleavage grains and the detached flakes were both conspicuous components of the drilling detritus. There was no observable change of scale of fracture of the constituent mineral grains in the detritus produced over the full range of bit pressures. This corroborated the results of the particle size distribution analysis of the coarse drilling detritus.

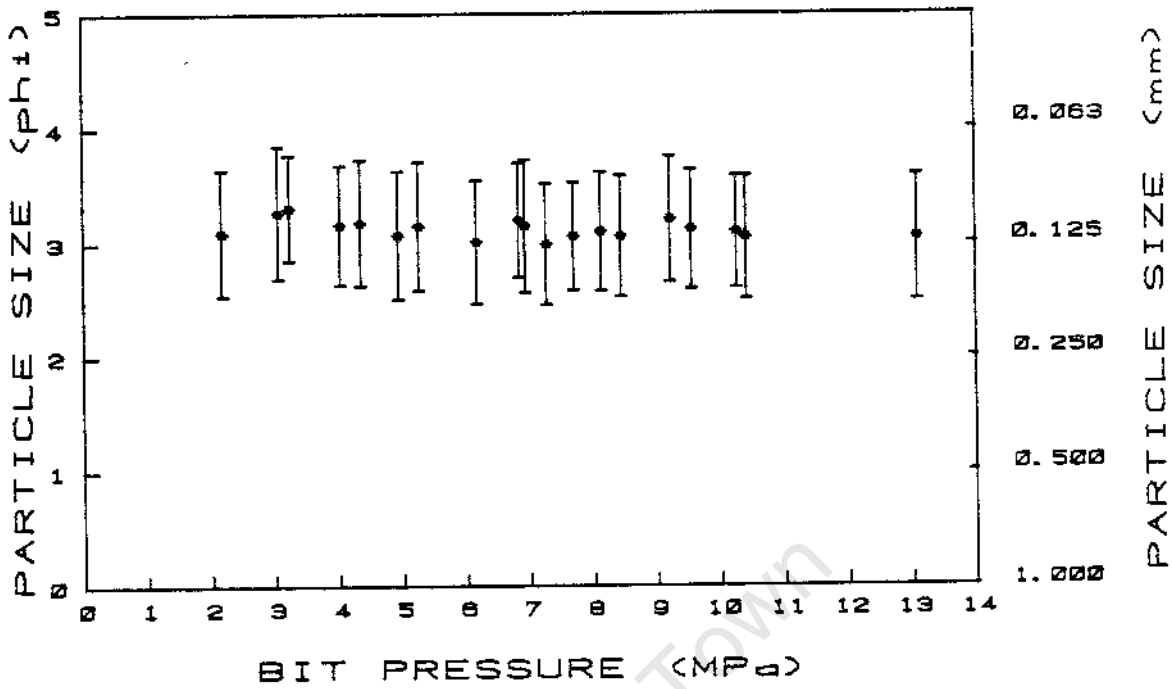

FIGURE 5.15 : Plot of particle size distribution of detritus between 2 mm and 0,063 mm against bit pressure for tests drilled in norite at set thrust (phi = -log2 diameter)

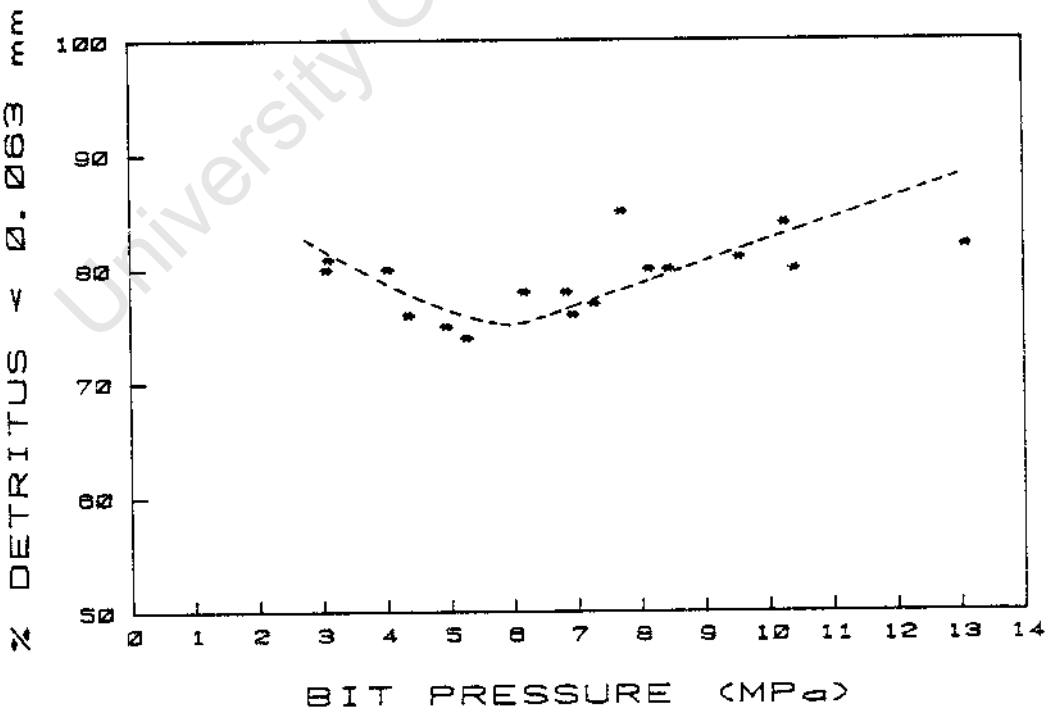

FIGURE 5.16 : Plot of percentage by mass of detritus under 0,063 mm in size against bit pressure for tests drilled in norite at set thrust, showing a minimum between 5 MPa and 6 MPa bit pressure

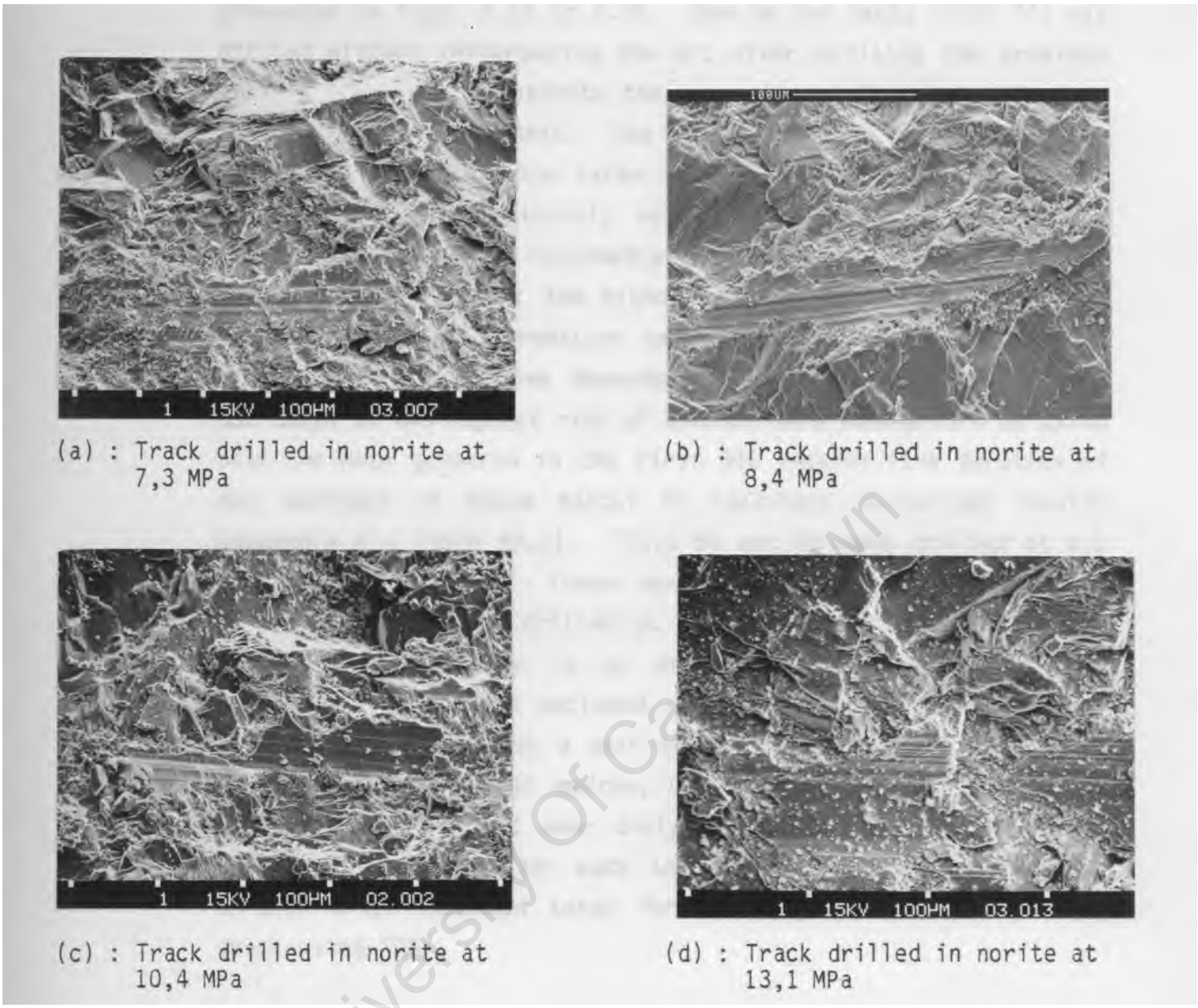

(a) : Track drilled in norite at 7,3 MPa

(b) : Track drilled in norite at 8,4 MPa

(c) : Track drilled in norite at 10,4 MPa

(d) : Track drilled in norite at 13,1 MPa

FIGURE 5.17: SEM of tracks drilled in norite at various set thrusts, showing similarity of appearance over full range of bit pressures corresponding to Mode 2 behaviour

5.4.2 Tests in Norite at Set Rate of Advance with Standard Bits

Twelve tests (TESTS 74 - 85) were drilled in norite with standard microbits at four set rates of advance ranging from 0,011 mm/rev to 0,1 mm/rev. This series of tests was aimed at evaluating the performance of the drilling machine and the response of norite to drilling under set rate of advance conditions. The results are

presented in Figs. 5.18 to 5.29. One of the tests (TEST 77) was drilled without resharpening the bit after drilling the previous test in order to demonstrate the persistence of Mode 1 behaviour over a double length test. The test lengths varied considerably because the tests at low rates of advance occupied the full 600 available sampling intervals before reaching 1 m of drilling length. The tests at intermediate set rates of advance were all over a metre long, but the highest rate of advance (0,1 mm/rev) caused stalling and premature termination of the test. Because Mode 1 behaviour is time dependent the results of all the tests but those at the highest rate of advance were standarised by using only the data gathered in the first 320 seconds (the duration of the shortest of these tests) to calculate normalised results (Appendix 5 : Table A5.1). TESTS 80 and 81 were drilled at 0,1 mm/rev and 3500 rpm. These were standardised to 200 seconds. TESTS 82 and 83 were drilled at reduced speeds of 2800 rpm and 2080 rpm respectively in an unsuccessful attempt to prevent stalling and have been excluded. However each test condition is represented by at least a pair of results. The geared rates of advance used were 0,011 mm/rev, 0,033 mm/rev, 0,044 mm/rev, and 0,10 mm/rev. Diamond wear analysis and detrital particle size analysis were done after each test and rock discs were punched through after selected tests for investigation of the drilling track using SEM.

Relationships Between the Drilling Variables

The standarised results of the nine comparable tests drilled at set rates of advance were plotted to illustrate the relationships between the drilling variables. There was a linear relationship between rate of advance and the net power consumption (Fig. 5.18) with a least squares best fit line of $y = 8980\ x + 13$ ($r = 1,00$). The relationship between rate of advance and bit pressure was also linear up to stalling conditions (Fig. 5.19) with a least squares linear regression line of $y = 42,1\ x + 1,7$ ($r = 0,98$). The intercept of the regression line represented an extrapolated threshold bit pressure of 1,7 MPa required to produce any penetration. By comparison with Fig. 5.6 it can be seen that the

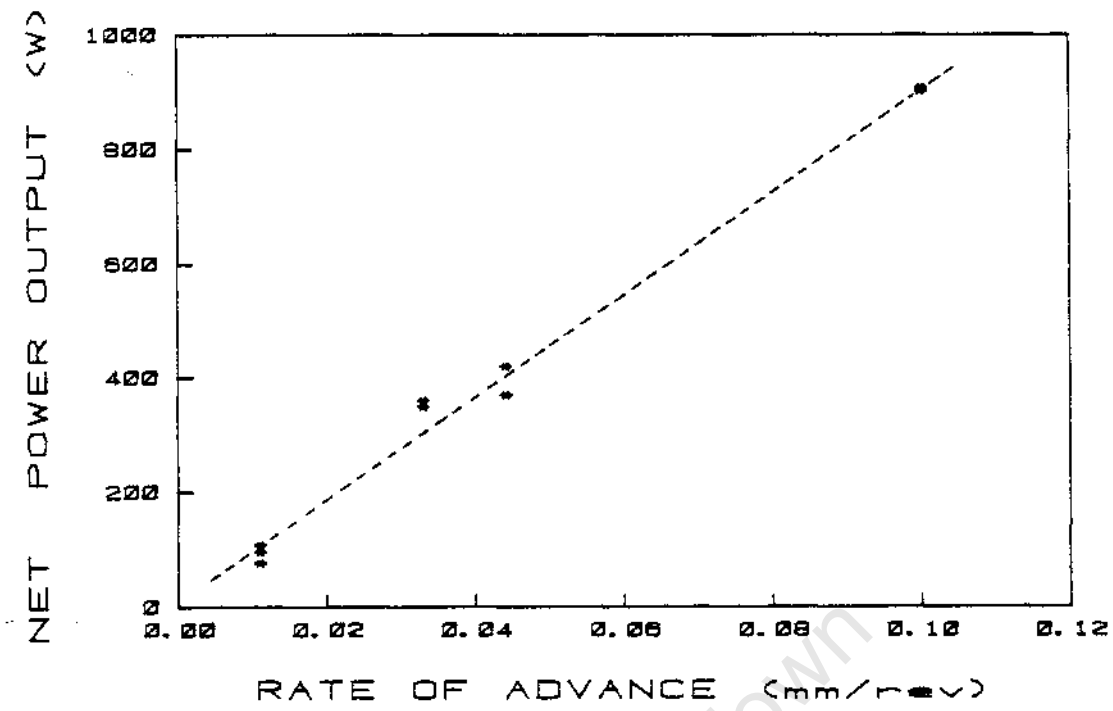

FIGURE 5.18 : Plot showing the linear relationship between net power consumption and rate of advance for tests drilled in norite at set rate of advance

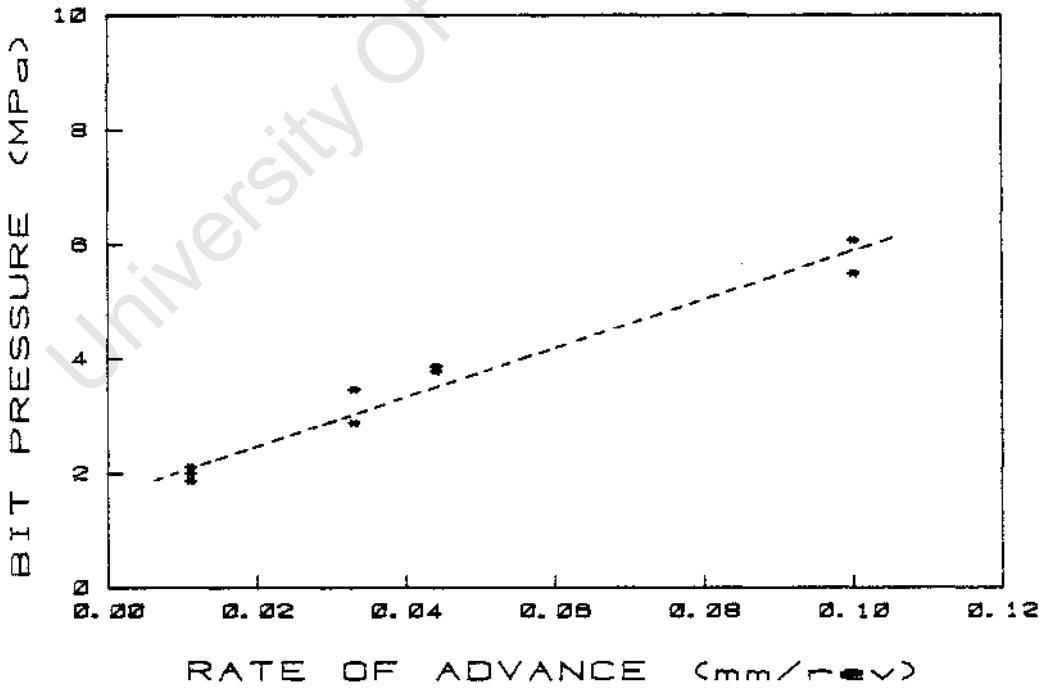

FIGURE 5.19 : Plot showing the linear relationship between the mean bit pressure and the rate of advance up to the stalling point for tests drilled in norite at set rate of advance

linear trends of power consumption below 6 MPa bit pressure are largely coincident. When attempting to drill at set rate of advance higher than 0,1 mm/rev to produce mean bit pressures in excess of 6 MPa, the drilling machine stalled.

The linear relationship between rate of advance and generated torque (Fig. 5.20) had a least squares best fit of $y = 19,2 x + 0,29$ ($r = 0,99$), suggesting a threshold torque of 0,29 Nm required to overcome the friction between the rock and the bit. The relationships of the two different sets of specific energy results with the rate of advance were similar to each other except for the values at 0,011 mm/rev (see Fig. 5.21). At low rates of advance associated with Mode 1 drilling behaviour the values for specific energy calculated from the net power consumption were characteristically always much lower than those derived from the torquemeter readings. At very low penetration rates or under conditions of no net penetration the torquemeter recorded the torque produced by simple friction between the bit and the rock. This was small (in the region of 0,3 Nm) but not negligible relative to the torque measured during drilling (about 3 Nm). However, the power required to overcome the sliding friction was negligible relative to the power consumed while drilling effectively. Hence the specific energy rose rapidly at low rates of penetration and for short tests such as those described here the values calculated from the torque were a more sensitive measure of specific energy. At very low rates of advance the specific energy was expected to rise rapidly to a theoretically infinite value when penetration virtually ceased. The specific energy reached an optimal minimum of about 600 MJm^{-3} above 0,044 mm/rev, corresponding to a bit pressure between 4 MPa and 5 MPa (see Figs. 5.19 & 5.21). This agreed with the results of the tests at set thrust in which a minimum specific energy of about 600 MJm^{-3} was achieved at about 5 MPa (see Fig. 5.8).

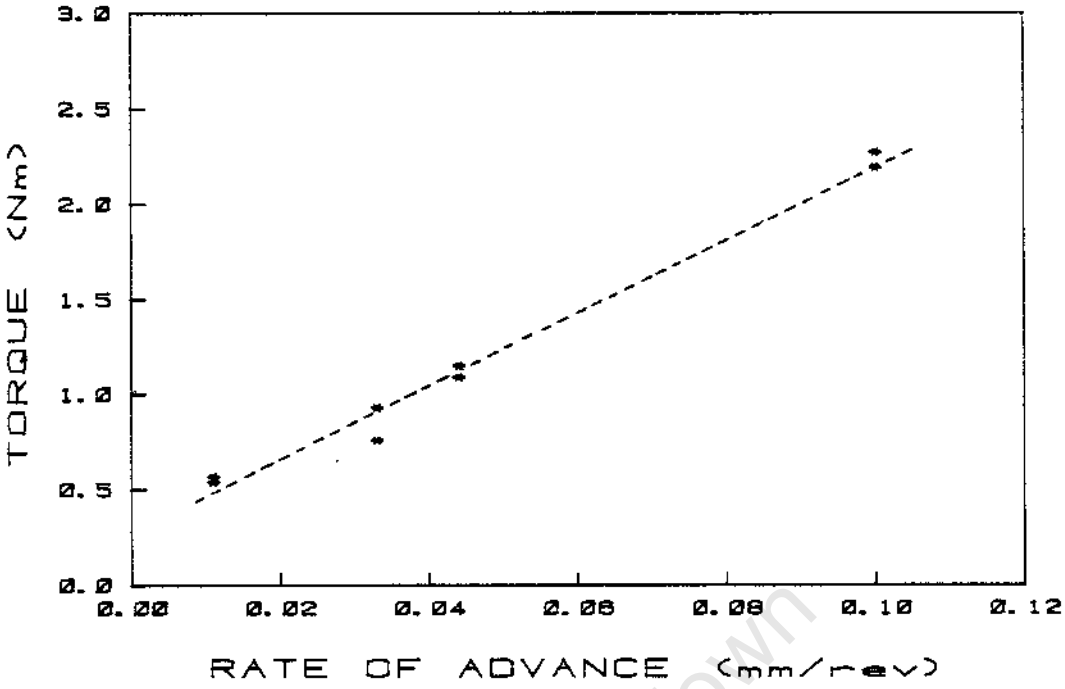

FIGURE 5.20 : Plot showing linear relationship between torque and rate of advance for tests drilled in norite at set rate of advance

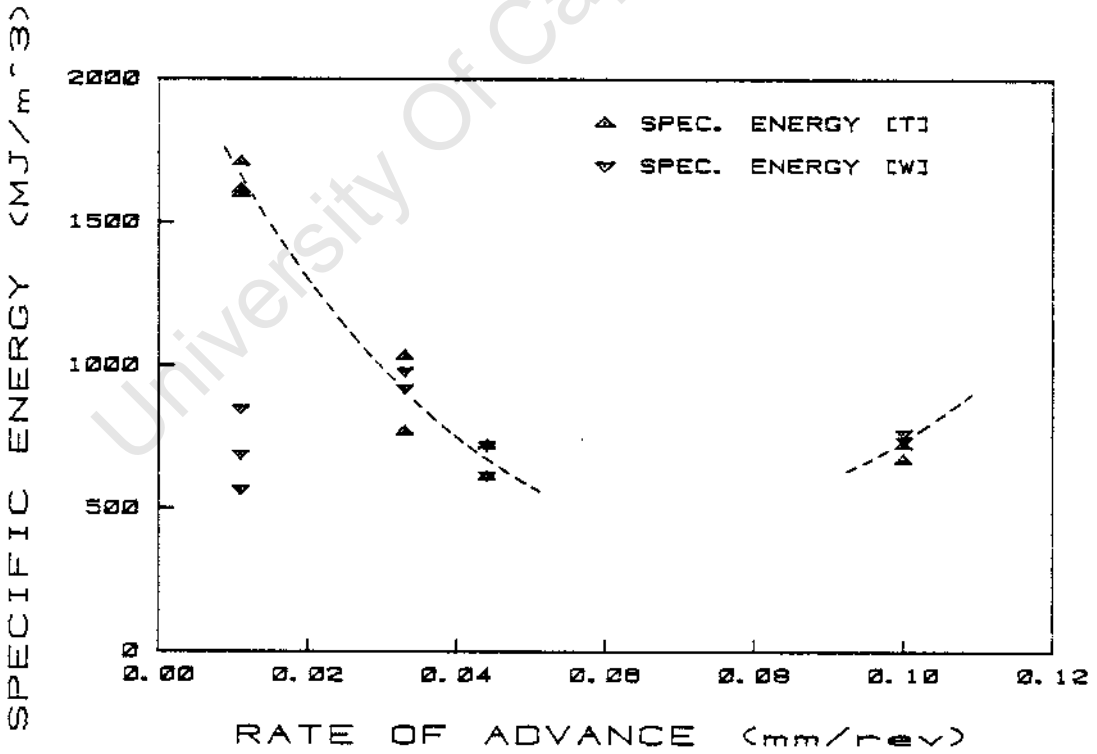

FIGURE 5.21 : Plot of specific energy against rate of advance for tests drilled in norite at set rate of advance, showing a minimum between 0,06 mm/rev and 0,08 mm/rev set rate of advance

Bit Wear and Diamond Wear

Specific bit wear was measured as linear axial wear and mass loss both normalised to 1 metre of drilling distance (Fig. 5.22). At low rates of advance with tests of long duration and minimal bit wear the values were generally low. One test at low rate of advance had a high normalised linear wear value because it was accidentally considerably shorter than the others and the initial wear rate was always relatively higher. At high rates of advance the rapid wear associated with the aggressive conditions during tests of short duration caused the normalised values to be both higher and more scattered. Bit wear rates were comparable with those of the tests at set thrust (see Figs. 5.9 & 5.10). The lower number of tests in the set rate of advance series made the identification of Mode 1 performance on the basis of bit wear alone more tenuous, but the tests at rates of advance below 0,1 mm/rev formed an identifiable group with little scatter.

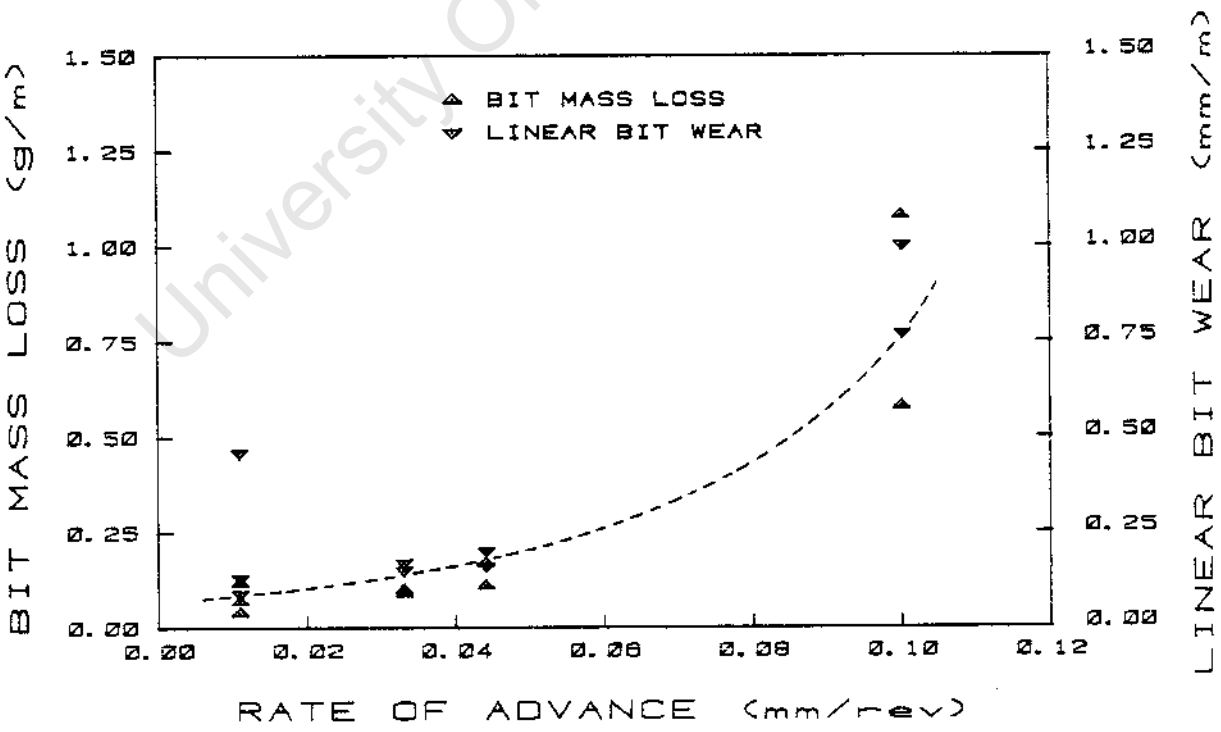

FIGURE 5.22 : Plot of specific bit mass loss against rate of advance for tests drilled in norite at set rate of advance, showing a rapid increase in bit wear at high rates of advance

The diamond wear type analysis of these tests showed a predominance of Type 1 over Type 2 wear at low rates of advance with a cross-over at an intermediate value of about 0,05 mm/rev (Fig. 5.23). This corresponded to a bit pressure between 4 MPa and 5 MPa as with the tests at set thrust (see Fig. 5.11). However, unlike the tests at set thrust the values for Type 0 wear (fresh stones) and Type 4 wear (macrofracture) were not constant. At the highest rate of advance fewer stones escaped wear and a larger proportion of stones were severely fractured. The percentages of Type 0 and Type 4 wear correspondingly tended to converge to a mean value of 15% at 0,1 mm/rev.

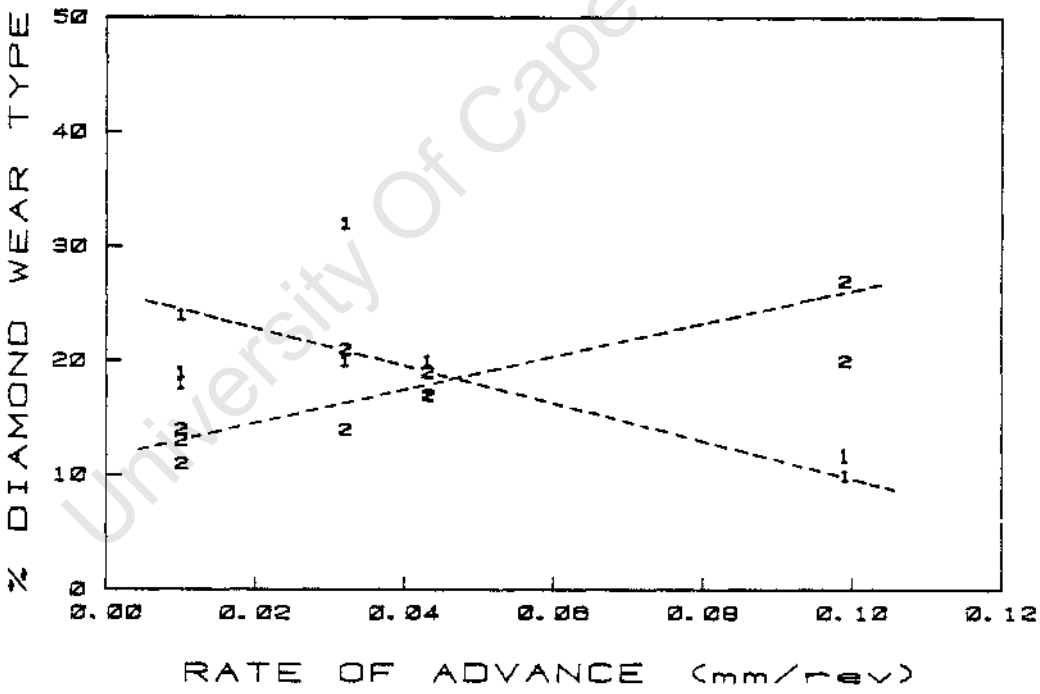

FIGURE 5.23 : Plot of diamond wear type percentage against bit pressure for tests drilled in norite at set rate of advance showing the change in predominant wear type at about 0,05 mm/rev set rate of advance

The test results plotted in Fig. 5.24 were typical of unstable Mode 1 drilling behaviour. TEST 77 was drilled with a bit dulled by the previous test to confirm that Mode I behaviour persisted as the bit pressure increased with protracted drilling at a low set rate of advance. The progressive increase in bit pressure and specific energy was due to the steady development of diamond wear flat area, i.e. an increase in the number of stones displaying Type lb wear. The preceding test, drilled with the same drilling parameters, had a mean bit pressure of 3,50 MPa and 22 stones had well developed wear flats. TEST 77 had a mean bit pressure of 7,32 MPa and 29 stones showed Type lb wear.

Fig. 5.25 shows SEM photographs of typical diamond wear from TEST 77. Wear proceded by abrasion and attrition of a point to produce Type la wear (Fig. 5.25(a)) or by abrasion of a flat face to produce Type lb wear (Fig. 5.25(b)). A further stage of Type lb wear obscured any possible association of the wear flat with a crystal face and revealed the presence of crystallographically controlled parallel steps transverse to the direction of the abrasion grooves on the wear flat (Fig. 5.25(c)). (Lines of transverse steps indicated by arrows). A wear flat could persist even on a fractured stone (Fig. 5.25(d)) and some stones were observed on which secondary wear flats had developed on the exposed points of the fractured diamonds.

Selected worn stones from tests drilled at the higher rates of advance were photographed in the SEM (Fig. 5.26). At 0,033 mm/rev Type lb wear predominated over Type 2b. The example of Type lb wear illustrated (Fig. 5.26(a)) showed signs of etching (1), typical grooving by abrasion (2) and the development of parallel transverse steps on the worn surface (3). The example of Type 2b wear (Fig. 5.26(b)) showed cleavage controlled fracture which produced sharp points and ridges without destroying the stone. Figs. 5.26(c & d) show Type 2 wear fractured stones with different degrees of fragmentation and protrusion produced at 0,044 mm/rev.

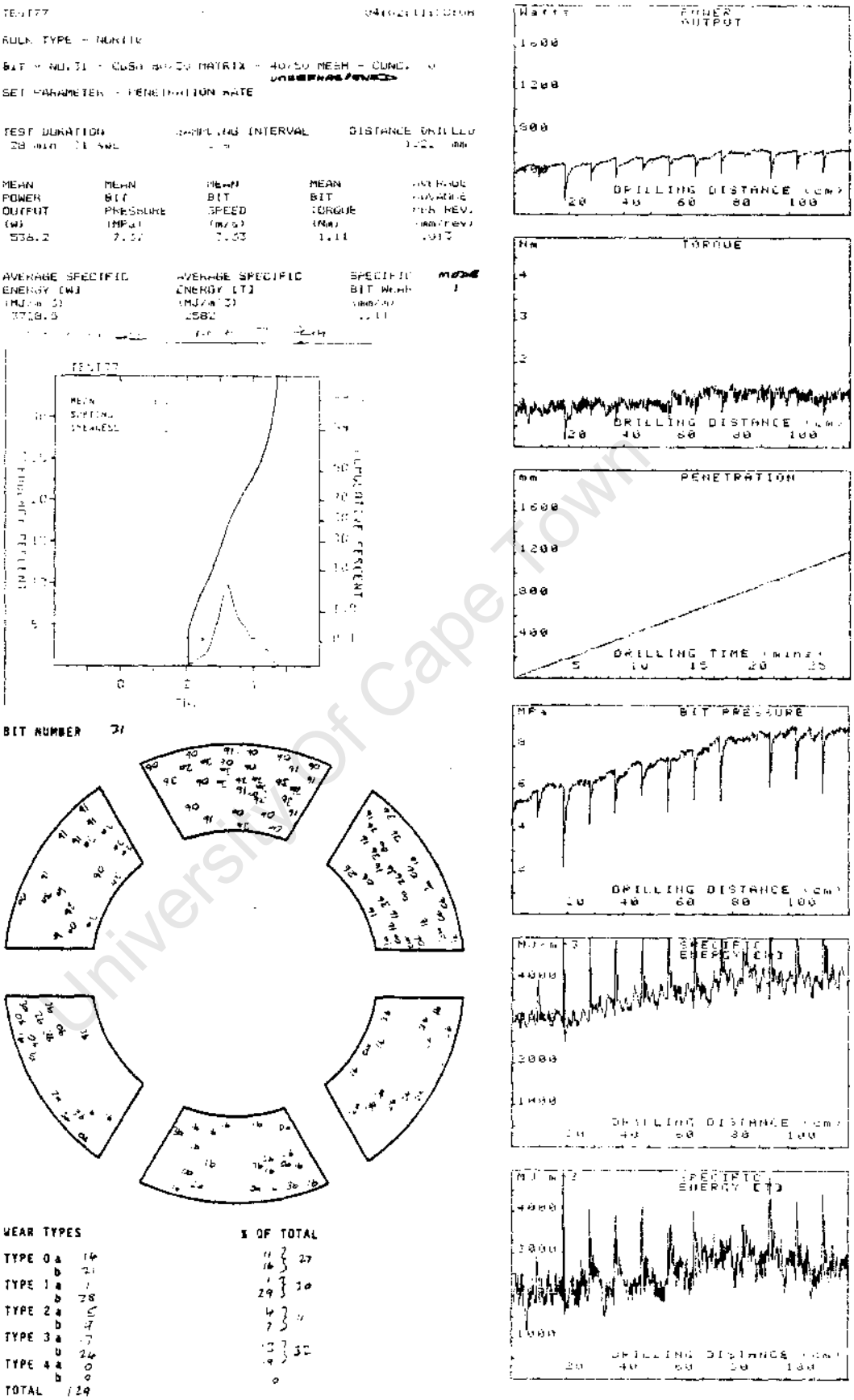

FIGURE 5.24: Full graphical record of TEST 77, typical of Mode 1 behaviour with decreasing penetration rate and a predominance of Type 1 wear over Type 2 wear

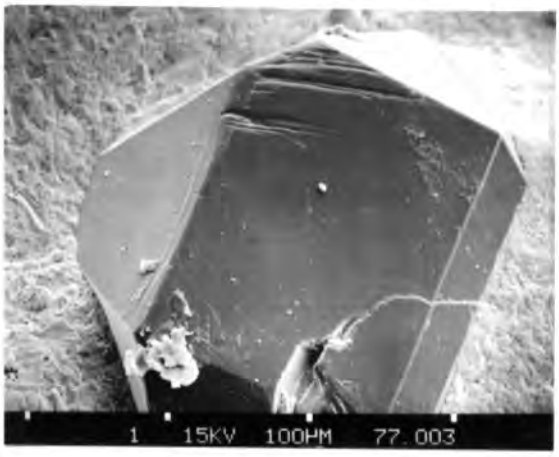

(a) : Type 1a - grooving and rounding on the apex of a stone with a fracture

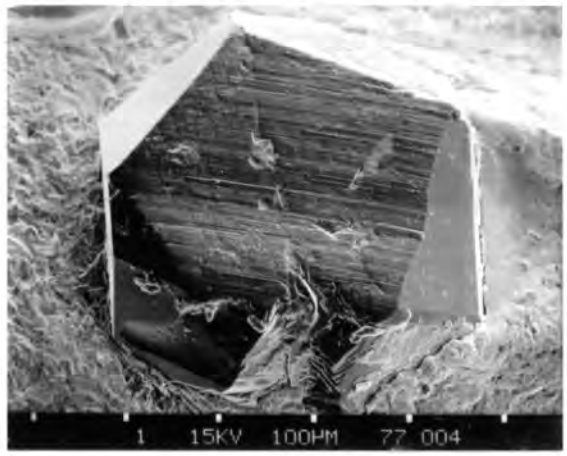

(b) : Type 1b - fully developed wear flat showing grooving

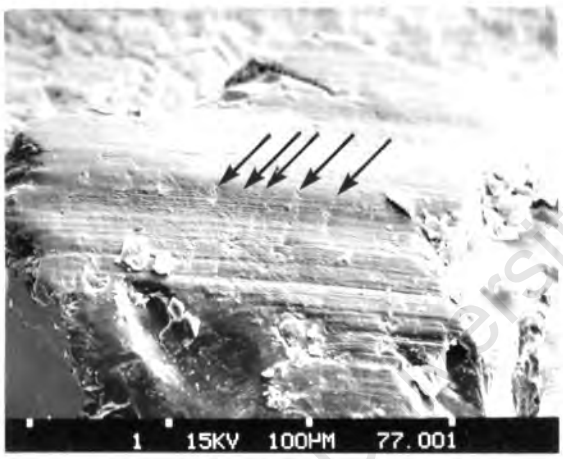

(c) : Type 1b - wear flat with parallel transverse steps on a partially fractured stone

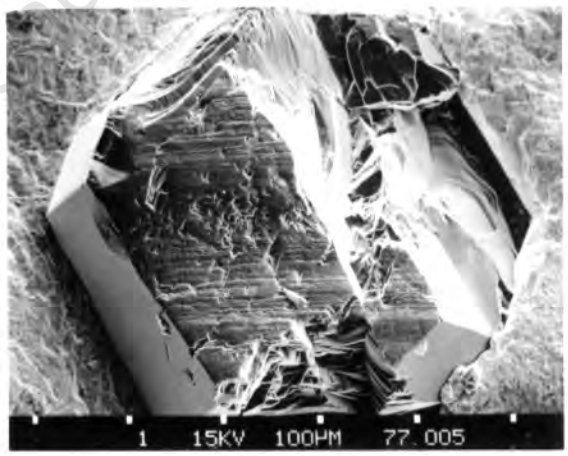

(d) : Type 1b - wear flat retained on partially fractured stone

FIGURE 5.25 : Typical Type 1 wear of diamonds at 0,011 mm/rev rate of advance in norite

The stones from bits drilled at 0,1 mm/rev were severely damaged. Many displayed Type 4a wear, broken off flush with the matrix and incapable of contributing to the drilling (Fig. 5.26(e)), or were masked by sintered drilling detritus adhering to the bit (Fig. 5.26(f)).

Drilling Detritus and Drilling Tracks

There was a trend of increasing mean particle size in the 2 mm to 63 micron fraction of the drilling detritus with increasing rate of advance (Fig. 5.27). The mean particle size increased from an average of 0,098 mm at 0,011 mm/rev to 0,132 mm at 0,1 mm/rev. The percentage by mass of detritus under 63 microns in size showed a corresponding trend decreasing slightly from an average of 78% to 74% with increasing rate of advance (Fig. 5.28). At the highest rate of advance of 0,1 mm/rev stalling and seizure made it impossible to create punch-through discs of rock. Punch-through discs were produced at the other three rates of advance and the drilling tracks photographed in the SEM.

Pairs of photographs at two different magnifications are presented in Fig. 5.29 for each rate of advance. The scale of fracture of the norite did not vary appreciably as can be seen from the left hand photograph of each pair except that the track produced at the lowest rate of advance appeared to be a bit smoother than the others. The photographs on the right hand side of each pair show the presence of mashed flakes even at the lower rates of advance and correspondingly low associated bit pressures. The width of individual flakes was determined by the size of the diamond surfaces that produced them by smearing mashed detritus onto the rock. Hence mashed flakes of widely diverse widths were present on all the discs.

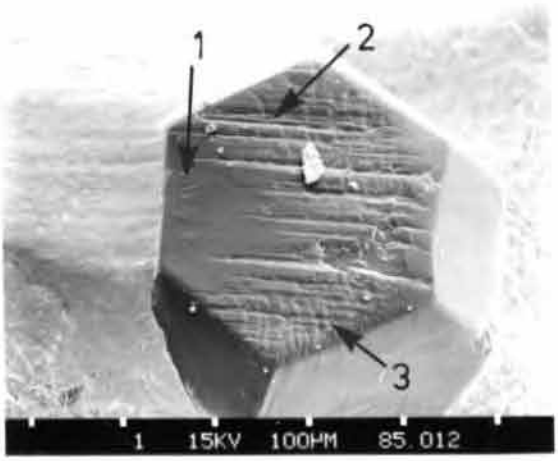

(a) : 0,033 mm/rev : Type 1b - wear flat

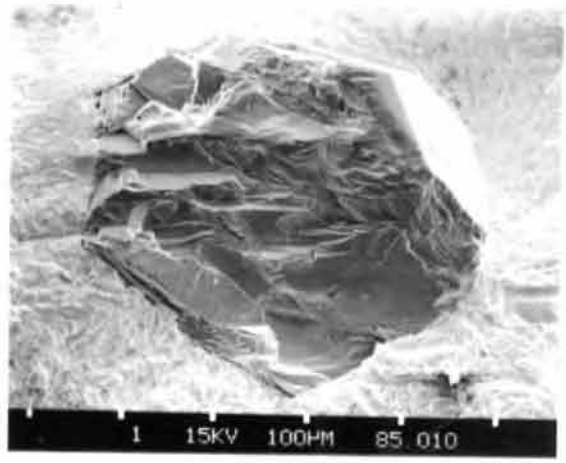

(b) : 0,033 mm/rev : Type 2b - microfracture

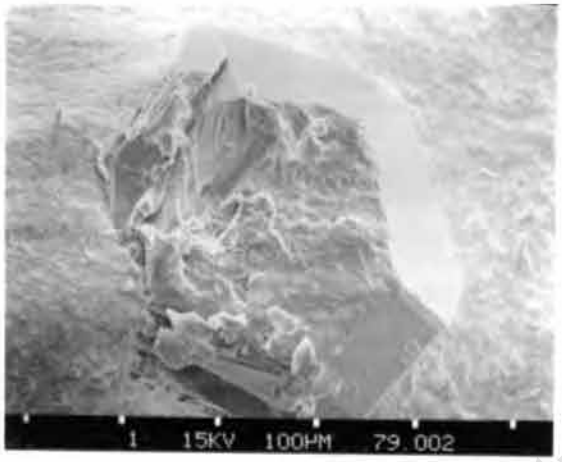

(c) : 0,044 mm/rev : Type 2b - microfracture

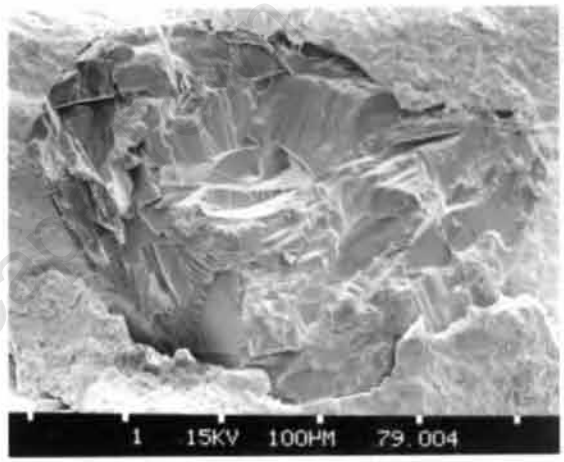

(d) : 0,044 mm/rev : Type 2b - advanced microfracture

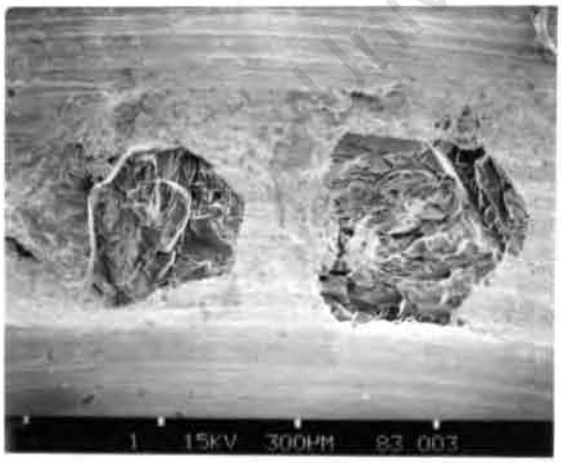

(e) : 0,1 mm/rev : Type 4a - fracture flush with the bit matrix

(f) : 0,1 mm/rev : Type 4a - stone masked by caked detritus

FIGURE 5.26 : Characteristic wear of diamonds drilled at different set rates of advance in norite. Numbered features are described in the text.

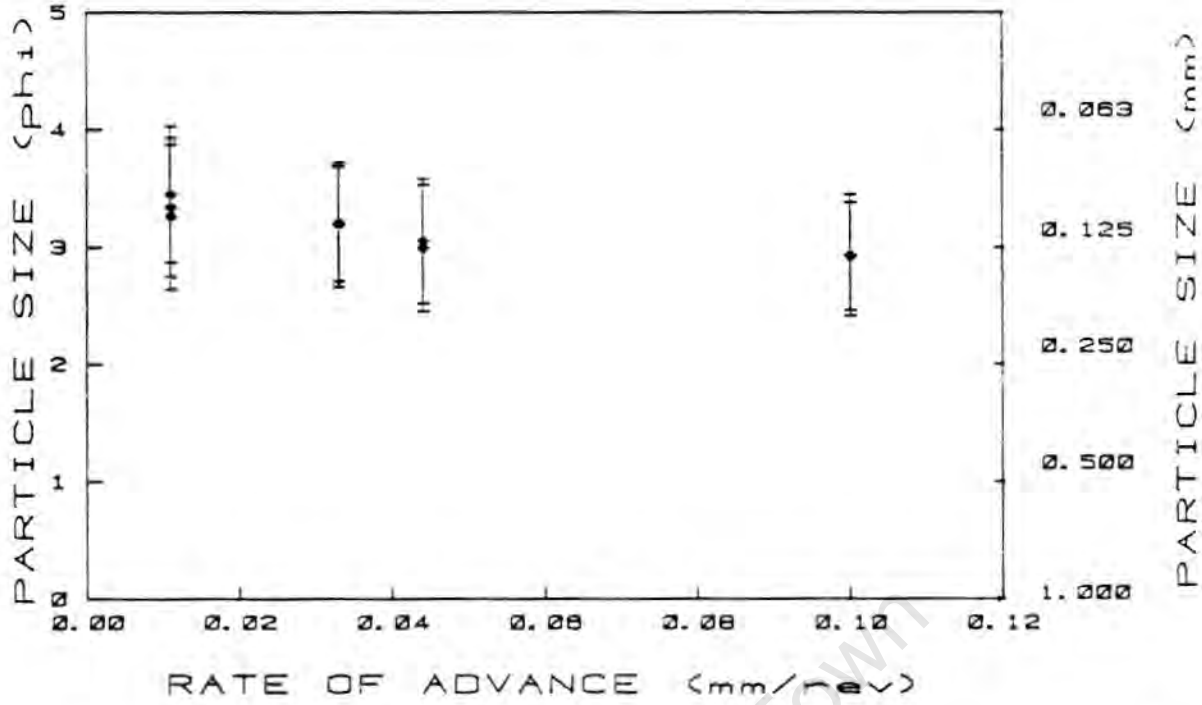

FIGURE 5.27 : Plot of particle size distribution of detritus between 2 mm and 0,063 mm against rate of advance for tests drilled in norite at set rate of advance

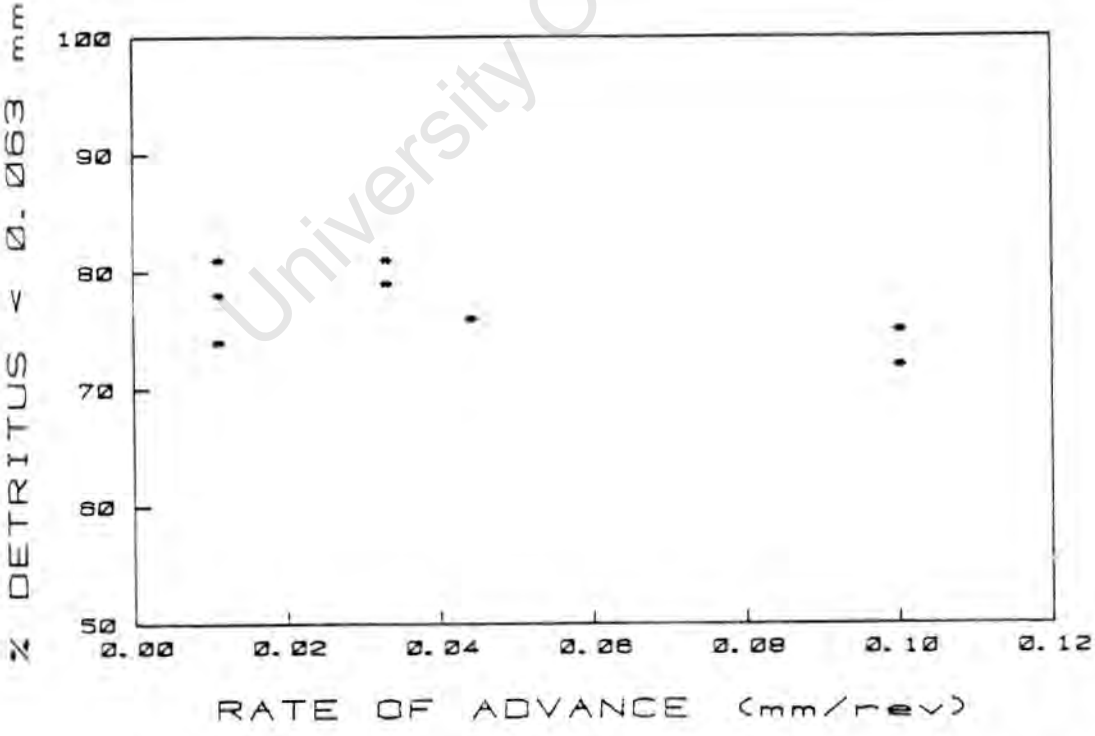

FIGURE 5.28 : Plot of percentage by mass of detritus under 0,063 mm in size against rate of advance for tests drilled in norite at set rate of advance, showing a decreasing trend with increasing rate of advance

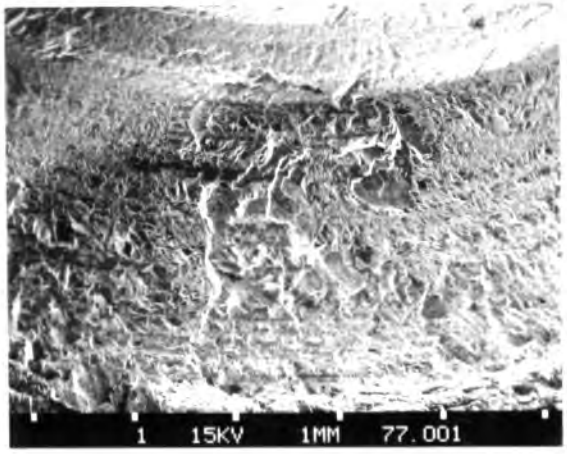

(a) : 0,011 mm/rev (± 10X)

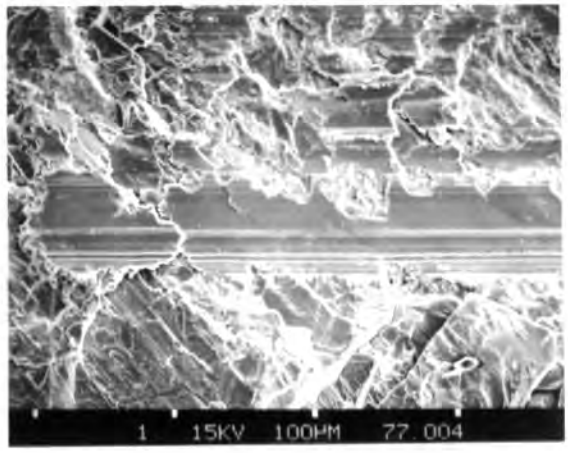

(b) : 0,011 mm/rev (± 100X)

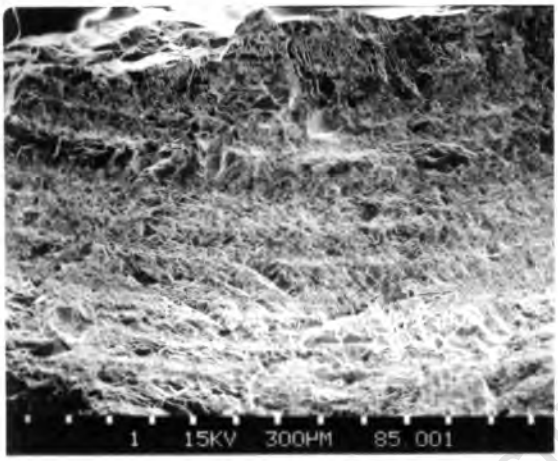

(c) : 0,033 mm/rev (± 10X)

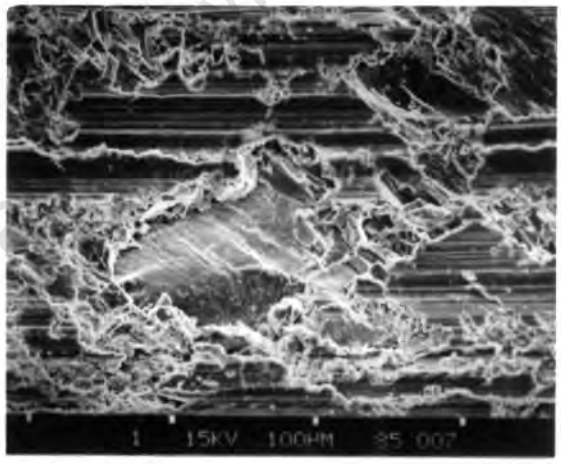

(d) : 0,033 mm/rev (± 100X)

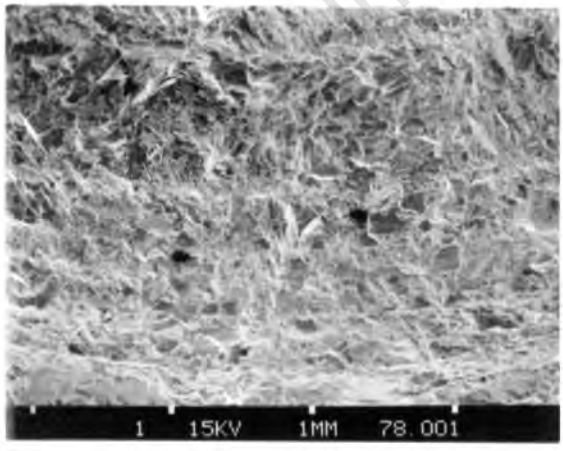

(e) : 0,044 mm/rev (± 10X)

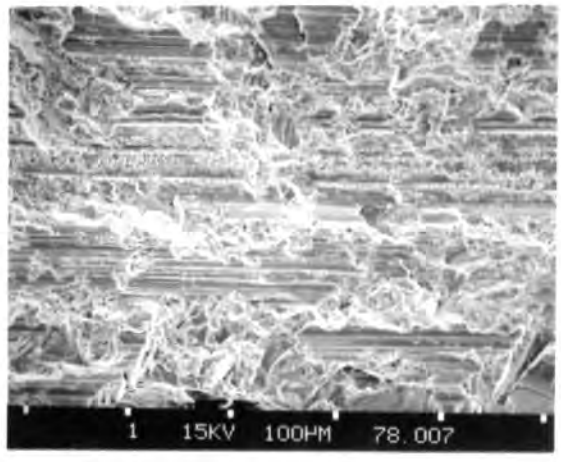

(f) : 0,044 mm/rev (± 100X)

FIGURE 5.29 : SEM photographs of drilling tracks produced at various set rates of advance in norite, showing uniformity of appearance

5.4.3 Tests in Norite at Set Rotational Velocity with Standard Bits

Four pairs of tests (TESTS 86 - 93) were drilled in norite using standard microbits at rotational velocities ranging from 1640 rpm to 3500 rpm (about 2 ms^{-1} to 4 ms^{-1} linear bit speed). A single set rate of advance of 0,044 mm/rev was used because this rate had produced stable drilling conditions with moderate bit wear in the set rate of advance tests. The two tests at 1640 rpm suffered severe vibration and were terminated early. They were standardised to 200 seconds whereas the other six tests were standarised to 300 seconds (Appendix 5, Table A5.2). The two tests at 1640 rpm displayed paradoxical Mode 2 behaviour, so their results were comparable with the others. Diamond wear type counts and detritus size distribution determinations were done for all the tests. SEM photographs were taken of the worn diamonds and the drilling tracks of three tests at different rotational speeds. The results are presented in Figs. 5.30 to 5.39.

Relationships Between the Drilling Variables

At a set rate of advance of 0,044 mm/rev, the bit pressure rose with increased rotational speed (Fig. 5.30) because the resulting linear pentration rate was higher and the bit was forced into the rock more rapidly. The relationship between mean bit pressure and mean bit speed had a least squares best fit line of $y = 0,46x + 2,44$ with a rather poor correlation coefficient of 0,78. The extrapolated pressure threshold for penetration was 2,44 MPa. The results for specific energy showed a complete divergence between those calculated from the power consumption and from the torque (Fig. 5.31). As explained earlier, for suboptimal drilling the specific energy calculated from the torque measurement is the more reliable. Of these tests only the ones at highest bit speed drilled effectively and the results of the tests below 2 ms^{-1} were largely invalidated by severe vibration.

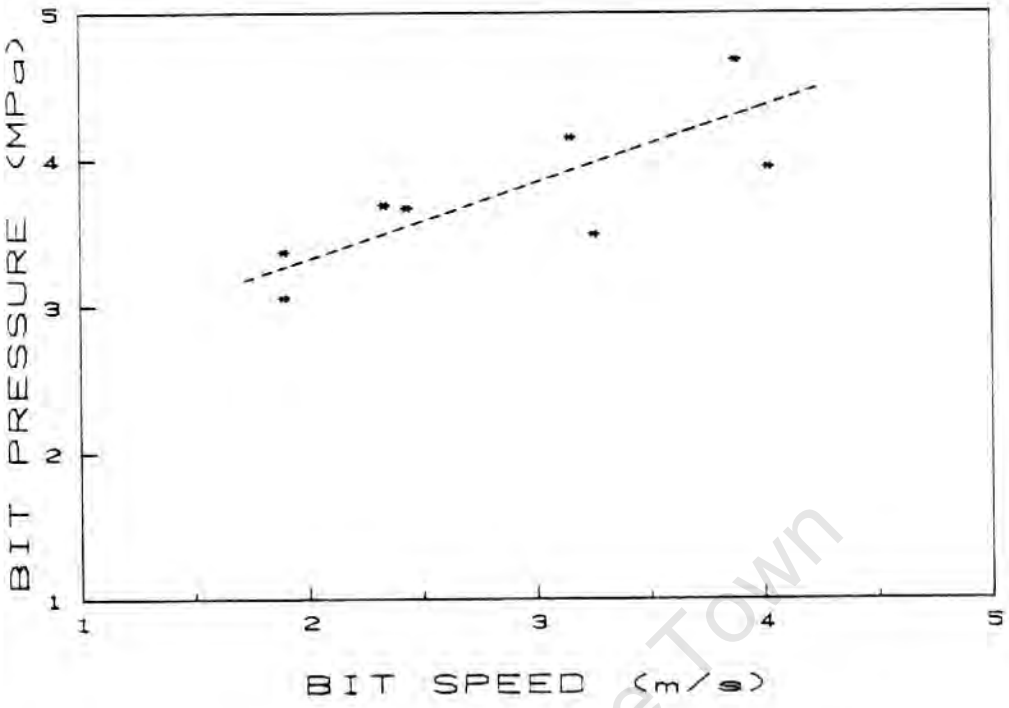

FIGURE 5.30 : Plot showing the linear relationship between the mean bit pressure and linear bit speed for tests drilled in norite at 0,044 mm/rev set rate of advance

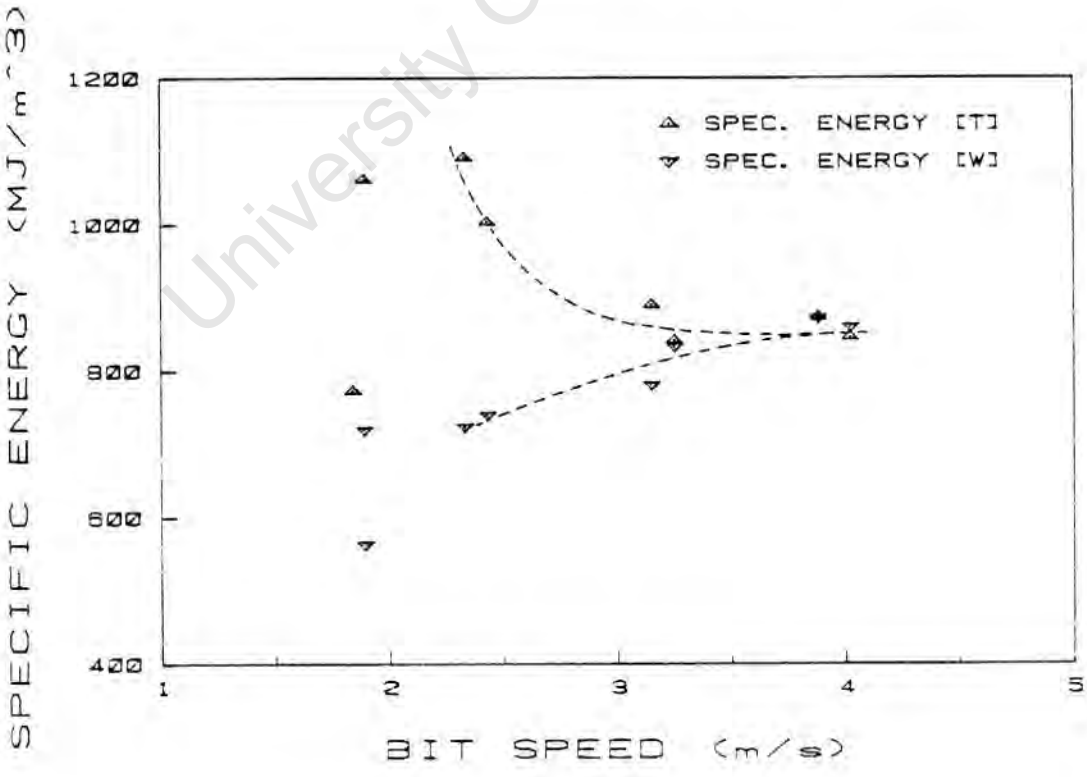

FIGURE 5.31 : Plot of specific energy against linear bit speed for tests drilled in norite at 0,044 mm/rev set rate of advance

Bit Wear and Diamond Wear

The bit wear values decreased with increasing bit speed (Fig. 5.32). There were also fewer stones lost from the bits at higher speed. The proportion of Type 3 wear (pull-outs) decreased as Type 1 and Type 2 wear converged at more optimal drilling conditions (Fig. 5.33). The vibration at low bit speeds was responsible for considerable bit damage. At low speeds steady penetration was aided by enhanced fracture of the diamonds under very unstable suboptimal conditions. The proportion of stones broken off flush with the matrix (Type 4) was low but nearly constant. The proportion of unworn stones (Type 0) was also nearly constant with a mean value of 25% (not plotted).

Selected worn diamonds drilled at various rotational velocities are illustrated in Fig. 5.34. The relationship between Type 1 and Type 2 wear is evident from Fig. 5.34(a). The central portion of the wear surface had broken up and microfractured (1) but was surrounded by relict Type 1 wear showing grooving (2) and transverse steps (3). The direction of movement of the stone was to the right (as in almost all of the SEM micrographs). Fig. 5.34(b) shows an area of Type 1 wear. Formerly straight abrasion grooves had been kinked by crystallo- graphically controlled steps in a diagonal orientation. The Type 2b wear illustrated in Fig. 5.34(c) was typical. Generally the degree of fracturing was more severe at the trailing edge. The bit and the diamonds which had been drilled at 1640 rpm with vibration had the appearance of being severely damaged. The stone illustrated in Fig. 5.34(d) had been broken down almost flush with the matrix. The stone shown in Fig. 5.34(e & f) had a variety of features including rounding of the leading edge (1), apical chipping (2), deep abrasion grooves (3) and what is probably a synthetic growth feature (at the bottom of the photograph (e)).

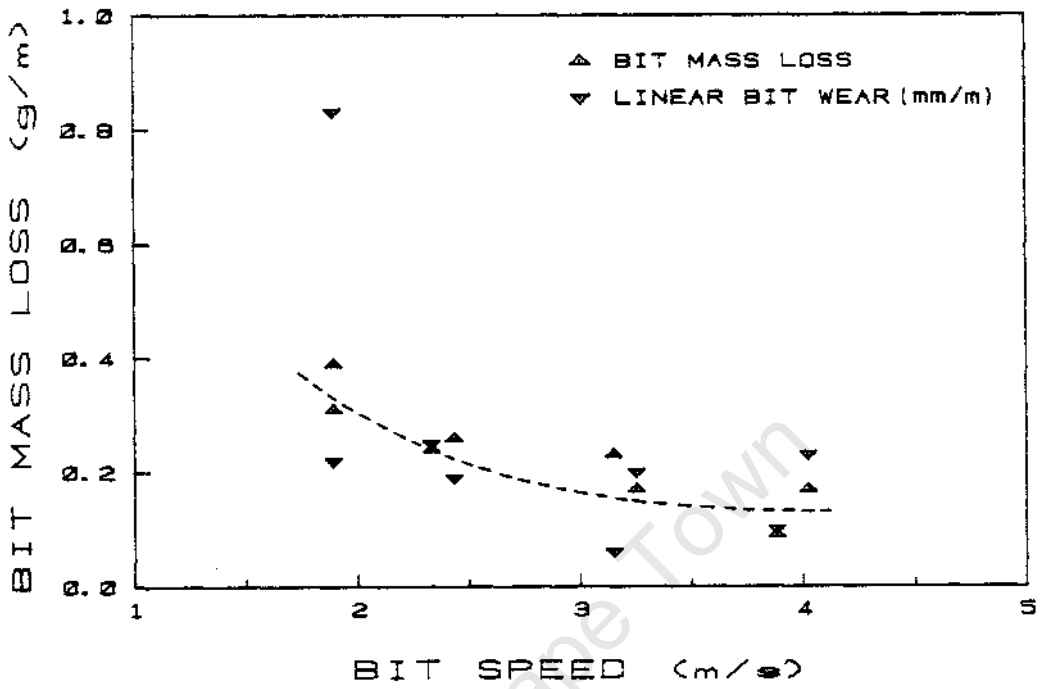

FIGURE 5.32 : Plot of specific bit mass loss against linear bit speed for tests drilled in norite at 0,044 mm/rev set rate of advance showing decreasing trend with increasing bit velocity

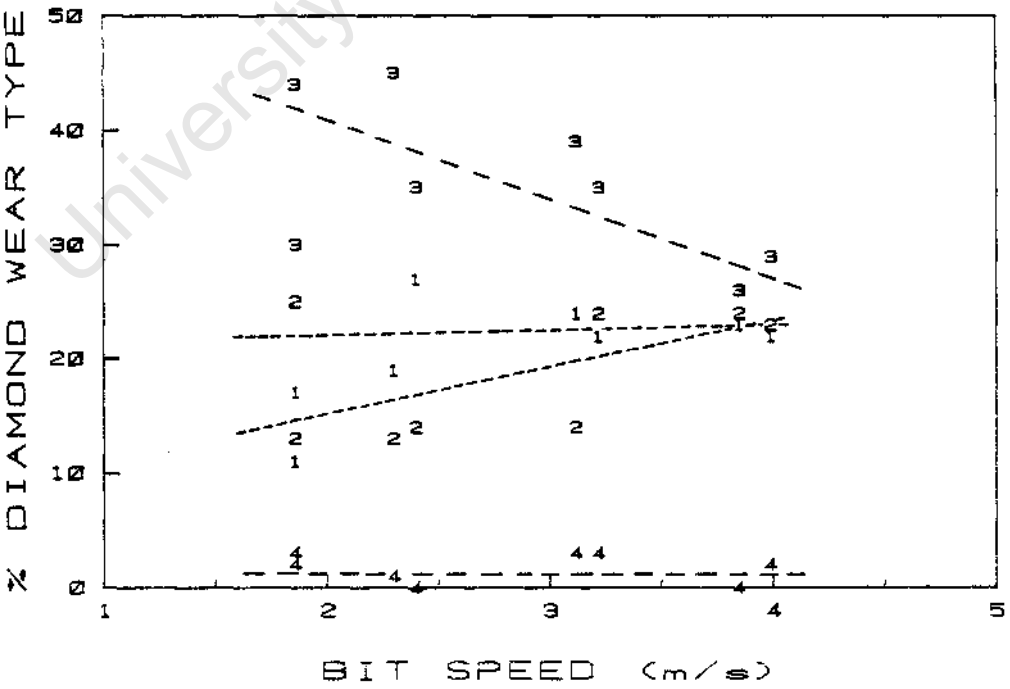

FIGURE 5.33 : Plot of diamond wear type percentage against linear bit speed for tests drilled in norite at 0,044 mm/rev set rate of advance

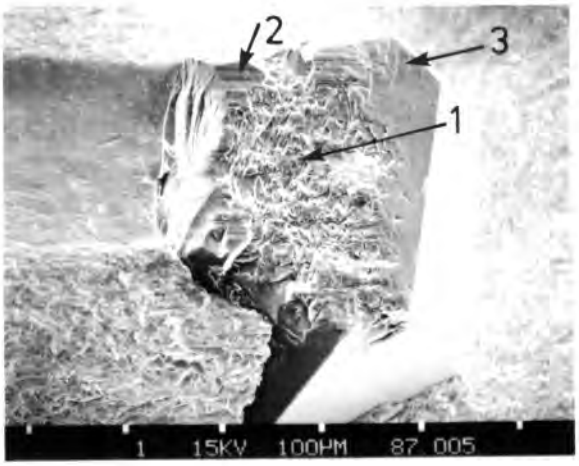

(a) : 3500 rpm
Type 2a wear

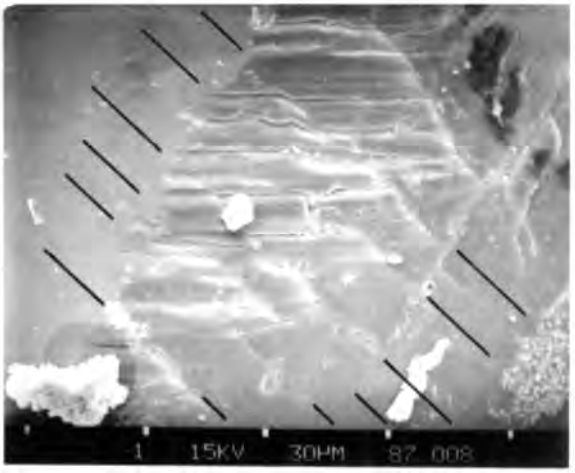

(b) : 3500 rpm
Type 1b wear

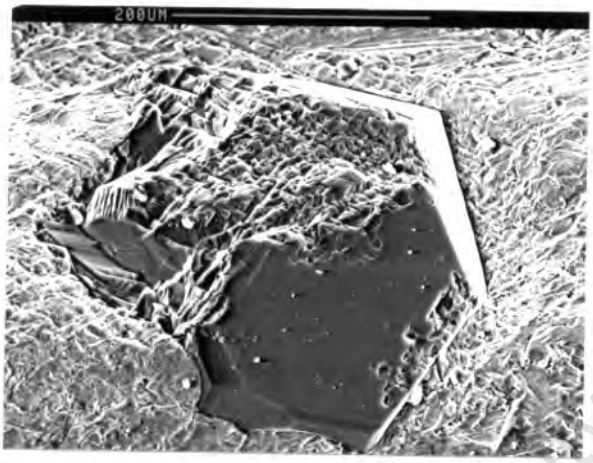

(c) : 2080 rpm
Type 2b wear

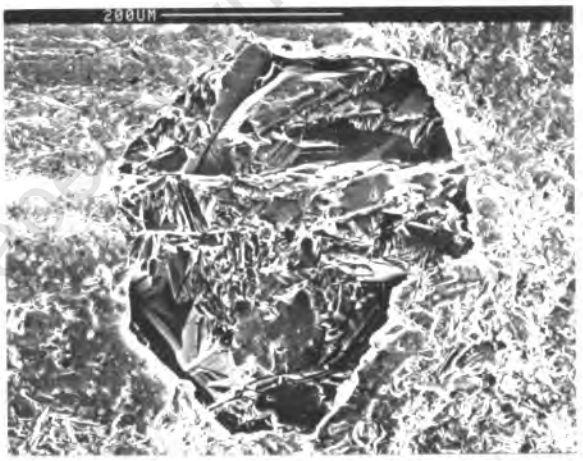

(d) : 1640 rpm
Type 4a wear

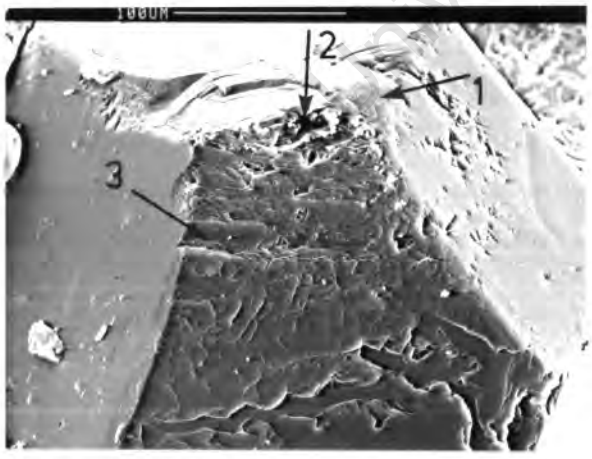

(e) : 1640 rpm
Type 1a wear

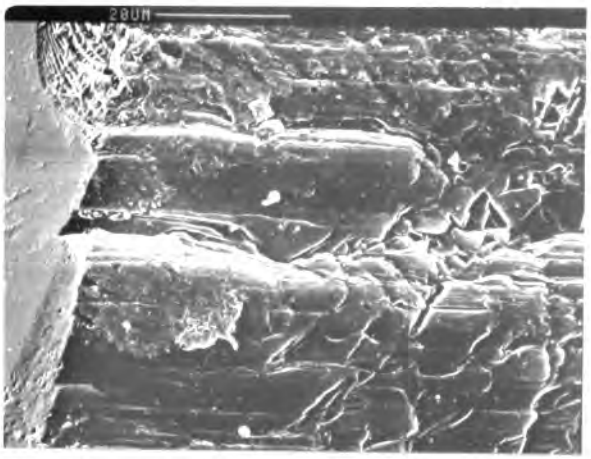

(f) : 1640 rpm
Detail of (e)

FIGURE 5.34 : Wear of selected diamonds drilled at different rotational speeds in norite. Numbered features are described in the text.

Drilling Detritus and Drilling Tracks

The particle size distribution of the coarse detritus did not vary significantly with rotational velocity (Fig. 5.35) but the percentage of fine particles increased from 70% to 80% with increasing rotational speed because of additional regrinding (Fig. 5.36). There was no appreciable difference in the appearance of the drilling tracks produced at different speeds (Fig. 5.37). Even the track produced at the lowest speed displayed mashed flakes of rock flour which had not been removed by the vibration of the bit on the rock. The scoring on the flakes was produced by asperities on the diamonds which had plastered the flakes onto the fractured norite.

Seizure

SEM photography of the used bit, the drilling detritus, and the drilling track produced by a test which stalled after drilling at 3500 rpm and 0,1 mm/rev set rate of advance was informative about the genesis of the mashed flakes. The bit face had tenaceous pads of sintered rock flour welded to the surface, in places coating and obscuring the diamonds (Fig. 5.38(a)). The mashed flake displayed layering and chatter marks. The hackly area resulted from parts of the flake adhering to the rock and being torn from the bit when they were separated. The remnants of these flakes were visible on the drilling track (Fig. 5.38(b)), their exposed surfaces smeared and showing evidence of plasticity (Fig. 5.38(c)). This was even more pronounced on some of the loose flakes recovered from the drilling detritus (Figs. 5.38(d - f)). Globules of molten material had flowed down the length of the flake. Other flakes had a very different appearance (Figs. 5.39(a - d)). They were curled, had annular plastic grooving caused by the passage of diamonds, a layered structure reflecting many passes of the same stone, possible quench cracks, and chatter marks on all but the most recent surfaces. The asperities of the detrital felspar grain shown in Fig. 5.39(d) appear to have been smeared out and to some extent plastered over by rock flour.

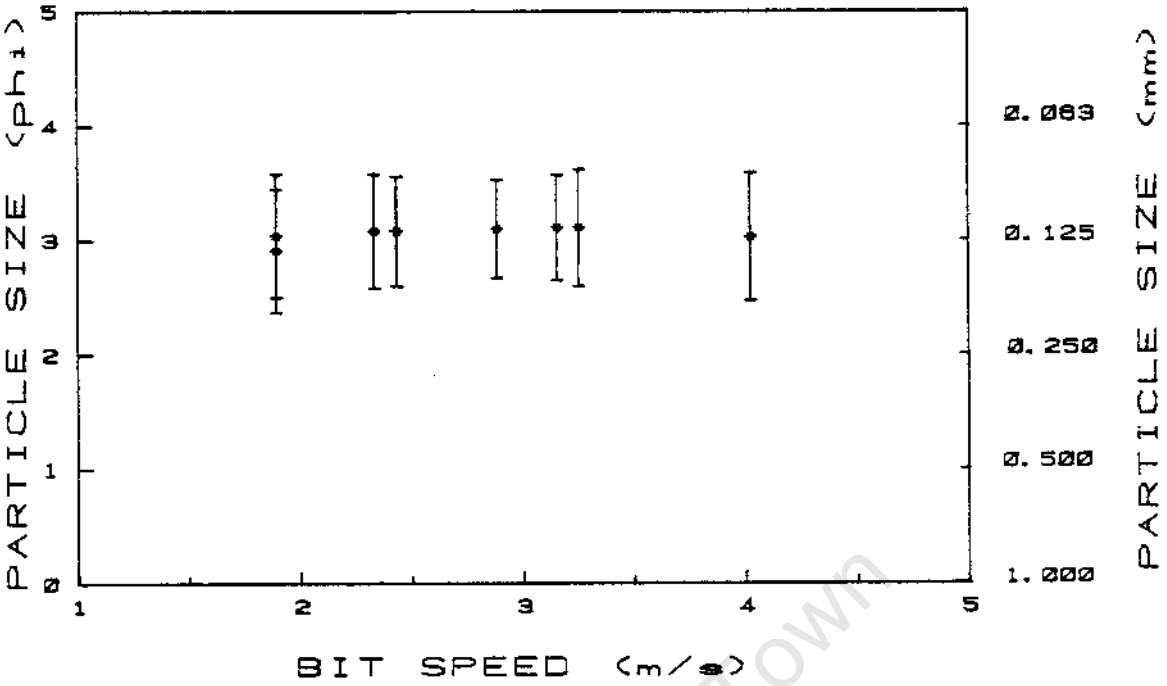

FIGURE 5.35 : Plot of particle size distributions of detritus between 2 mm and 0,063 mm against linear bit speed for tests drilled at 0,044 mm/rev set rate of advance

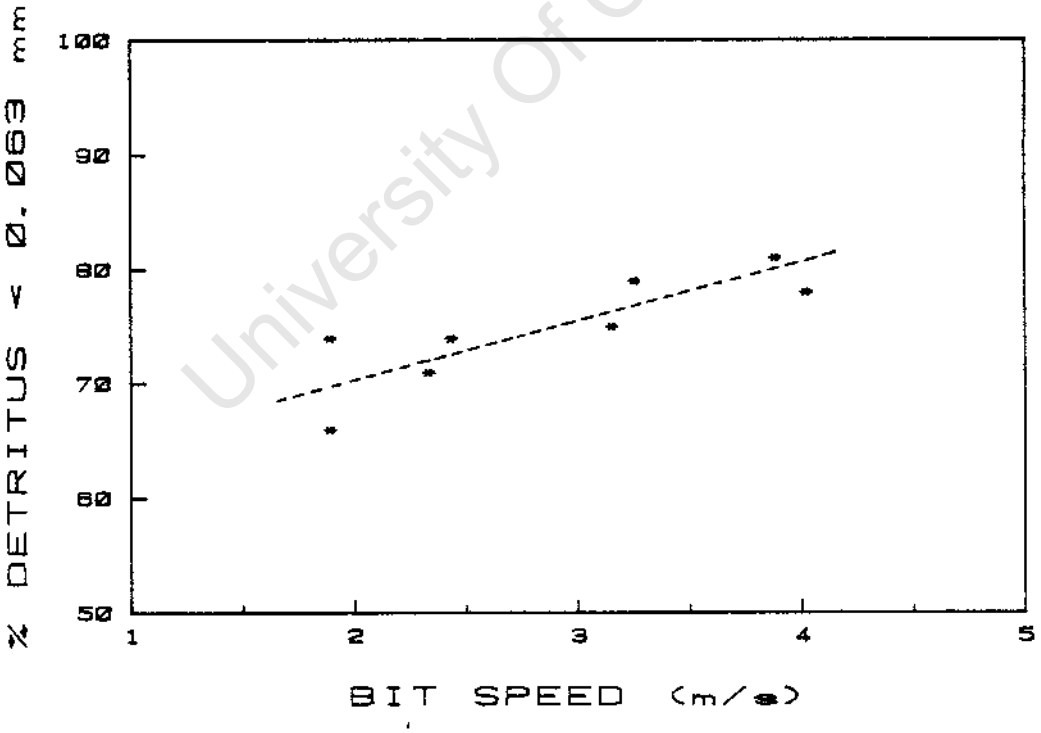

FIGURE 5.36: Plot of percentage by mass of detritus under 0,063 mm in size against linear bit speed for tests drilled in norite at 0,044 mm/rev set rate of advance, showing increasing trend with increasing bit velocity

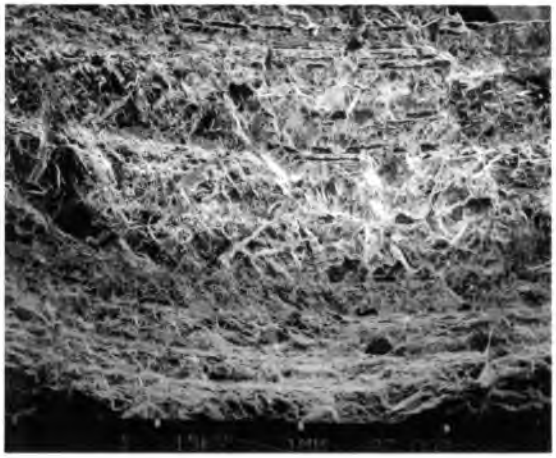

(a) : 3500 rpm - Drilling track produced at highest rotational speed

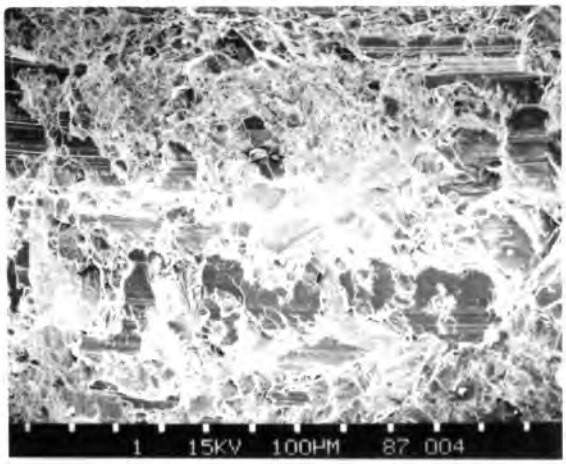

(b) : 3500 rpm - Detail of (a) - mashed flakes and fractured felspar

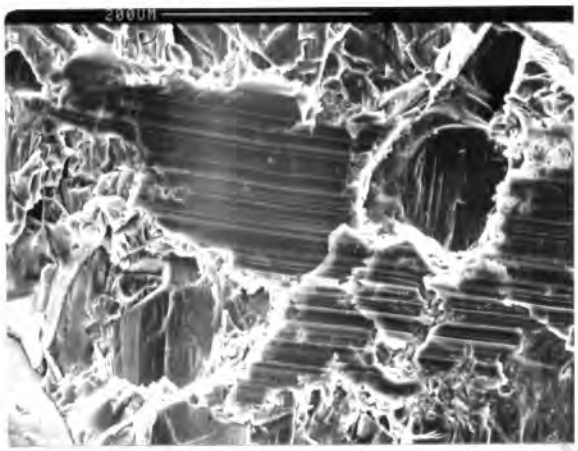

(c) : 2080 rpm - Mashed flakes produced at intermediate speed

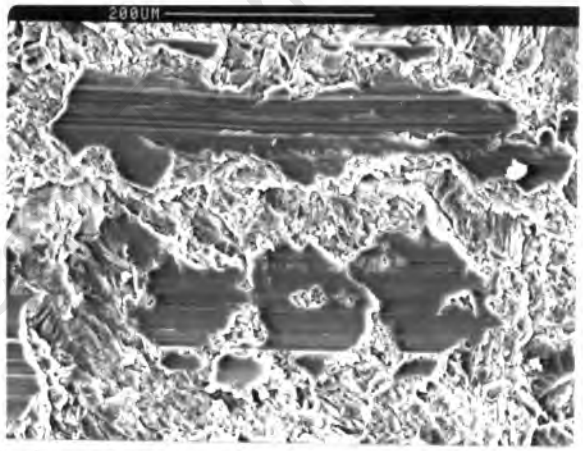

(d) : 2080 rpm - Striated flake on fractured felspar

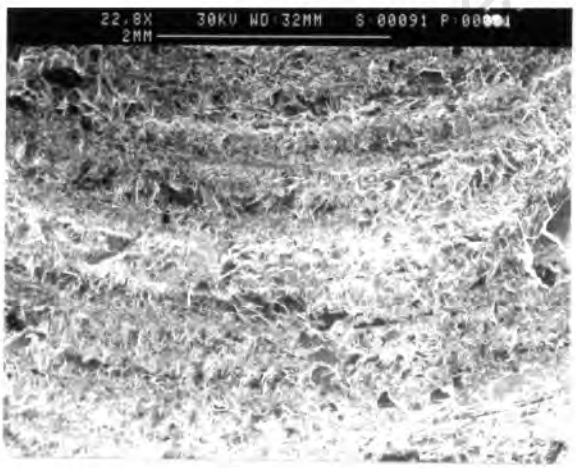

(e) : 1640 rpm - Drilling track produced at lowest rotational speed

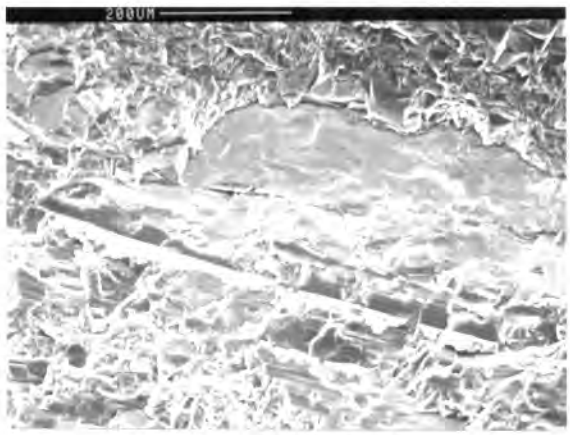

(f) : 1640 rpm - Detail of (e) - Mashed flake on cleaved mineral grains

FIGURE 5.37 : SEM photographs of drilling tracks produced in norite at different rotational speeds

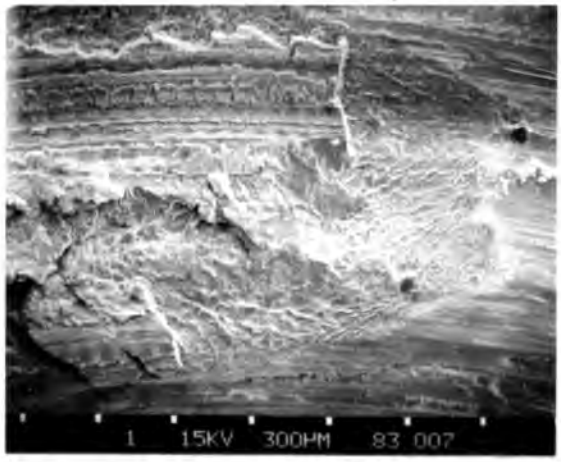

(a) : Sintered rock flour adhering to the bit face after seizure

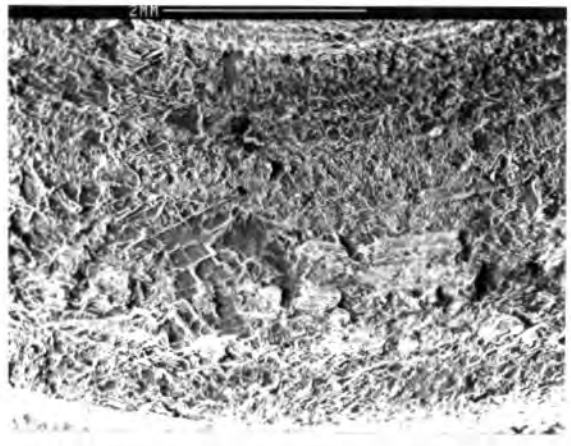

(b) : Drilling track with adhering remnants of flakes

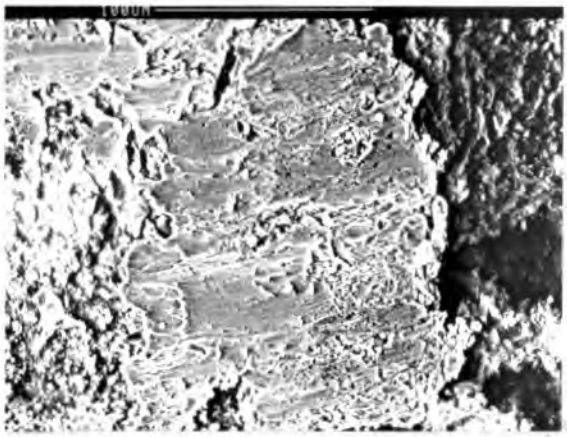

(c) : Detail of (b) - surface of flake welded to drilling track

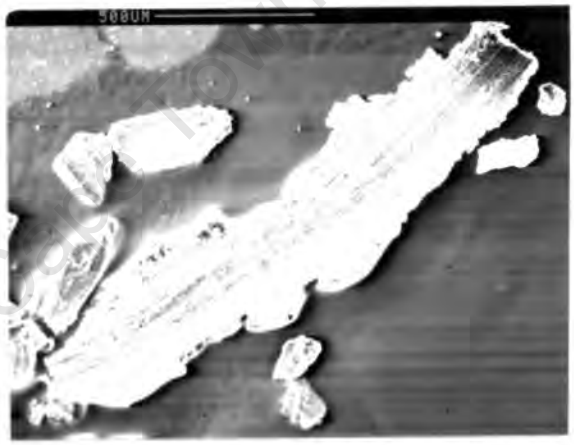

(d) : Flake recovered from the drilling detritus

(e) : Detail of surface of a sintered flake

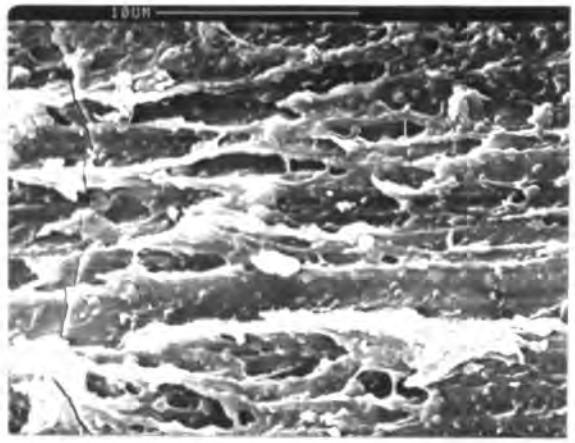

(f) : Detail of (e) showing vitreous flow

FIGURE 5.38 : SEM photographs of the bit, drilling track and detritus from a test in norite which terminated by seizure

(a) : Sintered flake showing plastic grooving

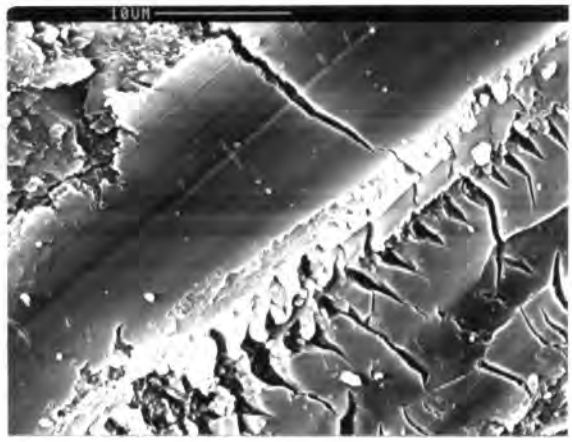

(b) : Detail of (a)

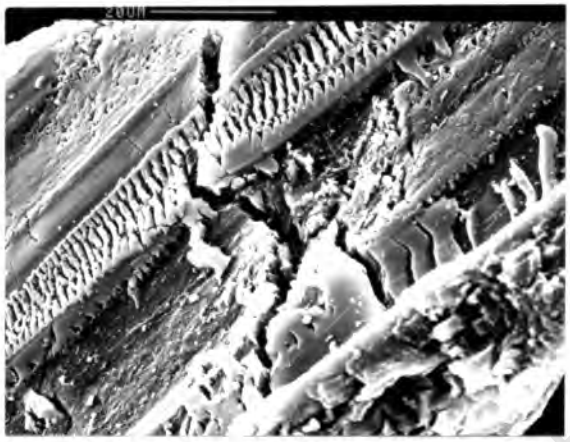

(c) : Sintered flake with transverse cracks

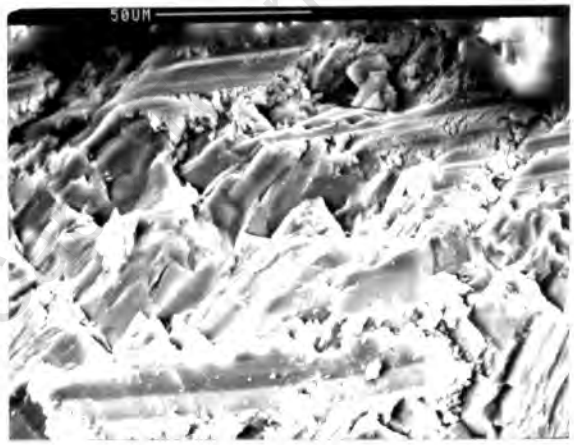

(d) : Detrital felspar grain with adhering flake material

FIGURE 5.39 : SEM photographs of the drilling detritus from a test in norite which terminated by seizure

5.4.4 Tests in Norite at Set Rate of Advance with Different Diamond Mesh Sizes

Fourteen tests (TESTS 94 - 107) were drilled in norite at 0,044 mm/rev set rate of advance and a nominal speed of 3500 rpm using microbits made up with different ranges of diamond size ranging from 20/30 US mesh to 60/80 US mesh as in Table 5.4 overleaf.

TABLE 5.4 : Bit formulations with different diamond mesh sizes

SIZE RANGE U.S. MESH	GRAIN SIZE RANGE (mm)*
20/30	0,84 - 0,59
30/40	0,59 - 0,42
40/50	0,42 - 0,297
50/60	0,297 - 0,250
60/80	0,250 - 0,177
20/30 & 40/50	0,84 - 0,297
40/50 & 60/80	0,42 - 0,177

* from : Hench & Gould (1971)

The mixed mesh bits were used to test the effect of a broad range of diamond size on performance. All the bits had a concentration of 30 so the bits with smaller diamonds had more exposed stones. With the exception of one test which drilled in Mode 2 but stopped prematurely due to bit failure, all the tests involved drilling an equal distance of about 1,5 m at a set rate of advance so the results were comparable without further standardising. It was found that diamond size strongly affected the bit opening and resharpening procedure. The coarse mesh size bits had to be drilled for at least 1 m in sandstone to remove the first layer of diamonds. The bits with the finest mesh size diamonds were very rapidly worn and were opened or reconditioned after drilling only 100 mm of the same material. Detritus size distribution analysis and diamond wear type counts were done for most of the tests. The results of this series of tests, aimed at evaluating the effect of diamond size on drilling performance, are presented in Figs. 5.40 to 5.49. For convenience of plotting the different mesh ranges are represented by the largest diamond size in the distribution.

Relationships Between the Drilling Variables

The mean reactive bit pressure at constant rate of advance rose with increasing diamond size (Fig. 5.40). The results obtained with the four mixed bits were very similar to the results obtained with bits containing diamonds corresponding only to the larger

sizes in the mixed distributions. This was also true for the specific energy data (Fig. 5.41). Effective drilling in Mode 2 without much variation in efficiency was possible using a wide range of diamond sizes from about 40 mesh to 60 mesh. The bits containing 30/40 mesh and 20/30 mesh stones drilled suboptimally, in Mode 1, but the mixed 20/30 plus 40/50 mesh bit drilled in Mode 2. Only half the stones in this latter bit fell into the 20/30 mesh interval and were too sparse to develop sufficient wear flat area to support the load and impede drilling. The 40/50 plus 60/80 mesh mixed bits performed no differently from the plain 40/50 mesh bits.

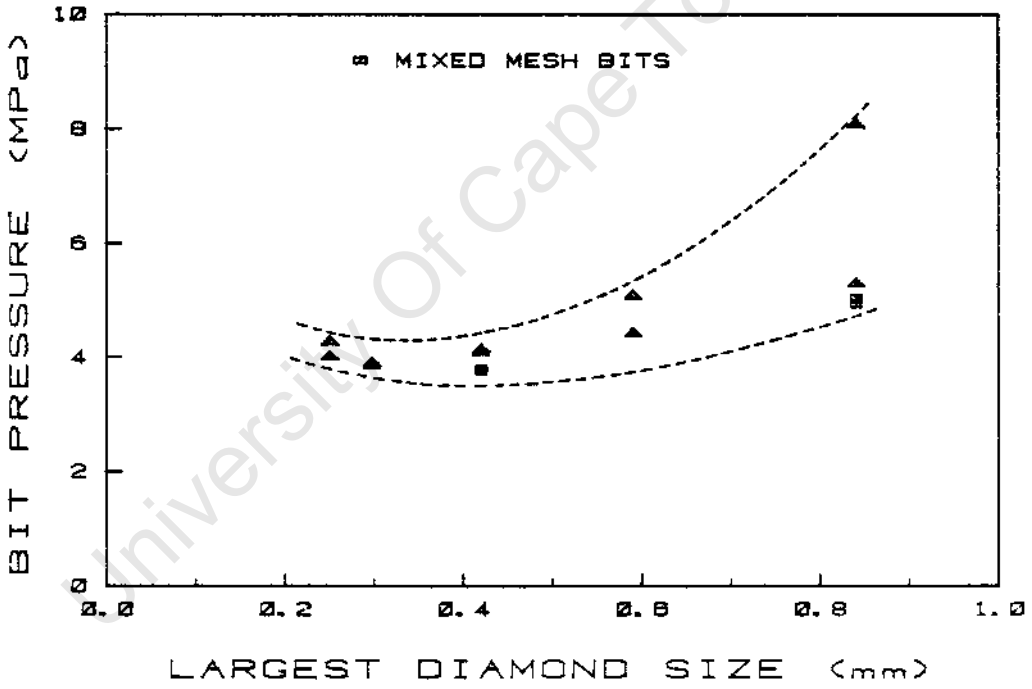

FIGURE 5.40 : Plot of mean bit pressure against diamond size for tests drilled in norite at 0,044 mm/rev set rate of advance showing a minimum at finer diamond size

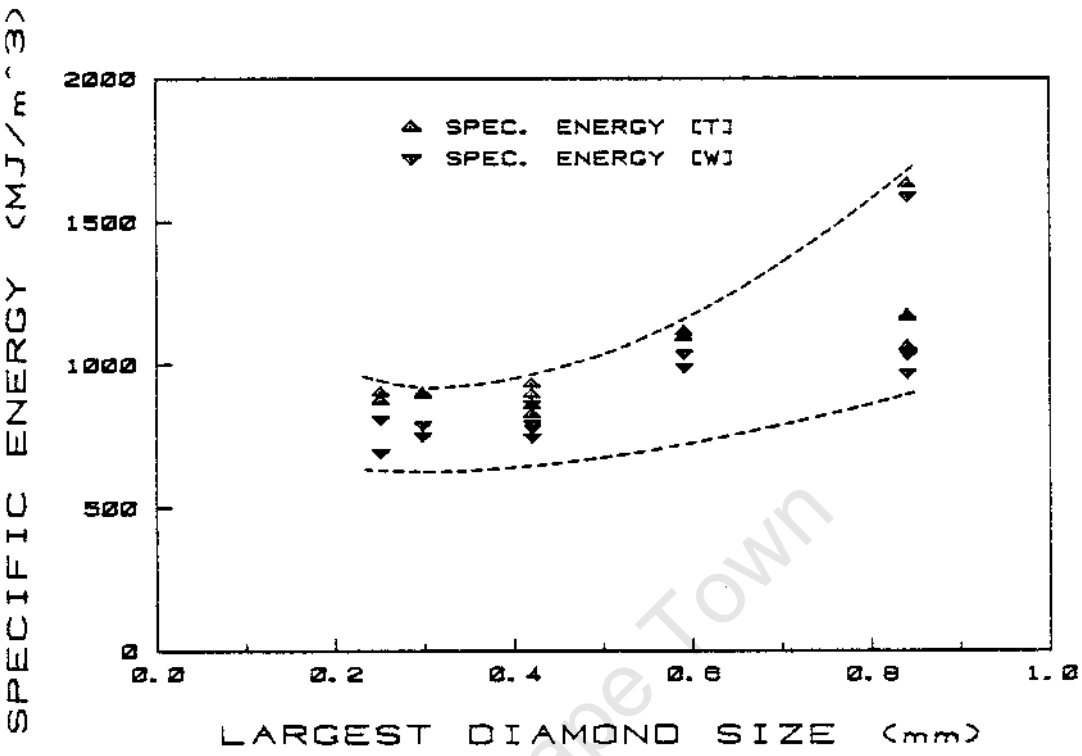

FIGURE 5.41 : Plot of specific energy against diamond size for tests drilled in norite at 0,044 mm/rev set rate of advance showing a minimum at finer diamond size

Bit Wear and Diamond Wear

The bit wear values, both specific bit mass loss and linear bit wear were very scattered for the coarse diamond mesh bits (Fig. 5.42). The relatively low number of stones in these bits led to unpredictable and uneven wear due to the crucial influence of the loss of individual stones. The bits with finer stones suffered less erratic wear with the bits containing the smallest diamonds wearing the least. When drilling norite the more numerous small stones in these bits shielded the matrix from wear. The mixed bits showed a different kind of shielding. There was a greater proportion of exposed but unworn stones on these bits due to shielding of the numerous smaller stones by the less numerous larger ones.

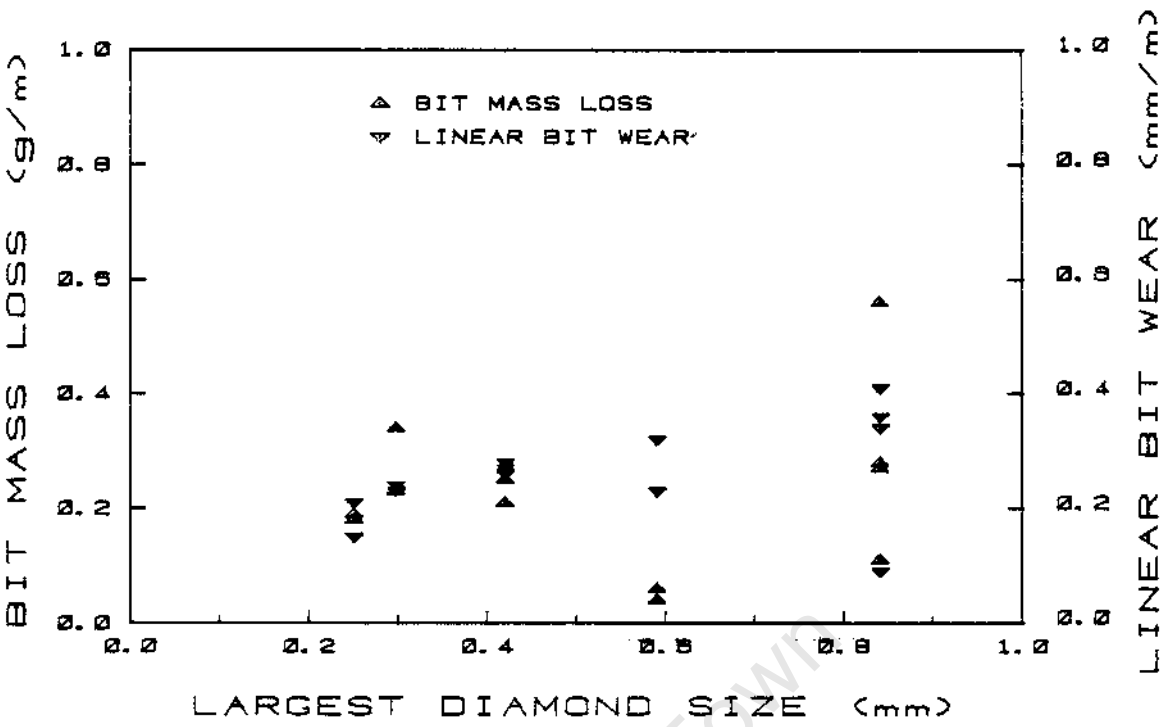

FIGURE 5.42 : Plot of bit wear against diamond size for tests drilled in norite at 0,044 mm/rev set rate of advance, showing less scatter for larger diamond sizes

The relation between Type 1 and Type 2 diamond wear is presented in Fig. 5.43 as the ratio of Type 2b to Type lb wear. The two coarse mixed mesh bits drilled in Mode 2 with wear Type 2b predominant because the effective concentration of the 20/30 mesh stones had been halved. The other 20/30 mesh bits drilled in Mode 1; the diamond wear count was done on only one of these bits. The 30/40 mesh bits also drilled suboptimally. All the remaining bits drilled in Mode 2 with no rise in bit pressure with drilling time. For a given concentration there was a diamond size boundary above which drilling took place in Mode 1 at 0,044 mm/rev. For concentration 30 the boundary was between 30 mesh and 40 mesh under the conditions described here. The 60/80 mesh bits drilled in Mode 2 despite the anomalous predominance of Type lb wear over Type 2b. Because the stones were physically so small, individual stones with wear flats were perhaps released by minimal matrix erosion before the total wear flat area on the bit face reached a critical value which impeded drilling.

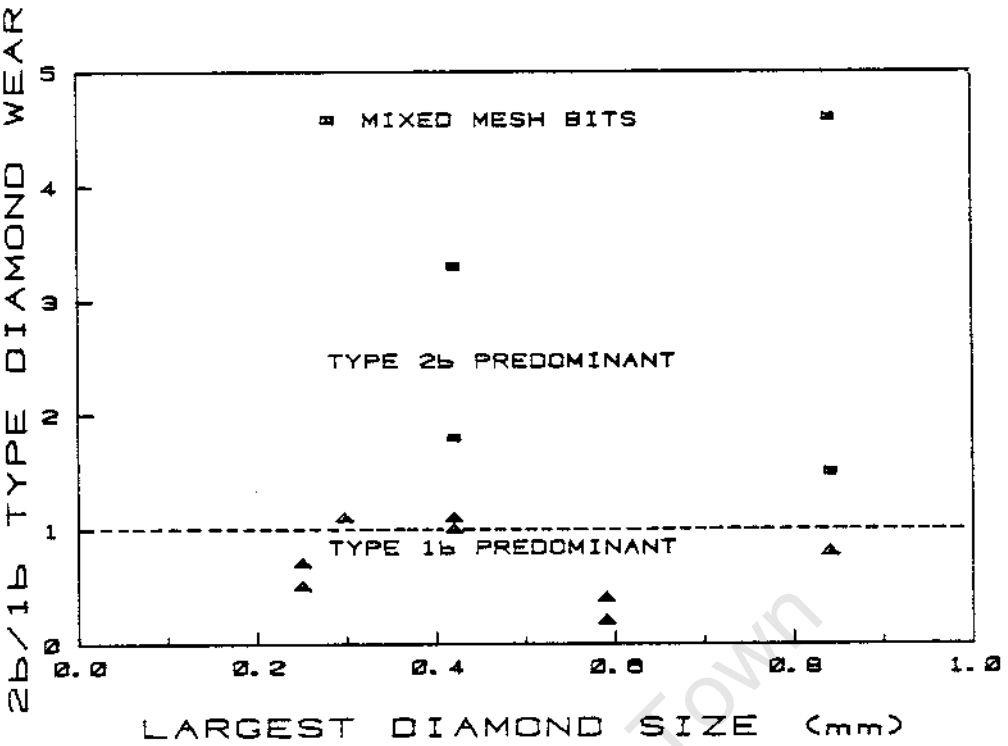

FIGURE 5.43 : Plot of Type 2b/Type lb wear ratio against diamond size for tests drilled in norite at 0,044 mm/rev set rate of advance, distinguishing the predominant wear type

The wear of selected diamonds on the single mesh size bits and mixed mesh bits is illustrated in Figs. 5.44 and 5.45 respectively. The coarsest diamonds of both the single and mixed mesh bits suffered a unique kind of clogging not observed on any other stones (Figs. 5.44(a & b) and 5.45(b & c)). Almost all the microfractured stones had caked detritus firmly packed between the asperities. This material had been scored by the passage of rock particles. In some cases the protruding diamond asperities had been grooved and worn to create small wear flats similar to Type lb wear (Fig. 5.44(b)). Ordinary Type lb wear was also present. The stones on the 30/40 mesh bits had a far more familiar appearance with ordinary Type 1 wear predominating (Fig. 5.44(c)). The wear of the stones on the finest mesh bits was unexceptional. Because of the small size of the stones each one clearly displayed a single unambiguous wear type (Figs. 5.44 (d - f)).

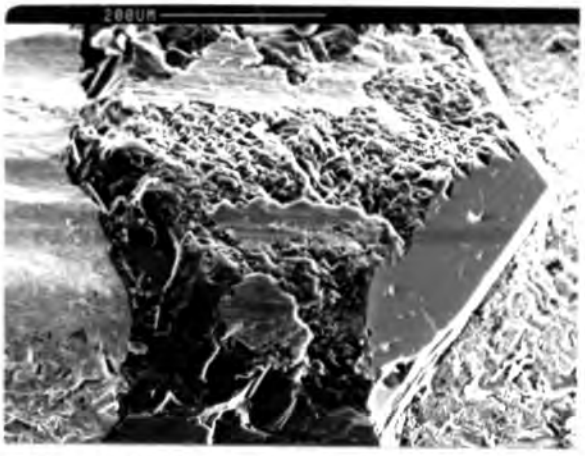

(a) : 20/30 mesh : Type 2b wear - caked with detritus

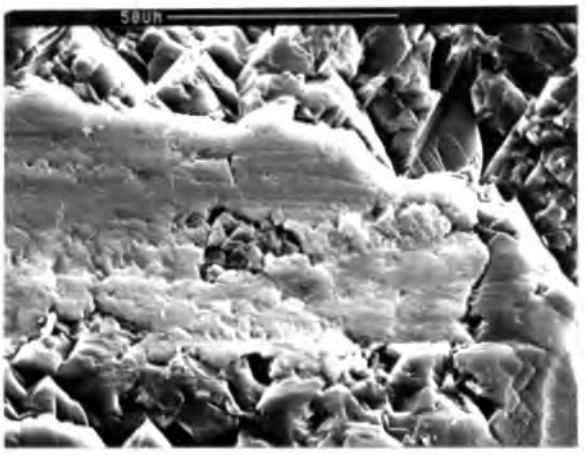

(b) : 20/30 mesh : Detail of (a) - note the rounding of diamond asperities

(c) : 30/40 mesh : Type 1b wear with transverse steps on lower diagonal edge

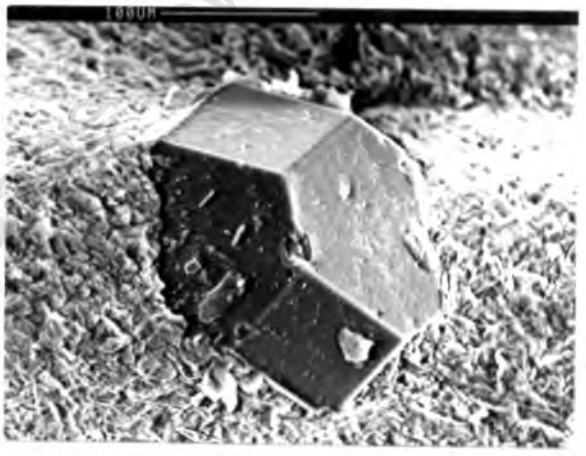

(d) : 60/80 mesh : Type 0b wear - fully exposed unworn stone

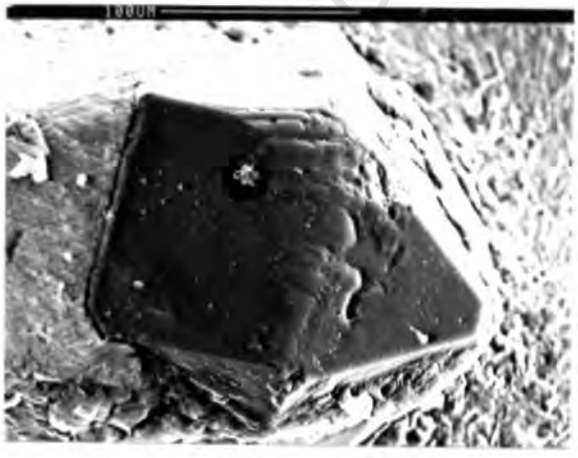

(e) : 60/80 mesh : Type 1b wear - grooved wear flat

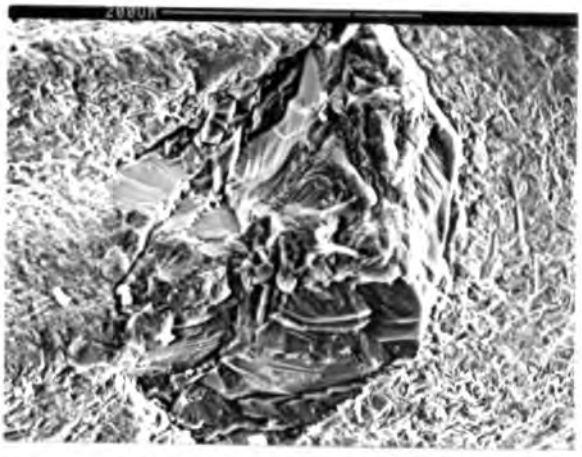

(f) : 60/80 mesh : Type 2b wear - microfracture

FIGURE 5.44 : Wear of selected diamonds from tests with various diamond sizes in norite

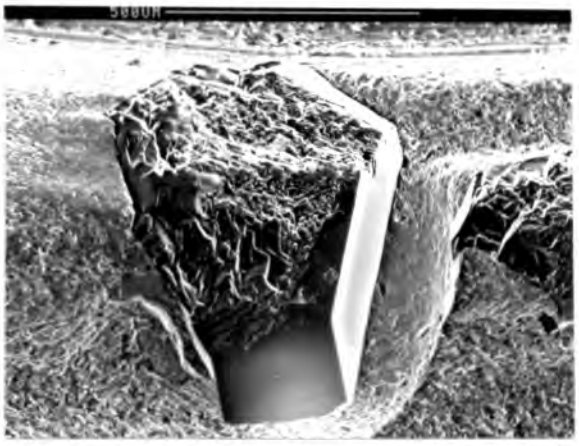

(a) : 20/30 mesh + 40/50 mesh : Typical Type 2b wear - microfracture

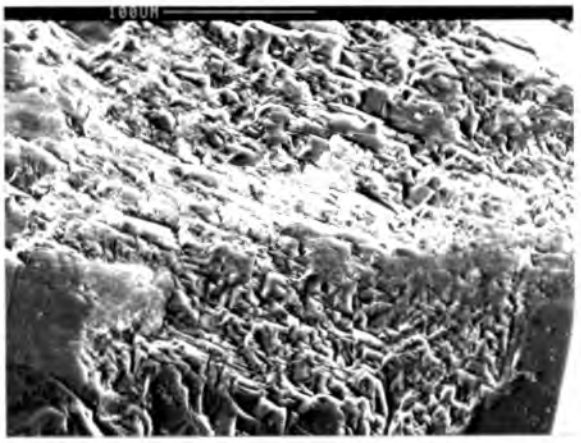

(b) : 20/30 mesh + 40/50 mesh : Detail of (a) - caking with detritus and rounding

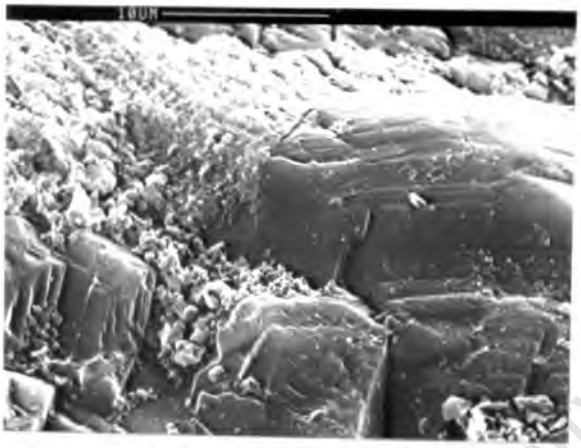

(c) : 20/30 + 40/50 mesh : Detail of (b) - rounded and grooved asperities

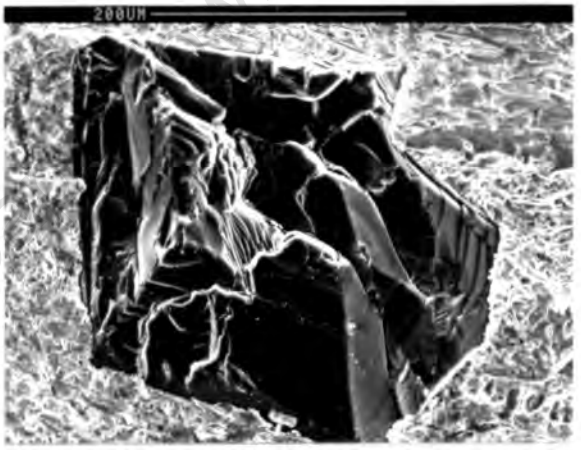

(d) : 40/50 + 60/80 mesh : Type 2b wear - severe fracture

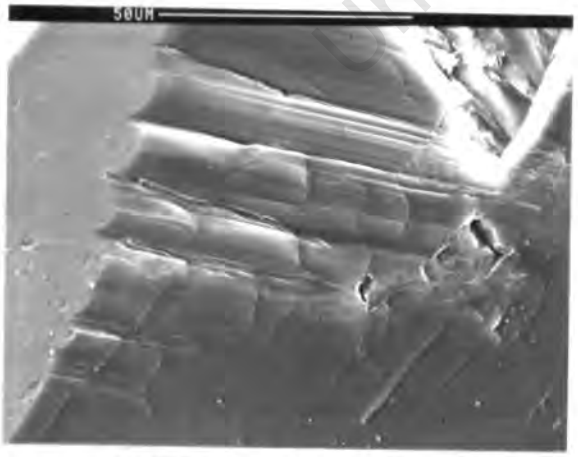

(e) : 40/50 + 60/80 mesh : Type 1b wear - deep grooving on flattened asperity

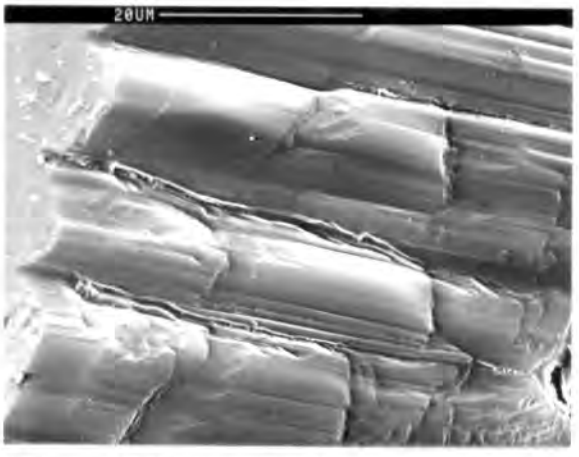

(f) : 40/50 + 60/80 mesh : Detail of (e) showing rounded ridges and transverse steps

FIGURE 5.45 : Wear of selected diamonds from tests with mixed mesh diamond sizes in norite

The coarsest stones on the mixed bits looked similar to those of the single mesh bits except that the degree of clogging was not so great (Fig. 5.45(a - c)). Fig. 5.45(d) shows that Type 2 wear did not always consist of fine microfracture and that a stone could break on a larger scale and still remain essentially intact. Figs. 5.45(e & f) show detail of the trailing edge of a particularly deeply grooved Type 1 wear surface. The crystallographically controlled transverse steps and fractures, the sinuous path of some of the wider grooves, the relative straightness of the narrow ones, and the smooth rounding of the intervening ridges are noteworthy.

Drilling Detritus and Drilling Tracks

The mean particle size of the coarse fraction of the drilling detritus increased with increasing diamond size from 0,098 mm with bits containing fine 60/80 mesh diamonds to 0,121 mm for the coarse 20/30 mesh bits (Fig. 5.46). The averages of the mean coarse detritus sizes produced by each diamond mesh size were calculated and plotted as mean drilled particle size against the largest grain size of each diamond mesh range (Fig. 5.47). It was evident that either large diamonds did not indent the rock to the same proportion of their diameter as the smaller ones, or regrinding reduced all the detritus particles to a nearly uniform size range irrespective of diamond size. The percentages of fine material under 63 microns for these tests were uninformatively scattered around an average value of 78% (and hence were not plotted).

Punch-through discs of rock were made with all the bits except the 40/50 mesh formulation which had already been studied under similar drilling conditions. SEM photographs of the drilling tracks are presented in Figs. 5.48 & 5.49. A comparison of all the photographs of the full width of the drilling tracks (at about 30X magnifiction) showed remarkably little difference between them.

The scale of fracture was determined by the rock fabric. The photographs of detail revealed mashed flakes on each sample and the cleavage controlled fracture of the mineral grains of the rock substrate. Figs. 5.48(c & d) show the many layered nature of some of the mashed flakes. They were built up by several passes of stones which mashed and partly sintered very fine rock flour into plastic masses smeared out under pressure between the hot diamonds and the rock surface. Plastic grooving of the flakes by asperities on the diamond surfaces was visible as well as tensional cracks on the edges of the most superficial layers of the flakes.

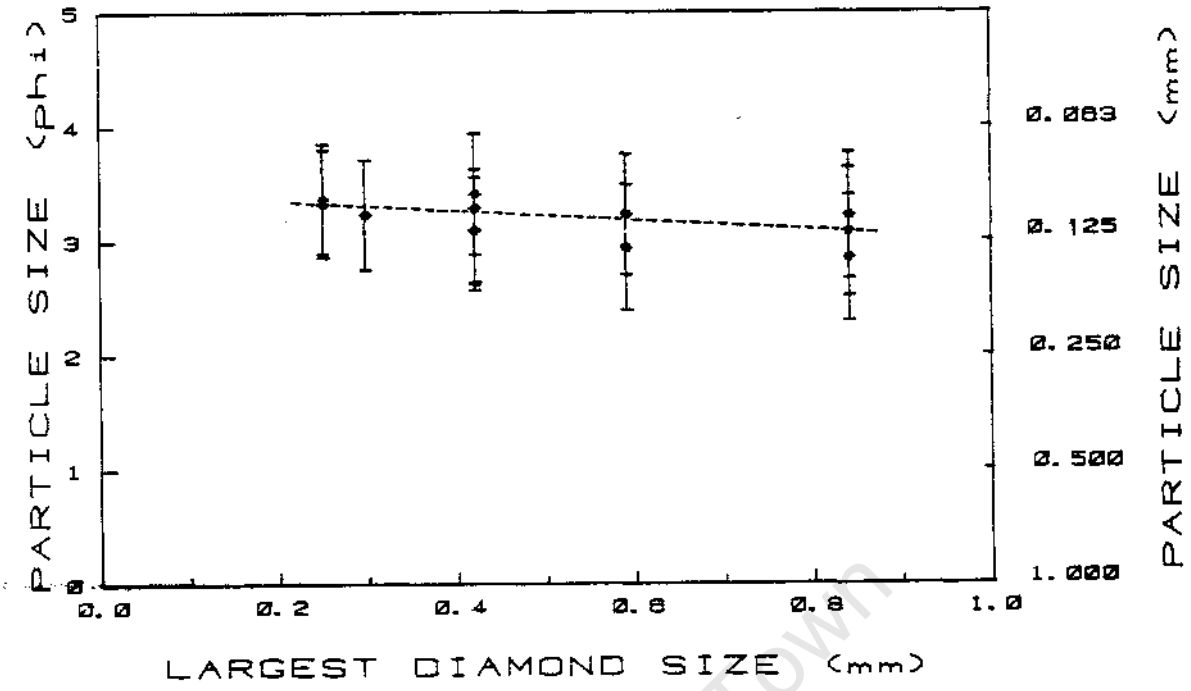

FIGURE 5.46 : Plot of particle size distribution of detritus between 2 mm and 0,063 mm against diamond size for tests drilled in norite at 0,044 mm/rev set rate of advance, showing increasing trend in mean detritus size with increasing diamond size

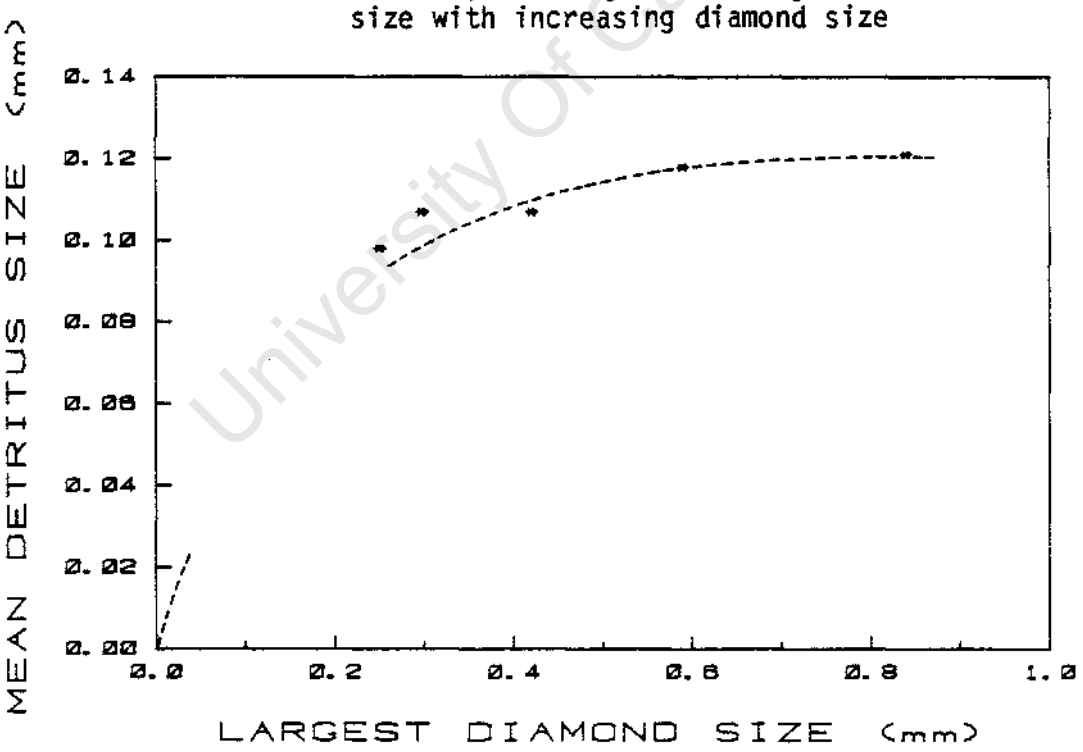

FIGURE 5.47: Plot of mean particle size of coarse detritus against diamond size for tests drilled in norite at 0,044 mm/rev showing negative exponential relationship between primary detritus size and diamond size

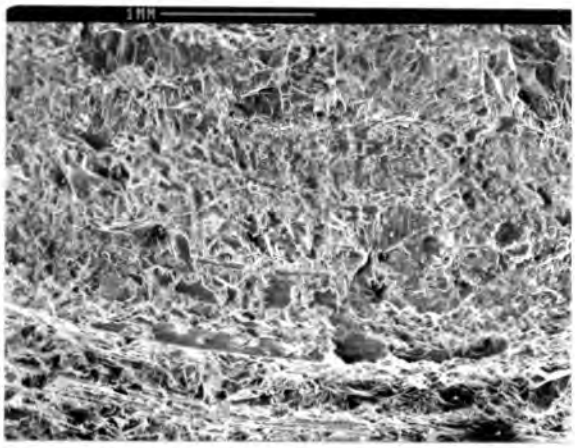

(a) : 20/30 mesh (coarse) : Drilling track

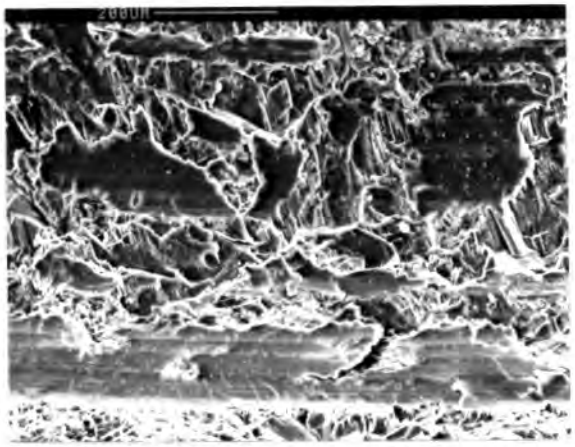

(b) : 20/30 mesh : Detail of (a) - mashed flakes on fractured felspar

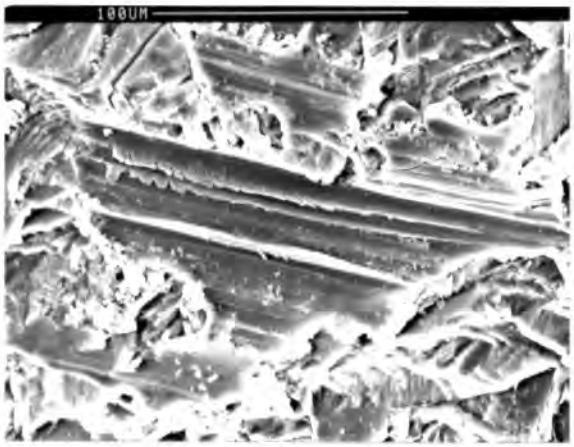

(c) : 20/30 mesh : Mashed flake showing layered structure

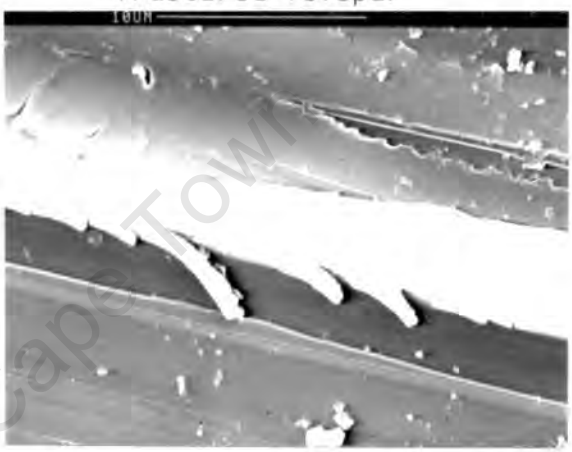

(d) : 20/30 mesh : Detail of (c) - plastic grooving and brittle tearing of compacted flake

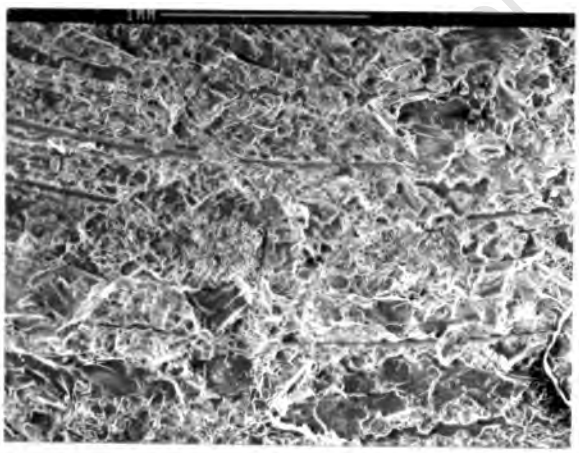

(e) : 50/60 mesh (fine) : Drilling track

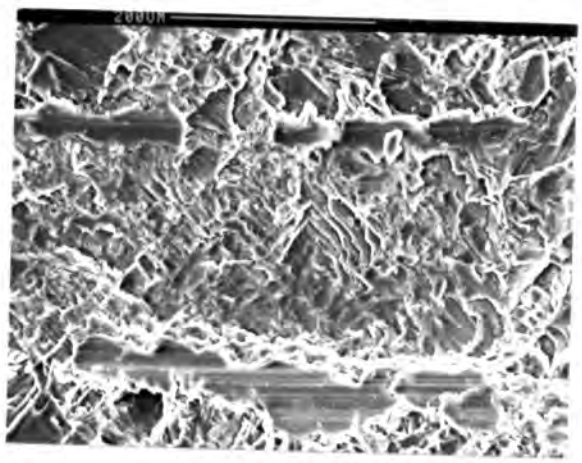

(f) : 50/60 mesh : Detail of (e) - striated flake on cleaved felspar

FIGURE 5.48 : Drilling tracks in norite produced at set rate of advance with bits containing various sizes of diamond

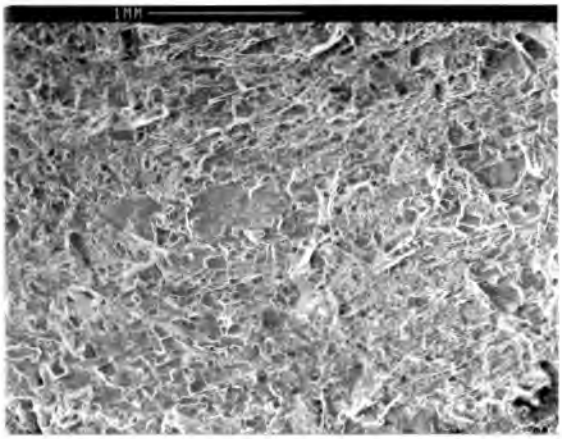

(a) : 60/80 mesh (finest) : Drilling track

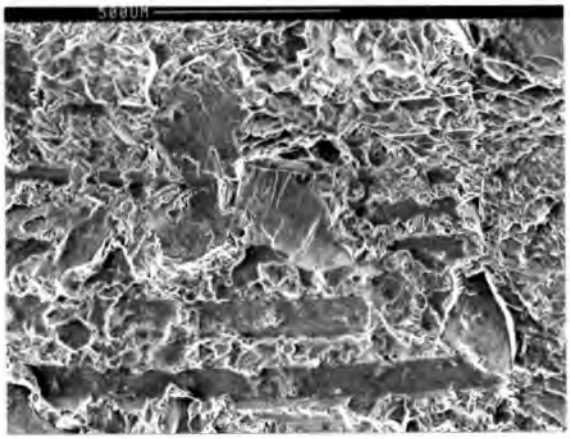

(b) : 60/80 mesh : Detail of (a) - drilling track

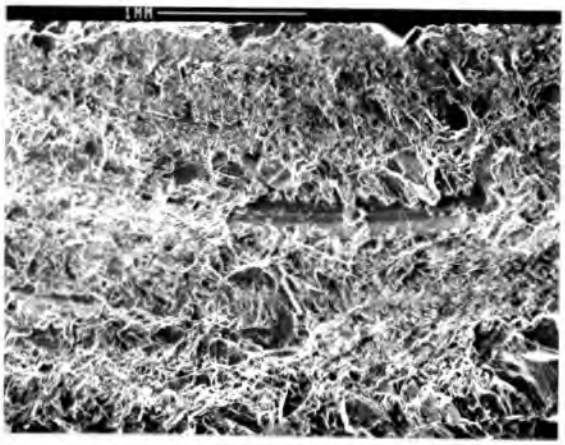

(c) : 20/30 + 40/50 (mixed) : Drilling track

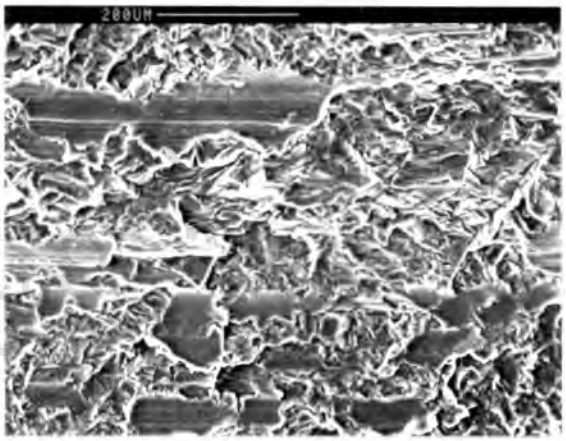

(d) : 20/30 + 40/50 (mixed) : Detail of (c)

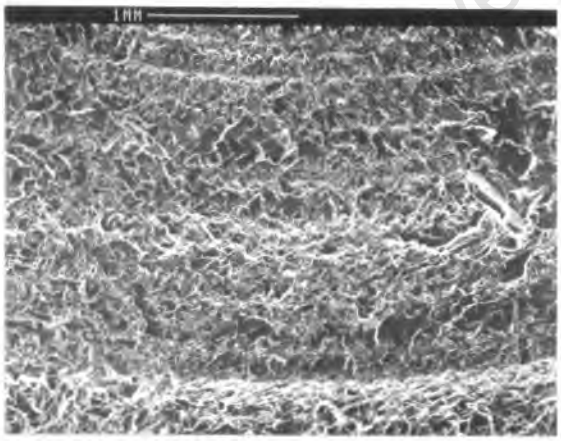

(e) : 40/50 + 50/60 (mixed) : Drilling track

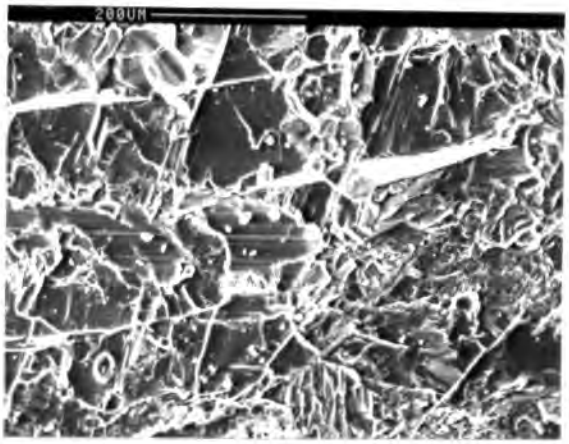

(f) : 40/50 + 50/60 (mixed) : Detail of (e)

FIGURE 5.49 : Drilling tracks in norite produced at set rate of advance with bits containing various sizes of diamond

5.4.5 Tests in Norite at Set Thrust with Different Diamond Mesh Size Bits

Forty seven tests (TESTS 108 - 143) were drilled in norite with microbits of concentration 30 containing nine different diamond mesh sizes ranging from 20/25 US mesh to 70/80 US mesh at set thrusts equivalent to bit pressures of 2,5 MPa, 5 MPa, 7,5 MPa, and 10 MPa. All the tests with the exception of four were 10 minutes long or were stopped after completing 16 holes (about 1,5 m), whichever occurred first. The exceptions terminated prematurely through bit failure, but these all drilled in Mode 2 and so their results were valid for comparison with the others.

Detritus size distributions were determined for all forty seven tests. Diamond wear counts were done for most of them. Eighteen bits were resharpened and re-used before the wear counts had been done so there were no diamond wear values for the tests conducted at 2,5 MPa and 5 MPa. The results of the whole series of tests, which was aimed at trying to find the optimum diamond size in terms of drilling performance and detritus size, are presented in Figs. 5.50 to 5.55. The lines and curves drawn on the plots are merely intended to draw the eye to salient features. Where more than one value was available for a point the average of these values has been plotted.

Relationships Between Diamond Size and the Drilling Variables

The rates of advance of the tests at 2,5 MPa bit pressure were uniformly low with no clear trend (Fig. 5.50). The tests at higher bit pressures had maximum rates of advance at values which indicated that the finer the diamonds the higher the pressures required to perform optimally. At 7,5 MPa and 10 MPa bit pressure the results obtained with the coarsest diamond mesh bits did not follow the prevailing trend; irregular bit wear due to sporadic loss of single large stones sustained penetration rate at the expense of bit life. For the tests drilled in Mode 2 the rate of

advance was strongly influenced by bit pressure especially for the intermediate diamond mesh sizes ranging from 35/40 mesh to 60 mesh. Higher bit pressures generated higher rates of advance without a very substantial increase in specific energy under the optimal operating conditions (see Fig. 5.51). The specific energy minima for the tests at bit pressures of 5 MPa and higher coincided with the rate of advance maxima. It should be noted that at high bit pressures the bits with coarser diamonds gave rise to relatively low rates of advance (and consequently high specific energy) when compared with bits containing smaller stones. When drilling at 2,5 MPa the specific energy had a maximum with bits of intermediate composition. At the highest bit pressure of 10 **MPa the range** of mesh sizes which operates effectively was narrower than at low bit pressures but the optimal rate of advance was much higher with the highest bit pressure.

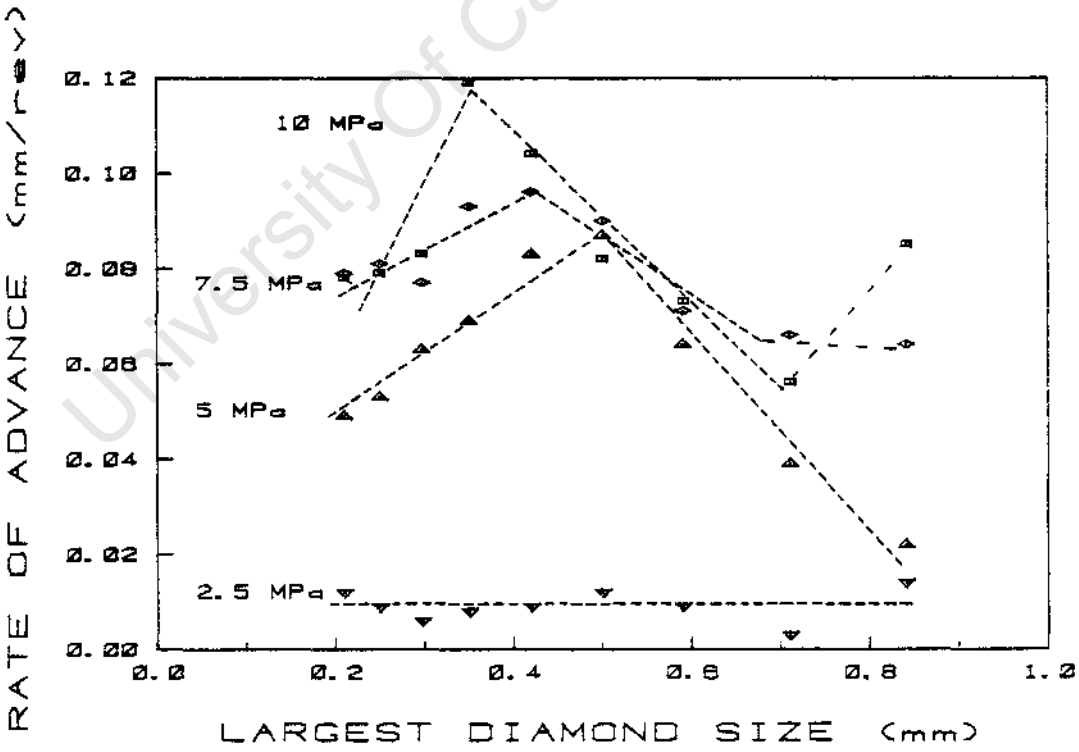

FIGURE 5.50 : Plot of rate of advance against diamond size for tests drilled in norite at set thrust showing maxima with finer diamonds for increasing bit pressure

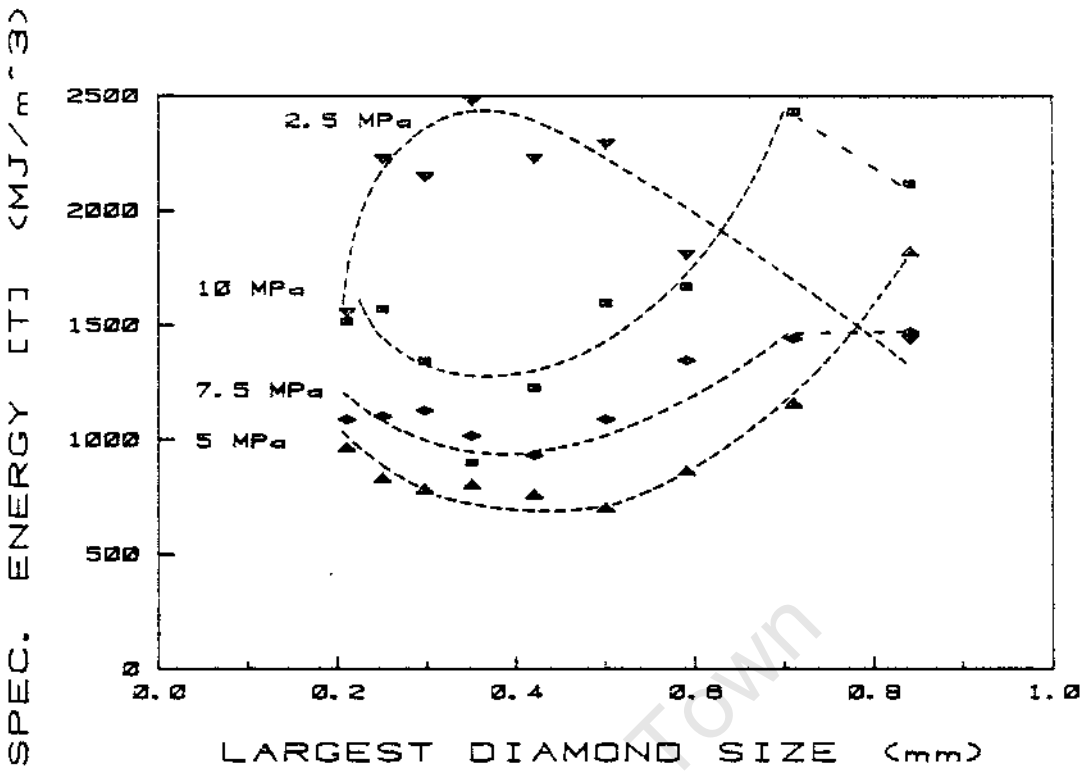

FIGURE 5.51 : Plot of specific energy against diamond size for tests drilled in norite at set thrust showing minima at intermediate diamond sizes for 5 MPa, 7,5 MPa and 10 MPa bit pressure

Bit Wear

The specific linear bit wear values were more scattered than the specific bit mass loss values although both sets of data followed the same trends. At the lowest bit pressure the bit wear values were scattered around a uniformly low value with no discernable trend (Fig. 5.52). With increasing bit pressure the wear of the bits with coarser diamonds increased rapidly. The wear results of the tests with bits with the two coarsest mesh sizes, 20/25 mesh and 25/30 mesh, were generally lower than the trend. This was due to inadequate initial standardisation of these bits. Retention of orientated diamonds on the bit face reduced the initial wear rates and thus lowered the net overall wear of the bits. At the intermediate bit pressure of 5 MPa the bit wear remained moderate over a wide range of diamond mesh sizes. At the highest two bit pressures there was little difference between the trends of bit wear. Moderate rates of wear were only obtained using bits with diamonds finer than 40 mesh at the concentration used.

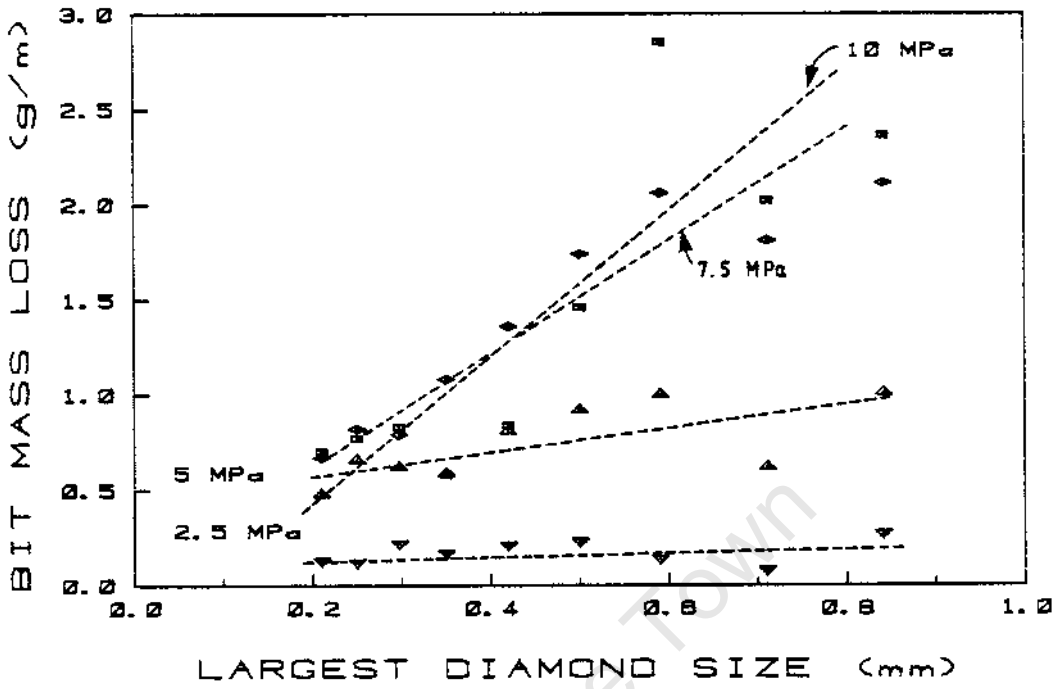

FIGURE 5.52 : Plot of specific bit mass loss against diamond size for tests drilled in norite at set thrust showing increased bit wear with increasing bit pressure and diamond size

Drilling Detritus

The mean size of the coarse fraction of the drilling detritus - between 2 mm and 63 micron - was dependent on diamond mesh size and to a lesser extent on bit pressure (Fig. 5.53). At the lowest bit pressure of 2,5 MPa the mean detritus sizes were scattered but at higher bit pressure the mean detritus sizes tended to increase slightly with an increase in bit pressure. With increasing diamond size the mean detritus size also increased, more so between the finer diamond sizes than the coarser ones. The diamond size and detritus size data have been listed for comparison in Table 5.5 and plotted in Fig. 5.54. The "size ratio" was calculated by expressing the mean detritus size as a percentage of the maximum diamond size in the bit. The effect of bit pressure was small, and the particle size ratio was determined largely by diamond size. The percentage of fine detritus below 63 micron in size was bit pressure dependant and also strongly influenced by diamond size (Fig. 5.55).

TABLE 5.5 : Comparative diamond size and detritus size data

DIAMOND SIZE		DETRITUS SIZE (mm) (SIZE RATIO AS (%))		
(US Mesh)	(mm)*	5 MPa	7,5 MPa	10 MPa
20/25	0,84 - 0,71	0,115 (14)	0,131 (16)	0,145 (17)
25/30	0,71 - 0,59	0,113 (16)	0,128 (18)	0,127 (18)
30/35	0,59 - 0,50	0,122 (21)	0,127 (22)	0,136 (23)
35/40	0,50 - 0,42	0,115 (23)	0,124 (25)	0,124 (25)
40/45	0,42 - 0,35	0,104 (25)	0,121 (29)	0,108 (26)
45/50	0,35 - 0,297	0,108 (34)	0,113 (35)	0,110 (34)
50/60	0,297 - 0,250	0,103 (35)	0,085 (29)	0,092 (31)
60/70	0,250 - 0,210	0,097 (39)	0,097 (39)	0,013 (45)
70/80	0,210 - 0,177	0,084 (40)	0,086 (41)	0,092 (44)

* from : Hench and Gould (1971)

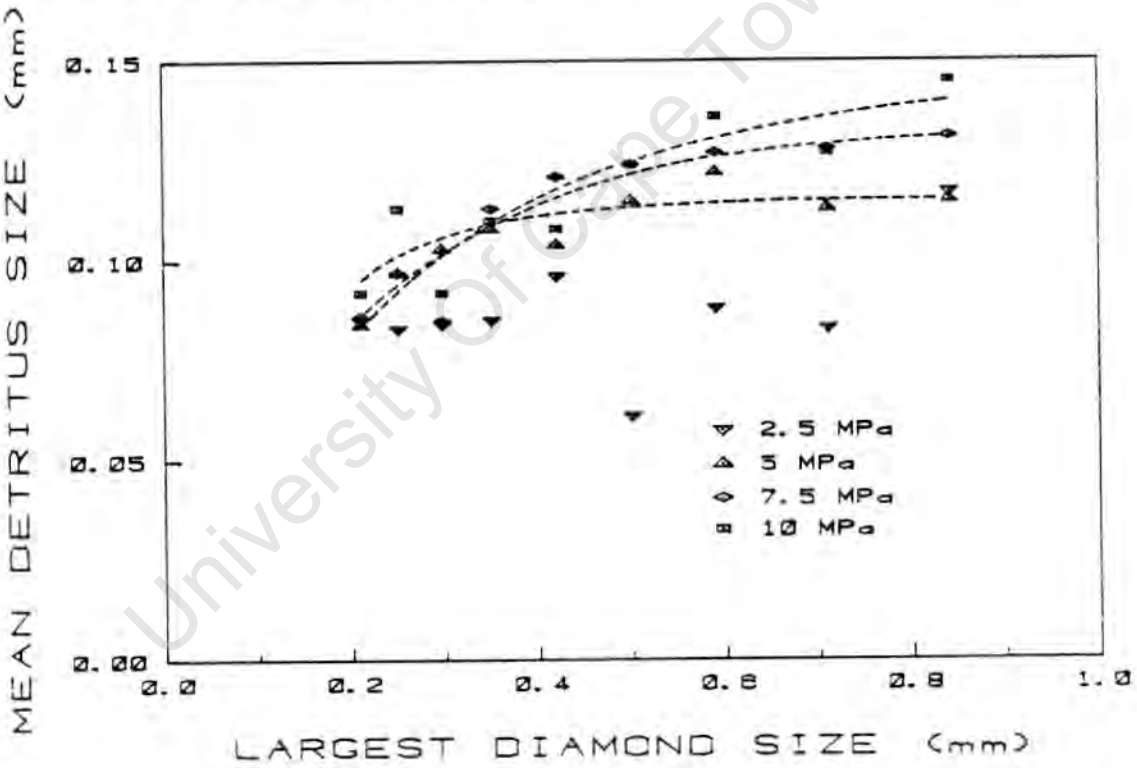

FIGURE 5.53 : Plot of mean particle size of coarse detritus against diamond size for tests drilled in norite at set thrust showing negative exponential relationship between particle size and diamond size

At the lowest bit pressure of 2,5 MPa all the tests drilled in Mode 1 with enhanced regrinding due to low rates of advance and little production of large particles. For bit pressures above 5 MPa the percentage of fine material increased with increasing bit pressure due to increasing comminution of rock particles in the reduced gap between the rock and the bit matrix.

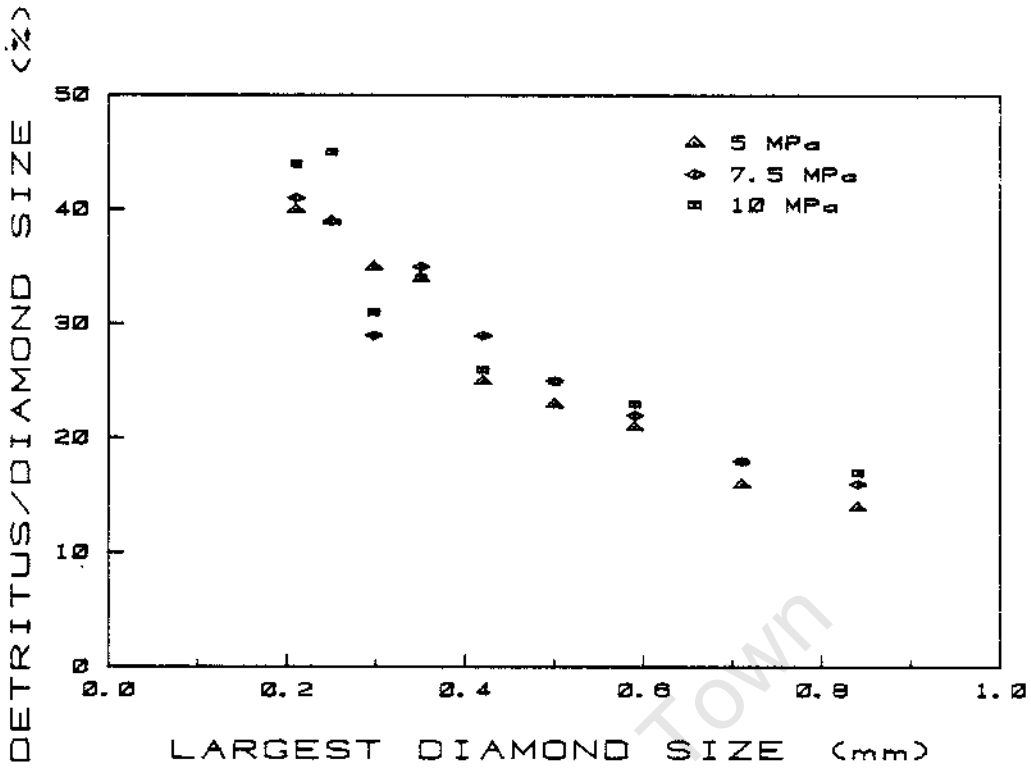

FIGURE 5.54 : Plot against the diamond size of mean particle size of coarse detritus as a percentage of the diamond size, showing the dependancy of detritus size on diamond size

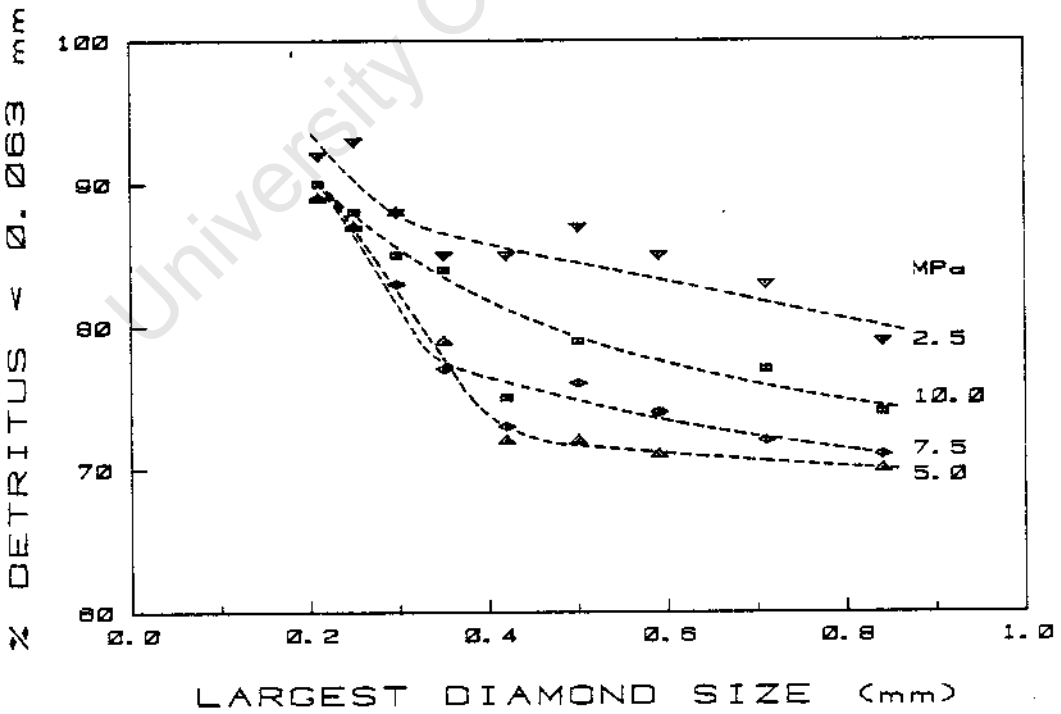

FIGURE 5.55 : Plot of percentage detritus by mass below 0,063 mm in size against diamond size for tests drilled in norite at set thrust showing strongly increasing percentage fines with finer diamonds

5.4.6 Tests at Set Rate of Advance with Two Different Diamond Sizes in Norite and Quartzite

Thirteen tests (TESTS 160 - 172) were drilled in norite and quartzite with 20/30 mesh and 50/60 mesh bits of concentration 30 at three different set rates of advance, excluding 0,1 mm/rev because previous tests at this rate of advance had tended to stall. Two tests at 0,011 mm/rev suffered severe vibration which temporarily disabled the torquemeter. The conditions of this test series are summarised in Table 5.6. The results are presented in Figs. 5.56 to 5.60.

TABLE 5.6 : Summary of results of comparative tests in norite and quartzite

ROCK	DIAMONDS (US Mesh)	RATE OF ADVANCE (mm/rev)	MODE	PERFORMANCE
Norite	20/30	0,011	2	Vibration damage
		0,033	1	Suboptimal
		0,044	1/2	Marginally operational
Norite	50/60	0,011	1	Suboptimal
		0,033	1/2	Marginally operational
		0,044	1/2	Marginally operational
Quartzite	20/30	0,011	2	Vibration damage
		0,033	1	Suboptimal
		0,044	1	Suboptimal
Quartzite	50/60	0,011	1	Suboptimal
		0,033	1	Suboptimal
		0,044	1	Marginally operational

Drilling Parameters

The trends in reactive bit pressure with changing rate of advance in drilling norite and a medium strength auartzite were determined more by diamond mesh size than by rock type (Fig. 5.56). The finer mesh bits experienced a smaller range of bit pressures with different rates of advance, with the coarsest bits at highest rate of advance producing the highest bit pressures. The data for the specific energy calculated from the torque was incomplete due to

the temporary failure of the torquemeter but the trends between these specific energy values and those calculated from the wattmeter were parallel. The specific energy values for the tests drilled at 0,011 mm/rev with 20/30 mesh bits were low because the tests were drilled in Mode 2 (see Fig. 5.57). This was due to the effect of severe vibration and consequent fracture of the diamonds.

The coarser mesh bits generally performed poorly in both rock types. The finer mesh bits approached more economical and optimal behaviour at high rate of advance, when the values of specific energy tended to be lower and converge for both rock types.

Bit Wear and Diamond Wear

The bit wear values were particularly high for the tests drilled at low rates of advance with 20/30 mesh stones (Fig. 5.58). This was due to the damage caused by vibration. The remainder of the bit wear values were moderate with a tendancy for the coarser bits to wear more rapidly at higher rates of advance. The wear of the 50/60 mesh bits was uniformly low because the more numerous 50/60 mesh diamonds masked the bit matrix more effectively. The effect of vibration was evident from the diamond wear counts. Spuriously high percentages of Type 2 wear at low rates of advance with the coarse diamond mesh bits were accompanied by relatively high counts of stones broken off flush with the matrix - about 10% Type 4 wear. The diamonds could not withstand impact.

On the basis of drilling performance and diamond wear the only tests of this series securely in the region of stable operation were those drilled in norite with the 50/60 mesh bits and the test at the highest rate of advance with the 20/30 mesh bit. The latter ended prematurely with the machine stalling as the drilling parameters moved momentarily out of the excessively narrow operating range of this bit in norite.

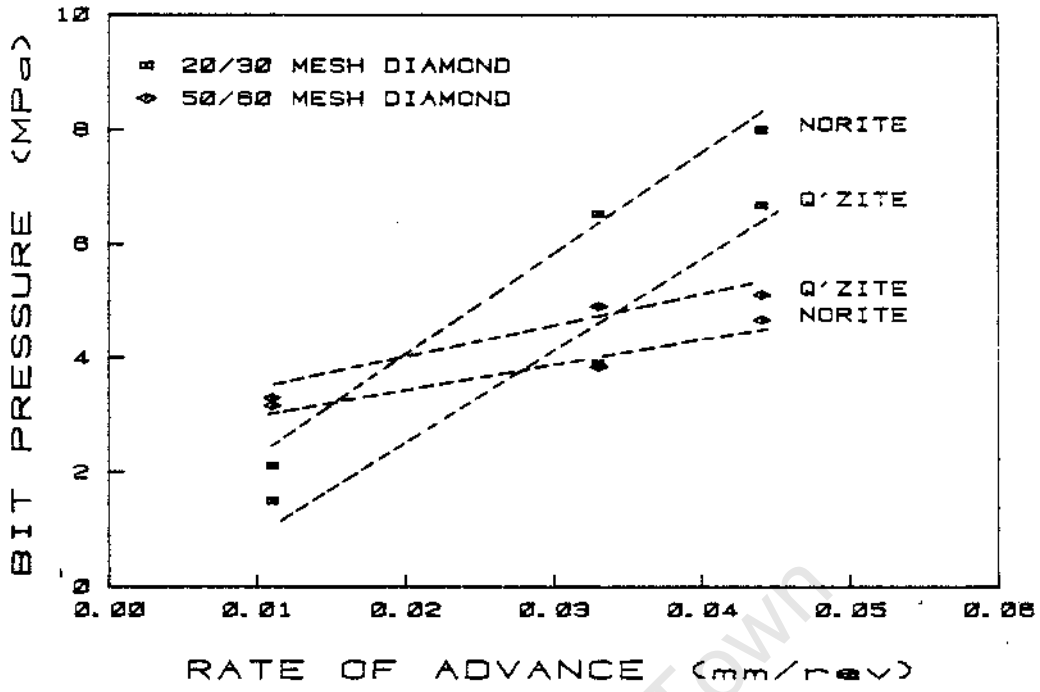

FIGURE 5.56 : Plot of mean bit pressure against rate of advance for tests drilled in norite and quartzite showing the difference in performance of bits with different diamond sizes

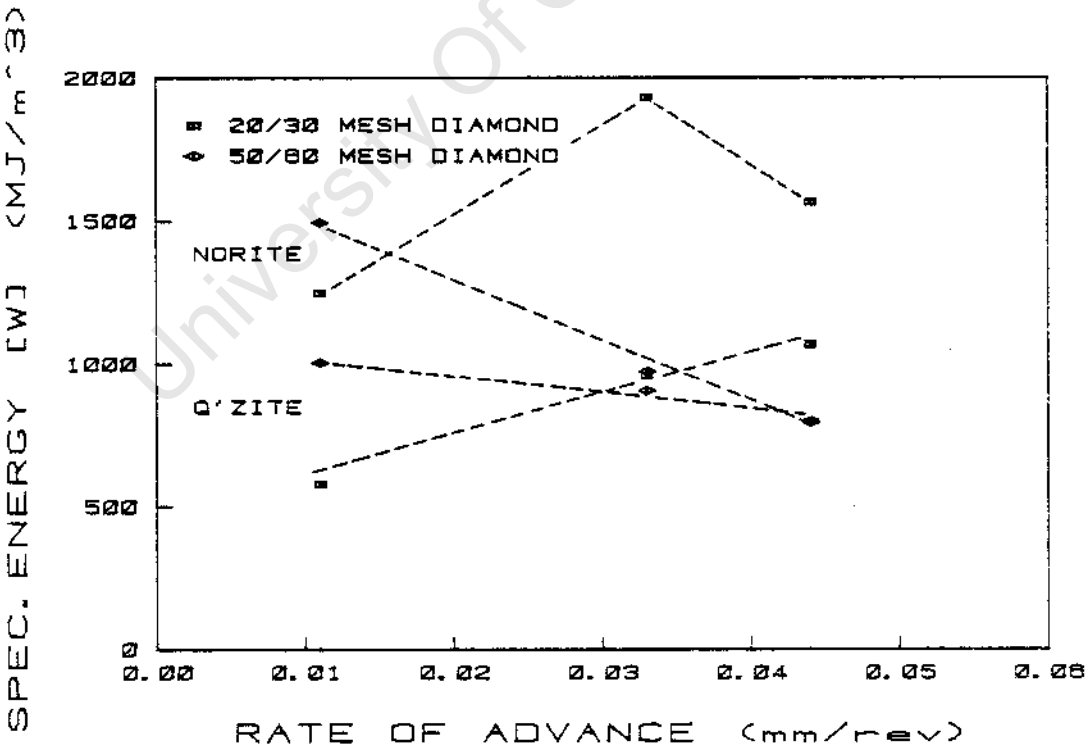

FIGURE 5.57 : Plot of specific energy against rate of advance for tests drilled in norite and quartzite at set rate of advance

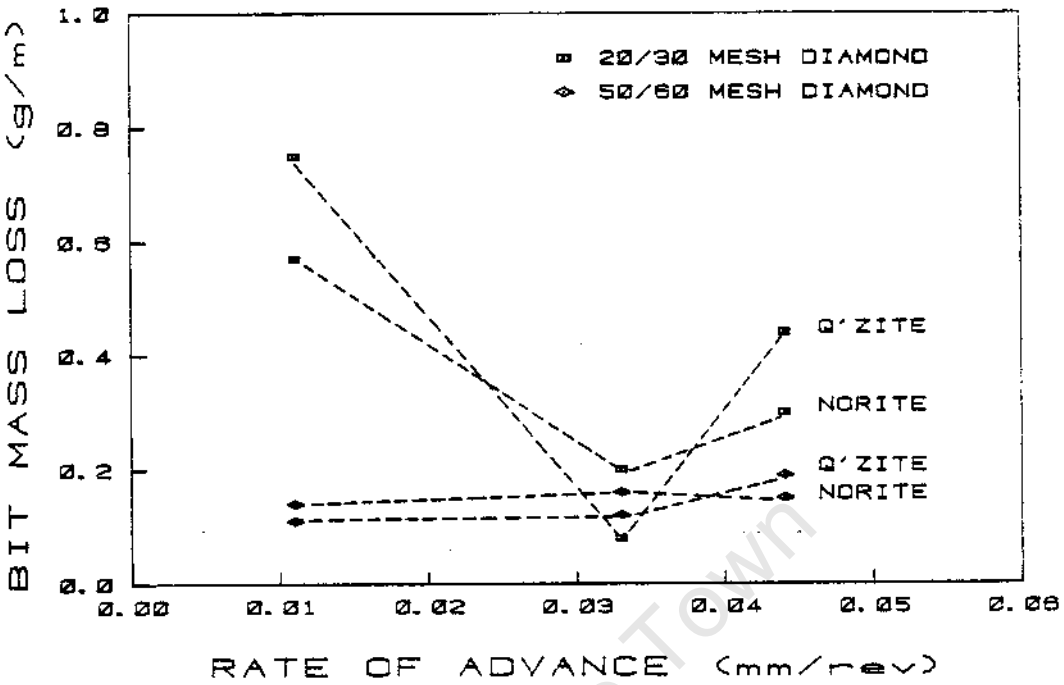

FIGURE 5.58 : Plot of specific bit mass loss against rate of advance for tests drilled in norite and quartzite at set rate of advance, showing more uniform behaviour of the finer 50/60 mesh bits

Drilling Detritus

Apart from one marginal exception at the lowest rate of advance the finer diamond bits consistently produced finer drilling detritus (Fig. 5.59). At the highest rate of advance the coarser mesh bits which drilled at considerably elevated bit pressures produced the largest particles. The results for the test drilled in quartzite at 0,011 mm/rev with the 20/30 mesh bit were somewhat anomalous. Very low bit pressure and specific energy, extreme bit wear, and relatively coarse detritus may have been due to the coarse diamonds excavating whole quartzite grains which had time to escape regrinding because of the low rate of advance. This interpretation is supported by the extremely low percentage of detritus below 63 microns in size (see Fig. 5.60).

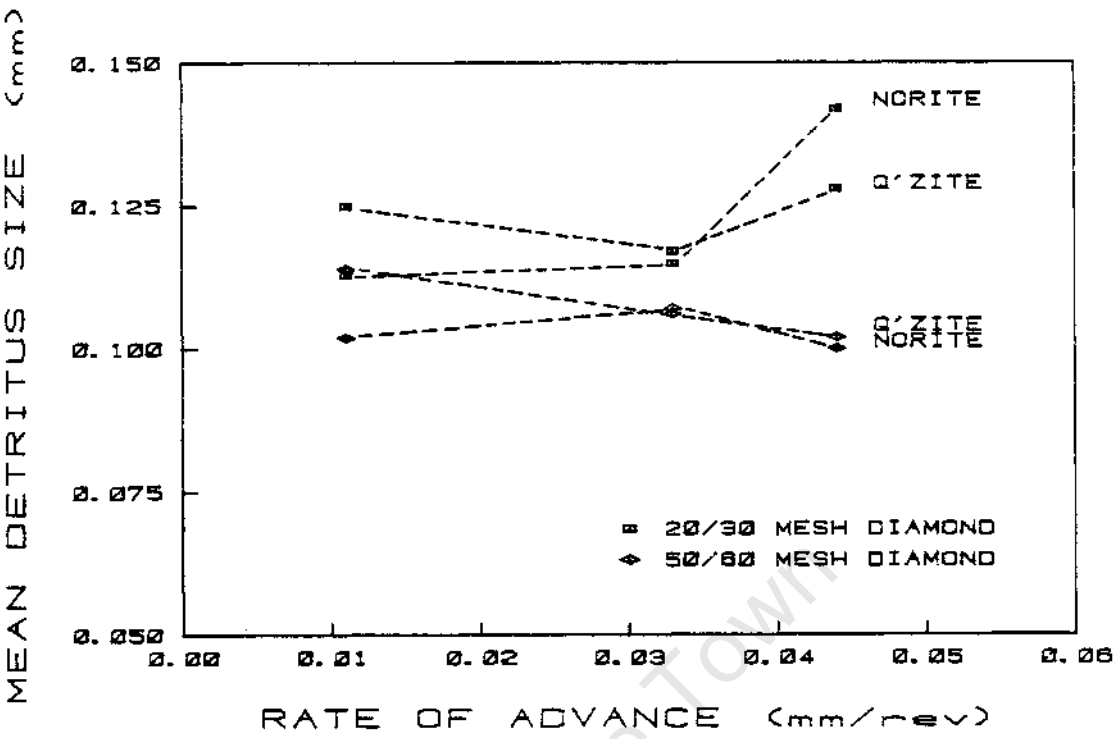

FIGURE 5.59: Plot of mean coarse detritus size against rate of advance for tests drilled in norite and quartzite at set rate of advance

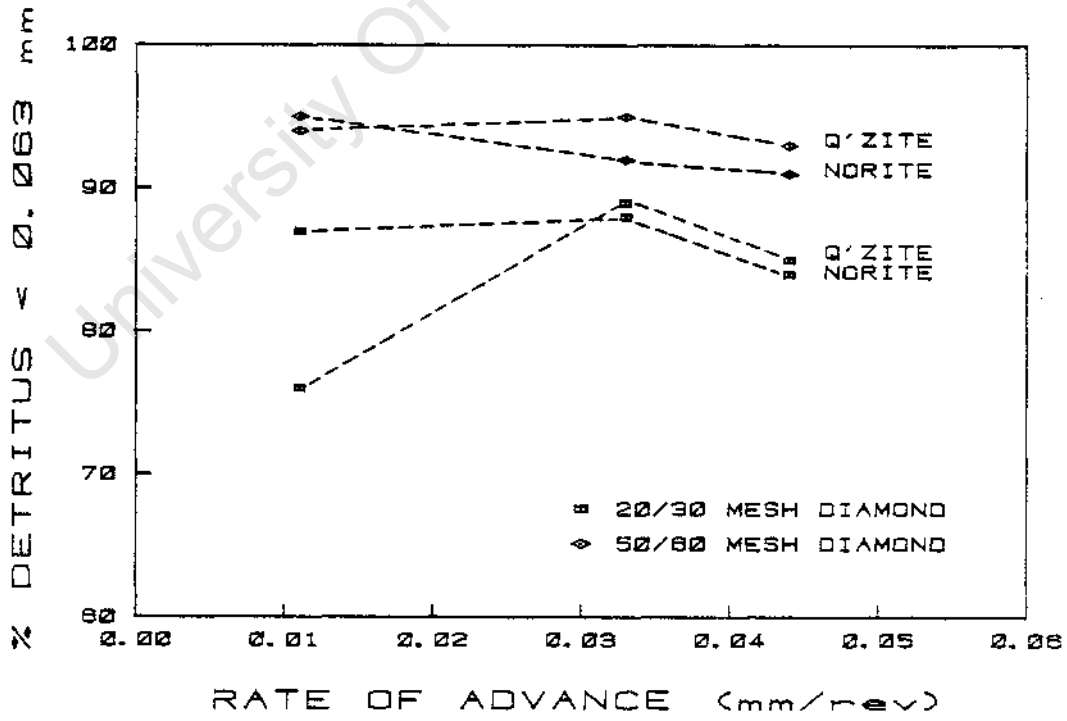

FIGURE 5.60 : Plot of percentage by mass of detritus under 0,063 mm in size against rate of advance for tests drilled in norite and quartzite at set rate of advance

Generally the drilling performance of these tests was determined by the diamond mesh size and not by differences in rock type. The one exception took place at the most uneconomical extreme of drilling performance.

Rock Fracture

Ring cracks were observed on punch-through discs produced in norite and quartzite under a range of loads. It was thought that these cracks might represent an extensive crack field ahead of the drill bit and specimens were drilled out of blocks of norite and quartzite to test this assumption. The specimens were produced by drilling at different set rates of advance with both 20/30 mesh and 50/60 mesh bits into both norite and quartzite. The drill bits were lifted off the rock as rapidly as possible by hand while drilling was in progress. The blocks were then sectioned and polished to expose the rock volume immediately ahead of the drill bit face.

No extensive crack field was observed and the only deformation visible by incident and transmitted light microscopy consisted of a crushed zone extending less than the average grain diameter, with the occasional crack extending into the first layer of crystals of the material exposed to the bit (see Fig. 5.61). Individual diamonds essentially encountered a series of coherent single crystals. The drilling process in the confined bulk of the rock consisted in the summation of the responses of these single crystals to the passage of each diamond under load.

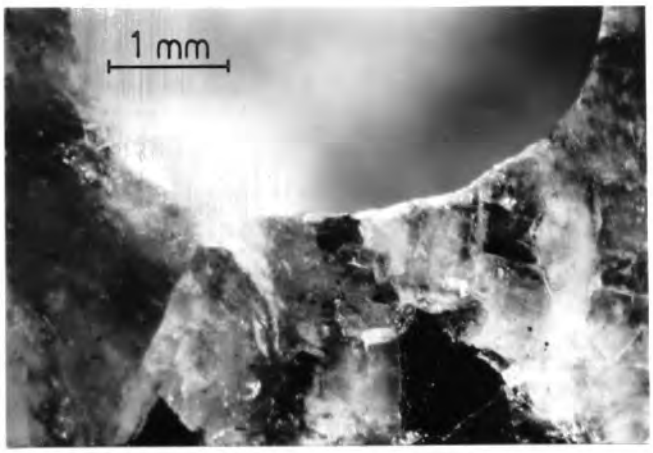

(a) : Norite
Magnification 20 X

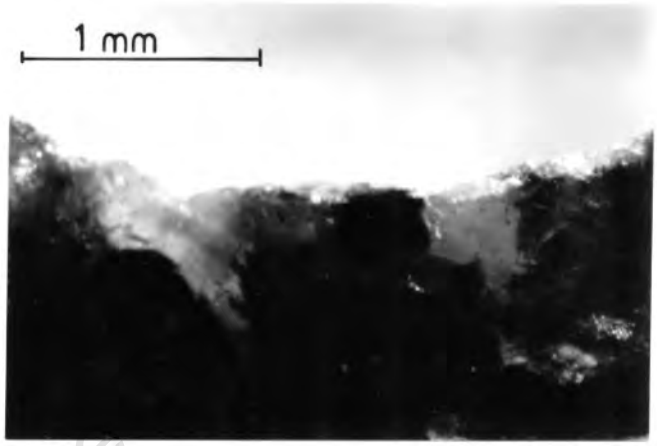

(b) : Norite
Magnification 40 X

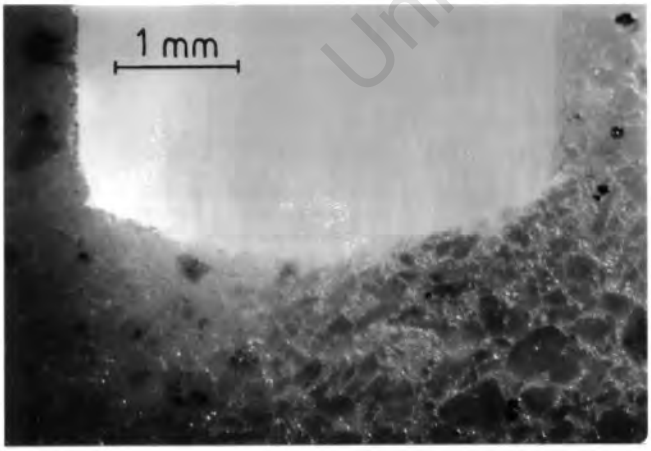

(c) : Quartzite
Magnification 20 X

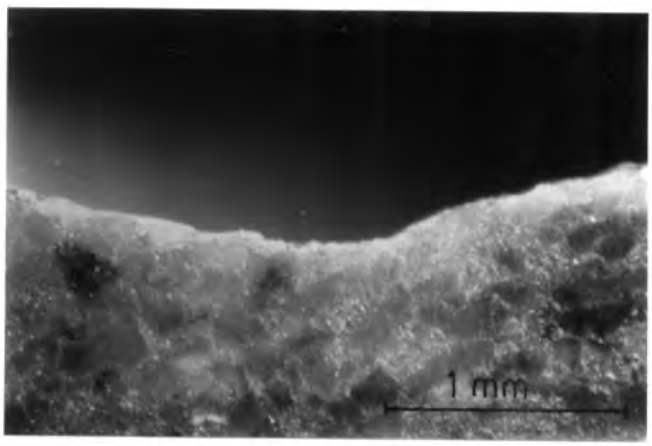

(d) : Quartzite
Magnification 40 X

FIGURE 5.61 : Photographs of sections through drilled tracks in norite and quartzite. Note the absence of an extensive crack field.

5.4.7 Comparative Tests at Both Set Thrust and Rate of Advance on Different Rock Types and Minerals with Standard Bits

A variety of ten different rock types and single crystal minerals were drilled with standard microbits under set rate of advance and set thrust conditions (TESTS 1 - 31, 45 - 52, 177 - 199, and 202 - 205). Not all the materials could be drilled with the full range of parameters used *and* the unavailability of sufficient volumes of some of the materials necessitated short tests for these. However, the majority of tests were 10 minutes long or involved drilling 16 holes (about 1,5 m). The nominal rotational velocity for all the tests was 3500 rpm. Diamond wear counts were done only on the tests drilled at set rate of advance. Detritus size distribution analysis was done for almost all the tests. A general summary of the conditions of this combined series of tests is presented in Table 5.7.

TABLE 5.7 : The materials drilled in comparative tests at set thrust and set rate of advance

TEST NUMBERS	SET PARAMETER	MATERIAL
1-31 & 45-52	BIT PRESSURE 0,5 to 11 MPa	Felspar Granite Light Norite Marble Quartz Syenite Sandstone
177-199 & 202-205	RATE OF ADVANCE 0,011 to 0,1 mm/rev	Calcite Dark Norite Felspar Granite Jaspilite Quartz Quartzite Sandstone Syenite

The granite, quartz and jaspilite could not be drilled effectively for the full 10 minutes or 16 holes for all the test conditions. Some of these tests were so short that their results were invalid. The others were standardised using the first 200 seconds for granite, 300 seconds for quartz, and 45 seconds for jaspilite (Appendix 5: Table A5.3). Where fewer than three points were available for a particular material the results have been excluded from the plots. These tests were intended to provide a comparative set of data to illustrate the differences in response between a variety of materials and the well characterised norite. The results of the tests are presented in Figs. 5.62 to 5.90.

Relationships' "Between the Drilling Variables

The values for the net power consumed in the drilling process were plotted against bit pressure for both sets of results - those drilled under set thrust (Fig. 5.62) and under set rate of advance (Fig. 5.63). Two groups were distinguishable on the basis of these results. The soft materials - sandstone, marble, and calcite - had threshold bit pressures below 1 MPa. The hard materials had threshold bit pressures ranging from 2 MPa to about 3,6 MPa. These threshold bit pressures were determined by linear regression and calculating the intercept on the abscissa at zero net power consumption. They are tabulated in Table 5.8.

TABLE 5.8 : Threshold bit pressures for drilling determined from the power consumption and torque values

MATERIAL	THRESHOLD BIT PRESSURES (MPa)		UNIAXIAL COMPRESSIVE STRENGTH (MPa)
	from POWER CONSUMPTION	from TORQUE	
Calcite	0,28	0,21	-
Marble	0,28	0,23	138
Sandstone	0,84	0,79	41
Dark Norite	2,00	1,36	287
Light Norite	2,13	1,88	209
Quartzite	2,13	1,90	250
Syenite	2,33	1,93	176
Jaspilite	2,37	2,16	489
Felspar	2,77	3,02	219
Granite	3,45	3,58	186
Quartz	3,58	3,57	360

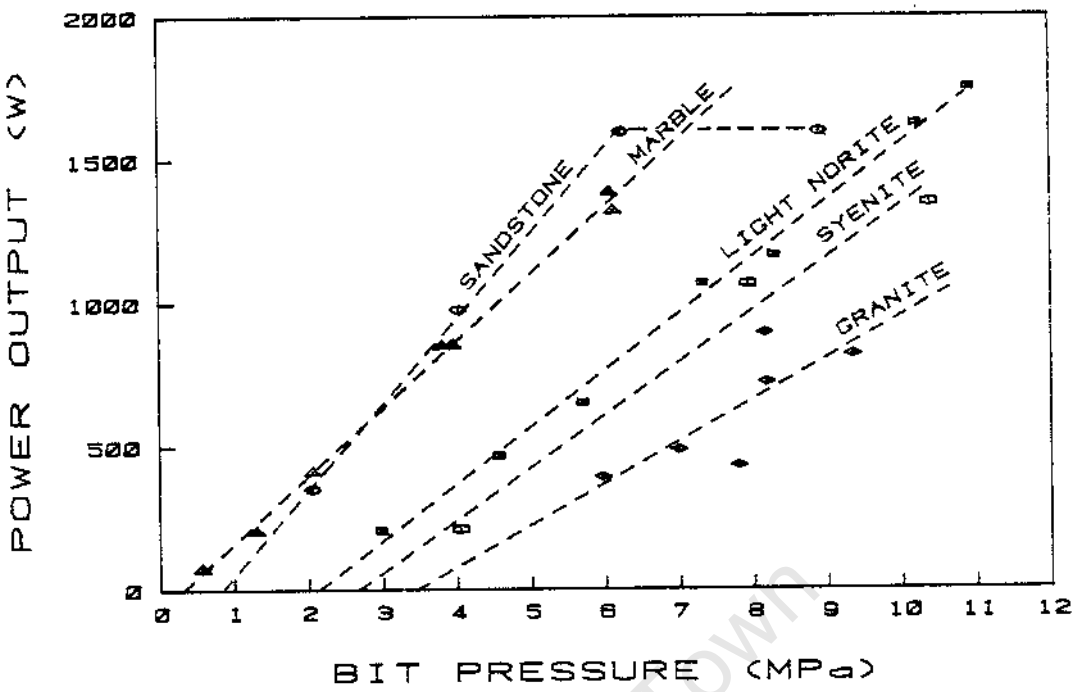

FIGURE 5.62 : Plot showing the predominantly linear relationships betwen net power consumption and bit pressure for tests drilled in a variety of rock types at set thrust

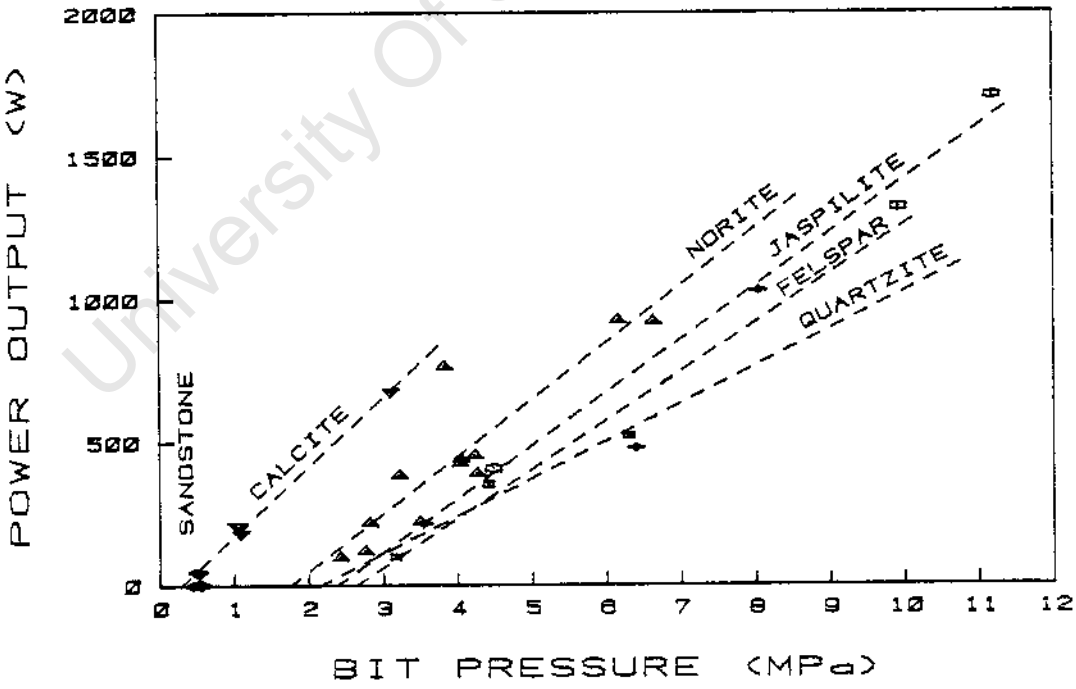

FIGURE 5.63 : Plot showing linear relationship between net power consumption and bit pressure for tests drilled in a variety of materials at set rate of advance

Under set thrust (Fig. 5.62) the relationship between power consumption and bit pressure was linear, particularly so for the materials which were drilled with relative ease - marble, light norite and syenite. The performance in granite was severely suboptimal resulting in greater scatter of the results. In sandstone, at bit pressures higher than a limit of 6 MPa the penetration rate was maintained but at the expense of the bit. Rapid wear of the bit matrix reduced the effective couple between the bit and the rock and lowered the power transmission. At set rate of advance (Fig. 5.63) all the rates used were too low to drill the sandstone optimally - hence very little power was used. The values for norite were augmented by the addition of the results of tests under equivalent conditions described in the section on set rate of advance testing in norite. The values for granite, quartz and jaspilite were consistently low in comparison with the other results because of the short duration of the tests in these materials.

The relationship between generated torque and the bit pressure was also linear for tests at set thrust and set rate of advance (Figs. 5.64 & 5.65). The results for granite were more scattered than for the other materials; and the soft abrasive sandstone was exceptional because of matrix wear as already mentioned. The threshold bit pressures obtained from the torque data are also tabulated in Table 5.8.

The ranking order of threshold bit pressure is almost identical for both sets of values in Table 5.8 although it should be noted that the value for jaspilite is undoubtedly too low because the values were calculated from only 45 seconds of drilling time. Excluding the result for jaspilite the linear best fit regression line between compressive strength and threshold bit pressure from the power data was:

$$y = 56\ x + 85\ (r = 0{,}672)$$

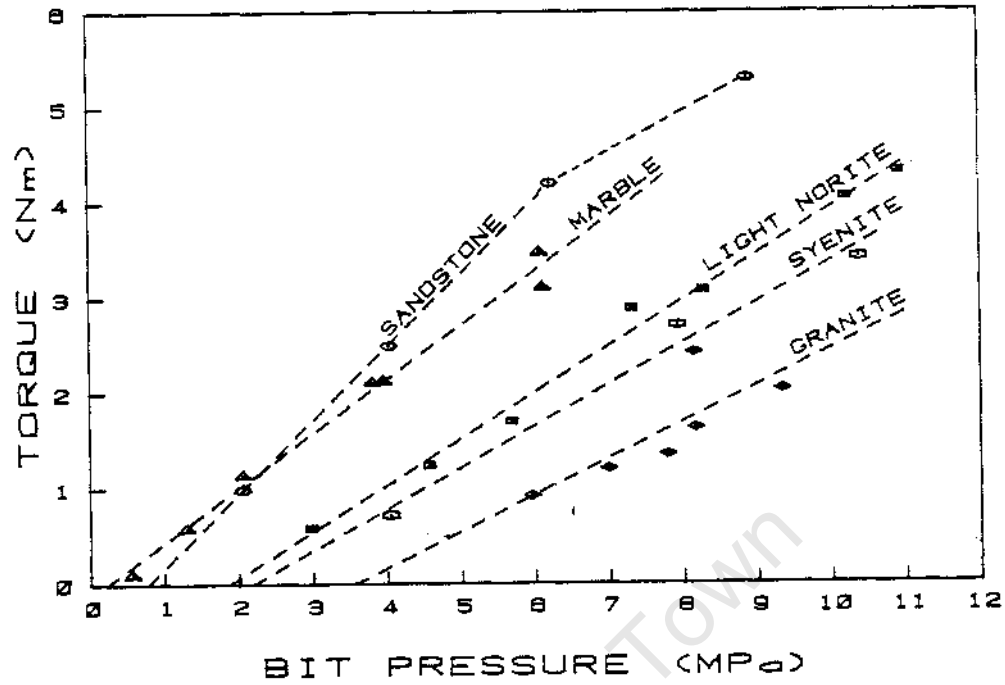

FIGURE 5.64 : Plot showing the linear relationships between torque and bit pressure for tests drilled in a variety of rock types at set thrust

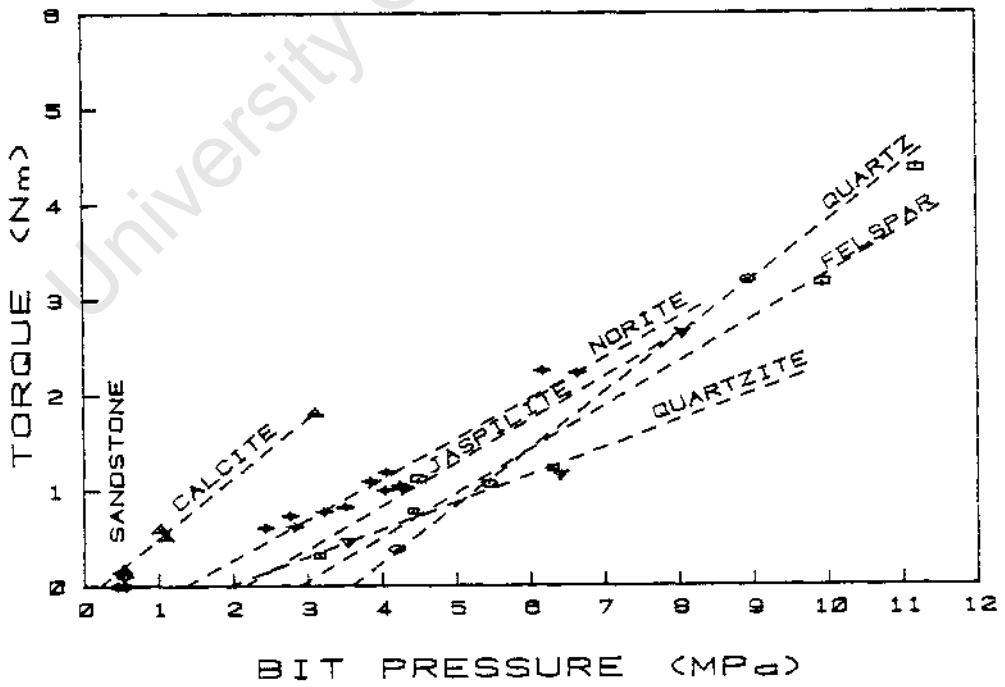

FIGURE 5.65 : Plot showing linear relationships between torque and bit pressure for tests drilled in a variety of materials at set rate of advance

For the tests at set thrust the rate of advance climbed steadily to a maximum and then levelled off or dropped for most rock types (Fig. 5.66). The results for light norite followed the same trend as the dark norite in the initial set thrust tests (see Fig. 5.6). The values for granite were very scattered and low because of the extremely suboptimal behaviour. The rates of advance in drilling sandstone were much higher than in the other rocks, with a slight drop at high bit pressure from the maximum of 0,33 mm/rev. (The plot for sandstone is referred to the right hand vertical axis). At set rates of advance ranging from 0,011 mm/rev to 0,044 mm/rev the reactive bit pressures of all but the anomalously low jaspilite and single crystal quartz were moderate (Fig. 5.67). At 0,1 mm/rev rate of advance the only two materials which did not cause stalling of the machine were calcite and sandstone. At 0,1 mm/rev the sandstone could be drilled easily without any tendency to develop excessive bit pressure.

Under set thrust conditions the specific energy of drilling (calculated from the torque) of each rock type except the granite had a minimum value (Fig. 5.68). This was at higher values of bit pressure for the stronger rocks and out of the range of feasible bit pressures with this drilling machine for the granite. For the softer rocks the curves were broad, indicating a wide operating range with the bits used. At set rate of advance the relationship between specific energy and advance per revolution was not so uniform (Fig. 5.69). At the feasible rates of advance few of the materials drilled in Mode 2 and most of the performance was severely suboptimal. At 0,044 mm/rev the jaspilite and quartz produced very high specific energies. There was a drop in the specific energy for both felspar and norite as they tended towards more optimal behaviour at 0,044 mm/rev. The two softest rocks were drilled with nearly uniform efficiency. Drilling sandstone at the lowest rates of advance required negligible power compared to the error in the measurement. The specific energy values for quartzite were essentially constant with all three tests in the suboptimal Mode 1 region of drilling. For convenience the drilling performance of the tests at set rate of advance are summarised in Table 5.9.

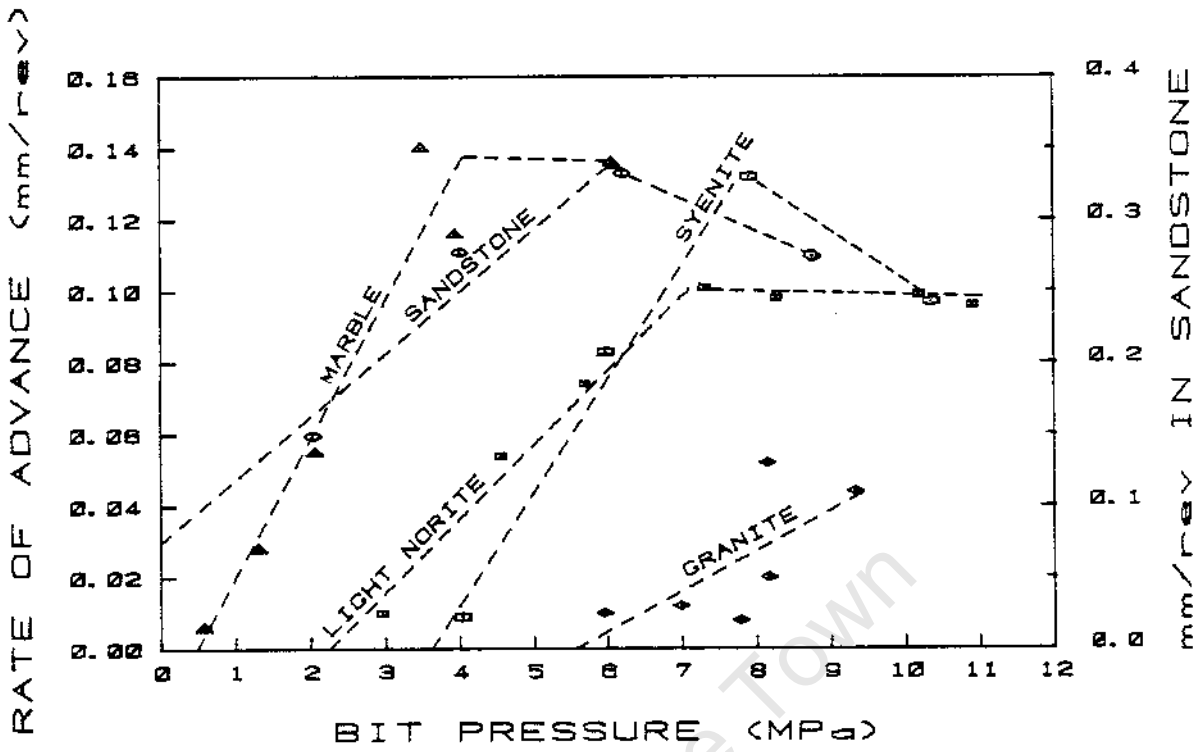

FIGURE 5.66 : Plot of rate of advance against bit pressure for tests drilled in a variety of rock types at set thrust (Sandstone - right hand axis)

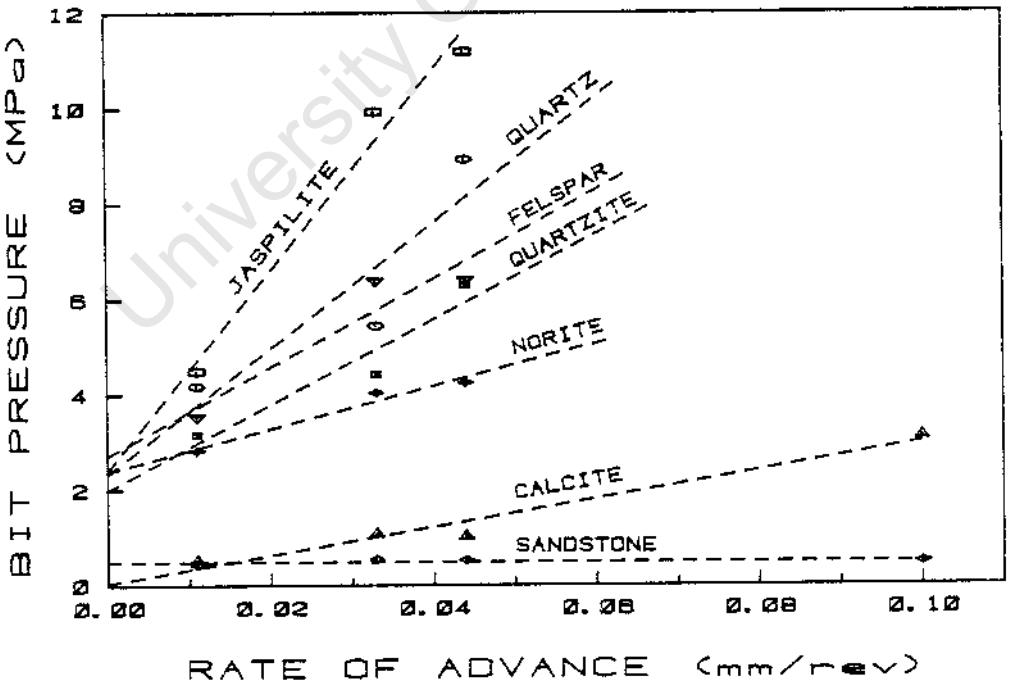

FIGURE 5.67 : Plot of mean bit pressure against rate of advance for tests drilled in a variety of materials at set rate of advance

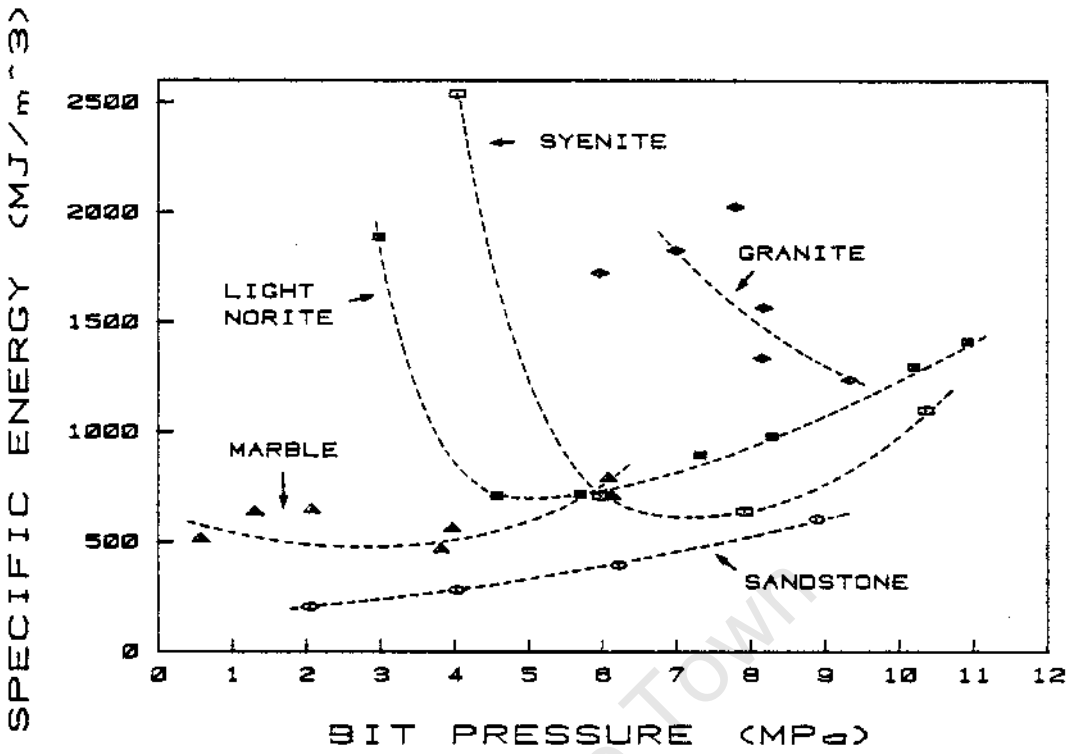

FIGURE 5.68 : Plot of specific energy against bit pressure for tests drilled in a variety of rock types at set thrust

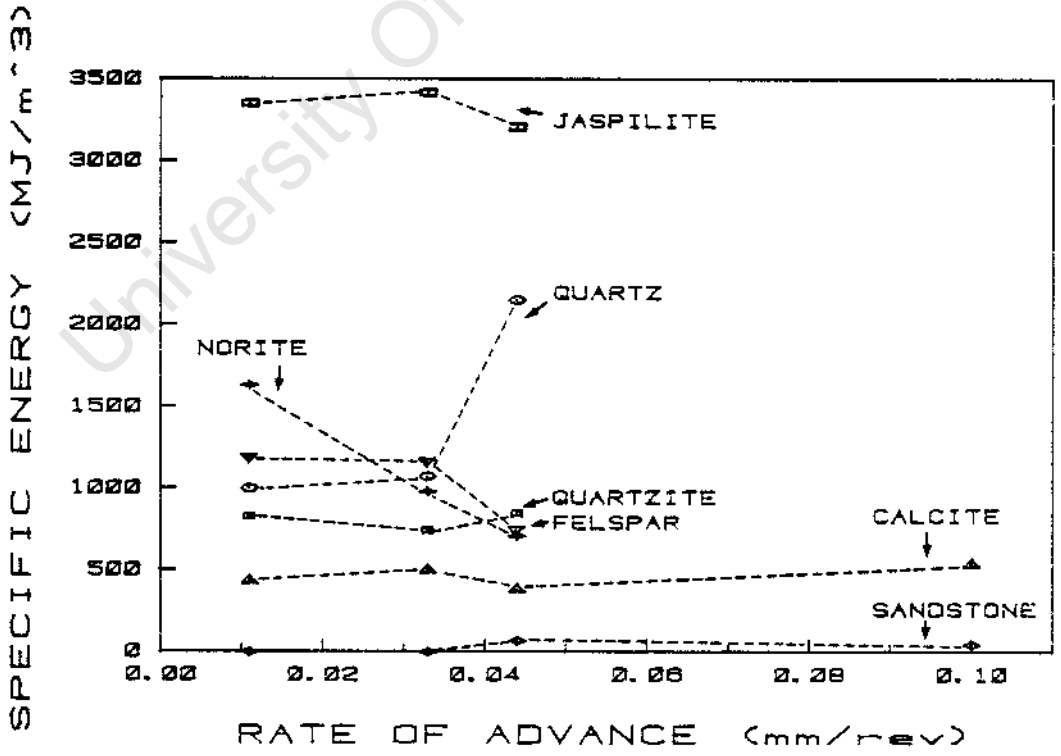

FIGURE 5.69 : Plot of specific energy against rate of advance for tests drilled in a variety of materials at set rate of advance

TABLE 5.9 : Summary of results of tests in rocks and single crystals at set rate of advance (L, M, H - low, medium, high)

MATERIAL	RATE OF ADVANCE (mm/rev)	SPECIFIC ENERGY	BIT PRESSURE	BIT WEAR	MAIN DIAMOND WEAR TYPE	COMMENT
Quartzite	0,011	L	M	L	0b + 1b	Suboptimal
	0,033	L	M	L	0b + 1b	Suboptimal
	0,044	L	M	L	0b + 1b	Marginal
Sandstone	0,011	L	L	M	0b + 2a	Operational
	0,033	L	L	L	0b + 2a	Operational
	0,044	L	L	L	0b + 2a	Operational
	0,1	L	L	H	0b + 2a	Operational
Jaspilite	0,011	H	H	H	4b	Suboptimal
	0,033	H	H	H	1b	Suboptimal
	0,044	H	H	H	1b	Suboptimal
Quartz	0,011	M	M	M	1b + 0b	Suboptimal
	0,033	M	M	H	1b	Suboptimal
	0,044	H	H	H	1b	Suboptimal
Calcite	0,011	L	L	L	0b + 2a	Operational
	0,033	L	L	L	0b + 2a	Operational
	0,044	L	L	L	0b + 2a	Operational
	0,1	L	M	H	0b + 2a	Operational
Felspar	0,011	M	M	L	0b + 1b	Suboptimal
	0,033	M	M	L	1b + 0b	Suboptimal
	0,044	L	M	L	1b + 0b	Marginal
Norite	0,011	M	M	L	0b+2a/1b	Suboptimal
	0,033	M	M	L	2a + 0b	Operational
	0,044	L	M	L	0b+2b/1b	Operational

Bit Wear

There was insufficient time during the shortest tests in resistant rocks for the bit wear rate to stabilise. This contributed for instance to scatter in the results for drilling granite at set thrust (Fig. 5.70). The tests in light norite were long and stable enough to produce very consistent results and for this rock the specific linear bit wear was directly proportional to bit

pressure. The syenite, containing about 5% free quartz, wore the bits at an almost constant rate irrespective of bit pressure. In marble the bit wear was paradoxically high at low bit pressure. This was due to damage caused by vibration at the very low thrust. At higher bit pressures the bit wear was uniform and low. In sandstone the bit wear was extremely high at high bit pressure (nearly 6 mm/m at 8,88 MPa) due to excavation of entire quartz grains and rapid bit matrix erosion.

At the penetration rates used for the tests at set rate of advance the bit mass loss values for tests in single crystal quartz and jaspilite were particularly high, rising steeply with increasing rate of advance (Fig. 5.71). In drilling the quartz this was due to the damage caused by large shard-like fragments and in jaspilite due to extreme damage to the bit caused by seizure. At 0,1 mm/rev the bit mass loss in sandstone was high but not suprisingly so. The high value for bit mass loss in calcite at 0,1 mm/rev is explained by the fact that at this high rate of advance, with correspondingly high torque and power consumption values, the production of large angular cleavage rhombs was promoted by the easy cleavage of calcite. These fragments did not have sufficient opportunity to escape without severely damaging the bit matrix.

Detritus Size Distributions

The coarse detritus size distributions support these observations. At set thrust (Fig. 5.72) there was considerable scatter in the means of the detritus size distributions for the 2 mm to 63 micron sized fraction but nevertheless a slightly increasing trend in mean particle size with bit pressure for all the materials except marble. The marble drilled easily at all thrusts because it is both soft and uniformly fine grained. The mean coarse detritus size values for the tests at set rate of advance (Fig. 5.73) when plotted against reactive bit pressure were far more scattered.

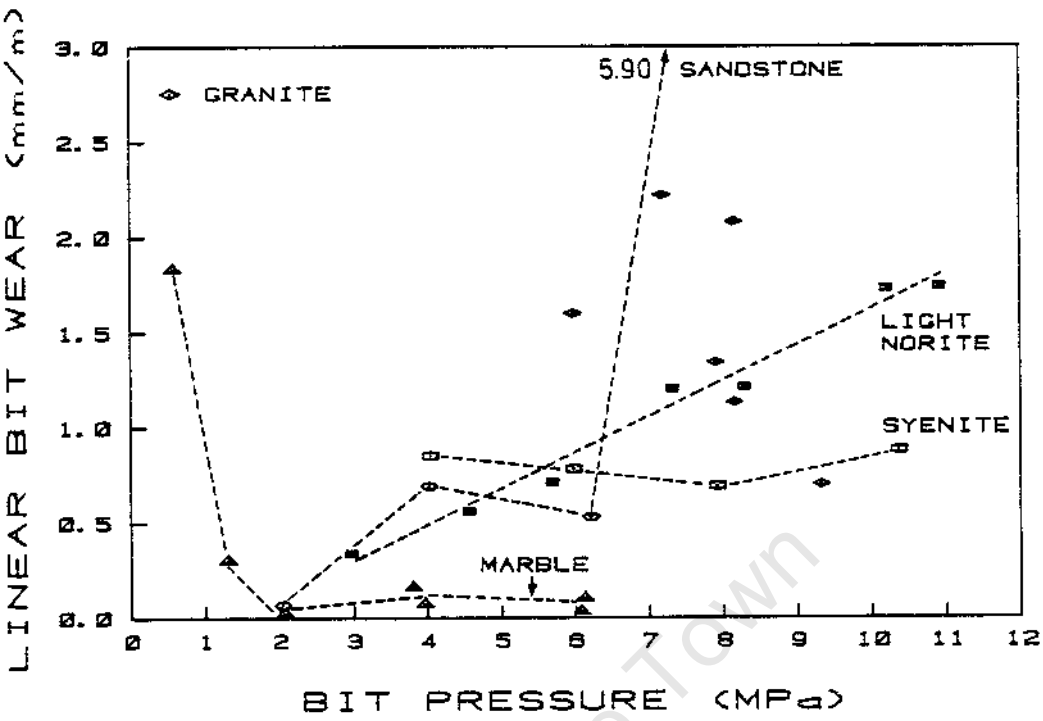

FIGURE 5.70 : Plot of specific linear bit wear against bit pressure for tests drilled in a variety of rock types at set thrust

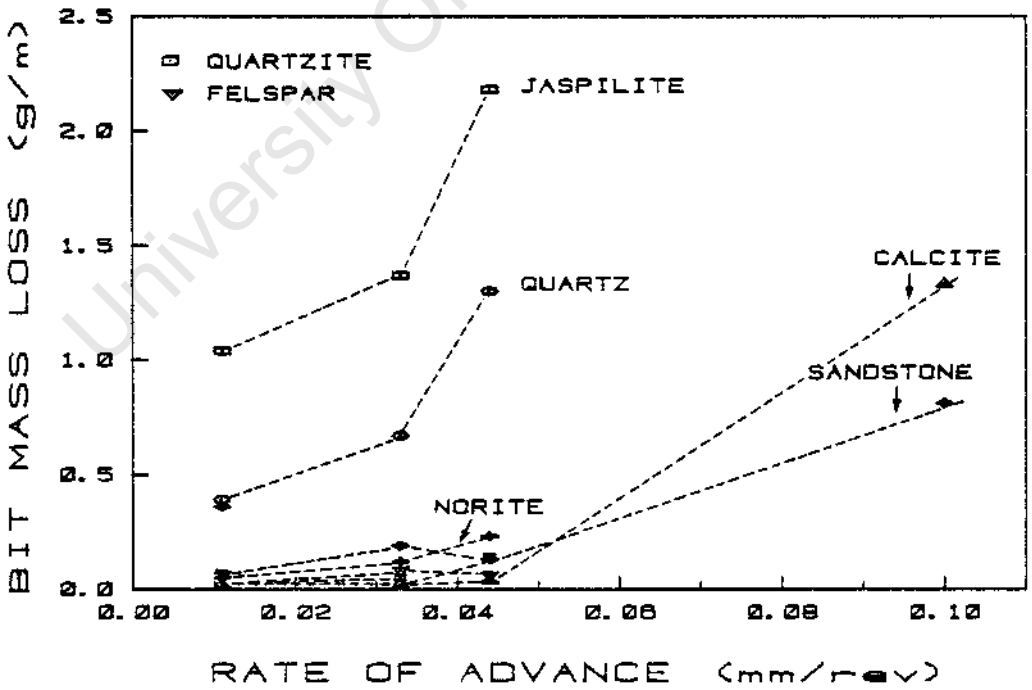

FIGURE 5.71 : Plot of specific linear bit wear against rate of advance for tests drilled in a variety of materials at set rate of advance

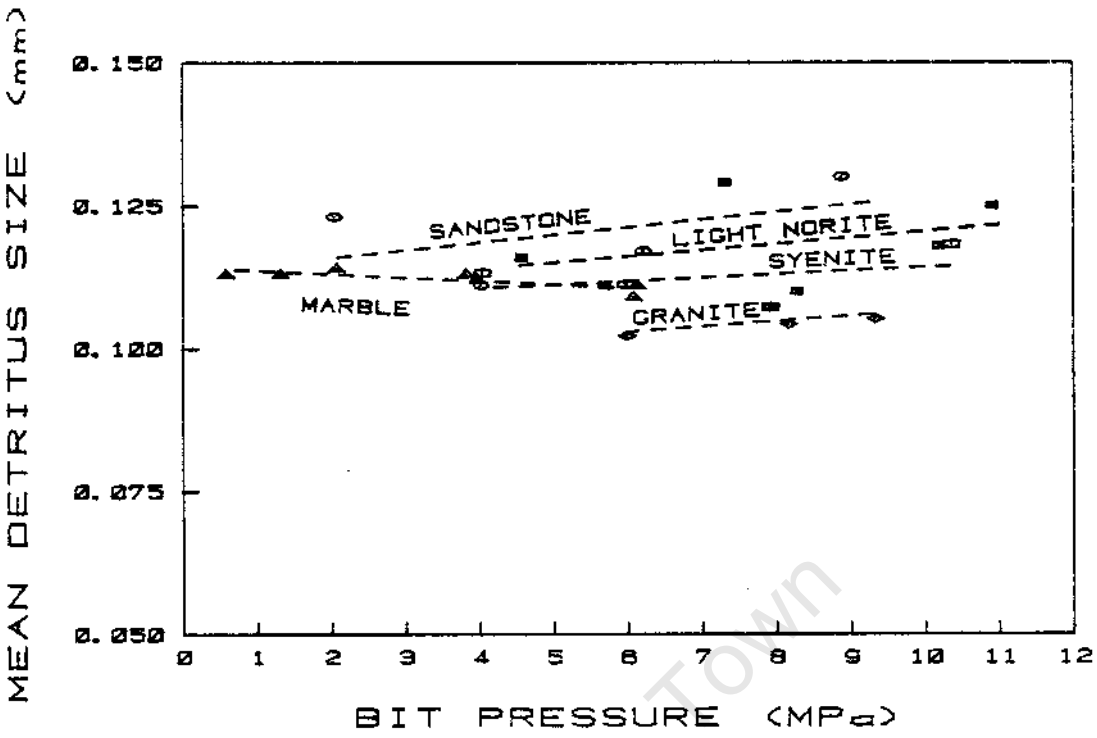

FIGURE 5.72 : Plot of mean coarse detritus size against bit pressure for tests drilled in a variety of rocks at set thrust

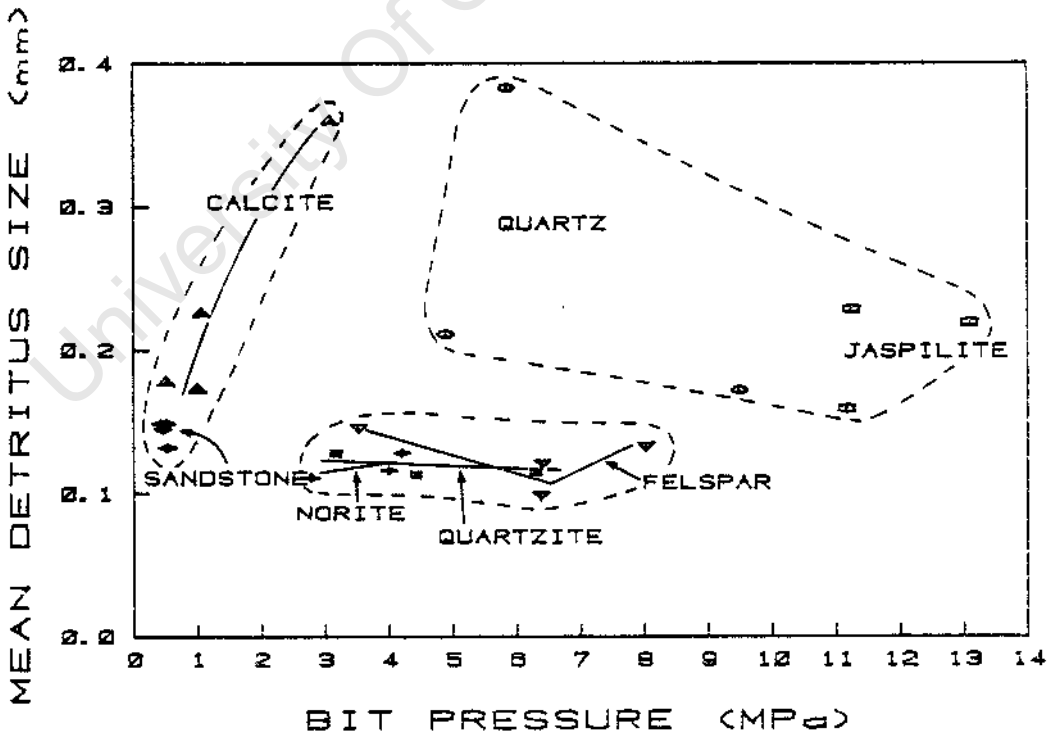

FIGURE 5.73 : Plot of mean coarse detritus size against mean bit pressure for tests drilled in a variety of materials at set rate of advance

The soft rocks drilled at relatively low pressures. The sandstone detritus was constant in size and essentially reflected the grain size of the rock. The percentage of material under 63 microns in size was uniformly low between 60% and 70% at all rates of advance (not plotted). The coarse detritus size of calcite rose steeply with increasing bit pressure at higher rates of advance due to the very easy cleavage. The percentage of fine material was moderate, between 74% and 85%. The materials of intermediate strength had finer mean coarse detritus size but with no uniform trends in the plotted values, and had relatively high percentages of reground fine material. The most resistant materials, quartz and jaspilite, produced a few distinctly larger coarse particles accompanied by high percentages (over 90%) of Tine material.

5.4.8 Microscopy of the Wear of Diamonds and Bit Matrix Under Set Thrust and Set Rate of Advance Conditions in a Variety of Materials

Scanning electron micrographs of the wear of diamonds which drilled under set thrust conditions are presented in Figs. 5.74 to 5.77. It should be noted that although the wear type distributions varied for bits drilled in different materials the nature of the diamond wear was similar. Identical wear features occurred on diamonds subjected to very different drilling conditions. The typical wear sequence in norite, from an unworn stone to failure of an abraded surface to produce a microfractured stone is shown in Figs. 5.74(a - d). The grooving on Type 1 wear surfaces may be shallow or deep, but the shallow grooves are straight whereas the deep grooves are often sinuous (see Figs. 5.74(e & f)). The wear of diamonds drilled in syenite (Fig. 5.75) and granite (Fig. 5.76) at the same bit pressures was indistinguishable from that in norite (Figs. 5.74) except that there were more wear flats. These displayed the characteristic grooving clearly with transverse ridges developed parallel to the cleavage planes (Figs. 5.76(c & d)). The diamonds on a bit drilled in the friable sandstone at 1 MPa showed considerable damage (Fig. 5.77) except for the stones most recently exposed (Fig. 5.77(a)).

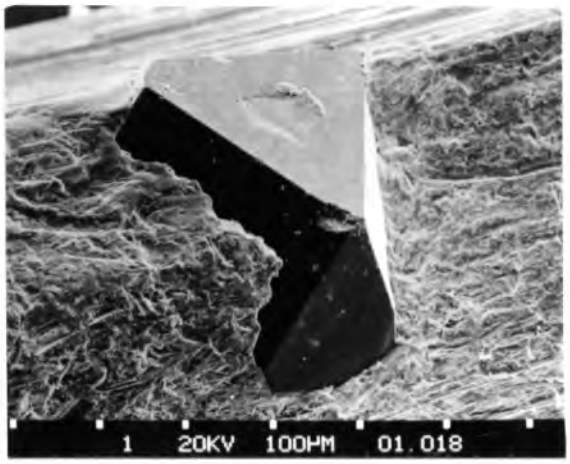

(a) : Type 0b - unworn stone

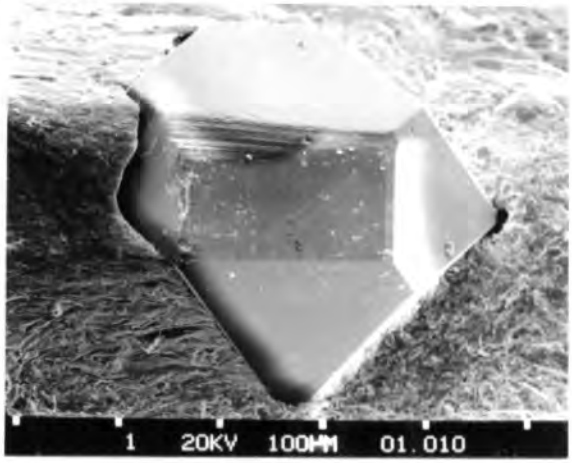

(b) : Type 1a - developing grooved wear flat

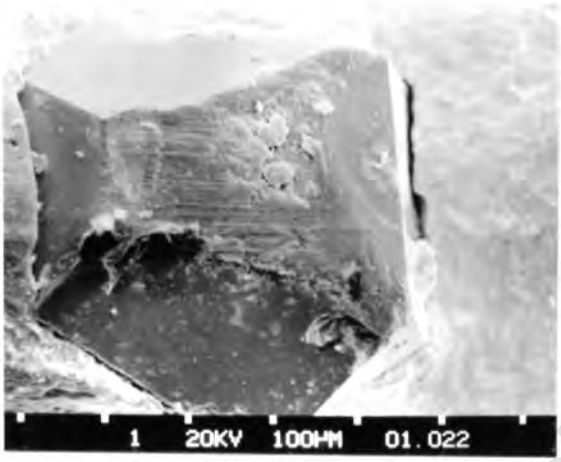

(c) : Type 1b - large wear flat

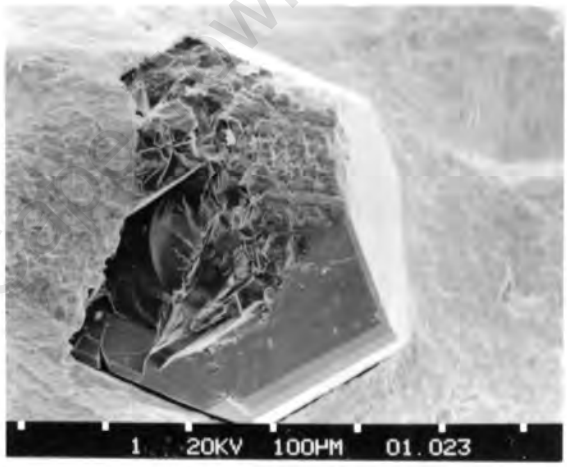

(d) : Type 1b/2b - progressive failure from trailing edge

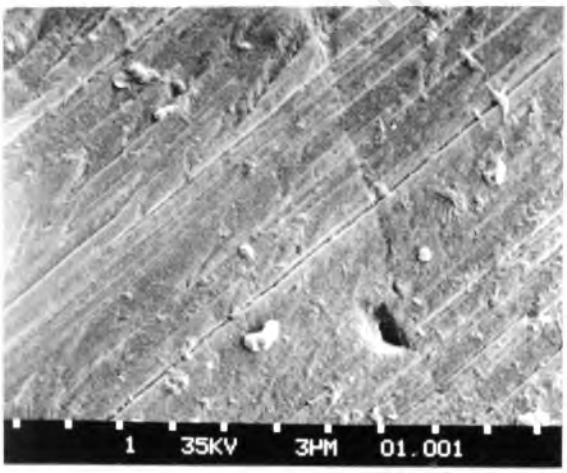

(e) : Type 1b - detail of grooved wear surface like (b)

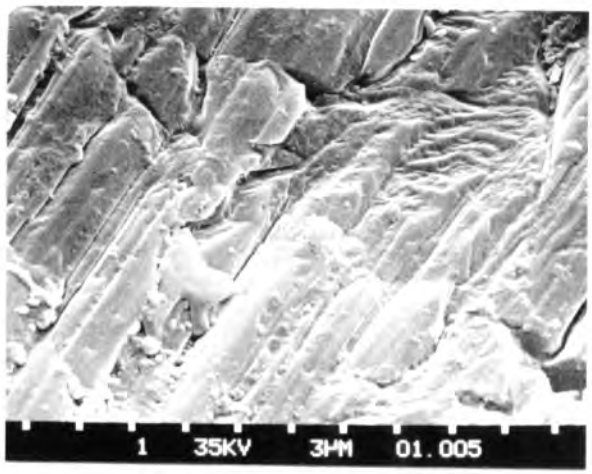

(f) : Type 1b - deeply grooved wear surface like (c)

FIGURE 5.74 : Wear of diamonds drilled in norite at 4 MPa bit pressure

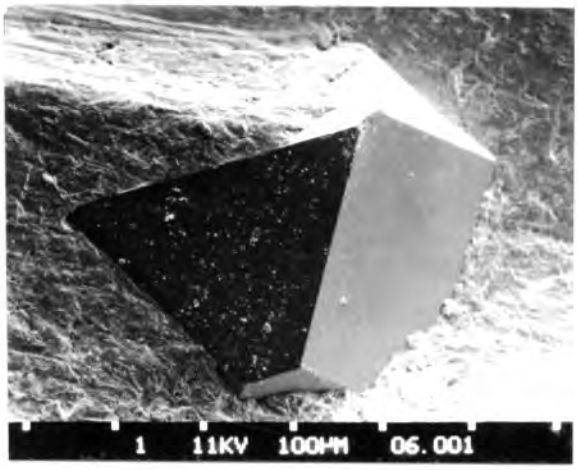

(a) : Type 0b - unworn stone

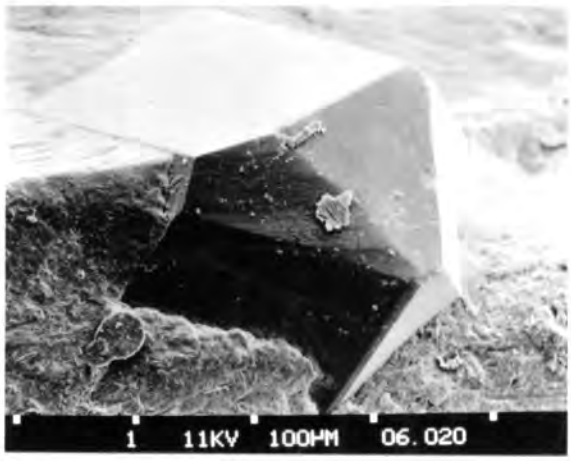

(b) : Type 1b - developing wear flat

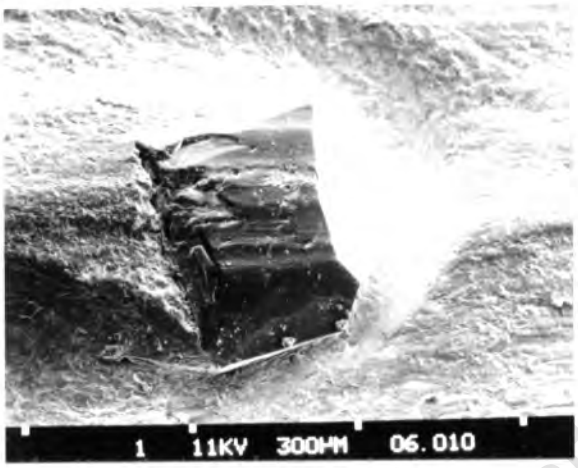

(c) : Type 1b - wear flat

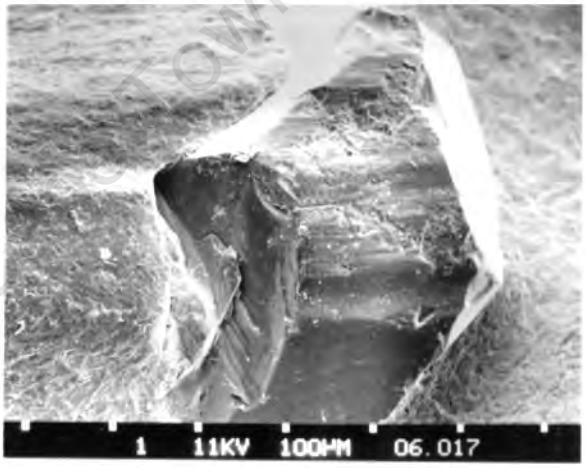

(d) : Type 1b - worn surface showing incipient failure

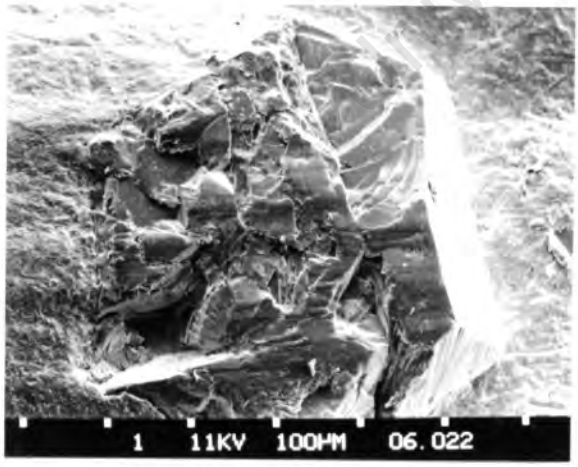

(e) : Type 1b/2b - progressive failure from trailing edge

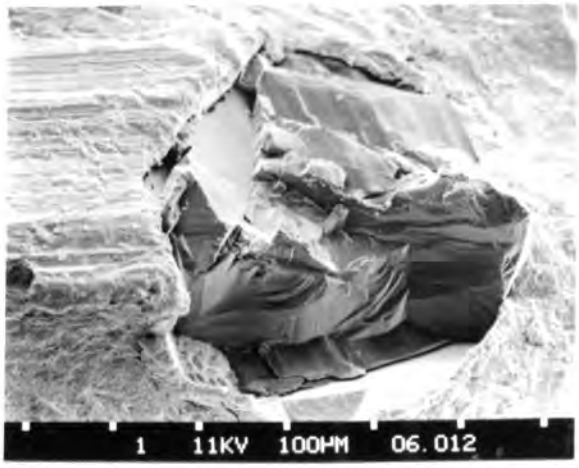

(f) : Type 2b - fractured stone

FIGURE 5.75 : SEM micrographs of wear of diamonds drilled in syenite at 4 MPa bit pressure

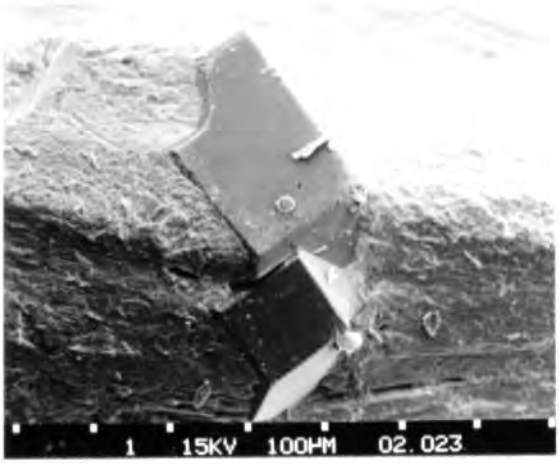

(a) : Type 0b - unworn twinned stone

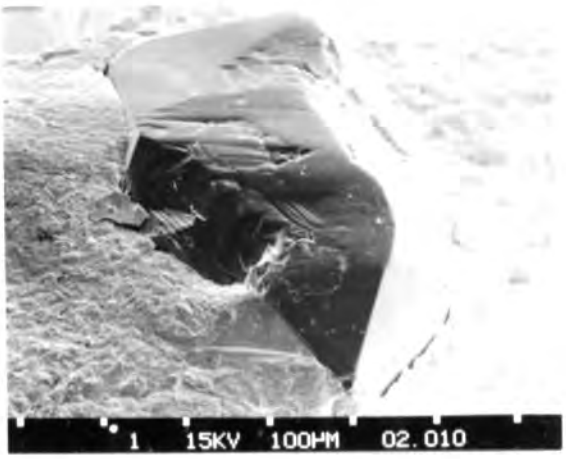

(b) : Type 1b - scored and rounded wear area

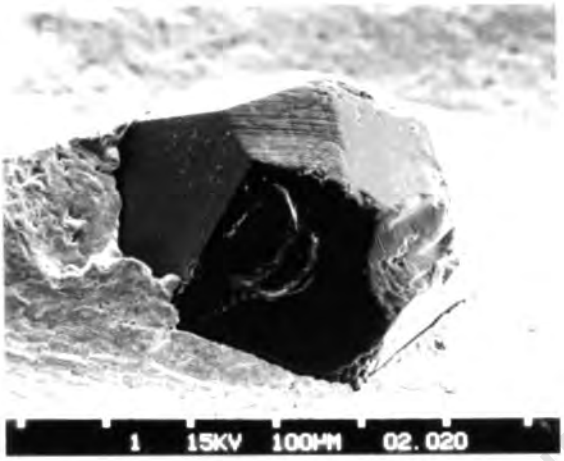

(c) : Type 1b - wear flat with transverse steps

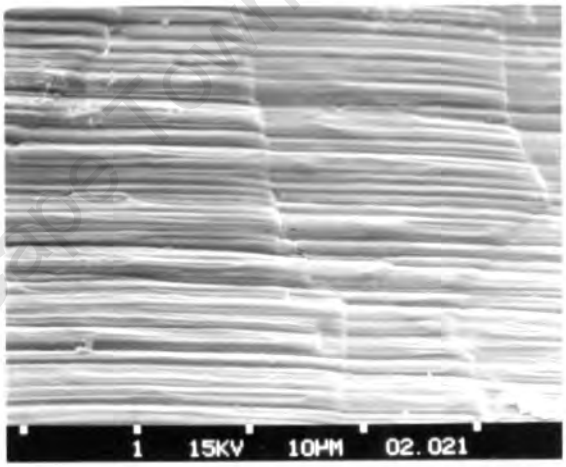

(d) : Detail of (c) - micro-grooving and transverse steps

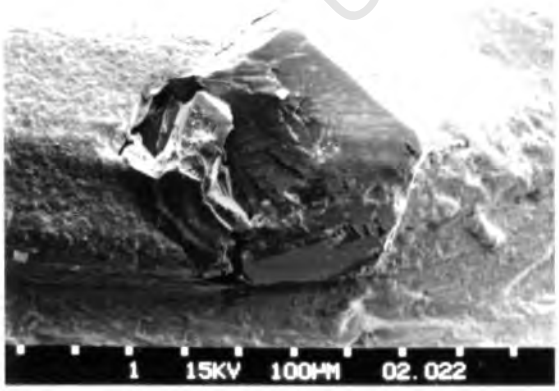

(e) : Type 1b/2b - progressive failure from trailing edge

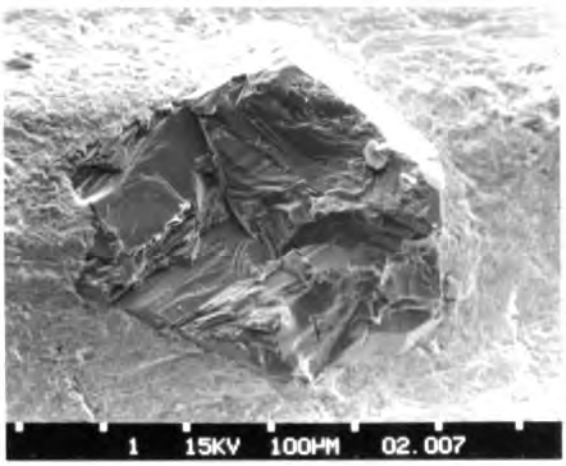

(f) : Type 2b - fractured stone

FIGURE 5.76 : SEM micrographs of wear of diamonds drilled in granite at 4 MPa bit pressure

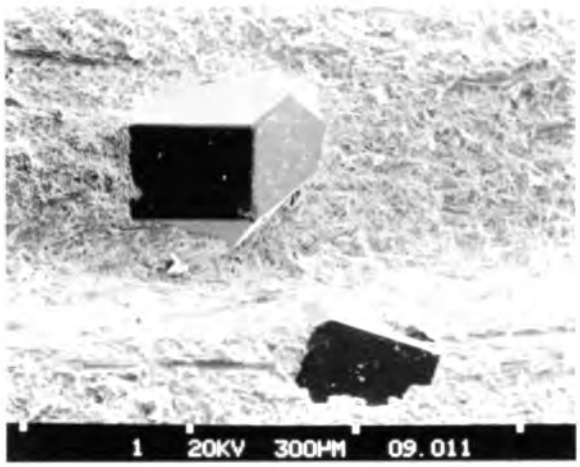

(a) : Type 0b - unworn stones

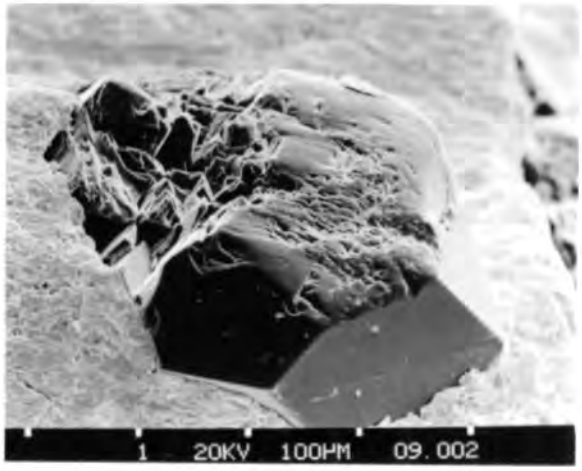

(b) : Type 1b - stone with disintegrating wear flat

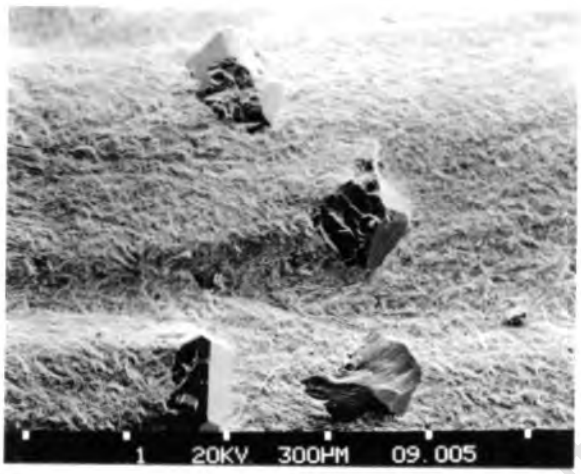

(c) : Type 2b - fractured stones with sharp points

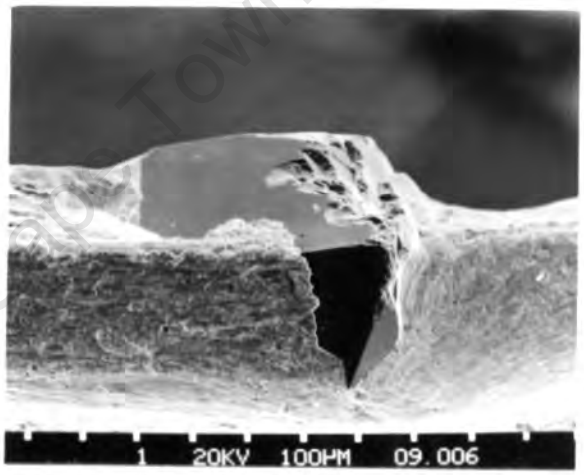

(d) : Type 2b - fractured stone

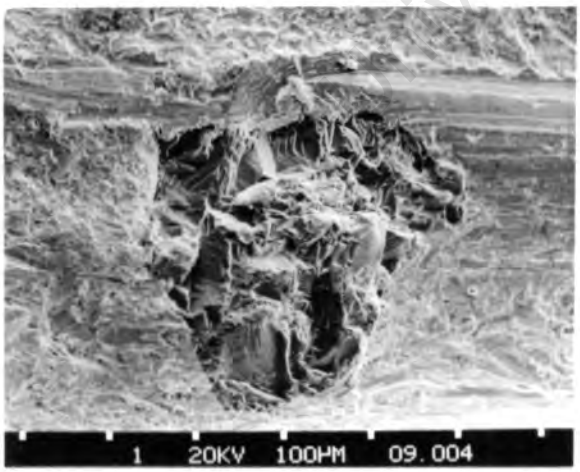

(e) : Type 2b - fractured stone

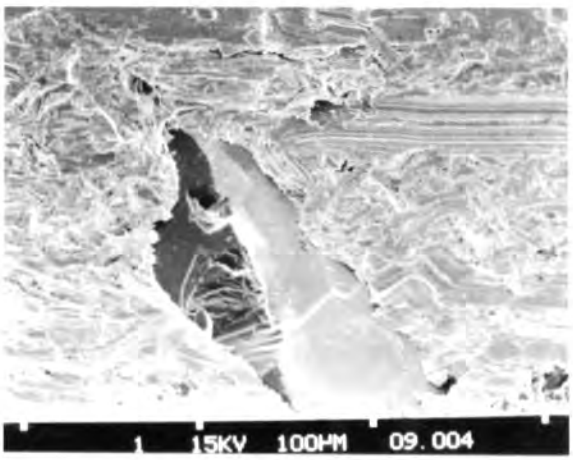

(f) : Type 2b - fractured stone

FIGURE 5.77 : SEM micrographs of wear of diamonds drilled in sandstone at 1 MPa bit pressure

The wear of the bit matrix in a variety of rocks is illustrated in Fig. 5.78. The typical topography produced by the flow of abrasive drilling slurry around an exposed diamond is illustrated in Fig. 5.78(a) with an example where the stone has just been lost while drilling syenite at 4 MPa. In the trough ahead of each stone the wear was by impact of drilled particles in the slurry dammed up by the obstruction (Fig. 5.78(b)). Immediately behind the stones the sheltered matrix formed "tails" (Fig. 5.78(c)), lightly scored and shaped by erosion by particles in the stream of drilling fluid. Typical matrix wear is shown in an example from a bit drilled in granite at 4 MPa. On the ridges between the stones the exposed matrix was scored by abrasion (Fig. 5.78(d)). These surfaces appear to have been produced by the same mechanisms responsible for the vigorous wear produced by sandstone drilled at 1 MPa. Plastic grooving and scoring resulted from ploughing of matrix material between the stones (Fig. 5.78(e)) and the removal of matrix by impact of particles on the more sheltered ridges behind the stones (Fig. 5.78(f)).

The wear of diamonds which drilled single crystal quartz and felspar at 8 MPa set bit pressure is illustrated in Fig. 5.79. The wear in felspar showed the typical development from rounding and grooving (Figs. 5.79(a)) through mixed wear involving break up of the surface (Fig. 5.79(b)) to crystallographically controlled microfracture (Fig. 5.79(c)). Similar wear features were produced in drilling quartz despite its mineralogical dissimilarity from felspar. In Fig. 5.79(d) it is clear that the break up of the flat exposed crystal face was controlled by the cleavage. (The direction of abrasion was from right to left). The disintegration of flat wear faces (Fig. 5.79(e)) and the appearance of microfracture (Fig. 5.79(f)) was not unusual despite the extreme difficulty encountered in drilling quartz.

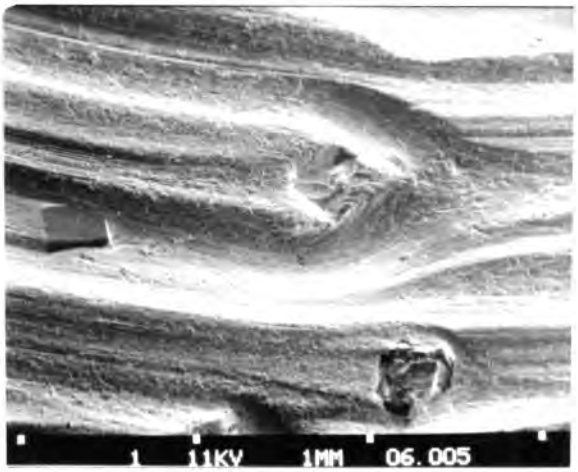

(a) : Typical bit matrix wear from drilling syenite at 4 MPa

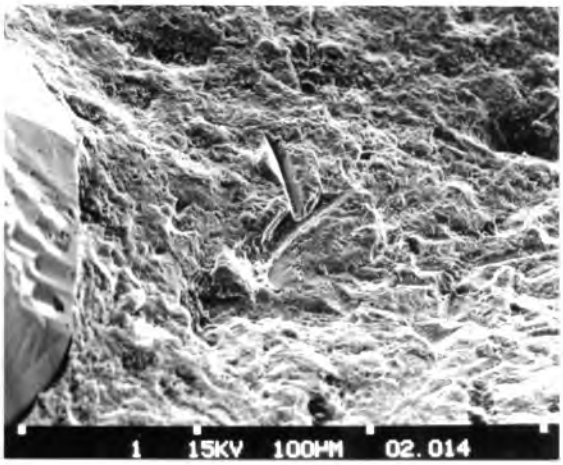

(b) : Bit matrix wear ahead of stone drilled in granite

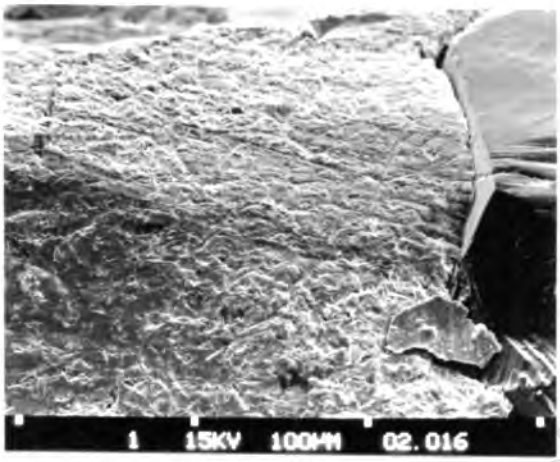

(c) : Bit matrix wear behind stone drilled in granite at 4 MPa

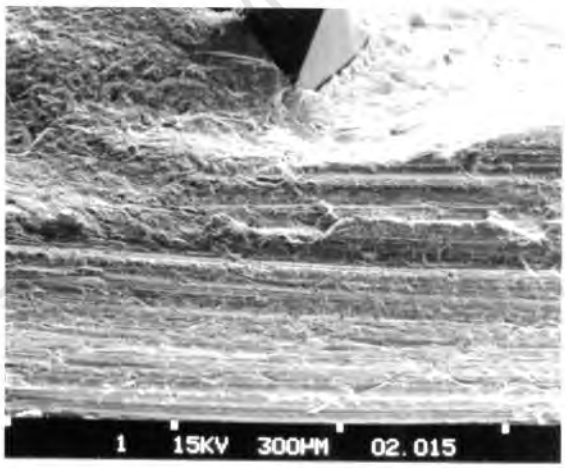

(d) : Bit matrix wear between stones drilled in granite

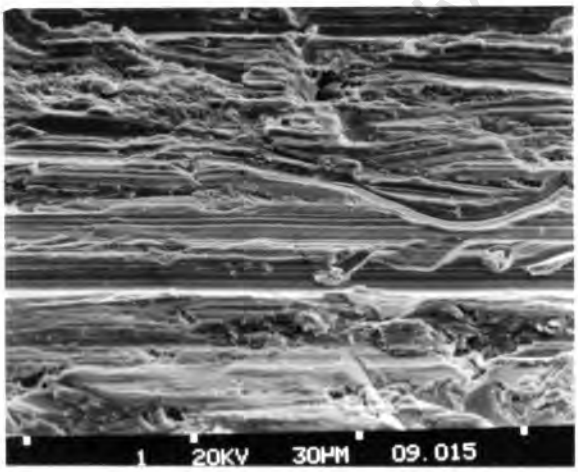

(e) : Wear of matrix between stones drilled in sandstone at 1 MPa

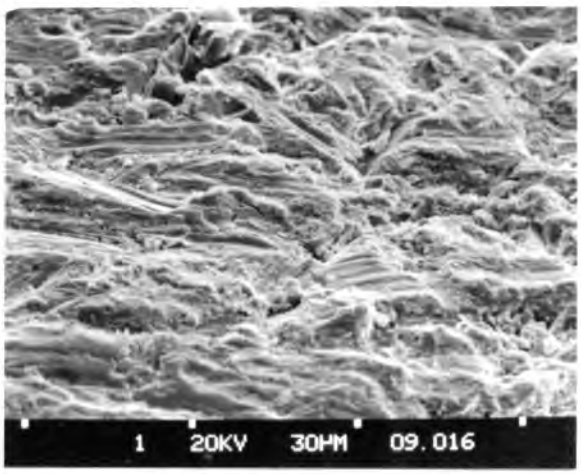

(f) : Wear of ridge behind a stone drilled in sandstone

FIGURE 5.78 : SEM micrographs of bit matrix wear from tests at set thrust in a variety of rocks

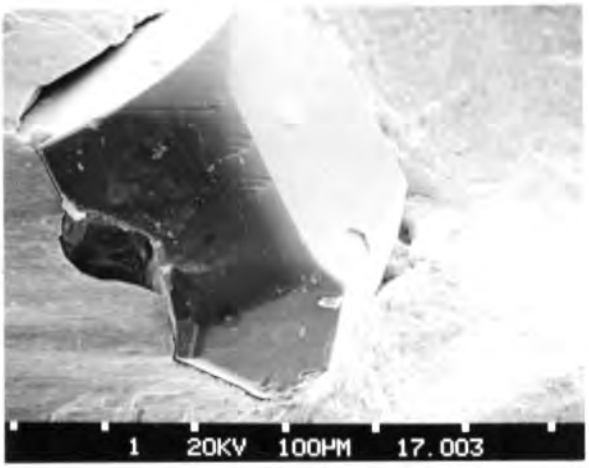

(a) : Type 1b - wear flat : Felspar

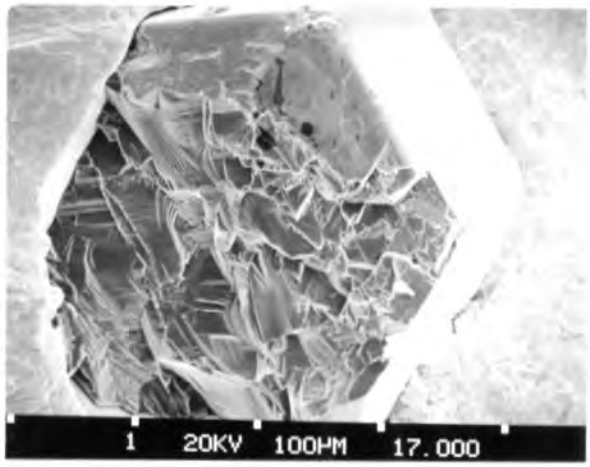

(b) : Type 2b - progressive failure : Felspar

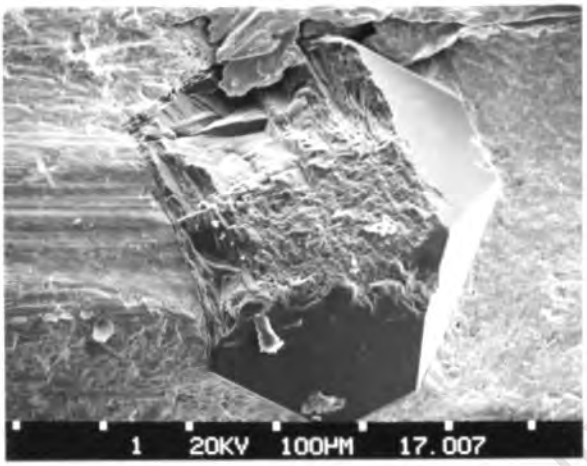

(c) : Type 2b - microfracture : Felspar

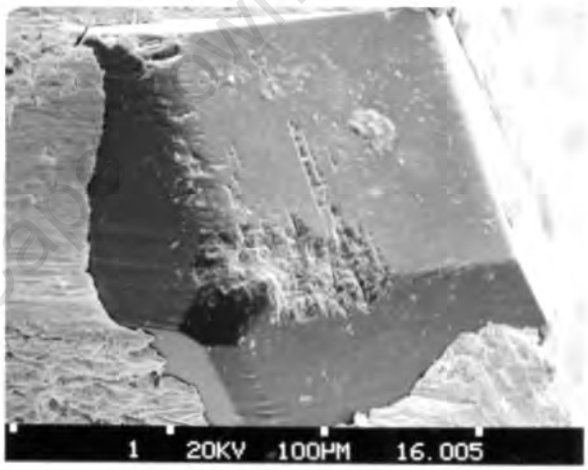

(d) : Type 2a - microcleavage : Quartz

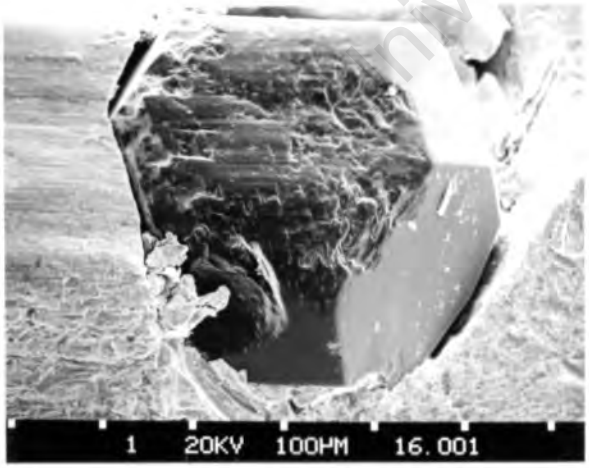

(e) : Type 1b/2b - progressive failure : Quartz

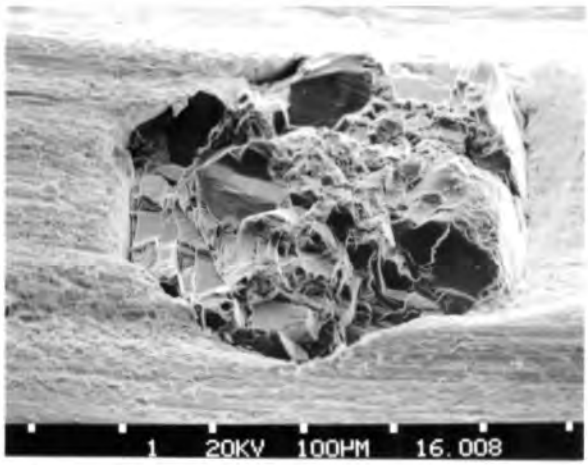

(f) : Type 2b - microfracture : Quartz

FIGURE 5.79 : SEM micrographs of wear of diamonds drilled in quartz and felspar under set thrust with 8 MPa bit pressure

Typical wear of the diamonds and the bit matrix drilled in a variety of materials at a set rate of advance of 0,044 mm/rev is illustrated in Figs. 5.80 to 5.83. After drilling quartzite in Mode 1 there was a predominance of abraded surfaces and wear flats (Fig. 5.80(a)) over fractured stones (Fig. 5.80(b)). Both these features were present on the diamonds which had drilled sandstone in Mode 2 very successfully (Figs. 5.80(d & e)) but fractured stones predominated. The bit matrix wear was far more severe in the soft abrasive sandstone than in the more strongly cemented quartzite (see Figs. 5.80(c & f)).

Jaspilite and quartz were both very difficult to drill and this was reflected in the wear of the diamonds (Fig. 5.81). In drilling jaspilite at set rate of advance the loads were so excessive that stones either failed very rapidly and thoroughly (Fig. 5.81(a)) or were forced into the bit matrix (Fig. 5.81(b)). This was the only situation in which significant Type 4b wear was encountered, with the smooth embedded stones supporting the load, avoiding fracture and hence impeding the progress of the drill. The bit wear was very smooth in appearance by the time this stage had been reached. Initially high bit wear had decreased as the penetration rate had dropped and the matrix had "polished" on the smooth, fine grained rock surface (Fig. 5.81(c)). In drilling quartz the diamonds were mostly smoothly rounded or more rarely severely fractured (Fig. 5.81(d)), sometimes nearly flush with the matrix (Fig. 5.81(e)). The matrix wear was severe and caused by scoring and gouging by the sharp angular shards of quartz (Figs. 5.81(e & f)).

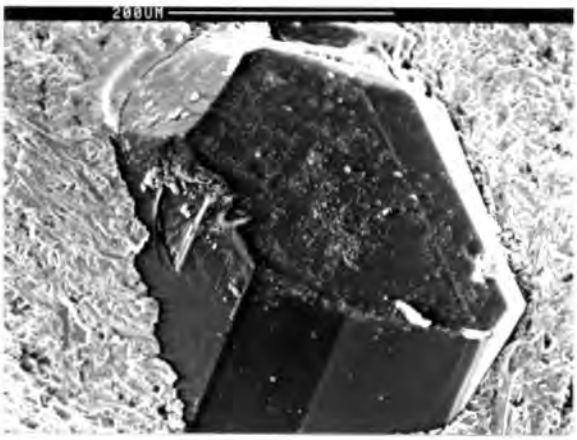

(a) : Type 1b - incipient wear on exposed face : Quartzite

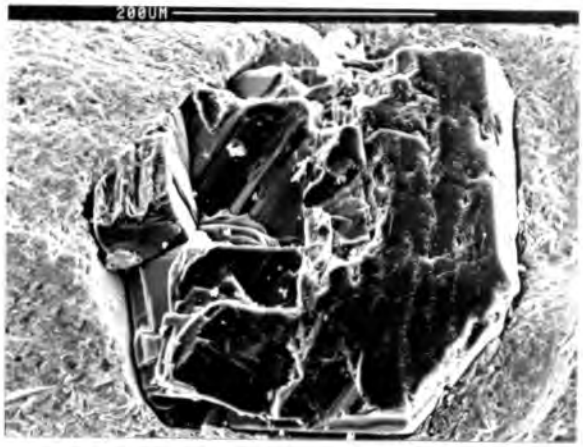

(b) : Type 2b - progressive failure of surface : Quartzite

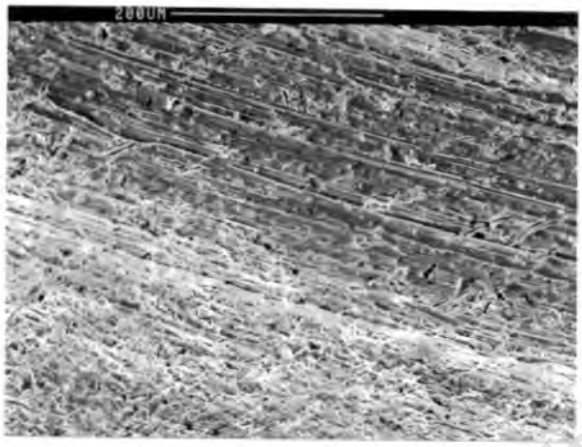

(c) : Matrix wear between stones after drilling in quartzite

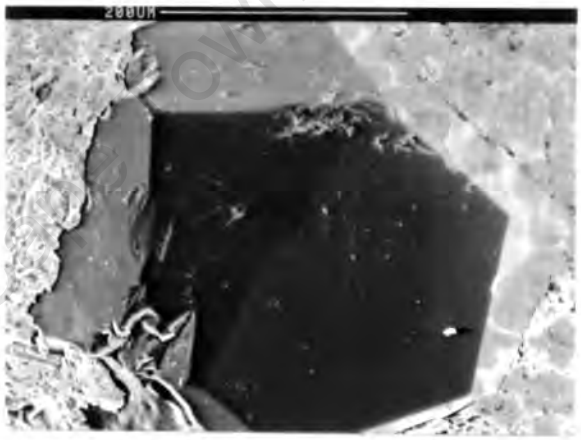

(d) : Type 1b - wear flat : Sandstone

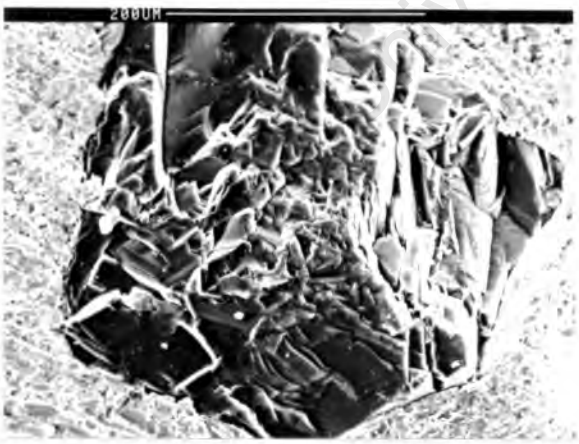

(e) : Type 2b - microfracture : Sandstone

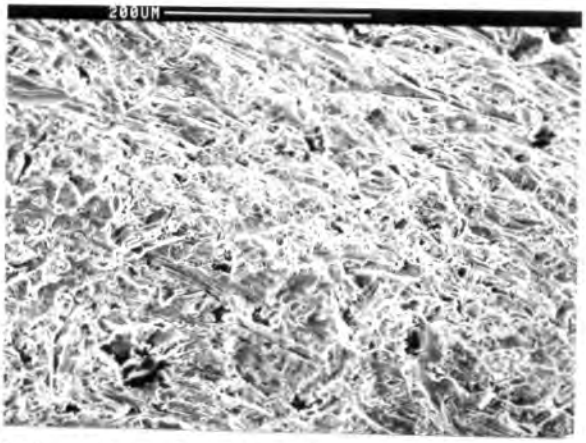

(f) : Matrix wear between stones after drilling in sandstone

FIGURE 5.80 : SEM micrographs of wear of diamonds and matrix wear of bits drilled at 0,044 mm/rev set rate of advance in quartzite and sandstone

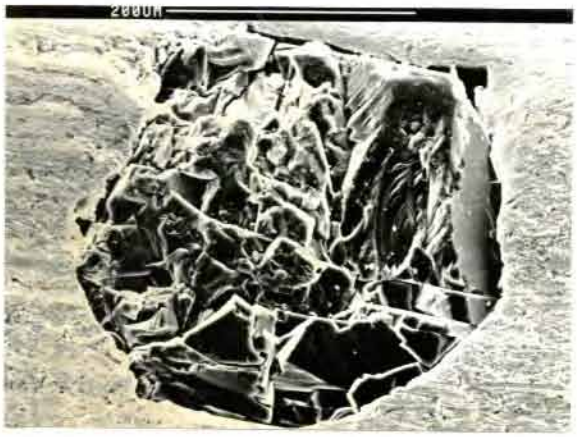

(a) : Type 2b - microfracture : Jaspilite

(b) : Type 4b - stone forced into matrix : Jaspilite

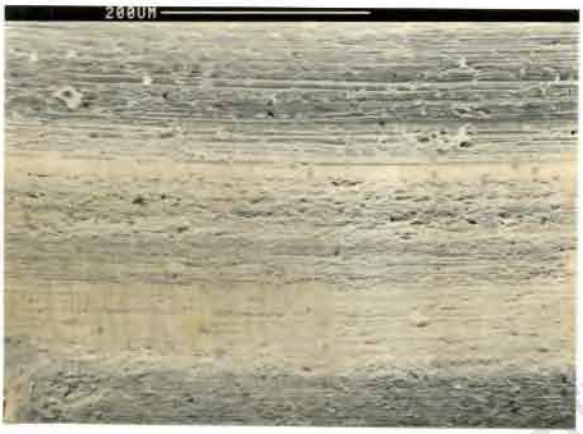

(c) : Matrix wear between stones after drilling in jaspilite

(d) : Type 2b - cleavage and microfracture : Quartz

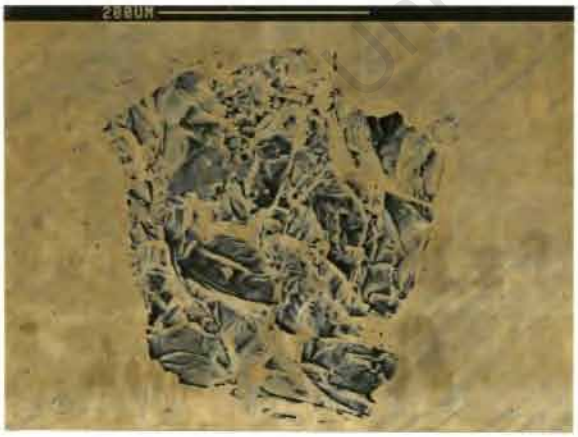

(e) : Type 4a - stone fractured until flush with the matrix : Quartz

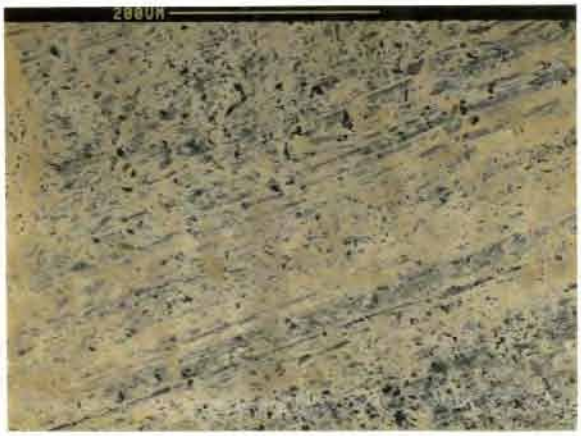

(f) : Matrix wear between stones after drilling in quartz

FIGURE 5.81 : SEM micrographs of diamond and matrix wear of bits drilled at 0,044 mm/rev in jaspilite and single crystal quartz

The wear of the diamonds and matrix after drilling single crystal felspar and norite at 0,044 mm/rev were indistinguishable with respect to the two materials (see Fig. 5.82) except for the higher incidence of wear flats when drilling the single crystal felspar. Wear flat development by abrasion and grooving (Figs. 5.82(a & d)), microfractured stones (Figs. 5.82(b & e)) and moderate matrix wear by abrasion and impact (Figs. 5.82(c & f)) were common to the bits drilled in both materials. The diamond wear in calcite was unusual in that there was very little evidence for abrasion (Fig. 5.83(a)). Some stones showed signs of thermal etching. With the absence of hard particles there was no abrasion to remove and obscure the effects of thermal degradation and the rounding of exposed points by etching (Fig. 5.83(b)). Apart from stones showing very little wear the predominant wear type was fractured stones (Fig. 5.83(c & d)) broken by impact, mostly with loose diamonds. Only the most exposed ridges of bit matrix showed scoring and abrasion by contact with the calcite surface (Fig. 5.83(e)). Elsewhere a curious rippled effect was common; caused by cavitation and flow erosion assisted by the small angular particles in the drilling slurry (Fig. 5.83(f)). It was only at much higher rates of advance that large cleavage fragments caused severe bit wear in drilling calcite.

5.4.9 Microscopy of Drilling Detritus and Drilling Tracks Produced by Drilling Under Set Thrust and Set Rate of Advance Conditions in a Variety of Materials

Optical micrographs taken at the same magnification of drilling detritus produced at about 6 MPa bit pressure under set thrust conditions in a variety of rock types are shown in Fig. 5.84. With the exception of sandstone the other rock types were dominated by minerals with relatively easy cleavages. These minerals represented the largest particles drilled from these rocks and all appear similar. There was no marked difference in detritus size from these rocks. Mashed flakes of compacted and sintered detritus were present in all the samples. The flakes were distinguished from mineral grains by being curved, striated and flat.

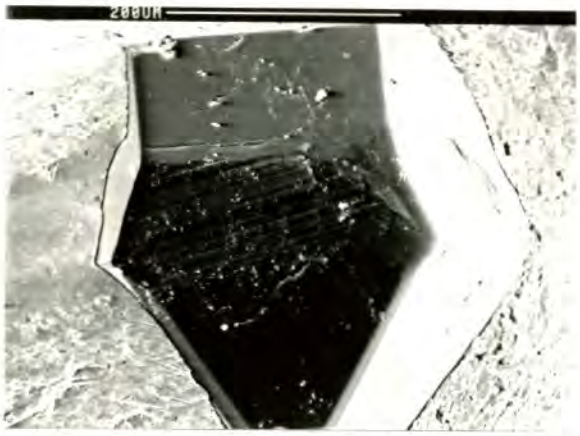

(a) : Type 1b - wear flat : Felspar

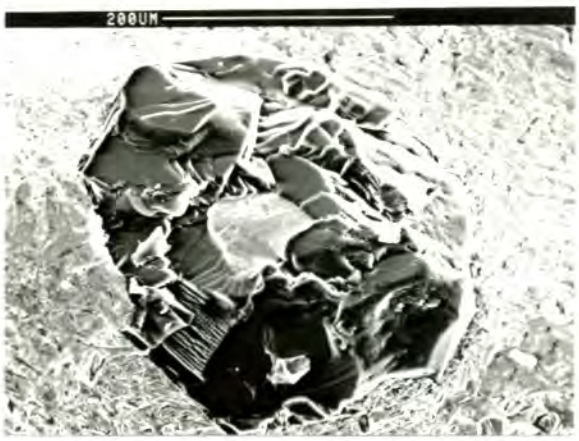

(b) : Type 2b - microfractured stone with sintered detritus : Felspar

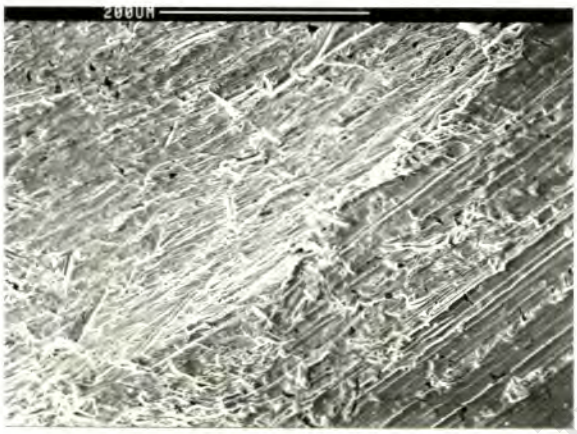

(c) : Matrix wear between stones after drilling single crystal felspar

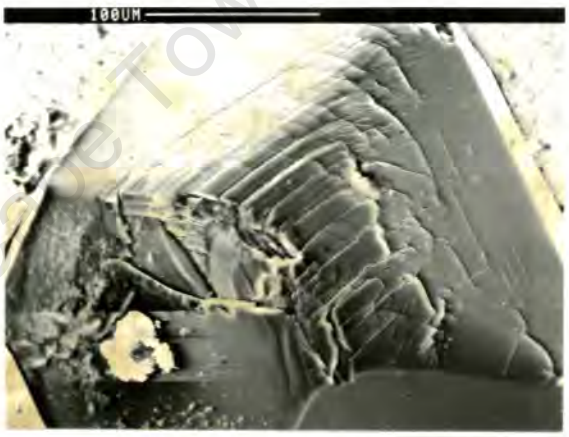

(d) : Type 1a - grooving and rounding : Norite

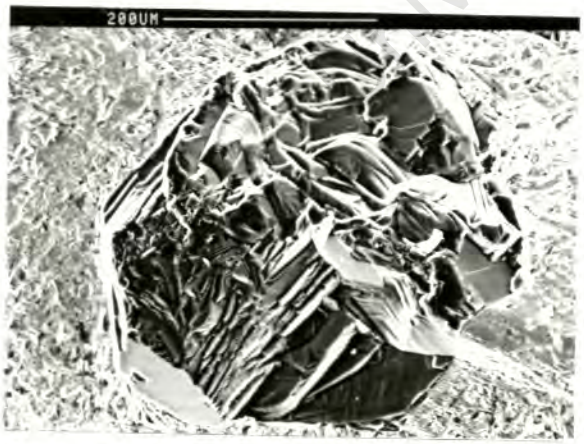

(e) : Type 2b - microfracture : Norite

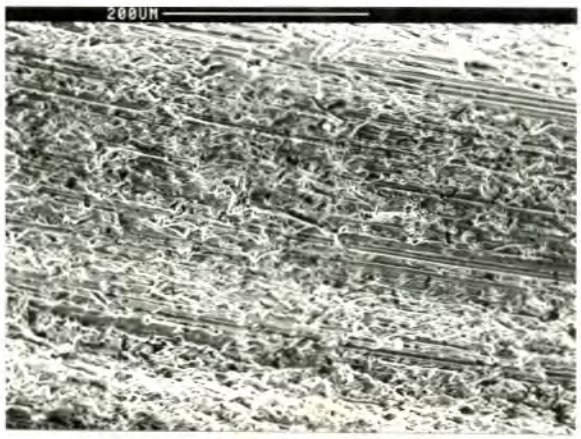

(f) : Matrix wear between stones after drilling norite

FIGURE 5.82 : SEM micrographs of diamond and matrix wear of bits drilled at 0,044 mm/rev in single crystal felspar and norite. Felspar is the major constituent of norite

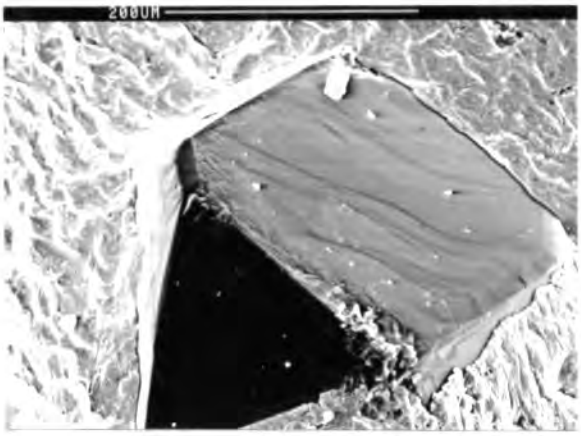

(a) : Type 0b - unworn stone

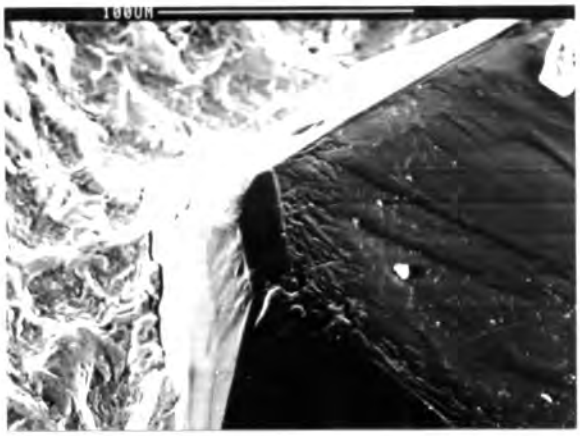

(b) : Detail of (a) - evidence of etching

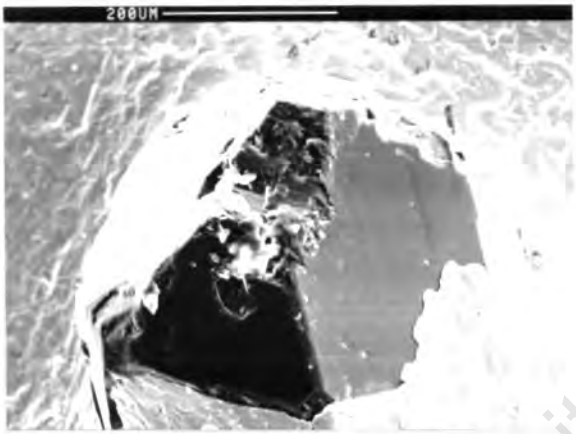

(c) : Type 2a - fracture of tip of stone

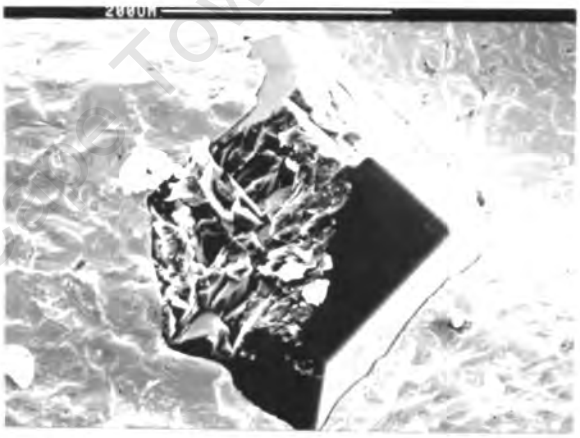

(d) : Type 2b - progressive fracture of stone

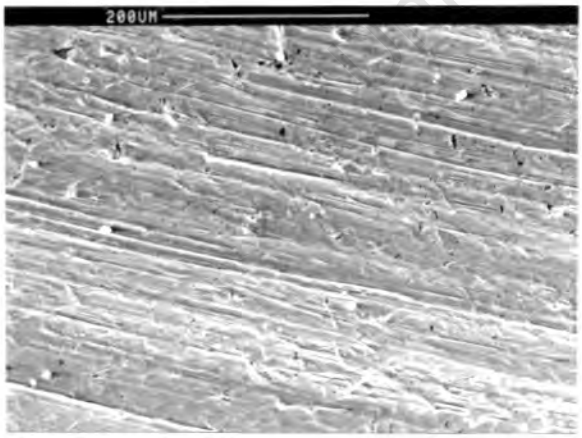

(e) : Matrix wear on exposed ridge

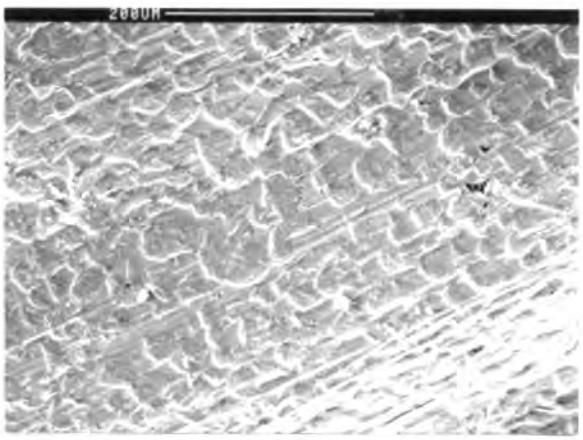

(f) : Matrix wear in lee of a stone

FIGURE 5.83 : SEM micrographs of diamond and matrix wear of bits drilled at 0,044 mm/rev in single crystal calcite

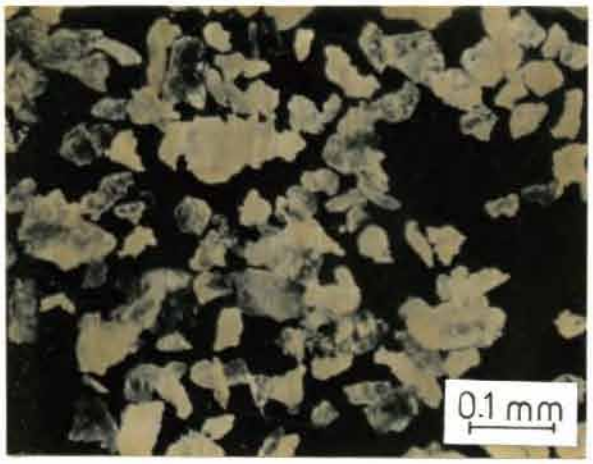

(a) : Light norite

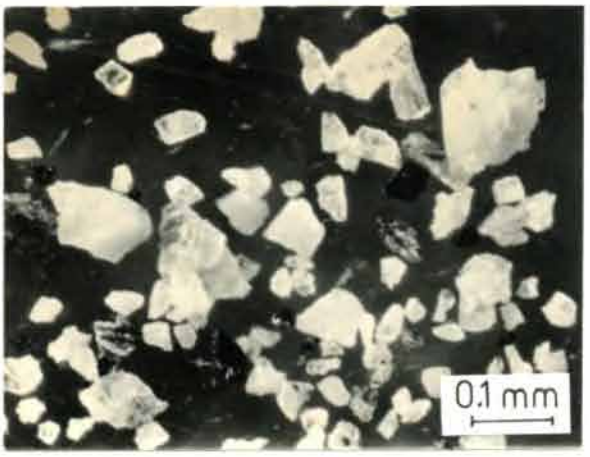

(b) : Syenite

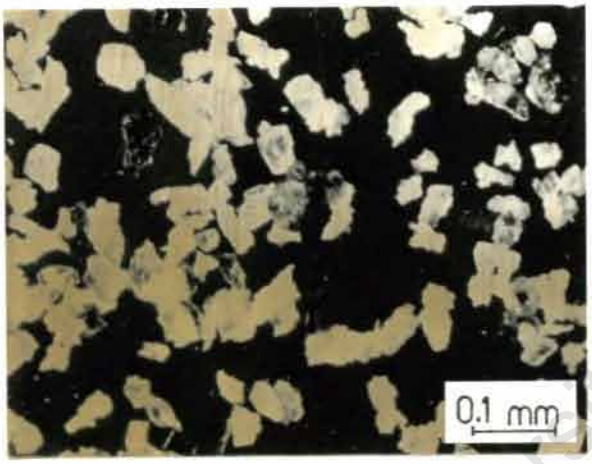

(c) : Granite

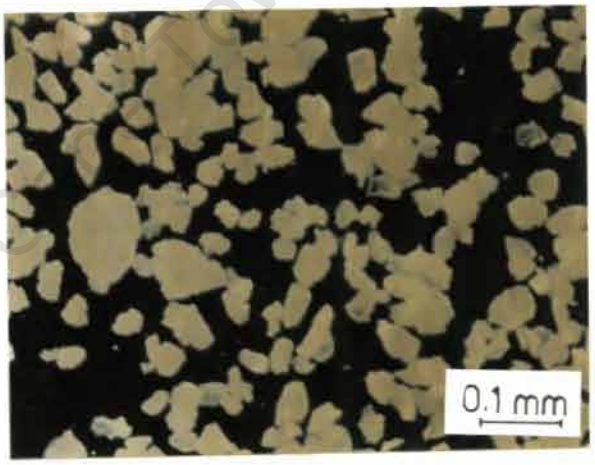

(d) : Marble

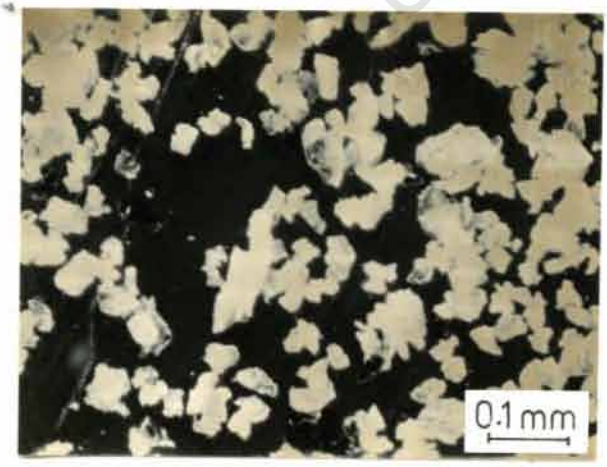

(e) : Sandstone

FIGURE 5.84 : Optical micrographs of drilling detritus from tests at set thrust

Scanning electron micrographs of detritus produced by drilling at a set rate of advance in a variety of materials are presented in Figs. 5.85 to 5.87. The quartzite consisted of grains cemented together by a micaceous matrix. Some of the grains were excavated intact with a coating of matrix although most of them had been fractured (Fig. 5.85(a)). The fine matrix was mashed into numerous flakes (Fig. 5.85(b)). The sharp angular sandstone grains were generally excavated intact (Fig. 5.85(c)), most of them free of adhering matrix (Fig. 5.85(d)). The single crystal quartz fractured into angular shards and sharp edged grains (Fig. 5.85(e & f)). Calcite broke by cleavage into angular rhombs (Figs. 5.86(a & b)) with the finer material being mashed into flakes. The cleavage fragments of single crystal felspar were also angular, but less so (Fig. 5.86(c)). The mashed flake of crushed felspar illustrated in Fig. 5.86(d)) was typical, showing scoring and transverse cracks. The detritus of drilling norite consisted mostly of cleavage fragments of felspar and pyroxenes (Fig. 5.86(e)) as well as the ubiquitous flakes (Fig. 5.86(f)). The generally very fine grained jaspilite broke into polycrystalline fragments (Figs. 5.87(a - c)) with the occasional single grain. Even some of this very resistant material consisting mostly of quartz was mashed into flakes (Fig. 5.87(d)).

The drilling tracks produced in single crystal felspar and quartz at set bit pressure of 8 MPa are illustrated by scanning electron micrographs at three different magnifications in Fig. 5.88. The fracture of the microcline felspar was controlled by the rectangular cleavage. The full width of the drilling track is illustrated in Fig. 5.88(a) showing the evenness of the fracture. At high magnification the tracks produced by individual diamonds can be identified by finer cleavage (Fig. 5.88(b)). The regular blocky cleavage is clear even at high magnification (Fig. 5.88(c)). The drilling track in quartz had the appearance of less homogeneous fracture (Fig. 5.88(d)). The crushing in the tracks by individual diamonds was fine but there was large scale conchoidal spalling producing large particles from the areas between the tracks of single stones (Fig. 5.88(e)). At high magnification the fracture at the bottom of the tracks in quartz appears random with no cleavage control (Fig. 5.88(f)).

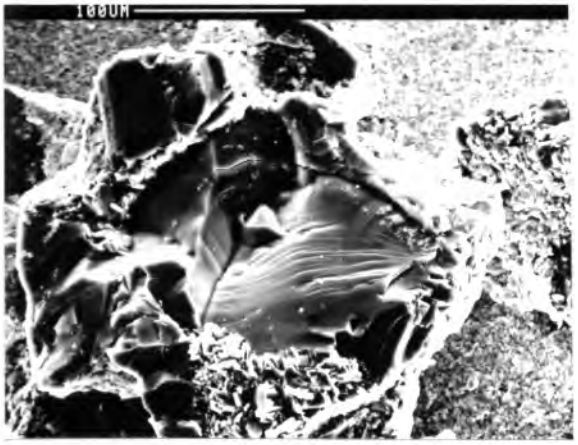

(a) : Quartzite particles with adhering rock matrix

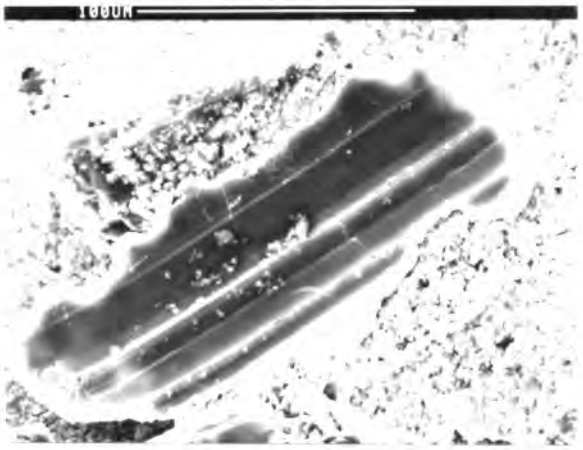

(b) : Mashed flake from drilling quartzite

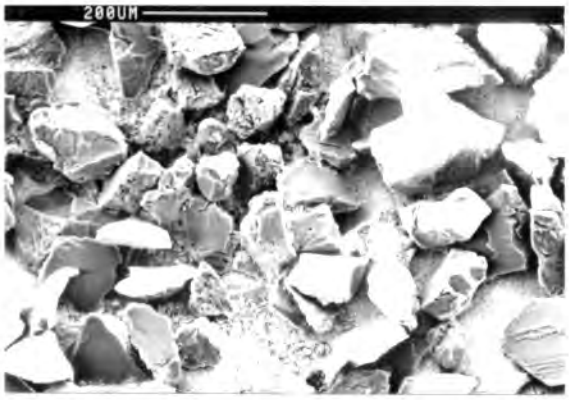

(c) : Sandstone detritus of loose grains

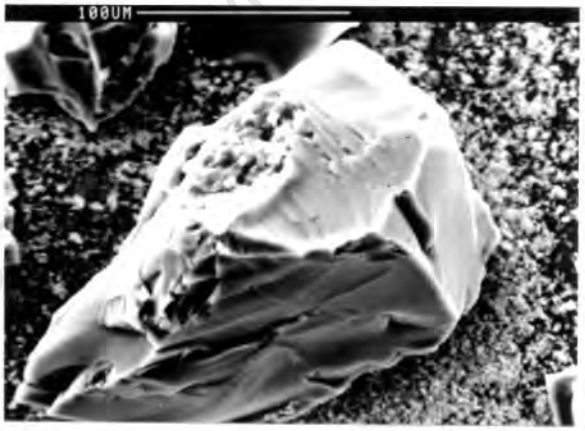

(d) : Quartz grain from sandstone

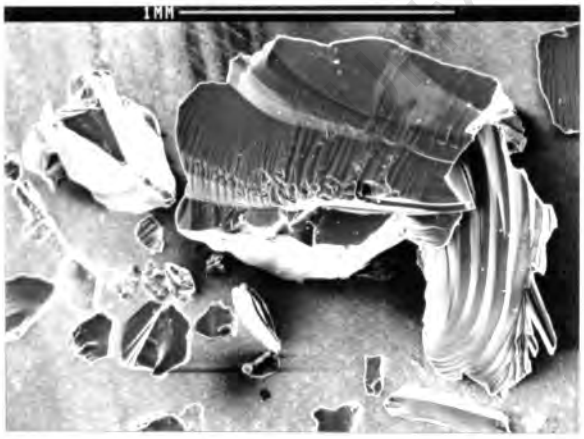

(e) : Quartz shard from drilling single crystal quartz

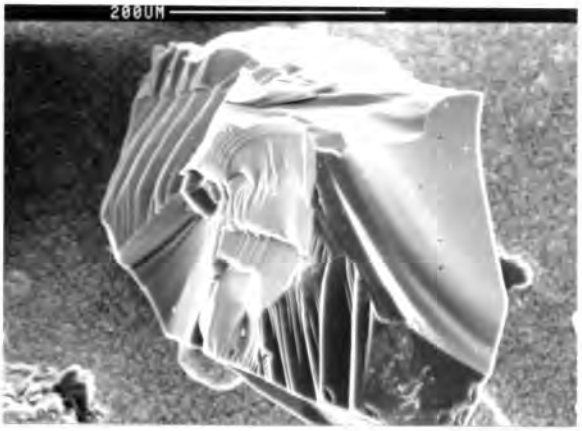

(f) : Quartz particle from drilling single crystal quartz

FIGURE 5.85 : SEM micrographs of detritus produced by drilling a variety of materials at 0,044 mm/rev set rate of advance

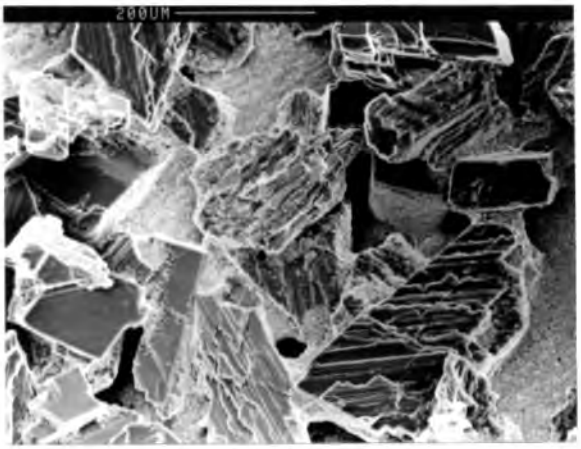

(a) : Cleavage fragments from single crystal calcite

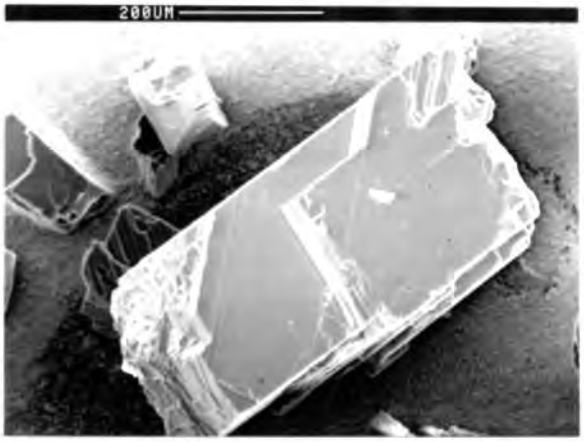

(b) : Single cleavage rhomb of calcite

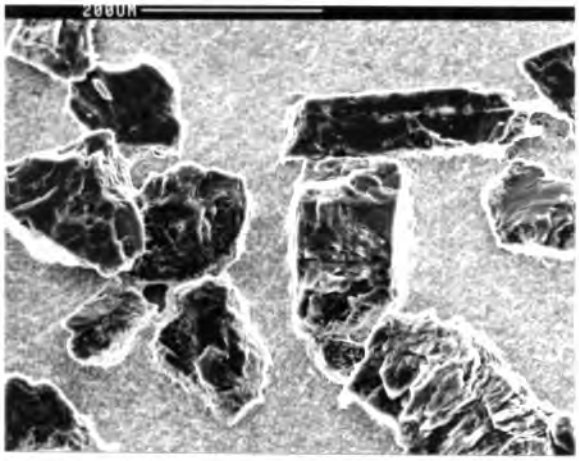

(c) : Cleaved grains of single crystal felspar

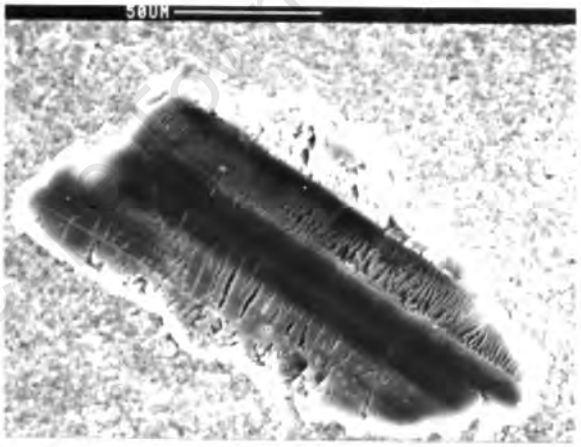

(d) : Mashed flake produced by drilling single crystal felspar

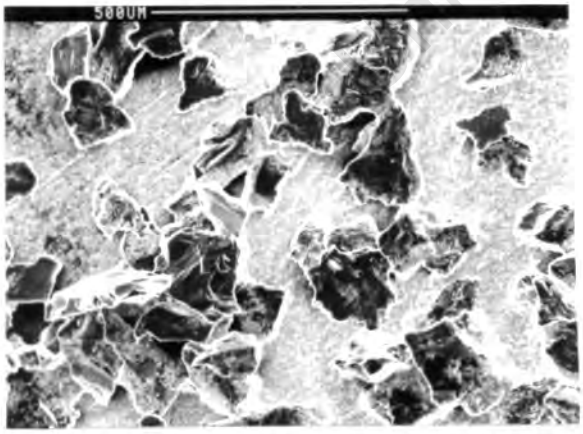

(e) : Particles produced by drilling norite

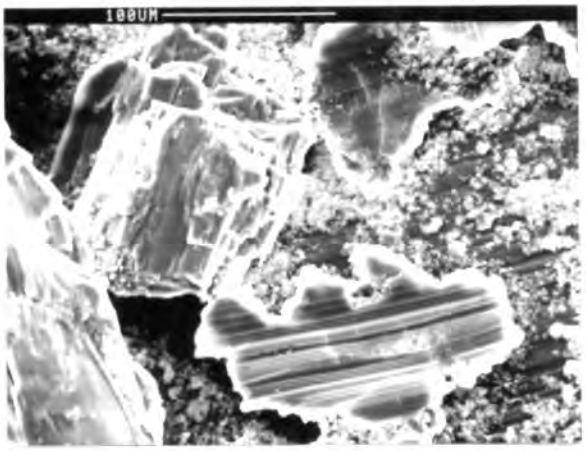

(f) : Mashed flake and angular detrital grain produced by drilling norite

FIGURE 5.86 : SEM micrographs of detritus produced by drilling a variety of materials at 0,044 mm/rev set rate of advance

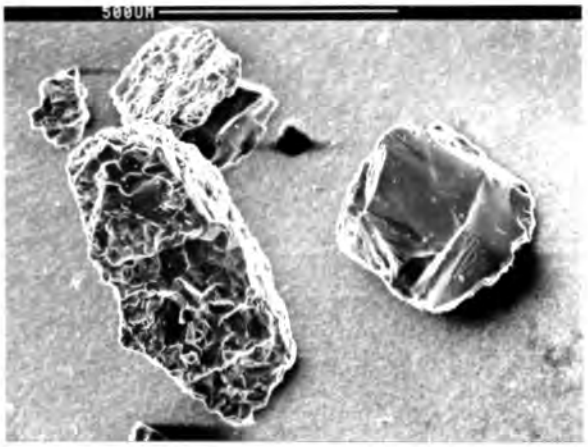

(a) : Large single grain and multigrained particle

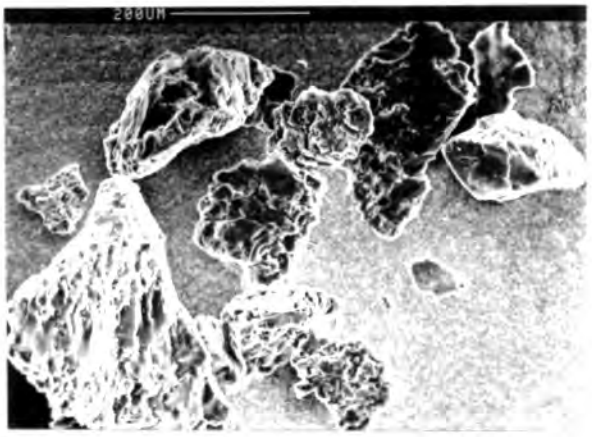

(b) : Typical particles

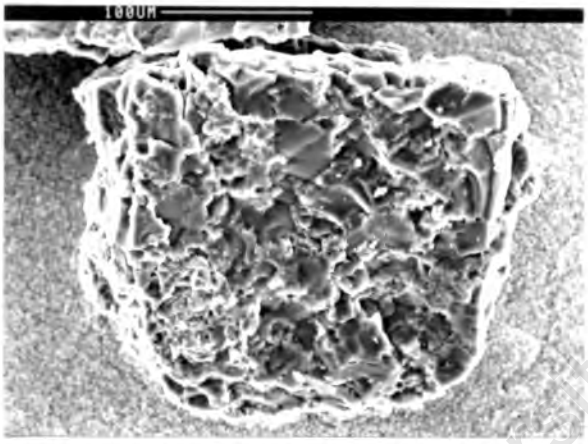

(c) : Single particle showing polycrystalline nature

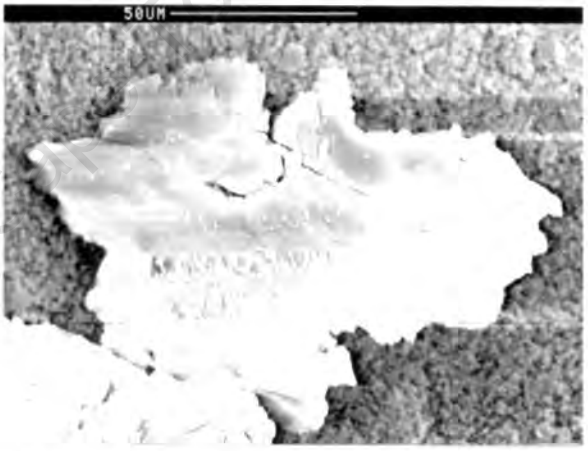

(d) : Mashed flake of finely ground rock flour

FIGURE 5.87 : SEM micrographs of detritus produced by drilling jaspilite at 0,033 mm/rev set rate of advance

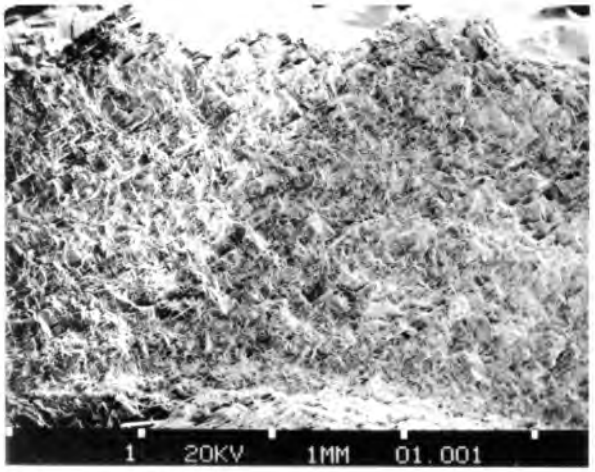

(a) : Drilling track produced at 8 MPa in felspar

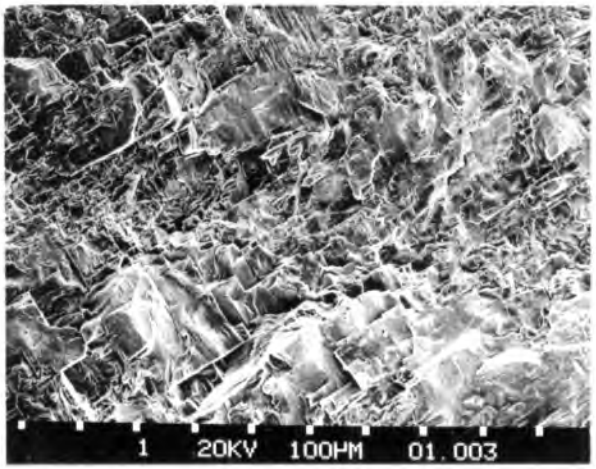

(b) : Detail of track of a single diamond in felspar

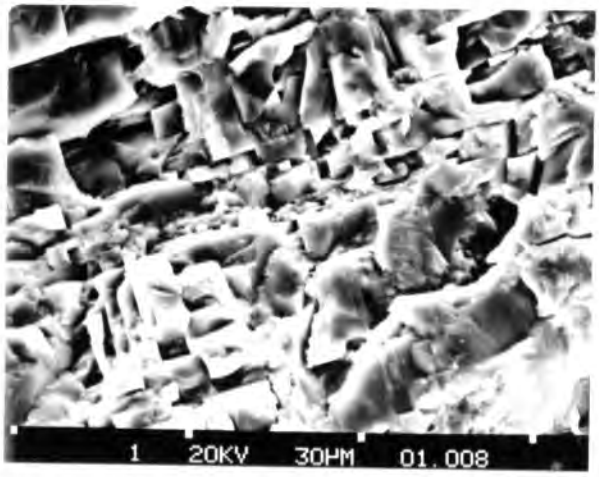

(c) : Detail of the cleavage fracture of felspar

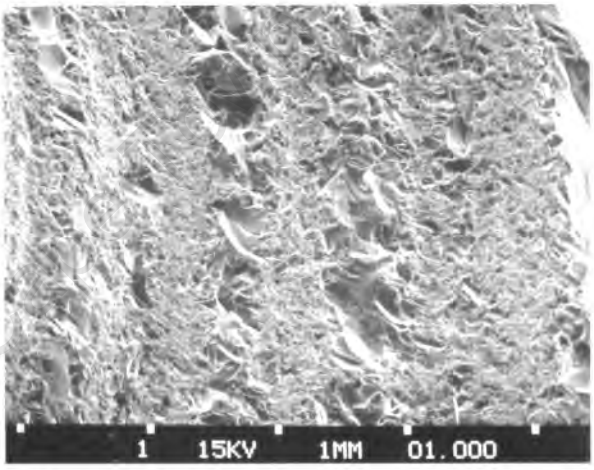

(d) : Drilling track produced in quartz at 8 MPa

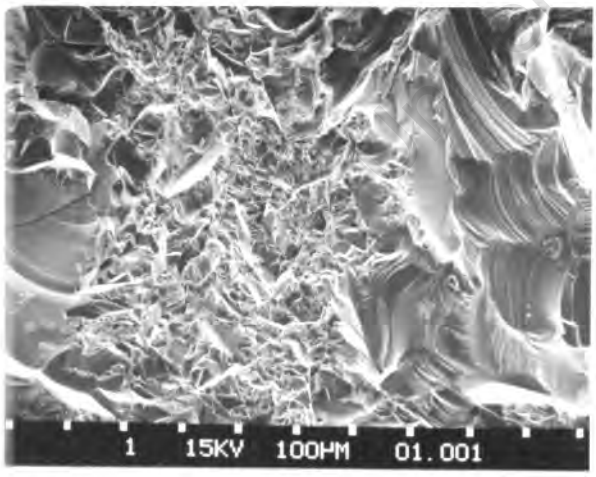

(e) : Detail of track of single diamond in quartz

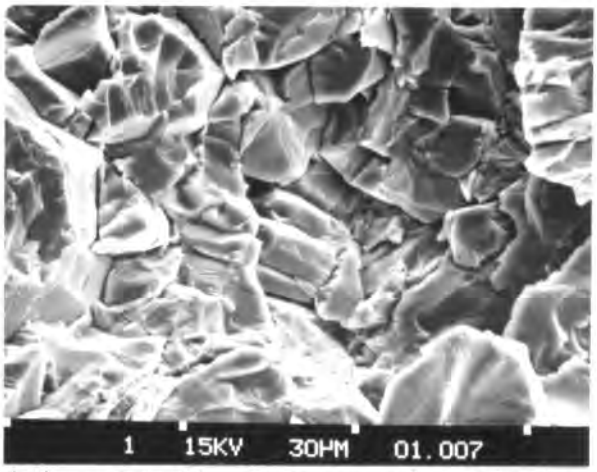

(f) : Detail of track of a single diamond in quartz

FIGURE 5.88 : SEM micrographs of drilled tracks in single crystal quartz and felspar

The scanning electron micrographs of the drilling tracks produced at set rate of advance in a variety of materials are presented in Figs. 5.89 and 5.90. It was only at the lowest rate of advance that punch-through discs could be produced successfully with a majority of materials. Even at 0,011 mm/rev the sandstone specimen was destroyed. The first micrograph of each pair was taken at low magnification to illustrate the whole width of the drilling track. The second micrograph was at a magnification of about 120X to illustrate the detail of the fracture. The micrographs of quartzite show the individual fractured quartz grains embedded in the micaceous matrix from which some of them have been excavated (Figs. 5.89(a & b)). Remnants of adhering mashed flakes can be seen at higher magnification. The even grained nature of the jaspilite is obvious at both low and high magnification (Fig. 5.89 (c & d)). Small fragments of mashed flakes are visible at high magnification. The single crystal quartz fractured very unevenly. The finer crushing caused by the passage of individual diamonds is clear at both magnifications (Figs. 5.89(e - f)). The track in calcite (Figs. 5.90(a & b)) showed that very few diamonds were in contact with the rock surface - there are seven distinct grooves with mashed material at the bottom of each. Particles were broken out from between the grooves by cleavage. The single crystal felspar also showed deep individual grooves with material removed between them by cleavage (Figs. 5.90(c & d)). This was less marked than in the calcite, partly because the cleavage of felspar is less readily opened than in calcite and because one of the two principle cleavages of the felspar was orientated perpendicular to the drilling direction. This accounts for the tabular appearance of the cleaved surfaces in Fig. 5.90(d). The norite track showed cleavage of the felspar and pyroxene grains in the rock and the presence of numerous mashed flakes adhering to the fractured surfaces (Fig. 5.90(e & f)).

The tracks of quartz, quartzite and norite produced at 0,033 mm/rev showed the same features as at 0,011 mm/rev with no appreciable difference in type or scale of fracture.

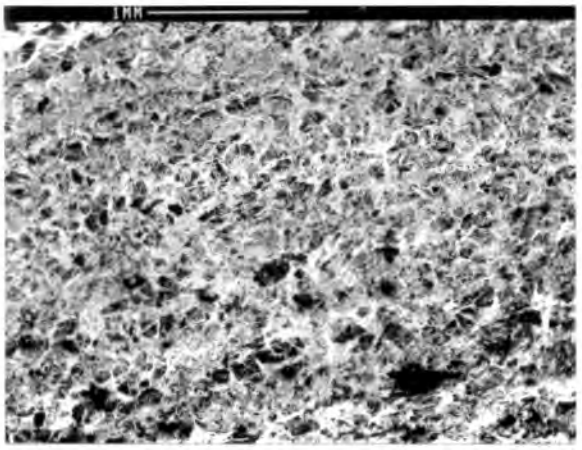

(a) : Drilled track in quartzite

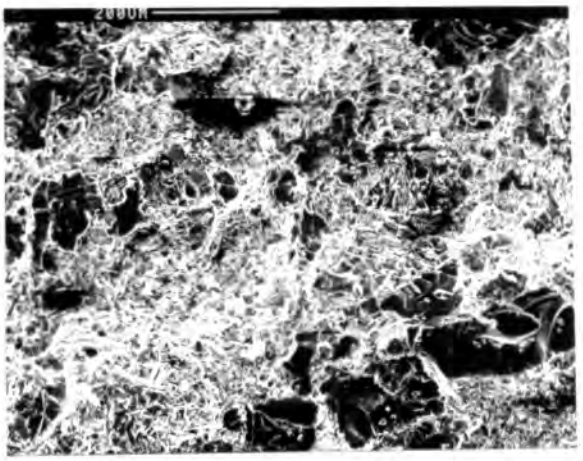

(b) : Detail of (a)

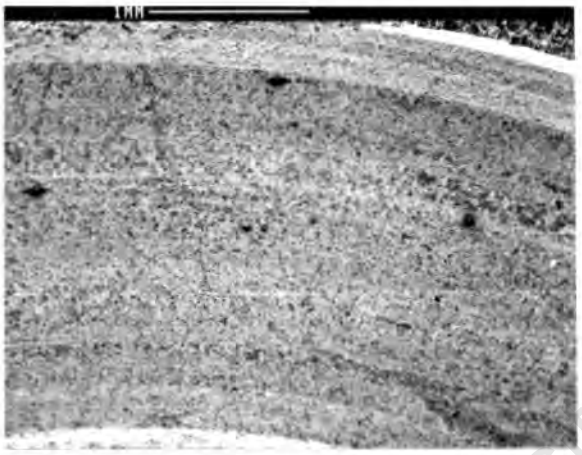

(c) : Drilled track in jaspilite

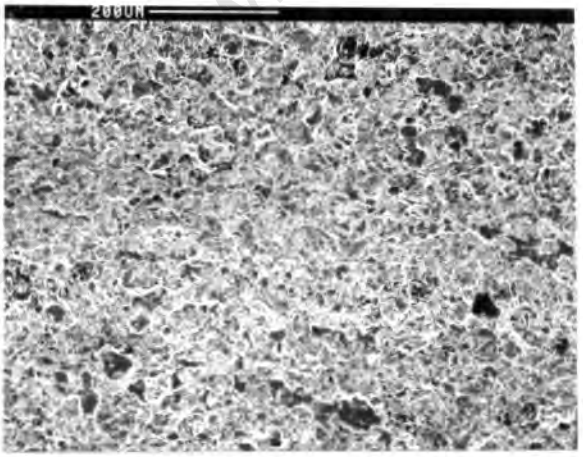

(d) : Detail of (c)

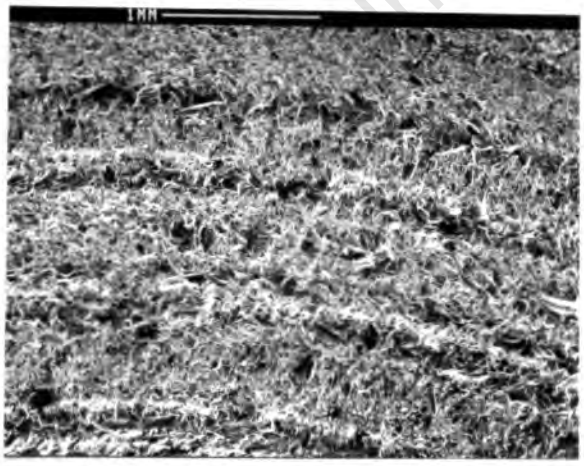

(e) : Drilled track in quartz

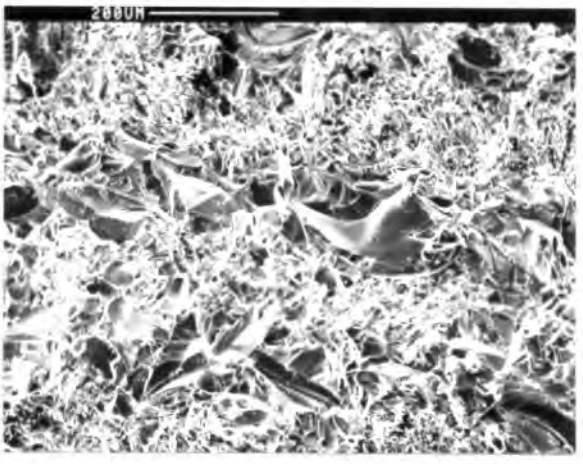

(f) : Detail of (e)

FIGURE 5.89 : SEM micrographs of drilled tracks produced at 0,011 mm/rev set rate of advance

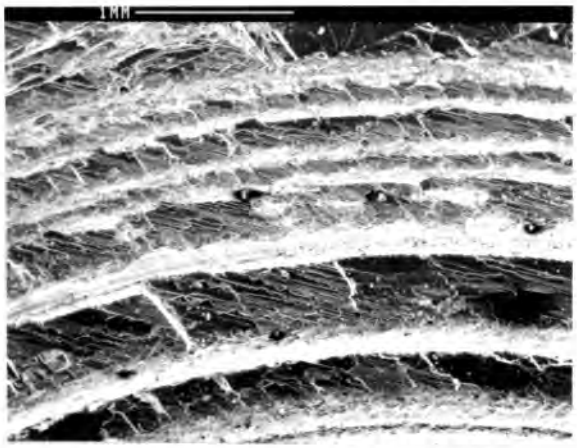

(a) : Drilled track in calcite

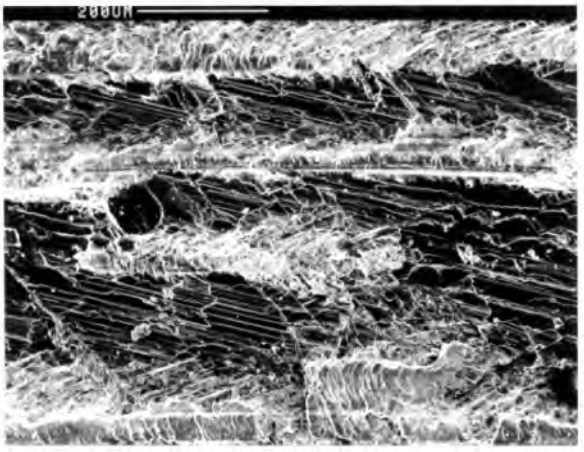

(b) : Detail of (a)

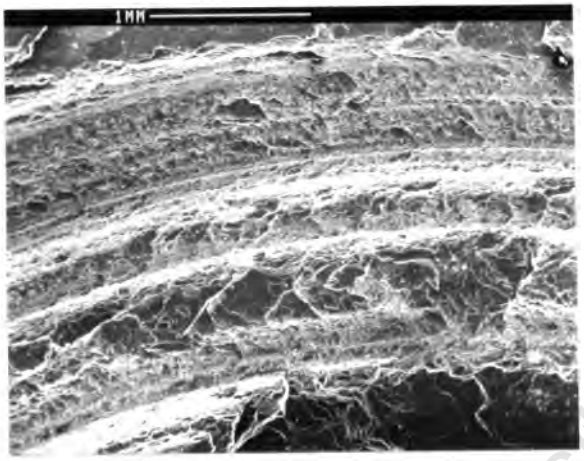

(c) : Drilled track in felspar

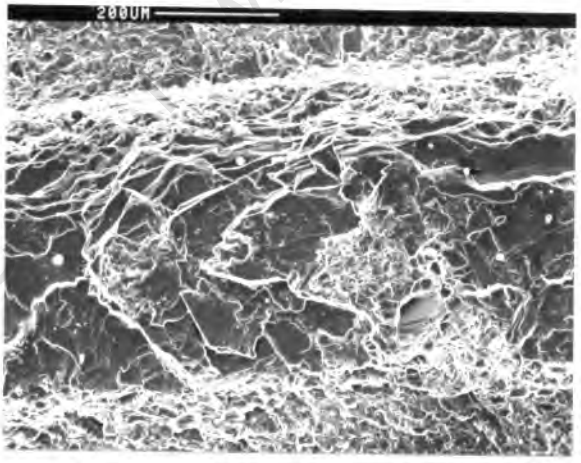

(d) : Detail of (c)

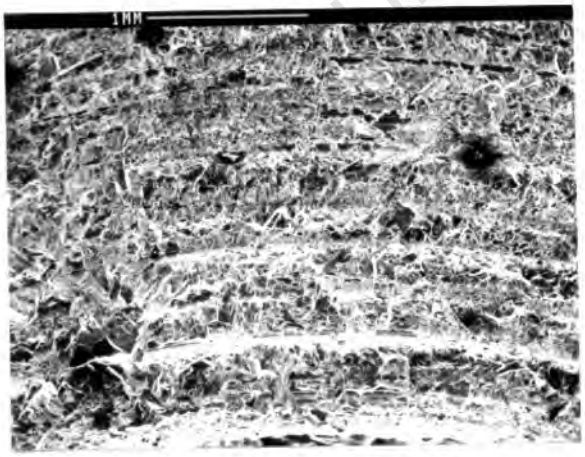

(e) : Drilled track in norite

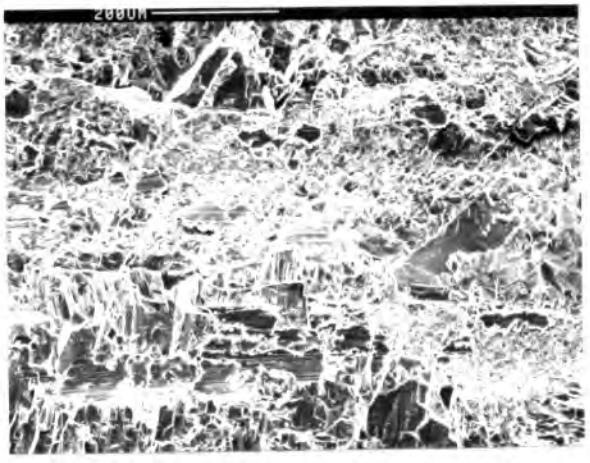

(f) : Detail of (e)

FIGURE 5.90 : SEM micrographs of drilled tracks produced at 0,011 mm/rev set rate of advance

5.5 THE EFFECT OF INCREASING CONCENTRATION

Three tests were drilled in norite with bits of 50 concentration to test the effect of an increase in diamond concentration. All three tests were at a nominal rotational velocity of 3500 rpm and involved drilling 16 holes (about 1,5 m). The first two were with 20/30 mesh bits and the last with a 50/60 mesh bit. The first one was at a set thrust of 7,5 MPa and the other two at a set rate of advance of 0,044 mm/rev. The results are tabulated in Table 5.10 with the results of equivalent tests with 30 concentration bits.

TABLE 5.10 : Results of concentration effect tests

TEST NO.	DIAMOND MESH (US MESH)	BIT PRESSURE (MPa)	RATE OF ADVANCE (mm/rev)	SPECIFIC ENERGY (MJm^{-3})	DRILLING MODE	SET PARAMETER
CONCENTRATION 50						
174	20/30	7,49	0,045	1442	1	Thrust
173	20/30	6,04	0,044	994	1	Rate of Advance
201	50/60	5,51	0,044	1019	1/2	Rate of Advance
CONCENTRATION 30						
117	20/25	7,61	0,054	1559	2	Thrust
160	20/30	4,74	0,044	997	2	Rate of Advance
161	50/60	4,67	0,044	732	2	Rate of Advance

The 50 concentration bits drilled suboptimally. The initial thrust was too low to maintain penetration. From this limited test series it appeared that the load per stone was an important variable. By comparison with the bits of 30 concentration the increased number of diamonds exposed on a 50 concentration bit raised the initial bit pressure level required for sustained Mode 2 behaviour. In the case of the tests at set thrust the initial bit pressure of 7,49 MPa gave rise to Mode 1 behaviour with a decreasing rate of advance when using the 50 concentration bit. In the case of the remaining two tests the initial bit pressure level was too low to keep the bit "open" and maintain steady drilling. Hence the bit pressure rose as the wear flat area increased.

5.6 COMPARISON OF BEHAVIOUR OF MICROBITS AND FULL-SCALE AXT BITS

The results of miscellaneous tests with full-scale bits done at Boart Research Centre were made available for comparison with tests using microbits. Three tests were selected that had been drilled in norite under conditions similar to those used for the microbits. A further nine tests were done by Boart Research Centre staff on a full-scale laboratory drilling machine. There are four sets of results presented here: at set rate of advance with different diamond sizes; at different rates of advance with 20/30 mesh 30 concentration bits; and with 50/60 mesh bits at both 30 and 50 concentration. Each AXT bit used for these tests had a bronze matrix, 32 mm inner diameter, 48 mm outer diameter, 4 waterways, and a bitpad surface area of approximately 845 11,111^{2}. The 'rotational velocity was about 1200 rpm giving a linear bit speed of about 3 ms^{-1}. The results are tabulated in Table 5.11. The second half of the table lists the results of corresponding tests using microbits. Few of the drilling conditions could be duplicated exactly and tests at 0,1 mm/rev were not possible because of stalling of the Arboga laboratory drill.

Although the correspondence between the results of drilling with full-scale bits and microbits at set rate of advance was not exact, both sets of results followed the same trends and had equivalent values of reactive bit pressure. The individual discrepancies in bit pressure and drilling mode could be explained in terms of differences in set rate of advance. Higher bit pressures and more optimal drilling with individual microbit tests were all related to higher rates of advance than those for the corresponding AXT bits. Although the specific energy values (where available) followed the same trends for both sets of data, they differed by a factor of about 5. Specific energy measurements of this nature are specific to each particular experimental rig and as such individual specific energy results were not directly comparable. Linear bit wear rates for tests in Mode 2, although highly variable, were of the order of 1 mm/m for both types of bits at set rate of advance.

TABLE 5.11 : Comparison of results of drilling with full-scale AXT bits and microbits

TEST	DIAMOND MESH (US MESH)	CONC.	BIT PRESSURE (MPa)	MODE	SPECIFIC ENERGY (MJm^{-3})	DRILLING DISTANCE (m)	RATE OF ADVANCE (mm/rev)
	AXT TESTS						
	20/30	30	5,2	1	-	2	0,070
	30/40	30	4,6	2	-	2	0,070
	40/50	30	3,4	2	-	2	0,070
	20/30	30	3,8	1	337	2	0,025
	20/30	30	5,5	1	262	2	0,040
	20/30	30	5,4	2	129	2	0,101
	50/60	30	3,2	1	286	2	0,028
	50/60	30	3,8	1/2	224	2	0,042
	50/60	30	3,9	2	117	2	0,100
	50/60	50	3,1	1	340	2	0,026
	50/60	50	3,5	1	240	2	0,041
	50/60	50	4,5	2	107	2	0,099
TEST	MICROBIT RESULTS						
97	20/30	30	5,3	1	1174	1,5	0,044
98	30/40	30	4,4++	1++	1098	1,5	0,044
78	40/50	30	4,1	2	746	1,5	0,044
165	20/30	30	6,5+	1	1651	1,5	0,033
97	20/30	30	5,3	1	1174	1,5	0,044
	20/30	30	-	-	-	-	0,1
169	50/60	30	3,8+	2+	1090	1,5	0,033
161	50/60	30	4,7+	2+	732	1,5	0,044
	50/60	30	-	-	-	-	0,1
	50/60	50	-	-	-	-	0,033
201	50/60	50	5,5+	1/2+	1019	1,5	0,044
	50/60	50	-	-	-	-	0,1

+ Higher bit pressure and more optimal drilling relates to higher rate of advance than corresponding AXT test.

++ Less optimal drilling relates to lower rate of advance than corresponding AXT test.

5.7 DIAMOND WEAR COUNTS ON AXT FULL-SCALE BITS

Five used AXT bits were received from Boart Research Centre. The diamond wear type frequencies were determined for comparison with the results from microbits. The diamond wear on a single impregnated pad from the

four on each AXT bit was assumed to be representative of the bit as a whole. The wear was evaluated by optical microscopy, and SEM of selected stones. The bit formulations (where known), drilling conditions, performance, and diamond wear counts are tabulated in Table 5.12.

TABLE 5.12 : Results of diamond wear counts on AXT bits

BIT	DESCRIPTION	ROCK TYPE	DRILLING DEPTH (m)	MODE	MEAN BIT PRESSURE (MPa)	RATE OF ADVANCE (mm/rev)
AXT 344	-	Granite	2,1	1	20,9	0,100
AXT 289	-	Granite	2,1	2	14,1	0,155
AXT 532	20/30# 30 Conc	Norite	2	2	5,4	0,101
AXT 533	50/60# 30 Conc	Norite	2	2	3,9	0,100
AXT 534	50/60# 50 Conc	Norite	2	2	4,5	0,009

	% DIAMOND WEAR TYPE									
BIT	0a	0b	1a	1b	2a	2b	3a	3b	4a	4b
AXT 344	8	4	6	31	6	13	13	19	1	0
AXT 289	13	10	5	13	4	22	12	21	0	0
AXT 532	13	11	7	18	9	27	9	4	2	0
AXT 533	9	16	9	6	11	12	18	18	1	0
AXT 534	14	20	7	6	9	13	17	12	1	0

AXT 344 was the only bit that had drilled in Mode 1. Type 1 wear predominated over Type 2; and in particular Type 1b (wear flats) predominated over Type 2b (microfractured stones) with a ratio of 31:13. The proportion of unworn stones (Type 0a + b) was low due to the diminished exposure of fresh stones because of low matrix wear. The other four bits had much higher proportions of freshly exposed stones, lower proportions of wear flats and higher numbers of sharp micro-fractured stones indicative of steady drilling with balanced bit wear in Mode 2. The diamond wear on the AXT bits did not differ in any appreciable way from the wear on microbits which had drilled under comparable conditions. Examples of SEM micrographs of worn diamonds from AXT 344 and AXT 289 are presented in Fig. 5.91. The Type 1b wear displayed by stones on bit AXT 344 showed typical grooving, transverse steps, and cleavage controlled break-up of the worn surfaces (Figs. 5.91(a - c)). The Type 2b wear on AXT 289 consisted of typical cleavage controlled microfracture creating sharp drilling points (Fig. 5.91(d - f)).

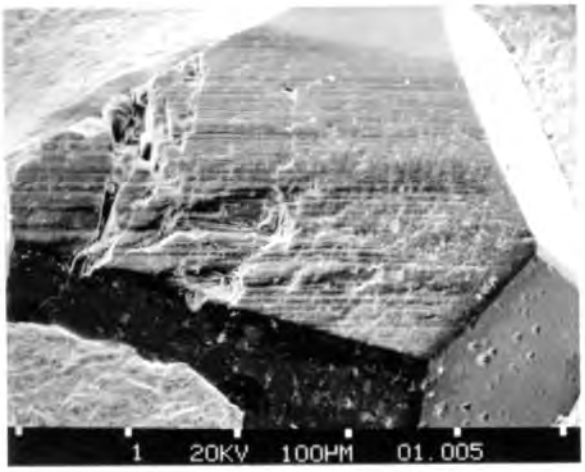

(a) : Type 1b - AXT 344 : grooved wear flat

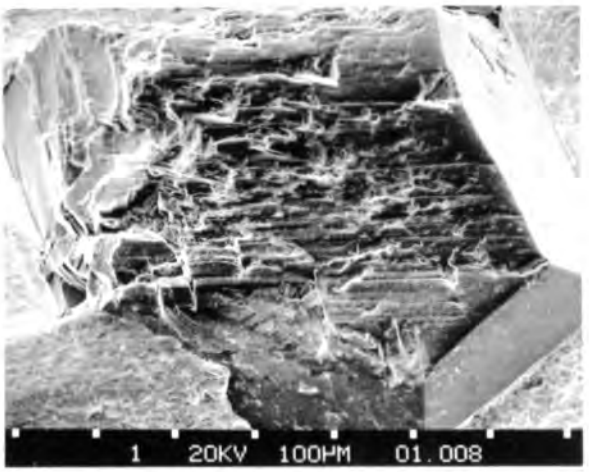

(b) : Type 1b - AXT 344 : fractured wear surface

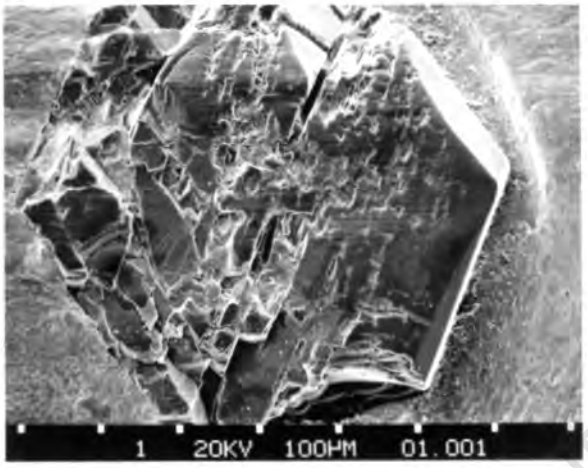

(c) : Type 1b - AXT 344 : cleavage fracture of worn surface

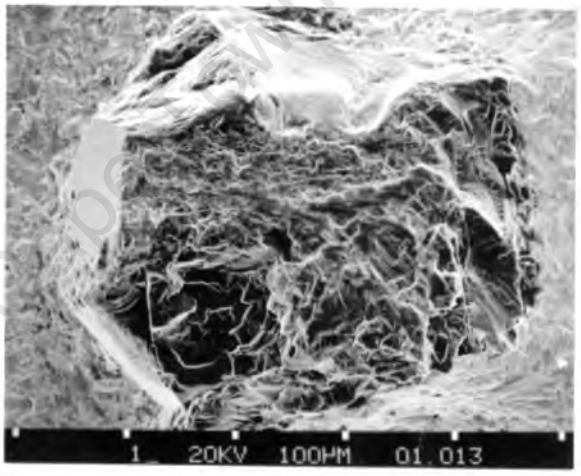

(d) : Type 2b - AXT 289 : micro-fracture

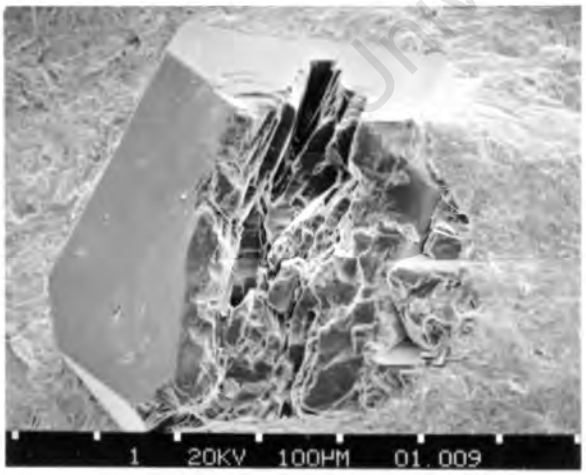

(e) : Type 2b - AXT 289 : microfracture

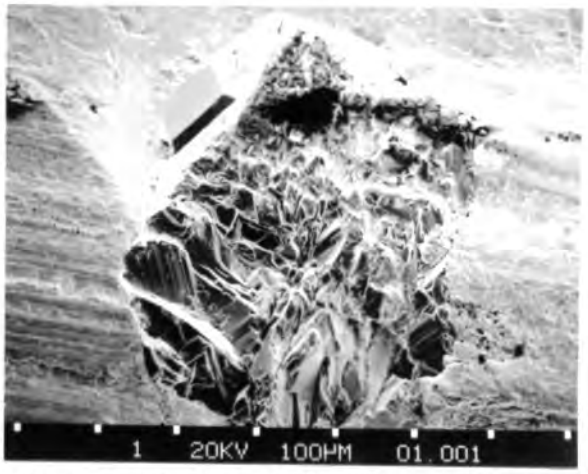

(f) : Type 2b - AXT 289 : micro-fracture

FIGURE 5.91 : Typical wear of diamonds on AXT bits drilled in Mode 1 (AXT 344) and Mode 2 (AXT 289)

5.8 DIAMOND WEAR DEVELOPMENT ON MICROBITS

Three sets of tests were drilled in norite with microbits to establish if there was a sequence of diamond wear development. A newly opened bit was drilled in Mode 2 at set thrust and the diamond wear monitored after regular intervals (TEST 73). A single bit was drilled at five successively higher set thrusts and diamond wear was monitored after each of the five tests (TESTS 144 to 148). Two specially made monolayer bits consisting of regular planar arrays of diamonds which could be characterised accurately were used. The first bit was used for two tests at set thrust and the second bit for a third test at set rate of advance. The wear development of particular stones could be followed by inspection at regular intervals (TESTS 175, 176 & 200).

5.8.1 Diamond Wear at Set Thrust

A newly opened bit was used for the nine tests, each about 185 mm long, at 6 MPa bit pressure and 3500 rpm nominal speed. They all drilled in Mode 2 with a constant bit pressure; a steady state had developed in less than 0,25 m of drilling (Fig. 5.92). Diamond wear was evaluated after each test. Occasionally it was difficult to assign a stone to either Type 1 or Type 2 wear with confidence. In these cases wear flats had been broken up by the development of microfracture or microfractured stones had worn to flats. Although individual points of microfractured stones displayed abrasion and rounding in the majority of cases the wear flats seemed to precede the fracturing of the stone. Without accurate plotting of position re-identification of individual stones was not possible after each test. However, the percentage incidence of Type 1 wear (rounding and flats) showed a steady decrease, reaching half its initial value of 22% after three runs and stabilizing at about 6% after a further three runs (Fig. 5.92). As this was the only clearly defined trend in the wear frequency percentages the implication was that the progression of wear types that a given stone might display was not simple. The development of other wear types from stones initially showing Type 1 wear flats was drilling distance dependent in the quasi-stable drilling mode.

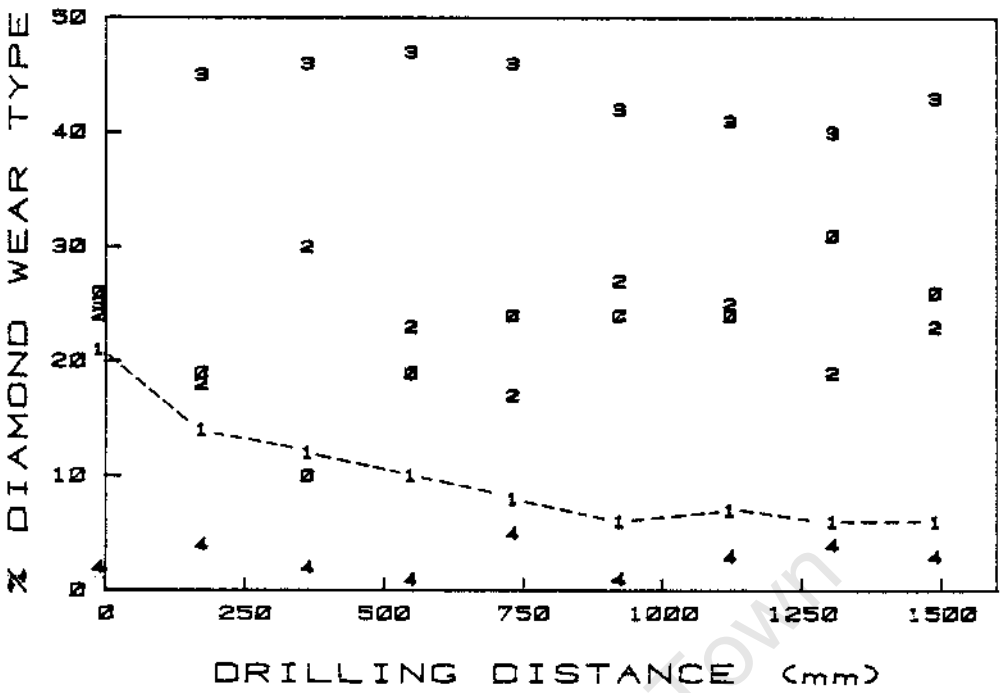

FIGURE 5.92 : Plot of diamond wear type percentage against drilling distance for tests drilled in norite at 6 MPa bit pressure, showing a decrease in wear flat development with the establishment of stable drilling

5.8.2 Diamond Wear with Stepwise Increasing Thrust

Five tests were drilled in norite at increasing set thrusts with a single standard microbit without reconditioning the bit between tests. The first bit pressure used was 2,4 MPa at which pressure the bit drilled in Mode 1 and ceased to penetrate the rock after 96 mm. Simply increasing the bit pressure to 5,6 MPa caused resumption of drilling in Mode 2. Wear flat generation had not been allowed to develop to the extent that the bit could not be "re-opened" without even higher regenerative loads. In terms of penetration rate there was a performance optimum at 7,5 MPa with a rate of advance of 0,106 mm/rev, and a slight drop at higher thrusts to mean values of 0,087 mm/rev at both 10,3 MPa and 12,5 MPa bit pressure. Diamond wear was evaluated after opening the bit and after each test of approximately 0,5 m length. The results are presented in Fig. 5.93.

As with the results of the previous test (see Fig. 5.92) all the diamond wear percentages (with the exception of Type 4) were fairly close to each other after opening the bit. With increasing thrust they diverged with subsequent drilling (Fig. 5.93). At 24 MPa bit pressure Type 1 wear predominated giving rise to Mode 1 drilling behaviour. At higher bit pressures this trend reversed with extreme divergence of the wear types at the highest thrusts with Type 2 wear predominating. Type 4a wear (macrofracture) also started to increase at the higher bit pressures.

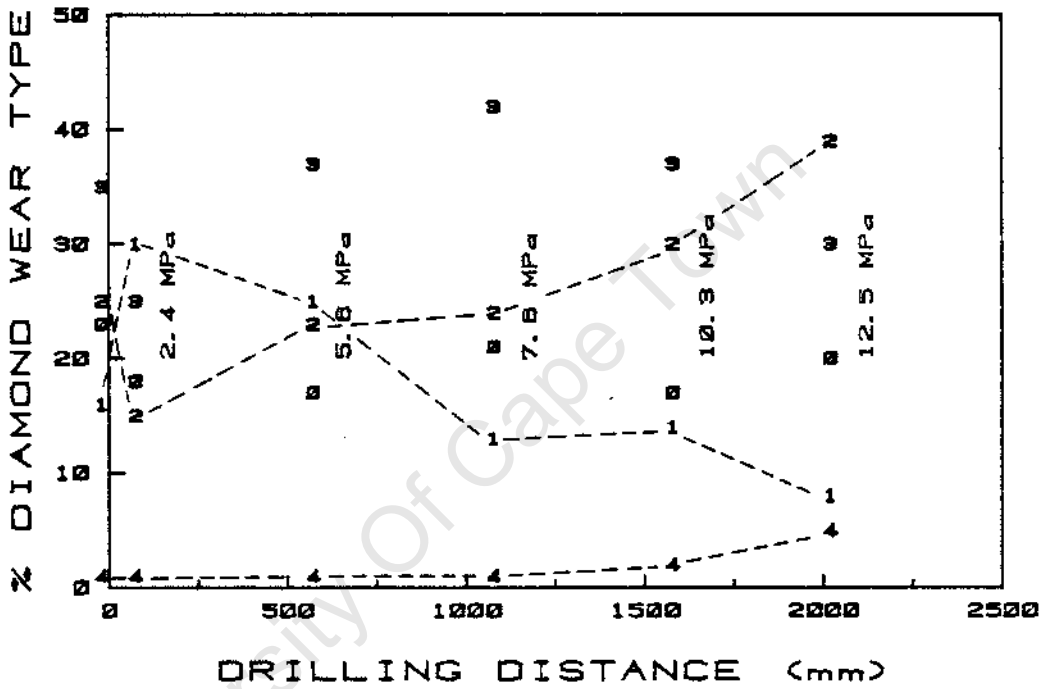

FIGURE 5.93 : Plot of diamond wear type percentage against drilling distance for tests drilled in norite at set thrust increments, showing the increase in microfracture (Type 2 wear) at higher thrusts

5.8.3 Diamond Wear Development on Monolayer Bits

Three long tests were drilled with the two monolayer bits to determine the sequence of diamond wear development of individual stones. The advantages of the monolayer bits were that due to the relatively dense placement of the stones bit wear was minimal if the correct bit pressures were maintained, and the bits were fully characterisable in terms of stone position and initial wear status.

The first two tests were drilled at set thrust with a I m lead-in using bit pressures from 4 MPa up to 8,5 MPa which latter was then maintained for the remaining 1,5 m of the two concatenated tests. Important features of the results (Fig. 5.94) were that after the first half of the test the diamond wear Type 2b (microfractured stones) dropped in number with a rise in Type 4a (failure flush with the matrix) and the other wear types established constant, low values.

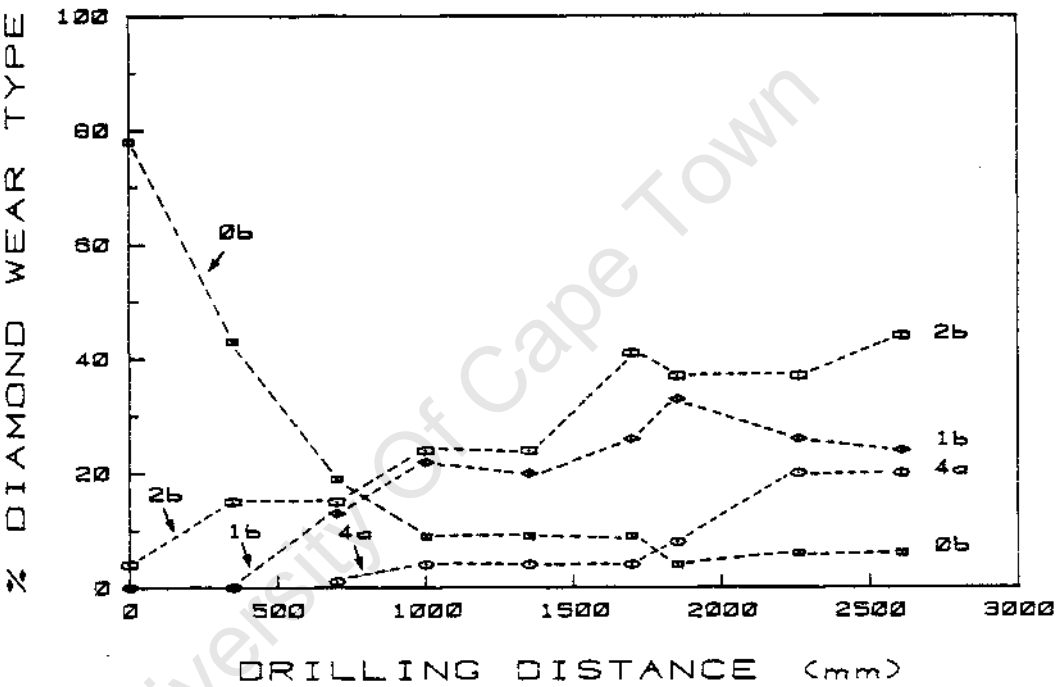

FIGURE 5.94 : Plot of diamond wear type percentage against distance drilled for a monolayer bit drilled in norite at set thrust increments showing development of diamond wear in Mode 2

The results for the test drilled at a set rate of advance of 0,033 mm/rev - which generated a mean bit pressure of 5,9 MPa - were very different (Fig. 5.95). Type lb wear predominated over Type 2b in the second half of the test with a steady increase in bit pressure approaching the limiting capacity of the drilling machine. The relatively high incidence of Type Ob stones (unworn) indicated that about 20% of the diamonds were not involved in the drilling process at all. This was due to the fact that the bit

face was not precisely perpendicular to the bit axis, sheltering some of the stones in the wedge created by the tilt. These tests were not done to optimise the operation of monolayer bits so the discrepancy in performance was useful in allowing a comparison of diamond wear development sequence in the two different modes of drilling behaviour.

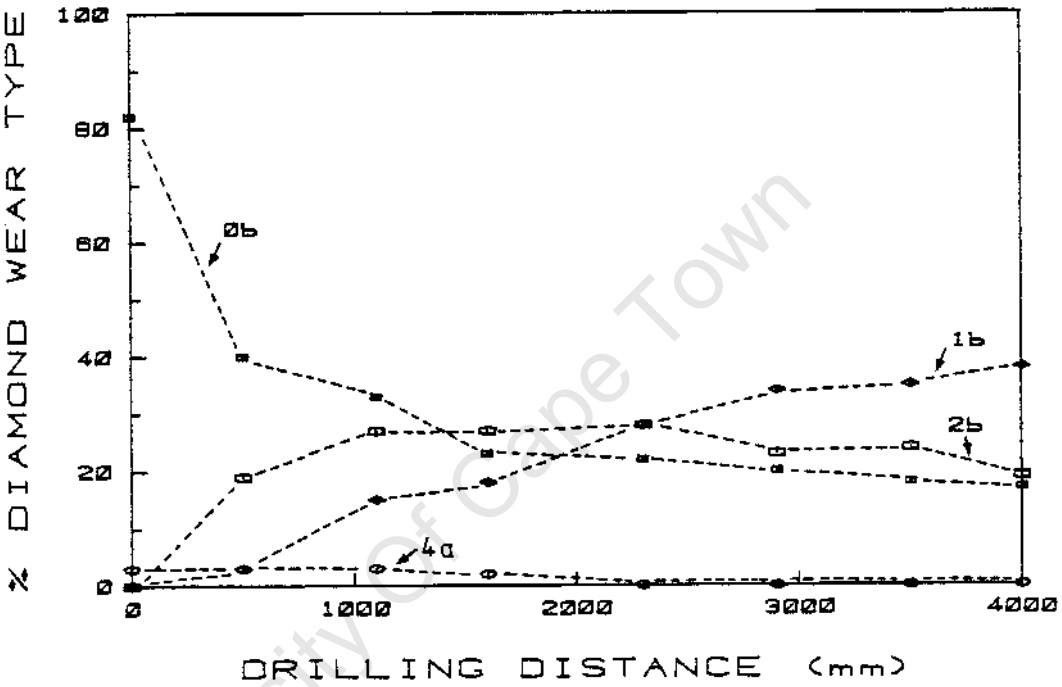

FIGURE 5.95 : Plot of diamond wear type percentage against distance drilled for a monolayer bit drilled in norite at 0,033 mm/rev set rate of advance showing development of diamond wear in Mode 1

Each stone was categorised at approximately regular intervals during the tests and full tables of wear development sequences were drawn up to record the history of each stone. A sequence of development was found to take place with stones progressing from either Type Ob or Type 2 initial conditions to states designated by higher numbers i.e. la, lb, or 2b, 4a. Apparent reversals did occur occasionally as some stones would develop wear features associated with less mature or with dynamically different wear states. A summary will clarify this.

30/40 MESH MONOLAYER 4 to 8,5 MPa 54 STONES
33 stones followed "main sequence" to higher-numbered wear types
21 stones suffered "reversals" of which
16 were Type lb to la and
5 were inter-type e.g. Type 2 to Type 1

20/30 MESH MONOLAYER 0,033 mm/rev 60 STONES
49 stones followed "main sequence" to higher-numbered wear types
11 stones suffered "reversals" of which
1 was Type lb to la and
10 were inter-type e.g. Type 2 to Type 1

Reversals from Type lb to la were considered to be an artefact of misclassification, the boundary between Type la and Type lb being gradationary anyway. The inter-type reversals (fewer than 15%) were different for each bit. The 30/40 mesh bit suffered more dynamic conditions and the diamond wear development reflected this. A few stones changed their characteristic wear type with several reversals, Type 2b stones usually being rounded and flattened to be classified as Type lb and then redeveloping the features characteristic of Type 2 stones. The development of a significant number of Type 4a stones was also indicative of the dynamic conditions.

The 20/30 mesh diamonds experienced more consistent main sequence development. The inter-type reversals were predominantly the development of permanent Type lb flats on previously Type 2b stones. Mode 1 drilling at suboptimal conditions produced insufficient microfracture and the diamonds developed progressively larger wear flats. A characteristic sequence of wear development was demonstrated by the bits drilling effectively in Mode 2. Most of the freshly exposed stones progressed through Type 1 rounding and wear flat development, and eventually microfractured to produce Type 2 wear (with a cyclical repetition of this stage possibly) until whole-scale failure reduced the stone to a Type 4a with ensuing loss in most cases.

The transition from Type 1 wear to Type 2 wear is illustrated by the SEM micrographs in Fig. 5.96 of a very large stone which displayed a number of different wear features simultaneously. In this case a single stone displayed a progression of wear types across the stone from leading edge to trailing edge. The stone was classified as an intermediate between Type 1 and Type 2 wear. The leading edge was rounded and followed by a wear flat area, characteristically grooved and crossed by transverse steps. In the middle of the exposed surface crystallographically controlled microfracture had started to develop which had progressed into considerably more severe cleavage and failure towards the trailing edge of the stone. With further drilling time at an appropriate

entire stone to produce typical Type 2b wear.

5.9 MEASUREMENT OF BIT FACE TOPOGRAPHY

Two bits were selected for a detailed study of the bit face topography. One was a 20/30 mesh bit, the other 50/60 mesh. Both were opened in sandstone by drilling 0,5 m at 5 MPa, then analysed using the reflex microscope interfaced with a computer. The position and elevation of all the diamonds were measured and readings taken on 1000 points of each bit matrix to enable the computer to construct relief maps of the bit faces. These were plotted with 0,1 mm contours. Both bits were then drilled in norite at 7,5 MPa for 0,5 m to generate diamond wear, and then remeasured with the reflex microscope. At the end of the last drilling run punch-through discs of rock had been produced with each bit and these were also measured by taking readings on 1000 points on the drilled track. An example of a contour plot is shown in Fig. 4.6.

Attempts were made to produce measurable indentations in a polished slab of norite at 10 MPa with both bits. The resulting identations were so small (and so few - about five per bit) that they could not be measured with the reflex microscope. An estimation of the mean protrusion of the diamonds exposed on each bit was made by subtracting the interpolated adjacent matrix elevation from the spot height of the apex of each stone. The results are presented in Table 5.13.

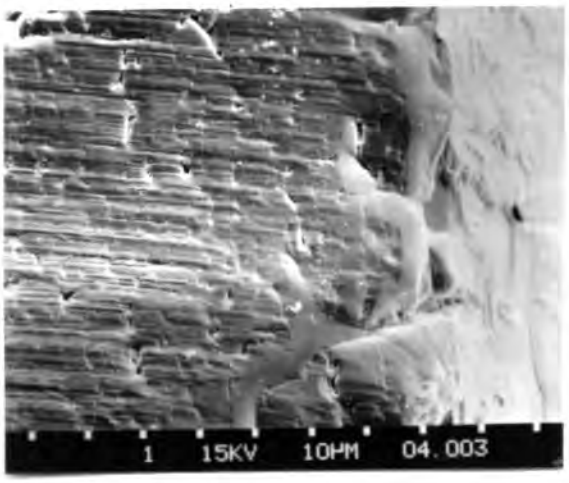

(a) : Rounded leading edge and wear flat with transverse steps

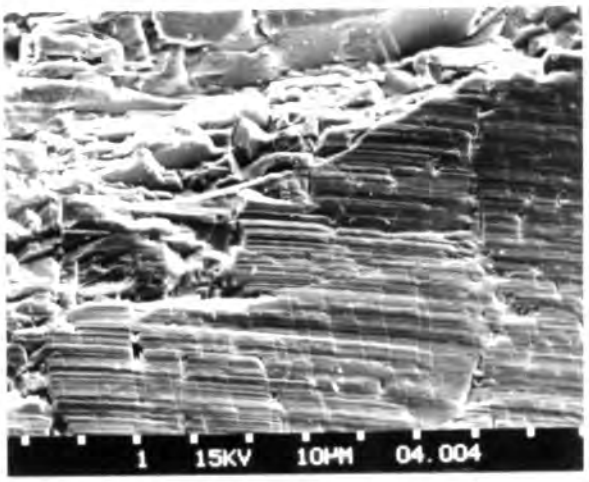

(b) : Grooved wear flat and microfracture

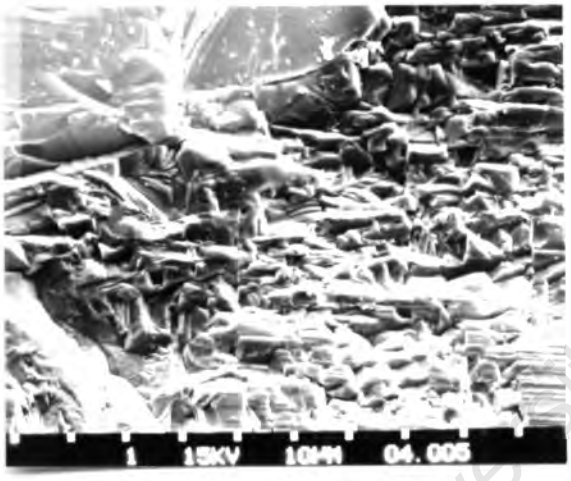

(c) : Microfractured area

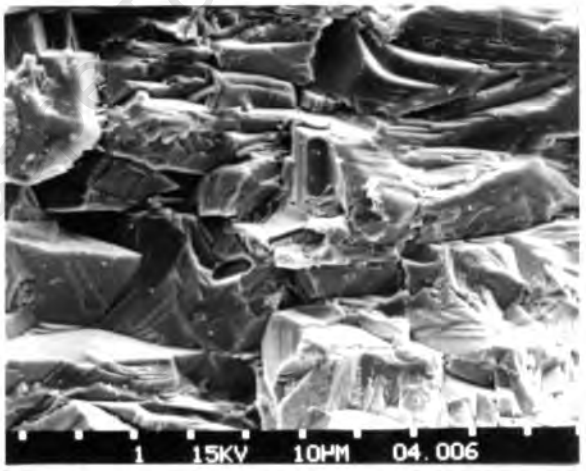

(d) : Large-scale fracture

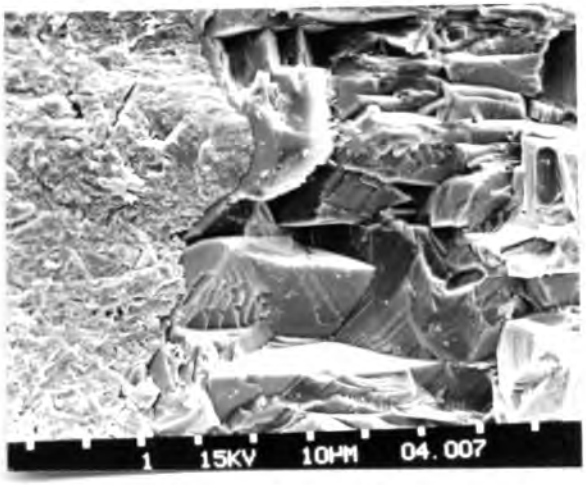

(e) : Failure at trailing edge

FIGURE 5.96 : SEM micrographs of diamond wear displayed on a single stone

TABLE 5.13 : Diamond protrusion measurement

	20/30 MESH OPENED	20/30 MESH DRILLED	50/60 MESH OPENED	50/60 MESH DRILLED
Mean protrusion of all stones (mm)	0,20 ± 0,12 (N = 36)	0,13 ± 0,09 (N = 28)	0,18 ± 0,11 (N = 137)	0,11 ± 0,08 (N = 125)
Mean protrusion of 8 most elevated stones (mm)	0,27 ± 0,15	0,17 ± 0,09	0,30 ± 0,02	0,10 ± 0,09
Mean protrusion of 8 most protuberant stones (mm)	0,37 ± 0,06	0,25 ± 0,04	0,41 ± 0,06	0,20 ± 0,04
Mean coarse detritus size (mm)	-	0,142	-	0,085
% Fine detritus (under 63 micron)	-	84	-	83

Even with a contour interval of 0,1 mm the measured relief at the bottom of the hole, reflected by the punch-through disc topography, was so irregular that the contour maps for the punch-through discs were not very informative. Broad grooves produced by individual diamonds, especially the coarser ones, were apparent but their depth could not be estimated reliably from the contour plots, nor could a particular groove be correlated with any individual diamond.

The most elevated stones were defined as those having the greatest absolute height reading for each bit plot. They undoubtedly participated in drilling. Some of the most protuberant stones were situated on the inner or outer margins of the bit but also contributed actively to the drilling. Comparison of the mean protrusion measurements of the most protuberant stones on the 20/30 mesh and 50/60 mesh bits showed that there was no significant difference between them after drilling 0,5 m. There was also no apparent relationship between the absolute protrusion and the mean of the detritus size in the 2 mm to 63 micron fraction.

5.10 ANALYSIS OF TORQUE AND CALCULATION OF COEFFICIENTS OF FRICTION

Drilling under set rate of advance in norite, the torque was linear with respect to set rate of advance over the operating range available (Fig. 5.20). However, under set thrust this linearity only held up to a limiting torque, and rate of advance (Fig. 5.97). At rates of advance above 0,08 mm/rev high torques were associated with penetration rates lower than expected. This scatter of results corresponded to the "plateau" region in Fig. 5.6 in which an increased bit pressure did not lead to the expected increase in penetration rate because of a compensatory drop in rotational velocity. Under both set thrust and set rate of advance minimum torques were required for any penetration to occur (Figs. 5.20 & 5.97).

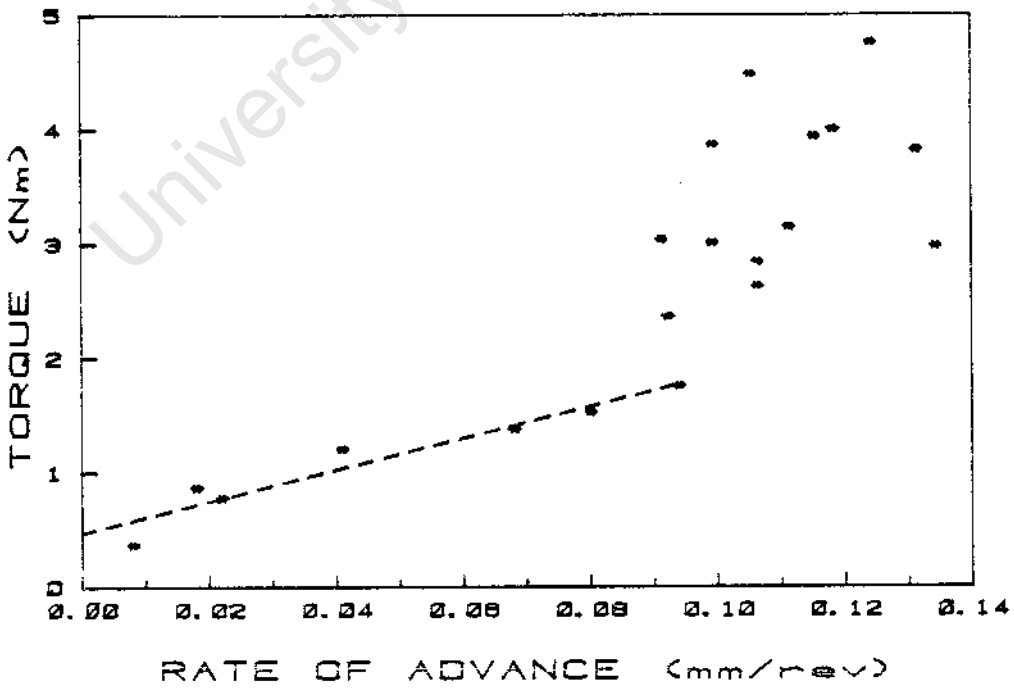

FIGURE 5.97 : Plot showing the linear relationship between torque and rate of advance up to 0,08 mm/rev for tests drilled in norite at set thrust

The coefficient of friction was estimated as the ratio of the tanjential force to the vertical force, i.e.

$$\mu = \frac{\text{Torque Force}}{\text{Thrust Force}} = \frac{T/r}{P \times A}$$

where T = torque (Nm)
r = 0,008 (m) radius of bit pad mid-point
P = bit pressure (MPa or N/mm^2)
A = bit face area (mm^2)

The results for the estimated sliding friction (μ) in norite were as follows:

	TORQUE THRESHOLD (Nm)	BIT PRESSURE (MPa)	ESTIMATED μ
Set thrust	0,475	2,3	0,18
Set rate of advance	0,29	1,9	0,13

The equivalent bit pressures were estimated from Figs. 5.3 and 5.19 and roughly agreed with the extrapolated value of about 2 MPa derived from Fig. 5.6.

The coefficient of friction for sliding could not be estimated by this method for different rock types. The torque was linear with respect to rate of advance only at low rates so there were not enough data points available from the limited number of tests performed in each rock for a valid determination of the threshold torque by linear regression. However because torque was linear with respect to bit pressure, threshold pressures could be calculated from this data for the different rock types (see Table 5.8). This pressure was the minimum required to penetrate the rock and overcome the sliding friction.

The rate of advance in a given rock was expected to be proportional to the friction controlling the torque transmitted to the rock for a given bit formulation. This expectation was tested by calculating the estimated coefficient of friction for each of the tests in the initial series at set thrust and set rate of advance.

The results are shown in Fig. 5.98. The tests that were suboptimal are designated by 1, those that were in Mode 2 are designated by 2, and those that were intermediate by an asterisk. The results are approximated by a straight line with a least squares best fit regression formula of y = 1,40 x + 0,18 (r = 0,92). The estimated threshold friction for penetration was about 0,18. The optimal rate of advance was between 0,06 mm/rev and 0,08 mm/rev with an estimated coefficient of friction in excess of 0,275. It was thought that this might represent a general threshold for drilling norite in mode 2 with the standard bits. The results of all the tests drilled in norite with standard microbits irrespective of rotational speed, thrust, or rate of advance were used to test this hypothesis.

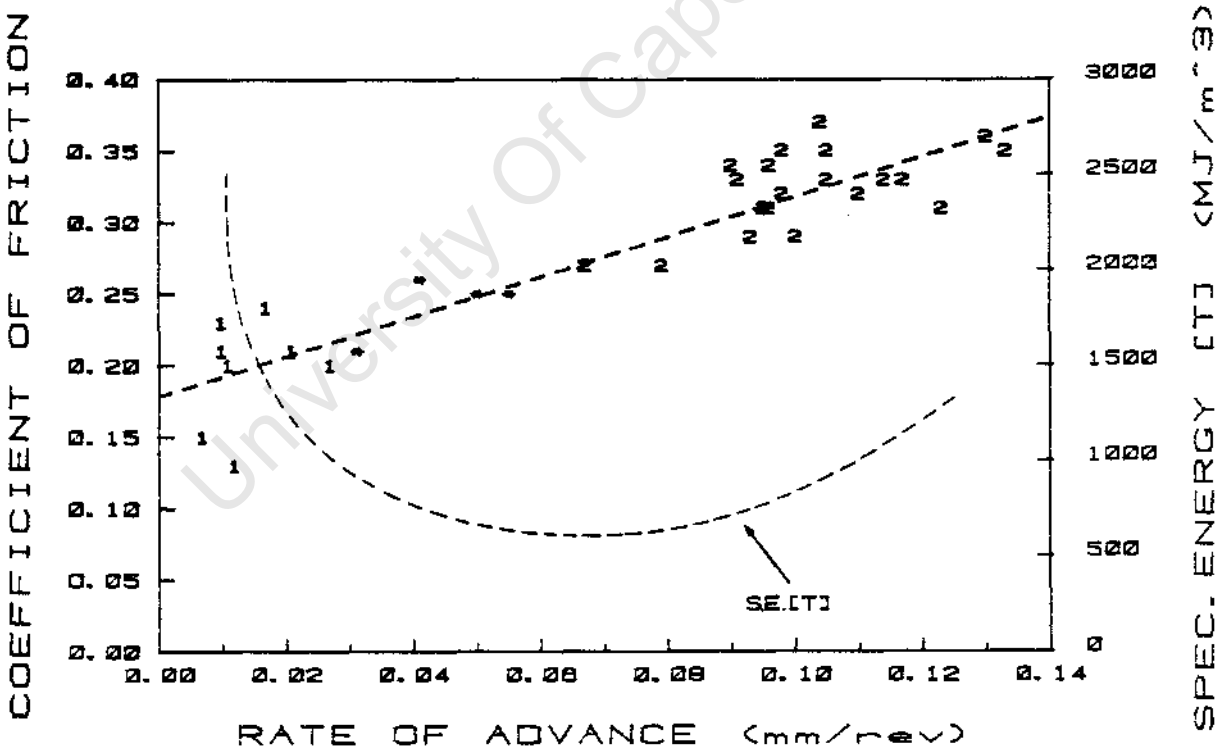

FIGURE 5.98 : Plot of estimated coefficient of friction against rate of advance for tests drilled in norite, showing the transition from Mode 1 to Mode 2 behaviour at about 0,05 mm/rev set rate of advance. The curve indicates specific energy.

The mean of the estimated coefficients of friction for all Mode 1 (including marginal) tests and the mean for all Mode 2 tests were calculated separately. They were as follows:

MODE 1 4 = 0,21 ± 0,045 (n = 38)
MODE 2 **4 =** 0,30 ± 0,047 (n = 89)

The effect of changing diamond size was evaluated by plotting the estimated coefficient of friction against rate of advance for fifty three tests at set thrust in norite with nine different diamond sizes ranging from 20/25 mesh to 70/80 mesh at concentration 30. Least squares linear best fit lines were fitted to the data and are shown in Fig. 5.99. There was no sensible trend in the slope of the lines with changing diamond size. The dispersion was caused by scatter in the results for individual mesh sizes. With all diamond sizes there was a transition from Mode I to Mode 2 drilling behaviour between 0,03 mm/rev and 0,06 mm/rev below a coefficient of friction of about 0,275. It was concluded that diamond size did not influence the relationship between coefficient of friction and rate of advance. The least squares best fit line for all fifty three points represented by Fig. 5.99 was y = 1,69 x + 0,18 (r = 0,82). The mean values for the coefficient of friction was as follows:

MODE 1 **4 =** 0,19 ± 0,042 (n = 14)
MODE 2 **4 =** 0,31 ± 0,041 (n = 39)

These results compare well with those calculated from the set thrust and rate of advance tests described above. Taken together they indicated that the relationship between coefficient of friction and rate of advance was approximately linear and unaffected by diamond size. The transition to stable Mode 2 behaviour occurred between 0,04 mm/rev and 0,06 mm/rev with an estimated coefficient of friction in the region of 0,25 to 0,28 in norite. The coefficients of friction for sliding between the bit and norite (estimated by regression from Figs. 5.20, 5.97 and 5.99) are tabulated for the tests drilled at set thrust, set rate of advance and with different diamond sizes in Table 5.14, From these results the mean coefficient of friction for sliding for microbits of concentration 30 in norite was calculated as 0,162 t 0,039. This is about half the estimated value for the coefficient of friction when drilling steadily in Mode 2.

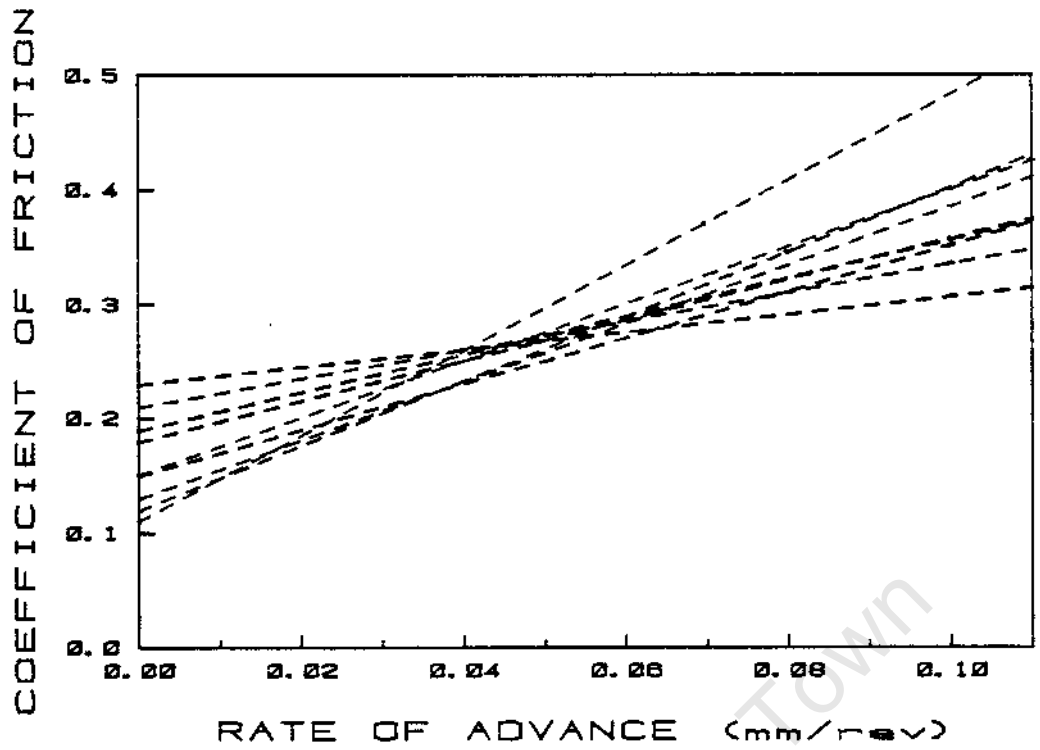

FIGURE 5.99 : Plot of estimated coefficients of friction against rate of advance for tests in norite at set rate of advance with different diamond size bits ranging from 20/25 mesh to 70/80 mesh

TABLE 5.14 : Estimated coefficients of friction for sliding in norite

TEST CONDITION	DIAMOND SIZE (US MESH)	ESTIMATED COEFFICIENT OF SLIDING FRICTION (μ)
Set Thrust	40/50	0,18
Set Rate of Advance	40/50	0,13
Set Rate of Advance	20/25	0,15
Set Rate of Advance	25/30	0,11
Set Rate of Advance	30/35	0,12
Set Rate of Advance	35/40	0,13
Set Rate of Advance	40/45	0,21
Set Rate of Advance	45/50	0,23
Set Rate of Advance	50/60	0,15
Set Rate of Advance	60/70	0,18
Set Rate of Advance	70/80	0,19

The estimated coefficient of friction was calculated for all the tests in rocks other than dark norite and plotted against rate of advance. Best fit straight lines were calculated by least squares regression and the resulting formulae tabulated with the regression coefficients in Table 5.15. The lines are plotted in Fig. 5.100. From the regression coefficients in Table 5.15 it can be seen that most of the relationships can be approximated reasonably with straight lines. The lowest regression coefficients were for the two softest materials. These materials presented relatively little resistance to drilling at all rates of advance. The estimated coefficient of friction at which transition took place from Mode 1 to Mode 2 varied for different materials. For quartzite and jaspilite the transition region was not reached in these tests and for these rocks a minimum value has been indicated. For sandstone, calcite and marble drilling was invariably in Mode 2 and so maximum values have been indicated in Table 5.15. Because of the very approximate nature of these values these estimates of coefficient of friction could not be correlated with the rock properties.

TABLE 5.15 : Formulae for the linear relationship between estimated coefficient of friction and rate of advance for different materials

MATERIAL	BEST LINE FIT	REGRESSION COEFFICIENT	ESTIMATED COEFFICIENT OF FRICTION FOR TRANSITION FROM MODE 1 TO MODE 2 (μ)
Quartzite	$y = 1,70x + 0,10$	$r = 0,81$	0,19
Sandstone	$y = 1,36x + 0,15$	$r = 0,98$	0,18
Syenite	$y = 1,31x + 0,14$	$r = 0,97$	0,27
Light norite	$y = 1,49x + 0,18$	$r = 0,87$	0,31
Granite	$y = 2,37x + 0,08$	$r = 0,97$	0,26
Jaspilite	$y = 4,16x + 0,14$	$r = 0,99$	0,33
Quartz	$y = 3,75x + 0,08$	$r = 0,91$	0,40
Felspar	$y = 1,92x + 0,09$	$r = 0,98$	0,20
Calcite	$y = 2,25x + 0,21$	$r = 0,78$	0,27
Marble	$y = 1,59x + 0,27$	$r = 0,76$	0,15
Dark norite	$y = 1,40x + 0,18$	$r = 0,92$	0,25

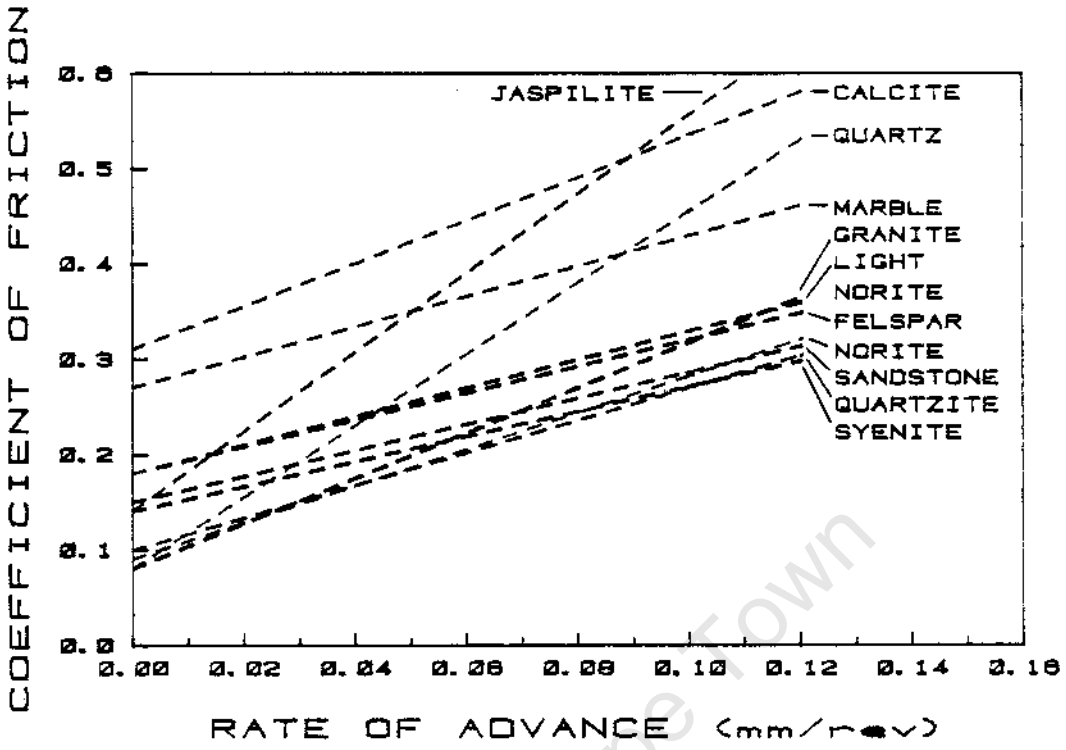

FIGURE 5.100 : Plot of the estimated coefficients of friction against rate of advance for tests drilled in a variety of materials at set rate of advance

5.11 CALCULATION OF FRACTURE ENERGY

The energy consumed in creating new primary surfaces could be estimated from the results of the laboratory drilling with microbits. Specific energy of drilling was measured. A value for the surface energy of a fresh surface had to be estimated. Assuming quartz to be a representative hard silicate mineral the surface energy of 2 Jm^{-2} (Ball & Payne 1976) was adopted. It was assumed that all the particles produced were spherical. The size distribution was described by two different measurements for different size ranges of each detritus sample. The coarse detritus always had a clearly defined peak in the region of 0,125 mm. The value of this mean was assumed to be representative of the coarse detritus size. The fine detritus was recorded simply as the percentage by mass of the material below 63 microns in size so a mean size for this fraction had to be assumed arbitrarily. A diameter of 1 micron was adopted.

Using standard formulae for the volume and surface area of a sphere the energy required to create the estimated new surface area was calculated for a unit volume of rock.

$$E_t = E_s \times F \times 4\pi(d/2)^2 \Big/ \frac{4}{3}\pi(d/2)^3$$

$$= E_s \times F \times \frac{6}{d}$$

where E_t = estimated energy for creating new surface
E_s = surface energy (assumed to be 2 Jm^{-2})
F = volume fraction of particular size range
d = diameter of mean particle size

Combining more than one size range (F1, F2 ...)

$$E_t = 6\, E_s \left(\frac{F_1}{d_1} + \frac{F_2}{d_2}\right)$$

The estimated energy required for new surface formation per cubic metre of rock was calculated for selected tests drilled in norite and other materials. The results have been compared with the measured specific energy calculated from the power consumption (Table 5.16 & 5.17).

TABLE 5.16 : Comparison of estimated fracture energy and measured specific energy for tests drilled in norite with a variety of diamond sizes

DIAMOND SIZE US MESH (30 CONC)	DETRITUS SIZE				ESTIMATED FRACTURE ENERGY (MJm^{-3})	MEASURED SPECIFIC ENERGY (MJm^{-3})
	COARSE (%)	(mm)	FINE (%)	(mm)		
20/30	32	0,139	68	0,001	4,1	1174
40/50	26	0,113	74	0,001	8,9	582
70/80	11	0,086	89	0,001	10,7	1089
-	assume 100	0,125	-	-	0,1	-
-	assume 100	0,001	-	-	12,0	-

TABLE 5.17 : Comparison of estimated energy for fracture and measured specific energy for tests drilled at 0,044 mm/rev set rate of advance in a variety of rocks with standard microbits

ROCK TYPE	DETRITUS SIZE				ESTIMATED ENERGY FOR FRACTURE (MJm^{-3})	MEASURED SPECIFIC ENERGY [W] (MJm^{-3})	ENERGY FOR FRACTURE (%)
	COARSE (%)	(mm)	FINE (%)	(mm)			
Quartzite	7	0,115	93	0,001	11,2	952,4	1,2
Sandstone	40	0,149	60	0,001	7,2	12,7	56,9
Jaspilite	6	0,159	94	0,001	11,3	3845,9	0,3
Quartz	10	0,173	90	0,001	10,8	2832,5	0,4
Calcite	15	0,173	85	0,001	10,2	380,1	2,7
Felspar	14	0,122	86	0,001	10,3	856,8	1,2
Norite	8	0,129	92	0,001	11,7	801,7	1,4
Syenite	9	0,106	81	0,001	9,7	1137,0	0,9
Granite	4	0,150	96	0,001	11,5	1394,4	0,8

Detailed discussion and evaluation of these results will be found in the next chapter in Section 6.7.

CHAPTER 6

DISCUSSION

This discussion of the experimental results is divided into nine sections. The first two consist of a discussion of the role of a predictive model in diamond drilling, and the presentation of a general performance model for impregnated diamond bit drilling. The remaining seven sections each cover a separate aspect of impregnated diamond bit drilling. In each case the results from these experiments are evaluated with respect to experimental and theoretical work summarised in the literature survey on impregnated bit drilling (Chapter 2). Where necessary pertinent material from the related fields of diamond sawing, surface set diamond bit drilling and diamond strength studies has been included.

6.1 PREDICTIVE DRILLING MODELS AND EXPERIMENTAL DRILLING

The central principle in the operation of an impregnated diamond bit is the balanced wear of the diamonds and the bit matrix. It has been shown in the previous chapter that the diamond wear depends *inter alia* on rock type and drilling mode which in turn depends on a variety of interactive factors. The bit matrix wear also depends on drilling mode and even more substantially on the rock type. Rocks are complex, inhomogeneous, variable materials with a very wide range of properties determined by their mineralogy, grain size, and the bonding between the grains. Because of the extreme range of variation in properties it is unlikely that the drillability of all rocks could be classified simply by a single physical parameter or even a single set of parameters. The interactions between the rock and the bit under different operating conditions are themselves interactive and complex. The degree of complexity is illustrated in Fig. 6.1. This diagram shows the principal variables and some important interactions between them when drilling under set thrust conditions.

The variable drilling parameters are placed in the outer columns, with frames around the particular parameters that were studied in the tests reported here. The dependent variables are in the central column. The lack of fundamental knowledge about some of these interactions and the difficulties in characterising the rock behaviour realistically make it impossible at this stage to formulate a coherent predictive model of drilling with impregnated diamond bits. It is likely that the difficulty of characterising the rock adequately will prohibit the establishment of a valid predictive model indefinitely. This means that there will be no realistic alternative to the practice of experimental drilling to test the behaviour of new bits and unfamiliar rocks.

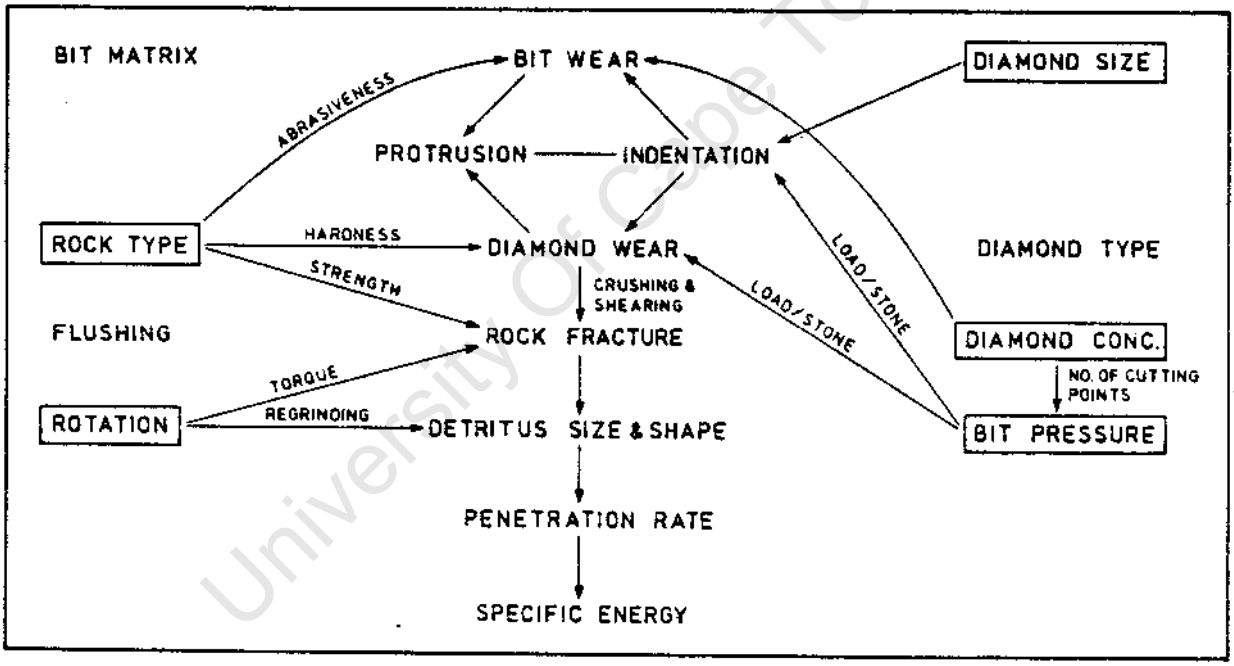

FIGURE 6.1 : Diagram of the principal variables and some important interactions between them in drilling under set thrust conditions

A detailed knowledge of the mechanism of diamond and bit matrix wear and of the rock failure, as well as the relationships between the drilling parameters and the performance variables is essential for the rational evaluation of the results of such experimental drilling. The performance characteristics cannot be interpreted without a clear understanding of

the complex interactions between the drilling parameters and performance variables and the effects that different rock properties have on these relationships. Fundamental research into these mechanisms is justified by this requirement alone even if the goal of a simple integrated performance model cannot be achieved.

For steady drilling it is necessary for the average pressure per active stone to exceed the indentation strength of the rock, given sufficient torque to overcome the shear strength. The ways of achieving this in the highly variable system of impregnated diamond bit drilling are multiferous. The drawback of most predictive models is that they restate the desirable effects of stable drilling without suggesting how to achieve them in practice. For instance the maintenance of a quasi-stable operating gap between the bit matrix and the rock (Cooper & Adams 1983) is a desirable consequence of optimal drilling but as an experimental tool to evaluate the performance of a bit it is of limited applicability because the size of the mean gap cannot be measured easily or reliably. The bit face is not flat, the gap is at the bottom of a hole, and the drilling variables fluctuate so much that measurement of water pressure or flow rate of the coolant and flushing medium is not a sufficiently accurate way of estimating the mean operating gap.

The characteristic diamond wear type frequencies associated with different modes of behaviour have been used as effective diagnostic tools in this research. The wear could be evaluated reliably, albeit tediously if a large number of stones were involved. This has proved, in conjunction with the performance variables, to act as a sensitive indicator of mode of behaviour. The diamond wear is a quantifiable variable directly related to the interaction between the bit and the rock. The wear state of the stones is the crucial controlling factor in the central role that diamonds play in the drilling process with impregnated bits. As such it is the most informative variable to monitor quantitatively and to evaluate qualitatively in assessing the bit performance in a given rock type.

The rock response tested by conventional drillability tests such as the Goodrich drillability test (Goodrich 1957) in which simplified model bits are drilled under standard conditions cannot have much bearing on

drilling with impregnated diamond bits. The crucial matrix wear and diamond wear are not taken into account by these methods which do not test the erosiveness of the drilling detritus nor the resistance of the rock to penetration by small diamond points. Under these circumstances there is no realistic alternative, either theoretical or experimental, to drilling rocks with impregnated diamond bits to assess bit performance.

For this purpose scale model impregnated bits have distinct advantages.

Some of the major advantages of laboratory drilling with microbits that were highlighted by this study are listed below:

i) The relatively low cost of the small bits compared to full-scale bits.
ii) The low numbers of stones to scrutinise in evaluation of the diamond wear.
iii) The convenience of manipulating the small bits under the optical microscope or in the SEM.
iv) The ease of transporting and handling small rock samples.
v) The relatively low volumes of water required to flush and cool the bit.
vi) The low torques and overall power consumption required which contributed to greater safety in the laboratory.
vii) The lower overall cost of the smaller drilling machine.

The most serious drawback of scaled testing with microbits is the possibility of uneven distribution of diamonds in the bit matrix. Because of the relatively low number of stones in a microbit inhomogeneities in distribution are far more serious than in full-scale bits. For the same reason bits with the larger mesh sizes and low numbers of stones are more likely to be seriously affected by the variation in performance caused by clumping of the stones.

Comparison of the results of tests drilled with 30 and 50 concentration microbits with full-scale AXT bits showed that there was a direct correspondence between bit pressures and diamond wear for similar drilling performance with equivalent bits of different size. In general the trends of results of testing with microbits are considered valid for

full-scale bits and the principles of drilling studied with microbits should be equally applicable to drilling the full-scale bits.

6.2 PROPOSED PERFORMANCE MODEL

Impregnated diamond bit drilling takes place in one of two different performance modes. It will be shown that a transition takes place from Mode 1 to Mode 2 drilling at the thrust level at which the average pressure per exposed stone equals the indentation strength (approximated by the compressive strength) of the material being drilled. In any particular case the thrust required to exceed the transition point depends on the rock strength, and the number, size, and wear status of the exposed stones. The drilling behaviour of impregnated diamond bits in a wide variety of materials can be explained with reference to a performance model based on these relationships (see Fig. 6.2).

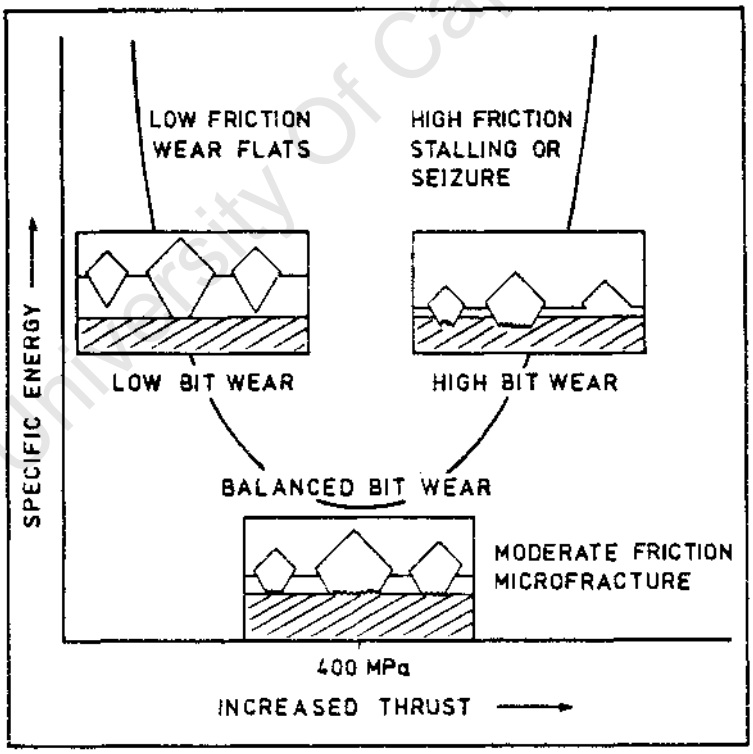

FIGURE 6.2 : Diagram illustrating the effect of increasing thrust through the transition at 400 MPa in drilling norite and the effect on diamond wear and the drilling performance as measured by the specific energy

At thrust levels below the transition few stones indent the rock and participate in drilling. The coefficient of friction between the bit and the rock is low, and wear flat development on the diamonds is promoted by sliding. Poor transmission of power to the rock leads to a low rate of production of detritus and matrix wear is low. Fresh diamonds are not exposed and penetration is impeded by the increasing diamond wear flat area. Consequently the penetration rate drops if drilling at set thrust, or the bit load increases if drilling at set rate of advance.

When drilling with increasing thrust up to the point of transition the torque, power required, and penetration rate increase linearly with increased thrust as a higher proportion of exposed stones indent the rock. The rotational speed remains essentially constant. At the transition all the fully exposed stones are active in drilling at a steady rate of penetration and constant load. Microfracture of the diamonds is promoted over wear flat generation with a higher coefficient of friction between bit and the rock. Rock fracture proceeds with an optimally low specific energy and a steady rate of detritus production and balanced bit wear. This is the optimal thrust at which to drill for any given combination of drill bit and rock type.

An increase in thrust level causes increased indentation of the diamonds up to a limit at which contact occurs between the bit matrix and the rock. In this range of operation the rate of advance does not increase appreciably because the rotational speed drops linearly with increased thrust and increased coefficient of friction between the bit and rock. The higher stress per stone promotes both increased diamond fracture and rock fracture with much greater matrix wear due to the larger detritus particles produced. The diminished clearance between rock and bit matrix causes more crushing of released particles. At still higher thrust levels insufficient clearance between the bit matrix and the rock prohibits effective flushing and cooling with the result that seizure occurs, often with fusion of the bit to the rock.

In drilling norite the transition occurred at an estimated average pressure per stone of 400 MPa irrespective of diamond size, or mode of control as will be shown. All the observed characteristics of drilling norite under 'a variety of conditions with a range of bits could be

explained with reference to the performance model based on the existence of this transition. A summary of the most important effects of changing the performance parameters on the drilling variables can be found in Chapter 7.

In principle the performance model is valid for a wide variety of rock types. The major effect of changing the rock type is to change the average pressure per stone at which the transition takes place. The stronger the rock the higher the pressure required, in some cases requiring high strength bit matrices to support the diamonds sufficiently to produce effective penetration at all.

6.3 COMPARISON OF DRILLING UNDER SET THRUST OR SET RATE OF ADVANCE

Diamond drilling is done under one of two modes of control. Either the thrust is set to produce a particular bit pressure or the feed rate is set to produce a constant rate of advance. Under set thrust the success of drilling a particular rock determines the rate of penetration; under set rate of advance the bit pressure results from the resistance of the rock to being drilled.

The results of the reproducibility tests and the initial test series in norite under set thrust and set rate of advance are compared here to demonstrate the differences in drilling between the two modes of control. From Table 4.3 it can be seen that the reproducibility errors associated with drilling at set rate of advance were higher than those from the drilling tests at set thrust. This was due to the fact that the tests at set rate of advance were drilled under less stable conditions. The feed rate used was lower than that generated by drilling under set thrust with a bit pressure of 6 MPa, and the mean reactive bit pressure of 4,2 MPa at set rate of advance was correspondingly lower. This caused an increase in Type 1 wear flats in the tests at set rate of advance. If these tests had been longer they would have suffered a noticable decrease in penetration rate with a concommitant increase in bit pressure and specific energy.

The results of the two initial test series in norite showed that the operating limits of the laboratory drilling rig were different in the two

different modes of control. Up to a bit pressure of 6 MPa the performance was substantially similar irrespective of mode of control. The specific energy of drilling reached a minimum of 600 MJm^{-3} at a bit pressure of about 5 MPa (Figs. 5.7, 5.8 & 5.21). The transition from Mode 1 to Mode 2 drilling behaviour took place between 4 MPa and 5 MPa and with a corresponding rate of advance between 0,04 mm/rev and 0,06 mm/rev (Figs. 5.11 & 5.23). There was only a slight variation in the detritus size under both types of control (Figs. 5.15 & 5.16 and 5.27 & 5.28). The relationships between power, torque and bit pressure were virtually identical up to 6 MPa and 0,1 mm/rev under both modes of control (Figs. 5.3 & 5.4 and 5.18, 5.19 & 5.20). At bit pressures above 6 MPa drilling proceeded at an average 0,12 mm/rev under set thrust up to a limit of 10 MPa above which the drill tended to stall (Fig. 5.6). The bit wear rate in this region above 6 MPa was high (Figs. 5.9 & 5.10). Under a set rate of advance of 0,1 mm/rev the drill stalled after drilling distances ranging from 233 mm to 682 mm with a mean bit pressure of 6 MPa (Fig. 5.19). From the result plots of the tests drilled at 0,1 mm/rev it was clear that the stalling had been preceded by a sudden and rapid rise in reactive bit pressure. The incidence of Type 4 wear (fracture of the diamonds flush with the matrix) was about 15% - much higher than the 2% average found on the bits drilled under set thrust.

At set thrust the vertical vibration of the bits was less constrained than under set rate of advance because of the gravity feed loading mechanism. At low bit pressures vibration was a problem but it proved that damage to the diamonds by the repeated impact caused by the vibration served to keep the bit "open" even at very low thrusts. Freedom to vibrate at high thrusts helped to keep the bit open perhaps less by damaging the diamonds than by inhibiting seizure of the bit to the rock. Resistant spots in the rock encountered at high loads under set thrust could be accommodated by a decrease in penetration rate.

Under set rate of advance the bit was forced into the rock by a geared mechanism with minimal compliance, especially at high rates of advance. The bit was not free to ride up over resistant asperities. A resistant patch of rock could cause excessive damage to the diamonds due to mechanical stress. A sudden increase in reactive pressure and the need

for more power than the limited laboratory rig could deliver caused stalling and seizure under these circumstances. The damage to the bits in terms of Type 4 diamond failure and bit matrix welded to the rock was evidence that this had happened (see Fig. 5.26(e & f)).

There are physical limitations to the amount of power that can be transmitted effectively to the rock. (i) All machines have a limit to the power they can provide although this is usually not the limiting factor of performance with full-scale drilling machines. (ii) If the strength of the bit matrix is exceeded then either the diamonds are forced into the metal or the impregnated pads shear off the bit. (iii) The effect of load on the diamonds is complex but if the strength of the stones is grossly exceeded then they fracture undesirably to generate Type 4 wear. (iv) The strength of the diamond to matrix bond is important in avoiding excessive pull-out and premature loss of stones leading to matrix contact with the rock, and possible seizure. At the upper end of practical thrust application none of these four limits must be exceeded.

At low thrust however, polishing of the diamonds to create large wear flats must be avoided. If the wear flat area becomes large enough then the stones cannot be broken by increasing the load without the risk of exceeding either the strength of the matrix (Bullen 1984) or, in the case of smaller machines, the available power. Vibration at low bit pressures may help to keep the bit open but this contributes to excessive matrix wear and loss of bit life.

Keeping these limits in mind the advantages and disadvantages of drilling under set thrust or set rate of advance can be summarised. Under set thrust the relative freedom of the bit to vibrate vertically may keep the bit open but in the laboratory study this happened only at the lowest, least economical thrusts, and with relatively high bit wear rates. Resistant rock can be accommodated by a drop in penetration rate, but at the risk of creating excessive wear flats or exceeding the power available to maintain penetration. At high thrusts the bit could be damaged by impact stress if a void were encountered in the rock (Hampe, Simon, Decker & Lundy 1973). The selection of the correct thrust is critical. There is a threat of excessive wear flat generation at too low a thrust and the risk of catastrophic damage to the bit at too high a

thrust. In the field situation it is generally difficult to maintain
III penetration at set thrust (Bullen 1984).

If the correct rate of advance for a given rock type and bit combination is selected then efficient drilling should be maintained for the life of the bit with low wear rates. The selected feed rate may be too high when a local hard spot is encountered with insufficient power available to maintain penetration and damage to the diamonds may result. At rates of advance that are too low there is the risk of wear flat generation which if not detected early enough can proceed to the extent that the bit cannot be re-opened without retracting the bit, and sandblasting or rasping the matrix or subjecting the diamonds to physical damage with a hammer.

6.4 THE ROLE OF THE DIAMONDS

Diamond wear and drilling performance have an interactive effect on each other and in this section on the role of the diamonds attention will be focussed mostly on the diamonds themselves but sometimes on the effect diamond wear behaviour has on drilling performance. There are five sub-sections concerned with the role of the diamonds: (i) The effect of varying drilling parameters on diamond wear, (ii) the effect of varying diamond parameters on performance, (iii) the sequence of diamond wear development, (iv) the effect of load per stone on drilling performance and (v) the mechanisms of diamond wear.

6.4.1 The Effect of Varying Drilling Parameters on Diamond Wear

Drilling norite at set thrust with the impregnated diamond microbits gave rise to two modes of behaviour. In mode 1 the penetration rate dropped from an initial maximum, eventually tending to zero with an increase in the number and size of wear flats on the diamonds. Above a transition at about 5 MPa bit pressure the rate of advance was more or less steady with a predominance of microfractured stones over wear flats (Fig. 5.11). These observations are in agreement with those of other researchers. Busch & Hill (1975) found a drop in penetration rate

to be caused by the "dulling" of the diamonds while steady drilling was associated with the presence of both wear flats and fractured stones in unspecified proportion. It has been generally acknowledged that the excessive development of wear flats must be avoided (Bullen 1983).

At set rate of advance the transition from Mode 1 to Mode 2 behaviour took place in norite at a rate of advance of about 0,06 mm/rev which corresponded to a bit pressure also of about 5 MPa. Mode 1 behaviour was associated with a predominance of wear flats (Fig. 5.23). At higher rates of advance the predominance of microfractured stones over wear flats was accompanied by a decrease in the number of unworn stones and an increase in failure by macrofracture. A uniform set of diamond failure mechanisms operated at equivalent bit pressures or rates of advance in norite irrespective of the mode of control. Comparison of the micrographs of stones worn in either Mode 1 or Mode 2 revealed no significant difference in the appearance of stones of the same wear type produced under different modes of control (see Figs. 5.14, 5.25 & 5.26). The differences in performance were determined by the relative proportions of different wear types (Miller 1985) rather than by distinct types of wear exclusive to each performance regime.

A reduction in rotational speed led to less optimal performance with an increase in the number of stones lost through pull-out (see Fig. 5.33). At low rotational speeds excessive vibration caused impact damage to some of the diamonds (Fig. 5.34(d)) and consequently a steady penetration rate was achieved despite severe bit wear. Bailey & Bullen (1979) have found in sawing studies that high peripheral speeds, although causing diamond fracture by impact, were preferrable to low speeds at which wear flats and pull-outs were caused by mechanical loading. This aggravated the problems caused by more severe vibration at low speeds.

There seem to be considerable similarities in the wear behaviour of diamonds in impregnated diamond bit drilling and sawing. The

illustrations of worn stones in the papers on rock sawing by Bailey & Bullen (1979), Büttner (1980) and Ertingshausen (1985) are directly comparable with illustrations of characteristically worn stones in this thesis. The fundamental fracture mechanisms are most probably the same despite the high peripheral speeds used in sawing. In the drilling experiments changing the rotational speed over the range of 1 ms^{-1} to 4 ms^{-1} had no discernable effect on the wear mechanisms of the diamonds apart from the damaging effects of the vibration at low speeds.

The effect of additives in the flushing medium was not studied in this experimental program. Selim et al (1969) and Cooper (1979) have found that additives that act as wetting agents reduce the diamond wear (presumably they reduce the generation of wear flats) and hence reduce the frequency of necessary resharpenings of the bit when drilling, as they did, in Mode 1. It was proposed that a thermal mechanism of oxidation or graphitisation may be responsible for the creation of wear flats. This explanation was also adopted by Ertingshausen (1985) in describing the development of wear flats in sawing. This will be discussed in more detail later.

In general high rotational speeds are desirable with no adverse effects in terms of diamond wear. However, the flushing mechanism must be efficient enough to remove the extra detritus effectively to avoid enhanced bit matrix wear at high speeds. The upper limit of effective bit pressure is determined more frequently by the mechanical strength of the bit matrix and the diamond-to-matrix bond than by the diamond properties.

6.4.2 The Effect of Varying Diamond Parameters on Performance

Diamond Type and Strength

Synthetic diamond grit is produced with a wide range of sizes, shapes and mechanical properties. Some types of synthetic are better suited to particular applications. For instance, Bullen & Bailey (1979) found that there was an important relationship

between penetration rate and grit type. In drilling granite the stronger SDA 100 grit achieved better penetration rates for longer without an increase in bit load above that used in drilling with the less robust SDA grit. However, at reduced bit load the stronger diamonds "polished" more rapidly with a drop in penetration rate. It can be inferred from these results that diamond fracture is crucial to the impregnated diamond bit drilling process. Diamond wear must not be encouraged to create wear flats and so diamond strength is an important variable. In applications where diamond fracture particularly needs to be encouraged (as in drilling very resistant formations like jaspilite) it would be preferrable to use more readily friable diamonds to maintain penetration, perhaps at the expense of bit life.

Direct measurement of the strength of diamonds is difficult due to the small size of the crystals and their high intrinsic strength. Indentation tests used to test the physical properties of relatively large natural crystals (Howes 1965, Bowden & Tabor 1965, Field 1979, Brookes 1979, Field & Freeman 1981) cannot easily be applied to small synthetic crystals. Impact and crushing tests (such as De Beers' Friatest) perhaps measure the response of the stones to the forces operating in circumstances involving considerable vibration rather than in the more stable state of steady drilling. Failure under compression is a function of the tensile and shear strength of the stone and represents the actual situation in diamond drilling more accurately than a test depending on impact. For a comprehensive review of strength testing methods for diamonds see Field & Freeman (1981).

In this study the compressive strength of the diamonds was measured by a technique modified from Field & Freeman (1981), using polished single crystal corundum anvils instead of high strength steel or diamond. The corundum anvils have the advantage of being harder than steel, less expensive than diamond, and can be cut and polished from readily available synthetic sapphire boules with an ordinary facetting machine. The corundum anvils underwent some plastic deformation as evidenced by slip lines on the polished surfaces after the tests (Fig. 6.3) but they suffered

mostly Hertzian cracking, which limited their life. The measured failure stress for SDA 100 diamond crystals in uniaxial compression was 4,44 GPa, a figure equivalent to half the stress of about 9,4 GPa measured between hardened steel anvils by Field & Freeman (1981). However, there is a twofold increase in the failure stress of diamond compressed between steel anvils as opposed to diamond anvils due to the constraining effect of the embedment of the diamonds in the steel. It is reasonable to assume the experimental value of 4,44 GPa is close to the failure stress that would have been obtained had the diamond strength been determined using diamond anvils.

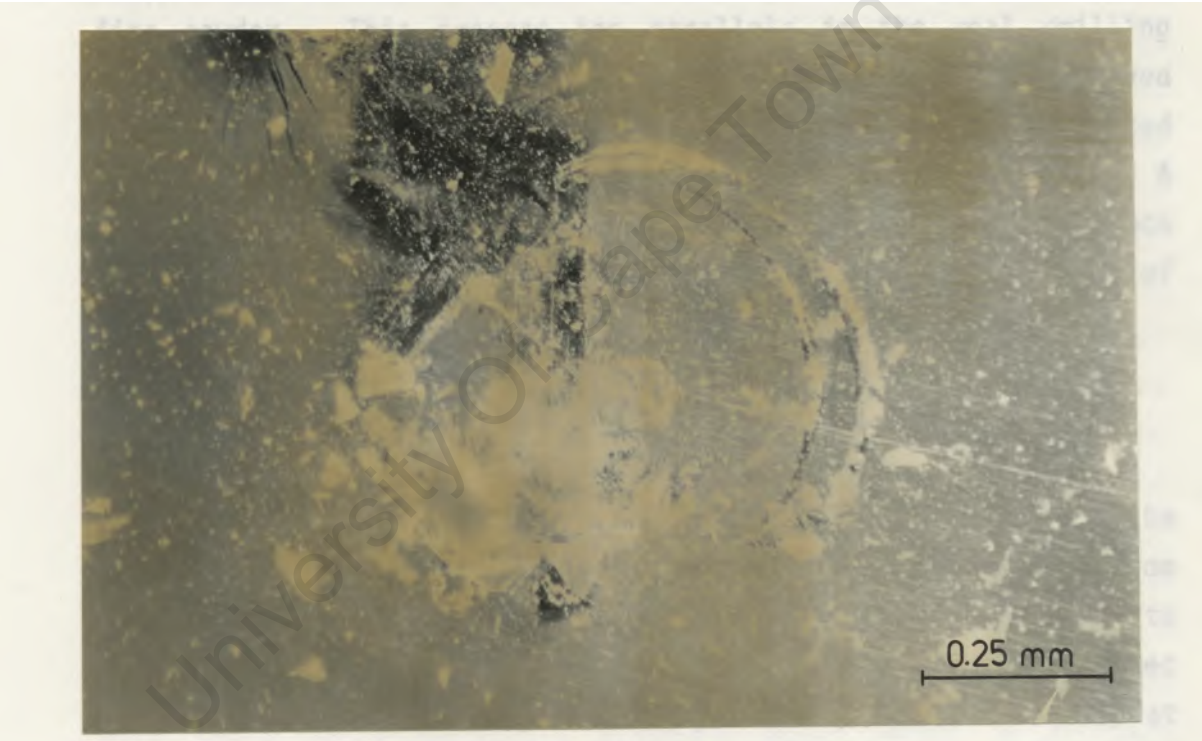

FIGURE 6.3 : Slip lines (straight) and Hertzian fracture (curved) in single crystal corundum anvils used in compression testing of diamonds

Although some plastic deformation of the corundum anvils took place there was very little embedment of the diamond. Hence the fractured stones would have received very little constraining support from the anvils - unlike the hardened steel anvils in which Field and Freeman (1981) found evidence of considerable embedment and hence elevation of the failure stress. The use of corundum anvils facilitated the measurement of final failure stress without the embedding effect, at a fraction of the cost of

using diamond anvils. The brittle Hertzian fracture of the corundum was a problem common to the use of diamond anvils as well. Possibly the use of a sintered polycrystalline diamond material with its high compressive strength and superior toughness might be more successful.

In common with Field & Freeman (1981) it was observed that diamond failure in uniaxial compression took place in a series of stages. At loads of a few tens of kilograms a single fracture formed, followed by the particle's going opaque due to subsequent multiple fracture. The fractured particle continued to support a load of up to ten times this value before disintegrating altogether into a fine powder. This process has parallels in the real drilling circumstances. Extensively fractured diamonds have been observed to be held together as a collection of interlocking sharp-pointed fragments supported by the surrounding matrix (e.g. Fig. 5.77(e) & 5.79(f)). These stones actively contributed to drilling the rock and could persist essentially intact for many thousands of revolutions of the drill bit.

Diamond Distribution and Concentration

The diamond distribution in the microbits ideally should be homogeneous. The diamonds act partially to shield the matrix from erosion and a uniform diamond distribution can be expected to promote uniform matrix wear across the bit face. If the stones are located in clumps they tend to protect the matrix locally at the expense of higher matrix wear in more exposed regions. Entire clumps of stones would tend to be lost simultaneously giving rise to uneven drilling performance as the total bit face characteristics change suddenly. The practical effects of clumping were evident in the initial reproducibility test series at set thrust (see Table 4.3) in which visibly obvious clumping of the stones caused the results of TEST 42 to be highly divergent from the norm for these tests. To obtain reliable and representative experimental results with microbits the distribution of stones must be as uniform as possible. The

performance of the larger bits is expected to be less susceptible to sudden local changes in distribution of stones on the bit face by the loss or persistence of individual clumps of self-supporting diamonds because the greater total number of stones would reduce the influence of individual clumps.

A full range of diamond concentration was not tested in the program but an increase from concentration 30 to 50 was found to increase the thrust requirement to maintain steady penetration for both microbits and full-scale bits (see Tables 5.10 & 5.12). Bamford et al (1979) found that a concentration of 30 produced the highest penetration rate when drilling sandstone at set thrust with impregnated diamond microbits. Frequent stoppages and high rates of matrix wear at lower concentration were ascribed to contact between the matrix and rock due to the low number of exposed stones. At high concentrations penetration rate tended to decrease; it was thought due to poor penetration of the numerous exposed stones. However, the effect of increasing diamond concentration is to decrease the mean distance between the stones as well as to increase the number of exposed points. The increased number of stones tends to mask the matrix between them more effeciently, inhibiting the matrix erosion and exposure of fresh stones. In conjunction with this the increased number of points lowers the pressure on each active stone to such an extent that wear flats develop at the expense of microfracture with a corresponding deterioration in drilling performance. This implies that there is a threshold pressure below which significant microfracture does not develop.

Diamond Size and Protrusion

The effect of diamond size in drilling performance in norite was considerable and this was reflected in the diamond wear. At a constant rate of advance and diamond concentration of 30 there was an optimal intermediate diamond size, above which drilling was in Mode 1 (Fig. 5.43). The coarsest diamonds tended to develop large wear flats, or rounding of the asperities of microfractured stones

occurred to act as Type 1 wear surfaces and impede drilling progress. In conjuction with the predominant wear flats the multiplicity of asperities all on approximately the same plane on these microfractured stones had an effect analogous to increasing the effective concentration. Hence more exposed points were available to support the load. Virtually all the microfractured stones on the coarse mesh bits had debris caked between the asperities (see Fig. 5.44(a & b)) so these stones also acted as pseudo-Type 1 wear surfaces to aggravate the Mode 1 behaviour. This particular type of caking may have been caused by the inability of the flushing water to penetrate between the large diamond surfaces and the rock to remove the detritus. This behaviour occurred to a lesser extent on the mixed 20/30 + 40/50 mesh bits (Figs. 5.45(a & b)). The concentration of large stones on the mixed bits was effectively halved and wear flat generation could not proceed to the point of impeding the penetration. With the coarse mesh bits there was a relationship between diamond size and concentration in keeping the total wear flat area below a critical threshold for undesirable Mode 1 behaviour. In terms of bit life mixed mesh bits may perform better than their simple coarse mesh analogues. The finer diamonds protect the bit matrix from the excessive erosive wear it would suffer at reduced diamond concentration.

The fine 60/80 mesh diamond bits behaved anomalously by drilling steadily although having a predominance of wear flats rather than microfractured stones (Fig. 5.43). With such small stones sufficient load could be transmitted through individual stones to maintain steady drilling despite the absence of microfracture. Individual wear flats simply could not develop to any appreciable extent because of the size of the stones (see Fig. 5.44(e)). Because of their small size individual stones with wear flats were released by minimal matrix wear before the total wear flat area on the bit face reached a critical value to impede drilling. With such small diamond mesh sizes a predominance of microfractured stones over those with wear flats was not necessary for drilling to proceed steadily. This implies that for a given rock type there is a critical wear flat area below which sufficient thrust

can be transmitted to the rock to cause continuous rock fracture. If this wear flat area is exceeded then the pressure beneath the individual diamonds is insufficient to cause rock failure; the wear flat area rises rapidly and the load can build up without effect on the rock. This inference will be tested later in this chapter.

The measurement of protrusion of the stones on the faces of two bits, one 20/30 mesh and the other 50/60 mesh, after drilling an equal distance in norite showed that the mean protrusion did not depend significantly on the diamond size (Table 5.13). However, the mean large detritus size was dependent on diamond mesh size. These relationships are illustrated in Fig. 6.4 with the arbitrary assumption of the indentation equal to 50 percent of the protrusion.

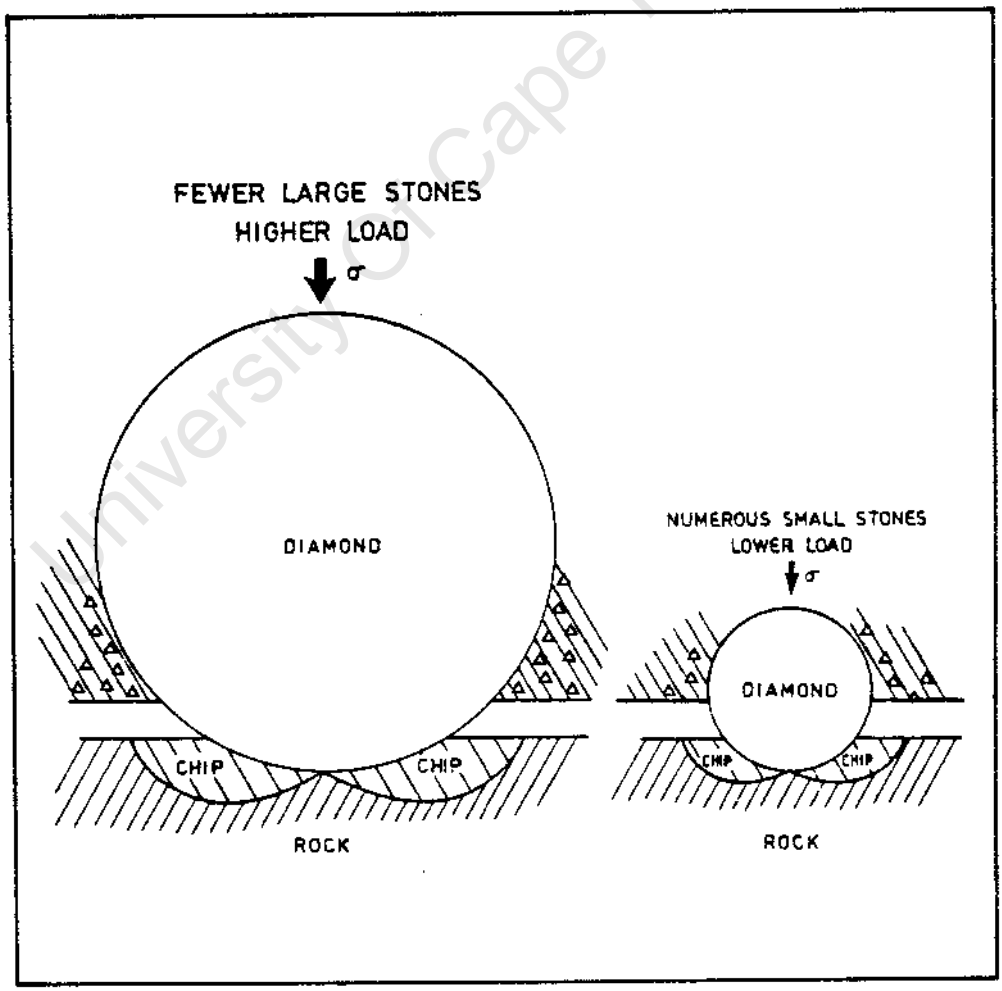

FIGURE 6.4 : Diagram illustrating the relationships between diamond size, protrusion, indentation and chip size in drilling at a set bit pressure of 5 MPa

There are fewer and larger stones on a 20/30 mesh bit so these carry a higher individual load. Even if they indent only to the same depth as the smaller stones on a 50/60 mesh bit the detritus particles produced by the larger diamonds can be expected to be larger because of the greater volume of the indentation. The mean gap size between bit matrix and rock is not crucial in determining the detritus size as the large particles may escape through the deep erosion grooves between the stones.

6.4.3 The Sequence of Diamond Wear Development

There is no published account of the sequence of wear type generation in impregnated bit drilling. However the development of diamond wear in sawing has been described by Ertingshausen (1985) as follows. (i) Wear flats develop in response largely to thermally driven mechanisms, the resulting load build-up leads to increased mechanical stress, and the stones fracture prior to disintegrating completely and falling out. (ii) Mechanical stress causes the stones to fracture, then the development of wear flats leads to high mechanical forces which pull the stones out of the matrix. Both mechanisms were thought to operate simultaneously in sawing.

There is some evidence of similar mechanisms operating in impregnated bit drilling. With both the standard impregnated diamond microbits and the monolayer bits drilled to test the diamond wear sequence it was found that in Mode 1 behaviour wear flats predominated over microfractured stones, and vica versa in Mode 2 behaviour. Hence the detailed wear sequences determined by analysis of the wear of the stones on the monolayer bits (Figs. 5.94 & 5.95) are considered valid for the microbits as well. Under both set thrust and set rate of advance conditions it was found that the large majority of stones progressed through a simple wear sequence. Initially unworn stones developed wear flats and then fractured (Fig. 5.96): alternatively they developed fracture very rapidly before being lost through pull-out or the severe fracturing associated with Type 4 wear. In Mode 2 drilling fewer than 15% of the stones which had suffered microfracture

then developed wear flats. The micrographs in Fig. 5.14 show a typical sequence of wear types in Mode 2 from unworn stones to loss by pull-out or failure of the stones by macrofracture. In Mode 2 there was very little evidence for the subsequent development of wear flats on microfractured stones except on the largest stones in the 20/30 mesh bits (see Figs. 5.44(b) & 5.45(c)). If bits which had operated in Mode 2 had reverted to Mode 1 behaviour then the development of wear flats on microfractured stones may have been more common. However, with the laboratory drill the limited power available prevented stones with extensive wear flats from being pulled out of the matrix. Instead, under set rate of advance conditions in Mode 1 the load simply built up to the limit of the capacity of the machine.

6.4.4 The Estimate of Load Per Stone

A number of lines of reasoning have led to the inference that for a given rock there is a critical pressure per stone below which microfracture tends not to occur and instead wear flat development is the dominant type of diamond wear. It is clearly impossible to measure the pressure on individual stones in an impregnated bit but an attempt was made to estimate the average pressure experienced by the load bearing stones. If the above inference is correct then for a given rock type there should be a transition from Mode 1 to Mode 2 drilling behaviour at a uniform estimated pressure per stone irrespective of diamond size, concentration, test length, or duration.

Three initial assumptions had to be made to facilitate such an estimate. (i) The load was carried entirely by the wear flats (ie. Type lb worn stones). (ii) The average diamond size in a bit was approximated validly by the median size. (iii) The wear flat area on each Type lb worn stone was equal to the area of the equatorial plane of an equivalent sphere. This was the maximum wear flat area theoretically possible before the stone fell out of the matrix. For each of the 119 tests drilled in norite with a microbit for which there was a record of the diamond wear three values were determined from the test record. (i) The number of

stones with wear flats (Type lb). (ii) The final bit pressure - from which the total load carried by the diamonds at the end of the test could be calculated. (iii) The diamond mesh size range - from which the average diamond size could be estimated.

For each test the average pressure per Type lb worn stone was calculated as follows:

$$\text{PRESSURE (MPa)} = \text{BIT } \frac{\text{FINAL MEASURED PRESSURE (MPa)} \times \text{BIT FACE AREA (mm)}}{n\,(d/2)^2 \times \text{NUMBER OF STONES WITH WEAR FLATS}}$$

where d = diameter of median stone size in mm.

The results of this calculation for all the tests drilled in norite ranged from just over 100 MPa to infinity (for bits with no Type lb wear stones). These values are tabulated in Appendix 6. The calculated values of estimated average pressure per stone falling below 1500 MPa were plotted in Fig. 6.5 against the measured final bit pressure for each test excluding those that displayed spurious Mode 2 behaviour due to vibration damage. The points representing tests drilled in Mode 1 were plotted with the symbol "1", tests drilled in Mode 2 were represented by "2", and "*" indicates tests that were intermediate. The estimated pressure per stone was less accurate for tests with few Type lb stones because of the assumption that Type lb stones alone carried the load. This is the reason for omitting the values above 1500 MPa from the plot. When drilling norite there is clearly a transition from Mode 1 to Mode 2 behaviour in the region of an estimated pressure per stone of about 400 MPa, irrespective of bit formulation. The horizontal spread of final bit pressures is due to the varying thrust requirements of bits with different diamond sizes or concentrations and hence different numbers of exposed stones.

An evaluation of the value of about 400 MPa for the transition must involve an appraisal of the assumptions made in the calculations. The assumption that the load was carried entirely by the wear flats would tend to cause the estimated pressure per

stone to be too high because some load would be carried by stones of the other wear types, the more so as the proportion of Type lb worn stones decreased. Even if it were assumed that the Type lb stones carried only half the load the estimate would be out only by a factor of 2. The assumption that the median stone size effectively represented the mesh size could not introduce much error for the narrow size ranges used. For instance, if the limiting values of 40 mesh and 50 mesh were used in the case of the 40/50 mesh distribution the two estimated pressures differ from each other also by a factor of 2 and the real value must lie between them.

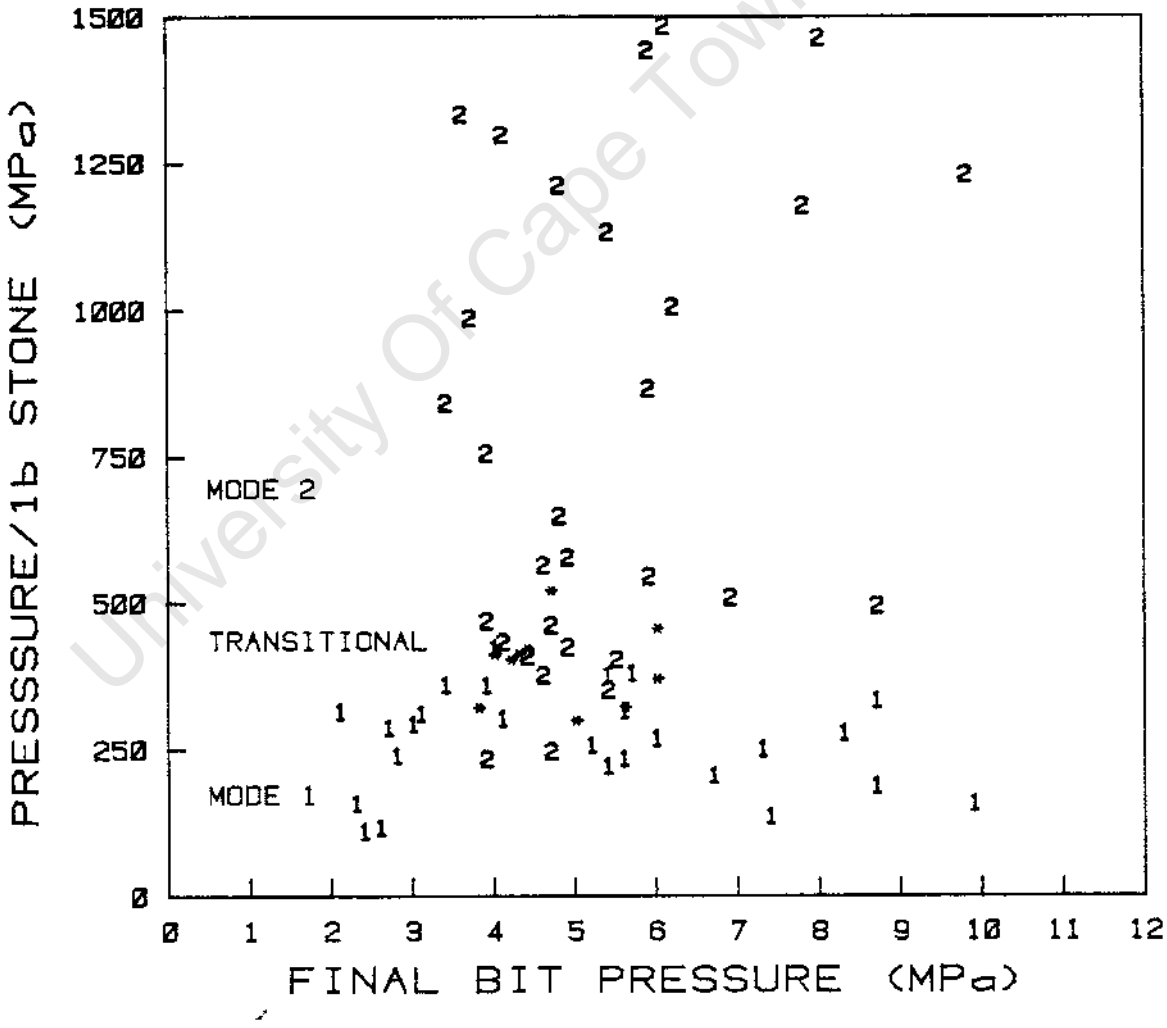

FIGURE 6.5 : Plot of estimated average pressure per active stone against the measured final bit pressure, showing the transition from Mode 1 to Mode 2 behaviour at about 400 MPa per stone

The assumption that the wear flat can be represented by the equatorial plane of an equivalent sphere is the most problematic. As this is the maximum area possible before loss of the stones using it in calculating the estimated pressure would tend to lower the value below the true value. The difference in pressure is proportional to the square of the change in wear area; so for instance assuming the wear flat area to be developed to only half of the diameter would raise the estimated pressure by a factor of four. However, the error introduced by this last assumption can be expected to be at least partially counterbalanced by the error inherent in the first assumption. Hence, the value of 400 MPa is of the correct order of magnitude as an estimate of the average pressure per wear flat at which microfracture becomes the predominant wear mechanism in drilling norite with SDA 100 in microbits.

There is insufficient information available to test the validity of the estimate of 400 MPa per Type lb stone for the transition from Mode 1 to Mode 2 drilling in materials other than norite, or for the full-scale bits. There is no reason to believe it is not valid for drilling norite with SDA 100 in full-scale bits. But it is expected that the value would be different in drilling different rock types because of the variation in their compressive strengths and abrasiveness.

6.4.5 Diamond Wear Mechanisms

There are considerable similarities and some important differences in the wear of diamonds and other hard abrasives used in machining operations. In the following section the development of various types of diamond wear including wear flats, microfracture and macrofracture in drilling with microbits will be discussed with reference to the physical properties of diamonds and the influence of the different materials drilled. It has been observed by Perrott (1979) that "the wear of diamonds in contact with minerals is not well understood". In fact the mechanisms of abrasion and wear of diamond in general are not well understood (Wilks & Wilks

1982). This research has produced information on the wear of single crystal synthetic diamonds drilling into a variety of materials using linear surface speeds from 1 ms^{-1} to 4 ms^{-1}. The range of bit pressures from 2 MPa to 13 MPa represents an average load per stone of up to 5 kgf. Of course individual stones may have experienced much higher loads.

Type 0 Wear

The crystals comprising SDA 100 grit are generally well formed (Fig. 5.1) and intergrowths (Fig. 5.76(a)) or morphological twins are rare. Very few stones escaped some form of wear even as they were being exposed by matrix erosion (Fig. 5.75(a); 5.77(a)). Glover (1980) found that sharp diamond points blunted rapidly in sliding on quartz over distances as short as 150 mm so it is not suprising that in drilling a wide variety of rocks bearing silicate minerals the exposed diamonds rapidly developed rounded corners or edges (Fig. 5.14(a)). These asperities reached temperatures in excess of 700 $^{\circ}$C (as will be demonstrated later) at which oxidation of diamond in the presence of air is possible (Evans 1976, 1979). As the initial rounding shows no evidence of grooving it was concluded that it was caused by oxidation, and perhaps graphitisation of the surface layers and not directly by a mechanical process. It has been noted that thermally activated mechanisms may play a crucial role in the wear of diamond at high speeds (Tabor 1979).

In calcite, which was too soft to cause grooving of the stones at all, a few of the exposed diamond points showed chevron markings at their tips. This may have been a sign of thermal etching (Fig. 5.83(a & b)). Identical features were observed in one other context - on the sheltered lee side of a wear flat on a stone drilled in norite (Fig. 5.26(a)). Usually in drilling silicate bearing rocks the rounded diamond points rapidly developed chipping (Figs. 5.44(d); 5.74(a)), or the onset of grooving (Fig. 5.80(a)) to form a wear flat.

Type 1 Wear

Wear flats developed on diamonds drilling all the silicate bearing rocks. The absence of wear flats after drilling calcite was informative. Calcite is soft and failed to abrade the diamonds visibly during the 10 minutes duration of the drilling tests. The rate of wear of diamond has been found to depend on the nature of the material being rubbed with a preparatory abrasion required, before the onset of wear, which also depends on the hardness of the rubbed materials (Crompton et al 1973, Wilks & Wilks 1979). The absence of wear flats after drilling calcite also proved that wear flats were not the product of abrasion by small released diamond particles. There were numerous fractured stones on the bits that had drilled calcite (Figs. 5.83(c & d)) which would have provided fine diamond particles. Thus the primary wear mechanism in the development of wear flats was physical abrasion of the diamond by sharp points of silicate minerals. All the wear flat surfaces were striated or grooved (eg. Figs. 5.25(a & b); 5.44(c & e), 5.74(b & c), 5.75(b & c), 5.76(c & d), 5.79(a), 5.80(d), 5.82(a & d)). Numerous examples have been illustrated to demonstrate that the features of wear flats are identical irrespective of the drilled material in which they developed. This applies also to the full-scale drilling with AXT bits (Fig. 5.91(a & b).

From the truncation of some of the faces it was clear that significant volumes of diamond had been removed in a maximum possible rubbing distance of 2,4 km. Some of the more detailed features of the wear flats were noteworthy. (i) The finer striations tended to be narrow and straight. At high magnification they appeared to have smooth sides and at least occasionally deep median cracks extending into the body of the stone (see Figs. 5.74(e); 5.76(d); 5.91(a)). (ii) The deeper grooving also appeared to have smooth sides and often smoothly rounded intervening ridges (Figs. 5.34(b, e & f); 5.45(e & f); 5.74(f); 5.82(d)). (iii) A third feature was almost invariably visible on the worn surfaces. Parallel steps had developed more or less transverse to the direction of abrasion. These were often

expressed on the worn surface as displacements which contributed to the kinking and sinuosity of the deeper grooves (Figs. 5.25(c); 5.26(a); 5.34(a & b); 5.45(e & f); 5.76(c & d)). These steps were crystallographically controlled and appeared on well developed crystals to be parallel to the 11111 cleavage planes.

Three explanations are possible for the origin of these steps. (i) They may be the expression of layers of slightly differing physical strength due to different densities of growth defects on the 11111 growth planes (Field 1979), (ii) they may be the result of the tensile opening of cleavage cracks on 11111 planes (Howes 1965) more or less perpendicular to the direction of abrasion, (iii) they may be slip steps produced in accordance with the 11111 <110> slip system of diamond (Brookes 1979) activated by frictional heating (Bowden & Tabor 1965). Cathodoluminescence studies which have been used to reveal structural control of variations in abrasion resistance of diamonds (Woods & Lang 1975) were not carried out on these stones so the first possibility could not be tested directly. Careful scrutiny of the steps in the SEM only occassionally showed the presence of cracks in the plane of the steps.

There was indirect evidence of high temperatures having been reached by the diamond surfaces. Sintered flakes of rock flour were a conspicuous component of the detritus produced by drilling the norite, the major constituent of which is plagioclase felspar of labradorite composition. This can be expected to melt between 1100 °C and 1150 °C at a pressure of 500 MPa in the presence of water (Deer, Howie & Zussman 1972). The wear flats experienced an estimated pressure of up to 400 MPa so the sintered rock flour can be expected to indicate local temperatures of about 1000 °C or more. Although there is little evidence for dislocation movement at room temperature in diamond (Hannink & Gane 1974, Wilks & Wilks 1979) plastic deformation would be possible in a surface layer at high temperatures in excess of 1000 °C temperature in drilling. This layer is expected to be thin because of the high thermal conductivity of diamonds.

The existance of a thin, plastic layer could explain the nature of the straight striations (see Fig. 6.6). A sharp asperity traversing the heated diamond surface generates high local pressures and ploughs an essentially plastic, narrow, straight track through the heated surface layer a few microns deep (see Fig. 5.74(e)). A brittle crack forms at the bottom of the plastic track in the cooler, less plastic body of the stone. Subsequent oxidation (and possibly graphitisation) erodes the plastically deformed material near the surface adjacent to the ploughed track and the median crack, allowing access to abrasive particles and erosive fluid which widen and deepen the crack to form the characteristic sinuosity of the deep grooves (see Figs. 5.45(e & f); 5.74(f)). The slip steps are caused by progressive build up of strain in the surface of the diamond and in conjunction with cleavage cracks displace the grooves to cause kinks and offsets (eg. Fig. 5.34(b)).

There is some controversy over the role of plastic grooving versus brittle chipping in the abrasion of diamond. It has been thought possible that if the deformed volume is sufficiently small and the pressure sufficiently high then plastic deformation can take place without the formation of cracks (Bowden & Tabor 1965) and that plastic grooving on a microscopic scale could contributed to the wear of diamond (Tabor 1979). On the other hand Wilks & Wilks (1979) considered the process of grinding of diamond on a skaife with diamond powder (at a linear surface speed of about 10 ms^{-1}) to take place by purely mechanical chipping and microcleavage to produce particles of the order of 5 nm. Chipping and micro-cleavage on this scale would not have been resolved by the SEM used for the experimental work with microbits but it is clear that some brittle cracking had taken place below the surface layer of diamond and there was considerable evidence that plastic deformation took place in the surface layers of the diamonds when drilling silicate minerals. The role of thermal ablation by oxidation (with or without graphitisation) was probably minor and confined to deepening and widening the wear grooves and rounding the ridges between them.

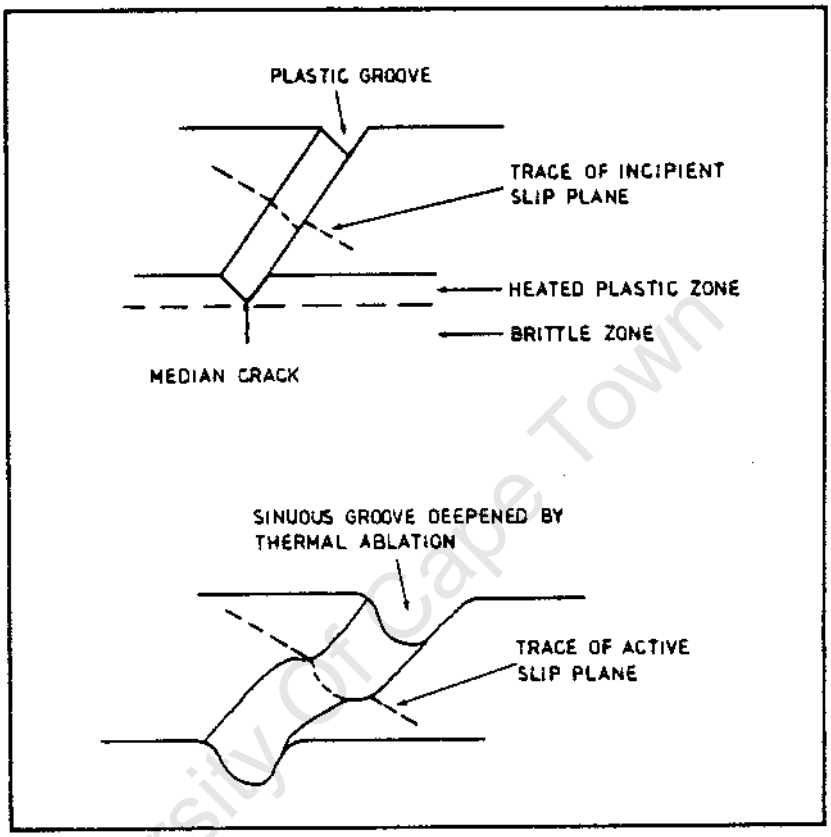

FIGURE 6.6 : Diagram illustrating the development of a deep rounded sinuous groove from an initially straight shallow groove in the heated, plastic surface layer of a diamond

Wilks & Wilks (1965) found no evidence of a controlling thermal mechanism in the abrasion of diamond and ascribed the amorphous carbon commonly produced by the grinding of diamond to the influence of high temperature on the fine diamond particles released by the process of microchipping. Under the optical microscope the matrix tails behind some of the larger wear flats on the microbits were characteristically smooth and appeared blackened, possibly by carbon produced in a similar way.

Wear flats eventually developed a plucked surface appearance and began to break up by brittle fracture, frequently but not always starting from the trailing edge which was more susceptible to failure in tension if the stone was not well supported by a tail of matrix (Figs. 5.34(a); 5.74(d); 5.75(d & e); 5.76(e); 5.77(f); 5.79(e); 5.91(b & c)). Occasionally a stone with a wear flat developed a single large fracture caused either by the impact of a loose diamond (Fig. 5.25(d)) or by the growth of a surface flaw until fracture occurred. The finer plucking involved the removal of fragments released by the coalescence of cleavage microcracks opened up by sustained fluctuating stresses on the surface (see Fig. 5.79(d)). It has been shown that above an estimated average pressure of the order of 400 MPa this process occurred more readily so that the predominant wear mechanism became one of microfracture and cleavage 'rather than wear flat generation.

Type 2 Wear

The microfracture of Type 2 wear appeared to be of two types. (i) Hackly fracture with what often looked like smooth conchoidal surfaces but which consisted of overlapping cleavage steps (eg. Figs. 5.26(b & c); 5.44(f); 5.45(d); 5.75(f); 5.76(f); 5.77(c & e); 5.79(b); 5.82(b & e); 5.91(d). (ii) Microfracture with numerous sharp points created by the coalescence of cleavage cracks to form blocky particles 1 to 10 microns in size (eg. Figs. 5.14(c); 5.34(c); 5.45(a); 5.79(c); 5.80(e); 5.91(d & f)). Numerous examples have been illustrated to demonstrate that both types of microfracture occurred on diamonds that had drilled a wide variety of silicate materials. The diamond wear in drilling the soft calcite was exceptional in one respect. There was no fine microcleavage in the diamonds and all the fractures were hackly (Figs. 5.83(c & d)). These were primarily due to high local forces caused by impact either with loose diamonds or hard asperities in the rock. The impact energy required to fracture diamonds is about a quarter of the energy required to cause them to fail by static loading (Field 1979) and most of these fractured stones had apparent impact sites.

The hackly fractures on diamonds drilled in the hard rocks were also the result of impact (Fig. 5.77(d)) but it is likely that some of them also represented the advanced stages of microcleavage. The microcleavage is strong evidence for a "fatigue-type" process in the wear of diamonds. A fatigue process by progressive subcritical crack growth has been recognised as generally important in the wear of diamond where cyclical stressing of the surface is involved (Bowden & Tabor 1965, Tabor 1979, Crompton et al 1973, Wilks & Wilks 1979). Brookes (1979) described experiments demonstrating the breakdown of hard crystals by the effect of cumulative microdeformation caused by the repeated sliding of a softer material on a diamond. The wear of diamond aggregates described by Brookes & Hooper (1982) also had striking similarities with the single crystals studied in rock drilling. The wear flats broke down progressively to form numerous aligned blocks about 10 microns in size. It was suggested that cracks passing through twin bands or encountering inclusions may have changed direction repeatedly to give rise to the blocky structure. The SDA 100 crystals used in drilling are remarkably free of external signs of twinning although microtwinning might be present. The high density of inclusions and growth defects on 11111 planes could account for the blocky microfracture of these stones.

If the transition from a wear flat to microfracture is the culmination of a fatigue type process then the physical meaning of the estimated pressure per stone at which the general transition from Type 1 to Type 2 behaviour takes place must be discussed. A few issues should be borne in mind. The estimate of 400 MPa was of the same order of magnitude as the compressive strength of norite measured in the laboratory and an order of magnitude less than the measured uniaxial compressive strength or the estimated tensile strength of diamond (Bowden & Tabor 1965, Field 1979, Field & Freeman 1981). Wear flats and microfractured stones were both present on almost all the bits drilled in either Mode 1 or Mode 2 so the wear mechanisms operated in both modes and it was the preponderance of wear types that altered in the transition from Mode 1 to Mode 2 behaviour. The results of the test drilled

in Mode 1 using a monolayer bit with initially unworn stones proved that the microfractured stones in bits that drilled in Mode 1 were not simply inherited from the bit opening procedure.

Consider a single diamond drilling a hard homogeneous material. The actual pressure per stone determines the extent of the indentation of the diamond into the material being drilled. If the pressure is below the indentation strength of the material, indentation does not take place. The torque induces sliding of the diamond over the surface and a wear flat may develop. As the pressure on the diamond is increased by an increase in thrust greater indentation is possible; the energy transmitted to the drilled material increases, with an increase in torque. There is less sliding and more fracture of the drilled material with much higher peak stresses on the diamond. Consequently, diamond fracture is promoted over wear flat development.

In applying this model of diamond wear to a whole bit drilling rock it must be kept in mind that it is the average effect of all the exposed stones that has to be considered although it is the individual stones that do the work. At a low average pressure per stone few stones will indent the rock, the energy transmitted will be low, most of the exposed diamonds will experience sliding and the development of wear flats. Those stones that do indent will experience higher stresses and be more liable to fracture. As the average pressure per stone is increased the number of stones indenting the rock will increase with a proportional decrease in sliding and an increase in torque, rock fracture and diamond fracture. At the point at which the average pressure per diamond exceeds the indentation strength of the rock the majority of exposed points will indent the rock. A further increase in load will cause greater depths of indentation rather than a greater number of indents, and sliding will be severely reduced in favour of rock and diamond fracture. A marked increase in bit wear would be expected at this point as almost all the available diamonds would be in contact with the rock and therefore contributing rock particles to the erosive slurry. The higher stress on all the active stones would promote fracture at the expense of wear flats.

If however, by drilling suboptimally, extensive wear flat areas had been allowed to develop, proportionally higher loads would be needed to produce the necessary pressure per stone on those diamonds to exceed the rock strength.

The fact that the estimated average pressure per stone (400 MPa) for the transition from Mode 1 to Mode 2 behaviour is of the same order of magnitude as the measured compressive strength of norite (287 MPa) can now be seen to be significant. The transition in drilling norite with the standard microbits occurred at a bit pressure of about 5 MPa or a corresponding rate of advance of 0,06 mm/rev. Below the transition wear flats predominated over microfracture, the rotational speed remained constant, the advance per revolution increased linearly with increasing bit pressure and bit matrix wear values were low. Above the transition microfracture predominated over wear flats, the rotational speed dropped with increasing bit pressure, the advance per revolution remained constant with increasing bit pressure and there was a sudden increase in bit matrix wear.

Microfractured stones could in turn progress to develop other wear features. Occasionally the asperities of the largest stones became caked with detritus with the protruding points suffering abrasion to small wear flats because of the lack of indentation of the stone (Fig. 5.44(a & b), 5.45(b & c)). Under high stress, usually associated with high loads, the fracture of Type 2b stones could be so extensive that they barely protruded from the matrix (Figs. 5.26(d); 5.77(f)). By this stage they were approaching the classification of Type 4 wear.

Type 4 Wear

Type 4 wear was defined to include all worn stones that no longer protruded from the matrix. The incidence of Type 4 wear increased slightly at higher bit pressures because of the higher stresses per stone. They had either fractured off below the level of the matrix by progressive disintegration (Figs. 5.14(e); 5.26(e & f); 5.34(d); 5.81(e)) or were stones with wear flats that had been

forced into the matrix so that the worn surfaces were flush with the matrix surface (Fig. 5.81(b)). The latter Only happened in drilling the very resistant jaspilite. In this case the pressure on the worn stones exceeded the compressive strength of the bronze of the matrix and some of the stones were forced into the matrix. This highly undesirable situation prohibited further drilling unless the bit was resharpened. In the field a similar situation is possible if wear flats are allowed to develop to such an extent that they are flush with the matrix. In practice this was never encountered in the laboratory except drilling jaspilite because the tests were not long enough.

Type 3 Wear

The loss of stones by pull-out or total disintegration is not strictly speaking a form of diamond wear nor generally caused by the diamond being pulled out of the matrix intact. But the mechanism does contribute to diamond wear. Loose diamonds occasionally left tracks in the bit matrix and some of these could be followed to impacts with other stones. Such impacts invariably cause extensive damage either in the form of fracture of the impacted stone or its complete removal from the matrix to form another pull-out. The number of pull-outs did not vary significantly in response to different drilling conditions. There was very little evidence for extensive pull-out by high mechanical forces on the diamonds. The general state of compression at the face of the drill bit would have tended to prevent the diamonds from being pulled out physically. This is unlike the situation in diamond sawing where impact and a compressive phase is followed by exposure of the diamond for at least half the rotation of the blade. Most of the diamonds in drilling were lost through release by matrix wear. Even highly fragmented stones would often be retained in the matrix as a collection of self-supporting fragments held in place by the restraining support of the surrounding metal. This allowed them to continue to operate effectively until released by matrix wear.

6.5 SELF SHARPENING BEHAVIOUR OF IMPREGNATED DIAMOND BITS

The literature on the self sharpening behaviour of impregnated diamond bits has been summarised in Section 2.7. In the microbit tests of this study the bit wear rate of tests which drilled suboptimally innorite in Mode 1 had a mean of 0,16 ± 0,14 g/m (n = 38). For the reproducibility tests drilled in Mode 2 under set thrust the mean bit mass loss was 0,40 ± 0,11 g/m (n = 11). The mean bit mass loss for the four tests which had stalled at high set rate of advance was 1,02 t 0,31 g/m (n = 4). Matrix wear was low in Mode 1 with relatively high numbers of wear flats. At intermediate thrusts and Mode 2 drilling there was a preponderance of microfractured stones over wear flats with a constant proportion of Type 3 wear or loss by pull-out (Figs. 5.11 & 5.12). There was no evidence of direct contact between the matrix and the rock in Mode 1 or Mode 2 drilling. It was only under stalling conditions that there was direct contact, resulting in seizure. At suboptimal drilling in Mode 1 the development of diamond wear flats predominated and the detritus was slightly finer. Because of the low penetration rate there was less detritus produced per revolution, so erosion of the bit matrix was reduced and fresh diamonds were not exposed. Eventually penetration ceased because the available load was borne by large, stable wear flats.

Effective drilling in Mode 2 depended on a balance of diamond loss and matrix wear rate. In the microbit tests there was no evidence of a build-up of wear flats and load followed by a sudden stripping of matrix to reveal a fresh layer of diamond as has been postulated for diamond sawing (Ertingshausen 1985) and drilling (Selim et al 1969, Bullen 1984). Under both set thrust and set rate of advance if drilling progressed in Mode 2 there was a steady but minor fluctuation in both bit pressure and torque apart from the peaks caused by switching on and off at the beginning and end of each test run (see Fig. 5.13). In the microbit tests a dynamic balance between the development of microfracture, the loss of stones, and the matrix wear had been achieved in Mode 2 drilling.

Sullen (1984) reported a bit load fluctuation of 50 kgf when drilling full-sized BOWL bits (with a contact area of 14,27 cm^2) at set rate of advance. This represented a bit pressure fluctuation of 0,34 MPa. This is unlikely to have represented any major event at the drill tip as it was only 2% of the full load required to drill. Bullen found no evidence in the matrix wear figures for cyclical stripping of the matrix (ibid). Bit matrix and rock contact can occur at thrusts higher than optimal and then wholesale removal of bit matrix by abrasion might be possible if sufficient power were available. With the laboratory drill it was not and seizure resulted from these conditions. The diamonds which fractured flush with the matrix because of the high forces involved tended to protect the surface and enhance its load bearing capacity (see Fig. 5.26(e & f)). The wear resistance 'of such a diamond reinforced surface has been described by Wapler, Spooner & Balfour (1980).

In summary; stable drilling with microbits was achieved by the promotion of microfracture, the suppression of the development of wear flats, and the steady erosion of the matrix by detritus particles created by the drilling process.

6.6 FRICTION, TORQUE AND ROTATIONAL VELOCITY

The resistive forces opposing rotation of the rock in drilling are a function of friction between the diamonds and the rock, the bit matrix and the rock, and particles trapped between the bit and the rock (Paone & Madson 1966, Spink 1972). This friction is determined largely by the tensile and shear strength of the rock and the volume of rock indented by the diamonds. The friction is thus influenced by rock properties, lubrication, thrust and the wear behaviour of the diamonds. The coefficient of friction for diamond drilling of hard rock has been estimated to be in the region of 0,4 (Clarke 1982).

Torque is a drilling variable frequently monitored in drilling in the field and in the laboratory. Torque is determined by the friction and the abrasion between the bit and the rock and as such it is affected by rock properties, number of exposed stones, bit thrust, extent of matrix contact, lubrication, rotational speed and the condition of the diamonds (Clarke 1979). Additives have been shown to improve drilling performance

(Joris & Maclaren 1967, Macmillan, Jackson & Westwood 1975, Strebig et al 1969, Mills 1978). Apart from the possible enhancement of the rock strength by a Rebinder-Westwood chemomechanical effect (Westwood & Mills 1977, Cuthrell 1978) the additives may promote wetting of the diamonds and facilitate removal of heat from the stones (Cooper 1979). This leads to less thermally activated diamond wear in the form of rounding of the stones and hence the maintenance of more efficient drilling conditions. A corresponding torque increase had been noted with the use of additives (Selim et al 1969) which could be explained by the reduction in wear and decrease in the sliding coefficient of friction. Hence greater torque could be transmitted to the rock. Selim et al (1969) and Clarke (1979) considered a finite torque at zero penetration rate to represent a threshold required to overcome the sliding friction.

At constant penetration rate the specific energy of drilling has been found to be proportional to torque (Selim et al 1969), indicating the fundamental importance of power transfer to the rock. Considering that the diamond wear is a dynamically changing variable, with the condition of the stones free to alter in the course of drilling, measurement of torque can be expected to indicate the state of the exposed diamonds in some way. This appears to be the case. Bullen (1984) considered the measurment of torque to be "the key to assessing the condition of the drill bit". Bullen found that if torque and penetration rate decreased then the diamonds were developing wear flats or the bit was "glazing over" with adhering detritus, but if the torque and penetration rate were constant then drilling was proceeding satisfactorily. The current study amplifies these observations substantially.

The miniture load cell used to measure torque force on the Arboga drilling machine enabled very low torques of the order of a fraction of a Newton metre to be measured accurately. The reproducibility of results even over a long period of time was good with an error of less than 15% for drilling in the stable Mode 2 (see Table 4.3). The load cell arrangement was far more successful in measuring low torques reliably than the strain-gauged beam employed on a similar machine by Siribumrungsukha (1980).

In the current study torque was found to drop steadily with decreasing penetration rate in Mode 1 drilling under set thrust conditions. Conversely, under set rate of advance the torque rose steadily with the rise in reactive load in Mode 1. This behaviour was also noted by Siribumrungsukha (1980). Torque on its own cannot be used to distinguish Mode 1 from Mode 2 behaviour. The relationship between torque and penetration rate has been studied by Paone & Madson (1966) who found a linear relationship up to a critical value of torque. Above this the torque increased less rapidly with increasing penetration rate. It was thought that above a maximum effective torque some unspecified rock property led to a reduction in friction and caused a drop in torque. At bit pressures in excess of 6 MPa with standard microbits in norite no significant improvement in drilling could be achieved by increasing the thrust. Bit wear increased suddenly (Fig. 5.9) with a wasteful rise in torque and energy consumption. Drilling could not be sustained in this region when drilling at set rate of advance.

Above 6 MPa bit pressure and about 0,08 mm/rev with the standard microbits increased thrust served only to force the diamonds into the rock up to the point that the matrix contacted the rock. This led to a sudden increase in torque and damage to the bit. The 40/50 mesh diamonds at 30 concentration drilled with an optimal minimum specific energy at moderate bit pressures. Improved performance in norite with this machine would only be achieved by a change in bit formulation.

An analysis of the friction in drilling norite led to a discriminating criterion for drilling in Mode 2 (see Section 5.10). The friction between the bit and the rock and hence the effective torque transfer depends primarily on the tensile and shear strength of the rock, and on the volume of the indentation of the diamonds (Clarke 1982). The volume of indentation at a given pressure depends on the compressive strength (itself related to the tensile and shear strengths) and on the diamond concentration and size as well as the wear condition of the exposed stones. The volume of indentation determines directly the volume of material removed per revolution.

Fig. 5.98 confirmed the linear relationship between estimated coefficient of friction and the penetration rate. As long as mechanical efficiency

can be maintained it is desirable for efficient rock fracture for the friction between the bit and the rock to be high. At a given thrust, the higher the friction the more effective the transmission of torque and hence power to the rock will be. However at excessively high thrusts, and high set rate of advance, energy is consumed in destroying the bit. Consequently an optimum thrust or corresponding rate of advance exists.

The approximate curve of specific energy derived from the torque and penetration rate measurement for these tests has been superimposed on Fig. 5.98 as a dotted line. The specific energy minimum corresponded to the drilling performance region just above the transition from Mode 1 to Mode 2 behaviour. The optimal rate of advance was between 0,06 mm/rev and 0,08 mm/rev with an estimated coefficient of friction in excess of 0,275. This represents a general threshold for steady drilling of norite in Mode 2 with the standard microbit formulation.

Any refinement of the drilling process which reduces the sliding friction without imparing the mechanical couple between the bit and the rock would be beneficial. Appropriate lubrication additives can achieve this goal in some rocks by acting as wetting agents (Joris & McLaren 1967, Strebig et al 1969), or possibly by strengthening the rock to encourage brittle fracture as opposed to sliding and ductile behaviour (MacMillan et al 1975, Mills & Westwood 1977). Surfactants affecting the rheological properties of the slurry around the bit affect the cooling and wear of the diamonds and hence the interaction between them and the rock (Cooper 1979). The effect of additives has not been studied in the current program. The mechanisms involved are poorly understood (Cuthrell 1978, Mills 1978) and in the light of the importance of friction and diamond wear to efficient drilling further research is required in this area.

If the demonstrated linear relationship between estimated coefficient of friction and rate of advance is valid for other rock types drilled with full-scale bits this relationship could form the basis of an easily applied drilling guide. Bit pressure, torque and rate of advance are variables easily measured in the field. Calculating the estimated coefficient of friction and plotting it against the rate of advance during drilling should enable the operator to locate the drilling performance on a line such as the one plotted in Fig. 5.98 for a given

rock type. This would indicate the mode of behaviour and assist the operator to decide in which direction to alter the drilling parameters to maintain steady drilling and appropriate diamond wear.

It has been shown that the relationship between the estimated coefficient of friction and the rate of advance is linear for a wide variety of materials. The estimated coefficient of friction associated with the pressure threshold required for initial penetration is inversely related to it and dependent on the mineralogy and bonding of the material. The transition from Mode 1 to Mode 2 drilling behaviour occurs at different rates of advance and corresponding coefficients of friction in different materials. The results of this very limited set of tests are strikingly consistent and suggest that a more detailed investigation with full-scale bits could form the basis of a simple operating guide when drilling a known rock type.

6.7 ENERGY IN ROCK DRILLING

The processes which consume energy in rock drilling have been discussed in detail by Simon (1963) and Spink (1972). The elastic strain energy required to load a larger volume of rock than that released by crack propagation represents about half the energy input. This is dissipated on unloading by crack propagation as stress waves and heat (Simon 1963). Most of the remaining energy is consumed in compacting and crushing material beneath the indenting diamonds. The energy consumed in actually forming primary new surfaces is considered to be negligible. Other possible sources of energy consumption have been listed generally by Spink (1972) as elastic hysteresis, plastic deformation such as ploughing without removing material, strain hardening, melting, chemical changes, annealing, mineralogical phase changes, secondary regrinding, and friction of the diamonds and bit matrix on rock, and the friction of rock particles trapped between the bit and the rock.

6.7.1 Fracture Energy

Under optimal drilling conditions in norite with a 40/50 mesh bit the estimated energy consumed in creating new surfaces was 8,9 MJm^{-3} (Table 5.16). This was about 1,5% of the total drilling

energy. This percentage dropped under less optimal drilling conditions using both coarser and finer mesh bits. Even if all the particles produced were assumed to be one micron in diameter then the estimated surface energy requirement was only 12 MJm^{-3} or about 1% of the total energy consumed. In calculating these figures it was assumed that all the detritus represented fresh, unreground particles. This was certainly not true. If the well defined mean of the coarse fraction can be assumed to represent the average grain size of primary particles then only about 0,01% of the energy consumed in drilling was used in primary fracture to release particles from the rock.

The estimated fracture energy was less than 2% of the measured specific energy for all the hard materials and rocks (Table 5.17). The value for calcite was not much higher although the calcite broke along the relatively easy cleavage. The true cleavage energy for calcite is much lower than the surface energy for quartz and this has contributed to a spuriously high value for the estimated surface energy in this case. The sandstone was drilled with very low specific energy because the diamonds excavated whole grains with minimal fracture. The estimated surface energy requirement was unrealistically high because the fracture that took place was through the poorly cemented rock matrix.

The bulk of the energy in drilling is therefore not used in primary rock fracture but principally in secondary grinding, crushing and compaction of detritus and rock beneath the diamonds, by compressive loading of the rock volume ahead of the drill bit, and in heat loss through friction. The relative magnitudes of these energy losses have not been determined as the partitioning is expected to vary with rock type (Clarke 1982). All these energy losses were included in the measured specific energy of drilling.

6.7.2 Specific Energy and Drilling Efficiency

As the energy required to create fresh surfaces in hard rock drilling is usually negligibly small the calculated specific energy can be seen as a measure of efficiency in the sense that the lower the specific energy the lower the energy wasted in dissipative processes. It is recognised generally that the specific energy of drilling at reasonable levels of efficiency approaches the same order to magnitude as the uniaxial compressive strength a_c (Bailey & Dean 1967). i.e.

$$ES = 0{,}3\ a_c \text{ to } 3\ a_c$$

No explanation has been found in the literature to account for this except the observation by Teale (1965) that since specific energy and compressive strength are dimensionally identical it is "not altogether suprising that a relationship of some kind should exist". An attempt will be made to offer an explanation here. Table 6.1 contains the measured minimum specific energy of drilling, the compressive strength as measured by unconfined uniaxial compression, and the ratio between the two (Es/a_c) for drilling a variety of materials. This data is plotted in Fig. 6.7.

With reference to Fig. 6.7 it can be seen that the plotted points for the more efficiently drilled materials do lie closer to the line equating specific energy to compressive strength. The most efficiently drilled material in terms of specific energy was sandstone which had an Es/a_c ratio of 1,69. This very friable material was drilled predominantly by excavation of whole grains from the weakly cemented rock matrix - there was a minimum of fracture and secondary comminution. This mechanism was unusual and material was removed with a near minimum of energy loss.

TABLE 6.1 : Minimum specific energy of drilling vs. compressive strength for a variety of materials

MATERIAL	BIT PRESSURE (MPa)	MINIMUM SPECIFIC ENERGY (MJm^{-3})	COMPRESSIVE STRENGTH (MPa)	EFFICIENCY PARAMETER E_s/σ_c
Sandstone (S)	0,5	69	41	1,69
Dark Norite (N)	5,3	582	287	2,03
Quartzite (Q)	4,4	744	250	2,98
Quartz (K)	4,9	1082	360	3,01
Light Norite (L)	5,0	640	209	3,06
Syenite (Y)	7,0	600	176	3,41
Marble (M)	3,8	472	138	3,42
Felspar (F)	6,4	749	219	3,42
Granite (G)	8,5	1231	186	6,62
Jaspilite (J)	11,2	3206	484	6,62

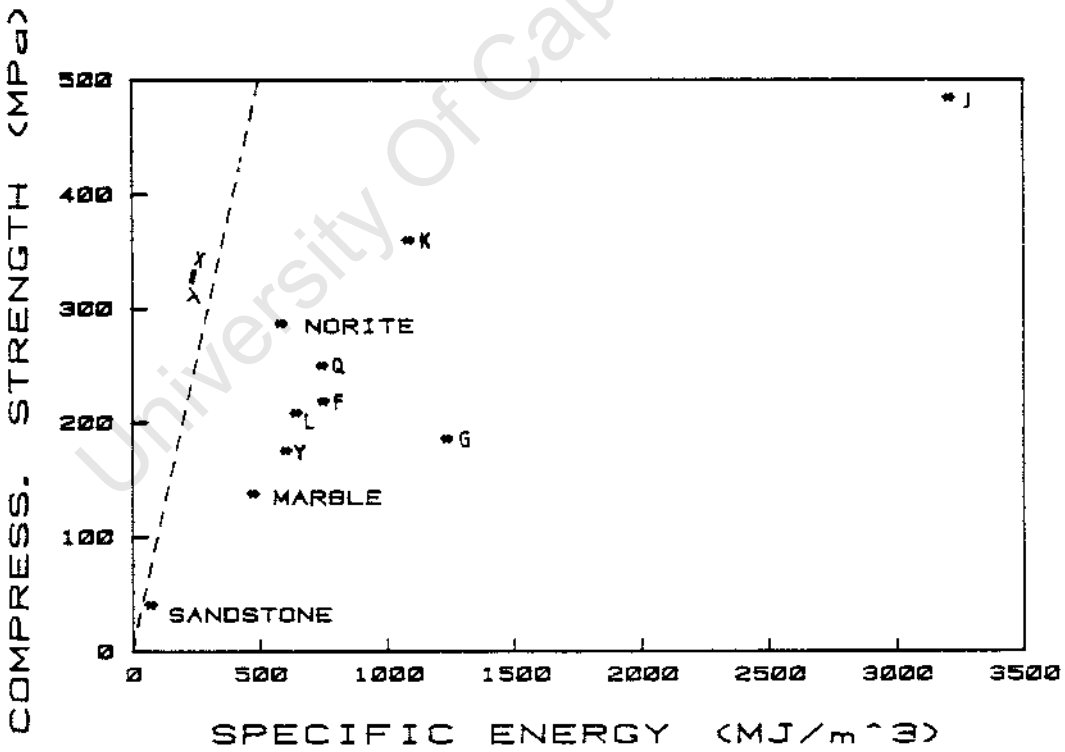

FIGURE 6.7 : Plot of uniaxial compressive strength against minimum measured specific energy for tests drilled in a variety of materials (for key to letters see Table G 1%

The rotary drilling process has been described as similar to that of a small element drag bit (Maurer 1967). A comparison of the mechanism of rock fracture using a drag bit element and fracture in uniaxial compression shows some signficant similarities (see Fig. 6.8). In the uniaxial compression test the cylindrical rock specimen is loaded until it fails in a combination of resolved shear stress and radial tension due to the axial compression. A horizontally moving diamond, loaded vertically so it is not free to ride up, impinging on a step or protuberance of rock stresses the material in a very similar way, to release a chip to the free surface by shear. In fine grained rocks at atmospheric pressure if the energy losses are kept to a minimum then this mechanism of brittle chip formation may be expected to be predominant. If the analogy between this mechanism and failure in uniaxial compression is valid then the relationship between unconfined compressive strength and minimum specific energy attainable in rotary drilling is to be expected.

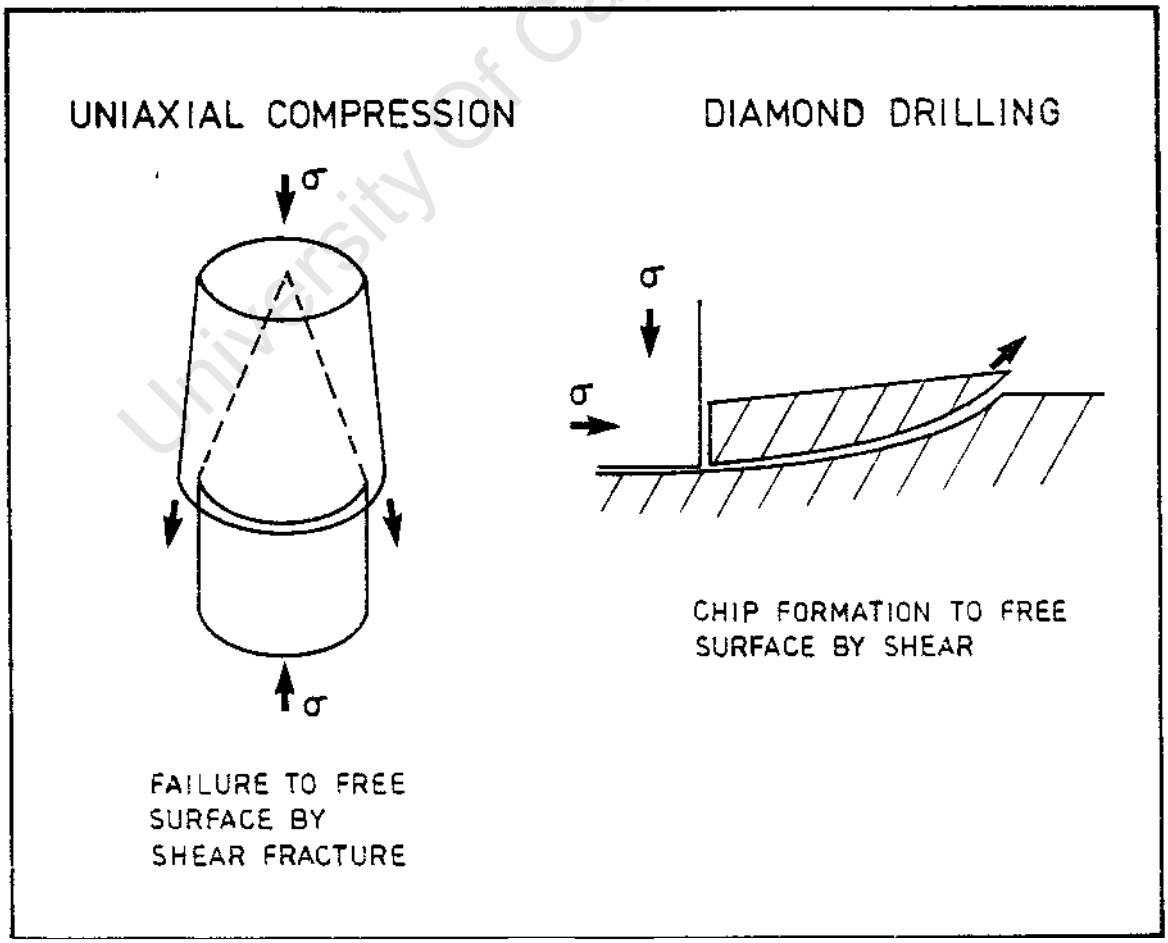

FIGURE 6.8 : Diagram to illustrate the similarities between compressive strength testing and rock drilling

Methods of rock removal very much more efficient than rotary drilling have been commented on by Bailey & Dean (1967). Manual picking can produce Es/a_c ratios well below unity. However, the rate of power transfer is also very low and the penetration rate not satisfactory. In rotary drilling the minimum attainable specific energy in a given rock may be determined ultimately by the rock fracture mechanism associated with drilling. To increase drilling rates either more power has to be transmitted to the rock or more efficient fracture mechanisms must be employed. In rotary drilling the application of power is limited by the strength of the materials comprising the drill string and bits. Innovation in materials design has led to progress in this direction (Fig. 6.9). Bits set with polycrystalline diamond compacts are capable of extremely high rates of penetration in hard rock (Tomlinson, Pipkin & Lammer 1985).

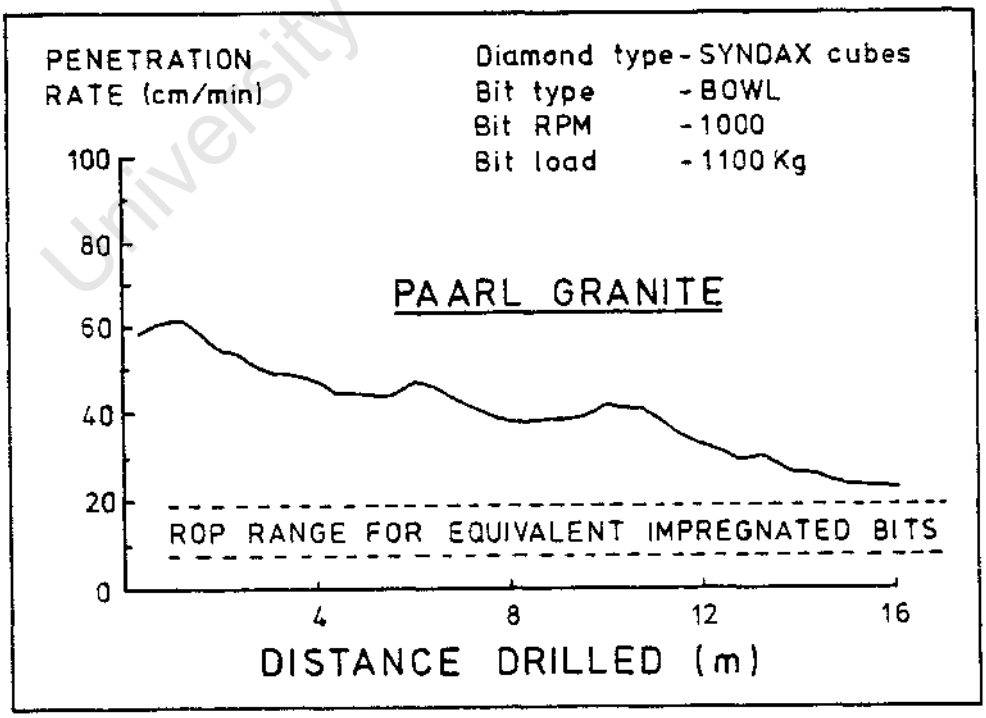

FIGURE 6.9 : Penetration rate as a function of depth drilled for a 30 element SYNDAX cube bit in Paarl granite (250 MPa) (from Tomlinson et al 1985)

The alternative of investigating more favourable loading geometries is more problematic. Bailey & Dean (1967) have shown that a degree of "intelligence", taking strategic advantage of prexisting fractures for instance, can lead to lower specific energies. They note however that is is difficult to envisage how this might be applied at the bottom of a narrow hole. Simon (1963) observed that the application of any energetically favourable loading geometry at the bottom of the hole rapidly leads to a complementarily unfavourable situation in which material must be broken from an essentially single free face, or from a reentrant angle, at the cost of efficiency. Even if a ratio of Es/a_c less than unity cannot be achieved in rotary drilling there is scope for decreasing the energy wasted on regrinding and friction. For instance, adequate flushing and well designed waterways, the use of appropriate flushing additives, the choice of optimal diamond type and size as well as the correct matrix composition for the rock being drilled all can contribute to reducing the net specific energy and increase the penetration rate.

In drilling norite with standard microbits the minimum specific energy obtained was 582 MJm^{-3} with an efficiency parameter Es/a_c of 2. The specific energy depended strongly on bit pressure both at set thrust and set rate of advance (Figs. 5.7, 5.8 & 5.21). The minimum specific energy occurred at a bit pressure between 5 MPa and 6 MPa with a rate of advance of about 0,1 mm/rev. This was just above the threshold of stable Mode 2 drilling, and involved moderate bit wear. Specific energy dropped with increasing rotational speed from 2,5 ms^{-1} to 4 ms^{-1} as more optimal conditions were approached at higher speeds (Fig. 5.31). With bits of constant concentration but different diamond mesh size the specific energy rose sharply with increasing diamond size at a set rate of advance of 0,044 mm/rev.

If sufficient power had been available to allow drilling to proceed at higher bit pressures with bits containing coarse mesh stones in higher concentration this may have been advantageous.

The larger stones produced coarser detritus (Fig. 5.47 & 5.53) which would have lowered the specific energy if penetration had been maintained. From Fig. 5.51 it is evident that drilling at bit pressures that are too low generated unacceptably high specific energies because of the generation of wear flats and subsequent loss of penetration rate. This is in direct conflict with the recommendations of Spink (1972) who found low net specific energies when drilling a variety of rocks with moderate to low bit pressures. A Hertzian mode of fracture was postulated to account for these results. However, Spink's tests were very short and no account was given of diamond wear so progressive dulling of the bit with the resulting decrease in penetration rate and increase in specific energy were not recorded.

In the present study the highest bit pressure for which there was sufficient power available to drill effectively was about 10 MPa. At this pressure the specific energy minimum in drilling norite was sharply defined for a particular diamond size (40/50 mesh) in the bits used (Fig. 5.51). Specific energy was also strongly influenced by diamond size in drilling both norite and a quartzite with similar compressive strengths (Fig. 5.57). This was because the mechanisms of rock removal and the extent of regrinding were directly affected by diamond size. At set rate of advance and set thrust the curves of specific energy plotted against bit pressure for drilling different types of rocks with standard microbits showed distinct minima for the less resistant materials (Figs. 5.68 & 5.69). These values have been tabulated in Table 6.1 and plotted in Fig. 6.7. The more resistant materials like granite and jaspilite had specific energy minima outside the operating range of the laboratory drilling machine.

For many rocks the drilling optimum in terms of specific energy does occur at relatively low thrusts and low rates of penetration (Simon 1963, Teal 1965, Spink 1972). The economics of drilling must be considered in terms of the combination of bit costs and time costs (Busch & Hill 1975).

In long hole drilling especially with wireline equipment it is advantageous to maximise the life of the bit to retain it down the hole. The time costs incurred in drawing the rods to replace the bit may outweigh the advantages to be gained by a rapid penetration rate at the expense of bit life. Under these conditions drilling at the energetic optimum which tends to coincide with moderate bit wear at lower penetration rates may be economic. In drilling short holes the advantages of high penetration rates can outweigh the cost of high energy consumption and more rapid bit wear rates.

Knowledge of the performance of particular bit designs in a variety of rock types is obviously necessary for the economic optimisation of any given drilling enterprise. The essential problem of transmitting more power to the rock with mechanical efficiency involves innovative materials design, the development of more efficient drilling machines, and the optimisation of performance through the application of the appropriate drilling parameters.

6.8 ROCK FRACTURE IN DIAMOND BIT DRILLING

A comprehensive theory of rock fracture in drilling with impregnated diamond bits is difficult to formulate due to the complexity of the drilling process and because the fundamental rock failure criteria are poorly understood (Maurer 1967). Those that have been studied are difficult to apply to the real situation because of the complex and diverse nature of different rock types (Simon 1967, Siribumrungsukha 1980). Individual minerals fracture in different modes, some of them idiosyncratically, and rocks may fail under tensile, shear or compressive stress (Rowlands 1975). The extant models for drilling with surface set bits (Rowley & Appl 1969, Peterson 1976, Moore, Walker & Appl 1978) cannot be applied to impregnated bit drilling because of the extreme difference in diamond size, the irregular arrangements of stones on the impregnated bit face, and the impossibility of achieving perfect flushing. The mechanism of rock drilling can be described simplistically as fracture induced by a combination of the vertical thrust force and the radial torque force. In practice these operate simultaneously in a

dynamic system resulting in a number of fracture mechanisms which must necessarily be considered separately in constructing a physical model of drilling. A detailed description of these fracture mechanisms can be found in Appendix 1.

At elevated confining pressures rocks appear to strengthen and undergo a brittle to ductile transition above a critical value for each rock type (Paone & Tandanand 1966, Garner 1967). The confining pressure at which the transition takes place ranges from about 7 MPa for soft limestones to over 30 MPa for some marbles and harder rocks (Cheatham & Gnirk 1967). The hydrostatic pressure exerted by the cutting fluid in diamond drilling is usually far lower than this transition threshold especially for the stronger rocks which tend to be drilled with diamonds (Rowlands 1975). Rowlands concluded that in most of the rocks drilled with diamonds predominantly brittle failure could be expected and the rocks would deform elastically up to the point of rupture (ibid).

However, plasticity and ductile behaviour may be a significant response of certain minerals as opposed to the rock as a whole. As the physical properties of each mineral constituent as well as the rock structure determines the fracture behaviour of the rock (Pfleider & Blake 1966) the interaction between the different fracture mechanisms is extremely complex and not readily amenable to theoretical analysis. Various modes of failure are superimposed on each other as a result of moving point loads traversing changing non-uniform stress distribution in the rock (Simon 1967). These modes of failure include compressive crushing, tensile cracking, failure by shear, Hertzian cracking, excavation and secondary crushing or grinding (see Appendix 1).

The interaction of these mechanisms depends on the drilling parameters; the rock structure and composition; the physical properties of the component minerals and the relations between them; the size, number and condition and relative position of the active diamonds; the composition and efficiency of the flushing medium and the geometry of the bit design. It is hardly suprising that no effective and coherent theoretical model of impregnated diamond bit drilling seems to exist.

The physical evidence for a variety of different fracture mechanisms in norite and other materials drilled in the laboratory with impregnated diamond microbits came from particle size distribution analyses of the drilling detritus, SEM and optical microscopy of this material and of the drilling tracks on punch-through rock discs, as well as selected sections cut through drilling tracks in norite and quartzite. Furthermore, in this study threshold bit pressures for penetration have been inferred for drilling a number of different materials (Table 5.8). The correlation with compressive strength was poor with a linear correlation coefficient of r = 0,672. However, this pressure threshold was not just for simple indentation but for drilling penetration. It was affected not only by the rock strength but also by other variables such as the number and condition of active stones which in turn was strongly influenced by the relative abrasion resistance of the materials.

6.8.1 Detritus Size Distribution

The size of the detritus produced in drilling norite depended most strongly on the diamond mesh size for the finer diamond sizes and on the bit pressure as well as the diamond size for the coarser mesh sizes at both set thrust and set rate of advance (Figs. 5.46, 5.47 & 5.53). The mean of the coarse detritus increased with increasing diamond size; and with increasing thrust for the larger diamond sizes (Fig. 5.53). The percentage of fine detritus (indicative of regrinding) decreased with increasing diamond size and had a minimum at optimal bit pressure (Figs. 5.16 & 5.55). These relationships were valid for all the tests drilled in norite. The effect of changing rate of advance was the same as a corresponding change in bit pressure (compare Figs. 5.15 and 5.53 with Figs. 5.27 and 5.59 respectively for the coarser detritus size). As rates of advance were increased towards more optimal peformance at a reactive bit pressure of about 6 MPa the percentage of fine detritus decreased slightly (Figs. 5.28, 5.60). The effect of increased rotational speed at a fixed set rate of advance was to increase the percentage of fine material

produced by regrinding (Fig. 5.36). There was no clear trend in the coarse fraction (Fig. 5.35).

For a given diamond size an increase in bit pressure (or rate of advance) increases the load per stone, causing the stones to indent the rock further and produce larger particles. This is in agreement with the findings of Pfleider & Blake (1953) and Fish (1961) who found that increased thrust (or penetration per revolution) produced larger fragments due to increased depth and intensity of fracture. On microbits operating below the optimal bit pressure the diamonds tend to develop broad wear flats which impede penetration and increase the extent of reginding. Garner (1967) found that sharp diamond points fractured rock more efficiently than blunt ones, and Fish (1961) and Maurer(1967) observed that as the tip radius of an indenter increased due to wear the thrust required to fracture rock rose rapidly. Above the optimal bit pressure with the microbits the gap between the rock and the bit matrix decreases which also enhances the reginding and raises the percentage of fine material produced. At reduced rotational speeds the released particles have more time to escape from the bit face so less regrinding takes place. The size of the primary particles seems to be unaffected by a drop in speed. Pfleider & Blake (1953) similarly found that the size and shape of released particles did not vary with speed but that at higher speeds intensity of fracture was greater and removed greater numbers of particles. As they tested whole stone surface set bits the regrinding phenomenon was not so apparent.

The effect on detritus size of changing the diamond size does not appear to have been studied before with impregnated bits. With a decrease in diamond size at constant concentration the smaller diamonds create progressively smaller indentations and hence produce finer detritus. With an increase in diamond size the relative increase in detritus size is less pronounced as the large diamonds indented the rock to a progressively smaller fraction of their size. As the diamond size gets larger the extent to which the stones indent the rock is determined almost entirely by the load so bit pressure becomes more important in determining

detritus size. In the tests with diamonds above 40/50 mesh diamond size the detritus size is determined predominantly by the bit pressure. Below 40/50 mesh diamond size the detritus is determined primarily by the diamond size.

The size of the coarse detritus produced depends on the volume of the indentations produced by the individual diamonds. This is affected directly by diamond size, diamond concentration, degree of protrusion, state of wear of the stones, the bit pressure, and the rock strength. The extent of regrinding is influenced directly by diamond wear flat area, the gap between the bit matrix and the rock, the rotational speed, and the flushing rate and pressure.

6.8.2 Fracture Patterns - The Drilling Tracks and Detrital Grains

The drilling tracks on the punch-through discs on norite were uniform in appearance for all drilling conditions (Figs. 5.17, 5.29, 5.37, 5.38(b), 5.48 & 5.49). There were no clear grooves although the tracks of single diamonds tended to be identifiable by annular rings of mashed flakes adhering to the rock. At all bit pressures the failure was by cleavage fracture of the felspar and pyroxene constituents with no apparent difference in intensity of fracture under different conditions. At extremely low rates of advance, and hence low bit pressure, the track was smoother (Fig. 5.29(a)) but the difference was subtle.

The appearance of the detritus grains themselves was also very uniform (see Figs. 5.84(a), 5.86(e & f)). The flat detached mashed flakes tended to be larger, curved and striated (Figs. 5.38(d) & 5.39(a to c)). The intact mineral grains were angular, blocky cleavage fragments (Figs. 5.86(e & f)). The uniformity of the appearance of the drilling tracks and the detritus suggested that norite was drilled by a uniform mechanism characterised by predominantly cleavage controlled tensile and shear fracture with minimal primary crushing. There was no apparent variation in the fracture mechanism under different drilling conditions and the drilling behaviour - suboptimal, quasi-stable, seizure - was

determined by the extent of regrinding, the diamond wear behaviour and the gap between the rock and the bit.

Microscopy of sections cut from the rock ahead of the drill bit operating at a wide range of pressures in norite revealed no extensive crack field ahead of the bit (Fig. 5.61). There was a zone of crushing and fracture confined largely to the first layer of crystals. Propagating cracks were evidently deflected along cleavage planes and either stopped or diverted at grain boundaries. This can be true only for impregnated bit drilling because of the small size of the diamonds relative to the mineral grains in the norite and the constraining effect of adjacent grains in a coherent rock.

6.8.3 Fracture in Different Materials

The detritus size distributions and the appearance of the drilling detritus and the tracks produced by drilling a variety of materials at set thrust and under set rate of advance conditions have been described in detail in Chapter 5. Each material had a characteristic failure mechanism within the operating region of impregnated bit drilling. It was clear that in impregnated diamond bit drilling, where the size of the diamonds is generally small with respect to the size of the crystal grains in the rock, the rock fracture under given conditions is largely determined by the physical properties of the constituent minerals and the nature of the relationship between them, that is the microstructure of the rock. This will be illustrated by discussing two topics, the role of cleavage and the effect of quartz content in different materials.

Single crystal microcline felspar and quartz are both relatively hard minerals with Mohs's hardness values of scratch resistance of 6 and 8 respectively (Hurlbut 1971). The relative ease with which the felspar could be drilled was largely due to its ready cleavage in two nearly orthogonal planes. A comparison of the drilling tracks produced at 8 MPa bit pressure in both microcline and quartz (Fig. 5.88) showed the influence of cleavage clearly. In

both specimens the scale of fracture was similar with the tracks of individual diamonds marked by finer fracture and crushing. Larger fragments were released from the ridges between the tracks. In the case of the felspar these were large blocky cleavage fragments and in the quartz they were large flat spalls with zig-zag fracture traces on conchoidal surfaces. The zig-zag fracture was due to competition between the weak rhombohedral cleavage planes of quartz (Ball 1974). At high magnification it can be seen how the cuboid nature of the felspar cleavage fragments promoted tneir easily being pried or flushed out of the drilling track, whereas the more angular quartz fragments tended to interlock and impede removal.

Calcite, the third single crystal material drilled, also illustrates the importance of cleavage (Fig. 5.90(a & b)). This was the only material, for which punch-through discs were produced, that displayed what appeared to be plastic grooving by the diamond points (Fig. 5.90(b)). However, the 'predominant mechanism of material removal was brittle failure by cleavage of large fragments between the tracks of individual stones. This was even more pronounced at higher loads when very large fragments were produced, raising the mean detritus size and wearing the bit matrix rapidly by abrasion. The ease of cleavage of the constituent minerals is an important factor in the drillability of any particular rock.

The percentage free quartz in a rock has been considered by a number of authors as an important variable in rock drillability (eg. Paone & Madson 1966, Singh 1973). The results of this study do not support this belief. The drilling performances of four different materials consisting predominantly of quartz (viz. single crystal quartz, sandstone, quartzite and jaspilite) differed widely and this could only be due to the microstructural differences which lead to different modes of fracture. The diamonds excavated mostly whole grains from the weakly cemented sandstone (Fig. 5.85(c)) whereas quartzite particles were both excavated and fractured (Figs. 5.85(a), 5.89(a & b)). The well bonded jaspilite fractured with difficulty into more rounded polycrystalline grains (Figs. 5.87(a to c)) but due to its very

fine grained nature was drilled with extreme difficulty producing smooth surfaces on the drilling tracks (Fig. 5.89(c & d)). The single crystal quartz having no grain boundaries to impede the propagation of fractures produced flatter spalls (Fig. 5.85(e & f)) with fracture surfaces sometimes approximating the logarithmic shape theoretically expected of an undeflected shear fracture trajectory (Maurer 1967). The effect of lack of grain boundaries in the single crystal quartz can be appreciated readily from Fig. 5.89(f). It has been demonstrated that the absolute size of the grains, the grain size relative to the diamonds size, and the nature of the cement between the grains is important in determining the different type and extent of fracture in different materials of essentially the same mineralogical composition.

It could be inferred from the petrographic descriptions of the syenite and granite, both hard, crystalline igneous rocks, that in these rocks quartz played a crucial role in their difference in drillability (see Fig. 4.1 and Appendix 3). The quartz in the syenite consists of small isolated grains easily fractured or excavated because of the relatively soft minerals around them. The higher proportion of quartz in the granite consists largely of highly intergrown masses of crystals with convoluted grain boundaries. These grains supported each other and resisted fracture in the same way as the jaspilite and made the granite highly resistant to drilling. The microstructural relationships between quartz and neighbouring grains is crucially important in determining the mode of failure of the rock as a whole and hence the drillability.

From the results of this study it would appear that a characteristic set of failure mechanisms exists for each rock type over the range of drilling with impregnated diamond bits. The transition from one mode of drilling behaviour to another depends not on a change in the mode of rock failure but on a change of total drilling performance caused by alterations in the diamond wear behaviour and drilling performance variables like thrust and the efficiency of flushing. It is thus of crucial importance to understand the diamond wear mechanism and to study the effect that

different rocks have on diamond wear behaviour, as well as to persue the more conventional study of the effect on performance of varying the drilling variables.

6.9 DRILLABILITY

Two different approaches have been taken commonly to evaluate the ease with which a particular rock may be drilled. A number of researchers have attempted to relate drilling performance to specific rock properties, either singly or in combination (eg. Paone & Bruce 1963, Paone et al 1966, Singh 1973, Siribumrungsukha 1980). Alternatively attempts have been made to establish a drillability index based on the drilling performance of a standard microbit, usually a rotary tungsten carbide chisel bit (eg. White 1969, Tsoutrelis 1969a). This is the basis of the Goodrich drillability test (Goodrich 1957).

There has been lack of agreement on the choice of the performance variable most appropriate to describe the ease of drilling. Paone & Madson (1966), Singh (1973) and Siribumrungsukha (1980) tried to relate penetration rate to a selection of rock properties including hardness, strength and abrasiveness. Teale (1965) and Bailey & Dean (1967) choose specific energy as a variable to describe drillability. Drillability evaluations based on microbit tests have usually included the determination of an additional factor; an index of wear of a standard metal bit after drilling a set distance under set conditions (White 1969, Tsoutrelis 1969a). There is no generally accepted method to determine drillability of rocks and no fully successful attempts at predicting the performance of impregnated diamond bits in different rocks have been described to date.

The tests drilled in a variety of materials and presented here were intended to enable a comparison to be made between the performance of impregnated microbits in norite with the response of other rocks. Despite the fact that this test series was not designed to establish the drillability of the materials some pertinent observations can be made.

Most of the tests were done under set rate of advance so penetration rate could not be used as a comparative criterion of performance. The

reactive load expressed as bit pressure could be used for the tests at set rate of advance. For those rocks drilled exclusively under set thrust conditions the tests at the nearest equivalent rates of advance had to be selected for comparison. The rate chosen was 0,044 mm/rev. Alternatively the specific energy could be used as a measure of drilling performance. The rock properties had been determined in terms of uniaxial compressive strength and relative abrasion resistance of drilled cores. Both of these were relatively easily determined and in addition uniaxial compressive strength has been found by a number of researchers to correlate strongly with drilling performance (Paone & Madson 1966, Maurer 1967, and Singh 1973).

Owing to the inherent scatter expected in the data due to the relatively low number of tests the significance of the relationships between the performance variables (mean bit pressure and specific energy) and the rock properties (relative abrasion resistance and uniaxial compressive strength) was tested by simple linear regression.

The most significant relationships were found to be as follows:

Specific energy vs. RAR x strength	y = 6,40x + 282 (r = 0,94)
Bit pressure vs. RAR	y = 9,84x + 1,55 (r = 0,90)
Specific energy vs. strength	y = 6,66x - 414 (r = 0,89)
Specific energy vs. RAR	y = 2595x - 18 (r = 0,84)

Mean bit pressure was best predicted by the RAR (Fig. 6.10). The specific energy was best predicted by the product of RAR and uniaxial compressive strength (Fig. 6.11). Considering the scatter expected in the results because of the low number of drilling tests involved this correlation was suprisingly good.

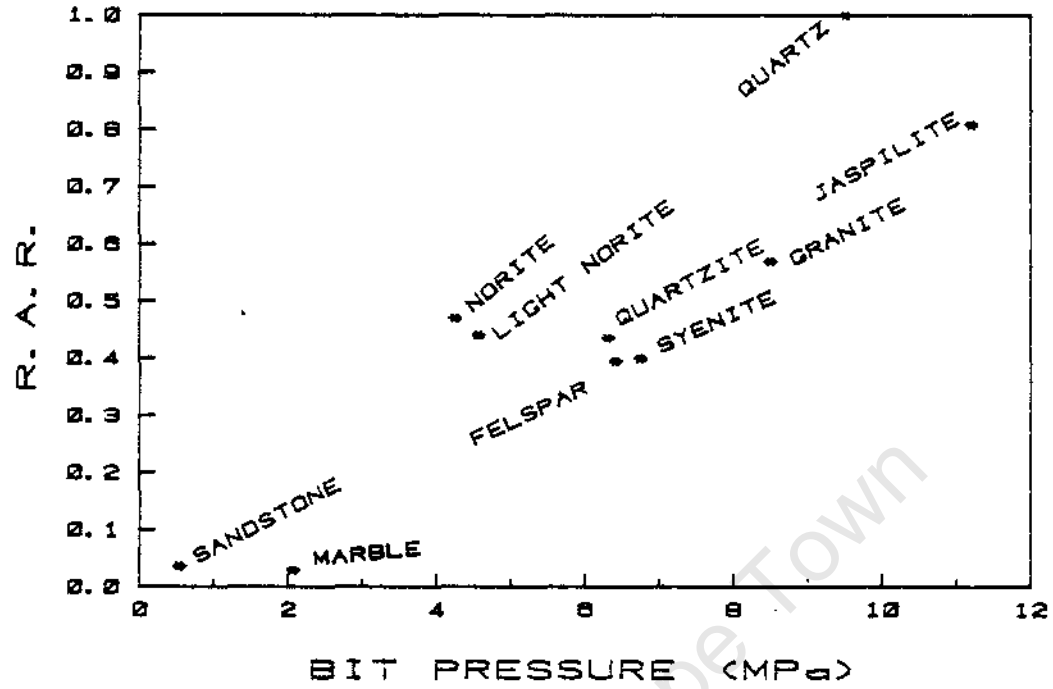

FIGURE 6.10 : Plot of relative abrasion resistance against mean bit pressure for tests drilled in a variety of materials at set rate of advance

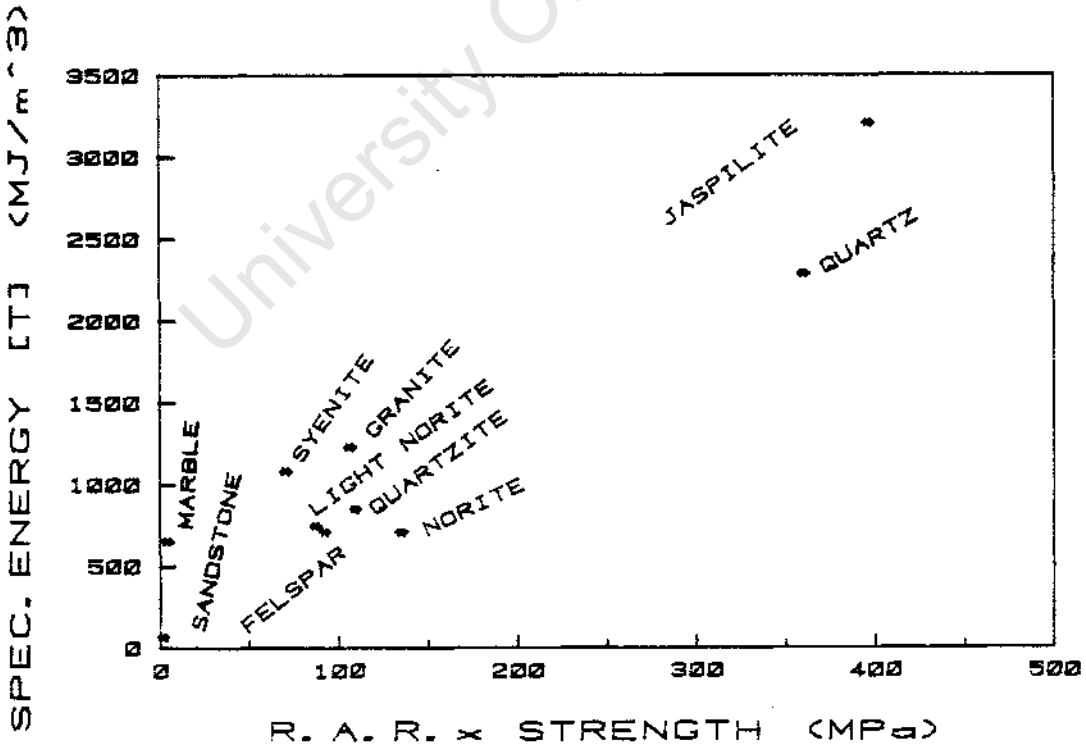

FIGURE 6.11 : Plot of specific energy against the product of relative abrasion resistance and compressive strength for tests drilled in a variety of materials

Uniaxial compressive strength in rocks depends directly on tensile strength and shear strength (Maurer 1967) and the relative abrasion resistance is affected directly by mineralogical composition and the rock fabric or structure. Together the two measured properties represent a variety of relevant rock properties and because they are easily determined could form the basis of a simple index of drillability.

However the relative abrasion resistance and uniaxial compressive strength do not predict the bit wear, which is affected very significantly by rock type. For instance at high bit pressures the wear of the bits drilling sandstone was extreme. This phenomenon is the basis of the bit conditioning procedure and has also been noted by Siribumrungsukha (1980). Such low strength, abrasive rocks with easily excavated grains of hard minerals like quartz are readily drilled but at the cost of high bit wear rates. Any standardised test of rock drillability must take bit wear into consideration (Singh 1973). In the experiments with microbits there was a disappointingly poor correlation between bit wear, in terms of bit mass loss, and the relative, abrasion resistance. Bit wear in impregnated diamond bit drilling did not proceed primarily by direct abrasion but by an erosive mechanism. The shape and size of the particles generated by drilling as well as their hardness affected the rate of bit matrix wear. This was illustrated by the high rate of bit wear associated with drilling single crystal calcite at high rates of penetration (see Fig. 5.71). The large angular cleavage fragments produced by the elevated loads damaged the bit matrix extensively despite the relative ease of abrasion of the soft calcite.

Attempts to predict the drilling performance in terms of measured rock properties have not been very successful (White 1969). The alternative of establishing rock drillability by standardised microbit tests has not yet been generally adopted. It has been shown though that as long as microbit tests are appropriately scaled so that the drilling parameters are similar to those of a full-size bit then the results of microbit tests are representative of equivalent full-scale performance (Singh 1973, Siribumrungsukha 1980). If the rock sample is representative then a laboratory drillability test with a microbit drill takes into account all the variables related to the rock properties. Drillability tests

involving the calculation of an abrasive index (White 1969) or penetration rate and bit wear (Tsoutrelis 1969a) tend to be more successful because they take into account the petrographic characteristics of the rock as well as the effect of bit wear. However, both the above methods do not consider the effect of appropriate bit formulation or geometry in drilling different rock types.

Any standarised bit will be more or less appropriate for drilling a specific rock type and in extreme cases a standarised bit, especially if it is a tungsten carbide bit intended to evaluate the diamond drillability as in the test of Tsoutrelis (1969a), may not be able to drill a given rock at all. It is clear that with different diamond bit formulations a variety of fracture mechanisms can occur in different materials. The limited tests drilled in a variety of rock types in this study have suggested that the relationship between the diamond size and the grain size of some rocks like quartzite can have a considerable effect on performance (see Figs. 5.59 and 5.60). In coarse grained rocks the relatively small diamonds traverse single grains causing predominantly intragranular fracture. If the diamond size approaches or exceeds the grain size of the rock entire grains can be excavated by propagation of intergranular fracture, possibly through weak rock matrix cement. This is certainly what occurred in drilling the sandstone.

To the conclusion of White (1969) that "the only way to determine the drillability of a rock is to drill it" might be added the requirement that it be drilled with a drill bit similar to that which will be used in the rock type in the field. A realistic laboratory drillability test for drilling with impregnated diamond bits would require a range of standardised tests to accommodate the extreme variation in rock properties and drilling response.

Rock drillability depends on a wide variety of rock properties, some of which (eg. the shape and arrangement of the abrasion resistant quartz grains in granites) cannot be measured directly with ease. There is hence no effective alternative to evaluating drillability by drilling the rock. The development of standardised laboratory tests with impregnated diamond microbits will make the determination considerably easier and more economical than testing with full-scale bits on large drilling machines.

CHAPTER 7

CONCLUSIONS

7.1 DRILLING MODE

In this study drilling with impregnated diamond bits took place in one of two modes of performance. Suboptimal drilling in Mode 1 was characterised by decreasing penetration rate or increasing reactive load depending on whether control was under set thrust or set rate of advance respectively. Optimal drilling in Mode 2 was characterised by a steady penetration rate and balanced matrix wear which allowed drilling to proceed for the full useful life of the bit. The transition from Mode 1 to Mode 2 behaviour took place at the thrust level at which the average pressure per exposed diamond was equal to the indentation strength of the material being drilled. This thrust level depended on the rock strength, and the size, number and state of wear of the exposed stones.

The optimum drilling thrust at which the specific energy was at a minimum and the penetration rate at a maximum occurred at and marginally above the thrust required for the transition. This was the equilibrium situation for steady bit performance with balanced diamond and bit wear.

7.2 DIAMOND WEAR

The diamond wear was one of the most informative experimental variables. Diamond wear progressed through the exposure of fresh stones to the development of wear flats by abrasion and thermal ablation in suboptimal drilling. Under optimal conditions cyclical loading of the diamond surface was sufficient to cause a fatigue type failure and resulting microfracture of the diamonds, generating numerous sharp points. At higher stresses more diamonds fractured completely or were lost through higher bit matrix wear.

7.3 PERFORMANCE MODEL

The behaviour of impregnated diamond microbits drilling norite is understandable in terms of a performance model based on the relationships

between drilling performance, diamond wear and rock fracture.' At low bit pressure suboptimal drilling in norite was associated with a low coefficient of friction and correspondingly low transfer of energy between the bit and the rock. Sliding of the diamonds promoted the development of wear flats and low penetration rates. As a result of the low penetration the production of detritus was scant, the bit wear was low, fresh stones were not exposed and the specific energy of drilling was high. With an increase in thrust more optimal drilling was achieved as the transition was approached. This took place at an estimated average pressure per stone of 400 MPa in norite irrespective of diamond size or concentration. At this stage all the exposed diamonds were in contact with the rock, the specific energy was at a minimum and the increased stresses per stone promoted microfracture over wear flat development. At pressures just above the transition drilling was optimal with balanced bit matrix wear, the maintenance of an optimal operating gap between the bit matrix and the rock, and sustained rock fracture by a process predominantly of indentation and shear. At higher pressures the diamonds were wastefully forced deeper into the rock with an increase in coefficient of friction, the clearance between the bit matrix and the rock was reduced, and the rotational speed dropped with a rise in specific energy and no gain in penetration rate. At the highest bit pressures stalling occurred with contact between the bit matrix and the rock, and with excessive fracture of the diamonds due to the high stresses involved.

7.4 EFFECTS OF ALTERING DRILLING PARAMETERS

There was a linear relationship between torque and the power requirement over the entire range of drilling at set thrust; but at set rate of advance this was true only up to the transition. Stalling occurred at the higher thrusts generated by correspondingly higher rates of advance. At set advance per revolution the bit could not ride up over resistant spots of rock and stalling occurred due to lack of power. The effect of reducing rotational speed at set advance per revolution was to move towards less optimal conditions due to the reduced bit pressures. At low speeds and low bit pressures vibration damaged the bit giving rise to wastefully high bit wear rates.

With increasing bit pressure the coarse detritus size increased as the transition was approached and then decreased slightly at higher pressures due to increased regrinding. The proportion of fine material produced was at a minimum at optimal bit pressures. At lower bit pressures low penetration rates and large wear flat areas produced more fine detritus and at higher pressures there was increased regrinding in the reduced operating gap.

7.5 EFFECTS OF ALTERING DIAMOND SIZE AND CONCENTRATION

The diamond size influenced drilling performance and the detritus size strongly. At constant concentration the bits with larger stones required higher bit pressure to drill optimally because of the unavoidably larger surfaces of the exposed stones. At a concentration of 30 there was an optimal diamond size of about 40 mesh at which the lowest bit pressures were necessary. Finer mesh stones required higher pressures for effective operation but achieved higher rates of advance despite the finer detritus produced. The more numerous fine stones sheltered the matrix from erosive wear so the bit wear was low and a larger total diamond surface could develop on the bits.

7.6 EFFECTS OF VARYING ROCK TYPE

A wide variety of rocks and minerals were classified broadly on the basis of their relative abrasion resistance and unaxial compressive strength into three groups with distinct drilling resistance and response. The threshold pressure for penetration as well as the thrust level of the transition rose with increasing resistance to drilling for different rock types. The bit wear mechanism and in some cases the diamond wear mechanism was strongly influenced by the widely differing rock properties which made prediction of penetration rates, diamond wear and bit matrix wear difficult. For instance, the bit opening procedure in soft abrasive sandstone depended on the rapid erosion of the bit matrix by drilling at moderate pressure. Fine mesh bits which would have performed well in norite due to reduced bit wear in this hard rock wore rapidly in drilling a short distance in sandstone because the loose abrasive sandstone grains were large relative to the diamonds. The general rock fracture mechanism is one principally of indentation of the rock by the diamonds and subsequent fracture by shear to free surfaces. The path of fracture is

strongly influenced by the cleavage of the constituent minerals and the bonding between adjacent grains in the rock. The rock properties strongly influence the drilling performance in ways that are not readily predictable. The complexity of the interactions between the drilling variables, and the highly variable and influential effect of the properties of different rocks make it impossible at this stage to establish a model that will predict successfully the performance of impregnated bits drilling in diverse rocks types. Consequently, experimental drilling is unavoidable in testing the drillability of rocks as well as to study the fundamental relationships between drilling parameters and variables. Drilling with microbits has a valid and important part to play in such investigations.

7.7 SUGGESTIONS FOR FURTHER RESEARCH

A number of issues suggest themselves as needing further study with impregnated diamond bits.

i) In the light of the importance of the coefficient of friction and transmission of power to the rock being drilled the effect of different flushing conditions and additives on diamond wear should be studied.

ii) The performance of bits with high strength matrices should be studied in drilling highly resistant rocks like granite to extend the performance model to materials that need to be drilled at bit pressures beyond the capability of the laboratory machine used in this study.

iii) The diamond wear mechanisms, especially the fatigue, of wear flats to develop microfracture, are worthy of further study to determine the precise nature of the strain build up in cyclically stressed diamond surfaces rubbing softer materials.

iv) A consequence of the observations of rock drilling reported here is that the routine testing of rocks by laboratory drilling is necessary to evaluate their resistance to drilling and to test the performance of different bit formulations and designs. Appropriate standard tests that take diamond wear into account still need to be formulated.

REFERENCES

ADAMSON, P.C. 1946. What goes on in the diamond-drill hole? Engineering and Mining Journal 147 (9): 70-3.

ANON. 1985. Metallurgy of diamond tools. Industrial Diamond Review 45 : 248-50.

ATKINS, B.C. 1983. The economic advantages of using manufactured diamond materials in drilling tools within the mining industry. Publication of Speciality Materials Department: 1-4. Ohio: General Electric.

ATKINS, B.C. 1985. Geoset drill diamond - further laboratory and field test developments. Proceedings of the South African Drilling Association Symposium: 156-83. Johannesburg: S.A. Drilling Association.

BAILEY, J.J. & DEAN, R.C. 1967. Rock mechanics and the evolution of improved rock cutting methods. In Fairhurst, C. Failure and breakage of rocks: 396-409. Proceedings of the Eighth Symposium on Rock Mechanics. University of Minnesota.

BAILEY, M.W. & BULLEN, C.J. 1979. Sawing in the stone and civil engineering industries. Industrial Diamond Review 39 : 48-52.

BALL, A. 1972. The propagation of fracture in quartz and quartzite. Research Report No. 7/72: 1-35. Johannesburg: Chamber of Mines.

BALL, A. 1974. The fracture of quartz: 1-24. Research Report No. 49/74. Johannesburg: Chamber of Mines.

BALL, A. & PAYNE, B.W. 1976. Tensile fracture of quartz crystals. Journal of Materials Science 11 : 731-40.

BAMFORD, W.E., BROWN, E.T. & SIRIBUMRUNGSUKHA, B. 1979. Mechanisms of diamond drilling. In Mansell, D.S. & Vasey, G.H. eds Fracture at Work: 7.1-7.25. Fourth Tewksbury Symposium on Fracture. Melbourne: Productivity Promotion Council of Australia.

BARBER, G.A. 1985. Deep observation and sampling of the Earth's continental crust. Proceedings of the South African Drilling Association Symposium: 13-35. Johannesburg: S.A. Drilling Association.

BIENIAWSKI, Z.T. 1967. Mechanism of brittle fracture of rock. Part 1 - Theory of the fracture process. International Journal of Rock Mechanics and Mining Sciences 4 : 395-406.

BLATT, H., MIDDLETON, G. & MURRAY. R. 1972. Origin of sedimentary rocks: 1-643. New Jersey: Prentice Hall.

BOSWELL, M. 1983. Industrial drilling machines. Proceedings of the South African Drilling Association Symposium: S1-S6. Johannesburg: S.A. Drilling Association.

BOWDEN, F.P. & TABOR, D. 1965. Deformation, friction and wear of diamond. In Berman, R. ed Physical properties of diamond: 184-220. Oxford: Clarendon Press.

BRACE, W.F., PAULDING, B.W. & SCHOLTZ, C. 1966. Dilatancy in the fracture of crystalline rocks. Journal of Geophysical Research 71 : 3939-53.

BROOKES, C.A. 1979. Indentation hardness. In Field, J.E. ed The properties of diamond: 383-402. London: Academic Press.

BROOKES, C.A. & HOOPER, R.M. 1982. Wear and hardness of new tool materials. Proceedings of the International Conference towards Improved Performance of Tool Materials: 32-6. London: The Metals Society.

BROOKES, C.A. & LAMBERT, W.A. 1982. Aspects of the indentation hardness of Amborite and Syndite. In Daniel, P. & Caveney, R.J. eds Advances in ultra-hard materials applications - Volume 1: 128-36. Charters: De Beers.

BULLEN, G.J. 1983. The challenge of synthetic versus natural diamond in hard rock drilling. In Daniel, P. & Caveney, R.J. eds Advances in ultra-hard materials application technology - Volume 2: 1-14. Charters: De Beers Industrial Diamond Division.

BULLEN, G.J. 1984. Hard rock drilling - some recent test results. Industrial Diamond Review 44 : 270-5. •

BULLEN, G.J. & BAILEY, M.W. 1979. SDA 100 in hard rock drilling. Industrial Diamond Review 39 : 352-5.

BUSCH, D.M. 1979. Industrial uses of diamond. In Field, J.E. ed The properties of diamond: 595-618. London : Academic Press.

BUSCH, D.M. & HILL, B.S. 1975. Concrete drilling with diamond impregnated bits. Industrial Diamond Review 35 : 172-6.

BUTTNER, A. 1980. Coolant additives in the sawing of granite. Industrial Diamond Review 40 : 332-5.

CHEATHAM, J.B. & GNIRK, P.F. 1967. The mechanics of rock failure associated with drilling at depth. In Fairhurst, C. ed Failure and breakage of rocks: 410-39. Proceedings of the Eighth Symposium on Rock Mechanics. University of Minnesota.

CLARKE, G.B. 1979. Principles of rock drilling. Colorado School of Mines Quarterly 74 : 74-9.

CLARKE, G.B. 1982. Principles of rock drilling and bit wear. Colorado School of Mines Quarterly 77 : 97-104.

COOPER, G.A. 1979. Some observations on environmental effects when diamond drilling. In Hockey, B.J. & Rice, W.R. eds The science of ceramic and surface finishing II: 115-38. National Bureau of Standards Special Publication 562. Washington: United States Government Printing Office.

COOPER, R. & ADAMS, G.R. 1983. Drilling with impregnated bits: a theoretical approach: 1-15. Unpublished manuscript. Krugersdorp: Boart Research Centre.

CROMPTON, D., HIRST, W. & HOWSE, M.G.W. 1973. The wear of diamond. Proceedings of The Royal Society of London, Series A. 333 : 435-54.

CUTHRELL, R.E. 1978. The role of ion aggregates in Rebinder-Westwood environmental effects on wear as monitored by acoustic emission. Journal of Applied Physics 49 : 432-36.

DEER, W.A., HOWIE, R.A. & ZUSSMAN, J. 1972. An introduction to the rock forming minerals: 1-528. London: Longman.

DUNN, K.J. & LEE, M. 1979. The fracture and fatigue of sintered diamond compact. Journal of Materials Science 14 : 882-90.

ENOMOTO, Y. & TABOR, D. 1980. The frictional anisotropy of diamond. Nature 283 : 51-2.

ERTINGSHAUSEN, W. 1985. Wear processes in sawing hard stone. Industrial Diamond Review 45 : 254-8.

EVANS, T. 1976. Diamonds. Contemporary Physics 17 : 45-70.

EVANS, T. 1979. Changes produced by high temperature treatment of diamond. In Field, J.E. ed The properties of diamond: 403-24. London: Academic Press.

FIELD, J.E. 1979. Strength and fracture properties of diamond. In Field, J.E. ed The properties of diamond: 282-324. London: Academic Press.

FIELD, J.E. & FREEMAN, C.J. 1981. Strength and fracture properties of diamond. Philosophical Magazine A. 43 : 595-618.

FISH, B.G. 1961. The basic variables in rotary drilling. Mine and Quarry Engineering 27 (2): 74-81.

FLEMMING, B.W. 1977. Depositional processes in Saldanha Bay and Langebaan Lagoon: 1-215. Stellenbosch: CSIR.

FRANK, F.C. & LAWN, B.R. 1967. On the theory of Hertzian fracture. Proceedings of the Royal Society of London, Series A 299 : 291-306.

FRITH, V. 1983. Quantitative characterisation of the porosity of porcelain using image analysis: 1-185. MSc Thesis. University of Cape Town.

GARNER, N.E. 1967. Cutting action of a single diamond under simulated borehole conditions. Journal of Petroleum Technology **19 :** 937-42.

GLOVER, G.J. 1980. The brittle and plastic response of quartz: 1-393. PhD Thesis. University of Cape Town.

GOODRICH, R.J. 1957. High pressure rotary drilling machines. Bulletin of the School of Mines and Metallurgy, University of Missouri **94 :** 25-45.

GRAHAM, J. 1972. Damage induced by a sliding diamond - an approach to hard rock drilling. Rock Mechanics 4 : 191-202.

'HAGEN, J.T. 1980. Shear deformation under pyramidal indentations in soda-lime glass. Journal of Materials Science **15 :** 1417-24.

HAMMERBACK, L. 1969. Time studies on diamond drilling factors influencing the performance of diamond bits. Proceedings of the Twenty Sixth Annual Meeting of the Canadian Diamond Drilling Association: 6-10. Toronto: Canadian Diamond Drilling Association.

HAMPE, W.R., SIMON, A.B., DECKER, W.E. & LUNDY, J.T. 1973. The moderate depth lunar drill programme - dry diamond drilling success. In Diamonds in industry - rock drilling: 51-63. Charters: De Beers.

HANNINK, R.H.J. & GANE, N. 1974. Transmission studies of Type IIb diamond prepared by ion beam machining. In Sanders, J.V. & Goodchild, D.J. eds Abstracts of Papers Presented at the Eighth International Congress on Electron Microscopy: 488-9. Canberra: The Australian Academy of Science.

HENCH, L.L. & GOULD, R.W. 1971. Characterisation of ceramics: 356. New York: Dekker.

HITCHENER, M.P. & WILKS, J. 1983. The wear of diamond and CBN grits during grinding. In Daniel, P & Caveney, R.J. eds Advances in ultra-hard materials application technology - Volume 2: 100-11. Charters: De Beers.

HOWES, V.R. 1965. Ring cracks of diamond surfaces. In Berman, R. ed Physical properties of diamond: 174-83. Oxford: Clarendon Press.

HUGHES, F.H. 1980. The early history of diamond tools. Industrial Diamond Review **40 :** 405-7.

HURLBUT, C.S. 1971. Dana's manual of mineralogy: 1-579. New York: John Wiley & Sons.

JORIS, A.C.T. & McLAREN, G. 1967. Additives to coolants used in diamond drilling and sawing in Australia. Mining and Minerals Engineering May: 190.

LAWN, B.R. 1968. Hertzian fracture in single crystals with the diamond structure. Journal of Applied Physics 39 : 4828-36.

LAWN, B.R. & SWAIN, M.V. 1975. Microfracture beneath point indentations in brittle solids. Journal of Materials Science 10 : 113-22.

LEVITT, C.M. & NABARRO, F.R.N. 1966. The impact strength of diamond under different rates of strain. Proceedings of The Royal Society of London, Series A. 293 : 259-74.

LIANDER, H. 1980. Diamond synthesis - the true story. Industrial Diamond Review 40 : 412-5.

LUNDBERG, B. 1974. Penetration of rock by conical indenters. International Journal of Rock Mechanics and Mining Sciences & Geomechanics Abstracts 11 : 209-14.

MACMILLAN, N.H., JACKSON, R.E. & WESTWOOD, A.R.C. 1975. Environment enhanced drilling in rock. Proceedings of the Fifteenth Symposium on Rock Mechanics: 469-500. Minneapolis: American Society of Civil Engineers.

MAURER, W.C. 1967. The state of rock mechanics knowledge in drilling. In Fairhurst, C. ed Failure and breakage of rocks: 355-95. Proceedings of the Eighth Symposium on Rock Mechanics. University of Minnesota.

MC WILLIAMS, J.R. 1957. Diamond drilling with impregnated bits. Proceedings of the Seventh Annual Drilling Symposium: 110-3. Minneapolis: University of Minnesota.

MILLER, D.E. 1984. The wear of diamonds in rock drilling with impregnated microbits. Proceedings of the Electron Microscopy Society of Southern Africa 14 : 167-8. Johannesburg: Electron Microscopy Society of Southern Africa.

MILLER, D.E. 1985. Rock drilling with impregnated diamond bits. South African Journal of Science 81 : 582-3.

MILLS, J.J. 1978. Environment-enhanced disintegration of hard rocks. Report No. MML TR 78-10c: 1-44. Martin Marietta Laboratories. Washington: National Science Foundation.

MILLS, J.J. & WESTWOOD, A.R.C. 1977. The wear of diamond-loaded bits: an analytical expression. Industrial Diamond Review 37 : 264-6.

MOLLER, J. & SPINK, K. 1973. The calibration of machines for specific energy experiments. Industrial Diamond Review 33 : 348-52.

MOORE, N.B., WALKER, B.H. & APPL, F.C. 1978. A model of performance and life of diamond drill bits. Journal of Pressure Vessel Technology, Transactions of the ASME 100 : 164-71.

NOEL, R.E.J. 1981. The abrasive-corrosive wear behaviour of metals: 1-158. MSc Thesis. University of Cape Town.

NORLING, R.G. undated. Rock drilling with diamond: 1-6. Charters: De Beers.

PAONE, J. & BRUCE, W.E. 1963. Drillability studies: diamond drilling. Report 6324: 1-26. Washington: United States Bureau of Mines.

PAONE, J., BRUCE, W.E. & VIRCIGLIO, P.R. 1966. Drillability studies. Report 6880: 1-29. Washington: United States Bureau of Mines.

PAONE, J. & MADSON, D. 1966. Drillability studies: impregnated diamond bits. Report 6776: 1-16. Washington: United States Bureau of Mines.

PAONE, J. & TANDANAND, S. 1966. Inelastic deformation of rock under a hemispherical drill bit. Report 6838: 1-26. Washington: United States Bureau of Mines.

PERROTT, C.M. 1979. Tool materials for drilling and mining. Annual Review of Materials Science 9 : 23-50.

PETERSON, J.L. 1976. Diamond drilling model verified in field and laboratory tests. Journal of Petroleum Technology 28 : 213-22.

PFLEIDER, E.P. & BLAKE, R.C. 1953. Research on the cutting action of the diamond drill bit. Mining Engineering **196 :** 187-95.

RAINER, D.M. 1980. De Beers research serves the industry. Industrial Diamond Review **40 :** 408-11.

REID, I.L. 1957. Use of impregnated diamond drill bits by Oliver Iron Division, United States Steel Corporation. Proceedings of the Seventh Annual Drilling Symposium: 105-9. Minneapolis: University of Minnesota.

ROWLANDS, D.C. 1971. Some basic aspects of diamond drilling. Proceedings of the First Australian-New Zealand Conference on Geomechanics - Volume 1: 222-31. Sydney: The Institution of Engineers.

ROWLANDS, D.C. 1972. Single diamond cutting of rock. Industrial Diamond Review 32 : 394-8.

ROWLANDS, D.C. 1975. Rock fracture by diamond drilling: 1-157. Thesis. University of Queensland.

ROWLEY, D.S. & APPL, F.C. 1969. Analysis of surface set diamond bit performance. Society of Petroleum Engineers Journal 9 (3): 301-10.

SASAKI, K., YAMAKADO, N., SHIOHARA, Z. & TOBE, M. 1962. Investigation of diamond core bit boring. Industrial Diamond Review 22 : 178-86.

SAVAGE, **J.** 1985. Deep hole wireline drilling. Proceedings of the South African Drilling Association Symposium: 252-61. Johannesburg: S.A. Drilling Association.

SCOTT, P.J. 1981. The reflex plotters: measurement without photographs. Photogrammetric Record **10 :** 435-46.

SEAL, M. 1981. The friction of diamond. Philosophical Magazine A. **43 :** 587-94.

SELIM, A.A., SCHULTZ, C.W. & STREBIG, K.C. 1969. The effects of additives on impregnated diamond bit performance. Society of Petroleum Engineers Journal 9 (4): 425-33.

SIMON, R. 1963. Energy balance in rock drilling. Society of Petroleum Engineers Journal 3 : 298-306.

SIMON, R. 1967. Rock fragmentation by concentrated loading. In Fairhurst, C. ed Failure and breakage of rocks: 440-60. Proceedings of the Eighth Symposium on Rock Mechanics. University of Minnesota.

SINGH, D.P. 1973. The drillability of rocks. Mineral Science and Engineering 5 : 255-60.

SIRIBUMRUNGSUKHA, B. 1980. Investigation into diamond drilling and rock drillability: microscale and fullscale impregnated bits: 1-103. MSc Thesis. University of Melbourne.

SPINK, K. 1972. The nature of the diamond drilling process. Industrial Diamond Review 32 : 230-42.

SPRUNT, E.S. & BRACE, W.F. 1974. Direct observation of microcavities in crystalline rocks. International Journal of Rock Mechanics and Mining Sciences & Geomechanics Abstracts 11 : 139-50.

STOKES, R.J. & VALENTINE, T.J. 1984. Wear mechanisms of ABN abrasive. Industrial Diamond Review 44 : 34-44.

STREBIG, K.C., SCHULTZ, C.W. & SELIM, A.A. 1969. How to effect a cost reduction in diamond drilling. Mining Engineering 21 (10): 73-5.

STREBIG, K.C., SELIM, A.A. & SCHULTZ, C.W. 1971. Effect of organic additives on impregnated diamond drilling. Report No. 7494: 1-31. Washington: United States Bureau of Mines.'

SVENDSEN, W. 1985. Deep exploration - a new challenge. Proceedings of the South African Drilling Association Symposium: 36-44. Johannesburg: S.A. Drilling Association.

TABOR, D. 1979. Adhesion and friction. In Field, J.E. ed The properties of diamond: 326-50. London: Academic Press.

TAPPONNIER, P. & BRACE, W.F. 1976. Development of stress-induced microcracks in Westerley Granite. International Journal of Rock Mechanics and Mining Sciences & Geomechanics Abstracts **13 :** 103-12.

TEALE, R. 1965. The concept of specific energy in rock drilling. International Journal of Rock Mechanics and Mining Sciences 2 : 57-73.

TOMLINSON, P.N., PIPKIN, N.J. & LAMMER, A. 1985. High performance drilling with SYNDAX 3. Proceedings of the South African Drilling Association Symposium: 140-155. Johannesburg: S.A. Drilling Association.

TSOUTRELIS, C.E. 1969(a). Determination of rock drillability in diamond drilling. Society of Mining Engineers, Transactions of the AIME 244 : 364-9.

TSOUTRELIS, C.E. 1969(b). Determination of the compressive strength of rock in situ or in test blocks using a diamond drill. International Journal of Rock Mechanics and Mining Science 6 : 311-21.

WANG, J.K. & LEHNHOFF, T.F. 1976. Bit penetration into rock - a finite element study. International Journal of Rock Mechanics and Mining Sciences & Geomechanics Abstracts **13 :** 11-6.

WAPLER, H., SPOONER, T.A. & BALFOUR, A.M. 1980. Diamond coatings for increased wear resistance. Tribology International February: 21-4.

WELCH, R.H. 1982. The role of synthetic diamonds in drilling. South African Mining and Engineering Journal January: 26-35.

WESTWOOD, A.R.C. & MILLS, J.J. 1977. Application of chemomechanical effects to fracture-dependent industrial processes. In Latanision, R.M. & Fourie, J.T. eds Surface effects in crystal plasticity: 835-62. Nato Advanced Study Institute Series. Leyden: Noordhoff.

WHITE, C.G. 1969. A rock drillability index. Quarterly of the Colorado School of Mines 64 (2): 1-68.

WILKS, E.M. & WILKS, J. 1965. The hardness and wear of diamond during grinding and polishing. In Berman, R. ed Physical properties of diamond: 221-50. Oxford: Clarendon Press.

WILKS, E.M. & WILKS, J. 1982. The abrasion resistance of natural and synthetic diamond. Wear 81 : 329-46.

WILKS, E.M. & WILKS, J. 1984. The abrasion resistance of brown diamonds. Industrial Diamond Review 44 : 82-5.

WILKS, J. & WILKS, E.M. 1979. Abrasion and wear of diamond. In Field, J.E. ed The properties of diamond. 352-82. London: Academic Press.

WILSON, D.A.P. 1941. Impregnated drill bits. South African Mining and Engineering Journal 52 : 605.

WOODS, G.S. 1971. Electron microscope observations of stacking faults and microtwins in synthetic diamond. Philosophical Magazine A 23 : 473-84.

WOODS, G.S. & LANG, A.R. 1975. Cathodoluminescence, optical absorption and X-ray topographic studies of synthetic diamonds. Journal of Crystal Growth 28 : 215-26.

WONG, C.J. 1981. Fracture and wear of diamond cutting tools. Journal of Engineering Materials and Technology, Transaction of the ASME 103 : 341-5.

APPENDIX 1 - ROCK FRACTURE MECHANISMS RELEVANT TO DIAMOND DRILLING

A number of mechanisms have been treated theoretically in isolation in the literature and although they act simultaneously to varying degrees in the real drilling situation they will be described here separately.

HERTZIAN CRACKING

A hard spherical indenter under increasing load on the face of a brittle solid (like a silicate mineral in a rock) produces an elastic indentation and then a shallow ring crack at a critical load proportional to the radius of the indenter. This dependency is known as Auerbach's Law. The crack can extend to form a typical Hertzian cone crack in the brittle solid if the stress reaches a suitable level (Frank & Lawn 1967, Lawn 1968). Herzian cracks have been studied extensively in diamond (Field & Freeman 1981) and observed in sliding indenter studies in glass and quartz (Graham 1972, Glover 1980). There is a lower limit to the indenter size for which Auerbach's Law is valid. For very small indenters the Hertz stress formulae are not valid because of the possible plastic flow produced by the high stress under a small indenter even in a brittle solid (Frank & Lawn 1967). It is doubtful if Auerbach's Law can be expected to apply as a fracture criterion in drilling with the diamond sizes used in impregnated bit drilling because the radius of curvature of the diamond asperities involved in drilling may well be below the lower limit. This was estimated by Rowlands (1975) to be 0,535 mm for a diamond indenter on glass.

CRUSHING

All rocks are highly imperfect, complex non-homogeneous materials containing minerals with widely differing strehgth properties. They are frequently porous, with porosities ranging up to 20 percent in some sedimentary rocks. Even dense crystalline rocks like granite contain microcavities accounting for up to one percent of the volume (Sprunt & Brace 1974). The presence of these cavities as well as healed fissures, grain boundaries and different degrees of compliance between adjacent minerals allow cracks to form under compressive stresses less than 0,75 of the peak stress (Tapponier & Brace 1976). Because

of the porosity even in apparently dense rock the axial thrust causes crushing to take place locally under an indenter (Simon 1967, Rowlands 1975). The crushing mechanism is brittle fracture in triaxial compression. This has been described in detail by Bieniawski (1967) who identified five stages prior to maximum deformation or rupture of norite under triaxial compression.

1) Under initial loading suitably orientated pre-existing cracks close.

2) Linear elastic deformation then takes place culminating in fracture initiation.

3) Stable fracture propagation proceeds until a critical energy release rate is reached.

4) Unstable fracture propagation rapidly leads to strength failure at the maximum stress.

5) Forking and coalescence of cracks accompanies the disintegration of the material into a crushed (but still load bearing) system.

Dilantancy due to grain boundary loosening, frictional sliding of grains and the opening of cracks subsequent to purely elastic compression at low stress has been described by Brace, Poulding & Scholtz (1966). The volume change of up to twice the elastic volume change that would have occurred if the rock were purely elastic may not only apparently strengthen the rock but also contribute to raising the overall stress in the adjacent unfractured rock (ibid). A minimum load for penetration, or indentation has been observed in a number of other studies (Paone & Tandanand 1966, Rowlands 1975, Siribumrungsukha 1980). Below this threshold the rock deformation is elastic and energy is primarily dissipated as frictional heating.

If the pressure threshold for crushing is exceeded then some crushing takes place. For a given indenter the depth of indentation can be expected to be linear with load (Paone & Tandanand 1966) up to a maximum defined by the protrusion of the stone. The volume of the crushing beneath the indenter depends on the indenter shape. A finite element simulation by Wang & Lehnhoff (1976) predicted a larger volume in compression beneath a blunt indenter than under a sharp wedge. This was in agreement with both the theoretical and

experimental observations made by Lundberg (1974) that indenters with large apical angles caused essentially only crushing as opposed to lateral chipping in granite. Blunt indenters require high loads to exceed the rock strength, and they promote crushing rather than chipping.

TENSILE FAILURE

If a sharp indenter with an included angle less than about 90° penetrates a rock vertical tensile cracks appear beneath the crushed zone (Simon 1967, Rowlands 1971). In the computer simulation of Wang and Lehnhoff (1976) a median tensile crack started to, propagate before the development of chips to the side of a wedge shaped indenter. The wedge geometry is responsible for imparting tensile stresses to the rock which cause cracks similar to the familiar median vent and radial cracks obtained by static indentation of brittle solids by Vickers diamond pyramids. The propagation of the tensile radial and median vent cracks in a relatively coarse grained polycrystalline material like a rock is complicated by interaction of these cracks with the grain boundaries and pre-existing flaws as well as by the cleavage of individual mineral grains.

SHEAR FAILURE

Outside the area of contact of the indenter and rock the mathematical solution of a point-load, or line-load model is applicable, assuming shear failure according to the Mohr-Coulomb criteria (Simon 1967). This theory predicts a maximum shear trajectory which would produce a lenticular chip by shear failure along a logarithmic spiral path of maximum shear (see Fig. A1.1). Large fragments produced by experimental carbide bits cutting in a variety of rock types have been shown to be lenticular in shape (Goodrich 1957, Fish 1961) and the fracture paths similar to logarithmic spirals (Maurer 1967).

In reality the particular path followed by a shear crack will be influenced by the logarithmic trajectory predicted by the Mohr-Coulomb theory but also by the location and orientation of flaws and cleavage traces with which it might interact (Simon 1967). A readily sheared rock matrix like a weak cement in a sandstone might cause deviation of the crack around grains, essentially excluding them from the shear fracture process (Rowlands 1971).

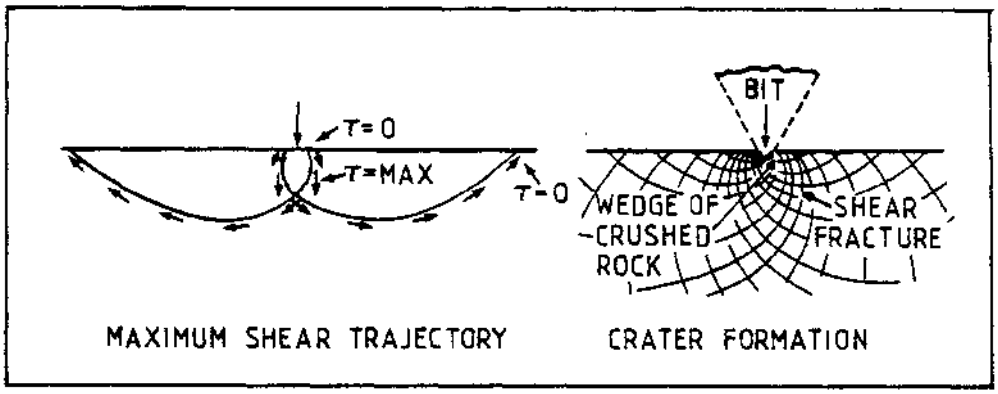

FIGURE A1.1 : Shear failure trajectories predicted using the Mohr-Coulomb criterion (after Maurer 1967)

So far the effects of rotation have not been considered. Rotational translation complicates the fracture mechanisms by superimposing them on each other and creating the possibility of new modes of failure.

HERTZIAN FRACTURE

A diamond indenter sliding on the surface of a brittle solid under load can produce a series of Hertzian cone cracks imposed in sequence upon each other. Graham (1972) noted the complexity and the depth of cracks produced in glass at relatively low loads (see Fig. 2.10) and described a variety of cracks; some extending ahead of the indenter, others looping back and some extending horizontally in the material from the bottoms of reverse cracks. Glover (1980) found that quartz could be cut by delamination if the partial cone cracks were suppressed by keeping the friction between the indenter and work piece low. This could only be achieved in drilling if the bit pressure were very low and the diamonds had relatively large radii. When this is the case low specific energies of drilling can be achieved in drilling brittle rock (Spink 1972). However, the penetration rate cannot be economic and as the diamond wear flat area increases it would be increasingly difficult to maintain penetration. There is no evidence to suggest that drilling can be maintained in this mode for any realistic length of time. Graham (1972) found that smaller indenters tended to crush silicate glass material in the track

creating very fine chips. The formation of "chatter cracks" was a random process and the threshold load could not be determined reliably.

CRUSHING

With rotation some lateral impact and crushing might occur (Pfleider & Blake 1953, Rowlands 1971). The torque on the bit is thought to cause an indenting diamond to stress the rock ahead of it; elastic straining is followed by sudden failure and the indenter accelerates into a freshly exposed face of material (Fig. A1.2). This may cause some crushing as in the drag bit model (Fish 1961, Maurer 1967). If impact is severe then it could require considerable elastic cushioning of the diamonds by the bit matrix to prevent the brittle stones from shattering.

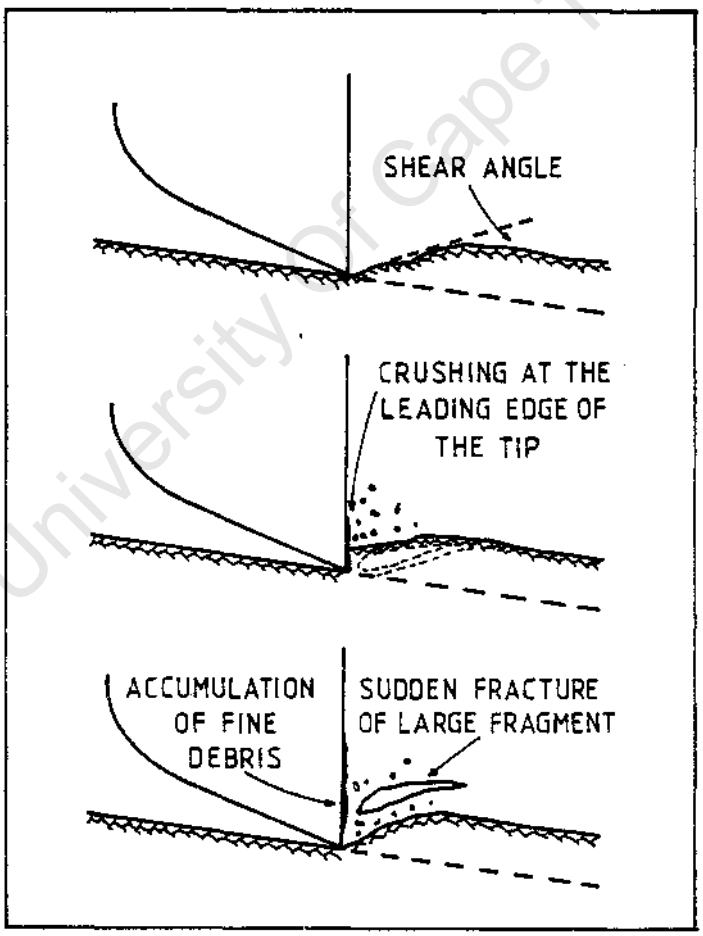

FIGURE A1.2 : Representation of the probable sequence of events at the drill tip during cutting (after Fish 1961)

TENSILE FRACTURE

Tensile fractures can be expected in the elastically stressed region in the wake of each diamond (Rowlands 1975) especially in association with suitably orientated cleavage planes in the rock. In addition tensile fractures may be expected in material ahead of the diamonds if an asperity of rock is impacted by a moving diamond or if a fragment is forced like a sharp indenter into the base of a protuberance. This is similar to the coal cutting model of Evans (Maurer 1967).

SHEAR FAILURE

The predominant mode of failure of a brittle material subject to a rotating indenter is shear (Paone & Tandanand 1966). The mechanism is illustrated in Fig. A1.3. In addition to shearing ahead of the diamond, the entrapment of fragments between the diamonds and the ridges of rock protruding between the tracks of the individual stones stresses the ridge. Material consequently breaks by shear to the free face (Pfleider & Blake 1953, Rowlands 1971, 1975).

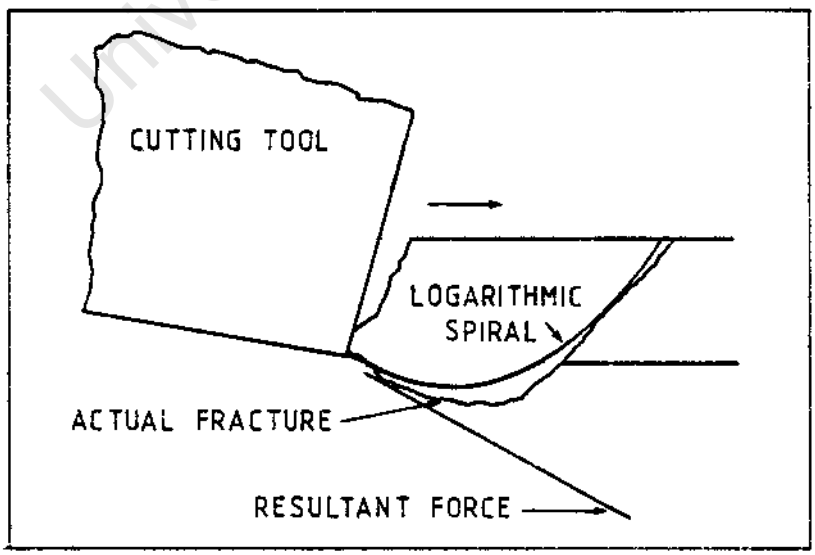

FIGURE A1.3 : Drag bit chip formation (after Maurer 1967)

GRINDING

Secondary crushing or grinding takes place between the diamonds and the rock. Unless perfect flushing is achieved (which is not realistically possible) detritus is present to be trapped beneath the stones, crushed still finer, or be compressed into mashed flakes of rock flour (Pfleider & Blake 1953). Garner (1967) found up to 50 percent by volume of the groove created by the passage of a diamond to be clogged with crushed detritus. Large accumulations of caked material can obstruct the indentation of the diamonds into the rock (Cheatham & Gnirk 1967). In the extreme case the diamonds ride on the sintered cake and penetration ceases, with the heat generated by friction leading to seizure.

EXCAVATION

In addition to causing fracture the rotation of the diamonds causes them to act as mechanical scoops, plucking out loose particles from the floor of the track and excavating fractured and ground material to be flushed away in the slurry. In some very friable rocks the energy required to propagate cracks through the rock matrix is so low that this excavation mechanism may be the one predominantly responsible for the removal of material. Multiple passes of a diamond over the same track complicates the balance of mechanisms still further. Rowlands (1972) found that a second cut removed less material at the same load than the initial one did.

LATERAL CRACKING ON PRESSURE UNLOADING

The irreversibly deformed zone beneath a hard indenter in a brittle solid gives rise to a residual stress in the material on unloading (Lawn & Swain 1975). These residual stresses are responsible on unloading for the propagation of lateral cracks (Hagan 1980) which can travel to the surface and release a chip of substantial volume. At least these lateral cracks contribute to the fracture in the bulk of the material being drilled.

APPENDIX 2 - COMPUTER PROGRAMS

Program "A"

"A" controls the data-logger, instructs it to read the instrument output voltages and stores the resulting data. It will be described in sections designated by their starting and finishing line numbers.

10 - 240 : Initializing section including dimensioning of variables and data arrays, and the determination of instrument calibration functions described in Chapter 3.

250 - 320 : Setting the date and time on the data-logger and running the drill for ten minutes to warm up.

330 - 410 : Taking twenty-four readings of the wattmeter with the drill running freely for calibration of power losses in the gears and the water swivel seals.

420 - 640 : Internal construction of a table like Table 3.1 using data from Table 3.1 for "total motor losses" and the newly measured value for "drill losses" to calculate a new calibration equation for the wattmeter. The coefficients of the best fit straight line to this data are stored for later use.

650 - 760 : Request for test parameters; rock type, bit description, set operation parameter, and expected test duration (to set the sampling rate).

770 - 800 : Instruction to lower the bit onto the reference steel cylinder to establish initial bit height by measuring and storing the mean of ten readings of the position of the LVDT: followed by instructions to insert the rock specimen.

810 - 900 : Measurement of zero readings on all instrument channels except the LVDT by taking mean of ten readings on each channel. Zero readings are stored for later use.

910 - 930 : Request for desired bit pressure (if the test is to be at set load force), calculation of required voltage output displayed on data-logger, lowering the bit onto the rock and adjusting the weight of the water bottle accordingly to produce the required load cell voltage output.

940 - 960 : The position of the bit on the top of the specimen is measured by sampling the LVDT output and storing 'the mean of ten readings.

970 - 990 : Instruction to turn on the water supply and the drilling machine. Monitoring the output of the wattmeter rapidly to sense the starting of the machine.

1000 - 1070 : Selection of appropriate timer and beginning of sampling routine. This consists of a long string sent to the data-logger which sets the digital voltmeter, an internal clock, establishes which channels to read and requests the values to be stored in an internal buffer.

1080 - 1100 : On request from the computer the channels are sampled sequentially in very rapid succession and the data stored in the buffer, then the buffer is read by the computer and the contents sorted into a data storage matrix. The value for the torque meter is tested. If overrange the test terminates with an alarm to prevent damage to the delicate miniature load cell. Switching off the drill also terminates the test.

1100 - 1150 : On completion of the test (six hundred data sets accumulated or early termination) the timers are switched off and the test duration measured from the internal clock.

1160 - 1170 : A reading of the position of the bit at the bottom of the drilled hole is taken by calculating the mean of ten readings of the LVDT output.

1180 - 1240 : All readings in the data matrix are corrected for non-zero initial values.

1250 - 1270 : The total test length is calculated and displayed with an option to drill another hole if the test is not complete. The data from successive holes within one test are concatenated to provide a continuous record as if it were one long test.

1280 - 1340 : The date and time are read from the data-logger and the bit lowered onto the steel reference cylinder again so that an estimate of linear bit wear can be calculated from the difference between this reading of the LVDT position and the one measured at the beginning of the test. This bit wear value is displayed with the total test duration and the sampling rate used.

1350 - 1500: Data storage starts with a listing of existing files on disc to avoid duplication. The creation of a new file and writing of

the data to disc from the matrix along with the test parameters follows. There is an option to create duplicate storage.

1510 - 1610 : A print-out of preliminary results on the HP85's internal printer consists of a listing of the test parameters, duration, length of test, and preliminary results.

1620 - 1870 : Some manipulation of the data to remove spurious terminal zeros and unexpected over-range readings precedes calculation of mean and average values for drilling variables using the calibration formulae described in Chapter 3 and the calculation formulae listed below. The results are printed as a temporary record before the data is subjected to program "B".

Formuli used in computation of drilling variables

$$\text{MEAN POWER OUTPUT (W)} = \frac{\Sigma(\text{NET POWER OUTPUT})}{N}$$

$$\text{MEAN BIT PRESSURE (MPa)} = \frac{\Sigma(\text{BIT LOAD})/\text{BIT FACE PAD AREA}}{N}$$

$$\text{MEAN BIT SPEED } (ms^{-1}) = \frac{\Sigma(\text{RPM})/60 \times \pi \times \text{BIT DIAMETER}}{N}$$

$$\text{MEAN BIT TORQUE (Nm)} = \frac{\Sigma(\text{TORQUE})}{N}$$

$$\text{MEAN ADVANCE/REV.(mm/rev)} = \frac{\Sigma(P2-P1)/Z \;/\; (\text{RPM})/60}{N}$$

$$\text{AVERAGE SPECIFIC ENERGY [W] } (MJm^{-3}) = \frac{\Sigma(\text{NET POWER OUTPUT}) \times Z}{\Sigma(P2-P1) \times \text{HOLE AREA}}$$

$$\text{AVERAGE SPECIFIC ENERGY [T] } (MJm^{-3}) = \frac{\frac{\Sigma(\text{TORQUE})}{N} \times \frac{\Sigma(\text{RPM})/N}{2\pi \times \text{BIT CIRCUMFERENCE}}}{\frac{\Sigma(P2-P1)}{N} \times 1/Z \times \text{HOLE AREA}}$$

$$\text{SPECIFIC BIT WEAR (mm/m)} = \frac{\text{LINEAR BIT WEAR}}{\text{TOTAL DISTANCE DRILLED}}$$

where: N = number of data sets used in calculation
P1 & P2 = two successive penetration readings
Z = sampling interval (1, 2 or 3 seconds)

Program "B"

"B" produces result plots for each test (eg. Figs. 5.13 & 5.24). It uses exactly the same computational routine as the end of program "A" to produce mean and average values of the drilling variables from the raw data stored on disc. The converted data is then used to produce plots of relevant variables against drilling distance or drilling time as appropriate. The spikiness of the plots is due to switching the drill on and off at the beginning and end of each test-run. The smoothing routine used for these plots intentionally does not remove the evidence of these episodes so as to avoid distorting the visual record unrealistically,.

Program "C"

"C" produces a table of unnormalised, or of standardised results (eg. Appendix 5) for a given test series. The raw data is read off disc, subjected to the standard computational routine common to the two previous programs, with the exception that if the data is to be normalised only the number of data sets corresponding to the length of the shortest test in the test series is read.

Program "D"

"D" reads the tabulated results produced and stored by "C" and collates them into summary results tables. These are a record of all the numerical results and can be found in Appendix 4.

PROGRAM LISTING - PROGRAM "A"

```
10 ! "A" - DRILLING TEST
20 ! THIS PROGRAM CONTROLS THE DATA LOGGER TO COLL
ECT 500 SETS OF DATA FROM THE DRILLING MACHINE
30 ! ROTATIONAL VELOCITY NOMINALLY 3500 rpm
40 ! THREE SAMPLING RATES CAN BE SELECTED
50 ! INITIALIZING VARIABLES
60 GOSUB 120 ! INITIALIZING AND SETTING CLOCK
70 GOSUB 310 ! WATTMETER CALIBRATION
80 GOSUB 650 ! DRILLING TEST
90 GOSUB 1380 ! DATA STORAGE
100 GOSUB 1510 ! PRINT RESULTS
110 END
120 CLEAR
130 OPTION BASE 1
140 COM SHORT X(500,5),B$(90),D$(14),M$(7),R$(20),
V$(30),A1,B1,F,N,P,T,W,Z
150 ! INSTRUMENT OUTPUT CONVERSION FORMULI
160 DEF FNF1(A) = A#199.8-.423 ! (W)
170 DEF FNF2(A) = A#1000#.3332/8.76#9.8/1000000 !
 (MN)
180 DEF FNF3(A) = A#907.7 ! (rpm)
190 DEF FNF4(A) = A#9.8#.26/4.817/.1856 ! (Nm)
200 DEF FNF5(A) = A#29.3 ! (mm)
210 DIM A$(60),T$(10),Y(24,4)
220 INTEGER M,O,Q
230 SHORT A,C1,C2,C3,C4,P1,P2,P3,P4
240 A1,B1,S1,S2,S3,S4,W=0 @ N=24
250 ! SETTING TIME
260 OUTPUT 709 ;"TD" @ ENTER 709 ; D$@ IF VAL(D$(7
,8))#0 THEN 290
270 DISP "SET DATE AND TIME USING :MMDDHHMMSS" @ B
EEP
280 INPUT D$@ OUTPUT 709 ;"TD"&D$
290 DISP "DATE AND TIME ARE SET ON HP3497A"
300 RETURN
310 ! WATTMETER CALIBRATION
320 DISP "SWITCH ON POWER AND RUN DRILL    FOR 10
MINUTES  THEN PRESS CONTINUE"
330 FOR I=1 TO 24
340 BEEP @ PAUSE
350 CLEAR 709
360 FOR I=1 TO 20
370 OUTPUT 709 ;"AC1SD1"
380 ENTER 709 ; A
390 W=W+A
400 NEXT I
410 DISP "SWITCH OFF DRILL" @ BEEP @ BEEP @ BEEP
420 W=INT(W/20#200+.5) ! WATTS
430 FOR I=1 TO 24
440 READ Y
450 DATA 100,102,105,109,115,122,130,140,148,160,1
73,188
460 DATA 203,220,235,255,270,290,310,340,370,386,4
06,450
470 Y(I,1)=Y#50
480 Y(I,2)=Y
490 Y(I,3)=Y(I,1)*Y(I,2)
500 Y(I,4)=Y(I,1)-W
510 IF Y(I,4)<0 THEN 520 ELSE 530
520 Y(I,4)=0 @ N=N-1
530 NEXT I
540 FOR I=25-N TO 24
550 S1=S1+Y(I,3)
560 S2=S2+Y(I,3)^2
570 S3=S3+Y(I,4)
580 S4=S4+Y(I,3)#Y(I,4)
590 NEXT I
600 A1=(S4-S1#S3/N)/(S2-S1^2/N)
610 B1=S3/N-A1#(S1/N)
620 DISP " OUTPUT=";INT(A1#10000+.5)/10000;"#INPUT
";INT(B1+.5)
630 DISP @ DISP "CALIBRATION OF POWER LOSSES COMPL
ETE"
640 RETURN
650 ! DRILLING TEST
660 A,C1,C2,C3,C4,N,O,P,P1,P2,P3,P4,T,W,Z=0 @ M=1
670 F=.000146 ! BIT PAD FACE AREA IN m^2
680 DISP "TEST PARAMETERS" @ BEEP
690 DISP "ROCK TYPE" @ INPUT R$
700 DISP "BIT NO." @ INPUT B$
710 DISP "MESH SIZE (eg.40/50)" @ INPUT B1$
720 B$=B$&" - CuSn 80/20 MATRIX - "&B1$&" MESH - C
ONC. 30"
730 DISP "SET PARAMETER" @ INPUT V$
740 DISP "ESTIMATE DURATION OF TEST AND    INPUT A
PPROPRIATE CODE"
750 DISP "MINUTES","CODE"
760 DISP "10","1" @ DISP "20","2" @ DISP "30","3"
@ BEEP @ INPUT I
770 DISP "LOWER BIT ONTO STEEL CYLINDER,   CHECK L
VDT, THEN PRESS CONTINUE" @ BEEP @ PAUSE
780 CLEAR 709 @ FOR I=1 TO 10 @ OUTPUT 709 ;"AC5SD
1" @ ENTER 709 ; A@ P1=P1+A @ NEXT I
790 DISP "INSERT ROCK SPECIMEN, UNCLAMP"
800 DISP " TURNTABLE, THEN PRESS CONTINUE" @ BEEP
@ PAUSE
810 CLEAR 709 @ FOR I=1 TO 10 @ OUTPUT 709 ;"AC1SD
1" @ ENTER 709 ; A@ C1=C1+A @ NEXT I
820 C1=INT(C1/10#1000+.5)/1000
830 CLEAR 709 @ FOR I=1 TO 10 @ OUTPUT 709 ;"AC2SD
1" @ ENTER 709 ; A@ C2=C2+A @ NEXT I
840 C2=INT(C2/10#1000+.5)/1000
850 CLEAR 709 @ FOR I=1 TO 10 @ OUTPUT 709 ;"AC3SD
1" @ ENTER 709 ; A@ C3=C3+A @ NEXT I
860 C3=INT(C3/10#1000+.5)/1000
870 DISP "CHANNEL 3 ZERO = ";C3 @ DISP @ DISP "IS
THIS VALUE REASONABLE? (Y/N)" @ BEEP
880 INPUT Y$@ IF Y$(1,1)="Y" THEN 890
890 CLEAR 709 @ FOR I=1 TO 10 @ OUTPUT 709 ;"AC4SD
1" @ ENTER 709 ; A@ C4=C4+A @ NEXT I
900 C4=INT(C4/10#1000+.5)/1000
910 CLEAR @ DISP "ENTER THE DESIRED BIT PRESSURE I
N MPa" @ BEEP @ INPUT A
920 DISP " DATA LOGGER READING - ";INT((A/(FNF2(1)
/F)+C3)#100000+.5)/100000
930 DISP "LOWER THE BIT TO SET THE LOAD    THEN PR
ESS CONTINUE" @ BEEP
940 CLEAR 709 @ OUTPUT 709 ;"AC2" @ PAUSE
950 CLEAR 709 @ FOR I=1 TO 10 @ OUTPUT 709 ;"AC5SD
1" @ ENTER 709 ; A@ P3=P3+A @ NEXT I
960 P3=INT(P3/10#1000+.5)/1000
970 DISP "TURN ON WATER AND THE MACHINE" @ BEEP
```

PROGRAM LISTING - PROGRAM "A" (Continued)

```
980 CLEAR 709 @ OUTPUT 709 ;"ARVR3V04VT1SD1SD0"
990 OUTPUT 709 ;"AC1" @ ENTER 709 ; A@ IF A<=.01 T
HEN 990
1000 CLEAR @ DISP "TEST RUNNING"
1010 ON Z GOTO 1020,1030,1040
1020 ON TIMER# 1,1000 GOTO 1070 @ GOTO 1050
1030 ON TIMER# 2,2000 GOTO 1070 @ GOTO 1050
1040 ON TIMER# 3,3000 GOTO 1070 @ GOTO 1050
1050 OUTPUT 709 ;;"ARAC1AE2AF1AL5SD0VA0VD4VN5VR5VS
1TE2"
1060 GOTO 1060
1070 IF N=600 THEN 1110
1080 N=N+1 @ OUTPUT 709 ;"VTJSV"&VAL$(N)&"VS" @ EN
TER 709 ; A$
1090 FOR J=1 TO 60 STEP 12 @ X(N,(J+11)/12)=VAL(A$
[J,J+10]) @ NEXT J @ IF X(N,4)>3.5 THEN 1110
1100 IF X(N,1)>.5 THEN 1060
1110 OFF TIMER# 1
1120 OFF TIMER# 2
1130 OFF TIMER# 3
1140 OUTPUT 709 ;"TE" @ ENTER 709 ; T$@ OUTPUT 709
 ;"TE0" @ T=VAL(T$)+T @ P4=0
1150 CLEAR @ DISP "CALCULATING - WAIT!"
1160 CLEAR 709 @ FOR I=1 TO 10 @ OUTPUT 709 ;"ACSS
01" @ ENTER 709 ; A@ P4=P4+A @ NEXT I
1170 P4=INT(P4/10*1000+.5)/1000
1180 FOR I=M TO N
1190 X(I,1)=X(I,1)-C1
1200 X(I,2)=X(I,2)-C2
1210 X(I,3)=X(I,3)-C3
1220 X(I,4)=X(I,4)-C4
1230 X(I,5)=X(I,5)-P3+P
1240 NEXT I @ P=P+ABS(P4-P3) @ M=N+1 @ P3=0
1250 ! TERMINATE TEST AND DISPLAY RESULTS
1260 DISP "DISTANCE DRILLED=";INT(FNF5(P)+.5);" mm
"
1270 DISP "IS THIS THE LAST TEST RUN?" @ BEEP @ IN
PUT L$@ IF L$[1,1]="N" THEN 930
1280 OUTPUT 709 ;"ARTO" @ ENTER 709 ; D$
1290 DISP "CLAMP TURNTABLE, LOWER BIT ONTO  STEEL
CYLINDER, PRESS CONTINUE" @ BEEP @ PAUSE
1300 CLEAR 709 @ FOR I=1 TO 10 @ OUTPUT 709 ;"ACSS
01" @ ENTER 709 ; A@ P2=P2+A @ NEXT I
1310 W=ABS(P2/10-P1/10)
1320 CLEAR @ DISP "BIT WEAR - ";INT(FNF5(W)*100+.5
)/100;" mm"
1330 DISP "TEST DURATION - ";INT(T/60);"min ";RMD(
T,60);"sec"
1340 DISP "SAMPLING INTERVAL - ";Z;"s"
1350 DISP @ DISP "DO YOU WANT TO STORE THE DATA"
1360 INPUT N$@ IF N$[1,1]="N" THEN 1520
1370 RETURN
1380 ! STORE RESULTS
1390 DISP "LOAD DATA DISC THEN PRESS        CONTIN
UE" @ BEEP @ PAUSE
1400 CAT ":,DATA" @ DISP "CHECK FILE NAMES THEN INP
UT NEW  TEST NUMBER" @ BEEP @ INPUT M$
1410 ON ERROR GOTO 1870
1420 O=N*5*8+2500 @ CREATE M$&".DATA",1,O @ ASSIGN
@ 1 TO M$&".DATA" @ OFF ERROR
1430 CLEAR @ DISP "WRITING TO DISC - WAIT!"
1440 PRINT@ 1 ; B$,D$,R$,V$,A1,B1,F,N,P,T,M,Z
1450 FOR I=1 TO N @ FOR K=1 TO 5 @ PRINT@ 1 ; X(I,
K) @ NEXT K @ NEXT I
1460 ASSIGN@ 1 TO * @ SECURE M$&".DATA","DM",2
1470 DISP "STORAGE COMPLETE"
1480 DISP "DO YOU WANT TO CREATE DUPLICATE STORAGE
 OF THE DATA" @ BEEP @ INPUT A$
1490 IF A$[1,1]="Y" THEN 1390
1500 RETURN
1510 ! PRINTING RESULTS
1520 A,Z1,Z2,Z3,Z4,Z5,Z6,Z7=0
1530 F2=.000201 ! HOLE CROSS-SECTIONAL AREA WITH 2
0 mm BITS
1540 PRINT M$;TAB(19);D$
1550 PRINT "ROCK TYPE ";R$
1560 PRINT "BIT ";B$
1570 PRINT "SET PARAMETER ";V$
1580 PRINT "TEST DURATION";INT(T/60);"min";RMD(T,6
0);"sec"
1590 PRINT "SAMPLING INTERVAL";Z;"sec"
1600 PRINT ;"DISTANCE DRILLED";INT(FNF5(P)+.5);"mm
"
1610 CLEAR @ DISP "CALCULATING - WAIT!"
1620 X(N,3)=X(N-1,3)
1630 FOR I=2 TO N-1
1640 IF X(I,1)>20 THEN 1650 ELSE 1660 ! REMOVES WA
TTMETER OVERRANGE READINGS
1650 X(I,1)=X(I+1,1)
1660 IF X(I,1)<=.5 THEN 1670 ELSE 1680
1670 X(I,1)=X(I-1,1) @ X(I,3)=X(I-1,3) @ X(I,4)=X(
I-1,4)
1680 Z1=Z1+(A1*FNF1(X(I,1))+B1)
1690 Z2=Z2+FNF2(X(I,2))/F
1700 Z3=Z3+FNF3(X(I,3))/60*PI*.02
1710 Z4=Z4+FNF4(X(I,4))
1720 Z5=Z5+FNF3(X(I,3))
1730 A=A+FNF5(X(I,5)-X(I-1,5))
1740 NEXT I
1750 Z6=Z1*Z*.000001/(A*.001*F2)
1760 Z7=Z4/(N-2)*(Z3/(N-2))/(PI*.02)*Z*PI*.000001/
(A/(N-2)*.001/Z*F2)
1770 PRINT "MEAN POWER OUTPUT";INT(Z1/(N-2)*10+.5)
/10;"W"
1780 PRINT "MEAN BIT PRESSURE";INT(Z2/(N-2)*100+.5
)/100;"MPa"
1790 PRINT "MEAN BIT SPEED";INT(Z3/(N-2)*100+.5)/1
00;"m/s"
1800 PRINT "MEAN BIT TORQUE";INT(Z4/(N-2)*100+.5)/
100;"Nm"
1810 PRINT "MEAN ADVANCE PER REV.";INT(FNF5(P)/(Z5
*T/((N-2)*60))*1000+.5)/1000
1820 PRINT "AVERAGE SPECIFIC ENERGY [MJ]";INT(Z6*10
+.5)/10;"MJ/m^3"
1830 PRINT "AVERAGE SPECIFIC ENERGY [TJ]";INT(Z7*10
+.5)/10;"MJ/m^3"
1840 PRINT "SPECIFIC BIT WEAR";INT(FNF5(W)/(FNF5(P
)*.001)*1000+.5)/1000;"mm/m"
1850 CLEAR @ DISP "END OF TEST"
1860 RETURN
1870 OFF ERROR @ DISP "ERRL=";ERRL;"  ERRN=";ERRN
@ PAUSE @ GOTO 1410
```

PROGRAM LISTING - PROGRAM "B"

```
10 ! "B" - COMPUTATION AND PLOTS
20 CLEAR
30 OPTION BASE 1
40 COM SHORT X(600,5),B$[90],D$[14],M$[7],R$[20],V
$[30],A1,B1,F,N,P,T,W,Z
50 DEF FNF1(A) = A#200 ! (N)
60 DEF FNF2(A) = A#1000#.3332/8.76#9.8/1000000 !
(MN)
70 DEF FNF3(A) = A#907.7 ! (rpm)
80 DEF FNF4(A) = A#9.8#.26/4.817/.1856 ! Nm
90 DEF FNF5(A) = A#29.3 ! (mm)
100 A,Q,Z1,Z2,Z3,Z4,Z5,Z6,Z7=0
110 F2=.000201 ! HOLE CROSS SECTIONAL AREA WITH 20
 mm BITS
120 PRINTER IS 706,80
130 PRINT CHR$(27)&"C"&CHR$(0)&CHR$(12)
140 DISP "CHECK PRINTER ON, PAPER ALIGNED"
150 DISP "LOAD DATA DISC THEN PRESS          CONTINU
E" @ BEEP @ PAUSE
160 CAT ".DATA" @ DISP "TYPE TEST NAME" @ BEEP @ I
NPUT M$
170 CLEAR @ DISP "READING FROM DISC - PLEASE WAIT!
"
180 ASSIGN# 1 TO M$&".DATA" @ READ# 1 ; B$,D$,R$,V
$,A1,B1,F,N,P,T,W,Z
190 FOR I=1 TO N @ FOR J=1 TO 5
200 READ# 1 ; X(I,J)
210 NEXT J @ NEXT I
220 ASSIGN# 1 TO *
230 CLEAR @ PRINT @ PRINT TAB(15);M$;TAB(61);D$
240 PRINT @ PRINT TAB(15);"ROCK TYPE - ";R$
250 PRINT @ PRINT TAB(15);"BIT - ";B$
260 PRINT @ PRINT TAB(15);"SET PARAMETER - ";V$
270 PRINT
280 PRINT @ PRINT TAB(15);"TEST DURATION";TAB(37);
"SAMPLING INTERVAL";TAB(59);"DISTANCE DRILLED"
290 PRINT TAB(15);INT(T/60);"min ";RMD(T,60);"sec"
;TAB(40);Z;"s";TAB(65);INT(FNF5(P)+.5);" mm"
300 CLEAR @ DISP "CALCULATING - PLEASE WAIT!"
310 X(N,3)=X(N-1,3)
320 FOR I=2 TO N-1
330 IF X(I,1)>20 THEN 340 ELSE 350 ! REMOVES #ATTM
ETER OVERRANGE
340 X(I,1)=X(I+1,1)
350 IF X(I,1)<=.5 THEN 360 ELSE 370
360 X(I,1)=X(I-1,1) @ X(I,3)=X(I-1,3) @ X(I,4)=X(I
-1,4)
370 Z1=Z1+(A1#FNF1(X(I,1))+B1)
380 Z2=Z2+FNF2(X(I,2))/F
390 Z3=Z3+FNF3(X(I,3))/60#PI#.02
400 Z4=Z4+FNF4(X(I,4))
410 Z5=Z5+FNF3(X(I,3))
420 A=A+FNF5(X(I,5))-X(I-1,5)
430 NEXT I
440 Z6=Z1#Z#.000001/(A#.001#F2)
450 Z7=Z4/(N-2)#(Z3/(N-2)*(PI#.02)#2#PI#.000001)/(
A2/(N-2)#.001/Z#F2)
460 PRINT @ PRINT @ PRINT TAB(15);"MEAN";TAB(28);"
MEAN";TAB(41);"MEAN";TAB(54);"MEAN";
470 PRINT TAB(67);"AVERAGE"
480 PRINT TAB(15);"POWER";TAB(29);"BIT";TAB(41);"B
IT";TAB(54);"BIT";TAB(67);"ADVANCE"
490 PRINT TAB(15);"OUTPUT";TAB(28);"PRESSURE";TAB(
41);"SPEED";TAB(54);"TORQUE";
500 PRINT TAB(67);"PER REV."
510 PRINT TAB(15);"(W)";TAB(28);"(MPa)";TAB(41);"(
m/s)";TAB(54);"(Nm)";TAB(67);"(mm/rev)"
520 PRINT TAB(15);INT(Z1/(N-2)#10+.5)/10;TAB(28);I
NT(Z2/(N-2)#100+.5)/100;
530 PRINT TAB(41);INT(Z3/(N-2)#100+.5)/100;TAB(54)
;INT(Z4/(N-2)#100+.5)/100;
540 PRINT TAB(67);INT(FNF5(P)/(25#T/((N-2)#60))#10
00+.5)/1000
550 PRINT
560 PRINT @ PRINT TAB(15);"AVERAGE SPECIFIC";TAB(3
7);"AVERAGE SPECIFIC";TAB(59);"SPECIFIC"
570 PRINT TAB(15);"ENERGY (WI";TAB(37);"ENERGY (TI
";TAB(59);"BIT WEAR"
580 PRINT TAB(15);"(MJ/m^3)";TAB(37);"(MJ/m^3)";TA
B(59);"(mm/m)"
590 PRINT TAB(15);INT(Z6#10+.5)/10;TAB(37);INT(Z7#
10+.5)/10;
600 PRINT TAB(59);INT(FNF5(W)/(FNF5(P)#.001)#1000+
.5)/1000
610 PRINT CHR$(12)
620 ! PLOTS
630 A=0
640 Y1=2000
650 Y2=5
660 Y3=2000
670 Y4=.2
680 Y5=3000
690 Y6=3000
700 CLEAR @ DISP "CALCULATING AGAIN - PLEASE WAIT!
"
710 FOR I=5 TO N @ FOR J=1 TO 4
720 X(I,J)=(X(I,J)+.8#X(I-1,J)+.6#X(I-2,J)+.4#X(I-
3,J)+.2#X(I-4,J))/3
730 NEXT J @ NEXT I
740 CLEAR @ DISP "CALCULATION COMPLETE FOR NOW!" @
 BEEP
750 PRINT TAB(15);M$;TAB(61);D$ @ PRINT @ PRINT
760 DISP @ DISP "PLOTTING INTRUCTIONS" @ DISP
770 DISP "TO COPY GRAPH - PRESS K1 WHEN    BEEP SO
UNDS" @ DISP
780 DISP "TO CHANGE Y AXIS - PRESS K2      DURING
PLOTTING"
790 ! DISP "TO AVOID PRINTING - PRESS K3 ON BEEP"
800 ON KEY# 1 GOTO 1900 @ ON KEY# 2 GOTO 1900 @ ON
 KEY# 3 GOTO 2060
810 DISP @ DISP "READ THESE INSTRUCTIONS AND THEN
PRESS CONTINUE" @ PAUSE
820 FOR K=1 TO 6
830 PEN 1 @ GCLEAR
840 ON K GOTO 850,920,1000,1080,1230,1310
850 Y=Y1 @ GOSUB 1660
860 LABEL "Watts" @ MOVE 1/2,.95#Y @ LABEL "POWER"
 @ MOVE 1/2,.9#Y @ LABEL "OUTPUT" @ PENUP
870 FOR I=5 TO N
880 Y=A1#FNF1(X(I,1))+B1
890 X=FNF5(X(I,5))
900 PLOT X,Y @ NEXT I @ GOTO 1890
910 NEXT K
```

PROGRAM LISTING - PROGRAM "B" (Continued)

```
920 Y=Y2 @ GOSUB 1660
930 LABEL "Na"
940 MOVE X/2,.95*Y @ LABEL "TORQUE" @ PENUP
950 FOR I=5 TO N
960 Y=FNF4(X(I,4))
970 I=FNF5(X(I,5))
980 PLOT X,Y @ NEXT I @ GOTO 1890
990 NEXT K
1000 Y=Y3 @ GOSUB 1420
1010 LABEL "mm"
1020 MOVE X/2,.95*Y @ LABEL "PENETRATION" @ PENUP
1030 FOR I=1 TO N
1040 Y=FNF5(X(I,5))
1050 I=I*Z
1060 PLOT X,Y @ NEXT I @ GOTO 1890
1070 NEXT K
1080 Y=Y4 @ GOSUB 1660
1090 IF V$[1,4]="LOAD" THEN 1100 ELSE 1150
1100 LABEL "MPa" @ MOVE X/2,.95*Y @ LABEL "BIT PRE
SSURE" @ PENUP @ Q=1
1110 FOR I=1 TO N
1120 Y=FNF2(X(I,2))/F
1130 I=FNF5(X(I,5))
1140 PLOT X,Y @ NEXT I @ GOTO 1890
1150 LABEL "mm/rev" @ MOVE X/2,.95*Y @ LABEL "ADVA
NCE/REV." @ PENUP
1160 FOR I=6 TO N
1170 A=X(I,5)-X(I-1,5)+.8*(X(I-1,5)-X(I-2,5))+.6*(
X(I-2,5)-X(I-3,5))+.4*(X(I-3,5)-X(I-4,5))
1180 X(I,2)=(A+.2*(X(I-4,5)-X(I-5,5)))/3
1190 Y=FNF5(X(I,2))/Z/(FNF3(X(I,3))/60)
1200 I=FNF5(X(I,5))
1210 PLOT X,Y @ NEXT I @ GOTO 1890
1220 NEXT K
1230 Y=Y5 @ GOSUB 1660
1240 LABEL "MJ/m^3"
1250 MOVE X/2,.95*Y @ LABEL "SPECIFIC" @ MOVE X/2,
.9*Y @ LABEL "ENERGY (W)" @ PENUP
1260 FOR I=6 TO N
1270 Y=(A1*FNF1(X(I,1))+B1)*Z*.000001/(FNF5(X(I,2)
)*.001*F2)
1280 I=FNF5(X(I,5))
1290 PLOT X,Y @ NEXT I @ GOTO 1890
1300 NEXT K
1310 Y=Y6 @ GOSUB 1660
1320 LABEL "MJ/m^3"
1330 MOVE X/2,.95*Y @ LABEL "SPECIFIC" @ MOVE X/2,
.9*Y @ LABEL "ENERGY (T)" @ PENUP
1340 FOR I=6 TO N
1350 Y=FNF4(X(I,4))*(FNF3(X(I,3))/60)*.000001*Z*P1
/(FNF5(X(I,2))*.001/Z*F2)
1360 I=FNF5(X(I,5))
1370 PLOT X,Y @ NEXT I @ GOTO 1890
1380 PENUP @ PRINT CHR$(12)
1390 CLEAR @ DISP "END OF TEST"
1400 END
1410 ! XAXIS=DRILLING TIME
1420 I=T
1430 SCALE 0,I,0,Y
1440 FRAME
1450 IF I<=60 THEN 1460 ELSE 1520
1460 XAXIS 0,10 @ YAXIS 0,.1*Y
1470 FOR I=10 TO I STEP 10
1480 MOVE I,-.04*Y @ LABEL VAL$(I)
1490 NEXT I
1500 MOVE .3*I,-.1*Y @ LABEL "DRILLING TIME (secs)"

1510 GOTO 1850
1520 XAXIS 0,60 @ YAXIS 0,.1*Y
1530 IF I>600 THEN 1590
1540 FOR I=60 TO I STEP 60
1550 MOVE I,-.04*Y @ LABEL VAL$(I/60)
1560 NEXT I
1570 MOVE .3*I,-.1*Y @ LABEL "DRILLING TIME (mins)"

1580 GOTO 1850
1590 XAXIS 0,300 @ YAXIS 0,.1*Y
1600 FOR I=300 TO I STEP 300
1610 MOVE I,-.04*Y @ LABEL VAL$(I/60)
1620 NEXT I
1630 MOVE .3*I,-.1*Y @ LABEL "DRILLING TIME (mins)"

1640 GOTO 1850
1650 ! XAXIS=DRILLING DISTANCE
1660 I=FNF5(P)
1670 SCALE 0,I,0,Y
1680 FRAME
1690 IF FNF5(P)<=200 THEN 1700 ELSE 1740
1700 XAXIS 0,10 @ YAXIS 0,.1*Y
1710 FOR I=20 TO I STEP 20
1720 MOVE I,-.04*Y @ LABEL VAL$(I/10)
1730 NEXT I @ GOTO 1830
1740 IF FNF5(P)<=500 THEN 1750 ELSE 1790
1750 XAXIS 0,100 @ YAXIS 0,.1*Y
1760 FOR I=100 TO I STEP 100
1770 MOVE I,-.04*Y @ LABEL VAL$(I/10)
1780 NEXT I @ GOTO 1830
1790 XAXIS 0,100 @ YAXIS 0,.1*Y
1800 FOR I=200 TO I STEP 200
1810 MOVE I,-.04*Y @ LABEL VAL$(I/10)
1820 NEXT I
1830 MOVE .3*I,-.1*Y @ LABEL "DRILLING DISTANCE (m
)"
1840 ! YAXIS
1850 FOR I=-.2*Y TO Y STEP .2*Y
1860 MOVE .02*X,I @ LABEL VAL$(I)
1870 NEXT I
1880 MOVE .02*X,.75*Y @ RETURN
1890 BEEP @ GOTO 1890
1900 GCLEAR @ CLEAR @ DISP "INPUT NEW Y AXIS MAXIM
UM." @ INPUT Y@ CLEAR
1910 ON K GOTO 1920,1930,1940,1950,1960,1970
1920 Y1=Y @ GOTO 950
1930 Y2=Y @ GOTO 920
1940 Y3=Y @ GOTO 1000
1950 Y4=Y @ GOTO 1080
1960 Y5=Y @ GOTO 1230
1970 Y6=Y @ GOTO 1310
1980 IF K=4 THEN 1990 ELSE 2000
1990 PRINT CHR$(12) @ PRINT TAB(15);M$;TAB(61);D$
@ PRINT @ PRINT
2000 PCOPY 706
2010 IF Q=1 THEN 2020 ELSE 2060
2020 CLEAR @ Q=0 @ DISP "DON'T PANIC - CALCULATING"
```

PROGRAM LISTING - PROGRAM "C"

```
2030 FOR I=6 TO N
2040 A=X(I,5)-X(I-1,5)+.8*(X(I-1,5)-X(I-2,5))+.6*(
X(I-2,5)-X(I-3,5))+.4*(X(I-3,5)-X(I-4,5))
2050 X(I,2)=(A+.2*(X(I-4,5)-X(I-5,5)))/3 @ NEXT I
@ Q=0
2060 ON K GOTO 910,990,1070,1220,1300,1380
```

```
10 ! "C" - TABULATION OF RESULTS
20 CLEAR
30 OPTION BASE 1
40 COM SHORT X(600,5),B$[90],D$[14],M$[7],R$[20],V
$[30],A1,B1,F,N,P,T,W,Z
50 DEF FNF1(A) = A*200 ! (W)
60 DEF FNF2(A) = A*1000*.3332/8.762*9.8/1000000 !
(MN)
70 DEF FNF3(A) = A*907.7 ! (rpm)
80 DEF FNF4(A) = A*9.8*.26/4.817/.1856 ! Nm
90 DEF FNF5(A) = A*29.3 ! (mm)
100 F2=.000201 ! HOLE CROSS SECTIONAL AREA WITH 20
 mm BIT
110 PRINTER IS 706,80
120 PRINT CHR$(27)&"C"&CHR$(0)&CHR$(12)
130 DIM Y(50,20),M$[50]
140 N=1 @ DISP "THIS PROGRAM TABULATES A MAXIMUM O
F 50 TESTS"
150 DISP "LOAD DATA DISC AND CHECK PRINTER IS ON L
INE THEN PRESS CONTINUE" @ BEEP @ PAUSE
160 CLEAR @ DISP "DO YOU WANT TO RECALL A TABLE
 FROM DISC";@ BEEP
170 INPUT A$@ IF A$[1,1]="Y" THEN 180 ELSE 270
180 CLEAR @ CAT ".TABLES"
190 DISP "INPUT NAME OF TABLE" @ BEEP
200 INPUT T$
210 ASSIGN@ 1 TO T$&".TABLES"
220 READ@ 1 ; C1,M$
230 FOR K=1 TO C1 @ FOR L=1 TO 20
240 READ@ 1 ; Y(K,L)
250 NEXT L @ NEXT K
260 ASSIGN@ 1 TO * @ GOTO 940
270 CLEAR @ DISP "HOW MANY TESTS DO YOU WANT TO
 TABULATE (MAX.=50)";
280 INPUT C1
290 DISP "INPUT TEST NUMBERS SEPARATELY eg. 32"
300 FOR C=1 TO 50
310 INPUT Y(C,1)
320 IF N=C1 THEN 350
330 N=N+1
340 NEXT C
350 FOR C=1 TO C1
360 CLEAR @ DISP "READING TEST";VAL$(Y(C,1));" FRO
M DISC - WAIT!"
370 A,Z1,Z2,Z3,Z4,Z5,Z6,Z7=0
380 T$="TEST"&VAL$(Y(C,1))
390 ON ERROR GOTO 1410
400 ASSIGN@ 1 TO T$&".DATA" @ READ@ 1 ; B$,D$,R$,V
$,A1,B1,F,N,P,T,W,Z
```

```
410 FOR K=1 TO N @ FOR L=1 TO 5
420 READ@ 1 ; X(K,L)
430 NEXT L @ NEXT K
440 ASSIGN@ 1 TO *
450 OFF ERROR
460 DISP "CALCULATING - WAIT!"
470 X(N,3)=X(N-1,3)
480 FOR I=2 TO N-1
490 IF X(I,1)>20 THEN 500 ELSE 510 ! REMOVES WATTM
ETER OVERRANGE
500 X(I,1)=X(I+1,1)
510 IF X(I,1)<=.5 THEN 520 ELSE 530
520 X(I,1)=X(I-1,1) @ X(I,3)=X(I-1,3) @ X(I,4)=X(I
-1,4)
530 Z1=Z1+(A1*FNF1(X(I,1))+B1)
540 Z2=Z2+FNF2(X(I,2))/F
550 Z3=Z3+FNF3(X(I,3))/60*PI*.02
560 Z4=Z4+FNF4(X(I,4))
570 Z5=Z5+FNF3(X(I,3))
580 A=A+FNF5(X(I,5)-X(I-1,5))
590 NEXT I
600 Z6=Z1*Z*.000001/(A*.001*F2)
610 Z7=Z4/(N-2)*(Z3/(N-2)/(PI*.02)^2*PI*.000001)/(
A/(N-2)*.001/Z*F2)
620 Y(C,2)=INT(Z1/(N-2)*1+.5)/1 ! MEAN POWER OUTPU
T (W)
630 Y(C,3)=INT(Z2/(N-2)*100+.5)/100 ! MEAN BIT PRE
SSURE (MPa)
640 Y(C,4)=INT(Z3/(N-2)*100+.5)/100 ! MEAN BIT SPE
ED (m/s)
650 Y(C,5)=INT(Z4/(N-2)*100+.5)/100 ! MEAN BIT TOR
QUE (Nm)
660 Y(C,6)=INT(FNF5(P)/(Z5*T/((N-2)*60))*1000+.5)/
1000 ! AVERAGE ADVANCE PER REV. (mm/rev)
670 Y(C,7)=INT(Z6*10+.5)/10 ! AVERAGE S.E.[W] (MJ/
m^3)
680 Y(C,8)=INT(Z7*10+.5)/10 ! AVERAGE S.E.[T](MJ/m
^3)
690 Y(C,9)=INT((Y(C,7)+Y(C,8))/2*10+.5)/10 ! AVERA
GE SPECIFIC ENERGY (MJ/m^3)
700 Y(C,12)=FNF5(P) ! TEST LENGTH
710 NEXT C
720 CLEAR @ DISP "DO YOU WANT TO INPUT BIT WEAR AN
ALYSIS RESULTS" @ INPUT A$
730 IF A$[1,1]="Y" THEN 770 ELSE 740
740 FOR C=1 TO C1 @ FOR P=10 TO 17 @ IF P=12 THEN
760
750 Y(C,P)=0
760 NEXT P @ NEXT C @ GOTO 850
770 CLEAR @ DISP "  - INPUT OF BIT WEAR RESULTS -"
 @ BEEP
780 DISP "FOR EACH TEST INPUT BIT WEAR     RESULTS
 IN REQUIRED ORDER,      SEPARATED BY A COMMA"
790 FOR C=1 TO C1
800 DISP "BIT WEAR RESULTS - TEST";Y(C,1)
810 DISP "SPECIFIC BIT WEAR (mm/m),SPECIFIC BIT MA
SS LOSS (g)"
820 INPUT Y(C,10),Y(C,11)
830 DISP "WEAR TYPES 0,1,2,3,4" @ INPUT Y(C,13),Y(
C,14),Y(C,15),Y(C,16),Y(C,17)
840 NEXT C
850 CLEAR @ DISP "DO YOU WANT TO INPUT PARTICLE SI
```

PROGRAM LISTING - PROGRAM "C" (Continued)

```
ZE DISTRIBUTION ANALYSIS RESULTS";@ INPUT A$
860 IF A$[1,1]="Y" THEN 880 ELSE 870
870 FOR C=1 TO C1 @ FOR P=18 TO 20 @ Y(C,P)=0 @ NE
XT P @ NEXT C @ GOTO 930
880 CLEAR @ DISP "- INPUT OF PARTICLE SIZE DISTRIB
UTION ANAYSIS RESULTS -" @ BEEP
890 DISP "FOR EACH TEST INPUT RESULTS SEPARATED BY
 COMMAS"
900 FOR C=1 TO C1
910 DISP "PARTICLE SIZE DISTRIBUTION ANALYSIS RESU
LTS - TEST";Y(C,1)
920 DISP "MEAN, SORTING, PERCENTAGE MUD (%)" @ INP
UT Y(C,18),Y(C,19),Y(C,20)@ NEXT C
930 CLEAR @ DISP "INPUT TABLE HEADING" @ INPUT H$
940 PRINT TAB(10);"DRILLING TEST RESULTS - "&H$ @
PRINT @ PRINT
950 IMAGE 10X,4A,X,4A,3X,4A,5X,4A,2X,4A,X,4(2X,7A)

960 PRINT USING 950 ; "TEST","MEAN","MEAN","MEAN",
"MEAN","AVERAGE","AVERAGE","AVERAGE","AVERAGE"
970 IMAGE 10X,3A,2X,5A,2X,3A,6X,3A,3X,3A,4X,7A,4X,
4A,5X,4A,3X,8A
980 PRINT USING 970 ; "NO.","POWER","BIT","BIT","B
IT","ADVANCE","S.E.","S.E.","SPECIFIC"
990 IMAGE 15X,6A,X,8A,X,5A,X,6A,X,8A,3X,3A,6X,3A,4
X,6A
1000 PRINT USING 990 ; "OUTPUT","PRESSURE","SPEED"
,"TORQUE","PER.REV.","(W)","(T)","ENERGY" @ PRINT
1010 IMAGE 16X,3A,4X,5A,3X,5A,2X,4A,2X,4(8A,X)
1020 PRINT USING 1010 ; "(W)","(MPa)","(m/s)","(Nm
)","(mm/rev)","(MJ/m^3)","(MJ/m^3)","(MJ/m^3)"
1030 PRINT
1040 IMAGE 10X,3D,3X,4D,2X,D.2D,4X,D.2D,3X,Z.2D,3
X,Z.3D,3(3X,4D.D)
1050 FOR C=1 TO C1
1060 PRINT USING 1040 ; Y(C,1),Y(C,2),Y(C,3),Y(C,4
),Y(C,5),Y(C,6),Y(C,7),Y(C,8),Y(C,9)
1070 NEXT C @ PRINT @ PRINT @ PRINT
1080 DISP "DO YOU WANT TO PRINT BIT WEAR TABLE";@
INPUT A$@ IF A$[1,1]="Y" THEN 1090 ELSE 1230
1090 IMAGE 10X,4A,2(X,8A),2X,4A,2X,2(A,2X,13A
1100 PRINT USING 1090 ; "TEST","SPECIFIC","SPECIFI
C","TEST","DIAMOND WEAR ANALYSIS","PARTICLE SIZE"
1110 IMAGE 10X,3A,2X,3A,6X,8A,X,6A,5X,14A,5X,12A
1120 PRINT USING 1110 ; "NO.","BIT","BIT MASS","LE
NGTH","% OF WEAR TYPE","DISTRIBUTION"
1130 IMAGE 15X,4A,5X,4A,8X,5(4X,A),2X,4A,2X,4A,2X,
3A
1140 PRINT USING 1130 ; "WEAR","LOSS","0","1","2",
"3","4","MEAN","S.D.","MUD" @ PRINT
1150 IMAGE 15X,6A,3X,5A,4X,4A,2(6X,2(5A,X),4A
1160 PRINT USING 1150 ; "(mm/m)","(g/m)","(mm)","(
phi)","(phi)","(%)" @ PRINT
1170 FOR C=1 TO C1
1180 IMAGE #10X,3D,3X,Z.2D,4X,Z,2D,5X,4D
1190 IMAGE 2X,2D.4(3X,2D),2X,D.0D,2X,Z.DD,2X,2D
1200 OUTPUT 706 USING 1180 ; Y(C,1),Y(C,10),Y(C,11
),Y(C,12)
1210 OUTPUT 706 USING 1190 ; Y(C,13),Y(C,14),Y(C,1
5),Y(C,16),Y(C,17),Y(C,18),Y(C,19),Y(C,20)
1220 NEXT C
1230 CLEAR @ DISP "END OF TABULATION"
1240 DISP "DO YOU WANT TO STORE THIS TABLE";@ BEEP

1250 INPUT A$@ IF A$[1,1]="Y" THEN 1260 ELSE 1400
1260 DISP "INSERT APPROPRIATE TABLES DISC AND PRES
S CONTINUE" @ BEEP @ PAUSE
1270 CLEAR @ CAT ".TABLES"
1280 DISP "CHECK FILES AND INPUT NAME OF NEW TABLE
" @ BEEP
1290 INPUT T$
1300 ON ERROR GOTO 1440
1310 CREATE T$&".TABLES",1,20*8+C1*1000
1320 ASSIGN# 1 TO T$&".TABLES"
1330 PRINT# 1 ; C1,H$
1340 FOR K=1 TO C1 @ FOR L=1 TO 20
1350 PRINT# 1 ; Y(K,L)
1360 NEXT L @ NEXT K
1370 ASSIGN# 1 TO *
1380 OFF ERROR
1390 DISP "RECORDING COMPLETE"
1400 CLEAR @ DISP "END" @ END
1410 DISP "PLEASE REPLACE DATA DISC THEN PRESS CON
TINUE"
1420 BEEP 100,5000 @ PAUSE
1430 GOTO 360
1440 DISP ERRL,ERRN @ GOTO 1300
```

PROGRAM LISTING - PROGRAM "D"

```
10 ! "D" FINAL TABULATION
20 DISP "THIS PROGRAM FULLY TABULATES UP TO 60 TES
TS RESULTS WITH CONSECUTIVE NUMBERS"
30 OPTION BASE 1
40 PRINTER IS 706,132
50 PRINT CHR$(27)&"C"&CHR$(0)&CHR$(12)
60 DIM A(60,28),Y(50,25),H$[80]
70 COM X
80 FOR I=1 TO 60 @ FOR J=1 TO 28
90 A(I,J)=0 @ NEXT J @ NEXT I
100 DISP "INSERT TABLES DISC & PRESS CONT" @ BEEP
@ PAUSE
110 DISP "INPUT FIRST AND LAST NUMBERS OF INTEREST
"
120 INPUT A3,A4
130 A2=A4-A3+1
140 A1=1
150 DISP "HOW MANY STORED TABLES ARE INVOLVED? INP
UT 0 TO REPRINT A TABLE";
160 INPUT N
170 IF N=0 THEN 1360
180 FOR I=1 TO N
190 DISP "INPUT NAME OF TABLES SEPARATELY" @ BEEP
200 INPUT T$
210 ASSIGN# 1 TO T$&".TABLES"
220 READ# 1 ; C1,H$
230 FOR K=1 TO C1 @ FOR L=1 TO 20
240 READ# 1 ; Y(K,L)
250 NEXT L @ NEXT K
260 ASSIGN# 1 TO *
270 FOR K=1 TO C1
280 A5=Y(K,1)
290 IF A5<A3 THEN 460
300 IF A5>A4 THEN 470
310 A=Y(K,1)-A3+1
320 A(A,1)=Y(K,1) ! NUMBER
330 A(A,3)=Y(K,12) ! LENGTH
340 A(A,4)=Y(K,2) ! POWER
350 A(A,5)=Y(K,4) ! SPEED
360 A(A,6)=Y(K,5) ! TORQUE
370 A(A,7)=Y(K,3) ! PRESSURE
380 A(A,8)=Y(K,6) ! ADVANCE
390 A(A,9)=Y(K,7) ! S.E.[W]
400 A(A,10)=Y(K,8) ! S.E.[T]
410 A(A,11)=Y(K,10) ! WEAR
420 A(A,12)=Y(K,11) ! LOSS
430 A(A,23)=Y(K,18) ! MEAN
440 A(A,24)=Y(K,19) ! S.D.
450 A(A,25)=Y(K,20) ! MUD
460 NEXT K
470 NEXT I
480 FOR A=A1 TO A2
490 X=A(A,1)
500 DISP "TEST"&VAL$(X)
510 DISP "INPUT ROCK TYPE CODE"
520 DISP "LIGHT NORITE : 1"
530 DISP "DARK NORITE  : 2"
540 DISP "SANDSTONE    : 3"
550 DISP "QUARTZ       : 4"
560 DISP "QUARTZITE    : 5"
570 DISP "JASPILITE    : 6"
580 DISP "SYENITE      : 7"
590 DISP "FELSPAR      : 8"
600 DISP "GRANITE      : 9"
610 DISP "CALCITE      :10"
620 DISP "MARBLE       :11"
630 DISP "GLASS        :12"
640 INPUT A(A,27)
650 DISP "INPUT MESH (eg. 20,30),CONC,MODE";@ INPU
T A(A,28),A(A,2),A(A,26)
660 DISP "DO YOU NEED TO INPUT DIAMOND WEAR";@ INP
UT Y$
670 IF Y$(1,1)#"Y" THEN 700
680 DISP "INPUT DIAMOND WEAR TYPES (0a,0b,1a etc.)
";
690 INPUT A(A,13),A(A,14),A(A,15),A(A,16),A(A,17),
A(A,18),A(A,19),A(A,20),A(A,21),A(A,22)
700 NEXT A
710 PRINT TAB(23);"DIAMOND DRILLING TESTS - SUMMAR
ISED RESULTS" @ PRINT @ PRINT CHR$(15)
720 IMAGE #3A,2X,4A,2X,4A,X,2(4A,X),2(4A,2X)
730 IMAGE #2(4A,2X),3(7A,X),2(3A,2X)
740 IMAGE 4X,21A,5X,13A,X,4A
750 IMAGE #21X,4A,X,5A,X,3(3A,3X),7A,3X
760 IMAGE #4A,4X,4A,2X,4A,X,4A
770 IMAGE 9X,14A,8X,12A
780 IMAGE #26X,4A,2X,3(5A,X),7A,3X
790 IMAGE #3A,5X,3A,8X,4A,X
800 IMAGE 29A,X,2(4A,X),3A
810 IMAGE #22X,2A,4X,A,4X,3A,3X,2A,4X,3A,2X,6A,2X,
2(6A,2X)
820 IMAGE 4A,X,3A,3X,3A,2X,3A,2X,A
830 OUTPUT 706 USING 720 ; "NO.","ROCK","MESH","CO
NC","TEST","MEAN","MEAN"
840 OUTPUT 706 USING 730 ; "MEAN","MEAN","AVERAGE"
,"AVERAGE","AVERAGE","BIT","BIT"
850 OUTPUT 706 USING 740 ; "DIAMOND WEAR ANALYSIS"
,"PARTICLE SIZE","MODE"
860 OUTPUT 706 USING 750 ; "LEN.","POWER","BIT","B
IT","BIT","ADVANCE"
870 OUTPUT 706 USING 760 ; "S.E.","S.E.","WEAR","M
ASS"
880 OUTPUT 706 USING 770 ; "% OF WEAR TYPE","DISTR
IBUTION"
890 OUTPUT 706 USING 780 ; "OUT.","SPEED","TORQ.",
"PRES.","PER REV"
900 OUTPUT 706 USING 790 ; "[W]","[T]","LOSS"
910 OUTPUT 706 USING 800 ; "0a 0b 1a 1b 2a 2b 3a 3
b 4a 4b","MEAN","SORT","MUD"
920 PRINT
930 OUTPUT 706 USING 810 ; "mm","N","m/s","Nm","MP
a","mm/rev","MJ/m^3","MJ/m^3"
940 OUTPUT 706 USING 820 ; "mm/m","g/s","pnt","pnt
","%"
950 PRINT
960 FOR A=A1 TO A2
970 N2,N3=A(A,28) @ N2=IP(N2) @ N3=FP(N3)*100
980 N1=A(A,1) @ N4=A(A,2) @ N5=A(A,3) @ N6=A(A,4)
@ N7=A(A,5) @ N8=A(A,6) @ N9=A(A,7)
990 M1=A(A,8) @ M2=A(A,9) @ M3=A(A,10) @ M4=A(A,11
) @ M5=A(A,12) @ M6=A(A,13) @ M7=A(A,14) @ M8=A(A,
```

PROGRAM LISTING - PROGRAM "D" (Continued)

```
15)
1000 M9=A(A,16)
1010 L1=A(A,17) @ L2=A(A,18) @ L3=A(A,19) @ L4=A(A
,20) @ L5=A(A,21) @ L6=A(A,22) @ L7=A(A,23) @ L8=A
(A,24)
1020 L9=A(A,25) @ K1=A(A,26)
1030 ON A(A,27) GOTO 1040,1050,1060,1070,1080,1090
,1100,1110,1120,1130,1140,1160
1040 N$="LNOR" @ GOTO 1170
1050 N$="DNOR" @ GOTO 1170
1060 N$="SSTN" @ GOTO 1170
1070 N$="QRTZ" @ GOTO 1170
1080 N$="QZIT" @ GOTO 1170
1090 N$="JASP" @ GOTO 1170
1100 N$="SYNT" @ GOTO 1170
1110 N$="FELS" @ GOTO 1170
1120 N$="GRAN" @ GOTO 1170
1130 N$="CALC" @ GOTO 1170
1140 N$="MARB" @ GOTO 1170
1150 N$="SSTN" @ GOTO 1170
1160 N$="GLAS" @ GOTO 1170
1170 IMAGE #3D,2X,4A,X,2D,A,DZ,2X,2D,2X,4D,X,4D,2X
,2(Z.2D,2X),DZ.2D,2X,Z.3D,2X,2(4D.D,2X)
1171 IMAGE #3D,2X,4A,X,2D,A,DZ,X,4A,X,4D,X,4D,2X,2
(Z.2D,2X),DZ.2D,2X,Z.3D,2X,2(4D.D,2X)
1180 IMAGE 2(Z.2D,X),10(2D,X),D.2D,X,Z.2D,X,2D,2X,
K
1181 IF N4=0 THEN 1182 ELSE 1190
1182 OUTPUT 706 USING 1171 ; N1,N$,N2,"/",N3,"MONO
",N5,N6,N7,N8,N9,M1,M2,M3 @ GOTO 1200
1190 OUTPUT 706 USING 1170 ; N1,N$,N2,"/",N3,N4,N5
,N6,N7,N8,N9,M1,M2,M3
1200 OUTPUT 706 USING 1180 ; M4,M5,M6,M7,M8,M9,L1,
L2,L3,L4,L5,L6,L7,L8,L9,K1
1210 NEXT A
1220 DISP "DO YOU WANT TO STORE THIS TABLE";@ BEEP

1230 INPUT Y$@ IF Y$[1,1]="Y" THEN 1430
1240 DISP "INSERT TABLES DISC & PRESS CONT." @ BEE
P @ PAUSE
1250 CLEAR @ CAT ".TABLES"
1260 DISP "CHECK FILES & INPUT NEW TABLE NAME" @ B
EEP @ INPUT T$
1270 ON ERROR GOTO 1350
1280 CREATE T$&".TABLES",1,(A2-A1+1)*28*8+1000
1290 ASSIGN# 1 TO T$&".TABLES"
1300 FOR A=A1 TO A2 @ FOR B=1 TO 28
1310 PRINT# 1 ; A(A,B)
1320 NEXT B @ NEXT A
1330 ASSIGN# 1 TO *
1340 OFF ERROR @ GOTO 1430
1350 DISP ERRL,ERRN @ GOTO 1270
1360 DISP "INPUT NAME OF TABLE TO PRINT";@ INPUT T
$
1370 ASSIGN# 1 TO T$&".TABLES"
1380 FOR A=A1 TO A2 @ FOR B=1 TO 28
1390 READ# 1 ; A(A,B)
1400 NEXT B @ NEXT A
1410 ASSIGN# 1 TO *
1420 GOTO 710
1430 CLEAR @ DISP "END"
1440 PRINT CHR$(18)
1450 END
```

APPENDIX 3 - PETROGRAPHIC DESCRIPTIONS

Gabbro norite	-	"Dark norite"
Plagioclase felspar	- 60%	Adhedral laths. Average grain size 2,5 mm. Estimated composition An. 58 (labradorite). Very fresh. Some grains extremely well zoned.
Orthopyroxene	- 22%	High proportion of converted pigeonite. Average grain size 2 to 3 mm. All grains anhedral. Probably hypersthene.
Clinopyroxene	- 18%	Anhedral grains, size 2 to 3 mm. Pale green. Fe-rich augite. Some exsolved orthopyroxene.
Biotite & opaques	-	Trace.
Gabbro norite	-	"Light norite"
Plagioclase felspar	- 55%	Anhedral to subhedral laths. Average 2,5 mm in length. Some alteration. Estimated composition An. 65 (labradorite).
Orthopyroxene	- 40%	Anhedral, 5 mm long poikilitic crystals. Fresh. Converted pigeonite.
Orthopyroxene	- 5%	Probably hypersthene - pinkish.
Granite	-	"Cape granite"
Alkali felspar	- 70%	i) Perthite - large crystals 4 to 10 mm long. ii) Orthoclase - closely associated with the quartz, slightly altered, smaller grains.
Quartz	- 20%	Clusters of crystals about 3 mm, strained.
Plagioclase felspar	- 6%	Smaller average grain size than alkali felspar. Highly sericitised.
Biotite	- 3%	Small platey crystals 1 mm long. Evenly distributed but associated with finer grained quartz and plagioclase.
Opaques	- 1%	Possibly magnetite

Quartz syenite	-	"Red granite"
Plagioclase felspar	- 60%	Large sericitised fractured laths with some recrystallisation along subgrain boundaries. Occur as clumps with few interstitial minerals.
Hornblende	- 20%	Large euhedral grains, often zoned.
Clinopyroxene	- 15%	Large laths or clumps of smaller equidimensional grains. Highly fractured and altered.
Quartz	- 2%	Seriate, fractured, with iron staining.
Opaques	- 2%	Associated with apatite, interstitially or as inclusions in hornblende and pyroxene. Anhedral to seriate.
Accessory minerals	- 1%	i) Calcite - triangular grains. ii) Zircon - few large fractured grains. iii) Apatite - euhedral grains associated with opaques.
Recrystallised limestone	-	"Marble"
Calcite	- 95%	Anhedral intergrown grains with maximum length about 1 mm. Most grains 0,25 to 0,5 mm long.
Opaques & clastic fragments	- 5%	Opaques are small inclusions in calcite grains. Very minor clastic material present.
Felspathic sublitharenite	-	"Sandstone"
Quartz	- 70%	Size of grains about 0,5 mm. Subangular to subrounded. Little recrystallisation.
Lithic fragments	- 10%	Average size about 0,4 mm. Rounded.
Matrix	- 10%	Very fine grained, micaceous.
Felspar	- 5%	Plagioclase and microcline present. Anhedral grains about 0,25 mm.
Opaques	- 5%	Probably haematite.

Ironstone	-	"Jaspilite"
Quartz	- 80%	Anhedral intergrown grains. Average size 0,05 mm.
Haematite	- 20%	Stringers of fine grains along foliation planes.
Quartz arenite	-	"Quartzite"
Quartz	- 80%	Subangular grains. Average size 0,25 mm. Some recrystallisation.
Matrix	- 20%	Siliceous, microcrystalline.
Muscovite	-	Trace.

APPENDIX 4 - TABLES OF SUMMARISED RESULTS

These tables consist of 28 columns of figures and include the results of the drilling tests and ancillary measurements made on the bits and drilling detritus. Where necessary clarifying notes accompany the column descriptions.

NO. : Test number

ROCK : Material drilled

LNOR light norite	QRTZ quartz
DNOR dark norite	QZIT quartzite
GRAN Cape granite	FELS felspar
SYNT syenite	JASP jaspilite
SSTN sandstone	CALC calcite
MARB marble	GLAS glass

MESH : Diamond size distribution in US mesh

CONC : Diamond concentration in the bit matrix

TEST LEN. : Total test length in millimetres

MEAN POWER OUT. : Corrected mean power output in Watts, calculated from the wattmeter readings and corrected for power losses in the drilling machine.

MEAN BIT SPEED : Mean linear bit speed in metres per second

MEAN BIT TORQUE : Mean bit torque in Newton metres, calculated from the output of the minature load cell

MEAN BIT PRES. : Mean bit pressure in megaPascals, calculated from the output of the thrust load cell

AVERAGE ADVANCE PER REV : Average advance per revolution in millimetres per revolution, calculated from the total test length and the total number of revolutions performed by the drill during the test

AVERAGE S.E. [W]: Average specific energy in megaJoules per cubic metre. calculated from the corrected power output derived from the wattmeter readings

AVERAGE S.E. [1]: Average specific energy in megaJoules per cubic metre, calculated from the torquemeter readings

BIT WEAR : Linear bit wear in millimetres per metre, calculated by normalising to 1 metre the value for bit wear measured with the micrometer jig

BIT MASS LOSS : Bit mass loss in grammes per metre, calculated by normalising to 1 metre the bit mass loss measured on a four-place balance

DIAMOND WEAR ANALYSIS : These ten columns consist of the figures for diamond wear evaluated by categorising each exposed stone in one of the categories defined in Chapter 4.

MEAN : Mean particle size of the coarse fraction of the detritus, ie. over 63 micron. phi -log2 (particle diameter)/1 mm

SORT : The sorting or standard deviation of the coarse fraction of the detritus

MUD : Percentage by mass of particles under 63 microns in the detritus. This figure was determined by wet sieving, drying and weighing the retained fraction.

MODE : Mode of drilling behaviour. 1 indicates lack of adequate diamond and matrix wear with progressive decrease in penetration rate or progressive build-up of load depending whether the drill is operating under set load force or set rate of advance conditions. 2 indicates effective drilling in a quasi-stable state with sufficient bit regeneration to maintain penetration without excessive load build-up. 4 indicates cessation of drilling because of stalling or immanent overload. 1.2 and 2.4 indicate marginal conditions which could not be resolved easily.

TABLE A4.1 : Summarised results of all the tests

DIAMOND DRILLING TESTS - SUMMARISED RESULTS

NO.	ROCK	MESH	CONC	TEST LEN.	MEAN POWER OUT.	MEAN BIT SPEED	MEAN BIT TORQ.	MEAN BIT PRES.	AVERAGE ADVANCE PER REV	AVERAGE S.E.	AVERAGE S.E.	BIT WEAR	BIT MASS LOSS	DIAMOND WEAR ANALYSIS % OF WEAR TYPE									PARTICLE SIZE DISTRIBUTION		MODE
														0a	0b	1a	1b	2a	2b	3a	3b	4a	4b	MEAN	SORT MUD	
				mm	W	m/s	Nm	MPa	mm/rev	MJ/m^3	MJ/m^3	mm/m	g/m											phi	phi	%
1	LNOR	40/50	30	832	651	3.44	1.70	5.69	0.074	802.3	719.2	0.71												3.17	0.46	2
2	LNOR	40/50	30	715	468	3.39	1.24	4.56	0.054	793.5	710.8	0.56												3.11	0.50	2
3	LNOR	40/50	30	331	208	3.56	0.59	2.97	0.010	1865.2	1888.8	0.39														1
4	LNOR	40/50	30	336	100	3.43	0.40	1.90	0.009	1063.5	1467.8	0.63												2.94	0.67	1
5	GRAN	40/50	30	226	388	3.66	0.94	7.17	0.013	2601.5	2304.7	2.22														1
6	GRAN	40/50	30	159	257	3.58	0.75	4.96	0.013	1678.7	1743.8	0.70														1
7	GRAN	40/50	30	190	110	3.97	0.32	3.13	0.005	1723.1	2009.6	0.46												3.49	0.76	1
8	GRAN	40/50	30	744	938	3.68	2.27	8.14	0.055	1304.7	1303.3	2.08												3.31	0.52	1
9	GRAN	40/50	30	294	283	3.82	1.09	7.39	0.008	2890.6	4245.8	1.34												3.23	0.61	1
10	GRAN	40/50	30	678	759	3.54	1.88	9.31	0.047	1429.6	1255.3	0.70												3.25	0.59	1
11	SYNT	40/50	30	986	1347	3.27	3.41	10.36	0.097	1332.4	1100.7	0.88												3.08	0.64	2
12	SYNT	40/50	30	763	1064	3.21	2.70	7.92	0.132	785.9	640.4	0.69												3.22	0.55	2
13	SYNT	40/50	30	707	737	3.36	1.88	5.98	0.083	825.8	709.4	0.78												3.17	0.57	1
14	SYNT	40/50	30	298	211	3.56	0.72	4.04	0.009	2107.3	2539.2	0.85												3.14	0.61	1
15	SSTN	40/50	30	1467	975	3.40	2.49	4.02	0.277	323.0	280.5	0.69												3.17	0.46	2
16	LNOR	40/50	30	1041	1165	3.36	3.08	8.28	0.098	1103.3	980.5	1.21												3.19	0.50	2
17	SSTN	40/50	30	1415	1595	3.24	4.19	6.21	0.332	463.5	394.3	0.53												3.09	0.48	2
18	SSTN	40/50	30	667	1596	3.17	5.29	8.88	0.274	574.9	604.1	5.90												2.94	0.55	2
19	SSTN	40/50	30	2040	350	3.94	0.98	2.05	0.149	185.9	204.7	0.07												3.02	0.52	2
20	GRAN	40/50	30	677	1382	3.58	3.38	10.17	0.078	1552.4	1359.1	1.47												3.06	0.74	2
21	GRAN	40/50	30	214	323	3.40	0.72	5.97	0.011	2816.1	2135.0	1.60												3.30	0.57	1
22	GRAN	40/50	30	386	563	3.45	1.32	8.14	0.021	2492.9	2015.3	1.13												3.27	0.59	1
23	GRAN	40/50	30	489	1334	3.08	3.20	10.22	0.085	1600.3	1180.7	1.48												3.19	0.48	2
24	MARB	40/50	30	916	204	3.46	0.58	1.30	0.028	650.7	641.7	0.30												3.15	0.47	2
25	MARB	40/50	30	191	73	3.38	0.10	0.57	0.006	1103.0	520.7	1.83												3.14	0.56	2
26	MARB	40/50	30	1056	410	3.70	1.14	2.06	0.055	632.5	652.5	0.02												3.13	0.57	2
27	MARB	40/50	30	1436	853	3.50	2.12	3.95	0.116	654.4	568.5	0.07												3.16	0.62	2
28	MARB	40/50	30	1392	1319	3.29	3.10	6.11	0.135	927.8	717.0	0.10												3.17	0.54	2
29	MARB	40/50	30	1409	848	3.43	2.11	3.80	0.140	553.2	472.5	0.16												3.14	0.46	2
30	MARB	40/50	30	1394	1384	3.29	3.47	6.06	0.136	969.1	798.2	0.03												3.20	0.55	2
31	LNOR	40/50	30	1321	1748	3.23	4.32	10.91	0.096	1765.4	1411.9	1.74												3.00	0.57	2
32	DNOR	40/50	30	524	850	3.74	2.18	6.15	0.065	1097.6	1053.7	0.66	0.32	11	7	6	3	1	21	26	21	3	1	3.02	0.55	2
33	DNOR	40/50	30	521	853	3.93	2.16	6.28	0.061	1110.7	1104.1	1.14	0.52	8	12	4	8	0	20	24	21	3	0	3.08	0.64	2
34	DNOR	40/50	30	514	908	3.96	2.18	6.11	0.056	1273.8	1210.3	1.05	0.31	4	7	6	2	3	31	16	24	6	1	3.29	0.54	2
35	DNOR	40/50	30	518	842	3.93	2.03	6.10	0.061	1096.9	1041.0	0.20	0.48	15	10	6	1	1	29	14	23	1	1	2.97	0.65	2
36	DNOR	40/50	30	499	878	3.80	2.35	6.29	0.060	1205.3	1224.6	1.08	0.64	10	11	13	1	0	29	21	14	1	0	3.15	0.52	2
37	DNOR	40/50	30	461	848	3.79	2.18	6.31	0.060	1175.4	1145.6	1.12	0.34	7	5	9	3	2	31	19	20	3	0	3.15	0.56	2
38	DNOR	40/50	30	510	711	3.85	1.87	6.27	0.052	1115.8	1131.7	0.19	0.27	6	6	6	4	0	35	17	24	3	0	3.26	0.52	2
39	DNOR	40/50	30	511	928	3.76	2.50	6.23	0.071	1089.3	1103.2	0.68	0.42	9	11	5	1	0	30	13	27	4	0	3.14	0.51	2
40	DNOR	40/50	30	495	856	3.90	2.30	6.18	0.061	1133.6	1186.6	0.70	0.33	5	5	5	0	0	39	16	25	5	0	3.21	0.50	2
41	DNOR	40/50	30	490	804	3.84	2.17	6.10	0.055	1190.4	1236.2	1.22	0.39	9	8	5	0	0	38	14	24	3	0	3.10	0.61	2
42	DNOR	40/50	30	496	553	3.90	1.54	6.02	0.036	1250.0	1356.1	0.28	0.11	8	6	8	15	0	20	22	15	7	0	3.37	0.57	1,2
43	DNOR	40/50	30	581	765	3.99	2.08	6.19	0.060	995.9	1078.6	0.54	0.33	2	9	6	2	1	43	11	23	2	0	3.22	0.57	2
44	GLAS	40/50	30	233	908	3.66	2.45	5.95	0.129	602.2	594.4	0.59	0.33													2
45	QRTZ	40/50	30	107	476	3.83	1.31	5.79	0.023	1762.9	1856.4	0.00	0.26													1
46	QRTZ	40/50	30	38	1807	3.37	4.32	9.49	0.100	1677.4	1349.1	0.16	0.74													1
47	LNOR	40/50	30	511	1624	3.58	4.05	10.19	0.099	1454.7	1296.6	1.73												3.08	0.66	2
48	LNOR	40/50	30	387	1067	3.73	2.89	7.31	0.101	889.2	896.7	1.20												2.95	0.62	2
49	LNOR	40/50	30	489	548	4.02	1.58	3.95	0.038	1105.5	1116.5	0.69												2.73	0.79	1
50	LNOR	40/50	30	649	352	3.96	0.88	2.38	0.024	1155.9	1150.0	0.05												2.83	0.72	1
51	QRTZ	40/50	30	198	1750	3.67	4.24	8.35	0.079	1894.8	1684.0	4.90	1.18	4	6	7	6	6	16	27	17	11	0	2.71	0.83	84 2
52	FELS	40/50	30	1209	1030	3.77	2.65	8.04	0.099	866.9	840.2	0.80	1.20	5	12	16	7	5	15	19	14	6	0	2.90	0.83	84 2

TABLE A4.2 : Summarised results of all the tests (Continued)

DIAMOND DRILLING TESTS - SUMMARISED RESULTS

NO.	ROCK	MESH	CONC	TEST LEN.	MEAN POWER OUT.	MEAN BIT SPEED	MEAN BIT TORQ.	MEAN BIT PRES.	AVERAGE ADVANCE PER REV	AVERAGE S.E.	AVERAGE S.E.	BIT WEAR	BIT MASS LOSS	DIAMOND WEAR ANALYSIS % OF WEAR TYPE								PARTICLE SIZE DISTRIBUTION			MODE
														0a	0b	1a	1b	2a	2b	3a	3b	4a	4b	MEAN	SORT	MUD	
				mm	W	m/s	Nm	MPa	mm/rev	MJ/m^3	MJ/m^3	mm/m	g/m											phi	phi	%	
53	DNOR	40/50	30	269	187	3.57	0.37	2.18	0.008	2079.9	1459.8	0.22	0.01	12	10	13	8	9	4	17	26	1	0	3.09	0.55	0	1
54	DNOR	40/50	30	1465	498	3.74	1.21	4.03	0.041	1019.9	924.0	0.19	0.21	9	12	15	11	6	13	12	21	0	0	3.16	0.52	80	1.2
55	DNOR	40/50	30	1429	900	3.74	2.37	6.17	0.092	818.8	805.1	0.78	0.92	16	7	6	5	11	15	13	21	5	0	3.01	0.54	78	2
56	DNOR	40/50	30	1461	1241	3.42	3.15	8.43	0.111	1017.9	883.9	0.60	0.77	10	11	7	4	11	12	15	28	2	0	3.06	0.53	80	2
57	DNOR	40/50	30	1453	1635	3.27	4.00	10.40	0.118	1321.9	1058.2	0.71	1.00	10	4	10	4	8	9	27	22	6	0	3.05	0.54	80	2
58	DNOR	40/50	30	1342	1779	2.81	4.76	13.08	0.124	1595.7	1198.0	0.92	1.28	8	8	5	4	9	15	23	22	5	0	3.05	0.55	82	2
59	DNOR	40/50	30	842	205	3.64	0.87	3.06	0.018	955.5	1478.1	0.12	0.11	13	10	11	11	6	5	19	24	0	0	3.27	0.58	80	1
60	DNOR	40/50	30	1498	563	3.50	1.53	4.94	0.080	627.0	594.7	0.27	0.37	9	8	7	9	6	16	22	22	2	0	3.07	0.56	75	2
61	DNOR	40/50	30	1460	1099	3.28	2.98	7.26	0.134	780.9	695.3	0.54	0.84	10	5	8	3	10	20	12	25	5	0	2.99	0.53	77	2
62	DNOR	40/50	30	1478	1188	3.26	3.01	8.12	0.099	1135.9	938.8	0.97	0.97	5	9	8	6	5	23	16	26	1	0	3.10	0.52	80	2
63	DNOR	40/50	30	1486	1562	3.20	3.87	9.54	0.099	1524.9	1206.2	1.02	1.23	9	9	7	4	8	22	15	24	1	0	3.12	0.52	81	2
64	DNOR	40/50	30	1532	1546	3.01	3.94	10.25	0.115	1389.0	1067.7	0.81	0.85	9	9	5	3	7	21	21	23	1	0	3.10	0.49	84	2
65	DNOR	40/50	30	778	303	3.73	0.78	3.24	0.022	1163.8	1124.1	0.23	0.12	12	12	8	15	5	12	9	29	0	0	3.31	0.46	83	1
66	DNOR	40/50	30	1360	558	3.55	1.38	4.35	0.068	724.7	637.2	0.46	0.46	16	9	11	6	10	16	15	15	2	0	3.18	0.55	76	2
67	DNOR	40/50	30	1461	783	3.31	1.76	5.26	0.094	781.6	582.1	0.55	0.51	8	12	11	4	11	10	24	19	0	0	3.15	0.56	74	2
68	DNOR	40/50	30	1372	1115	3.52	2.84	6.93	0.106	917.3	823.4	0.76	0.82	5	12	8	5	8	14	23	21	3	0	3.15	0.58	76	2
69	DNOR	40/50	30	1663	1513	3.24	3.82	9.21	0.131	1096.9	897.2	1.52	0.96	8	15	6	2	9	22	21	19	0	0	3.21	0.55	0	2
70	DNOR	40/50	30	364	1620	3.03	4.48	10.39	0.105	1600.8	1342.1	1.62	2.58	9	17	2	1	8	17	34	11	0	1	2.75	0.81	71	2
71	DNOR	40/50	30	1365	1034	3.53	2.63	6.83	0.106	857.3	774.8	0.66	0.95	5	12	6	3	5	12	23	33	0	0	3.20	0.50	78	2
72	DNOR	40/50	30	1366	1146	3.44	3.04	7.69	0.091	1134.3	1035.7	0.88	0.90	13	12	9	5	13	14	16	22	1	0	3.06	0.47	85	2
73	DNOR	40/50	30											10	16	4	2	10	13	23	20	3	0				2
74	DNOR	40/50	30	433	99	4.10	0.61	2.43	0.011	715.1	1808.8	0.46	0.12	15	17	5	13	10	5	14	21	0	0	3.26	0.62	78	1
75	DNOR	40/50	30	1222	122	4.05	0.73	2.76	0.011	890.3	2160.6	0.13	0.07	15	10	3	16	6	8	15	26	1	0	3.34	0.59	74	1
76	DNOR	40/50	30	1279	224	3.66	0.82	3.50	0.012	1572.0	2104.1	0.09	0.04	13	17	2	22	8	3	11	24	1	0	3.45	0.58	81	1
77	DNOR	40/50	30	1222	536	3.33	1.11	3.32	0.013	3728.5	2582.0	0.03	0.03	11	16	1	29	4	7	13	19	0	0	3.41	0.51	80	1
78	DNOR	40/50	30	1495	442	3.64	1.19	4.05	0.050	759.9	745.7	0.20	0.17	9	21	6	12	8	9	15	20	0	0	2.99	0.54	0	1.2
79	DNOR	40/50	30	1012	366	3.37	1.10	3.83	0.055	609.0	615.0	0.16	0.11	12	17	4	13	10	9	13	20	2	0	3.05	0.53	76	1.2
80	DNOR	40/50	30	623	927	3.70	2.25	6.16	0.097	803.4	721.3	1.00	1.08	4	10	2	7	17	10	17	11	3	19	2.92	0.46	72	2.4
81	DNOR	40/50	30	483	923	3.67	2.23	6.63	0.101	771.1	683.9	0.77	0.58	5	10	6	4	9	11	18	25	7	4	2.93	0.52	75	2.4
82	DNOR	40/50	30	233	838	3.94	2.67	7.32	0.096	911.8	854.1	1.29	1.12	13	10	12	8	12	12	9	8	16	1	3.06	0.51	69	2.4
83	DNOR	40/50	30	682	520	2.30	2.60	5.44	0.097	732.1	842.8	0.85	1.30	8	10	8	11	13	10	21	4	13	0	2.90	0.59	70	2.4
84	DNOR	40/50	30	1093	386	3.85	0.78	3.22	0.031	1016.9	794.3	0.17	0.10	15	14	6	14	8	13	10	20	0	0	3.19	0.53	79	1.2
85	DNOR	40/50	30	1398	393	4.04	1.02	4.27	0.028	1078.0	1134.8	0.15	0.09	8	17	6	26	11	4	2	27	0	0	3.20	0.49	81	1
86	DNOR	40/50	30	1430	496	3.87	1.28	5.03	0.044	900.4	899.8	0.10	0.09	16	11	6	17	10	14	4	21	0	0	3.10	0.43	81	1.2
87	DNOR	40/50	30	1437	474	4.01	1.20	4.13	0.042	871.1	886.6	0.23	0.17	12	12	10	12	7	16	9	20	2	0	3.03	0.56	78	1.2
88	DNOR	40/50	30	1461	355	3.15	1.26	4.59	0.043	810.5	907.8	0.06	0.23	9	11	11	12	8	7	10	30	3	0	3.11	0.46	75	1.2
89	DNOR	40/50	30	1279	373	3.24	1.15	3.74	0.041	868.4	866.9	0.20	0.17	11	8	7	15	11	13	17	18	2	0	3.11	0.51	79	1.2
90	DNOR	40/50	30	943	230	2.33	1.47	3.77	0.042	726.5	1084.1	0.25	0.24	6	16	8	12	6	8	15	29	1	0	3.08	0.50	71	1.2
91	DNOR	40/50	30	555	125	1.89	0.95	2.83	0.041	504.4	718.8	0.22	0.31	13	17	6	6	6	7	19	25	3	0	2.91	0.54	66	2
92	DNOR	40/50	30	939	232	2.42	1.28	3.95	0.040	743.5	993.6	0.19	0.26	6	18	13	14	3	11	2	33	0	0	3.08	0.48	74	1
93	DNOR	40/50	30	254	180	1.89	1.38	3.37	0.042	720.8	1045.1	0.83	0.39	13	13	14	4	14	12	4	26	2	0	3.04	0.54	74	2
94	DNOR	40/50	30	1409	463	4.12	1.22	4.14	0.041	861.7	932.9	0.28	0.21	4	12	9	12	12	12	6	30	2	0	3.09	0.47	79	2
95	DNOR	40/50	30	1416	428	4.04	1.20	4.09	0.042	793.0	897.7	0.26	0.21	8	15	5	15	9	16	8	22	1	0	3.10	0.53	82	2
96	DNOR	20/30	30	1484	815	4.10	2.04	8.08	0.039	1588.5	1631.6	0.09	0.56											3.08	0.56	61	1
97	DNOR	20/30	30	1515	551	4.07	1.54	5.30	0.041	1033.7	1173.6	0.36	0.11	7	2	5	29	5	24	12	15	0	0	2.85	0.55	68	1
98	DNOR	30/40	30	1537	556	4.05	1.45	5.08	0.041	1039.2	1097.8	0.23	0.04	4	8	3	21	8	18	6	31	1	0	2.94	0.55	64	1
99	DNOR	30/40	30	1509	533	4.15	1.45	4.42	0.040	989.1	1117.4	0.32	0.06	1	25	7	22	6	9	10	19	1	0	3.23	0.53	84	1
100	DNOR	50/60	30	1433	428	4.26	1.14	3.90	0.040	789.0	896.1	0.24	0.23	10	13	10	13	12	14	6	20	2	0	3.23	0.48	79	2
101	DNOR	50/60	30	1102	405	4.18	1.16	3.86	0.040	750.3	900.3	0.23	0.34														2
102	DNOR	60/80	30	1542	448	4.03	1.24	4.27	0.043	808.9	904.2	0.21	0.18	13	16	9	17	9	9	7	18	3	0	3.33	0.47		2
103	DNOR	60/80	30	1520	378	3.98	1.20	4.01	0.043	692.1	874.3	0.15	0.19	11	15	12	14	10	10	1	25	3	0	3.37	0.48		2

TABLE A4.3 : Summarised results of all the tests (Continued)

DIAMOND DRILLING TESTS - SUMMARISED RESULTS

NO.	ROCK	MESH	CONC	TEST LEN.	MEAN POWER OUT.	MEAN BIT SPEED	MEAN BIT TORQ.	MEAN BIT PRES.	AVERAGE ADVANCE PER REV	AVERAGE S.E. (W)	AVERAGE S.E. (T)	BIT WEAR	BIT MASS LOSS	DIAMOND WEAR ANALYSIS % OF WEAR TYPE								PARTICLE SIZE DISTRIBUTION			MODE
														0a	0b	1a	1b	2a	2b	3a	3b	4a	4b	MEAN	SORT	MUD	
				mm	W	m/s	Nm	MPa	mm/rev	MJ/m^3	MJ/m^3	mm/m	g/m											phi	phi	%	
104	DNOR	20/30	IO	1482	516	4.12	1.38	4.93	0.040	968.5	1065.0	0.34	0.27	10	13	14	5	8	23	4	22	0	0	3.22	0.55	75	2
105	DNOR	20/30	IO	1440	572	3.91	1.63	5.05	0.044	1043.8	1165.2	0.41	0.28	9	12	12	12	9	18	4	25	0	0				2
106	DNOR	40/80	IO	1480	419	3.95	1.18	3.80	0.044	746.6	827.8	0.27	0.27	21	11	8	6	9	11	9	25	1	0	3.41	0.53	84	2
107	DNOR	40/80	IO	1422	437	4.08	1.19	3.75	0.043	776.6	859.1	0.26	0.25	15	14	10	4	8	13	8	27	1	0	3.29	0.65	81	2
108	DNOR	20/25	IO	538	366	3.86	1.03	5.07	0.015	2037.8	2222.4	0.77	0.08											3.45	0.67	70	1
109	DNOR	25/30	IO	1396	547	3.76	1.43	5.05	0.039	1170.3	1155.1	0.52	0.62											3.14	0.58	0	2
110	DNOR	30/35	IO	1421	683	3.85	1.75	4.99	0.064	873.4	859.8	0.83	1.00											3.03	0.60	71	2
111	DNOR	35/40	IO	1423	725	3.77	1.94	4.88	0.087	693.0	698.6	0.75	0.92											3.12	0.59	72	2
112	DNOR	40/45	IO	1414	739	3.69	2.01	4.83	0.083	752.2	756.9	0.60	0.81											3.27	0.59	72	2
113	DNOR	45/50	IO	1427	564	3.91	1.78	4.91	0.069	648.9	800.1	0.37	0.59											3.21	0.48	79	2
114	DNOR	50/60	IO	1359	584	3.85	1.57	4.73	0.063	753.0	780.1	0.70	0.62											3.28	0.52	88	2
115	DNOR	60/70	IO	1385	548	4.00	1.41	4.83	0.053	804.5	827.9	0.29	0.66											3.37	0.49	87	2
116	DNOR	70/80	IO	1394	564	4.22	1.50	4.85	0.049	858.6	962.0	0.30	0.48											3.58	0.50	89	2
117	DNOR	20/25	IO	1393	1015	3.67	2.70	7.81	0.054	1595.0	1558.9	1.76	2.17	9	3	0	6	6	15	39	21	0	0	3.10	0.13	68	2
118	DNOR	25/30	IO	1180	1185	3.55	3.15	7.67	0.061	1697.6	1603.9	0.00	0.00	6	0	11	0	6	11	33	33	0	0	3.04	0.70	68	2
119	DNOR	30/35	IO	1057	1224	3.76	3.10	7.82	0.071	1412.6	1346.9	1.75	2.06	4	6	2	6	8	19	27	23	4	0	2.98	0.75	74	2
120	DNOR	35/40	IO	840	1213	3.72	3.47	7.80	0.092	1102.8	1176.7	1.76	2.22	5	11	7	0	14	16	20	25	2	0	3.08	0.66	70	2
121	DNOR	40/45	IO	1379	1176	3.75	2.98	7.62	0.089	1099.8	1045.7	1.34	1.83	1	13	4	3	18	13	22	18	6	0	3.07	0.75	68	2
122	DNOR	45/50	IO	1374	1106	3.72	3.02	7.54	0.093	1001.3	1017.5	0.66	1.08	10	18	6	2	10	8	25	21	1	0	3.15	0.58	77	2
123	DNOR	50/60	IO	1348	1078	3.74	2.80	7.46	0.077	1160.1	1127.1	0.61	0.79	11	12	8	5	5	16	25	16	2	0	3.56	0.56	83	2
124	DNOR	60/70	IO	1443	908	3.74	2.86	7.55	0.081	936.0	1102.4	0.58	0.82	6	19	7	1	11	20	16	18	2	0	3.36	0.48	87	2
125	DNOR	70/80	IO	1261	1049	3.77	2.77	7.52	0.079	1093.8	1089.3	0.53	0.67	14	14	11	2	13	17	14	15	1	0	3.54	0.56	89	2
126	DNOR	20/25	IO	492	155	3.98	0.67	2.72	0.013	945.5	1623.2	0.25	0.32											3.28	0.76	74	1
127	DNOR	25/30	IO	119	90	3.90	0.32	2.61	0.003	2277.6	3131.7	0.45	0.08											3.59	0.70	83	1
128	DNOR	30/35	IO	308	87	3.77	0.49	2.76	0.009	848.6	1812.3	0.31	0.14											3.50	0.68	85	1
129	DNOR	35/40	IO	431	181	3.77	0.87	2.62	0.012	1263.1	2294.0	0.19	0.23											4.04	0.28	87	1
130	DNOR	40/45	IO	340	134	3.75	0.67	2.61	0.009	1186.7	2230.2	0.55	0.21											3.38	0.70	85	1
131	DNOR	45/50	IO	294	107	3.83	0.63	2.54	0.008	1091.0	2480.6	0.39	0.17											3.55	0.57	85	1
132	DNOR	50/60	IO	223	112	3.80	0.42	2.34	0.006	1518.4	2152.2	0.28	0.22											3.58	0.66	88	1
133	DNOR	60/70	IO	326	116	3.82	0.63	2.71	0.009	1074.0	2228.8	0.25	0.12											3.59	0.57	93	1
134	DNOR	70/80	IO	432	147	3.83	0.62	2.57	0.012	1020.8	1558.7	0.18	0.13											3.56	0.52	92	1
135	DNOR	70/80	IO	1443	1548	3.24	3.84	10.17	0.078	1887.3	1516.1	0.52	0.70	16	14	14	4	12	13	15	14	1	0	3.44	0.53	90	2
136	DNOR	60/70	IO	1408	1523	3.22	3.95	10.16	0.079	1879.9	1570.2	0.58	0.77	14	14	7	6	9	17	18	14	1	0	3.14	0.55	88	2
137	DNOR	50/60	IO	1386	1468	3.18	3.59	9.94	0.083	1728.7	1343.1	0.59	0.83	13	16	6	7	9	18	13	14	4	0	3.44	0.55	85	2
138	DNOR	45/50	IO	1476	1512	3.15	3.73	10.07	0.119	1248.2	969.8	0.61	0.67	10	11	9	3	9	22	11	23	0	0	3.25	0.57	81	2
139	DNOR	40/45	IO	1409	1653	3.58	4.14	10.44	0.104	1367.7	1227.9	0.63	0.84	13	10	6	4	7	15	13	27	5	0	3.21	0.60	75	2
140	DNOR	35/40	IO	1423	1616	3.41	4.20	10.35	0.082	1802.4	1597.9	1.23	1.46	5	13	2	2	7	17	25	22	7	0	3.01	0.56	79	2
141	DNOR	30/35	IO	700	1503	3.42	3.86	10.19	0.073	1898.3	1667.9	2.65	2.85	3	5	2	3	18	18	28	17	5	0	2.88	0.63	74	2
142	DNOR	25/30	IO	680	1547	3.33	4.00	10.35	0.056	2573.4	2212.7	2.22	2.38	6	23	6	0	11	17	15	13	9	0	2.89	0.62	79	2
143	DNOR	20/25	IO	594	1707	3.22	4.46	10.56	0.085	1945.4	1637.4	3.31	4.71	3	0	3	0	21	7	34	24	7	0	2.75	0.70	71	2
144	DNOR	40/50	IO	96	121	3.82	0.56	2.42	0.003	2806.1	6702.4	0.20	0.06	7	11	11	19	4	11	13	22	1	0				1
145	DNOR	40/50	IO	497	505	3.58	1.32	5.60	0.051	853.5	801.0	0.33	0.24	9	8	7	16	5	18	20	17	1	0				2
146	DNOR	40/50	IO	505	1108	3.25	2.87	7.61	0.106	961.1	834.7	0.48	1.06	9	12	8	5	3	21	25	17	1	0				2
147	DNOR	40/50	IO	501	1545	3.06	4.20	10.26	0.087	1788.9	1487.9	1.21	1.43	7	10	9	5	10	20	21	16	2	0				2
148	DNOR	40/50	IO	441	1836	2.91	4.58	12.49	0.087	2217.7	1611.4	1.02	1.11	10	10	5	3	17	22	21	9	5	0				2
149	DNOR	20/25	IO	364	150	3.63	0.56	2.51	0.011	1236.8	1661.9	0.07	0.21	14	3	8	16	3	11	25	17	3	0	2.90	0.97	81	1
150	DNOR	20/25	IO	933	640	3.57	1.66	5.18	0.027	2050.7	1900.6	2.01	2.31	16	0	11	0	5	33	0	5	0	0	2.80	0.72	76	2
151	DNOR	20/25	IO	1481	1273	3.52	3.27	7.70	0.074	1616.6	1379.5	1.01	2.05	7	13	7	3	10	27	3	20	10	0	2.80	0.71	74	2
152	DNOR	20/25	IO	1145	1491	2.99	3.78	10.49	0.045	3424.8	2597.1	1.97	2.74	5	5	5	5	0	27	18	32	5	0	2.83	0.74	77	2
153	DNOR	25/30	IO	1559	1117	3.24	2.92	7.69	0.071	1509.7	1277.4	1.33	1.81	8	19	0	2	4	25	21	19	2	0	2.91	0.67	75	2
154	DNOR	25/30	IO	1166	1356	2.88	3.61	10.10	0.042	3480.7	2650.6	1.98	1.65	8	12	6	2	8	22	20	14	6	0	3.08	0.64	82	2
155	DNOR	35/40	IO	1566	1118	3.14	2.83	7.42	0.088	1261.9	1001.9	1.05	1.26	5	21	5	1	13	21	11	21	1	0	2.96	0.66	79	2
156	DNOR	40/45	IO	1588	1033	3.14	2.70	7.43	0.103	996.4	815.1	1.19	0.89	10	18	8	3	4	26	21	11	0	0	3.04	0.61	78	2
157	DNOR	45/50	IO	1538	1281	2.80	3.10	9.98	0.116	1226.0	830.3	0.34	0.48	8	16	9	5	6	16	22	15	3	0	3.13	0.61	87	2
158	DNOR	20/25	IO	617	183	3.34	0.84	3.67	0.019	885.6	1038.7	0.15	0.27	7	23	5	20	5	8	23	7	2	0	3.15	0.63	83	1
159	DNOR	20/25	IO	834	425	3.64	1.62	4.78	0.024	1522.8	1327.5	0.97	0.64	0	0	16	19	0	28	13	25	0	0	3.18	0.72	85	2

TABLE A4.4 : Summarised results of all the tests (Concluded)

DIAMOND DRILLING TESTS - SUMMARISED RESULTS

NO.	ROCK	MESH	CONC	TEST LEN.	MEAN POWER OUT.	MEAN BIT SPEED	MEAN BIT TORQ.	MEAN BIT PRES.	AVERAGE ADVANCE PER REV	AVERAGE S.E. [W]	AVERAGE S.E. [T]	BIT WEAR	BIT MASS LOSS	DIAMOND WEAR ANALYSIS % OF WEAR TYPE									PARTICLE SIZE DISTRIBUTION			MODE
														0a	0b	1a	1b	2a	2b	3a	3b	4a	4b	MEAN	SORT	MUD	
				mm	W	m/s	Nm	MPa	mm/rev	MJ/m^3	MJ/m^3	mm/m	g/m											phi	phi	%	
160	DNOR	20/30	30	316	564	3.74	1.44	4.74	0.045	1043.2	997.2	1.70	1.25	3	3	9	13	13	13	19	16	13	0	2.74	0.66	71	2
161	DNOR	50/60	30	1525	447	3.71	1.10	4.67	0.047	800.4	732.3	0.09	0.15	14	16	12	7	9	10	9	23	0	0	3.32	0.57	91	2
162	QZIT	20/30	30	1571	602	3.51	1.47	6.68	0.050	1069.3	919.1	0.37	0.44	10	3	3	44	5	15	10	5	5	0	2.97	0.68	85	1
163	QZIT	50/60	30	1572	455	3.50	1.13	5.11	0.051	795.6	690.8	0.23	0.19	9	5	4	30	4	18	16	14	0	0	3.29	0.49	93	1
164	DNOR	20/30	30	422	176	3.72		2.12	0.012	1247.8		0.93	0.57	8	10	13	8	5	10	21	15	10	0	3.14	0.64	87	2
165	DNOR	50/60	30	431	216	3.63	0.68	3.16	0.012	1494.6	1708.1	0.10	0.14	15	20	9	9	10	7	12	18	1	0	3.29	0.57	95	1
166	QZIT	20/30	30	426	83	3.63	0.23	1.50	0.012	579.9	580.1	0.42	0.75	6	13	3	9	9	28	13	13	6	0	3.00	0.77	76	2
167	QZIT	50/60	30	432	145	3.61	0.58	3.30	0.013	1005.5	1445.7	0.07	0.11	9	15	8	15	6	9	16	19	3	0	3.13	0.53	94	1
168	DNOR	20/30	30	1108	718	3.74	1.64	6.53	0.031	1930.8	1651.2	0.27	0.20	13	5	5	28	15	15	5	15	0	0	3.12	0.74	88	1
169	DNOR	50/60	30	1057	374	3.75	1.11	3.84	0.032	976.4	1090.2	0.17	0.16	13	18	5	5	10	8	17	23	1	0	3.23	0.60	92	2
170	QZIT	20/30	30	1130	373	3.72	0.87	3.91	0.032	960.3	829.1	0.15	0.08	11	8	5	24	3	16	24	8	3	0	3.10	0.63	89	1
171	QZIT	50/60	30	1113	348	3.70	0.92	4.91	0.032	905.5	884.8	0.14	0.12	5	9	5	33	5	9	15	18	1	0	3.24	0.53	95	1
172	DNOR	20/30	30	1080	846	3.76	1.98	8.00	0.045	1567.4	1379.9	0.17	0.30	9	2	7	10	11	22	33	4	2	0	2.82	0.63	84	2
173	DNOR	20/30	50	1494	645	3.46	1.59	6.04	0.050	1164.2	994.0	0.18	0.20	8	15	8	21	11	7	16	13	0	0	2.94	0.64	82	1
174	DNOR	20/30	50	1428	775	3.35	2.09	7.49	0.045	1591.7	1441.7	0.41	0.41	6	5	5	23	5	15	16	26	0	0	2.98	0.59	84	1
175	DNOR	30/40	MONO	1259	327	3.61	0.83	5.75	0.012	2320.9	2126.9			0	9	24	20	19	24	0	0	4	0				1
176	DNOR	30/40	MONO	1410	731	3.62	1.75	8.83	0.045	1385.7	1197.5			0	6	6	24	0	44	0	0	20	0				2
177	QZIT	40/50	30	435	102	3.79	0.32	3.17	0.012	701.3	830.3	0.21	0.07	8	33	2	15	7	5	10	20	0	0	2.97	0.61	97	1
178	SSTN	40/50	30	434	0	3.72	0	0.44	0.012	0	0	0.07	0.36	8	26	11	15	16	5	8	11	0	0	2.75	0.44	71	2
179	JASP	40/50	30	222	1043	3.63	2.47	11.27	0.011	7962.9	6843.5	2.07	1.04	1	1	1	11	0	6	1	7	0	72	2.13	0.93	97	1
180	QRTZ	40/50	30	437	208	3.77	0.42	4.91	0.012	1421.0	1081.9	0.32	0.39	11	13	4	18	7	8	29	9	1	0	2.24	0.77	91	1
181	CALC	40/50	30	443	44	3.74	0.17	0.53	0.012	294.4	431.6	0.09	0.02	9	33	2	3	22	1	16	14	0	0	2.48	0.69	84	2
182	FELS	40/50	30	422	216	3.68	0.46	3.54	0.012	1530.2	1191.7	0.17	0.06	12	16	3	15	9	8	20	17	0	0	2.77	0.65	88	1
183	DNOR	40/50	30	424	220	3.70	0.62	2.82	0.012	1553.4	1631.8	0.09	0.05	11	24	6	12	13	7	13	14	0	0	3.16	0.63	91	1
184	QZIT	40/50	30	1308	522	3.79	1.23	6.30	0.045	952.4	849.3	0.11	0.14	11	9	4	39	1	4	11	21	0	0	3.12	0.60	93	1
185	SSTN	40/50	30	1722	8	3.85	0.11	0.53	0.048	12.7	69.2	0.04	0.13	6	30	7	17	18	7	5	10	0	0	2.75	0.54	60	2
186	JASP	40/50	30	98	1709	3.27	4.36	11.19	0.042	3845.9	3206.2	1.22	2.18	4	3	4	21	10	9	16	8	10	15	2.65	0.78	94	1
187	QRTZ	40/50	30	892	1409	3.34	3.41	9.50	0.046	2832.5	2285.3	1.04	1.30	3	4	4	46	6	10	19	7	1	0	2.53	0.92	90	1
188	CALC	40/50	30	1019	212	3.67	0.59	1.02	0.047	380.1	385.4	0.01	0.04	11	23	5	2	17	8	11	22	1	0	2.52	0.40	85	2
189	FELS	40/50	30	1186	483	3.64	1.16	6.41	0.048	856.8	749.3	0.20	0.06	7	17	4	22	6	9	26	9	0	0	3.04	0.62	86	1
190	DNOR	40/50	30	1501	454	3.82	1.05	4.24	0.046	801.7	710.4	0.19	0.23	4	24	4	13	10	13	14	17	1	0	2.95	0.51	92	2
191	QZIT	40/50	30	1168	354	3.78	0.78	4.42	0.033	890.5	744.2	0.11	0.05	10	11	7	19	10	1	20	22	0	0	3.15	0.50	88	1
192	SSTN	40/50	30	1195	0	4.02	0	0.55	0.031	0	0	0.12	0.19	4	40	4	12	20	2	6	12	0	0	2.92	0.51	69	2
193	JASP	40/50	30	178	1641	3.29	4.08	13.11	0.028	5496.7	4500.7	1.69	1.37	7	1	6	34	1	8	16	15	3	9	2.19	0.90	92	1
194	QRTZ	40/50	30	829	452	3.86	1.11	5.86	0.031	1157.9	1096.4	0.57	0.67	13	7	9	29	3	7	25	7	0	0	1.38	0.71	99	1
195	CALC	40/50	30	1177	183	3.89	0.51	1.98	0.032	463.7	500.6	0.00	0.02	10	27	4	1	18	6	16	18	0	0	2.14	0.42	74	2
196	FELS	40/50	30	1121	479	3.79	1.16	6.39	0.031	1275.0	1168.0	0.04	0.08	9	18	9	20	2	6	15	22	0	0	3.32	0.57	90	1
197	DNOR	40/50	30	1153	428	3.79	1.00	4.04	0.032	1108.0	982.0	0.15	0.12	10	13	8	8	17	10	16	18	0	0	3.10	0.54	87	2
198	SSTN	40/50	30	2290	48	4.01	0.15	0.48	0.103	36.2	46.0	0.17	0.81	10	42	8	8	11	1	5	14	1	0	2.79	0.58	64	2
199	CALC	40/50	30	632	278	3.68	1.81	3.10	0.104	550.6	541.2	0.13	1.33	6	35	10	2	17	7	13	10	0	0	1.47	0.86	85	2
200	DNOR	20/30	MONO	3339	535	3.82	1.42	5.90	0.030	1435.6	1459.7			0	17	13	38	10	19	3	0	0	0				1
201	DNOR	50/60	50	1438	528	4.10	1.36	5.51	0.041	969.4	1019.3	0.08	0.12	8	21	6	10	8	10	17	17	2	0				1,2
202	SYNT	40/50	30	1520	606	3.98	1.45	6.74	0.042	1127.0	1081.6	0.13	0.13	8	8	7	20	4	15	19	9	0	0	3.24	0.64	81	1
203	GRAN	40/50	30	1489	733	3.88	1.67	8.49	0.042	1394.4	1231.7	0.50	0.24	7	3	6	32	1	10	32	10	0	0	2.74	0.90	96	1
204	SYNT	40/50	30	417	128	4.33	0.42	2.38	0.010	913.8	1317.5	0.34	0.17	13	21	6	20	6	7	17	11	0	0	3.03	0.58	88	1
205	GRAN	40/50	30	398	266	4.23	0.59	6.56	0.010	1998.6	1870.7	0.05	0.27	12	20	3	27	7	6	13	12	0	0	2.81	0.77	94	1

APPENDIX 5 - STANDARDISED TEST RESULTS

TABLE A5.1 : Standardised results of set rate of advance tests in norite

TEST NO.	MEAN POWER OUTPUT (W)	MEAN BIT PRESSURE (MPa)	MEAN BIT SPEED (ms^{-1})	MEAN BIT TORQUE (Nm)	AVERAGE ADVANCE PER.REV. (mm/rev)	AVERAGE S.E. [W] (MJm^{-3})	AVERAGE S.E. [T] (MJm^{-3})
STANDARDISED TO 320 SECONDS							
74	96	2.11	4.15	0.54	0.011	688.9	1617.7
75	77	1.87	4.07	0.57	0.011	565.2	1709.7
76	108	2.00	3.76	0.54	0.011	846.7	1599.8
78	420	3.79	3.67	1.15	0.044	721.3	721.3
79	370	3.87	3.36	1.09	0.044	616.8	612.1
84	350	2.88	3.87	0.76	0.033	919.9	768.3
85	360	3.46	4.06	0.93	0.033	981.8	1034.2
STANDARDISED TO 200 SECONDS							
80	907	5.49	3.77	2.27	0.1	765.9	723.6
81	901	6.07	3.73	2.19	0.1	739.4	672.0

TABLE A5.2 : Standardised results of bit tests at set rotational speed in norite

TEST NO.	MEAN POWER OUTPUT (W)	MEAN BIT PRESSURE (MPa)	MEAN BIT SPEED (ms^{-1})	MEAN BIT TORQUE (Nm)	AVERAGE ADVANCE PER.REV. (mm/rev)	AVERAGE S.E. [W] (MJm^{-3})	AVERAGE S.E. [T] (MJm^{-3})
STANDARDISED TO 300 SECONDS							
86	477	4.68	3.88	1.23	0.044	872.1	873.8
87	465	3.95	4.02	1.14	0.042	859.8	846.4
88	340	4.15	3.15	1.23	0.043	781.1	890.0
89	358	3.49	3.25	1.11	0.041	832.8	841.6
90	228	3.69	2.33	1.48	0.042	723.8	1091.0
92	229	3.67	2.43	1.28	0.040	740.2	1003.6
STANDARDISED TO 200 SECONDS							
91	141	3.06	1.89	1.02	0.041	563.3	773.4
93	179	3.37	1.89	1.40	0.042	720.0	1061.5

TABLE A5.3 : Standardised results for tests in granite, quartz and jaspilite

TEST NO.	MEAN POWER OUTPUT (W)	MEAN BIT PRESSURE (MPa)	MEAN BIT SPEED (ms^{-1})	MEAN BIT TORQUE (Nm)	AVERAGE ADVANCE PER.REV. (mm/rev)	AVERAGE S.E. [W] (MJm^{-3})	AVERAGE S.E. [T] (MJm^{-3})
GRANITE : STANDARDISED TO 200 SECONDS							
5	486	6.98	3.83	1.20	0.012	1928.5	1825.9
8	894	8.14	3.86	2.41	0.052	1286.1	1335.8
9	431	7.78	3.99	1.35	0.008	1619.1	2024.2
10	818	9.32	3.71	2.03	0.044	1342.5	1236.5
21	393	5.95	3.57	0.92	0.010	2069.6	1723.7
22	721	8.16	3.60	1.63	0.020	1923.1	1564.9
203	594	5.85	3.93	1.47	0.042	1118.6	1085.1
205	173	4.26	4.26	0.42	0.010	1297.8	1330.0
QUARTZ : STANDARDISED TO 300 SECONDS							
180	171	4.18	3.79	0.38	0.012	1183.5	999.2
187	1336	8.93	3.42	3.19	0.045	2637.1	2150.9
194	435	5.45	3.88	1.07	0.031	1117.5	1070.8
JASPILITE : STANDARDISED TO 45 SECONDS							
179	410	4.49	3.85	1.12	0.011	3191.7	3352.2
186	1709	11.19	3.27	4.36	0.042	3845.9	3206.2
193	1320	9.93	3.63	3.17	0.025	3924.8	3417.3

APPENDIX 6 - RESULTS OF CALCULATIONS OF ESTIMATED PRESSURE PER STONE

TEST NO.	NO. OF 1b WORN STONES	FINAL BIT PRESSURE (MPa)	MEDIAN STONE SIZE (mm)	DRILLING MODE	AVERAGE PRESSURE (MPa)
32	5	6,2	0,359	2	1775
33	9	6,3	0,359	2	1006
34	3	6,1	0,359	2	2934
35	2	6,1	0,359	2	4409
36	2	6,3	0,359	2	2275
38	5	6,3	0,359	2	1809
39	1	6,2	0,359	2	9006
40	0	6,2	0,359	2	-
41	0	6,1	0,359	2	-
42	19	6,0	0,359	1,2	457
43	3	6,2	0,359	2	2973
53	10	2,2	0,359	1	315
54	14	4,0	0,359	1,2	415
55	6	6,2	0,359	2	1484
56	6	8,4	0,359	2	2028
57	5	10,4	0,359	2	3001
58	6	13,1	0,359	2	3146
59	15	3,1	0,359	1	294
60	11	4,9	0,359	2	648
61	4	7,3	0,359	2	2617
62	8	8,1	0,359	2	1464
63	6	9,5	0,359	2	2295
64	5	10,3	0,359	2	2958
65	15	3,2	0,359	1	312
66	2	4,4	0,359	2	3144
67	5	5,3	0,359	2	1518
68	6	6,9	0,359	2	1667
69	2	9,2	0,359	2	6657
70	1	10,4	0,359	2	15019
71	3	6,8	0,359	2	3280
72	6	7,7	0,359	2	1850
74	14	2,8	0,359	1	288
75	17	2,9	0,359	1	246
76	26	5,7	0,359	1	316
77	38	8,8	0,359	1	334
78	15	4,3	0,359	1,2	414
79	17	3,8	0,359	1,2	322
80	7	5,5	0,359	2	1133
81	3	8	0,359	2	2884
82	6	6,0	0,359	2	1443
83	10	6,0	0,359	2	866
84	20	4,2	0,359	1	303
85	29	5,0	0,359	1,2	300
86	25	5,6	0,359	1,2	323
87	15	4,2	0,359	1,2	404
88	13	4,7	0,359	1,2	521

TEST NO.	NO. OF 1b WORN STONES	FINAL BIT PRESSURE (MPa)	MEDIAN STONE SIZE (mm)	DRILLING MODE	AVERAGE PRESSURE (MPa)
89	15	4,4	0,359	1,2	423
90	14	4,0	0,359	1,2	412
91	6	3,5	0,359	2	842
92	16	4,0	0,359	1	360
93	4	3,7	0,359	2	1334
94	15	4,8	0,359	2	462
95	18	4,7	0,359	2	377
97	12	6,8	0,715	1	206
98	15	6,1	0,505	1	296
99	15	5,3	0,505	1	258
100	24	4,2	0,274	2	433
102	60	4,0	0,230	2	234
103	30	4,0	0,230	2	469
104	5	5,0	0,569	2	577
105	9	5,5	0,569	2	351
106	11	4,3	0,299	2	756
107	8	3,8	0,562	2	987
117	2	7,6	0,775	2	1178
118	0	7,8	0,650	2	-
119	3	7,8	0,545	2	1631
120	0	7,8	0,460	2	-
121	2	7,6	0,455	2	3423
122	3	7,5	0,324	2	4457
123	5	7,5	0,274	2	3692
124	2	7,5	0,230	2	13281
125	3	7,5	0,194	2	12336
135	14	10,2	0,194	2	3587
136	14	10,2	0,230	2	2549
137	20	9,9	0,274	2	1231
138	6	10,1	0,324	2	2970
139	5	10,4	0,359	2	3012
140	2	10,4	0,460	2	4552
141	2	10,2	0,545	2	3186
142	0	10,4	0,650	2	-
143	0	10,6	0,775	2	-
144	22	2,4	0,359	1	159
145	20	5,6	0,359	2	404
146	6	7,6	0,359	2	1830
147	6	10,3	0,359	2	2468
148	3	12,5	0,359	2	5998
149	7	2,5	0,775	1	111
150	0	5,2	0,775	2	-
151	1	7,7	0,775	2	2382
152	1	10,5	0,775	2	3245
153	1	7,7	0,650	2	3382
154	1	10,1	0,650	2	4442
155	1	7,4	0,460	2	6526
156	3	7,4	0,455	2	2223
157	10	10,0	0,324	2	1768

TEST NO.	NO. OF 1b WORN STONES	FINAL BIT PRESSURE (MPa)	MEDIAN STONE SIZE (mm)	DRILLING MODE	AVERAGE PRESSURE (MPa)
158	7	2,7	0,775	1	118
159	6	4,8	0,775	2	247
160	4	4,5	0,715	2	409
161	10	4,9	0,274	2	1213
162	17	8,8	0,715	1	188
163	60	5,7	0,274	1	235
164	3	2,4	0,715	2	291
165	24	3,5	0,274	1	361
166	3	1,0	0,715	2	121
167	36	5,5	0,274	1	378
168	11	8,4	0,715	1	278
169	8	4,2	0,274	2	1299
170	9	5,5	0,715	1	222
171	73	7,4	0,274	1	251
172	5	7,0	0,715	2	509
173	4	6,0	0,715	2	545
174	20	7,5	0,715	1	136
175	11	5,8	0,505	1	381
176	13	8,8	0,505	2	495
183	14	4,1	0,359	1	423
190	17	5,0	0,359	2	424
197	12	4,7	0,359	2	564
200	23	10,1	0,715	1	158
201	40	6,0	0,274	1,2	371